LLNL: UCRL-TM-231628

LBNL: LBNL-62783

Beam Physics with Intense Space-Charge

Lecturers:
John J. Barnard and Steven M. Lund
Lawrence Livermore National Lab

Grader and Simulation Lectures:
Rami A. Kishek
University of Maryland

Course Notes:
United States Particle Accelerator School
Held 12-23 June, 2006
Waltham, Massachusetts
Sponsored by Boston University

Beam Physics with Intense Space Charge

Instructors: John Barnard and Steven Lund, Lawrence Livermore National Laboratory
and Rami Kishek, University of Maryland

Purpose and Audience

The purpose of this course is to provide a comprehensive introduction to the physics of beams with intense space charge. This course is suitable for graduate students and researchers interested in accelerator systems that require sufficient high intensity where mutual particle interactions in the beam can no longer be neglected. *Prerequisites: undergraduate level Electricity and Magnetism and Classical Mechanics. Some familiarity with plasma physics, special relativity, and basic accelerator physics is recommended but not required.*

Objectives

This course is intended to give the student a broad overview of the dynamics of beams with strong space charge. The emphasis is on theoretical and analytical methods of describing the acceleration and transport of beams. Some aspects of numerical and experimental methods will also be covered. Students will become familiar with standard methods employed to understand the transverse and longitudinal evolution of beams with strong space charge. The material covered will provide a foundation to design practical architectures.

Instructional Method

Lectures will be given during morning sessions, followed by afternoon discussion sessions, which will engage the student on the material covered in lecture. Daily problem sets will be assigned that will be expected to be completed outside of scheduled class sessions. Problem sets will generally be due the morning of the next lecture session. A final take home exam will be given on the second Thursday, and will cover the contents of the entire course. Two instructors and a teaching assistant will be available to for guidance during evening homework sessions.

Course Content

In this course, we will introduce you to the physics of intense charged particle beams, focusing on the role of space charge. The topics include:

particle equations of motion, the paraxial ray equation, and the Vlasov equation; 4-D and 2-D equilibrium distribution functions (such as the Kapchinskij-Vladimirskij, thermal equilibrium, and Neuffer distributions), reduced moment and envelope equation formulations of beam evolution; transport limits and focusing methods; the concept of emittance and the calculation of its growth from mismatches in beam envelope and from space-charge non-uniformities using system conservation constraints; the role of space-charge in producing beam halos; longitudinal space-charge effects including small amplitude and rarefaction waves; stable and unstable oscillation modes of beams (including envelope and kinetic modes); the role of space charge in the injector; and algorithms to calculate space-charge effects in particle codes. Examples of intense beams will be given primarily from the ion and proton accelerator communities with applications from, for example, heavy-ion fusion, spallation neutron sources, nuclear waste transmutation, etc.

Reading Requirements

Extensive class notes will be provided that will serve as the primary reference. *(to be provided by the USPAS)* "The Theory and Design of Charged Particle Beams" by Martin Reiser (Wiley & Sons 1994) will be provided as a supplemental reference.

Credit Requirements

Students will be evaluated based on performance: final exam (20 % of course grade), homework assignments (80 % of course grade).

```
US Particle Accelerator School
  sponsored by Boston University
Waltham, Massachusetts
Monday June 12 - Friday June 23, 2006

LLNL: UCRL-??To Add??
LBNL: LBNL-??To Add??


"Beam Physics with Intense Space Charge"

Lecturers:
John J. Barnard and Steven M. Lund
Lawrence Livermore National Laboratory

Simulation Lectures and Grader:
Rami A. Kishek
University of Maryland


List of Files:

  .txt => ascii text format
  .pdf => Adobe Acrobat pdf
  .ppt => Microsoft Power Point (produced by OpenOffice Conversion)
  .xls => Microsoft Excel       (produced on OpenOffice Conversion)
  .odp => Open Document Presentation (Open Office)
  .odw => Open Document Writer       (Open Office)
  .ods => Open Document Spread Sheet (Open Office)


   JJB - Notes by J.J. Barnard
   SML - Notes by S.M. Lund
   RAK - Notes by R.A. Kishek

Class material can be found in the following files and directories:

00_cover.pdf
00_cover.ppt
  Cover used in paper printing of class material.

00_outline.txt
00_outline.pdf
  Outline and file list (this file).

00_overview.txt
00_overview.pdf
  Class overview in text and pdf formats.

00_schedule.pdf
00_schedule.xls
  Actual schedule of class lectures.

01_intro.pdf   (JJB)
  Introductory lecture surveying basic concepts.

02_envelope_eqns.pdf  (JJB)
  Introduction to envelope equations.

03_currentlimits.pdf (JJB)
  Introduction to current limits.

04_tpe.pdf  (SML)
  Transverse particle equations of motion.

05_ted_full.pdf  (SML)
05_ted_ho.pdf
05_ted_app_a.pdf
```



```
05_ted_app_b.pdf
  Transverse equilibrium distributions.

06_ca.pdf (SML)
  Transverse particle resonances with application to rings.

07_injector_longitudinal_I.pdf  (JJB)
  Injectors and longitudinal physics, part I.

08_longitudinal_II.pdf  (JJB)
  Longitudinal physics, part II.

09_longitudinal_III.pdf  (JJB)
  Longitudinal physics, part III.

10_tce_full.pdf  (SML)
10_tce_ho.pdf
10_tce_sec9.pdf
  Centroid and envelope evolution including envelope modes and stability.

11_env_modes_halo.pdf  (JJB)
  Continuous focusing envelope modes and beam halo.

12_tks.pdf (SML)
  Transverse kinetic stability: conservation constraints, kinetic stability
  bounds, normal modes on a KV beam, and other beam stability topics.

13_pressure_scattering_electrons.pdf  (JJB)
  Vacuum, scattering, and electron effects.

14_heavyionfusion_finalfocus.pdf  (JJB)
  Heavy ion fusion overview and final focus.

15_sims_rak.pdf  (RAK)
15_sims_sml.pdf    (SML)
  Numerical simulations of beams.

16_summary_jjb.pdf  (JJB)
  Summary of lectures by J.J. Barnard.

grades_evaluations  (directory)
  Note: This directory is only distributed to the instructors.

  grades_evaluations.pdf
    Summary of all grades on problem sets and final and class evaluations.

  students.pdf
    Listing of students and institutions, and credit status.

  students_prelim.txt
    Preliminary listing of students signed up before the class along
    with overall statistics of classes from the school.


movies  (directory)
  Note: This directory is not included in most distributions (large file size)

  ESQfastrise_zx.mpg
    3D injector simulation with a fast rise voltage pulse.

  ESQslowrise_zx.mpg
    3D injector simulation with a slow rise voltage pulse.

  hcx.mov
    Simulation of the HCX experiment from the source.

  hollow_movie.mpg
    Simulation on the evolution of a nonuniform density beam.
```

```
photos  (directory)
class1.jpg            john.jpg       steve.jpg       studyroom2.jpg
class2.jpg            john_lec1.jpg  steve_lec1.jpg  studyroom3.jpg
class.listening1.jpg  john_lec2.jpg  steve_lec2.jpg
class.listening2.jpg  rami.jpg       studyroom1.jpg


problems (directory)
  Note: This directory is only distributed to the instructors.

  All files pdf scans of handwritten problems and solutions

  01_set1_problems.pdf    Problem  Set #1
  01_set1_solutions.pdf   Solution Set #1

  02_set2_problems.pdf    Problem  Set #2
  02_set2_solutions.pdf   Solution Set #2

  03_set3_problems.pdf    Problem  Set #3
  03_set3_solutions.pdf   Solution Set #3

  04_set4_problems.pdf    Problem  Set #4
  04_set4_solutions.pdf   Solution Set #4

  05_set5_problems.pdf    Problem  Set #5
  05_set5_solutions.pdf   Solution Set #5

  06_set6_problems.pdf    Problem  Set #6
  06_set6_solutions.pdf   Solution Set #6

  07_set7_problems.pdf    Problem  Set #7
  07_set7_solutions.pdf   Solution Set #7

  08_set8_problems.pdf    Problem  Set #8
  08_set8_solutions.pdf   Solution Set #8

  09_final_problems.pdf   Problem  Set #9  (Final Exam counts for 2 sets)
  09_final_solutions.pdf  Solution Set #9

  10_replacement_problems.pdf   More difficult replacement problems (not used)

  SML: Collections of problems and solutions sorted by topic
       (only a subset were used in this class)

  ps_tpe.pdf   Transverse particle equations of motion
  ps_ted.pdf   Transverse equilibrium distributions
  ps_tce.pdf   Transverse centroid and envelope descriptions of beam evolution
  ps_ca.pdf    Circular accelerators and resonance effects in rings
  ps_st.pdf    Simulation techniques for intense beams


simulations (directory)
  Note:  This directory not included in most distributions.  Material was
  not used in this class (RAK gave in-class illustrations)

  ag-slice.py
     Python input script for example WARP PIC code simulations.   This file
     was used in one interactive class session to carry out example
     simulations by making simple variants of this example run.  See script
     header for instructions on running this script and viewing the output
     files.

  ag-slice.000.cgm
     cgm output file produced by WARP simulation ag-slice.py


Course Outline:
```



```
Note:  This outline and the distribution files are arranged in logical
presentation order.  In the actual class, there were deviations from
this order due to practical constraints.  The actual order of material
presented can be found in 00_schedule.pdf.

"Beam Physics with Intense Space-Charge"


Lecturers: John J. Barnard and Steven M. Lund
Lawrence Livermore National Laboratory

Simulations and Grading: Rami A. Kishek
University of Maryland

1.  Introduction to the Physics of Beams and Basic Parameters  (JJB)
01_intro.pdf  pdf scan, handwritten notes and slides

  1.1 Particle equations of motion
  1.2 Dimensionless parameters: Perveance, phase advance, space charge
      tune depression
  1.3 Plasma physics of beams: collisions, Debye Length
  1.4 Klimontovich equation, Vlasov equation, Liouville's theorem
  1.4 Emittance and brightness


2.  Envelope Equations-I  (JJB)
02_envelope_eqns.pdf  pdf scan, handwritten notes and slides

  2.1 Paraxial Ray Equation
  2.2 Envelope equations for axially symmetric beams
  2.3 Cartesian equations of motion
      2.3.1 Quadrupole focusing
      2.3.2 Space charge force for elliptical beams
  2.4 Envelope equations for elliptically symmetric beams


3.  Current Limits in Accelerators and Centroid equations-I (JJB)
03_currentlimits.pdf  pdf scan, handwritten notes and slides

  3.1 Axisymmetric beams
     3.1.1 Solenoids
     3.1.2 Einzel Lenses
  3.2 Elliptically symmetric beams
     3.2.1 Derivation of space charge term in envelope equation with
           elliptical symmetry
     3.2.2 Current limit for quadrupoles using Fourier transforms
  3.3 Current limit for continuous focusing
     3.3.1 Calculation of sigma_0 (using matrix multiplication)
     3.3.2 Comparison of quadrupole current limit (from Fourier transform,
     and matrix methods)
  3.4 Centroid equations (first order moments)
     3.4.1 Space charge and focusing forces
  3.5 Image forces (effect on centroid and envelope)


4.  Transverse Particle Equations of Motion (SML)
04_tpe.pdf  pdf scan, handwritten notes and slides

  4.1  Particle equations of motion
    4.1.1 Derivation of transverse equations
      - Basic form
      - Including bending and dispersive terms
  4.2  Transverse particle equations of motion in linear focusing channels
    4.1.1 Continuous focusing
    4.2.2 Quadrupole focusing
    4.2.3 Solenoidal focusing
    Appendix A: Transformation of solenoidal focused particle equations of
                motion to uncoupled form
  4.3  Description of applied focusing fields
```

```
    4.3.1 Overview
    4.3.2 Multipole descriptions
  4.4 Transverse particle equations of motion with nolinear applied fields
  4.5  Linear equations of motion without space-charge, acceleration, and
       momentum spread
    4.5.1 Hill's equation
    4.5.2 Orbit stability and eigenvalue structure
  4.6  Floquet's theorem and the phase-amplitude form of the particle orbit
    4.6.1 Floquet's theorem
    4.6.2 Phase amplitude form of the particle orbit
    4.6.3 Particle phase advance
    Appendix A: Calculation of w(s) from principal orbit functions
  4.7  The Courant-Snyder invariant and single-particle emittance
    4.7.1 Derivation of the Courant-Snyder invariant
    4.7.2 Interpretation and uses
  4.8 The betatron formulation of the particle orbit
    4.8.1 Formulation
    4.8.2 Envelope of particle orbits
  4.9  Momentum spread effects
    4.9.1 Overview and equations
    4.9.2 Dispersion function
  4.10  Acceleration and normalized emittance
    4.10.1 Transformation of orbit equations to standard form
    4.10.2 Normalized emittance
    Appendix A: Accelerating fields and calculation of gamma*beta
  References


5.  Transverse Equilibrium Distribution Functions (SML)
05_ted_full.pdf    combined file
05_ted_ho.pdf      slides only, handout form (2 per page)
05_ted_app_a.pdf   appendix A, pdf scan, handwritten notes
05_ted_app_b.pdf   appendix B, pdf scan, handwritten notes

  5.1  Vlasov model
    5.1.1 Vlasov-Poisson system
    5.2.2 Review: lattices: continuous, solenoidal, and quadrupole
    5.2.3 Review: Undepressed particle phase advance
  5.2  Vlasov equilibria
    5.2.1 Equilibrium conditions
    5.2.2 Single particle equations of motion with linear space-charge
    5.2.2 Plasma physics approach to beam physics
  5.3 The KV equilibrium distribution
    5.3.1 Hill's equation with linear space-charge forces
    5.3.2 Courant-Snyder invariants for a uniform density elliptical beam
    5.2.3 KV envelope equations
    5.2.4 Canonical form of the KV distribution function
    5.2.5 Matched envelope structure
    5.2.6 Depressed particle orbits
    5.2.7 rms equivalent beams
    5.2.6 Discussions/comments on the KV model
  5.4  The continuous focusing limit of the KV distribution
    5.4.1 Wavenumbers of particle oscillations
    5.4.2 Distribution form
  5.5  Equilibrium distributions in continuous focusing channels
    5.5.1 Equilibrium form
    5.5.2 Poisson's equation
    5.5.3 Moments
    5.5.4 Example distributions
  5.6 Continuous focusing: the waterbag equilibrium distribution
    5.6.1 Distribution form
    5.6.2 Poisson's equation
    5.6.3 Equilibrium properties
  5.7  Continuous focusing: the thermal equilibrium distribution
    5.7.1 Overview
    5.7.2 Distribution form
    5.7.3 Poisson's equation
    5.7.4 Equilbirum properties
  5.8  Continous focusing: Debye screening in a thermal equilibrium beam
```



```
    5.8.1 Poisson's equation for the perturbed potential due
          to a test particle
    5.8.2 Solution for characteristic Debye screening
  5.9  Continuous focusing: the density inversion theorem
    5.9.1 Relation of density profile to the full distribution function
    5.9.2 Example application to the KV distribution
  5.10 Comments on the plausiblility of smooth, non-KV Vlasov equilibria
       in periodic focusing lattice
    5.10.1 Discussion
  Appendix A: Self-fields of a uniform density elliptical beam in free space
    Derivation #1: direct
    Derivation #2: simplified
  Appendix B: Canonical transformas of the KV distribution
    Canonical transforms
    Simplified moment calculations
  References


6.  Transverse Particle Resonances with Application to Rings (SML)
06_ca.pdf  pdf scan, handwritten notes and slides

  6.1 Overview
  6.2 Floquet coordinates
  6.3 Perturbed Hill's equation in Floquet coordinates
  6.4 Sources and forms of perturbation terms
  6.5 Unperturbed solution and relation to a simple harmonic oscillator
  6.6 Perturbation analysis of perturbed Hill's equation and resonances
  6.7 Tune restrictions resulting from resonances and machine operating points
  6.8 Effects of space-charge


7.  Injectors and Longitudinal Physics Part I (JJB)
07_injector_longitudinal_I.pdf  pdf scan, handwritten notes and slides

  7.1  Diodes and Injectors
    7.1.1 Space-charge limited flow and child-Langmuir law
    7.1.2 Pierce electrodes
    7.1.3 Transients in injectors and Lampel-Tiefenback solution
  7.2 Injector Choices


8.  Longitudinal Physics Part II (JJB)
08_longitudinal_II.pdf  pdf scan, handwritten notes and slides

  8.1  Acceleration -- introduction
  8.2  Space charge of short bunches (in rf-accelerators)
  8.3  Space charge of long bunches (g-factor model)
  8.4  Longitudinal 1D Vlasov equation
  8.5  Longitudinal fluid equation
  8.4  Longitudinal space charge waves
  8.5  Longitudinal rarefaction waves and bunch end control


9.  Longitudinal Physics Part III (JJB)
08_longitudinal_III.pdf  pdf scan, handwritten notes and slides

  9.1  Longitudinal cooling from acceleration
  9.2  Longitudinal resistive instability
  9.3  Bunch compression
  9.4  Longitudinal envelope equation
  9.4  Neuffer distribution function


10. Centroid and Envelope Descriptions of Beam Evolution (SML)
10_tce_full.pdf  combined pdf file
10_tce_ho.pdf    slides in handout form (2 per page)
10_tce_sec9.pdf  pdf scan, handwritten notes and slides

  10.1 Overview
```

```
  10.2 Derivation of centroid and envelope equations of motion
    10.2.1 Statistical averages
    10.2.2 Particle equations of motion
    10.2.3 Distribution assumptions
    10.2.4 Self-Fields: direct and image
    10.2.5 Coupled centroid and envelope equations
  10.3 Centroid equations of motion
    10.3.1 Solution structure and stability
    10.3.2 Driving error terms and image charge effects
  10.4 Envelope equations
    10.4.1 KV evelope equations: properties of terms
  10.5 Matched solution
    10.5.1 Definition
    10.5.2 Symmetries
  10.6 Envelope perturbations
    10.6.1 Mismatch perturbations and mismatch modes
    10.6.2 Driving perturbtions
    10.6.2 Decoupled modes
    10.6.3 General mode limits
   10.7 Envelope modes in continuous focusing
    10.7.1 Homogeneous solution properties
    10.7.2 Driven modes
   10.8 Envelope modes in periodic focusing
    10.8.1 Solenoidal focusing
    10.8.2 Quadrupole focusing
   10.9 Transport limit scaling based on envelope models
    10.9.1 Overview
    10.9.2 Example calculation for a periodic FODO quadrupole
           transport channel
    10.9.3 Discussion on application of formulas in design
    10.9.4 Results of more detailed models
  10.10 Formulation and use of 1st order coupled moment approaches
        (to be added in future notes)
    10.10.1 Motivation
    10.10.2 Example illustration - dispersive effects
 References


11. Continuous Focusing Envelope Modes and Beam Halo  (JJB)
11_env_modes_halo.pdf  pdf scan, handwritten notes and slides

  11.1 Envelope modes of unbunched beams in continuous focusing
  11.2 Envelope modes of bunched beams in continuous focusing
  11.3 Halos from mismatched beams
    11.3.1 What is halo? Why do we care
    11.3.2 Qualitative picture of halo formation: mismatches
           resonantly drive particles to large amplitude
    11.3.3 Core/particle models
    11.3.4 Amplitude phase analysis


12. Transverse Kinetic Stability (SML)
12_tks.pdf  slides, handout form (2 per page)

  12.1 Overview: machine operating points
    12.1.1 Notions of beam stability
    12.1.2 Tiefenback experimental results for quadrupole transport
  12.2 Overview: collective modes and transverse kinetic stability
    12.2.1 Possibility of collective internal modes
    12.2.2 Vlasov model review
    12.2.3 Plasma physics approach to beam physics
  12.3 Linearized Vlasov equation
    12.3.1 Equilibrium and perturbations
    12.3.2 Linear Valsov equation
    12.3.3 Method of characteristics
    12.3.4 Discussion
  12.4 Collective modes on a KV equilibrium beam
    12.4.1 KV equilibrium
    12.4.2 Linearized equations of motion
```



```
    12.4.3 Solution of equations
    12.4.4 Mode properties
    12.4.5 Physical mode components based on fluid model
    12.4.6 Periodic focusing results
  12.5 Global conservation constraints
    12.5.1 Conserved quantities
    12.5.2 Uses of conservation constraints
  12.6 Kinetic stability theorem
    12.6.1 Conserved free energy
    12.6.2 Expansion in perturbations
    12.6.3 Perturbation bound and a sufficient condition for stability
    12.6.4 Interpretation and example applications
  12.7 rms emittance growth and nonlinear forces
    12.7.1 Equations of motion
    12.7.2 Coupling of nonlinear forces to rms emittance evolution
  12.8 rms emittance growth and nonlinear space-charge forces
    12.8.1 Equations of motion
    12.8.2 rms equivalent beam forms
    12.8.3 Wangler's theorem
  12.9 Uniform density beams and extreme envery states
    12.9.1 Variational formulation
    12.9.2 Self-field energy minimization
  12.10 Collective relaxation and rms emittance growth
    12.10.1 Conservation constraints
    12.10.2 Relaxation processes
    12.10.3 Emittance growth bounds from space-charge nonuniformities
  12.11 Phase mixing and Landau damping in beams
    (to be added in future versions)
  References


13. Pressure, Scattering, and Electron Effects (JJB)
13_pressure_scattering_electrons.pdf  pdf scan, handwritten notes and slides

  13.1 Beam/beam Coulomb collisions
  13.2 Beam/residual-gas scattering
  13.3 Charge-changing processes
  13.4 Wall effects
    13.4.1 gas pressure instability
  13.5 Electron cloud processes
    13.5.1 Multiple-bunch beam-induced multipacting
    13.5.2 Single-bunch beam-induced multipacting
  13.6 Electron-ion instability


14. Heavy Ion Fusion and Final Focus (JJB)
14_heavyionfusion_finalfocus.pdf  pdf scan, handwritten notes and slides

  14.1 An application of intense beams: Heavy Ion Fusion
    14.1.1 Requirements
    14.1.2 Targets for inertial confinement fusion
    14.1.3 Accelerator
    14.1.4 Drift compression
    14.1.5 Final focus
  14.2 Final focus
    14.2.1 Predicting spot size using envelope equation
           and estimate of effects from chromaticity
  14.3 Experiments for Heavy Ion Fusion


15. Numerical Simulations (RAK)
15_sims_rak.pdf  pdf

  Overview
  Particle Tracking and Numerical Methods
  Computation in Beams: Field Solvers
  Particle in Cell Codes
  Advanced Computing Topics
  Testing: A Case Study on Validation
```

```
15. Numerical Simulations (SML)
15_sims_sml.pdf  pdf scan, handwritten notes and slides
  Note: From SML handouts 2004 USPAS, used as handout for additional
        information.

  15.1 Why numerical simulation?
  15.2 Classes of intense beam simulations
    15.2.1 Particle methods
    15.2.2 Distribution methods
    15.2.3 Moment methods
  15.3 Numerical methods
    15.3.1 Discretizations
      - Derivatives
      - Integrals
    15.3.1 Application to moment methods
      - Euler and Runge-Kutta advances
      - Example application
  15.4 Numerical methods for particle and distribution methods
    15.4.1 Field discretizations
    15.4.2 Particle methods and PIC codes for solving Valsov's equation
      - Leapfrog advance
      - Field solution
      - Particle weighting
      - Advance cycle
      - Initialization
      - Numerical convergences
      - Examples
    15.4.1 Distribution methods
      - Similarities with PIC method
      - Distribution advance
      - Examples
  15.5 Overview of the WARP PIC code
  References


16. Summary of Lectures by John J. Barnard (JJB)
16_summary_jjb.pdf  pdf scan, handwritten notes and slides

  16.1 Emittance and phase space review
  16.2 Particle equations of motion (radial and Cartesian)
  16.3 Summary of 6 statistical envelope equations and two equations based
       on particular distribution functions
  16.4 Current limits
  16.5 Using envelope equations to estimate spot size
  16.6 Longitudinal dynamics summary
  16.7 Instability summary
  16.8 Halo summary
  16.9 Electron, gas, pressure, and scattering effects summary
  16.10 Summary of HIF
```

Course Title: Beam Physics with Intense Space Charge
US Particle Accelerator School, June 12-23, 2006, Waltham, Massachusetts

Course Instructors: John J. Barnard (JB) and Steven M. Lund (SL), Lawrence Livermore National Laboratory
Rami Kishek (RK), University of Maryland

	Monday 6/12	Tuesday 6/13	Wednesday 6/14	Thursday 6/15	Friday 6/16
9:00 am to 10:30 am	Organization/Intro Envelope Equations and Modes JB	Envelope Equations Current Limits JB	Injectors/Longitudinal Beam Physics I JB	Longitudinal Beam Physics II JB	Longitudinal Beam Physics III. JB
10:30 am o 12:00 noon	Transverse Particle Eqs. of Motion I SL	Transverse Particle Equations of Motion II SL	Transverse Distribution Funcs. I SL	Transverse Distribution Funcs. II SL	Simulation Techniques I RK
12:00 noon to 1:00 pm	Lunch	Lunch	Lunch	Lunch	Lunch
1:00 pm to 2:00 pm	Transverse Particle Eqs. of Motion SL	Transverse Particle Eqs. of Motion II SL	Tran. Dist. Funcs. SL	Tran. Dist. Funcs. SL	Circular Accelerators SL
2:00pm to 3:00 pm		Recitation RK	Recitation RK	Recitation RK	Recitation RK
3:00 pm to 4:00 pm					
Evenings 6-?	Homework 1	Homework 2	Homework 3	Homework 4	Homework 5

	Monday 6/19	Tuesday 6/20	Wednesday 6/21	Thursday 6/22	Friday 6/23
9:00 am to 10:30 am	Modes in Continuous Focusing and Halo JB	Pressure/Scattering/ Electron Effects JB	Heavy Ion Fusion/ Final Focusing JB	Review of Material JB	To Be Determined
10:30 am o 12:00 noon	Transverse Centroid and Envelope Eqs. I SL	Transverse Centroid and Envelope Eqs. II SL	Transverse Kinetic Stability I SL	Simulation Techniques II SL	Final Exam Review JB/SL/RK
12:00 noon to 1:00 pm	Lunch	Lunch	Lunch	Lunch	
1:00 pm to 2:00 pm	Tran. Cen. Env. Eqs. I SL	Tran. Cen. Env. Eqs. II SL	Tran. Kin. Stability II SL	Sim. Techs. III RK	
2:00pm to 3:00 pm	Recitation RK	Recitation RK	Recitation RK	Recitation RK	
3:00 pm to 4:00 pm					
4:00 pm to 5:00 pm					
Evenings 6-?	Homework 6	Homework 7	Homework 8	Take-home final	

Homework: collaboration with other students in class, and hints from grader or instructors allowed. (80% of grade)
Take-home final: no collaboration allowed (20% of grade)

John Barnard
Steven Lund
USPAS
June 2006

I. Introduction

(related reading in parentheses)

Particle motion (Reiser 2.1)
Equation of motion (Reiser 2.1)
Dimensionless quantities (Reiser 4.2)

Plasma physics of beams (Reiser 3.2, 4.1)

Emittance and brightness (Reiser 3.1 - 3.2)

PARTICLE EQUATIONS OF MOTION / DIMENSIONLESS QUANTITIES

CONSIDER THE LORENTZ FORCE ON A PARTICLE UNDER THE INFLUENCE OF ELECTRIC AND MAGNETIC FORCES.

$$\frac{d\underline{p}}{dt} = q(\underline{E} + \underline{v} \times \underline{B}) \qquad [\text{SI units}]$$

$$\underline{p} = \gamma m \underline{v} \qquad \gamma^2 = \frac{1}{1-\beta^2} \qquad \beta = \frac{v}{c}$$

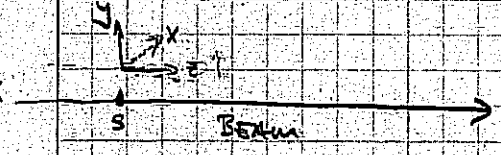

CONSIDER THE X-COMPONENT OF THE MOTION (TRANSVERSE TO THE STREAMING MOTION OF THE PARTICLE)

TRANSFORM TO S AS THE INDEPENDENT VARIABLE.

$$dt = \frac{ds}{v_z} \quad \Rightarrow \quad v_x = \frac{dx}{dt} = v_z x' \qquad ' = \frac{d}{ds}$$

$$m v_z \frac{d}{ds}(\gamma v_z x') = q(\underline{E} + \underline{v} \times \underline{B})_x$$

$$\gamma m v_z^2 x'' + x' m v_z \frac{d}{ds}(\gamma v_z) = q(\underline{E} + \underline{v} \times \underline{B})_x$$

$$\Rightarrow \quad x'' + \left[\frac{1}{\gamma v_z}\frac{d}{ds}(\gamma v_z)\right] x' = \frac{q}{\gamma m v_z^2}(\underline{E} + \underline{v} \times \underline{B})_x$$

NOW CONSIDER AN UNBUNCHED BEAM OF UNIFORM DENSITY ρ AND CIRCULAR CROSS SECTION

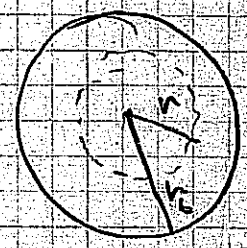

$$\underline{\nabla} \cdot \underline{E} = \frac{\rho}{\varepsilon_0}$$

$$2\pi r E_r = \pi r^2 \frac{\rho}{\varepsilon_0} \qquad \text{(Gauss' theorem)}$$

$$\lambda = \pi r_b^2 \rho$$

$$E_r = \frac{\rho}{2\varepsilon_0} r = \frac{\lambda}{2\pi\varepsilon_0}\frac{r}{r_b^2} \qquad E_x = E_r \cos\theta = E_r\left(\frac{x}{r}\right) = \frac{\lambda}{2\pi\varepsilon_0}\frac{x}{r_b^2}$$

Similarly $\underline{\nabla} \times \underline{B} = \mu_0 \underline{J}$

$$2\pi r B_\theta = \mu_0 \rho v_z \pi r^2 \qquad \text{(Stokes theorem)}$$

$$B_\theta = \frac{\mu_0 \lambda v_z}{2\pi}\frac{r}{r_b^2} \qquad B_y = \frac{\mu_0 \lambda v_z}{2\pi}\frac{x}{r_b^2} \qquad (B_z = 0)$$

Let $(\underline{E} + \underline{v} \times \underline{B})_x = (E_x - v_z B_y)^{self} + (E_x + v_y B_z - v_z B_y)^{ext}$

$$\Rightarrow \quad x'' + \left[\frac{1}{\gamma v_z}\frac{d}{ds}\gamma v_z\right] x' = \frac{q}{\gamma m v_z^2}\frac{\lambda}{2\pi\varepsilon_0}\frac{x}{r_b^2}\left[1 - \mu_0\varepsilon_0 v_z^2\right] + \frac{q}{\gamma m v_z^2}(\underline{E} + \underline{v} \times \underline{B})_x^{ext}$$

USING $\mu_0\varepsilon_0 = \frac{1}{c^2}$

Assuming $\beta_x^2 + \beta_y^2 \ll \frac{1}{\gamma^2} \Rightarrow \gamma^2 \simeq \frac{1}{1 - v_z^2/c^2}$ (PARAXIAL APPROXIMATION)

($\Rightarrow \tilde{\beta}_x^2 + \tilde{\beta}_y^2 \ll 1$; HERE ~ INDICATES VALUE IN COMOVING FRAME [NON-RELATIVISTIC MOTION IN COMOVING FRAME].)

LUMPING EXTERNAL FORCE INTO A LINEAR FIELD:

$$x'' + \frac{1}{\gamma v_z}\frac{d}{ds}(\gamma v_z)\, x' \cong \frac{q}{\gamma^3 m v_z^2}\frac{\lambda}{2\pi\epsilon_0}\frac{x}{r_b^2} - \underbrace{K(z)\,x}_{\text{EXTERNAL FORCES}}$$

$$\equiv Q\frac{x}{r_b^2} - K(z)\,x$$

$$Q \equiv \frac{q\lambda}{2\pi\epsilon_0\gamma^3 m v_z^2} \equiv \text{GENERALIZED PERVEANCE} \longrightarrow \begin{cases} \dfrac{\lambda}{4\pi\epsilon_0 V} & \text{for } \gamma^2 v_z^2 \ll c^2 \\[2ex] \dfrac{\lambda}{2\pi\epsilon_0 V\left(\frac{qV}{mc^2}\right)^2} & \text{for } \gamma^2 v_z^2 \gg c^2 \end{cases}$$

$$= \frac{(q/e)}{(m/m_{amu})}\,\frac{2I}{I_0}\,\frac{1}{\gamma^3\beta^3} \qquad I_0 = \frac{4\pi\epsilon_0\, m_{amu}\, c^3}{e} \cong 31\ \text{MA}$$

here $qV \equiv (\gamma - 1)\, mc^2$

Also note in non-relativistic limit $Q = \left(\frac{m}{2q}\right)^{1/2}\frac{1}{4\pi\epsilon_0 c}\left(\frac{I}{V^{3/2}}\right)$

(same scaling as original term perveance characterizing impedance).

$$Q \simeq \frac{\Phi_{SELF}}{V} = \frac{\int_0^{r_b}(E_r - v_z B_\theta)\,dr}{V} = \frac{\text{POTENTIAL ENERGY OF BEAM PARTICLE}}{\text{KINETIC ENERGY OF " "}}$$

SOMETIMES PERIODIC FOCUSING IS EMPLOYED

$$K(z) = K(z+S)$$

$$S = \text{PERIOD}$$

FOR SOME PURPOSES A SUITABLE CONSTANT CAN BE FOUND WHICH CAPTURES SLOW VARIATION OF THE PARTICLE MOTION. (SMOOTH FOCUSING APPROX.)

$$\Rightarrow \boxed{x'' + \frac{1}{\gamma v_z}\frac{d}{ds}(\gamma v_z)\, x' = Q\frac{x}{r_b^2} - k_{\beta 0}^2\, x}$$

$k_{\beta 0} \equiv$ "UNDEPRESSED BETATRON FREQUENCY"

$\sigma_0 \equiv k_{\beta 0} S$ = UNDEPRESSED PHASE ADVANCE

If $\frac{dv_z}{dz} = 0$ [drifting beams]

$$x'' = -\left[k_{\beta 0}^2 - \frac{Q}{r_b^2}\right] x$$

$$= -k_{\beta 0}^2 \underbrace{\left[1 - \frac{Q}{k_{\beta 0}^2 r_b^2}\right]}_{\equiv \left(\frac{\sigma}{\sigma_0}\right)^2 = (\text{"TUNE DEPRESSION"})^2} x \equiv -k_\beta^2 x$$

"DEPRESSED BETATRON FREQUENCY"

EFFECT OF SPACE CHARGE IS TO LOWER FREQUENCY OF HARMONIC OSCILLATIONS

$\frac{\sigma}{\sigma_0} = 0 \Rightarrow$ FULLY TUNE DEPRESSED

$\frac{\sigma}{\sigma_0} = 1 \Rightarrow$ NO SPACE-CHARGE DEPRESSION

Space charge reduces betatron phase advance

Without space charge: $x = x_i \cos\left[k_{\beta 0}(s - s_i)\right] + \frac{x_i'}{k_{\beta 0}} \sin\left[k_{\beta 0}(s - s_i)\right]$

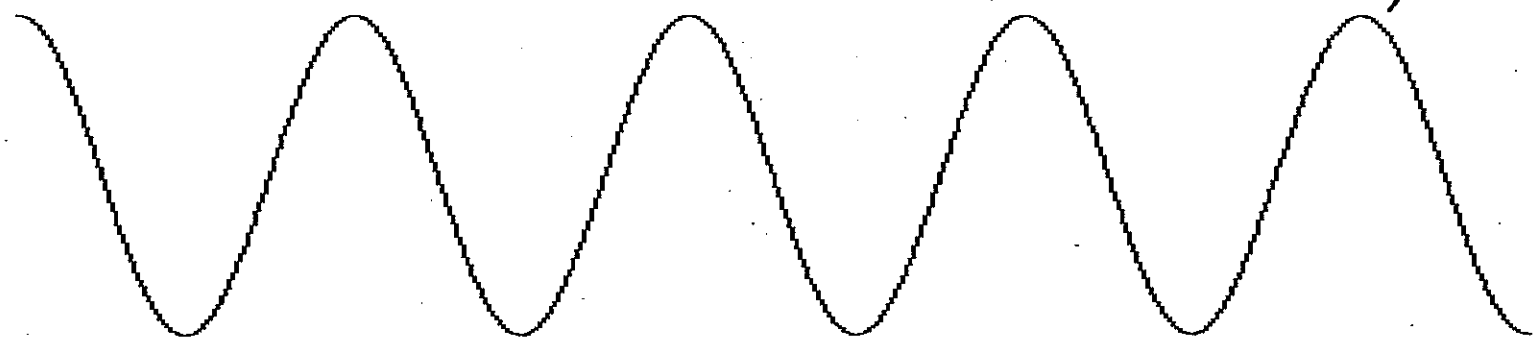

With space charge:

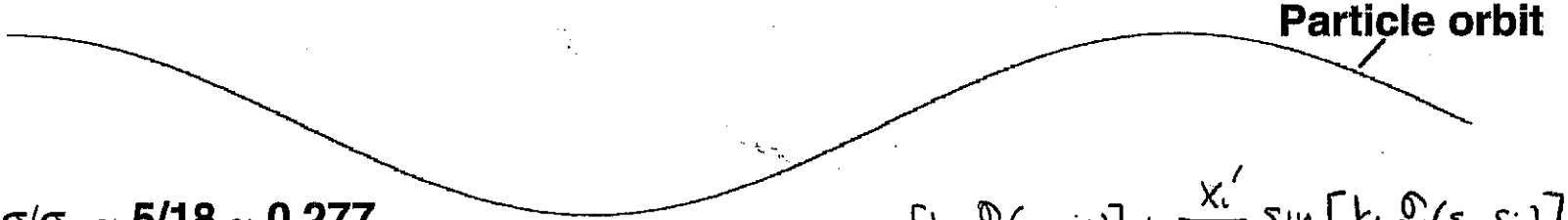

σ/σ_0 ~ **5/18 ~ 0.277**

$$x = x_i \cos\left[k_{\beta 0}\frac{\sigma}{\sigma_0}(s - s_i)\right] + \frac{x_i'}{\left(\frac{\sigma}{\sigma_0}\right)k_{\beta 0}} \sin\left[k_{\beta 0}\frac{\sigma}{\sigma_0}(s - s_i)\right]$$

Beam envelope

J. BARNARD

5

BENDING BEAMS

RETURNING TO PARTICLE EQUATION WITH ARBITRARY E, & B:

$$x'' + \left[\frac{1}{\gamma v_z}\frac{d}{ds}(\gamma v_z)\right] x' = \frac{q}{\gamma m v_z^2}\left(\underline{E} + \underline{v}\times\underline{B}\right)_x$$

IF EXTERNAL FORCE IS PROPORTIONAL TO $-x$

$\Rightarrow$ FOCUSING (HARMONIC OSCILLATIONS)

HOWEVER, IF $\underline{E} + \underline{v}\times\underline{B}$ = CONSTANT

$\Rightarrow$ BENDING

EXAMPLE: If $B = B_y \hat{e}_y$

$\underline{v} = v_0 \hat{e}_z + v_x \hat{e}_x$ where $v_0 \gg v_x$

$$\Rightarrow \quad x'' = \frac{q B_y}{\gamma m v_z} = \frac{B_y}{[B\rho]} \qquad [B\rho] \equiv \text{RIGIDITY} = \frac{\gamma m v_z}{q} = \frac{p}{q}$$

$$x' = \frac{B_y}{[B\rho]} z + x_0'$$

$$x = \frac{B_y}{[B\rho]}\frac{z^2}{2} + x_0' z + x_0$$

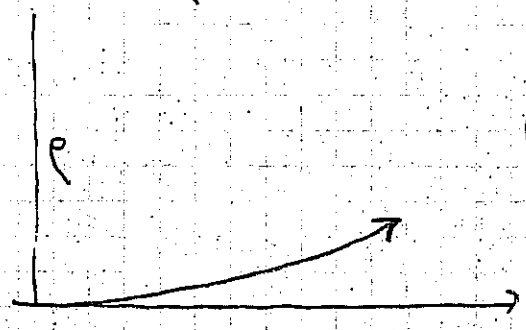

ρ = RADIUS OF CURVATURE OF ARC $= \dfrac{[B\rho]}{B_y}$

(BENDING CAN ALSO BE CARRIED OUT WITH ELECTRIC FIELDS E_x = const).

PLASMA PHYSICS OF BEAMS

PHYSICS OF SPACE-CHARGE $\equiv$ PHYSICS OF SELF-FIELDS

$\equiv$ PLASMA PHYSICS OF PARTICLE BEAMS

PLASMA PARAMETER

$$q\bar{\Phi}_{IP} = \frac{1}{4\pi\varepsilon_0}\frac{q^2}{r}$$

$$\simeq \frac{1}{4\pi\varepsilon_0} n_0^{1/3} q^2$$

AVERAGE POTENTIAL ENERGY $q\bar{\Phi}_{IP}$ OF PARTICLE DUE TO ITS NEAREST NEIGHBOR (q = charge of particle)

IF $q\bar{\Phi}_{IP} << k_B T \Rightarrow$ PLASMA (weakly coupled plasma)

DEFINE $$\lambda_D = \frac{(kT/m)^{1/2}}{(n_0 q^2/\varepsilon_0 m)^{1/2}} = \frac{v_{TH}}{\omega_p} = \left(\frac{kT\varepsilon_0}{n_0 q^2}\right)^{1/2} = \text{DEBYE LENGTH}$$

= SHIELDING DISTANCE EVEN IN NON-NEUTRAL PLASMA

DEFINE $\Lambda = \frac{4\pi}{3} n_0 \lambda_D^3 \equiv$ PLASMA PARAMETER

$$\sim \left(\frac{k_B T}{q\bar{\Phi}_{IP}}\right)^{3/2} >> 1$$

KLIMONTOVICH EQUATION

REF. "INTRO. TO PLASMA THEORY", D.R. NICHOLSON WILEY, 1983.

Let $N(\underline{x},\underline{v},t) = \sum_{i=1}^{N_0} \delta(\underline{x}-\underline{X}_i(t))\,\delta(\underline{v}-\underline{V}_i(t))$

No particles; $\underline{X}_i$, $\underline{V}_i$ are position and velocity of ith particle

$\dot{\underline{X}}_i = \underline{V}_i \qquad m\dot{\underline{V}}_i = q\underline{E}^m[\underline{X}_i(t),t] + q[\underline{V}_i \times \underline{B}^m[\underline{X}_i(t),t]]$ (non-relativistic)

$N(x,v,t)$ = "density" of particle in phase space

$$\int N\, d^3x\, d^3v = N_0$$

Let $u = x - X_i(t)$

$\frac{\partial}{\partial x} f(u) = f'(u)$

$\frac{\partial}{\partial t} f(u) = f'(u)(-\dot{X}(t)) = -\dot{X}(t)\frac{\partial}{\partial x} f(u)$

Taking derivative:

$$\frac{\partial N}{\partial t}(x,v,t) = -\sum_{i=1}^{N} \dot{\underline{X}}_i(t)\cdot\nabla_x\left[\delta(\underline{x}-\underline{X}_i(t))\,\delta(\underline{v}-\underline{V}_i(t))\right]$$

$$-\sum_{i=1}^{N_0} \dot{\underline{V}}_i(t)\cdot\nabla_v\left[\delta(\underline{x}-\underline{X}_i(t))\,\delta(\underline{v}-\underline{V}_i(t))\right]$$

MAXWELL'S EQUATIONS:

$$\underline{\nabla}\cdot\underline{E}^m = \left(\frac{1}{\epsilon_0}\right)\overbrace{q\int d^3v\, N(x,v,t)}^{\rho^m} \qquad \underline{\nabla}\cdot\underline{B}^m = 0$$

$$\nabla\times\underline{E}^m = -\frac{\partial \underline{B}^m}{\partial t} \qquad \nabla\times\underline{B}^m = \mu_0\underbrace{q\int d^3v\,\underline{v}\,N(x,v,t)}_{\underline{J}^m} + \frac{\partial \underline{E}^m}{\partial t}$$

$$\Rightarrow \frac{\partial N}{\partial t}(x,v,t) = -\sum_{i=1}^{N_0} \underline{V}_i(t)\cdot\nabla_x\left[\delta(\underline{x}-\underline{X}_i(t))\,\delta(\underline{v}-\underline{V}_i(t))\right]$$

$$-\sum_{i=1}^{N_0}\left(\left(\frac{q}{m}\right)\underline{E}^m + \left(\frac{q}{m}\right)[\underline{V}_i\times\underline{B}^m[\underline{X}_i(t),t]]\right)\cdot\nabla_v\left[\delta(x-X_i)\,\delta(v-V_i(t))\right]$$

Note that $\underline{V}_i(t)\,\delta(\underline{v}-\underline{V}_i(t)) = \underline{v}\,\delta(\underline{v}-V_i(t))$ so,

∇_x = spatial gradient

∇_v = gradient w.r.t. 3 velocity variables

$$\Rightarrow \frac{\partial N}{\partial t}(\underline{x},\underline{v},t) = -\underline{v}\cdot\nabla_x\sum_{i=1}^{N_0}\delta(\underline{x}-\underline{X}_i(t))\,\delta(\underline{v}-\underline{V}_i(t))$$

$$-\left(\frac{q}{m}\underline{E}^m(\underline{x},t) + \frac{q}{m}(\underline{v}\times\underline{B}^m(\underline{x},t))\right)\cdot\nabla_v\sum_{i=1}^{N_0}\delta(x-X_i(t))\,\delta(v-V_i(t))$$

$$\boxed{\frac{\partial N}{\partial t}(\underline{x},\underline{v},t) = -\underline{v}\cdot\nabla_x N(\underline{x},\underline{v},t) + \frac{q}{m}(\underline{E}^m + \underline{v}\times\underline{B}^m)\cdot\nabla_v N(\underline{x},\underline{v},t)}$$

Klimontovich Equation

Total derivative along an orbit:

$$\frac{D}{Dt} = \frac{\partial}{\partial t} + \left.\frac{d\underline{x}}{dt}\right|_{\text{ORBIT}} \cdot \nabla_x + \left.\frac{d\underline{v}}{dt}\right|_{\text{ORBIT}} \cdot \nabla_v$$

$$\Rightarrow \boxed{\frac{D}{Dt} N(\underline{x}, \underline{v}, t) = 0}$$

Note that $N = 0$ or ∞, nothing in between.

Let $$f(x, v, t) = \frac{\int^{\Delta x^3, \Delta v^3} N(\underline{x}, \underline{v}, t)\, d^3x\, d^3v}{\Delta x^3\, \Delta v^3}$$

over some box in phase space. Δx & Δv are the size of box

$$\equiv \langle N(\underline{x}, \underline{v}, t) \rangle$$

Assume $n^{-1/3} \ll \Delta x \ll \lambda_D$ so that $f(x, v, t)$ is smooth function.

Then

$N = f + \delta f$	$f = \langle N \rangle$	$\langle \delta f \rangle = 0$
$E^m = E + \delta E$	$E = \langle E^m \rangle$	$\langle \delta E \rangle = 0$
$B^m = B + \delta B$	$B = \langle B^m \rangle$	$\langle \delta B \rangle = 0$

$$\Rightarrow \underbrace{\frac{\partial f}{\partial t} + \underline{v} \cdot \nabla_x f + \frac{q}{m}(\underline{E} + \underline{v} \times \underline{B}) \cdot \nabla_v f}_{\text{SMOOTHLY VARYING PART}} = -\frac{q}{m} \underbrace{\langle (\delta \underline{E} + \underline{v} \times \delta \underline{B}) \cdot \nabla_v \delta f \rangle}_{\text{AVERAGE OF "SPIKEY" QUANTITIES}}$$

"DISCRETE PARTICLE EFFECTS" OR "COLLISIONS"

If collisions are neglected (set RHS to zero):

VLASOV - EQUATION

$$\frac{\partial f}{\partial t} + \underline{v} \cdot \nabla_x f + \frac{q}{m}(\underline{E} + \underline{v} \times \underline{B}) \cdot \nabla_v f = 0$$

$$\Rightarrow \boxed{\frac{Df}{Dt} = 0}$$

PHASE SPACE DENSITY CONSTANT ON TRAJECTORIES. (LIOUVILLE'S THEOREM)

THE RHS IS DUE TO COLLISIONS WITH NON-SMOOTH FIELDS:

VERY HEURISTICALLY

$$-\frac{q}{m}\left\langle \left(\delta\underline{E} + \underline{v}\times\delta\underline{B}\right)\cdot\nabla_v \delta f\right\rangle \sim \nu_c f$$

$$\nu_c \sim \sigma n v$$

$\sigma \sim \pi r_c^2$ where r_c is given by $kT \sim \frac{q^2}{4\pi\varepsilon_0 r_c}$

(for large angle collisions)

$$\Rightarrow \nu_c \sim \pi\left(\frac{q^2}{4\pi\varepsilon_0 kT}\right)^2 n_0\left(\frac{kT}{m}\right)^{1/2}$$

← (VERY ROUGH, BUT MAIN SCALING IS CORRECT, WITH LOGARITHMIC CORRECTION FACTORS)

ON LHS of VLASOV EQUATION:

$$\frac{q}{m}E\,\nabla_v f \sim \left(\frac{q\lambda_D n_0}{\varepsilon_0}\right)\frac{f}{v_{TH}}$$

where $v_{TH} \sim \sqrt{\frac{kT}{m}}$

$$\frac{\text{COLLISION TERM}}{\text{LHS}} \sim \frac{1}{16\cdot\lambda_D^3 n_0} = \frac{1}{16\Lambda}$$

Accelerator beams are non-neutral plasmas

Accelerator beams for Heavy Ion Fusion

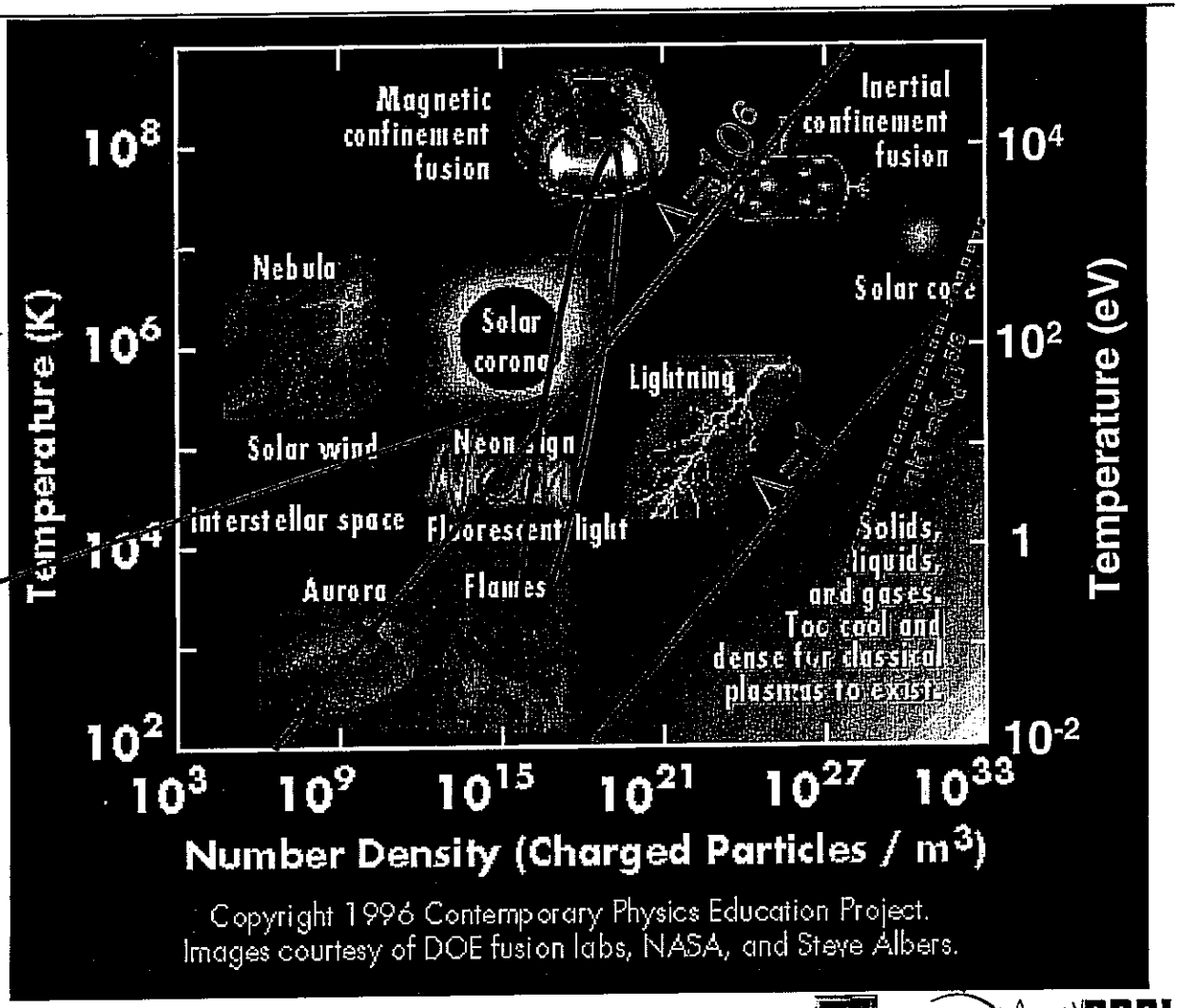

Copyright 1996 Contemporary Physics Education Project.
Images courtesy of DOE fusion labs, NASA, and Steve Albers.

DESCRIPTION OF THE BEAM

LIOUVILLE'S THEOREM: $\frac{df}{dt} = 0$ along a trajectory in phase space.

Let $dN = f\, dx\, dy\, dz\, dp_x\, dp_y\, dp_z$

The continuity equation in phase space is:

$$\frac{\partial f}{\partial t} + \underline{\nabla} \cdot (f \underline{v}) = 0$$

where $\underline{v} = \frac{d}{dt}\begin{pmatrix} q_1 \\ q_2 \\ q_3 \\ p_1 \\ p_2 \\ p_3 \end{pmatrix}$ & $\underline{\nabla} \cdot \underline{a} = \frac{\partial a_1}{\partial q_1} + \frac{\partial a_2}{\partial q_2} + \frac{\partial a_3}{\partial q_3} + \frac{\partial a_{p_1}}{\partial p_1} + \frac{\partial a_{p_2}}{\partial p_2} + \frac{\partial a_{p_3}}{\partial p_3}$

($\underline{v}$ & $\underline{\nabla}$ are the 6-D velocity & divergence, respectively).

If the system is governed by a Hamiltonian $H(\underline{q}, \underline{p}, t)$

$$\dot{q}_i = \frac{\partial H}{\partial p_i} \qquad \dot{p}_i = \frac{-\partial H}{\partial q_i}$$

Now, $\underline{\nabla} \cdot \underline{v} = \sum_{i=1}^{3} \frac{\partial \dot{q}_i}{\partial q_i} + \frac{\partial \dot{p}_i}{\partial p_i} = \sum_{i=1}^{3} \frac{\partial^2 H}{\partial q_i \partial p_i} - \frac{\partial^2 H}{\partial p_i \partial q_i} = 0$

$$\Rightarrow \frac{\partial f}{\partial t} + f \underbrace{\underline{\nabla} \cdot \underline{v}}_{0} + \underline{v} \cdot \nabla f = 0$$

$$\Rightarrow \boxed{\left.\frac{df}{dt}\right|_{\substack{6D \\ \text{trajectory}}} = 0}$$

Emittance & Brightness

LIOUVILLE'S EQUATION OR VLASOV EQUATION $\Rightarrow \dfrac{dN}{dx\,dy\,dz\,dp_x\,dp_y\,dp_z} = \text{const}$

IF $x'' = f(x)$ AND NOT FUNCTIONS $(y \,\&\, z)$
$y'' = f(y) =$ " " " $(x, \& z)$
$z'' = f(z) =$ " " " $(x, \& y)$

THEN $\dfrac{dN}{dx\,dp_x} = \text{const}$; $\dfrac{dN}{dy\,dp_y} = \text{const}$ & $\dfrac{dN}{dz\,dp_z} = \text{const}$

separately.

1ST DEFINITION:
EMITTANCE: USE TRACE-SPACE OF ALL PARTICLES IN A GIVEN SLICE OF BEAM.

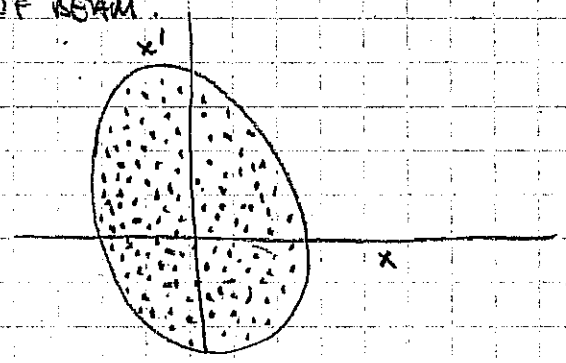

INSTEAD OF p_x USE $x' \equiv \dfrac{V_x}{V_z}$ (FOR NON-ACCELERATING PARAXIAL BEAM, x' PROPORTIONAL TO MOMENTUM)

EMITTANCE $\equiv \dfrac{1}{\pi} \cdot$ AREA OF SMALLEST ELLIPSE WHICH ENCLOSES ALL PARTICLES. (TRACE-SPACE DEFINITION)

(INTUITIVELY, PRODUCT OF WIDTH IN x, TIMES WIDTH IN x', SO IT IS ESSENTIALLY (WITHIN FACTOR OF π) = PHASE SPACE AREA OF BEAM.

2ND DEFINITION INVOLVES STATISTICAL ANALOGUES OF 2ND ORDER QUANTITIES (SUCH AS rms).

$$\epsilon_x \equiv 4\left(\langle x^2\rangle\langle x'^2\rangle - \langle xx'\rangle^2\right)^{1/2}$$

FOR an upright uniform beam (in phase space): $\langle x^2\rangle = \dfrac{r_x^2}{4}$ $\langle x'^2\rangle = \dfrac{x'^2_{max}}{4}$
& $\langle xx'\rangle = 0$

$$\Rightarrow \epsilon_x = r_x x'_{max} = \frac{\text{Area}}{\pi}$$

NORMALIZED EMITTANCE

For a beam that is accelerating, return to x, p_x as definition of phase space area:

$$p_x = \gamma m v_x = \gamma m v_z x' \qquad \text{AGAIN, ASSUMING } v \simeq v_z$$

$$\Rightarrow \epsilon_{Nx} \equiv 4\gamma\beta\left(\langle x^2\rangle\langle x'^2\rangle - \langle x x'\rangle^2\right)^{1/2} = \gamma\beta\,\epsilon_x$$

$$= \frac{4}{m}\left(\langle x^2\rangle\langle p_x^2\rangle - \langle x p_x\rangle^2\right)^{1/2}$$

SINCE EMITTANCE IS THE AVERAGE PHASE SPACE AREA OF BEAM (AVERAGING OVER EMPTY SPACE) THE EMITTANCE IN GENERAL GROWS AS A BEAM FILAMENTS (ENGULFING EMPTY SPACE).

BRIGHTNESS

THE DENSITY OF PARTICLES IN 6-D PHASE SPACE IS:

$$\frac{dN}{dx\,dy\,dz\,dp_x\,dp_y\,dp_z} = f \quad \longleftarrow \text{MICROSCOPIC DENSITY}$$

DEFINE A QUANTITY $\bar{f}$ WHICH IS THE PHASE-SPACE DENSITY IN AN AVERAGE SENSE

$$\bar{f} = \left\langle \frac{dN}{dx\,dp_x\,dy\,dp_y\,dz\,dp_z} \right\rangle = \frac{(I\Delta t)/q}{\pi^3 \epsilon_{Nx}\epsilon_{Ny}\epsilon_{Nz}}$$

Note $f(\underline{x},\underline{p})$ = constant along a trajectory, whereas $\bar{f}$ usually is a decreasing function of z.

NORMALIZED BRIGHTNESS $B_N \equiv \dfrac{I}{\epsilon_{Nx}\epsilon_{Ny}}$

IS A USEFUL MEASURE OF 4D AVERAGE PHASE SPACE DENSITY, (if Δt = constant, & $\perp,\parallel$ motion is uncoupled.)

For non-accelerating beams the unnormalized brightness B (also if Δt = const. & $\perp,\parallel$ motion uncoupled):

$$\Rightarrow B \equiv \frac{I}{\epsilon_x \epsilon_y} \quad \text{MEASURES PHASE SPACE DENSITY.}$$

Emittance constant for linear force profile & matched beams

Linear force profile ($x'' = -k^2 x$) => Phase space area preserved, ellipse stays elliptical.

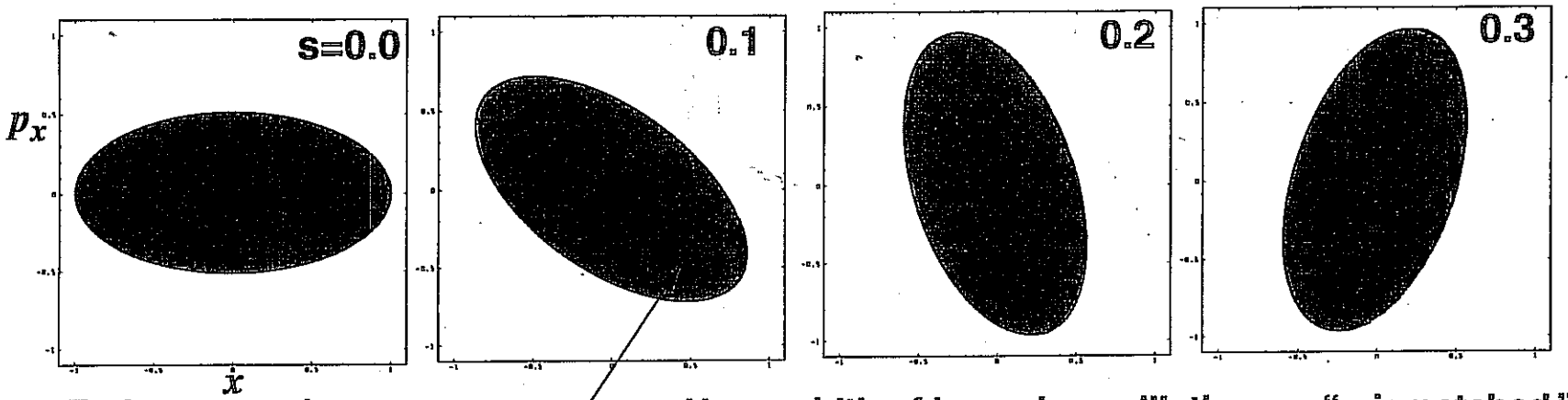

Emittance = phase space area

Emittance constant if forces linear

Here, width of beam is oscillating or "mismatched."

Non-linear forces (e.g. $x'' = -k^2 x + \varepsilon x^3$) $\Rightarrow$ position-dependent frequency

$\Rightarrow$ phase mixing, increasing effective area $\Rightarrow$ Emittance increases if forces non-linear

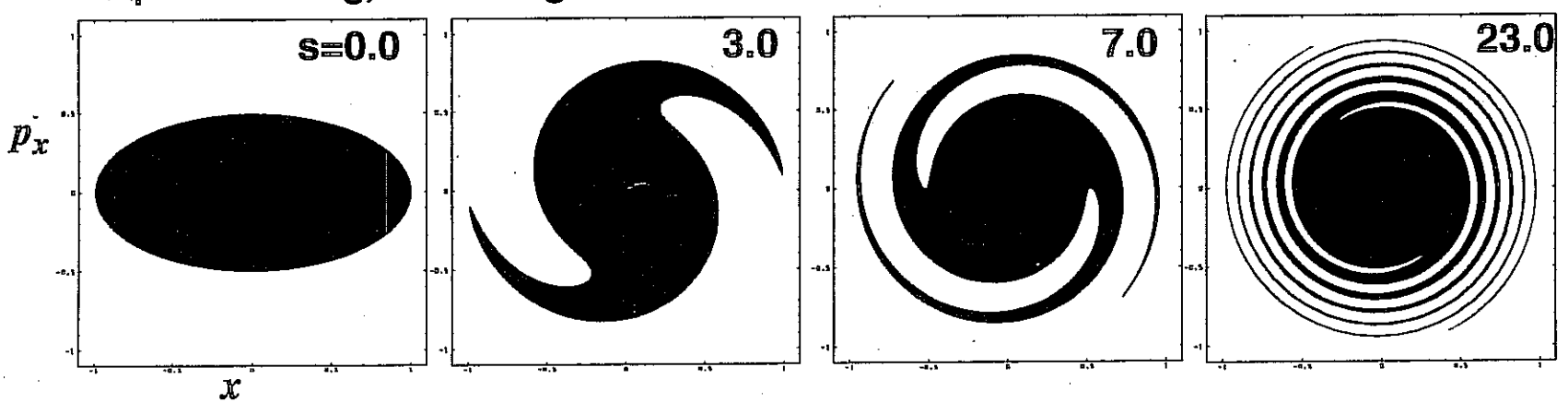

John Barnard
Steven Lund
USPAS
June 2006

II. Envelope Equations

Paraxial Ray Equation

Envelope equations for axially symmetric beams

Cartesian equation of motion

Envelope equations for elliptically symmetric beams

START WITH NEWTON'S EQUATION WITH THE LORENTZ FORCE:

$$\frac{d\underline{p}}{dt} = q(\underline{E} + \underline{v} \times \underline{B})$$

In cartesian coordinates:

$$\frac{d}{dt}(\gamma m \dot{x}) = \dot{\gamma} m \dot{x} + \gamma m \ddot{x} = q(E_x + \dot{y} B_z - \dot{z} B_y)$$

$$\frac{d}{dt}(\gamma m \dot{y}) = \dot{\gamma} m \dot{y} + \gamma m \ddot{y} = q(E_y + \dot{z} B_x - \dot{x} B_z)$$

$$\frac{d}{dt}(\gamma m \dot{z}) = \dot{\gamma} m \dot{z} + \gamma m \ddot{z} = q(E_z + \dot{x} B_y - \dot{y} B_x)$$

In cylindrical coordinates: (use $\frac{d\hat{e}_r}{dt} = \hat{e}_\theta \dot{\theta}$; $\frac{d\hat{e}_\theta}{dt} = -\hat{e}_r \dot{\theta}$)

$$\frac{d}{dt}(\gamma m \dot{r}) - \gamma m r \dot{\theta}^2 = q(E_r + r\dot{\theta} B_z - \dot{z} B_\theta) \qquad \text{(I)}$$

$$\frac{1}{r}\frac{d}{dt}(\gamma m r^2 \dot{\theta}) = q(E_\theta + \dot{z} B_r - \dot{r} B_z) \qquad \text{(II)}$$

$$\frac{d}{dt}(\gamma m \dot{z}) = q(E_z + \dot{r} B_\theta - r\dot{\theta} B_r) \qquad \text{(III)}$$

<u>When $\frac{\partial}{\partial \theta} = 0$:</u>

$$\underline{E} = -\nabla\Phi - \frac{\partial \underline{A}}{\partial t} = \hat{e}_r\left[-\frac{\partial \Phi}{\partial r} - \frac{\partial A_r}{\partial t}\right] + \hat{e}_\theta\left[-\frac{\partial A_\theta}{\partial t}\right] + \hat{e}_z\left[-\frac{\partial \Phi}{\partial z} - \frac{\partial A_z}{\partial t}\right]$$

$$\underline{B} = \nabla \times \underline{A} = \hat{e}_r\left[-\frac{\partial}{\partial z}(A_\theta)\right] + \hat{e}_\theta\left[\frac{\partial A_r}{\partial z} - \frac{\partial A_z}{\partial r}\right] + \hat{e}_z\left[\frac{1}{r}\frac{\partial}{\partial r}(r A_\theta)\right]$$

$$q r(E_\theta + \dot{z} B_r - \dot{r} B_z) = q\left(-\frac{\partial r A_\theta}{\partial t} - \dot{z}\frac{\partial r A_\theta}{\partial z} - \dot{r}\frac{\partial}{\partial r}(r A_\theta)\right)$$

$$= -q\left[\frac{\partial}{\partial t} + \underline{v}\cdot\frac{\partial}{\partial \underline{x}}\right](r A_\theta)$$

$$= -q\frac{d(r A_\theta)}{dt} \qquad \text{(IV)}$$

Eqtn II & IV $\Rightarrow$ $\frac{d}{dt}(\gamma m r^2 \dot{\theta} + q r A_\theta) = 0$

$$\underline{p} = p_r \hat{e}_r + p_\theta^* \hat{e}_\theta + p_z \hat{e}_z$$

where $p_r = \gamma m \dot{r}$

$p_\theta^* = \gamma m r \dot{\theta}$

$p_z = \gamma m \dot{z}$

$$\frac{d\underline{p}}{dt} = \dot{p}_r \hat{e}_r + p_r \dot{\hat{e}}_r + \dot{p}_\theta^* \hat{e}_\theta + p_\theta^* \dot{\hat{e}}_\theta + \dot{p}_z \hat{e}_z$$

$$\Rightarrow \frac{d\underline{p}}{dt} = (\dot{p}_r - p_\theta^* \dot{\theta}) \hat{e}_r + (p_r \dot{\theta} + \dot{p}_\theta^*) \hat{e}_\theta + \dot{p}_z \hat{e}_z$$

WHERE WE HAVE USED:

$$\frac{d\hat{e}_r}{dt} = \hat{e}_\theta \dot{\theta} \quad \& \quad \frac{d\hat{e}_\theta}{dt} = -\hat{e}_r \dot{\theta}$$

$$\Rightarrow \frac{d\underline{p}}{dt} = \left[\frac{d}{dt}(\gamma m \dot{r}) - \frac{d}{dt}(\gamma m r \dot{\theta}^2)\right] \hat{e}_r$$

$$+ \underbrace{\left[\gamma m r \dot{\theta} + \frac{d}{dt}(\gamma m r \dot{\theta})\right]}_{= \frac{1}{r}\frac{d}{dt}(\gamma m r^2 \dot{\theta})} \hat{e}_\theta$$

$$+ \frac{d}{dt}(\gamma m \dot{z}) \hat{e}_z$$

(NOTE: ON THIS PAGE $p_\theta^* \equiv \theta$-component of MECHANICAL MOMENTUM

NOT TO BE CONFUSED WITH $P_\theta = \gamma m r^2 \dot{\theta} + q r A_\theta \equiv \theta$-component

OF <u>CANONICAL</u> <u>ANGULAR</u> MOMENTUM)

CONSERVATION OF CANONICAL ANGULAR MOMENTUM

DEFINE $p_\theta = \gamma m r^2 \dot{\theta} + q r A_\theta$

$$\frac{d}{dt} p_\theta = 0$$ (CONSERVATION OF CANONICAL ANGULAR MOMENTUM)

NOTE THAT THE FLUX ENCLOSED BY A CIRCLE OF RADIUS r

$$\psi = \int \underline{B} \cdot d\underline{A} = \int (\nabla \times \underline{A}) \cdot d\underline{A} = \oint \underline{A} \cdot d\underline{l} = 2\pi r A_\theta$$

$$p_\theta = \gamma m r^2 \dot{\theta} + \frac{q}{2\pi} \psi$$ IS CONSERVED ALONG AN ORBIT IN AXISYMMETRIC GEOMETRIES

"EXTERNAL" (REISER SECTION 3.3)

ELECTRIC & MAGNETIC FIELDS WITH RADIAL SYMMETRY

J. BALMAIN

(B)

CONSIDER THE EXTERNAL FIELD: (TIME STEADY VACUUM SOLUTIONS)

$$\nabla \times \underline{B} = 0 \quad \& \quad \nabla \times \underline{E} = 0$$

$$\nabla \cdot \underline{B} = 0 \quad \& \quad \nabla \cdot \underline{E} = 0 \quad \Rightarrow \quad \underline{E} \ \& \ \underline{B} = -\underline{\nabla}\Phi$$

Let $\Phi = \sum_{\nu=0}^{\infty} f_{2\nu}(z) r^{2\nu}$ $\quad \nabla^2 \phi = 0 \Rightarrow \Phi = \sum_{\nu=0}^{\infty} \frac{(-1)^{\nu}}{\nu!} \frac{\partial^{2\nu} f(0,z)}{\partial z^{2\nu}} \left(\frac{r}{2}\right)^{2\nu}$

$$\Rightarrow \Phi = \Phi(0,z) - \frac{1}{4}\frac{\partial^2 \Phi(0,z)}{\partial z^2} r^2 + \frac{1}{64}\frac{\partial^4 \Phi(0,z)}{\partial z^4} r^4$$

Let $B_z(0,z) = B(z)$ & let $\Phi(0,z) = V(z)$

$$B_z(r,z) = B(z) - \frac{r^2}{4}\frac{\partial^2 B}{\partial z^2} + \frac{r^4}{64}\frac{\partial^4 B}{\partial z^4} + \cdots$$

$$B_r(r,z) = -\frac{r}{2}\frac{\partial B}{\partial z} + \frac{r^3}{16}\frac{\partial^3 B}{\partial z^3} + \cdots$$

$$\Phi(r,z) = V(z) - \frac{1}{4}V'' r^2 + \frac{r^4}{64}\frac{\partial^4 V}{\partial z^4}$$

$$\Rightarrow \quad E_r = \frac{1}{2}V'' r - \frac{r^3}{16}\frac{\partial^4 V}{\partial z^4}$$

Also, $\psi \cong \pi r^2 B(z)$

$$\nabla^2 \phi = \frac{1}{r}\frac{\partial}{\partial r}\left(r\frac{\partial \phi}{\partial r}\right) + \frac{\partial^2 \phi}{\partial z^2} = 0$$

$$f(r,z) = \sum_{\nu=0}^{\infty} f_{2\nu}(z)\, r^{2\nu} = f_0 + f_2 r^2 + f_4 r^4$$

$$\sum_{\nu=1}^{\infty} \left[2\nu + 2\nu(\nu-1)\right] f_{2\nu}\, r^{2\nu-2} + \sum_{\nu=0}^{\infty} f_{2\nu}''\, r^{2\nu} = 0$$

PARAXIAL RAY EQUATION

$$(\mathrm{I}) \Rightarrow \underbrace{\frac{d}{dt}(\gamma m \dot{r})}_{\text{INERTIAL}} - \underbrace{\gamma m r \dot{\theta}^2}_{\text{CENTRIFUGAL}} = q\Big(\underbrace{\frac{V''}{2} r}_{E_r \text{ external}} + \underbrace{r\dot{\theta} B}_{v_\theta B_z \text{ external}}\Big) + q\Big(\underbrace{E_r^{self} - v_z B_\theta^{self}}_{\text{SELF FIELDS}}\Big)$$

Now use s as independent variable $v_z dt = ds$

$$v_z \frac{d}{ds}\left(\gamma m v_z r'\right) - \gamma m v_z^2 r \theta'^2 = q\left(\frac{V''}{2} r + r v_z \theta' B\right) + q\left(E_r^{self} - v_z B_\theta^{self}\right)$$

EXPANDING 1st term and $v_z \cong v$; AND DIVIDING BY $\gamma m v^2$:

$$r'' - r\theta'^2 + \frac{\gamma'}{\beta^2 \gamma} r' = \frac{q}{\gamma m \beta^2 c^2}\left(\frac{V''}{2} r + r\beta c \theta' B + E_r^{self} - v_z B_\theta^{self}\right) \qquad (P1)$$

Using CANONICAL MOMENTUM, eliminate θ' via

$$\theta' = \frac{p_\theta - \frac{q\psi}{2\pi}}{\gamma m r^2 \beta c} = \frac{p_\theta}{\gamma m r^2 \beta c} - \frac{qB}{2\gamma \beta m c} \equiv \frac{p_\theta}{\gamma m r^2 \beta c} - \frac{\omega_c}{2\gamma\beta c}$$

where we define $\omega_c \equiv \frac{qB}{m}$.

ADDING THE TWO θ' TERMS IN THE EQUATION (P1)

$$-r\theta'^2 - \frac{r\omega_c \theta'}{\gamma\beta c} = \frac{-p_\theta^2}{\gamma^2 m^2 r^3 \beta^2 c^2} + \frac{p_\theta \omega_c}{\gamma^2 m \beta^2 c^2 r} - \frac{r\omega_c^2}{4\gamma^2\beta^2 c^2} - \frac{p_\theta \omega_c}{\gamma^2 m \beta^2 c^2 r} + \frac{r\omega_c^2}{2\gamma^2\beta^2 c^2}$$

$$= \frac{-p_\theta^2}{\gamma^2 m^2 r^3 \beta^2 c^2} + \frac{r\omega_c^2}{2\gamma^2\beta^2 c^2}$$

So equation (P1) becomes:

$$r'' + \frac{\gamma'}{\beta^2\gamma} r' = \frac{q}{\gamma m \beta^2 c^2}\left(\frac{V''}{2} r\right) + \frac{r\omega_c^2}{2\gamma^2\beta^2c^2} + \frac{p_\theta^2}{\gamma^2 m^2 r^3 \beta^2 c^2} + \frac{q}{\gamma m \beta^2 c^2}\left[E_r^{self} - v_z B_\theta^{self}\right] \quad (P2)$$

Now $\gamma' mc^2 = q\frac{\underline{E}\cdot\underline{v}}{v_z}$ so $\gamma'' = \left(V'' + \frac{\partial^2\phi^{self}}{\partial z^2}\right)\frac{q}{mc^2}$

CALCULATING $\frac{q}{\gamma m\beta^2c^2}\left[\frac{V''}{2}r + E_r^{self} - v_z B_\theta^{self}\right]$:

$$\nabla^2\phi^{self} = -\frac{\rho}{\varepsilon_0} \Rightarrow \frac{1}{r}\frac{\partial}{\partial r}\left(r\frac{\partial\phi}{\partial r}\right) = -\frac{\rho}{\varepsilon_0} - \frac{\partial^2\phi^{self}}{\partial z^2}$$

$$\Rightarrow \frac{\partial}{\partial r}\left(r\frac{\partial\phi}{\partial r}\right) = -\frac{r\rho(r)}{\varepsilon_0} - \frac{r\partial^2\phi^{self}}{\partial z^2}$$

$$r\frac{\partial\phi}{\partial r} = -\frac{1}{2\pi\varepsilon_0}\int_0^r 2\pi r\,\rho(r)\,dr - \frac{r^2}{2}\frac{\partial^2\phi}{\partial z^2}$$

$$= -\frac{1}{2\pi\varepsilon_0}\lambda(r) - \frac{r^2}{2}\frac{\partial^2\phi^{self}}{\partial z^2}$$

$$\Rightarrow E_r^{self} = \frac{\lambda(r)}{2\pi\varepsilon_0 r} + \frac{r}{2}\frac{\partial^2\phi^{self}}{\partial z^2}$$

$$\nabla\times\underline{B} = \mu_0\underline{J} \Rightarrow 2\pi r B_\theta = \mu_0\int_0^r 2\pi r\, J_z(r)\,dr = \mu_0 v_z\lambda(r)$$

$$B_\theta^{self} = \frac{\mu_0 v_z\lambda(r)}{2\pi r} = \frac{v_z}{c^2}\frac{\lambda(r)}{2\pi\varepsilon_0 r}$$

$$\left[\frac{V''}{2}r + E_r^{self} - v_z B_\theta^{self}\right] = \left[\frac{r}{2}\underbrace{\left(V'' + \frac{\partial^2\phi^{self}}{\partial z^2}\right)}_{-\frac{mc^2}{q}\gamma''} + \underbrace{\left(1 - \frac{v_z^2}{c^2}\right)}_{1/\gamma^2}\frac{\lambda(r)}{2\pi\varepsilon_0 r}\right]$$

So equation (P2) becomes: "THE PARAXIAL RAY EQUATION:"

$$\underbrace{r'' + \frac{\gamma'}{\beta^2\gamma} r'}_{\text{INERTIAL}} + \underbrace{\frac{\gamma''}{2\beta^2\gamma} r}_{\substack{E_r \\ \text{(CONVERGENCE OF FIELD LINES)}}} + \underbrace{\left(\frac{\omega_c}{2\gamma\beta c}\right)^2 r}_{\substack{V_\theta B_z \\ \text{- CENTRIFUGAL}}} - \underbrace{\left(\frac{p_\theta}{\gamma\beta m c}\right)^2 \frac{1}{r^3}}_{\text{CENTRIFUGAL}} - \underbrace{\frac{q}{\gamma^3 m v_z^2} \frac{\lambda(r)}{2\pi\epsilon_0 r}}_{\text{SELF FIELD}} = 0$$

MOMENT EQUATIONS

Vlasov eqtn: $\frac{\partial f}{\partial s} + x' \frac{\partial f}{\partial x} + x'' \frac{\partial f}{\partial x'} + y' \frac{\partial f}{\partial y} + y'' \frac{\partial f}{\partial y'} = 0$

Let $g = g(x, x', y, y')$; $N = \iiiint f \, dx \, dx' \, dy \, dy'$

MULTIPLY VLASOV equation by g & $\frac{1}{N}\iiiint dx\, dx'\, dy\, dy'$

$$\int dx\, dx'\, dy\, dy \left[g \frac{\partial f}{\partial s} + g x' \frac{\partial f}{\partial x} + g x'' \frac{\partial f}{\partial x'} + g y' \frac{\partial f}{\partial y} + g y'' \frac{\partial f}{\partial y'} \right] = 0$$

$$\Rightarrow \frac{d}{ds}\langle g \rangle + \underbrace{\overbrace{\frac{1}{N}\iiint g f \Big|_{x=-\infty}^{\infty}}^{\text{INTEGRATE BY PARTS}}}_{\to 0} - \underbrace{\frac{1}{N}\iiiint \frac{\partial g}{\partial x} f x'}_{= \langle x' \frac{\partial g}{\partial x} \rangle} + \cdots = 0$$

$$\Rightarrow \frac{d}{ds}\langle g \rangle = \langle x' \frac{\partial g}{\partial x} \rangle + \langle x'' \frac{\partial g}{\partial x'} \rangle + \langle y' \frac{\partial g}{\partial y} \rangle + \langle y'' \frac{\partial g}{\partial y'} \rangle$$

But $\frac{dg}{ds} = \frac{\partial g}{\partial x} x' + \frac{\partial g}{\partial x'} x'' + \frac{\partial g}{\partial y} y' + \frac{\partial g}{\partial y'} y''$

$$\Rightarrow \frac{d}{ds}\langle g \rangle = \langle g' \rangle$$

So $\frac{d}{ds}\langle x^2 \rangle = 2\langle x x' \rangle$

$\frac{d}{ds}\langle x'^2 \rangle = 2\langle x' x'' \rangle$ etc...

$\frac{d}{ds}\langle x x' \rangle = \langle x x'' \rangle + \langle x'^2 \rangle$

ENVELOPE EQUATION FOR AXISYMMETRIC BEAMS

LET $r_b^2 = 2\langle r^2\rangle = 2(\langle x^2\rangle + \langle y^2\rangle) = 4\langle x^2\rangle$ for an axisymmetric beam

$$2 r_b r_b' = 4\langle r r'\rangle \quad \Rightarrow \quad r_b' = \frac{2\langle r r'\rangle}{r_b}$$

$$r_b'' = \frac{2\langle r r''\rangle + 2\langle r'^2\rangle}{r_b} - \frac{2\langle r r'\rangle}{r_b^2}\left(\frac{2\langle r r'\rangle}{r_b}\right)$$

$$= 2\frac{\langle r r''\rangle}{r_b} + \frac{4\langle r^2\rangle\langle r'^2\rangle - 4\langle r r'\rangle^2}{r_b^3}$$

WHAT IS $\langle r r''\rangle$?

RECALL EQUATION P1 (ON PATH TO HARRIS LAW EQUATION):

$$r'' - r\theta'^2 + \frac{\gamma'}{\beta^2\gamma} r' = \frac{q}{\gamma m \beta^2 c^2}\left(\frac{V''}{2} r + r\beta c\theta' B + E_r^{self} - v_z B_z^{self}\right)$$

P1 may be rewritten:

$$r'' - r\theta'^2 + \frac{\gamma'}{\beta^2\gamma} r' = \frac{q}{\gamma m \beta^2 c^2}\left[\frac{-mc^2}{q}\gamma''\frac{r}{2} + \frac{\lambda(r)}{\gamma^2 2\pi\epsilon_0 r} + r\beta c\theta' B\right]$$

$\Rightarrow$

$$\boxed{r'' + \frac{\gamma'}{\beta^2\gamma} r' + \frac{\gamma''}{2\beta^2\gamma} r - \frac{q}{\gamma^3 m v_z^2}\frac{\lambda(r)}{2\pi\epsilon_0 r} \underbrace{\frac{-\omega_c}{\gamma\beta c}\theta' r - r\theta'^2}_{} = 0}$$

What is $\langle r r''\rangle$?

$$\langle r r''\rangle + \frac{-\omega_c}{\gamma\beta c}\langle\theta' r^2\rangle - \langle r^2\theta'^2\rangle + \cdots = 0$$

$$\langle p_\theta\rangle^2 = \gamma^2 m^2 \beta^2 c^2 \langle r^2\theta'\rangle^2 + \frac{\omega_c^2}{4} m^2 \langle r^2\rangle^2 + \omega_c \gamma m^2 \beta c \langle r^2\theta'\rangle\langle r^2\rangle$$

$$\Rightarrow \frac{-\omega_c}{\gamma\beta c}\langle\theta' r^2\rangle = \frac{-\omega_c}{\gamma\beta c}\left[\frac{\langle p_\theta\rangle^2}{\omega_c \gamma m^2 \beta c \langle r^2\rangle} - \frac{\omega_c\langle r^2\rangle}{4\gamma\beta c} - \frac{\gamma\beta c}{\omega_c}\frac{\langle r^2\theta'\rangle^2}{\langle r^2\rangle}\right]$$

$$\Rightarrow \langle r r''\rangle = \frac{\langle p_\theta\rangle^2}{\gamma^2 m^2 \beta^2 c^2 \langle r^2\rangle} - \frac{\omega_c^2\langle r^2\rangle}{4\gamma^2\beta^2 c^2} - \frac{\langle r^2\theta'\rangle^2}{\langle r^2\rangle} + \langle r^2\theta'^2\rangle + \cdots = 0$$

$\Rightarrow$

$$\langle r r'' \rangle = \frac{\gamma'}{\beta^2 \gamma} \langle r r' \rangle + \frac{\gamma''}{2\beta^2 \gamma} \langle r^2 \rangle - \frac{q}{\gamma^3 m v_z^2} \frac{\langle \lambda(r) \rangle}{2\pi \epsilon_0} +$$

$$\frac{\langle p_\theta \rangle^2}{(\gamma m \beta c)^2 \langle r^2 \rangle} - \frac{\omega_c^2 \langle r^2 \rangle}{4(\gamma^2 \beta c)^2} - \frac{\langle r^2 \theta' \rangle^2}{\langle r^2 \rangle} + \langle r^2 \theta'^2 \rangle$$

$$r_b'' = \frac{2\langle r r'' \rangle}{r_b} + \frac{4\langle r^2 \rangle \langle r'^2 \rangle - 4\langle r r' \rangle}{r_b^3}$$

$$= \frac{\gamma'}{\beta^2 \gamma} \frac{2\langle r r' \rangle}{r_b} + \frac{\gamma''}{2\beta^2 \gamma} \frac{2\langle r^2 \rangle}{r_b} - \frac{2q}{\gamma^3 m v_z^2} \frac{\langle \lambda(r) \rangle}{2\pi \epsilon_0} \frac{1}{r_b}$$

$$+ \frac{\langle p_\theta \rangle^2}{(\gamma m \beta c)^2} \frac{2}{\langle r^2 \rangle r_b} - \frac{\omega_c^2}{4(\gamma \beta c)^2} \frac{2\langle r^2 \rangle}{r_b} - \frac{2\langle r^2 \theta' \rangle^2}{r_b \langle r^2 \rangle}$$

$$+ \frac{2\langle r^2 \theta'^2 \rangle}{r_b} + \frac{4\langle r^2 \rangle \langle r'^2 \rangle - 4\langle r r' \rangle^2}{r_b^3}$$

USING $r_b^2 \equiv 2\langle r^2 \rangle$ & $r_b' = \dfrac{2\langle r r' \rangle}{r_b}$

ENVELOPE EQUATION

$$\Rightarrow \boxed{r_b'' + \frac{\gamma'}{\beta^2 \gamma} r_b' + \frac{\gamma''}{2\beta^2 \gamma} r_b + \left(\frac{\omega_c}{2\gamma \beta c}\right)^2 r_b + \frac{-4\langle p_\theta \rangle^2}{(\gamma m \beta c)^2 r_b^3} - \frac{\varepsilon_r^2}{r_b^3} - \frac{Q}{r_b} = 0}$$

WHERE $\varepsilon_r^2 = 4(\langle r^2 \rangle \langle r'^2 \rangle - \langle r r' \rangle^2 + \langle r^2 \rangle \langle r^2 \theta'^2 \rangle - \langle r^2 \theta' \rangle^2)$

ENVELOPE EQUATION -- CONTINUED

$$\boxed{r_b'' + \frac{\gamma'}{\beta^2\gamma} r_b' + \frac{\gamma''}{2\beta^2\gamma} r_b + \left(\frac{\omega_c}{2\gamma\beta c}\right)^2 r_b - \frac{4\langle p_\theta\rangle^2}{(\gamma m\beta c)^2 r_b^3} - \frac{\varepsilon_r^2}{r_b^3} - \frac{Q}{r_b} = 0}$$

COMPARE WITH THE SINGLE PARTICLE PARAXIAL RAY EQUATION:

$$\underbrace{r'' + \frac{\gamma'}{\beta^2\gamma} r'}_{\text{INERTIAL}} + \underbrace{\frac{\gamma''}{2\beta^2\gamma} r}_{E_r} + \underbrace{\left(\frac{\omega_c}{2\gamma\beta c}\right)^2 r}_{v_\theta B_z - \text{CENTRIFUGAL}} - \underbrace{\left(\frac{p_\theta}{\gamma m\beta c}\right)^2 \frac{1}{r^3}}_{\text{CENTRIFUGAL}} - \underbrace{\frac{q}{\gamma^3 m v_z^2} \frac{\lambda(r)}{2\pi\varepsilon_0 r}}_{E_r - v_z B_\theta \text{ self field}} = 0$$

$$\varepsilon_r^2 = 4\left(\langle r^2\rangle\langle r'^2\rangle - \langle rr'\rangle^2 + \langle r^2\rangle\langle r^2\theta'^2\rangle - \langle r^2\theta'\rangle^2\right)$$

NOTE THAT FOR AXISYMMETRIC BEAMS ($\rho = \rho(r)$ ONLY)

$$\langle r^2\rangle = \langle x^2\rangle + \langle y^2\rangle = 2\langle x^2\rangle$$

$$\Rightarrow 2\langle rr'\rangle = 4\langle xx'\rangle$$

$$\& \quad \langle x'^2\rangle + \langle y'^2\rangle = 2\langle x'^2\rangle = \langle r'^2\rangle + \langle r^2\theta'^2\rangle$$

DEFINE $\varepsilon_x^2 = 16\left(\langle x^2\rangle\langle x'^2\rangle - \langle xx'\rangle^2\right)$

$$\Rightarrow \boxed{\varepsilon_r^2 = \varepsilon_x^2 - 4\langle r^2\theta'\rangle^2}$$

EXAMPLES OF
SYSTEMS WITH AXIAL SYMMETRY

- PERIODIC SOLENOIDS

- EINZEL LENSES

- CONTINUOUS FOCUSING

EXAMPLES OF
SYSTEMS WITHOUT AXIAL SYMMETRY

- ELECTRIC OR MAGNETIC QUADRUPOLE

⟹ USE CARTESIAN COORDINATES WITH
ELLIPTICAL SPACE CHARGE SYMMETRY

TOPS
35500

(11)

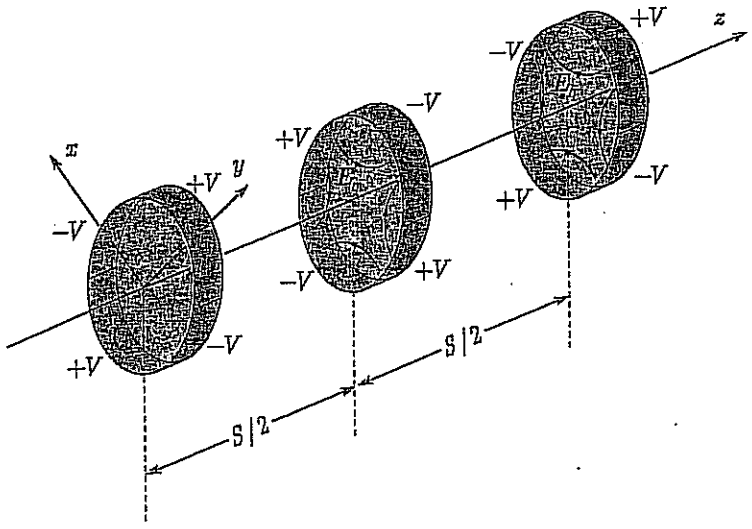

Figure 3.3. Schematic of conductor configuration with applied voltages producing an alternating-gradient quadrupole electric field with axial periodicity length S.

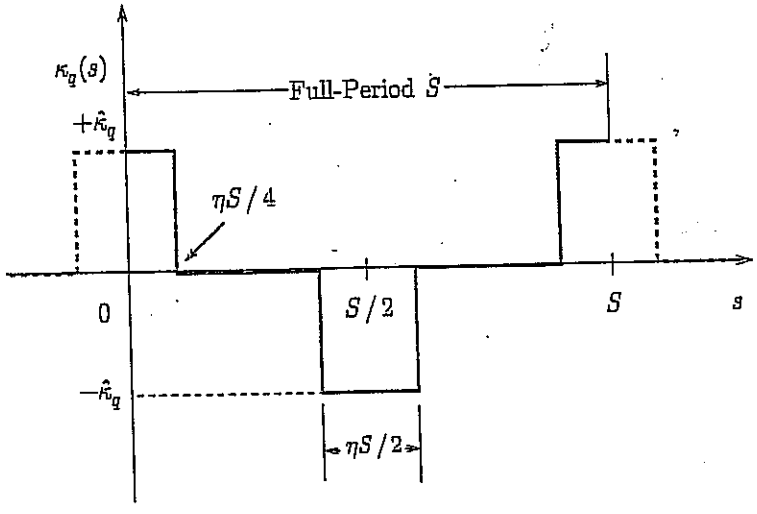

Figure 3.7. Alternating step-function model of a periodic quadrupole lattice with filling factor η for the lens elements. The figure shows a plot of the quadrupole coupling coefficient $\kappa_q(s)$ versus s for one full period (S) of the lattice. Such a configuration is often called a FODO transport lattice (acronym for focusing-off-defocusing-off).

FIGURES FROM DAVIDSON & QIN 2003

(12)

figure from
Davidson & Qin, 2003.

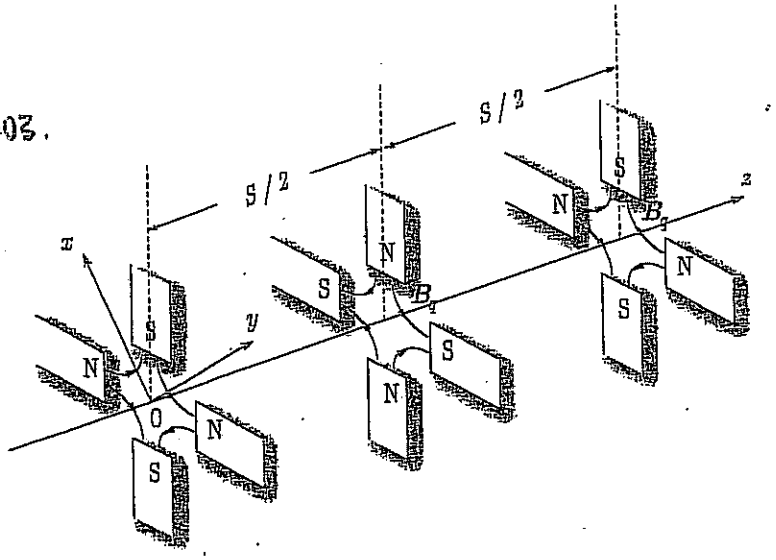

Figure 3.1. Schematic of magnet sets producing an alternating-gradient quadrupole field with axial periodicity length S.

J. BARNARD
13

FROM REISER, p. 112

$E_x = -E'x$
$E_y = E'y$

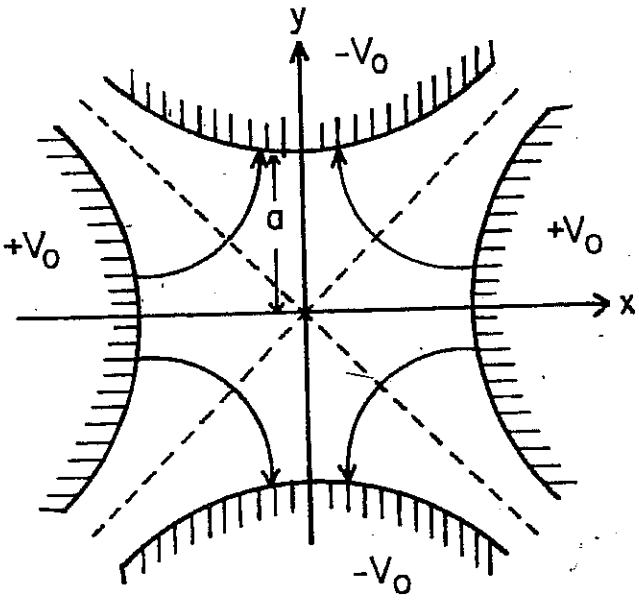

$F_x = -qE'x$
$F_y = qE'y$

ELECTROSTATIC QUADS

Figure 3.15. Electrodes and force lines in an electrostatic quadrupole.

$B_x = B'y$
$B_y = B'x$

$F_x = -qV_z B'x$
$F_y = qV_x B'y$

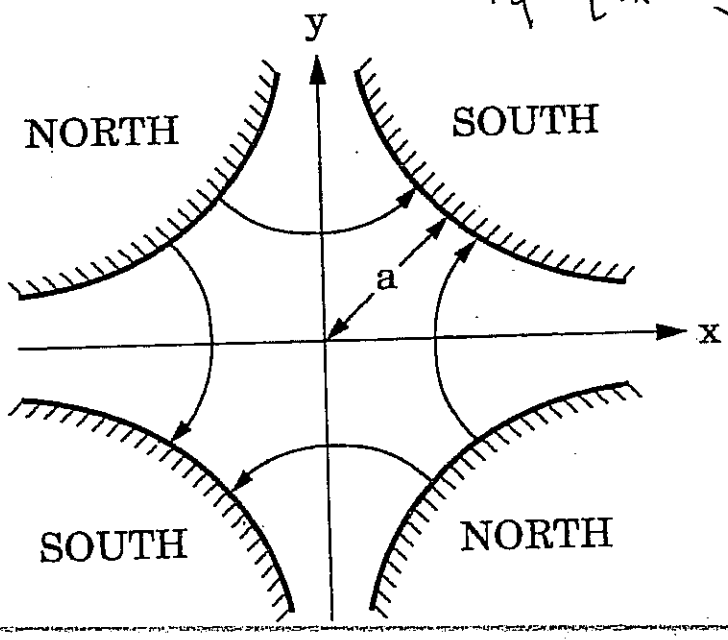

MAGNETIC QUADS

QUADRUPOLE FOCUSING

Now, relax radial symmetry:

For $\nabla \cdot B = 0$ & $\nabla \times B = 0$

EXPAND FIELD IN CYLINDRICAL "MULTIPOLES":

$$E_r, B_r = \sum_{n=1}^{\infty} f_n r^{n-1} \cos(n\theta)$$

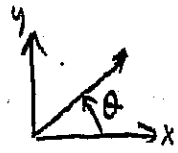

$E_x = E_r \cos\theta - E_\theta \sin\theta$
$E_y = E_r \sin\theta + E_\theta \cos\theta$

$$E_\theta, B_\theta = \sum_{n=1}^{\infty} f_n r^{n-1} \sin(n\theta)$$

$n=1 \Rightarrow$ dipole $\begin{cases} E_r = f_1 \cos\theta \\ E_\theta = -f_1 \sin\theta \end{cases} \Rightarrow \begin{matrix} E_x = f_1 \\ E_y = 0 \end{matrix}$

$n=2 \Rightarrow$ quadrupole $\begin{cases} E_r = f_2 r \cos 2\theta \\ E_\theta = -f_2 r \sin 2\theta \end{cases} \Rightarrow \begin{matrix} E_x = f_2 x \\ E_y = -f_2 y \end{matrix}$

NOTE: ABOVE EXPANSION IS VALID WHEN <u>E or B ≠ function(z)</u>. FOR MAGNETS OF FINITE AXIAL EXTENT, FOR EACH FUNDAMENTAL n-pole, A SET OF HIGHER ORDER MULTIPOLES WITH SAME AZIMUTHAL SYMMETRY ARE REQUIRED TO SATISFY $\nabla^2\phi = 0$.

FOR EXAMPLE FOR A FUNDAMENTAL QUADRUPOLE THE FIELD MAY BE EXPANDED:

$$E_r = \sum_{\nu=0}^{\infty} f_{2,\nu}(z)\,[1+\nu]\, r^{1+2\nu} \cos[2\theta]$$

$$E_\theta = \sum_{\nu=0}^{\infty} -f_{2,\nu}(z)\, r^{1+2\nu} \sin[2\theta]$$

$$E_z = \sum_{\nu=0}^{\infty} \frac{1}{2}\frac{df_{2,\nu}}{dz}\, r^{2+2\nu} \cos 2\theta$$

with $f_{2,\nu+1}(z) = \dfrac{-1}{4(\nu+1)(\nu+3)} \dfrac{d^2 f_{2,\nu}(z)}{dz^2}$

SEE LUND, S. M. (1996) FOR EXAMPLE. HIF note 96-1 LLNL.

Heavy ion accelerators use alternating gradient quadrupoles to focus (confine) the beams (non-neutral plasmas)

Space-charge forces and thermal forces act to expand beam

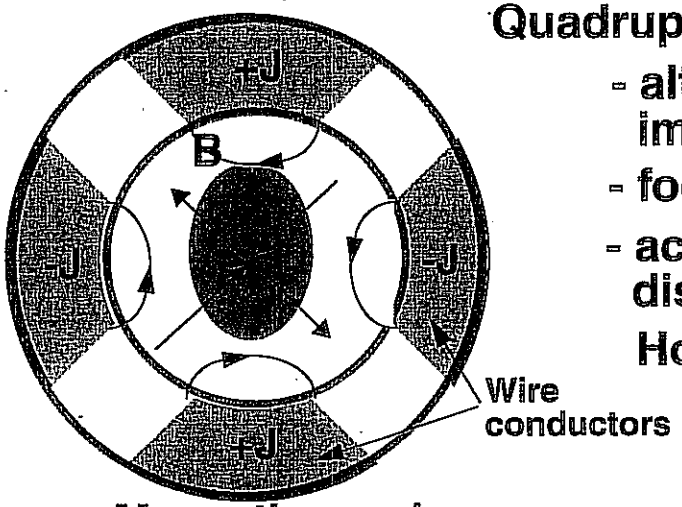

Magnetic quad

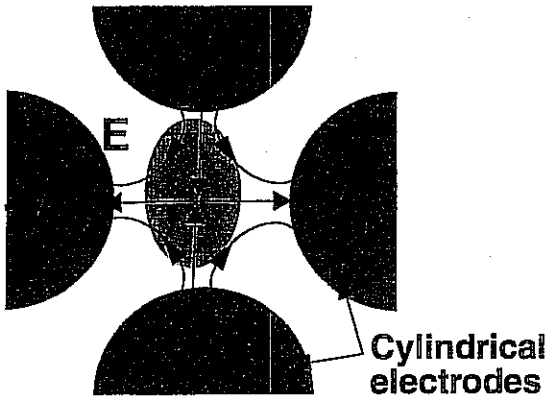

Electric quad

Quadrupoles (magnetic or electric):

- alternately provide inward then outward impulse
- focus in one plane and defocus in other
- act as linear lenses. (Force proportional to distance from axis).

Horizontal (x) plane:

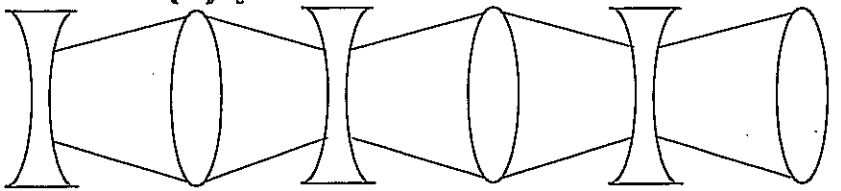

Vertical (y) plane:

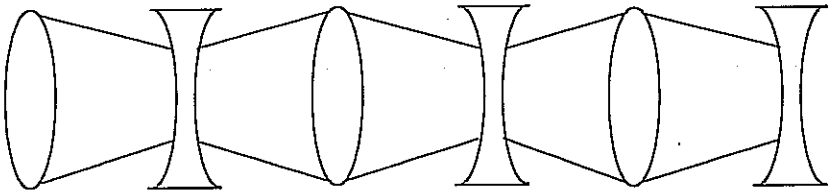

Average displacement is larger in focusing lenses so the net effect is focusing.

J. Barnard

16

Space charge reduces betatron phase advance

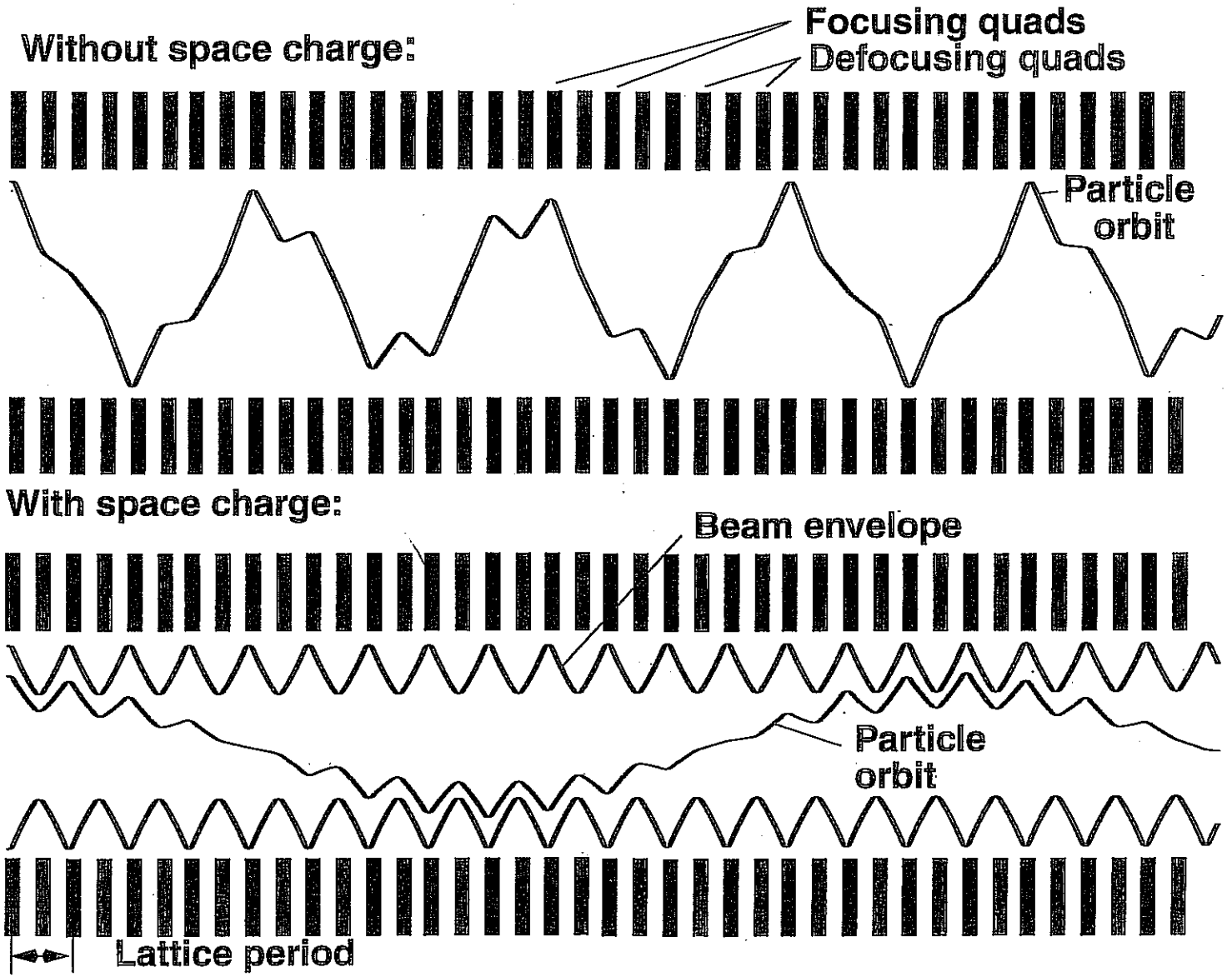

J. Barnard

John Barnard
Steven Lund
USPAS
June 2006

Elliptical Beam Envelope Equations -- cont'd

Current limits

A. Axisymmetric
   1. Solenoids
   2. Einzel lens
B. Quadrupolar
   1. Derivation of envelope equations with elliptic symmetry
   2. Current limit using fourier transform method
   3. Alternative methods

Centroid motion

YESTERDAY, WE DERIVED THE PARAXIAL RAY EQUATION FOR PARTICLES IN AXISYMMETRIC SYSTEMS:

$$\underbrace{r'' + \frac{\gamma'}{\beta^2\gamma} r'}_{\text{INERTIAL}} + \underbrace{\frac{\gamma''}{2\beta^2\gamma}}_{E_r} + \underbrace{\left(\frac{\omega_c}{2\gamma\beta c}\right)^2 r}_{\substack{V_\theta B_z \\ -\text{CENTRIFUGAL}}} - \underbrace{\left(\frac{p_\theta}{\gamma\beta m c}\right)^2 \frac{1}{r^3}}_{\text{CENTRIFUGAL}} - \underbrace{\frac{q}{\gamma^3 m v_z^2} \frac{\lambda(r)}{2\pi\epsilon_0 r}}_{\text{SELF-FIELD}} = 0$$

$$\theta' = \frac{p_\theta}{\gamma m r^2 \beta c} - \frac{\omega_c}{2\gamma\beta c}$$ ← CONSTANCY & DEFINITION OF CANONICAL MOMENTUM

ENVELOPE EQUATION FOR AXISYMMETRIC BEAM

$$r_b'' + \frac{\gamma' r_b'}{\beta^2\gamma} + \frac{\gamma''}{2\beta^2\gamma} r_b + \left(\frac{\omega_c}{2\gamma\beta c}\right)^2 r_b - \frac{4\langle p_\theta\rangle^2}{(\gamma m\beta c)^2 r_b^3} - \frac{\epsilon_r^2}{r_b^3} - \frac{Q}{r_b} = 0$$

$$\epsilon_r^2 \equiv 4\left(\langle r^2\rangle\langle r'^2\rangle - \langle r r'\rangle^2 + \langle r^2\rangle\langle r^2\theta'^2\rangle - \langle r^2\theta'\rangle^2\right)$$

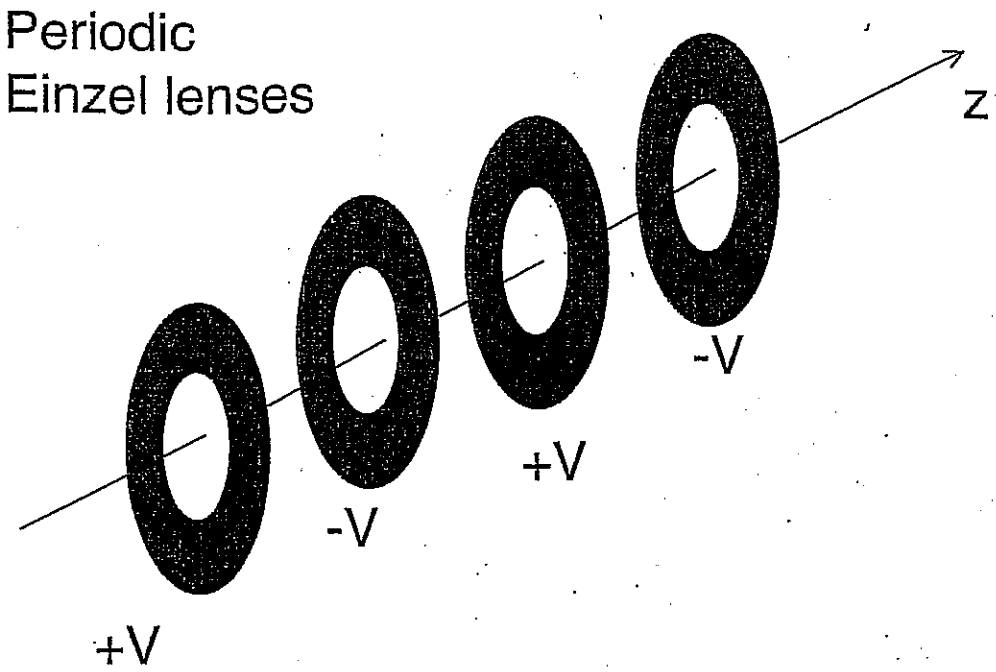

PERIODIC SOLENOIDS

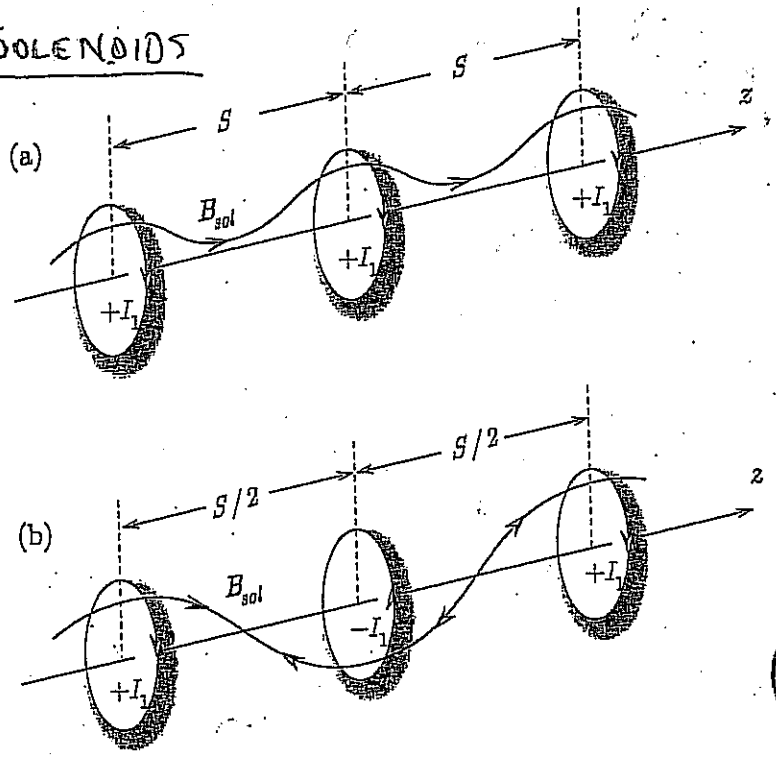

(FIGURE FROM DAVIDSON & QIN, 2003) p. 55 "PHYSICS OF INTENSE (HIGH-CURRENT) PARTICLE BEAMS IN HIGH ENERGY ACCELERATORS"

Figure 3.2. Schematic of magnet sets producing a periodic focusing solenoidal field with axial periodicity length S. In Fig. 3.2 (a), successive coils are spaced by S and have the same current polarity $+I_1, +I_1, \cdots$. In Fig. 3.2 (b), successive coils are spaced by $S/2$ and have alternating current polarities $+I_1, -I_1, +I_1, \cdots$.

SOLENOIDAL FOCUSING

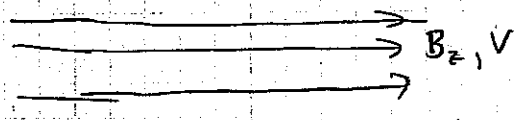

Let $\gamma' = \gamma'' = 0$

FOR MAXIMUM TRANSPORT $P_\theta = 0$ & $\varepsilon_r^2 = 0$

$$\Rightarrow \quad r_b'' + \left(\frac{\omega_c}{2\gamma\beta c}\right)^2 r_b = \frac{Q}{r_b}$$

FOR A MATCHED BEAM:

$$Q_{max} = \left(\frac{\omega_c}{2\gamma\beta c}\right)^2 r_b^2$$

HEURISTICALLY:

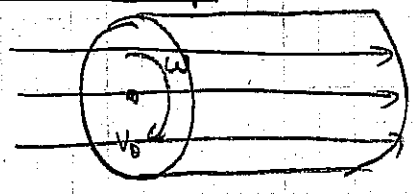

$V_\theta = \omega r$

$$m\omega^2 r + Q m V_z^2 \left(\frac{r}{r_b^2}\right) = q \underbrace{\omega r}_{V_\theta} B_z$$

centrifugal force — SPACE CHARGE FORCE — MAGNETIC FORCE INWARD

$$\Rightarrow \quad \omega^2 + \frac{QV^2}{r_b^2} = \omega\omega_c$$

$\omega\omega_c - \omega^2 =$ MAXIMUM WHEN $\omega = \frac{\omega_c}{2}$

$$\Rightarrow \quad Q_{max} = \left(\frac{\omega_c^2}{4}\right)\left(\frac{r_b^2}{V^2}\right)$$

EINZEL LENS

J. BARNARD

5

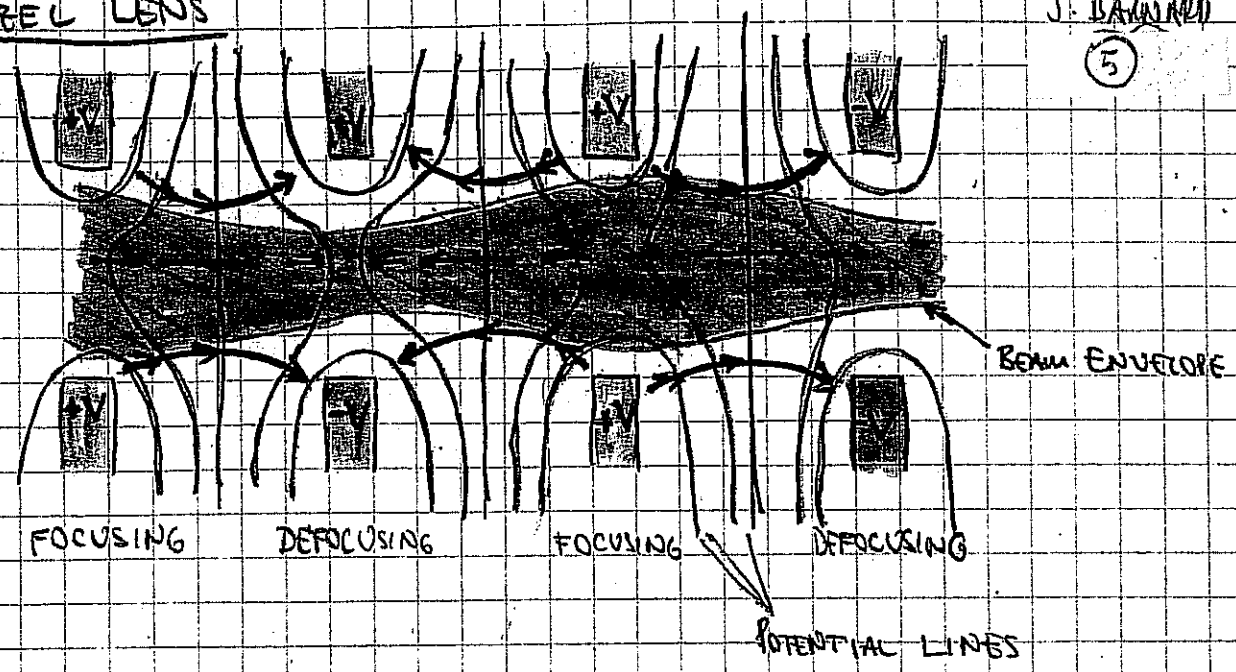

FOCUSING OCCURS AT LARGE RADIUS THAN DEFOCUSING

$\Rightarrow$ NET INWARD FORCE

EINZEL LENS – ANALYSIS (DERIVATION FROM ED LEE)

NOW, LET $\omega_c = \langle P_\theta \rangle = \varepsilon_r^2 = 0$

$$\Rightarrow r_b'' + \frac{\gamma'}{\beta^2\gamma} r_b' + \frac{\gamma''}{2\beta^2\gamma} r_b - \frac{Q}{r_b} = 0$$

ALSO ASSUME $\beta \ll 1$, NON-RELATIVISTIC BEAM $\rightarrow \gamma' \simeq \beta\beta'$, $\gamma'' \simeq \beta'^2 + \beta''\beta$

$$r_b'' + \frac{\beta'}{\beta} r_b' + \left[\frac{1}{2}\frac{\beta'^2}{\beta^2} + \frac{1}{2}\frac{\beta''}{\beta}\right] r_b - \frac{Q}{r_b} = 0$$

To eliminate r_b' term try substitution

$$r_b = \left(\frac{\beta_0}{\beta}\right)^{1/2} R$$

$$r_b' = \left(\frac{\beta_0}{\beta}\right)^{1/2} R' - \frac{1}{2}\left(\frac{\beta}{\beta_0}\right)^{-3/2} \frac{R}{\beta_0}\beta'$$

$$r_b'' = \left(\frac{\beta_0}{\beta}\right)^{1/2} R'' - \left(\frac{\beta}{\beta_0}\right)^{-\frac{3}{2}} \frac{R'}{\beta_0}\beta' + \frac{3}{4}\left(\frac{\beta}{\beta_0}\right)^{-\frac{5}{2}} \frac{R}{\beta_0^2}\beta'^2 - \frac{1}{2}\left(\frac{\beta}{\beta_0}\right)^{-\frac{3}{2}} \frac{R}{\beta_0}\beta''$$

$$\Rightarrow \left(\frac{\beta_0}{\beta}\right)^{1/2} R'' + \frac{3}{4}\left(\frac{\beta}{\beta_0}\right)^{-\frac{5}{2}} \frac{\beta'^2}{\beta_0^2} R = \frac{Q}{R}\left(\frac{\beta}{\beta_0}\right)^{1/2}$$

$$\Rightarrow \boxed{R'' = \frac{Q}{R}\left(\frac{\beta}{\beta_0}\right) - \frac{3}{4}\left(\frac{\beta'}{\beta}\right)^2 R}$$

National Brand 42-182 100 SHEETS Made in U.S.A.

EINZEL LENS - CONTINUED

MODEL: LET $\phi = \phi_0 \cos\left(\frac{\pi z}{L}\right)$

$$\frac{1}{2} m v^2 + q\phi = \text{constant}$$

$$\Rightarrow \quad v^2 = v_0^2 + \frac{2q\phi}{m} \cos\left(\frac{\pi z}{L}\right)$$

$$v' = \frac{-q\phi_0}{mv}\left(\frac{\pi}{L}\right) \sin\left(\frac{\pi z}{L}\right)$$

If $\left(\frac{2q\phi_0}{m}\right) << v_0^2$: $\left(\frac{\beta'}{\beta}\right)^2 \cong \left(\frac{q\phi_0}{m v_0^2}\right)^2 \left(\frac{\pi}{L}\right)^2 \sin^2\left(\frac{\pi z}{L}\right)$

FOR EQUILIBRIUM LOOK AT D.C. COMPONENT: $\sin^2(x) = \frac{1}{2} - \frac{1}{2}\cos 2x$

$$R'' = 0 \quad \Rightarrow \quad \frac{Q}{\bar{R}} = \frac{3}{4} \overline{\left(\frac{\beta'}{\beta}\right)^2}\, \bar{R}$$

$$R \equiv \left(\frac{\beta}{\beta_0}\right)^{1/2} r_b \quad \Rightarrow \quad \bar{R} = r_b$$

$$\overline{\left(\frac{\beta'}{\beta}\right)^2} = \frac{1}{2}\left(\frac{q\phi_0}{m v_0^2}\right)^2 \left(\frac{\pi}{L}\right)^2$$

$$\Rightarrow \quad Q_{max} = \frac{3\pi^2}{8}\left(\frac{q\phi_0}{m v_0^2}\right)^2 \left(\frac{r_b}{L}\right)^2$$

National® Brand 42-182 100 SHEETS Made in U.S.A.

QUADRUPOLE ANALYSIS

J BRANNON

EQUATION OF MOTION

RETURN TO x, y COORDINATES

$$x'' + \frac{1}{\gamma v_z}\frac{d}{ds}(\gamma v_z)x' = \frac{-q}{\gamma^3 m v_z^2}\frac{\partial \varphi}{\partial x} \pm \begin{cases} \frac{qB'}{\gamma m v_z^2}x & \text{for magnetic quads} \\ \frac{qE'}{\gamma m v_z^2}x & \text{for electric quads} \end{cases}$$

Let $\frac{\gamma m v_z}{q} = \frac{p}{q} \equiv [B\rho] \equiv$ RIGIDITY

$$y'' + \frac{1}{\gamma v_z}\frac{d}{ds}(\gamma v_z)y' = \frac{-q}{\gamma^3 m v_z^2}\frac{\partial \varphi}{\partial y} \mp \begin{cases} \frac{B'}{[B\rho]}y & \text{magnetic} \\ \frac{qE'}{\gamma m v_z^2}y & \text{electric} \end{cases}$$

ENVELOPE EQUATION

$$r_x^2 = 4\langle x^2\rangle; \quad r_y^2 = 4\langle y^2\rangle$$

$$r_x' = \frac{4\langle x x'\rangle}{r_x}$$

$$r_x'' = \frac{4\langle x x''\rangle}{r_x} + \frac{\varepsilon_x^2}{r_x^3}; \qquad \varepsilon_x^2 = 16\left(\langle x^2\rangle\langle x'^2\rangle - \langle x x'\rangle^2\right)$$

$$r_y'' = \frac{4\langle y y''\rangle}{r_y} + \frac{\varepsilon_y^2}{r_y^3} \qquad \varepsilon_y^2 = 16\left(\langle y^2\rangle\langle y'^2\rangle - \langle y y'\rangle^2\right)$$

For magnetic focusing:

$$r_x'' + \frac{1}{\gamma v_z}\frac{d}{ds}(\gamma v_z)\, r_x' + \frac{4q}{\gamma^3 m v_z^2}\frac{\langle x \frac{\partial \varphi}{\partial x}\rangle}{r_x} \pm \frac{B'}{[B\rho]}r_x - \frac{\varepsilon_x^2}{r_x^3} = 0$$

$$r_y'' + \frac{1}{\gamma v_z}\frac{d}{ds}(\gamma v_z)\, r_y' + \frac{4q}{\gamma^3 m v_z^2}\frac{\langle y \frac{\partial \varphi}{\partial y}\rangle}{r_y} \pm \frac{B'}{[B\rho]}r_x - \frac{\varepsilon_y^2}{r_y^3} = 0$$

(for electric focusing $\frac{B'}{[B\rho]} \to \frac{qE'}{\gamma m v_z^2}$)

SPACE CHARGE TERM WITH ELLIPTICAL SYMMETRY

NOW DEFOCUSING IN ONE DIRECTION AND FOCUSING IN THE OTHER $\Rightarrow$ RADIAL SYMMETRY SHOULD BE REPLACED BY ELLIPTICAL SYMMETRY:

$$\rho = \rho\left(\frac{x^2}{r_x^2} + \frac{y^2}{r_y^2}\right)$$

CAN BE SHOWN THAT

$$\left\langle x \frac{\partial \phi}{\partial x} \right\rangle = \frac{-\lambda}{4\pi\varepsilon_0} \frac{r_x}{r_x + r_y}$$

$$\left\langle y \frac{\partial \phi}{\partial y} \right\rangle = \frac{-\lambda}{4\pi\varepsilon_0} \frac{r_y}{r_x + r_y}$$

DEFINING $Q = \dfrac{2q\lambda}{4\pi\varepsilon_0 \gamma^3 m v_z^2}$

$$\boxed{\begin{aligned} r_x'' + \frac{1}{\gamma v_z}\frac{d}{ds}(\gamma v_z) r_x' - \frac{2Q}{r_x + r_y} \mp \frac{B'}{[B\rho]} r_x - \frac{\varepsilon_x^2}{r_x^3} &= 0 \\ r_y'' + \frac{1}{\gamma v_z}\frac{d}{ds}(\gamma v_z) r_y' - \frac{2Q}{r_x + r_y} \pm \frac{B'}{[B\rho]} r_y - \frac{\varepsilon_y^2}{r_y^3} &= 0 \end{aligned}}$$

(for Electric Focusing $\dfrac{B'}{[B\rho]} \to \dfrac{qE'}{\gamma m v_z^2}$)

SPACE CHARGE TERM WITH ELLIPTICAL SYMMETRY II

ELLIPTICAL SYMMETRY: $\rho = \rho\left(\frac{x^2}{r_x^2} + \frac{y^2}{r_y^2}\right)$

CAN BE SHOWN THAT $\left\langle x \frac{\partial \varphi}{\partial x} \right\rangle = \frac{-\lambda}{4\pi\varepsilon_0} \frac{r_x}{r_x + r_y}$

(Sacherer, 1971)

& $\left\langle y \frac{\partial \varphi}{\partial y} \right\rangle = \frac{-\lambda}{4\pi\varepsilon_0} \frac{r_y}{r_x + r_y}$

OUTLINE OF PROOF: (from R. Ryne)

Let $\chi = \frac{x^2}{r_x^2+s} + \frac{y^2}{r_y^2+s}$

DEFINE $\eta(\chi)$ such that $\rho(x,y) = \left.\frac{d\eta(\chi)}{d\chi}\right|_{s=0} = \hat{\rho}(\chi)\big|_{s=0}$

So $\rho = \hat{\rho}\left(\frac{x^2}{r_x^2} + \frac{y^2}{r_y^2}\right) = \hat{\rho}(\chi)\big|_{s=0}$

DEFINE $\Psi(x,y) = \frac{-r_x r_y}{4\varepsilon_0} \int_0^\infty \frac{\eta(\chi)\, ds}{\sqrt{r_x^2+s}\,\sqrt{r_y^2+s}}$

It follows that $\frac{\partial^2 \Psi}{\partial x^2} + \frac{\partial^2 \Psi}{\partial y^2} = -\frac{\rho}{\varepsilon_0}$ AND SO IS A SOLUTION OF POISSON'S EQUATION (since $\Psi \to 0$ as $x, y \to \infty$)

WHAT IS $\left\langle x \frac{\partial \Psi}{\partial x} \right\rangle$?

$$\left\langle x \frac{\partial \Psi}{\partial x} \right\rangle = \frac{-r_x r_y}{4\lambda\varepsilon_0} \int_{-\infty}^{\infty} dx \int_{-\infty}^{\infty} dy\, x\, \rho(x,y) \int_0^\infty \frac{\eta' \frac{\partial \chi}{\partial x}\, ds}{\sqrt{r_x^2+s}\,\sqrt{r_y^2+s}}$$

where $\lambda = \int_{-\infty}^{\infty} dx \int_{-\infty}^{\infty} dy\, \rho(x,y)$

So $$\left\langle x \frac{\partial \psi}{\partial x} \right\rangle = \frac{-2 r_x r_y}{4 \lambda \varepsilon_0} \int_{-\infty}^{\infty} dx \int_{-\infty}^{\infty} dy \; x^2 \hat{\rho}\left(\frac{x^2}{r_x^2} + \frac{y^2}{r_y^2}\right) \int_0^{\infty} \frac{\hat{\rho}\left(\frac{x^2}{r_x^2+s} + \frac{y^2}{r_y^2+s}\right) ds}{(r_x^2+s)^{3/2}(r_y^2+s)^{1/2}}$$

Let $r\cos\theta = \dfrac{x}{\sqrt{r_x^2+s}}$ $\qquad r\sin\theta = \dfrac{y}{\sqrt{r_y^2+s}}$

$\det J = \sqrt{r_x^2+s}\,\sqrt{r_y^2+s}\; r$ $\qquad$ where J is the Jacobian $dx\,dy = \det J \cdot dr\,d\theta$

$$\Rightarrow \left\langle x \frac{\partial \psi}{\partial x} \right\rangle = \frac{-r_x r_y}{\lambda 2 \varepsilon_0} \int_0^{\infty} dr \int_0^{2\pi} d\theta \int_0^{\infty} ds \; r^3 \hat{\rho}(r^2)\, \rho\left(\frac{r_x^2+s}{r_x^2} r^2\cos^2\theta + \frac{r_y^2+s}{r_y^2} r^2 \sin^2\theta\right)$$

Let $$r'^2 = \frac{r_x^2+s}{r_x^2} r^2\cos^2\theta + \frac{r_y^2+s}{r_y^2} r^2 \sin^2\theta$$
$$= r^2\left[1 + s\left(\frac{\cos^2\theta}{r_x^2} + \frac{\sin^2\theta}{r_y^2}\right)\right]$$

with r fixed $\quad 2r'dr' = r^2\left(\dfrac{\cos^2\theta}{r_x^2} + \dfrac{\sin^2\theta}{r_y^2}\right) ds$

$$\Rightarrow \left\langle x \frac{\partial \psi}{\partial x} \right\rangle = \frac{-r_x r_y}{2\lambda \varepsilon_0} \int_0^{\infty} dr \int_0^{2\pi} d\theta \int_r^{\infty} dr' \; \frac{2r'dr'\, r^3 \rho(r^2)\, \hat{\rho}(r'^2) \cos^2\theta}{r^2\left(\frac{\cos^2\theta}{r_x^2} + \frac{\sin^2\theta}{r_y^2}\right)}$$

$$\int_0^{2\pi} \frac{\cos^2\theta \; d\theta}{\frac{\cos^2\theta}{r_x^2} + \frac{\sin^2\theta}{r_y^2}} = \frac{2\pi\, r_x^2 r_y}{r_x + r_y}$$

$$\Rightarrow \left\langle x \frac{\partial \psi}{\partial x} \right\rangle = \frac{-r_x^3 r_y^2}{\lambda 2\pi \varepsilon_0 (r_x + r_y)} \int_0^{\infty} dr\, 2\pi r\, \hat{\rho}(r^2) \int_r^{\infty} dr'\, 2\pi r' \rho(r'^2)$$

Recall $$\lambda = \int_{-\infty}^{\infty}\int_{-\infty}^{\infty} dx\,dy\,(x,y) = \int_{-\infty}^{\infty}\int_{-\infty}^{\infty} dx\,dy\; \hat{\rho}\left(\frac{x^2}{r_x^2} + \frac{y^2}{r_y^2}\right)$$

Let $\dfrac{x}{r_x} = r\cos\theta \quad \dfrac{y}{r_y} = r\sin\theta \quad \det J = r_x r_y r$

$$\Rightarrow \lambda = \int_0^{\infty} dr \int_0^{2\pi} d\theta\; \rho(r^2)\, r_x r_y r = 2\pi r_x r_y \int_0^{\infty} dr\, r\, \rho(r^2)$$

Now $\int_0^\infty r\,dr \int_r^\infty r'\,dr'\ \hat{\rho}(r^2)\,\hat{\rho}(r'^2) = \frac{1}{2}\underbrace{\int_0^\infty dr\ r\,\hat{\rho}(r^2)}_{\lambda/2\pi r_x r_y}\ \underbrace{\int_0^\infty dr'\ r'\,\hat{\rho}(r'^2)}_{\lambda/2\pi r_x r_y}$

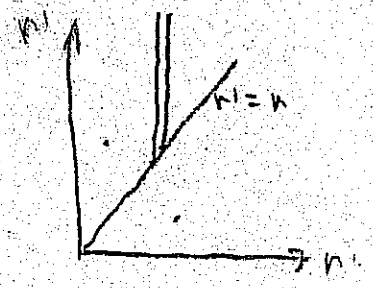

$\hat{\rho}(r^2)\,\hat{\rho}(r'^2)$ is the same on switching r & r'.

So $$\left\langle x\frac{\partial\psi}{\partial x}\right\rangle = \frac{-r_x^3 r_y}{\lambda\, 2\pi\epsilon_0 (r_x - r_y)}\left[\frac{1}{2}\,\frac{\lambda}{2\pi r_x r_y}\cdot\frac{\lambda}{2\pi r_x r_y}\right]$$

$$= \frac{-\lambda}{4\pi\epsilon_0}\,\frac{r_x}{r_x + r_y}$$

J. BARNARD

CURRENT LIMIT FOR QUADRUPOLES (FODO)

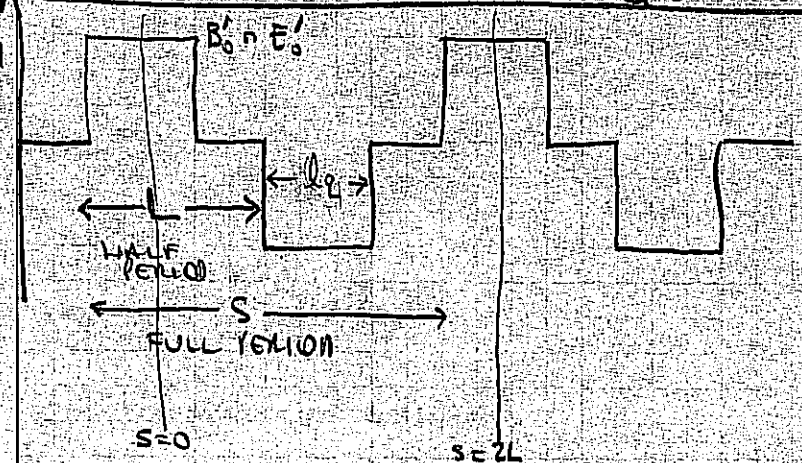

$$k = \begin{cases} \dfrac{B_0'}{[B\rho]} & \text{MAGNETIC} \\ \dfrac{qE_0'}{\gamma m v_z^2} & \text{ELECTRIC} \end{cases}$$

$$r_x'' + k f(s) r_x - \frac{2Q}{r_x + r_y} = 0$$

(NOTE WE HAVE SET $\epsilon = 0$).

$$r_y'' - k f(s) r_y - \frac{2Q}{r_x + r_y} = 0$$

$$f(s) = \begin{cases} 1 & 0 < s < \eta L/2 \\ -1 & L - \frac{\eta L}{2} < s < L + \eta L/2 \\ 1 & 2L - \eta L/2 < s < 2L \\ 0 & \text{otherwise} \end{cases}$$

$$\frac{1}{2L}\int_0^{2L} f(s) \cos\left(\frac{\pi s}{L}\right) ds = \left(\frac{2}{\pi}\right) \sin\left(\frac{\pi \eta}{2}\right)$$ = fourier amplitude at fundamental lattice frequency

Let $r_x = r_b\left(1 + \delta \cos\left(\frac{\pi s}{L}\right)\right)$

$r_y = r_b\left(1 - \delta \cos\left(\frac{\pi s}{L}\right)\right)$

Let $k f(s) \rightarrow k\left(\frac{2}{\pi}\right)\sin\left(\frac{\eta\pi}{2}\right) \cos\left(\frac{\pi s}{L}\right)$

COLLECTING "FAST" TERMS AND "SLOW" TERMS

$$\left[\frac{-\pi^2}{L^2} r_b \delta + k r_b \left(\frac{4 \sin\left(\frac{\eta\pi}{2}\right)}{\pi}\right)\right] \cos\left(\frac{\pi s}{L}\right) = 0 \quad \text{(fast)}$$

$$\delta k r_b \left(\frac{2 \sin\left(\frac{\eta\pi}{2}\right)}{\pi}\right) = \frac{Q}{r_b} \quad \text{(slow)}$$

Fast $\Rightarrow$ $\delta = \dfrac{2kL^2}{\pi^3} \sin\left(\dfrac{\eta\pi}{2}\right)$ & $Q_{max} \cong \dfrac{\eta^2 k^2 L^2}{\pi^2}\left(\dfrac{\sin\left(\frac{\eta\pi}{2}\right)}{\left(\frac{\eta\pi}{2}\right)}\right)^2 r_b^2$

National® Brand 42-182 100 SHEETS Made in U.S.A.

CONTINUOUS FOCUSING

$$r_x'' = -k_{\beta 0}^2 x + \frac{2Q}{r_x + r_y} - \frac{\epsilon^2}{r_x^2}$$

$$r_y'' = -k_{\beta 0}^2 y + \frac{2Q}{r_x + r_y} - \frac{\epsilon^2}{r_y^2}$$

CURRENT LIMIT BALANCES PERVEANCE & EXTERNAL FOCUSING ($r_x = r_y = r_b$):

$$k_{\beta 0}^2 r_b = \frac{Q_{max}}{r_b}$$

Effective $k_{\beta 0}^2$ FOR QUADRUPOLES FOUND FROM DOMINANT FOURIER COMPONENT

$$k_{\beta 0}^2 = \frac{\eta^2 k^2 L^2}{\pi^2} \left(\frac{\sin\left(\frac{\eta\pi}{2}\right)}{\frac{\eta\pi}{2}} \right)^2 \qquad \text{where } k = \frac{B'}{[B\rho]}$$

FOR CONTINUOUS FOCUSING: $k_{\beta 0}^2 = \frac{\sigma_0^2}{4L^2}$

ELIMINATING L:

$$Q_{max} = \frac{\eta k \sigma_0}{2\pi} \left(\frac{\sin\frac{\eta\pi}{2}}{\frac{\eta\pi}{2}} \right) r_b^2 \quad \leftarrow$$

PERVEANCE LIMIT FOR FODO QUADRUPOLES

Envelope instabilities set upper limit on "single particle" phase advance σ_0

Experimental data (Tiefenback, 1986) from LBL's Single Beam Transport Experiment (SBTE)

$\sigma_0 < 85^0$

Experimental limits on beam stability in terms of σ and σ_0

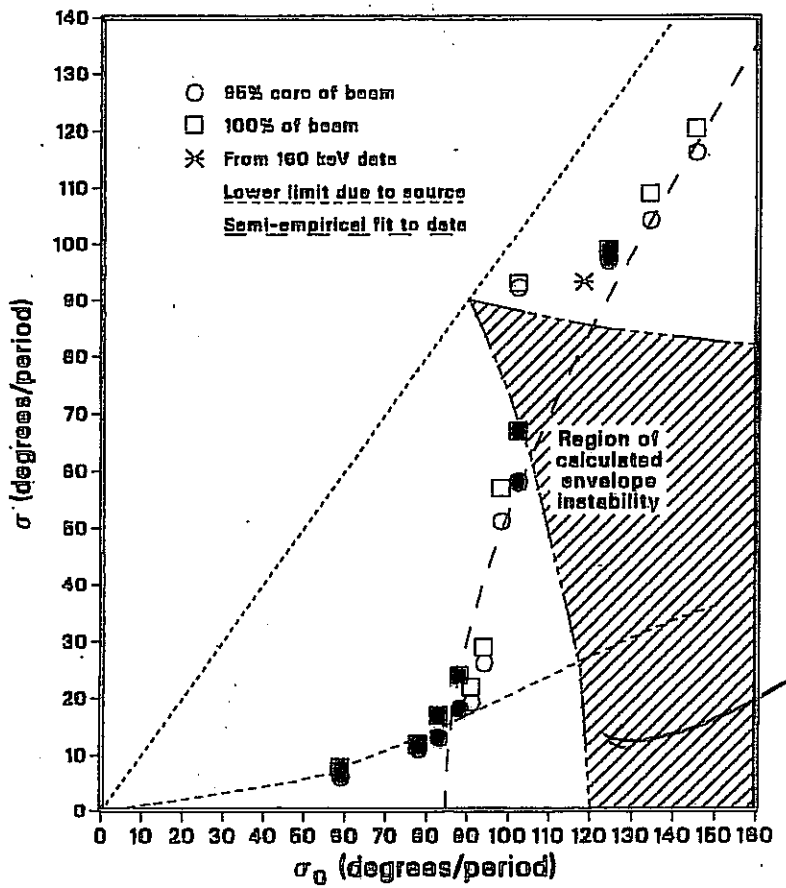

SEE LUND & CHAWLA 2006, NIMPR-A, FOR HIGHER ORDER PARTICLE-LATTICE RESONANCES WHICH CLARIFIES $\sigma_0 = 85^0$ LIMIT

SEE STAUCKMEIR & REISER, PARTICLE ACCELERATORS 14, 227, (1984) & LUND & BUKH, PRSTAB, 7 024801 (2004)

J. BARNARD

QUADRUPOLE CURRENT LIMIT — CONTINUED

$$Q_{max} \cong \frac{\eta k \Theta_0}{2\pi} \left(\frac{\sin \frac{\eta \pi}{2}}{\frac{\eta \pi}{2}} \right) r_b^2$$

$$\text{here } k = \begin{cases} \dfrac{dB/dx}{[B\rho]} \sim \dfrac{B}{[B\rho]\, r_p} & \text{(MAGNETIC QUAD FODO)} \\[2ex] \dfrac{q\, dE/dx}{\gamma m v_z^2} \sim \dfrac{2 q V_q}{\gamma m v_z^2 r_p^2} & \text{where } V_q = \frac{1}{2}\frac{dE}{dx} r_p^2 \quad \text{(ELECTRIC QUAD FODO)} \end{cases}$$

So

$$Q_{max} \cong \frac{\eta \Theta_0}{2\pi} \left(\frac{\sin \frac{\eta \pi}{2}}{\frac{\eta \pi}{2}} \right) \begin{cases} \dfrac{B\, r_b}{[B\rho]} \left[\dfrac{r_b}{r_p} \right] \\[2ex] \dfrac{2 q V_q}{\gamma m v_z^2} \left[\dfrac{r_b^2}{r_p^2} \right] \end{cases}$$

Summary of Current Limits From Different Focusing Methods

Einzel Lens

$$Q_{max} \cong \frac{3\pi^2}{8}\left(\frac{q\phi_0}{m v_0^2}\right)^2\left(\frac{r_b}{L}\right)^2$$

Solenoids

$$Q_{max} = \left(\frac{\omega_c r_b}{2\gamma\beta c}\right)^2$$

Quadrupole Focusing

$$Q_{max} \cong \frac{\eta\phi_0}{2\pi}\left(\frac{\sin\frac{\eta\pi}{2}}{\frac{\eta\pi}{2}}\right)\left[\frac{B r_b}{[B\rho]}\left[\frac{r_b}{r_p}\right] \quad \frac{2qV_q}{\gamma m v_z^2}\left[\frac{r_b^2}{r_p^2}\right]\right]$$

MAGNETIC

Electric

For Non-Relativistic Beams

$$\lambda_{max} \propto \frac{\phi_0^2}{V} \qquad \lambda_{max} \propto \frac{q}{m} B^2 r_p^2 \qquad \lambda_{max} \propto \begin{cases} B\, V^{1/2}\, r_p \\ V_q \end{cases}$$

Note
ϕ_0 = Voltage between Einzel lenses
V_q = Voltage on a quad relative to ground
V = particle energy / q

FIRST ORDER MOMENTS DESCRIBE "CENTROID" EVOLUTION

$$x'' = -\frac{\theta_0^2}{4L^2}x + \frac{Q(x-\langle x\rangle)}{r_b^2}$$

$$\frac{d}{ds}\langle x\rangle = \langle x'\rangle$$

$$\frac{d}{ds}\langle x'\rangle = \langle x''\rangle = -\frac{\theta_0^2}{4L^2}\langle x\rangle + \cancelto{0}{\frac{Q}{r_b^2}\left(\langle x\rangle - \langle x\rangle\right)}$$

$$\Rightarrow \frac{d^2\langle x\rangle}{ds^2} = -\frac{\theta_0^2}{4L^2}\langle x\rangle$$

$\Rightarrow$ MOTION OF CENTROID IS UNAFFECTED BY SPACE-CHARGE EXCEPT THROUGH IMAGE CHARGES

IMAGE FORCES (SUMMARY ONLY)

cf. REISER SEC 4.4.4

To linear order:

$$\frac{d^2\langle x\rangle}{ds^2} \cong \left(\frac{\theta_0^2}{4L^2} - \frac{Q}{r_p^2}\right)\langle x\rangle$$

IMAGES ATTRACT BEAM TO $1/r$ REDUCING FOCUSING FIELD

ENVELOPES ARE ALSO EFFECTED BY IMAGES (cf eg. Lee, Close, & Smith, Proc. 1987 IEEE PAC, p. 1126)

To lowest order:

$$\frac{d^2 r_x}{ds^2} = \cdots + \frac{2Q}{r_x + r_y} + \frac{fQ}{r_p^2} r_x$$

$$\frac{d^2 r_y}{ds^2} = \cdots + \frac{2Q}{r_x + r_y} + \frac{fQ}{r_p^2} r_y$$

$$f = \frac{r_x^2 - r_y^2}{4r_p^2} + \frac{\langle x\rangle^2}{r_p^2}\left[1 + \frac{3}{2}\frac{(r_x^2 - r_y^2)}{r_p^2} + \frac{3}{8}\frac{(r_x^2 - r_y^2)^2}{r_p^4}\right]$$

IMAGE FORCES

Let $x_c = \langle x \rangle$

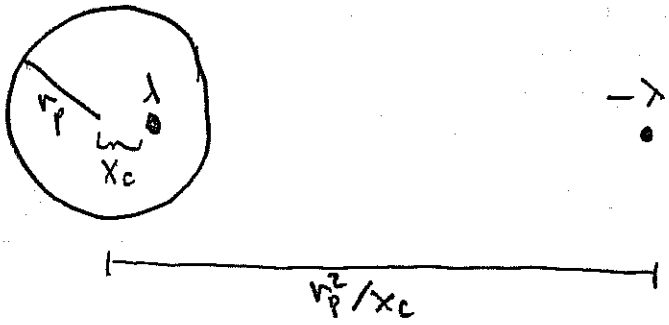

$$E_x = \frac{\lambda}{2\pi\varepsilon_0} \frac{1}{r_p^2/x_c - x_c} \simeq \frac{\lambda}{2\pi\varepsilon_0} \frac{x_c}{r_p^2}$$

IMAGE CURRENTS ALSO CAN GIVE RISE TO

$$|B_y| = \beta E_x$$

$$F_x = (1 - \beta^2)\, q E_x$$

$$\Rightarrow \frac{d^2\langle x \rangle}{ds^2} \cong \frac{-\sigma_0^2}{4L^2}\langle x \rangle + \frac{Q}{r_p^2}\langle x \rangle$$

J.J. Barnard and S.M. Lund
US PAS, June 2006

Transverse Particle Equations of Motion

Outline:

§1 Particle Equations of Motion
- Derivation of transverse equations
  - Basic form
  - Including bending and dispersive terms

§2 Transverse Particle Equations of Motion in Linear Focusing Channels
- Continuous Focusing
- Quadrupole Focusing
- Solenoidal Focusing

§3 Description of Applied Focusing Fields.
- Overview
- Multipole descriptions

§4 Transverse Particle Equations of Motion with Nonlinear Applied Fields
- Approach 1 : Explicit 3D
- Approach 2 : Perturbed linear

§5 Linear Equations of Motion without Space-Charge, Acceleration, and Momentum Spread
- Hill's Equation
- Orbit Stability and eigenvalue structure

§6 Floquet's Theorem and the Phase-Amplitude form of the Particle Orbit.

- Floquet's theorem
- Phase amplitude form of the particle orbit
- Particle phase advance.

§7 The Courant-Snyder Invariant and Single-Particle Emittance

- Derivation - Courant Snyder Invariant.
- Interpretation and uses.

§8 The Betatron Formulation of the Particle Orbit

- Formulation
- Envelope of particle orbits.

§9 Momentum Spread Effects

- Overview and equations
- Dispersion function

§10 Acceleration and Normalized Emittance.

- Transformation of orbit equations to standard form
- Normalized emittance.

References

J.J. Barnard and S.M. Lund
USPAS, June 2006

§1 Particle Equations of Motion

The Lorentz force on a particle of charge q and mass m at coordinate $\vec{x}(t)$ is given by: (SI units)

$$\boxed{\frac{d}{dt}\vec{p}_i(t) = q\left[\vec{E}(\vec{x}_i,t) + \vec{v}_i(t)\times\vec{B}(\vec{x}_i,t)\right]}$$

i = particle index
t = time

$\vec{p}_i(t) = m\,\gamma_i(t)\,\vec{v}_i(t)$ — particle momentum

$\vec{v}_i(t) = c\,\vec{\beta}_i(t)$ — particle velocity, c = speed of light in vacuum

$\gamma_i(t) = \dfrac{1}{\sqrt{1-\vec{\beta}_i^{\,2}(t)}}$

where

	Total-Field		Applied-Field		Self-Field
Electric Field:	$\vec{E}(\vec{x},t)$	=	$\vec{E}_a(\vec{x},t)$	+	$\vec{E}_s(\vec{x},t)$
Magnetic Field:	$\vec{B}(\vec{x},t)$	=	$\vec{B}_a(\vec{x},t)$	+	$\vec{B}_s(\vec{x},t)$

Applied Field sources:

- Focusing Optics
- Dipole Bends
- Accelerating Fields

Focusing Optics (Examples)

Electric Quadrupole — Magnetic Quadrupole — Solenoid

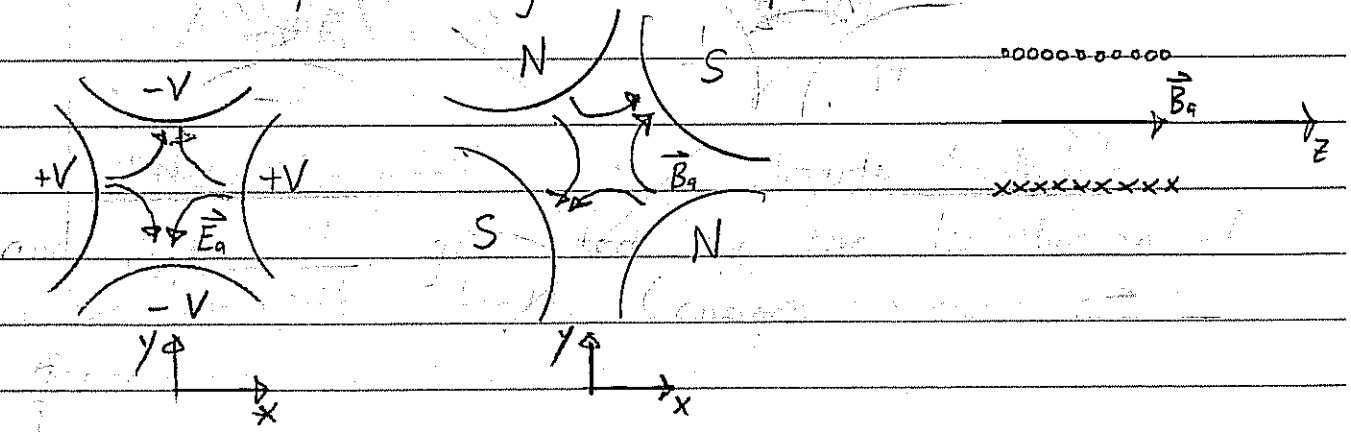

Dipole Bends (Examples)

Electric Dipole
x-direction bend

Magnetic Dipole
x-direction bend.

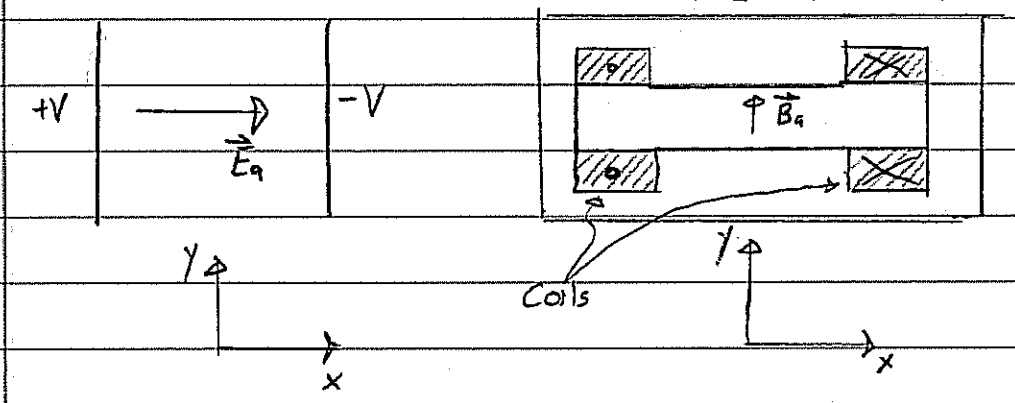

Bend is typically x-plane

Accelerating Fields (Examples)

RF Cavity

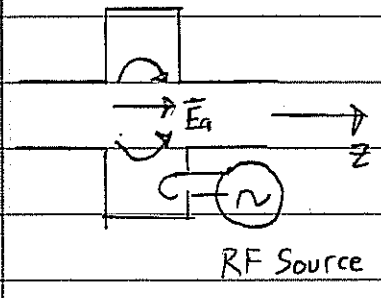

Induction Cell

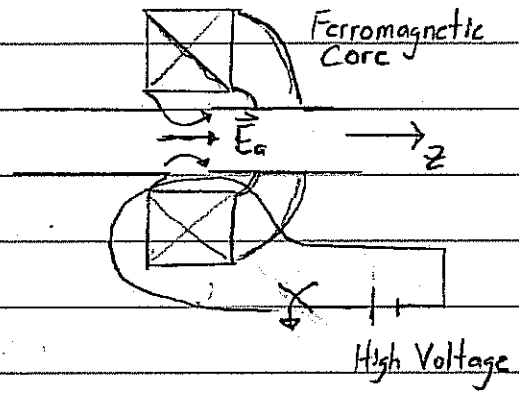

Applied field structures are often arranged in a regular (periodic) lattice for transport / acceleration.

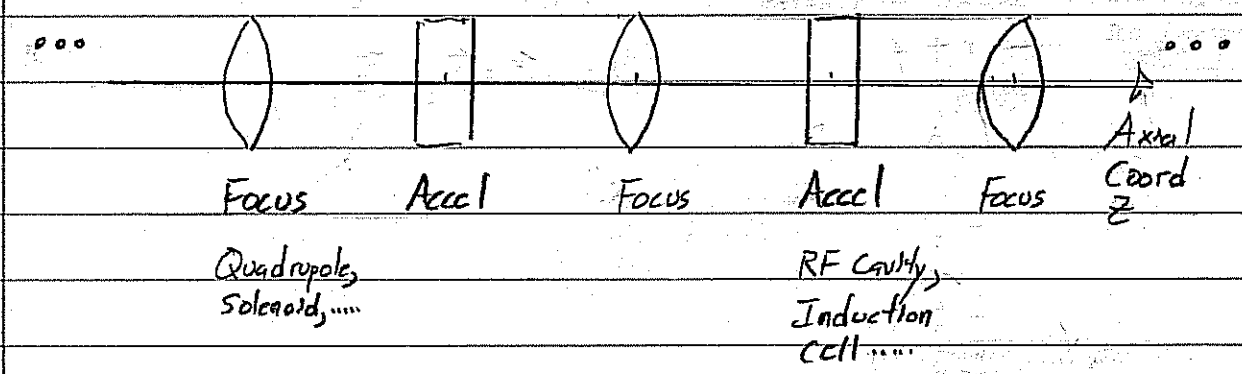

Example - Linear FODO Lattice:

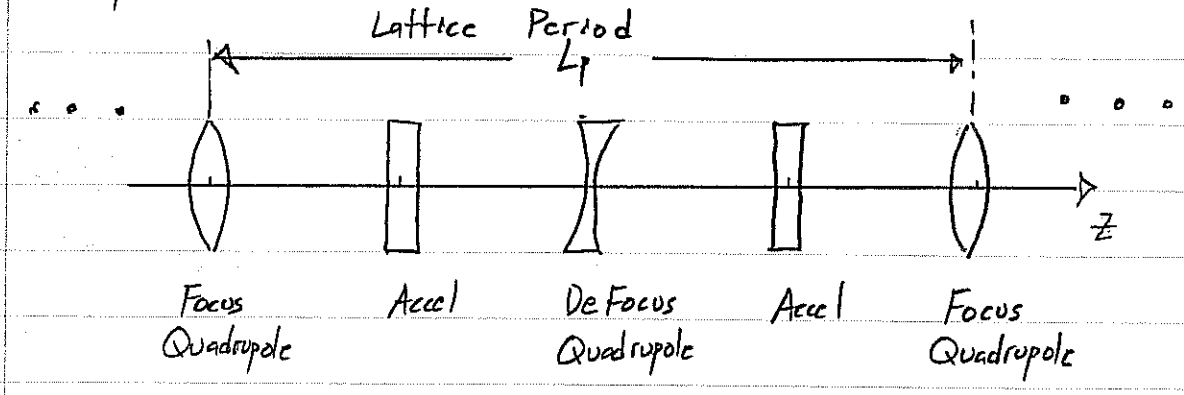

Some lattices for rings may also incorporate bends and more complicated periodic focusing structures.

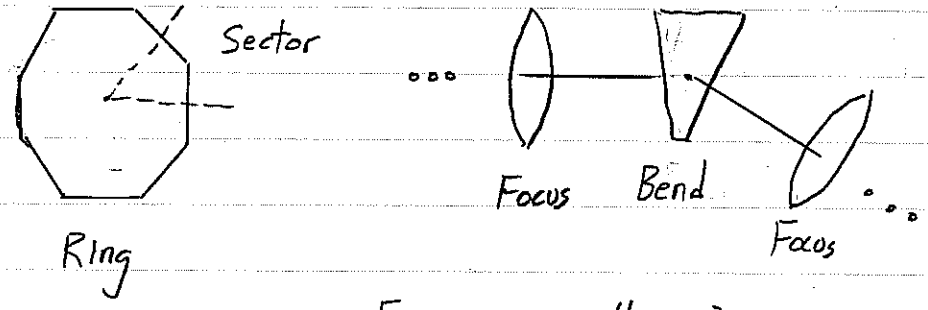

Focus usually 3 or more Focus/Defocus Quadrupoles (Triplet etc).

Self-Fields

Are generated by the distribution of beam particles
- charges
- currents

Particle at Rest

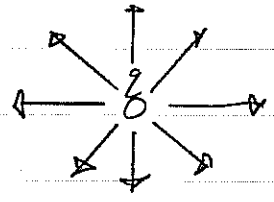

$\vec{E}_s$, $\vec{B}_s = \vec{0}$

Particle in Motion (Relativistic)
See Jackson, "Classical Electrodynamics"

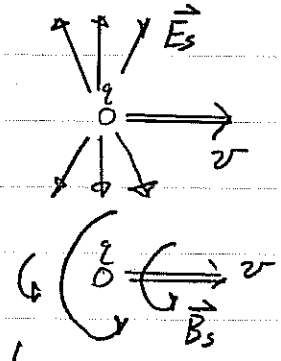

"Boost" Lab-Frame $\vec{E}_s$ field to moving frame

- Superimpose for particles in beam distribution
- Accelerating particles also radiate.

$\vec{E}$ and $\vec{B}$ satisfy the Maxwell Equations, and the linear structure of the Maxwell Equations can be exploited to express:

Applied Fields (often quasi-static)

$$\nabla \cdot \vec{E}_a = \frac{\rho_a}{\varepsilon_0} \qquad \nabla \times \vec{B}_a = \mu_0 \vec{J}_a + \frac{1}{c^2}\frac{\partial \vec{E}_a}{\partial t}$$

$$\nabla \times \vec{E}_a = -\frac{\partial}{\partial t}\vec{B}_a \qquad \nabla \cdot \vec{B}_a = 0$$

$$\frac{1}{\mu_0 \varepsilon_0} = c^2$$

ρ_a = applied charge density

$\vec{J}_a$ = applied current density

+ Boundary Conditions on $\vec{E}_a, \vec{B}_a$

Self Fields

$$\nabla \cdot \vec{E}_s = \sum_i q_i \frac{\delta(\vec{x}-\vec{x}_i(t))}{\varepsilon_0} \qquad \nabla \times \vec{B}_s = \mu_0 \sum_{i=1}^{N} q_i \vec{v}_i \delta(\vec{x}-\vec{x}_i(t)) + \frac{1}{c^2}\frac{\partial \vec{E}_s}{\partial t}$$

$$\nabla \times \vec{E}_s = -\frac{\partial}{\partial t}\vec{B}_s \qquad \nabla \cdot \vec{B}_s = 0$$

$\sum_{i=1}^{N}$ = sum over all N particles in beam

$\delta(\vec{x})$ = Dirac-delta function

+ Boundary Conditions on $\vec{E}_s, \vec{B}_s$ from material structures, radiation conditions etc.

In accelerator beams, there is ideally a single species of ion, many particles, and the motion of the "bunch" is highly directed:

Directed Motion

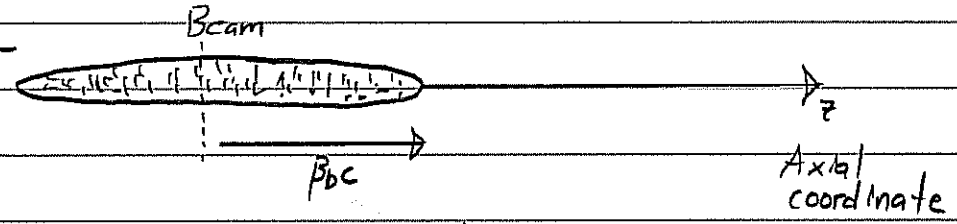

ion velocity

$$\frac{d\vec{x}_i}{dt} = \vec{v}_i = \beta_b c\,\hat{z} + \delta\vec{v}_i$$

β_b = Mean axial Relativistic factor of beam

$$|\delta\vec{v}_i| \ll \beta_b c \Rightarrow \text{Paraxial Approx.}$$

Many Particles

$$\sum_i q_i \delta(\vec{x} - \vec{x}_i(t)) \simeq \rho(\vec{x}, t)$$ continuous charge density

$$\sum_i q_i \vec{v}_i \delta(\vec{x} - \vec{x}_i(t)) \simeq \beta_b c\, \rho(\vec{x}, t)\hat{z}$$ continuous axial current density

Moreover, the evolution is typically sufficiently slow for heavy ions where in the Maxwell equations we can neglect radiation and approximate the self-field Maxwell equations (see Intro. lecture by J.J. Barnard, Electrostatic approximation) as:

$$\boxed{\begin{aligned} \vec{E}_s &= -\nabla\phi \\ \vec{B}_s &= \nabla\times\vec{A}; \quad \vec{A} = \frac{\beta_b}{c}\phi\,\hat{z} \\ \nabla^2\phi &= \frac{\partial}{\partial\vec{x}}\cdot\frac{\partial}{\partial\vec{x}}\phi = \frac{-\rho}{\varepsilon_0} \end{aligned}}$$

and Boundary conditions on ϕ

The force acting on the beam particles can be resolved into applied and self-field components:

$$\boxed{\vec{F}_i(\vec{x}_i,t) = q\vec{E}(\vec{x}_i,t) + q\vec{v}_i(t)\times\vec{B}(\vec{x}_i,t)}$$

$$\vec{E} = \vec{E}_a + \vec{E}_s$$
$$\vec{B} = \vec{B}_a + \vec{B}_s$$

Applied:

$$\boxed{\vec{F}_a = q\vec{E}_a + q\vec{v}_i\times\vec{B}_a}$$

Self:

$$\boxed{\vec{F}_s = q\vec{E}_s + q\vec{v}_i\times\vec{B}_s}$$

The self-field force can then be expressed as (see also J.J. Barnard, Intro. Lectures):

$$\vec{F}_s = q\left(\vec{E}_s + \vec{v}_i\times\vec{B}_s\right)$$

$$\simeq q\Big[\underbrace{-\nabla\phi}_{\text{Transverse and Longitudinal}} + \underbrace{\beta_b c\cdot\hat{z}\times\left(\nabla\times\frac{\beta_b}{c}\phi\hat{z}\right)}_{\text{Transverse Only}}\Big]$$

$$\vec{F}_s \simeq -q(1-\beta_b^2)\nabla_\perp\phi - q\frac{\partial\phi}{\partial z}\hat{z}$$

$$\boxed{F_s \simeq -\frac{q}{\gamma_b^2}\nabla_\perp\phi - q\frac{\partial\phi}{\partial z}\hat{z}}$$

where

$$\boxed{\gamma_b \equiv \frac{1}{\sqrt{1-\beta_b^2}}}$$ is the axial relativistic factor of the beam

The particle equations of motion become:

Transverse:

$$\boxed{\frac{d}{dt}\left(m\gamma_i \vec{v}_{\perp i}\right) \simeq q\vec{E}_\perp^{\,a} + q\beta_b c\,\hat{z}\times\vec{B}_\perp^{\,a} + qB_z^a\,\vec{v}_{\perp i}\times\hat{z} - \frac{q}{\gamma_b^2}\nabla_\perp\phi}$$

applied terms

self term

Longitudinal

$$\boxed{\frac{d}{dt}\left(m\gamma_i v_{zi}\right) \simeq qE_z^a - q\left(v_{xi}B_y^a - v_{yi}B_x^a\right) - q\frac{\partial\phi}{\partial z}}$$

Applied terms

self-term

In the remainder of this lecture, we only analyze <u>transverse dynamics</u>. Longitudinal dynamics will be covered in lectures by J. J. Barnard.

- Except near injector, acceleration is typically slow
  - Fractional changes in β_b and γ_b are small over characteristic lattice period of a periodic accelerator lattice.
- Can often regard γ_b, β_b as specified functions of s given by the "acceleration schedule"

In transverse accelerator dynamics, it is convenient to employ the axial coordinate of a slice of beam particles in the accelerator as the independent variable:

$$\boxed{\begin{aligned} \beta_b &= \sum_{\substack{i=1 \\ \text{slice}}}^{N} \frac{v_{zi}}{c} \\ s &\equiv s_i + c\int_{t_i}^{t} d\tilde{t}\, \beta_b(\tilde{t}) \end{aligned}}$$

Notation Comment:

v_{zi} ~ i = particle index

t_i, s_i } initial time, s (same for all particles)

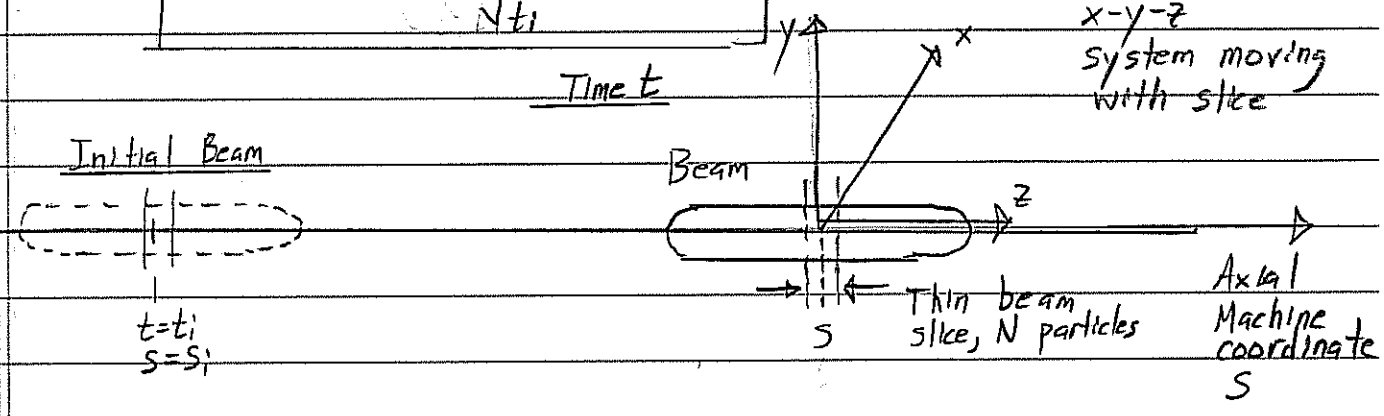

Transform:

$$dt = \frac{ds}{\beta_b c} \Rightarrow v_x = \frac{dx_i}{dt} \simeq \beta_b c \frac{dx_i}{ds} \equiv \beta_b c\, x_i'$$

Denote: etc.

$$\boxed{' \equiv \frac{d}{ds}}$$

$$\boxed{\begin{aligned} v_x &= \frac{dx}{dt} \simeq \beta_b c\, x' \\ v_y &= \frac{dy}{dt} \simeq \beta_b c\, y' \end{aligned}}$$

x', y' ~ angles trajectory makes with z-axis.

Paraxial Approx:

$x'^2, y'^2 \ll 1$

$\Rightarrow v_x^2, v_y^2 \ll v_z^2$

Transform transverse particle equation of motion:

$$\frac{d}{dt}\left(m\gamma_i \frac{d\vec{x}_{\perp i}}{dt}\right) = m v_{zi}\frac{d}{ds}\left(\gamma_i v_{zi}\frac{d}{ds}\vec{x}_{\perp i}\right)$$

$$= \underbrace{m\gamma_i v_{zi}^2 \frac{d^2}{ds^2}\vec{x}_{\perp i}}_{\text{Term 1}} + \underbrace{m\frac{d}{ds}\vec{x}_{\perp i}\, v_{zi}\frac{d}{ds}\left(\gamma_i v_{zi}\right)}_{\text{Term 2}}$$

But:

Term 1: $m\gamma_i v_{zi}^2 \frac{d^2}{ds^2}\vec{x}_{\perp i} \simeq m\gamma_b\beta_b^2 c^2 \frac{d^2}{ds^2}\vec{x}_{\perp i} = m\gamma_b\beta_b^2 c^2 \vec{x}_{\perp i}''$

Term 2: $m\frac{d}{ds}\vec{x}_{\perp i}\, v_{zi}\frac{d}{ds}\left(\gamma_i v_{zi}\right) \simeq m\frac{d}{ds}\vec{x}_{\perp i}\,\beta_b c\frac{d}{ds}\left(\gamma_b\beta_b c\right)$

$$\simeq m\,\beta_b c\left(\gamma_b\beta_b c\right)'\vec{x}_{\perp i}'$$

Summary:

$$\Rightarrow \boxed{m\frac{d}{dt}\left(\gamma_i\frac{d\vec{x}_{\perp i}}{dt}\right) \simeq m\gamma_b\beta_b^2 c^2\left[\vec{x}_{\perp i}'' + \frac{1}{(\gamma_b\beta_b)}\frac{d}{ds}(\gamma_b\beta_b)\,\vec{x}_{\perp i}'\right]}$$

Also, for the applied field component terms:

$$\boxed{q B_z^a\,\vec{v}_{\perp i}\times\hat{z} = q B_z^a\,\beta_b c\,\vec{x}_{\perp i}'\times\hat{z}}$$

Using these results the transverse particle equations of motion on pg 7 become:

Drop particle "i" subscripts to clean up notation:

Transverse Particle Equations of Motion

$$\vec{x}_\perp'' + \frac{(\gamma_b \beta_b)'}{(\gamma_b \beta_b)} \vec{x}_\perp' = \frac{q}{m\gamma_b \beta_b^2 c^2} \vec{E}_\perp^a + \frac{q}{m\gamma_b \beta_b c} \hat{z} \times \vec{B}_\perp^a$$

$$+ \frac{q B_z^a}{m\gamma_b \beta_b c} \vec{x}_\perp' \times \hat{z} - \frac{q}{\gamma_b^3 \beta_b^2 c^2} \nabla_\perp \phi$$

$\vec{E}_a$ = Applied Electric Field
$\vec{B}_a$ = Applied Magnetic Field

$$\nabla^2 \phi = \frac{\partial}{\partial \vec{x}} \cdot \frac{\partial}{\partial \vec{x}} \phi = \frac{-\rho}{\varepsilon_0}$$

and boundary conditions on ϕ

$$' \equiv \frac{d}{ds}$$

Note:

- γ_b factors different in applied and self-field terms.
- In $-\frac{q}{\gamma_b^3 \beta_b^2 c^2} \nabla_\perp \phi$ contributions to γ_b^3 come from:
  - $\gamma_b \Rightarrow$ kinematics
  - $\gamma_b^2 \Rightarrow$ leading order self-magnetic field corrections.

Overview:

S.M. Lund

Much transverse accelerator physics centers on understanding the evolution of beam particles in 4-dimensional $x-x'$, $y-y'$ phase-space.

Often phase-space projections in $x-x'$ and $y-y'$ are analyzed

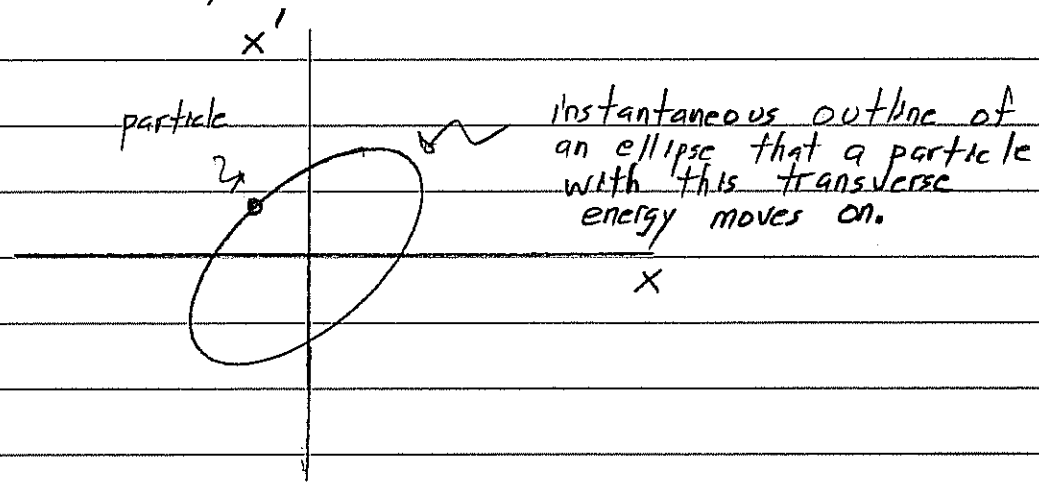

When forces acting on particles are linear, particles tend to move on ellipses of constant area (which may elongate/shrink and rotate) in phase-space. Nonlinear forces can distort orbits and cause undesireable effects, growing effective phase-space area.

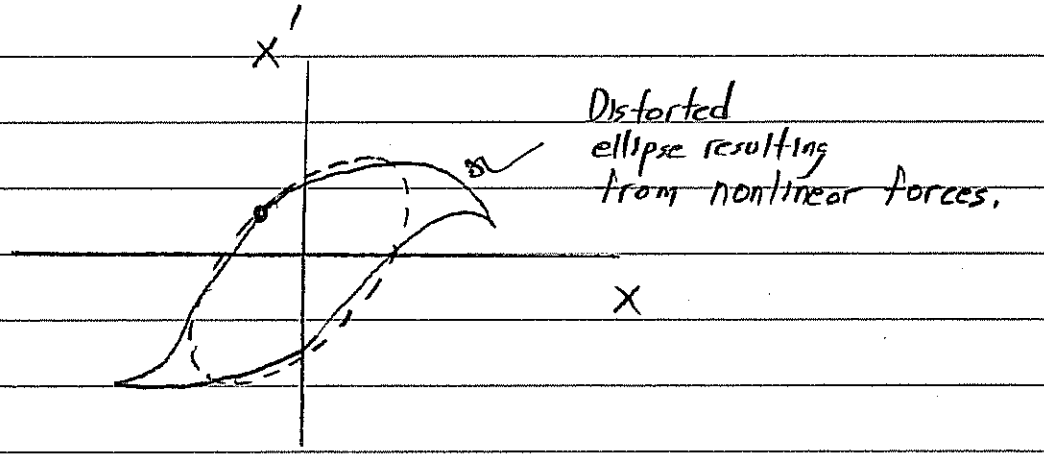

The effective phase-space volume of a distribution of beam particles is of fundamental interest.

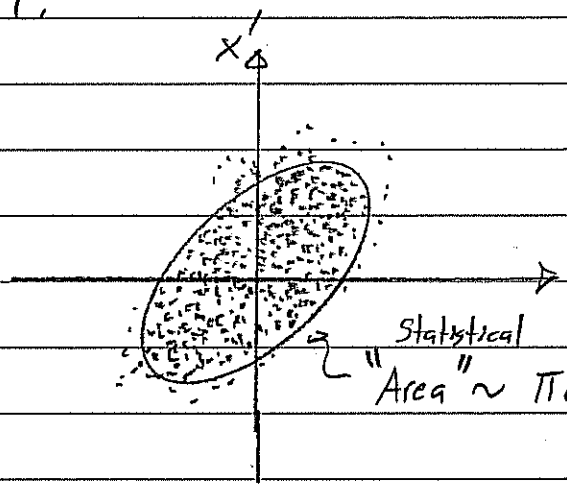

Effective area measure in x-x' phase-space is the x-emittance:

$$\varepsilon_x = 4\left[\langle x^2\rangle_\perp \langle x'^2\rangle_\perp - \langle x x'\rangle^2\right]^{1/2}$$

We will find in statistical beam descriptions:

Larger phase-space areas (larger emittances) $\Rightarrow$ Harder to achieve small beam spots on target.

Smaller phase-space areas (smaller emittances) $\Rightarrow$ Easier to achieve small beam spots on target

Much of advanced accelerator physics seeks to understand and control emittance growth due to nonlinear applied fields and space-charge effects. In the remainder of this lecture we will review basic accelerator physics for the transverse dynamics of a particle moving in applied fields. Later we will generalize concepts to include space-charge.

Bent Coordinate System to analyze particle equations of motion with dipole bends and spread in axial particle momentum

The previous equations of motion can be applied to dipole bends provided the x-y-z coordinate system is fixed. In practice, it can be more convienient to employ coordinates that follow the beam in a bend.

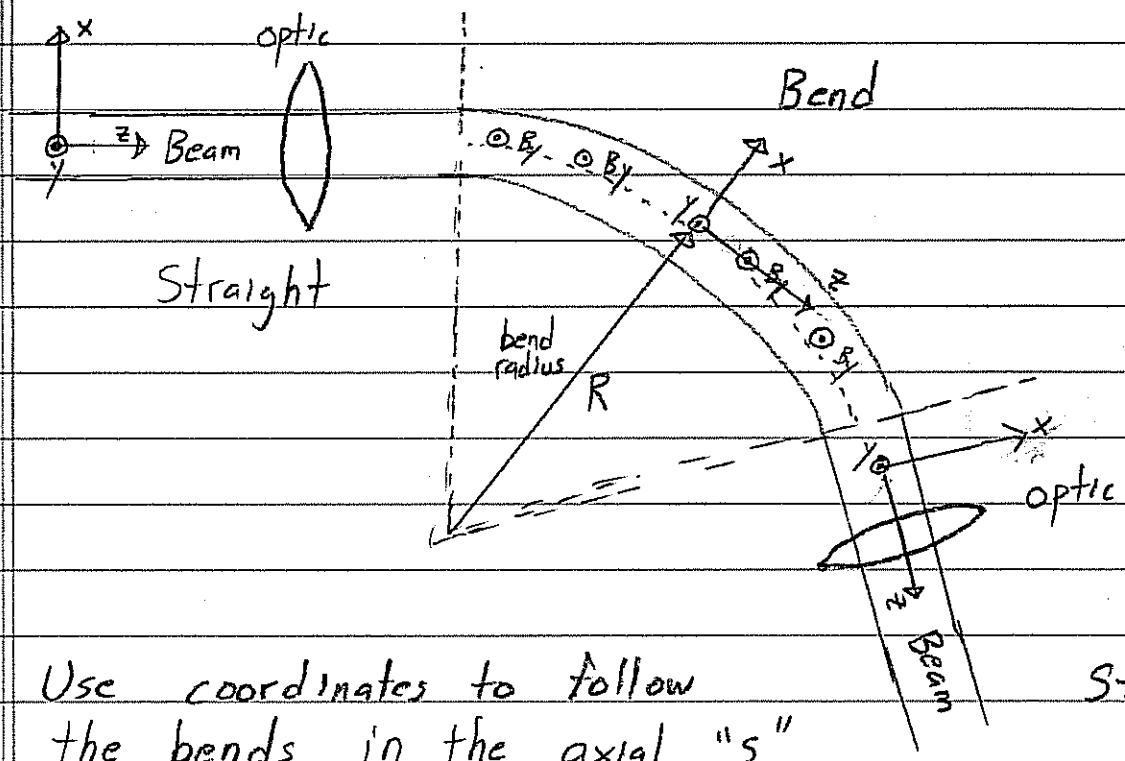

Use coordinates to follow the bends in the axial "s" coordinate.

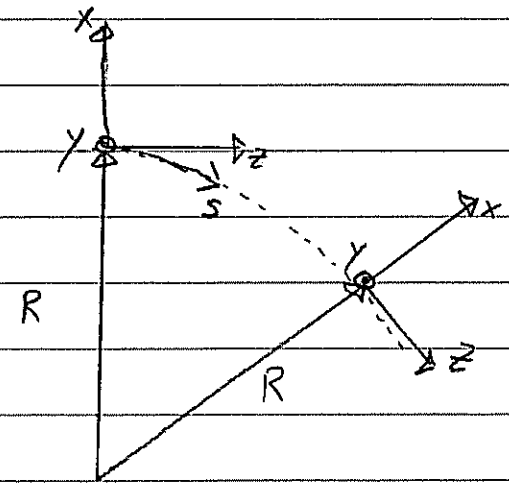

x-y-z local cartesian system

Using this system, dipoles are adjusted given the mean beam energy / momentum to bend the required amount for a bend radius R. Usually, bends are only in one plane, say the x-plane, and are implemented by a <u>dipole</u> B_y^a or E_x^a applied field.

Denote:

$$\boxed{p_o = m\gamma_b\beta_b c \quad = \quad \text{design momentum}}$$

Then the x-bending radius R of the design momentum particle p_o = const in a constant applied magnetic field $\vec{B}^a = B_y^a\hat{y}$ = const is given by

$$\boxed{\frac{1}{R} = \frac{qB_y^a}{p_o}}$$

B_y^a = const
R = const.

Often this is expressed in terms of the "particle rigidity" $[B\rho]$ (read as one symbol and called "B-rho").

$$\boxed{[B\rho] \equiv \frac{p_o}{q} = \frac{m\gamma_b\beta_b c}{q}}$$

Then

$$\boxed{\frac{1}{R} = \frac{B_y^a}{[B\rho]}}$$

Comment: Different design formulas will result for electric bends with $E_x^a \neq 0$ (see problems)

In straight sections $R \to \infty$, and bends can be positive or negative radius R (direction of curve) depending on the sign of B_y^0 and $[B\rho]$. Practical machines are often made from discrete element dipoles and straight sections with seperated function optics. (See the sketch of a practical ring on the next page). For a ring, such dipoles are tuned with the particle rigidity such that the orbit makes a complete lap through the machine. Dipoles must be adjusted as the particles gain energy to maintain a closed orbit in the machine aperture. The need to synchronously adjust bending dipoles and focusing elements with the gains in particle energy is the origin of the name "Synchrotron" for such machines. The total bending strength of a synchrotron in tesla-meters limits ultimate achievable particle energy / momentum in the machine.

Typical Seperated Function Lattice Period

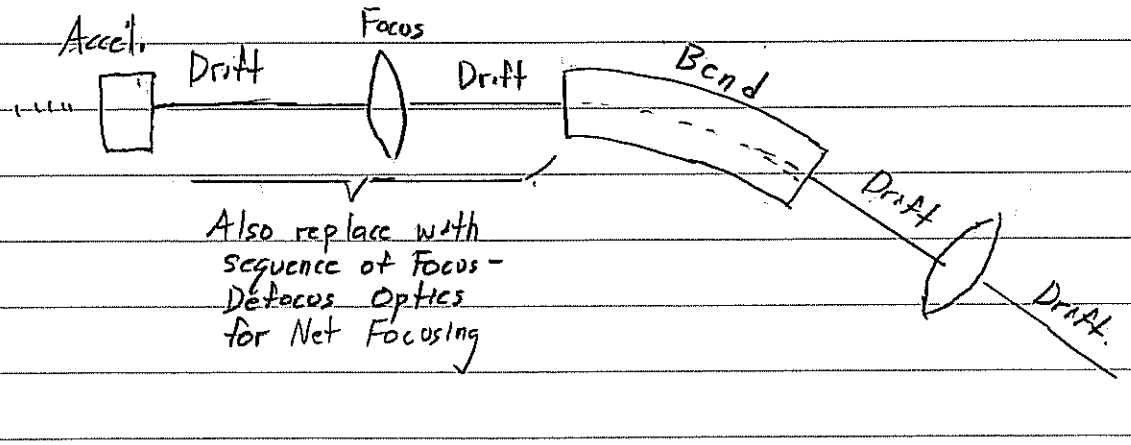

SIS – 18 Synchrotron
GSI, Germany
18 Tesla–Meter Bending Strength

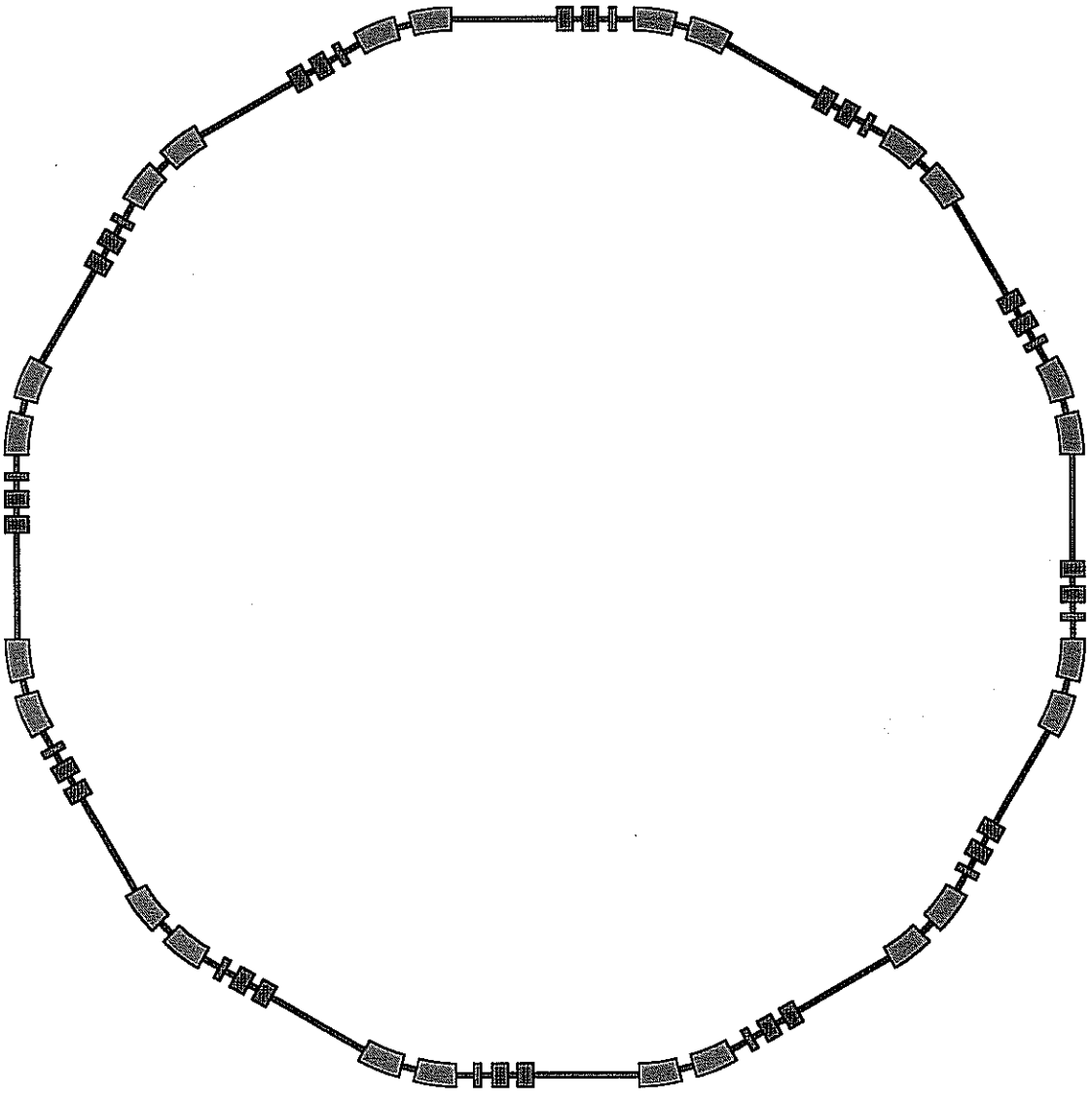

Acceleration Cells
Not Shown

Diplole Bending Magnets

Quadrupole Focusing Magnets (Triplets)

Off momentum effects:

$$\boxed{p_s = m\gamma_b\beta_b c = \text{design momentum.}}$$

For momentum errors:

$$\boxed{\begin{aligned} p_s &= p_o + \delta p \\ p_o &= m\gamma_b\beta_b c = \text{"design-momentum"} \\ \delta p &= \text{"off-momentum"} \end{aligned}}$$

This will modify the particle equations of motion, particularly in cases where there are bends since particles with different momenta will be bent at different radii.

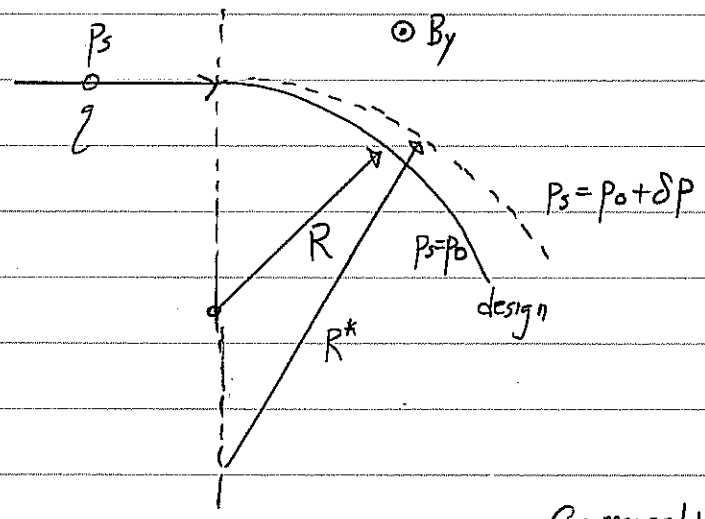

Comment: It is not common to have acceleration in bends. However, dipoles bends and quadrupole focusing magnets are sometimes combined.

Without presenting algebraic detail (see standard accelerator texts such as Edwards and Syphers) the particle equations of motion for a coasting beam with design momentum p_o become (the full derivation is beyond the scope of this class).

$$x''(s) + \frac{(\gamma_b\beta_b)'}{(\gamma_b\beta_b)}x'(s) + \left[\frac{1}{R^2(s)}\frac{1-\delta}{1+\delta}\right]x(s) = \frac{\delta}{1+\delta}\frac{1}{R(s)} + \frac{q}{m\gamma_b\beta_b^2c^2}\frac{E_x^q}{(1+\delta)^2}$$

$$-\frac{q}{m\gamma_b\beta_b c}\frac{B_y^q}{1+\delta} + \frac{q B_s^q}{m\gamma_b\beta_b c}\frac{y'(s)}{1+\delta} - \frac{q}{m\gamma_b^3\beta_b^2c^2}\frac{1}{1+\delta}\frac{\partial\phi}{\partial x}$$

$$y''(s) + \frac{(\gamma_b\beta_b)'}{(\gamma_b\beta_b)}y'(s) = \frac{q}{m\gamma_b\beta_b^2c^2}\frac{E_y^q}{(1+\delta)^2} + \frac{q}{m\gamma_b\beta_b c}\frac{B_x^q}{1+\delta}$$

$$\frac{-q B_s^q}{m\gamma_b\beta_b c}\frac{x'(s)}{1+\delta} - \frac{q}{m\gamma_b^3\beta_b^2c^2}\frac{1}{1+\delta}\frac{\partial\phi}{\partial y}$$

$$\delta \equiv \frac{\delta p}{p_o} = \text{Fractional Momentum Error.}$$

$p_o = m\gamma_b\beta_b c$ = design momentum, $\frac{1}{R} = \frac{B_y^q\big|_{dipole}}{[B\rho]}$, $[B\rho] = p_o/q$

Comments:

- Design bends only in x and E_x^q, B_y^q contain <u>no</u> dipole field terms. These components are set consistent with the design bend radius $R(s)$
- x and y equations differ significantly due to the bends modifying the x-equation when $R(s) \not\to \infty$.
- Equations contain only low-order terms in δ.

J.J. Barnard and S.M. Lund
USPAS, June 2006

✓

§2 Transverse Particle Equations of Motion in Linear* Focusing Channels

* No Bends and Linear Applied Fields

The transverse particle equations of motion previously derived in §1 can be expressed as:

$$\boxed{\begin{aligned} x'' + \left[\frac{1}{\gamma_b\beta_b}\frac{d}{ds}\left(\gamma_b\beta_b\right)\right]x' &= \frac{q}{m\gamma_b\beta_b^2c^2}E_x^a - \frac{q}{m\gamma_b\beta_b c}B_y^a + \frac{q}{m\gamma_b\beta_b c}B_z^a y' \\ &\quad - \frac{q}{m\gamma_b^3\beta_b^2c^2}\frac{\partial\phi}{\partial x} \\ y'' + \left[\frac{1}{\gamma_b\beta_b}\frac{d}{ds}\left(\gamma_b\beta_b\right)\right]y' &= \frac{q}{m\gamma_b\beta_b^2c^2}E_y^a + \frac{q}{m\gamma_b\beta_b c}B_x^a - \frac{q}{m\gamma_b\beta_b c}B_z^a x' \\ &\quad - \frac{q}{m\gamma_b^3\beta_b^2c^2}\frac{\partial\phi}{\partial y} \end{aligned}}$$

Assumptions:

- Paraxial equations: $x'^2, y'^2 \ll 1$
- Dispersive effects neglected; $v_z = \beta_b c$ for all particles, but acceleration (β_b may vary in s) is allowed.
- Electrostatic and leading-order (in β_b) self-magnetic interactions included.
- Fixed x-y-z coordinate system (no local bends).

To complete the description of the $\perp$ particle equations of motion, the applied focusing fields

$$\boxed{\begin{array}{ll} \text{electric:} & E_x^a,\ E_y^a,\ E_z^a \\ \text{magnetic:} & B_x^a,\ B_y^a,\ B_z^a \end{array}}$$

must be specified as a function of s and the $\perp$ particle coordinates x, y. Also the consistent change in axial velocity with $\beta_b c$ must be evaluated due to E_z^a and possibly time-varying electromagnetic fields (as in RF cavities). Here we restrict ourselves to $\vec{E}_a, \vec{B}_a$ <u>resulting from applied focusing structures</u>. In intense beam accelerators and transport lattices, focusing structures are designed to optimize <u>linear focusing forces</u> with:

Linear Focusing

$$\boxed{\begin{array}{l} E_x^a \simeq (\text{function of } s) \cdot (x \text{ or } y) \\ E_y^a \simeq (\text{function of } s) \cdot (x \text{ or } y) \\ \\ B_x^a \simeq (\text{function of } s) \cdot (x \text{ or } y) \\ B_y^a \simeq (\text{function of } s) \cdot (x \text{ or } y) \\ B_z^a \simeq (\text{function of } s) \end{array}}$$

We now review some common situations that realize these forms:

1/ Continuous Focusing
2/ Quadrupole Focusing
3/ Solenoidal Focusing

Continuous Focusing

$$\boxed{\begin{cases} \vec{B}^a = 0 \\ E_x^a = -\dfrac{m\gamma_b\beta_b^2c^2k_{\beta 0}^2}{q}x \qquad E_y^a = -\dfrac{m\gamma_b\beta_b^2c^2k_{\beta 0}^2}{q}y \end{cases} \qquad k_{\beta 0}^2 = \text{const.}}$$

Then the $\perp$ equations of motion reduce to:

$$\boxed{\vec{x}_\perp'' + \left[\frac{1}{\gamma_b\beta_b}\frac{d}{ds}(\gamma_b\beta_b)\right]\vec{x}_\perp' + k_{\beta 0}^2\vec{x}_\perp = \frac{-q}{m\gamma_b^3\beta_b^2c^2}\frac{\partial\phi}{\partial\vec{x}_\perp}}$$

This situation is realized by a stationary (mass $\to\infty$), partially neutralizing uniform background of charges. To see this we apply Poisson's equation to the applied field to calculate the neutralizing charge density:

$$\boxed{\rho_a = \varepsilon_0\nabla\cdot\vec{E}^a = -\frac{2m\varepsilon_0\gamma_b\beta_b^2c^2k_{\beta 0}^2}{q} = \text{const.}}$$

- Unphysical model, but very commonly employed since it simply represents the <u>average</u> action of more physical focusing fields.
  - Demonstrate this later in some simple problems
- We will find that continuous focusing can provide reasonably good estimates for more realistic focusing models if $k_{\beta 0}^2$ is appropriately identified in terms of relevant factors.

In more physical situations one requires that quasistatic focusing fields in the aperture satisfy the vacuum Maxwell Equations in the beam region:

$$\boxed{\begin{array}{ll} \nabla \cdot \vec{E}^q = 0 & \nabla \cdot \vec{B}^q = 0 \\ \nabla \times \vec{E}^q = 0 & \nabla \times \vec{B}^q = 0 \end{array}}$$

These equations constrain the 3D form of the vacuum fields resulting from spatially localized lenses. But the following situations can be exploited to optimize linear focusing in practical lattices: We will cover two common cases:

1) Alternating Gradient Quadrupoles
   - Electric Quadrupoles
   - Magnetic Quadrupoles
2) Magnetic Solenoids.

Alternating Gradient Quadrupole Focusing

A) Electric Quadrupoles: $(\vec{B}^q = 0)$

In the axial center of an electric quadrupole:

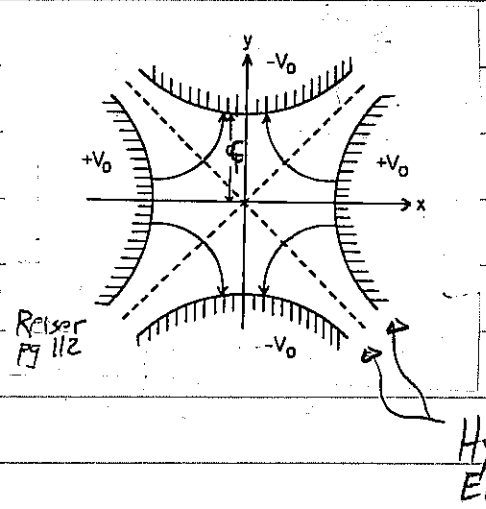

2D Fields

$$E_x^q = -\frac{2V_0}{r_p}\frac{x}{r_p} = -E_q' x$$

$$E_y^q = \frac{2V_0}{r_p}\frac{y}{r_p} = E_q' y$$

$$G = \frac{2V_0}{r_p^2} = -\frac{\partial E_x^q}{\partial x} = \frac{\partial E_y^q}{\partial y} = \text{Electric Gradient}$$

V_0 = pole voltage

r_p = "pipe" aperture radius

For a lattice of finite length quadrupoles with alternating gradient

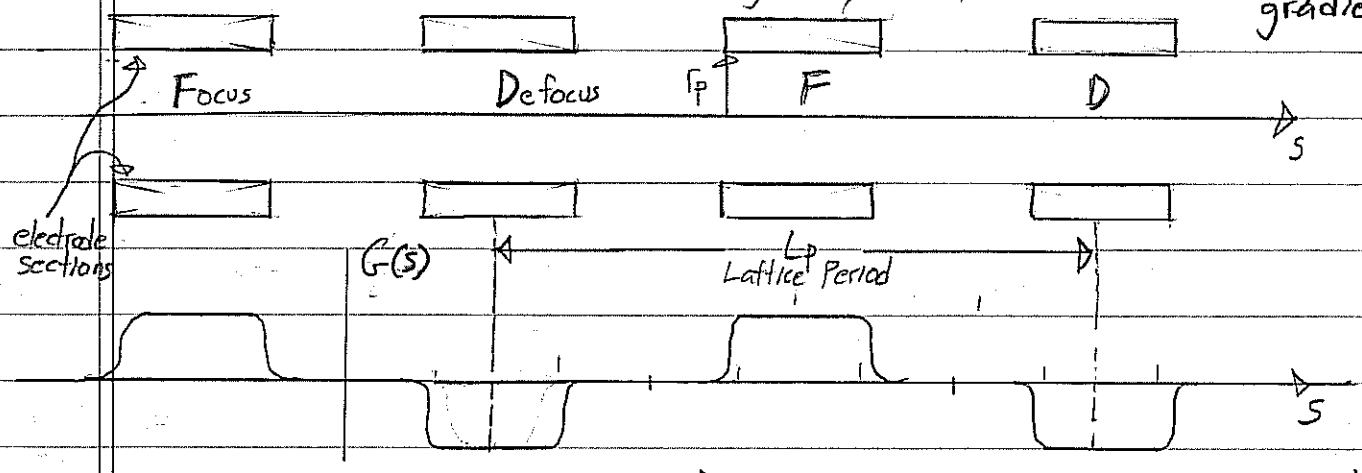

Equations of motion: Not focusing in both planes by alternating "Focus" and "Defocus" quadrupoles.

$$x'' + \left[\frac{1}{\gamma_b\beta_b}\frac{d}{ds}(\gamma_b\beta_b)\right]x' + \kappa_q(s)x = \frac{-q}{m\gamma_b^3\beta_b^2c^2}\frac{\partial\phi}{\partial x}$$

$$y'' + \left[\frac{1}{\gamma_b\beta_b}\frac{d}{ds}(\gamma_b\beta_b)\right]y' - \kappa_q(s)y = \frac{-q}{m\gamma_b^3\beta_b^2c^2}\frac{\partial\phi}{\partial y}$$

$$\kappa_q(s) \equiv \frac{q\,G(s)}{m\gamma_b\beta_b^2c^2} = \frac{G(s)}{\beta_b c\,[B\rho]}$$

B) Magnetic Quadrupoles ($\vec{E}^a = 0$)

In the center of a magnetic quadrupole:

2D Fields

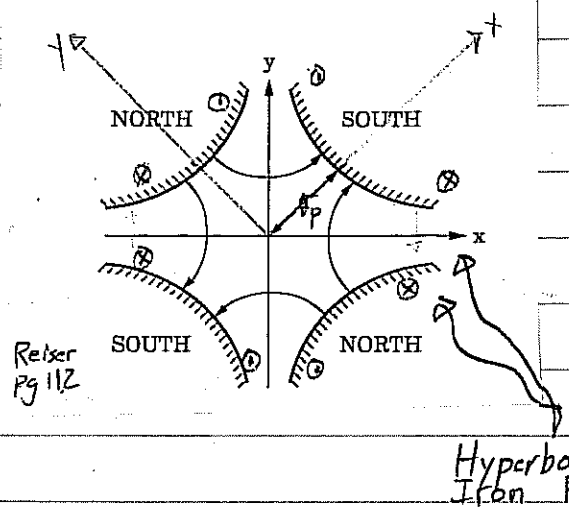

Reiser Pg 112

$$B_x^a = B_0 \frac{y}{r_p}$$

$$B_y^a = B_0 \frac{x}{r_p}$$

$$G \equiv \frac{B_0}{r_p} = \frac{\partial B_x^a}{\partial y} = \frac{\partial B_y^a}{\partial x} = \text{Magnetic Gradient}$$

$B_0 = |\vec{B}_a|_{r=r_p}$ = pole Field

r_p = "pipe" aperture radius

For a lattice of finite length quadrupoles with alternating gradient.

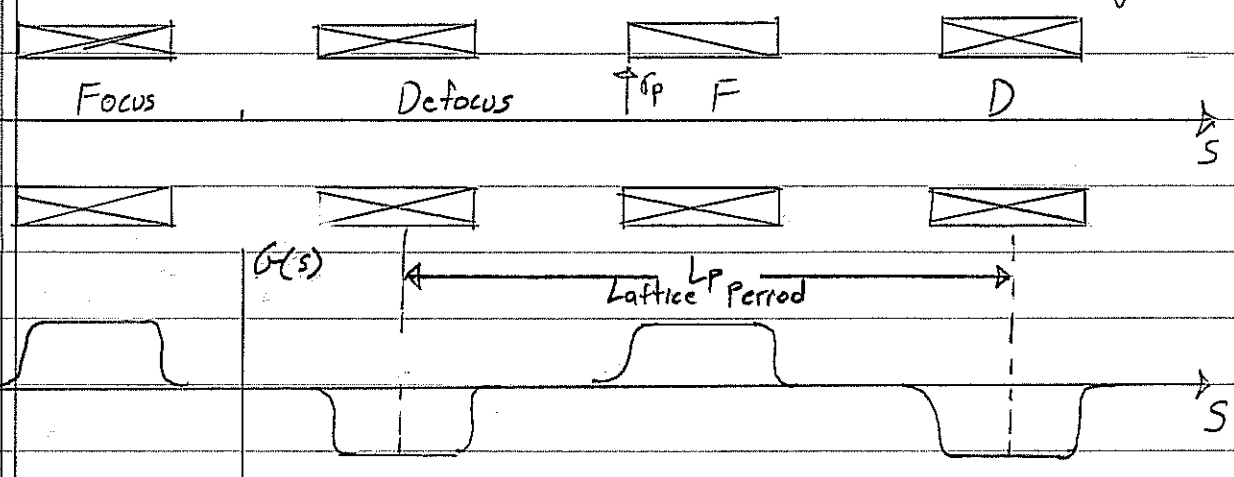

Equations of motion:

$$x'' + \left[\frac{1}{\gamma_b\beta_b}\frac{d}{ds}(\gamma_b\beta_b)\right]x' + \kappa_q(s)\,x = \frac{-q}{m\gamma_b^3\beta_b^2c^2}\frac{\partial\phi}{\partial x}$$

$$y'' + \left[\frac{1}{\gamma_b\beta_b}\frac{d}{ds}(\gamma_b\beta_b)\right]y' - \kappa_q(s)\,x = \frac{-q}{m\gamma_b^3\beta_b^2c^2}\frac{\partial\phi}{\partial y}$$

$$\kappa_q(s) = \frac{q\,G(s)}{m\gamma_b\beta_b c} = \frac{G(s)}{[B\rho]}$$

* Equations are the same as for the electric case with diff. $\kappa_q(s)$.

Quadrupole Skew Couplings

Consider a quadrupole "actively" rotated through a positive angle ψ about the z-axis.

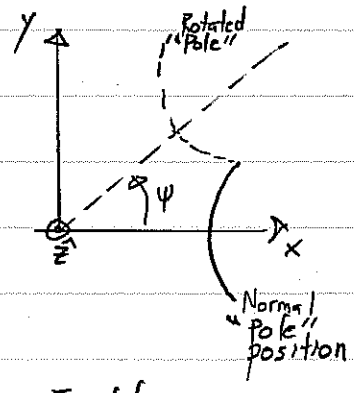

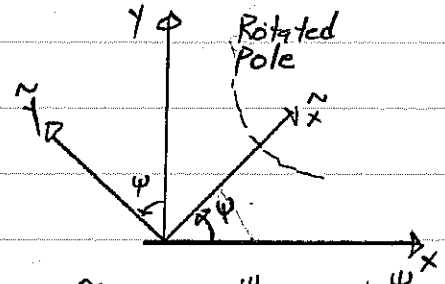

$$\tilde{x} = x\cos\psi + y\sin\psi$$
$$\tilde{y} = -x\sin\psi + y\cos\psi$$

Normal Orientation Fields:

Electric:

$$E_x^q = -Gx$$
$$E_y^q = Gy$$

Magnetic

$$B_x^q = Gy$$
$$B_y^q = Gx$$

Rotated Fields

Electric

$$E_x^q = E_{\tilde{x}}^q \cos\psi - E_{\tilde{y}}^q \sin\psi \qquad E_{\tilde{x}}^q = -G\tilde{x} = -G(x\cos\psi + y\sin\psi)$$
$$E_y^q = E_{\tilde{x}}^q \sin\psi + E_{\tilde{y}}^q \cos\psi \qquad E_{\tilde{y}}^q = G\tilde{y} = G(-x\sin\psi + y\cos\psi)$$

collect components:

$$E_x^q = -G(x\cos^2\psi + y\sin\psi\cos\psi) - G(-x\sin^2\psi + y\sin\psi\cos\psi)$$
$$= G(\sin^2\psi - \cos^2\psi)x - G\,2\sin\psi\cos\psi\, y$$
$$= -G\cos(2\psi)x - G\sin(2\psi)y$$

$$E_y^q = -G(x\sin\psi\cos\psi + y\sin^2\psi) + G(-x\sin\psi\cos\psi + y\cos^2\psi)$$
$$= -G\sin(2\psi)x + G\cos(2\psi)y$$

Magnetic

$$B_x^q = B_{\tilde{x}}^q \cos\psi - B_{\tilde{y}}^q \sin\psi \qquad B_{\tilde{x}}^q = G\tilde{y} = G(-x\sin\psi + y\cos\psi)$$

$$B_y^q = B_{\tilde{x}}^q \sin\psi + B_{\tilde{y}}^q \cos\psi \qquad B_{\tilde{y}}^q = G\tilde{x} = G(x\cos\psi + y\sin\psi)$$

collect components:

$$B_x^q = G(-\sin\psi\cos\psi\, x + \cos^2\psi\, y) - G(\sin\psi\cos\psi\, x + \sin^2\psi\, y)$$
$$= -G\sin(2\psi)\, x + G\cos(2\psi)\, y$$

$$B_y^q = G(-\sin^2\psi\, x + \sin\psi\cos\psi\, y) + G(\cos^2\psi\, x + \sin\psi\cos\psi\, y)$$
$$= G\cos(2\psi)\, x + G\sin(2\psi)\, y$$

Then the equations of motion become for <u>both</u> electric and magnetic focusing:

$$\boxed{\begin{aligned} x'' + \frac{(\gamma_b\beta_b)'}{(\gamma_b\beta_b)} x' + k_q\cos(2\psi)\, x + k_q\sin(2\psi)\, y &= \frac{-q}{m\gamma_b^3\beta_b^2c^2}\frac{\partial\phi}{\partial x} \\ y'' + \frac{(\gamma_b\beta_b)'}{(\gamma_b\beta_b)} y' - k_q\cos(2\psi)\, y + k_q\sin(2\psi)\, x &= \frac{-q}{m\gamma_b^3\beta_b^2c^2}\frac{\partial\phi}{\partial y} \end{aligned}}$$

where as before

$$k_q = \begin{cases} \dfrac{G}{\beta_b c[B\rho]} & ;\ \text{Electric Focusing} \\ \dfrac{G}{[B\rho]} & ;\ \text{Magnetic Focusing} \end{cases}$$

For $\psi \neq 0, \pi, 2\pi, \ldots$, applied field terms $\propto k_q$ in the x-equation of motion depend on y and vice-versa for the y-equation of motion. Such "skew" coupling, while still being linear, considerably complicate the particle dynamics. Unless otherwise specified, quadrupoles are considered "normal" oriented. However, skew error terms or intentional skews can be important for some machines.

Solenoidal Focusing

$$\boxed{\begin{aligned} \vec{E}^a &= 0 \\ \vec{B}^a &= -\frac{1}{2} B_z^{a\prime}(s)\, \vec{x}_\perp + \hat{z}\, B_z^a(s) + \text{Higher order Terms.} \end{aligned}}$$

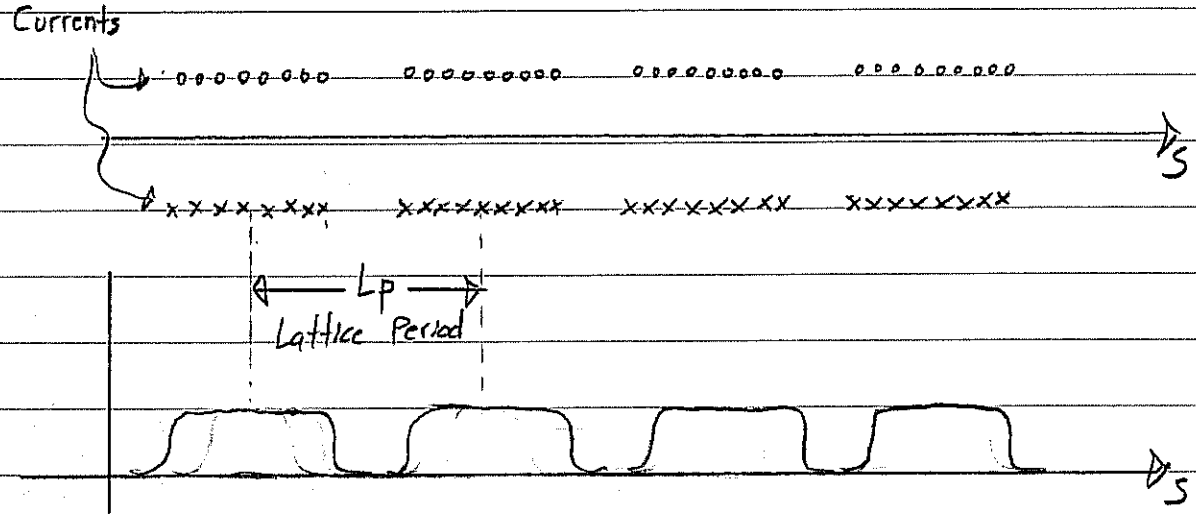

Equations of motion:

$$\boxed{\begin{aligned} x'' + \left[\frac{1}{\gamma_b \beta_b}\frac{d}{ds}(\gamma_b \beta_b)\right] x' &= \frac{\omega_c'(s)}{2\gamma_b \beta_b c}\, y + \frac{\omega_c(s)}{\gamma_b \beta_b c}\, y' - \frac{q}{m\gamma_b^3 \beta_b^2 c^2}\frac{\partial \phi}{\partial x} \\ y'' + \left[\frac{1}{\gamma_b \beta_b}\frac{d}{ds}(\gamma_b \beta_b)\right] y' &= -\frac{\omega_c'(s)}{2\gamma_b \beta_b c}\, x - \frac{\omega_c(s)}{\gamma_b \beta_b c}\, x' - \frac{q}{m\gamma_b^3 \beta_b^2 c^2}\frac{\partial \phi}{\partial y} \end{aligned}}$$

Here:

$$\omega_c = \frac{q\, B_z^a(s)}{m} = \text{cyclotron frequency of applied magnetic field}$$

These equations are linearly cross-coupled in the applied field terms

- x equation depends on $B_z' y$, $B_z y'$
- y equation depends on $B_z' x$, $B_z x'$

The linear cross-coupling in the applied field can be transformed away through a (s-varying) transformation to a rotating "Larmor" frame (see Appendix A). If the beam is axisymmetric

$$\frac{\partial \phi}{\partial \vec{x}_\perp} = \frac{\partial \phi}{\partial r}\frac{\partial r}{\partial \vec{x}_\perp} = \frac{\partial \phi}{\partial r}\frac{\vec{x}_\perp}{r}$$

then the equations of motion can be expressed in uncoupled form as (see Appendix A):

$$\boxed{\begin{aligned} \tilde{x}'' + \frac{(\gamma_b\beta_b)'}{(\gamma_b\beta_b)}\tilde{x}' + \kappa(s)\tilde{x} &= \frac{-q}{m\gamma_b^3\beta_b^2c^2}\frac{\partial\phi}{\partial r}\frac{\tilde{x}}{r} \\ \tilde{y}'' + \frac{(\gamma_b\beta_b)'}{(\gamma_b\beta_b)}\tilde{y}' + \kappa(s)\tilde{y} &= \frac{-q}{m\gamma_b^3\beta_b^2c^2}\frac{\partial\phi}{\partial r}\frac{\tilde{y}}{r} \end{aligned}}$$

Here:

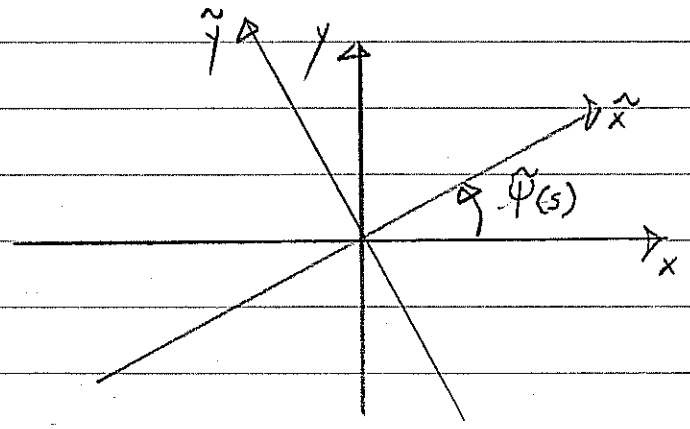

Rotating Frame variables with $\sim$

$$\kappa(s) = \frac{\omega_c^2(s)}{4\gamma_b^2\beta_b^2c^2}$$ Solenoid focusing strength.

$$\tilde{x}(s) = x\cos\tilde{\psi}(s) + y\sin\tilde{\psi}(s)$$
$$\tilde{y}(s) = -x\sin\tilde{\psi}(s) + y\cos\tilde{\psi}(s)$$

$$\tilde{\psi}(s) = \frac{-1}{2\gamma_b\beta_b c}\int_{s_i}^{s} d\tilde{s}\,\omega_c(\tilde{s})$$

s_i outside chain of magnets.

It has been shown that in certain reasonable approximations in a <u>linear</u> focusing channels including:

1) Continuous Focusing
2) Alternating Gradient Quadrupole Focusing
   - Electric
   - Magnetic
3) Solenoidal Focusing

that the transverse particle equations of motion can be cast in the form:

$$\boxed{\begin{aligned} x'' + \left[\frac{1}{\gamma_b\beta_b}\frac{d}{ds}(\gamma_b\beta_b)\right]x' + \kappa_x(s)x &= \frac{-q}{m\gamma_b^3\beta_b^2c^2}\frac{\partial\phi}{\partial x} \\ y'' + \left[\frac{1}{\gamma_b\beta_b}\frac{d}{ds}(\gamma_b\beta_b)\right]y' + \kappa_y(s)y &= \frac{-q}{m\gamma_b^3\beta_b^2c^2}\frac{\partial\phi}{\partial y} \\ \kappa_x(s) &= x\text{-lattice focusing function} \\ \kappa_y(s) &= y\text{-lattice focusing function} \end{aligned}}$$

- Continuous Focusing: $\kappa_x = \kappa_y = k_{\beta 0}^2 = \text{const.}$
- Quadrupole focusing: $\kappa_x(s) = -\kappa_y(s) \equiv \kappa_q(s)$
- Solinoidal focusing: $\kappa_x(s) = \kappa_y(s) \equiv \kappa(s)$

Before studying space-charge effects, it is instructive to analyze these equations neglecting space-charge:

$$\frac{\partial\phi}{\partial x} = \frac{\partial\phi}{\partial y} \longrightarrow 0$$

and acceleration:

$$\frac{1}{\gamma_b\beta_b}\frac{d}{ds}(\gamma_b\beta_b) \longrightarrow 0$$

In this simple case, the x- and y- equations have identical form:

$$\boxed{\begin{aligned} x'' + \kappa_x(s)\,x &= 0 \\ y'' + \kappa_y(s)\,y &= 0 \end{aligned}}$$

Later we will show (KV Model) that linear space charge forces may also be included in κ_x and κ_y.

Usually, κ_x and κ_y will be periodic functions of s.

$$\boxed{\begin{aligned} \kappa_x(s+L_p) &= \kappa_x(s) \\ \kappa_y(s+L_p) &= \kappa_y(s) \end{aligned} \qquad L_p = \text{lattice period}}$$

But this <u>need not</u> be the case. Most of the analysis that follows is presented for the periodic case for simplicity in interpretation, but holds in general for matching sections and other non-periodic lattices where $\kappa_x(s)$ and $\kappa_y(s)$ may change form strongly

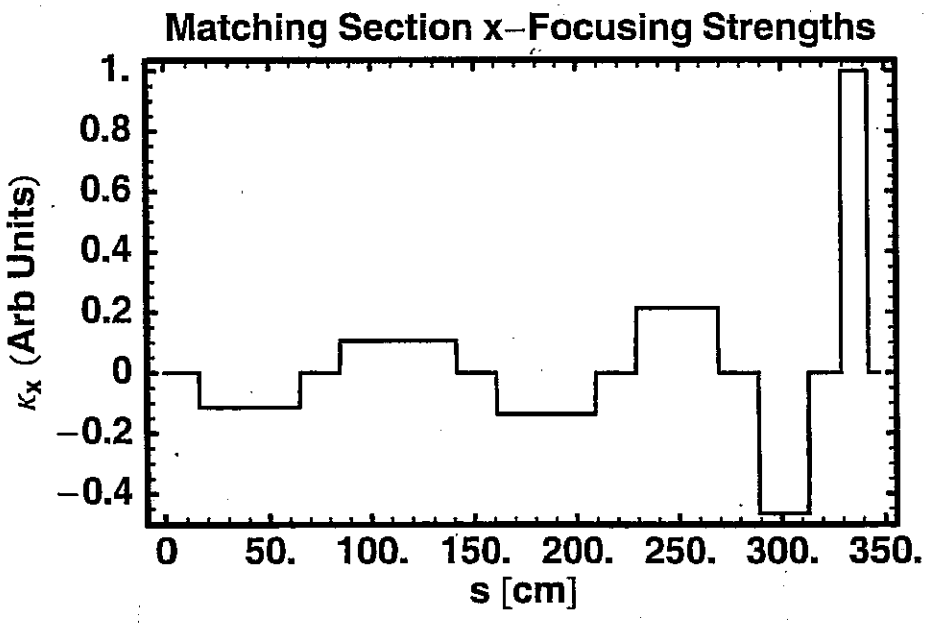

Piecewise Constant Linear Focusing Functions for Periodic Lattices

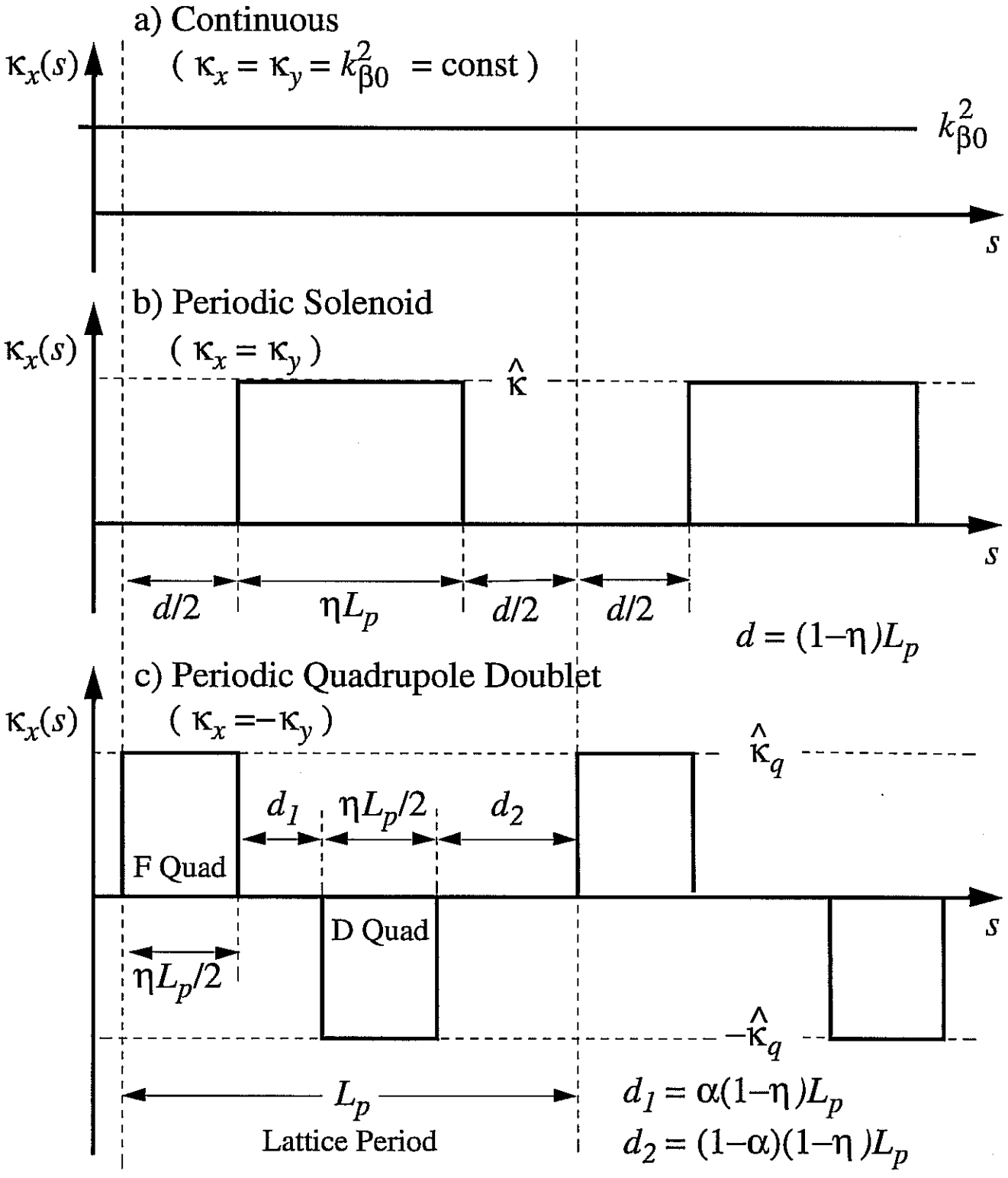

The equations presented in this section apply to a single particle moving in a beam. In the remaining sections we will carry out analysis of the equations neglecting space-charge effects ($\phi \to 0$) as is conventional in the standard theory of low-intensity accelerators. What we learn from this treatment will later aid analysis of high intensity beams where space-charge cannot be neglected. For example, we will later see that the x and y particle equations of motion can be applied to analyze the evolution of the beam in the absence of image charges:

$$x \longrightarrow x_c = \langle x \rangle_\perp \qquad x\text{-Centroid}$$
$$y \longrightarrow y_c = \langle y \rangle_\perp \qquad y\text{-Centroid}$$

By making appropriate variable substitutions, much of the analysis that follows can be applied to intense beams.

J.J. Barnard and S.M. Lund, USPAS June 2006

§2 Appendix A: Transformation of Solenoidal Focused Particle Eq. of Motion to Uncoupled Form

Solenoid Equations of motion:

$$\boxed{\begin{aligned} x'' + \left[\frac{1}{\gamma_b\beta_b}\frac{d}{ds}(\gamma_b\beta_b)\right]x' &= \frac{\omega_c'(s)}{2\gamma_b\beta_b c}\,y + \frac{\omega_c(s)}{\gamma_b\beta_b c}\,y' - \frac{q}{m\gamma_b^3\beta_b^2c^2}\frac{\partial\phi}{\partial x} \\ y'' + \left[\frac{1}{\gamma_b\beta_b}\frac{d}{ds}(\gamma_b\beta_b)\right]y' &= -\frac{\omega_c'(s)}{2\gamma_b\beta_b c}\,x - \frac{\omega_c(s)}{\gamma_b\beta_b c}\,x' - \frac{q}{m\gamma_b^3\beta_b^2c^2}\frac{\partial\phi}{\partial y} \end{aligned}}$$

To simplify algebra introduce the complex coordinate

$$\boxed{z = x + iy}$$

Then the two equations can be expressed as a single complex equation:

$$z'' + \left[\frac{1}{\gamma_b\beta_b}\frac{d}{ds}(\gamma_b\beta_b)\right]z' + \frac{i\omega_c'}{2\gamma_b\beta_b c}\,z + \frac{i\omega_c}{\gamma_b\beta_b c}\,z' = \frac{-q}{m\gamma_b^3\beta_b^2c^2}\left(\frac{\partial\phi}{\partial x} + i\frac{\partial\phi}{\partial y}\right)$$

For axisymmetric potential ϕ:

$$\frac{\partial\phi}{\partial x} + i\frac{\partial\phi}{\partial y} = \frac{\partial\phi}{\partial r}\frac{z}{r} \qquad r = \sqrt{x^2+y^2}$$

and the equation of motion becomes:

$$\boxed{z'' + \frac{(\gamma_b\beta_b)'}{(\gamma_b\beta_b)}z' + \frac{i\omega_c'}{2\gamma_b\beta_b c}\,z + \frac{i\omega_c}{\gamma_b\beta_b c}\,z' = \frac{-q}{m\gamma_b^3\beta_b^2c^2}\frac{\partial\phi}{\partial r}\frac{z}{r}}$$

Following Wiedemann, Vol. II pg 82, S.M. Lund A2/

Introduce the complex variable $\tilde{z}$ and a (real) phase function $\tilde{\psi}(s)$ by:

$$\boxed{\tilde{z} = z\, e^{-i\tilde{\psi}(s)} \equiv \tilde{x} + i\tilde{y}}$$

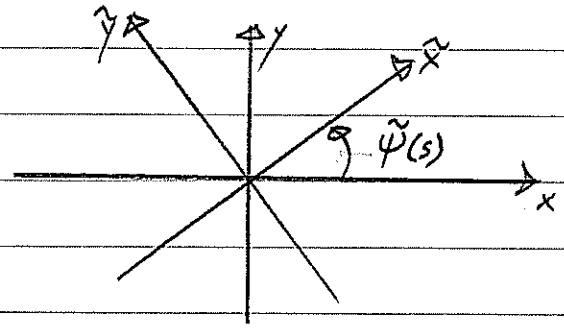

Note:
$|\tilde{z}| = r$

Then

$$z = \tilde{z}\, e^{i\tilde{\psi}}$$
$$z' = (\tilde{z}' + i\tilde{\psi}'\tilde{z})\, e^{i\tilde{\psi}}$$
$$z'' = (\tilde{z}'' + 2i\tilde{\psi}'\tilde{z}' + i\tilde{\psi}''\tilde{z} - \tilde{\psi}'^2\tilde{z})\, e^{i\tilde{\psi}}$$

and the complex equations of motion become:

$$\boxed{\begin{aligned}\tilde{z}'' &+ \left[2i\tilde{\psi}' + \frac{i\omega_c}{\gamma_b\beta_b c} + \frac{(\gamma_b\beta_b)'}{(\gamma_b\beta_b)}\right]\tilde{z}' + \left[i\tilde{\psi}'' - \tilde{\psi}'^2 - \frac{\omega_c}{\gamma_b\beta_b c}\tilde{\psi}' + \frac{i\omega_c'}{2\gamma_b\beta_b c} + i\tilde{\psi}'\frac{(\gamma_b\beta_b)'}{(\gamma_b\beta_b)}\right]\tilde{z} \\ &= \frac{-q}{m\gamma_b^3\beta_b^2 c^2}\frac{\partial\phi}{\partial r}\frac{\tilde{z}}{r}\end{aligned}}$$

Choose $\tilde{\psi}(s)$ (free to make this choice .... note that it eliminates the imaginary terms in [ ]s.)

$$\boxed{\tilde{\psi}' = -\frac{\omega_c}{2\gamma_b\beta_b c}}$$

Then $\tilde{\psi}'' = \dfrac{-\omega_c'}{2\gamma_b\beta_b c} + \dfrac{\omega_c}{2c}\dfrac{(\gamma_b\beta_b)'}{(\gamma_b\beta_b)^2}$ and the equation reduces to

$$\boxed{\tilde{z}'' + \frac{(\gamma_b\beta_b)'}{(\gamma_b\beta_b)}\tilde{z}' + \frac{\omega_c^2}{4\gamma_b^2\beta_b^2 c^2}\tilde{z} = -\frac{q}{m\gamma_b^3\beta_b^2 c^2}\frac{\partial\phi}{\partial r}\frac{\tilde{z}}{r}}$$

Or using $\tilde{z} = \tilde{x} + i\tilde{y}$, the equations are now decoupled in the $\tilde{x}, \tilde{y}$ variables!

Uncoupled $\Rightarrow$ form same as for continuous or quadrupole focusing.

$$\boxed{\begin{aligned} &\tilde{x}'' + \frac{(\gamma_b\beta_b)'}{(\gamma_b\beta_b)}\tilde{x}' + \kappa_s(s)\tilde{x} = \frac{-q}{m\gamma_b^3\beta_b^2c^2}\frac{\partial\phi}{\partial r}\frac{\tilde{x}}{r} \\ &\tilde{y}'' + \frac{(\gamma_b\beta_b)'}{(\gamma_b\beta_b)}\tilde{y}' + \kappa_s(s)\tilde{y} = \frac{-q}{m\gamma_b^3\beta_b^2c^2}\frac{\partial\phi}{\partial r}\frac{\tilde{y}}{r} \\ &\text{Solenoidal focusing force} \quad \kappa_s(s) \equiv \frac{\omega_c^2(s)}{4\gamma_b^2\beta_b^2c^2} \qquad \omega_c(s) = \frac{qB_z(s)}{m} \end{aligned}}$$

The transformation can be effected by integrating the equation for $\tilde{\psi}'$

$$\boxed{\tilde{\psi}(s) = -\frac{1}{2\gamma_b\beta_b c}\int_{s_i}^{s} d\tilde{s}\ \omega_c(\tilde{s})}$$

Where s_i some value of s where the solenoidal field $B_z(s)$ is zero, (i.e., outside the lattice of magnets). Then the transformation is given by:

$$\boxed{\begin{aligned} \tilde{x} &= \mathrm{Re}\left[(x+iy)e^{-i\tilde{\psi}(s)}\right] = x\cos\tilde{\psi}(s) + y\sin\tilde{\psi}(s) \\ \tilde{y} &= \mathrm{Im}\left[(x+iy)e^{-i\tilde{\psi}(s)}\right] = -x\sin\tilde{\psi}(s) + y\cos\tilde{\psi}(s) \end{aligned}}$$

Since $\tilde{\psi}' = -\frac{1}{2}\left(\frac{\omega_c}{\gamma_b\beta_b c}\right)$, note that the $\tilde{x}, \tilde{y}$ frame is rotating at 1/2 the local (s-varying) cyclotron frequency. This rotating frame is refered to as the "Larmor" frame. For a

uniform solenoid with $B_z(s) = \text{const}$, $\tilde{\psi}' = -\frac{1}{2}\left(\frac{\omega_c}{\gamma_b \beta_b c}\right) = \text{const}$, and the Larmor frame is uniformly rotating as is well-known.

Note that at the initial condition with $B_z = 0$,

$$\tilde{x}(s=s_i) = x(s=s_i) = x_i$$
$$\tilde{x}'(s=s_i) = x'(s=s_i) = x_i'$$

$$\tilde{y}(s=s_i) = y(s=s_i) = y_i$$
$$\tilde{y}'(s=s_i) = y'(s=s_i) = y_i'$$

The rotation matrix of the transformation can be explicitly worked out:

$$\tilde{x} = x\cos\tilde{\psi} + y\sin\tilde{\psi}$$
$$\tilde{x}' = -x\tilde{\psi}'\sin\tilde{\psi} + x'\cos\tilde{\psi} + y\tilde{\psi}'\cos\tilde{\psi} + y'\sin\tilde{\psi}$$

$$\tilde{y} = -x\sin\tilde{\psi} + y\cos\tilde{\psi}$$
$$\tilde{y}' = -x\tilde{\psi}'\cos\tilde{\psi} - x'\sin\tilde{\psi} - y\tilde{\psi}'\sin\tilde{\psi} + y'\cos\tilde{\psi}$$

collecting terms and using $\tilde{\psi}' = -\frac{1}{2}\frac{\omega_c}{\gamma_b\beta_b c}$;

$$\boxed{\begin{pmatrix} x \\ x' \\ y \\ y' \end{pmatrix} = \begin{pmatrix} \cos\tilde{\psi} & 0 & \sin\tilde{\psi} & 0 \\ \frac{\omega_c}{2\gamma_b\beta_b c}\sin\tilde{\psi} & \cos\tilde{\psi} & -\frac{\omega_c}{2\gamma_b\beta_b c}\cos\tilde{\psi} & \sin\tilde{\psi} \\ -\sin\tilde{\psi} & 0 & \cos\tilde{\psi} & 0 \\ \frac{\omega_c}{2\gamma_b\beta_b c}\cos\tilde{\psi} & -\sin\tilde{\psi} & \frac{\omega_c}{2\gamma_b\beta_b c}\sin\tilde{\psi} & \cos\tilde{\psi} \end{pmatrix} \begin{pmatrix} \tilde{x} \\ \tilde{x}' \\ \tilde{y} \\ \tilde{y}' \end{pmatrix}}$$

J.J. Barnard and S.M. Lund
US PAS, July 2006

§3 Description of Applied Focusing Fields

Applied fields for focusing, bending, and acceleration enter the equations of motion via

$\vec{E}^a$: Applied Electric Field
$\vec{B}^a$: Applied Magnetic Field

Generally, these fields are produced by sources outside an aperture of radius r_p. For example, for electric and magnetic quadrupoles:

Transverse Cross-Sections

Electric Quadrupole

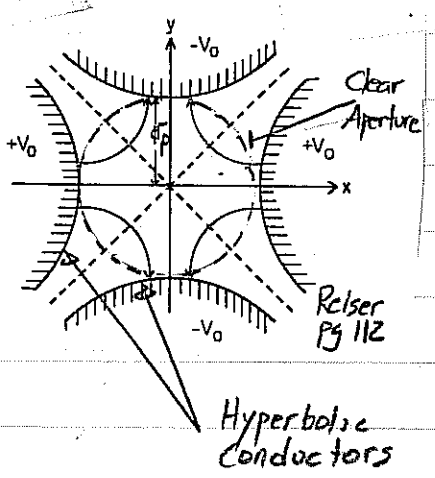

Magnetic Quadrupole

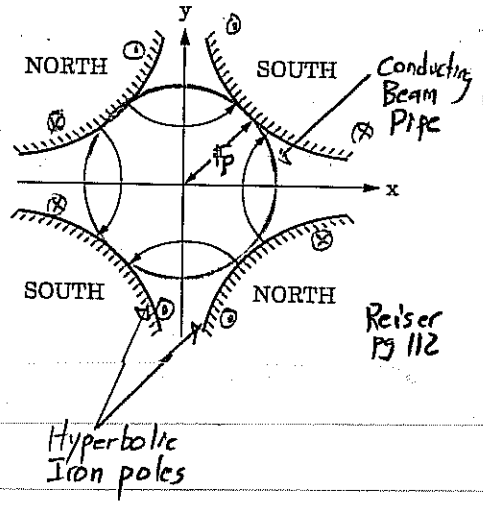

The fields within the aperture of these and similiar elements satisfy the vacuum Maxwell Equations:

$$\boxed{\begin{aligned} \nabla \cdot \vec{E}^a &= 0 & \nabla \cdot \vec{B}^a &= 0 \\ \nabla \times \vec{E}^a &= -\frac{\partial \vec{B}^a}{\partial t} & \nabla \times \vec{B}^a &= \frac{1}{c^2}\frac{\partial \vec{E}^a}{\partial t} \end{aligned}}$$

In many cases of interest, the fields are static or a quasistatic approximation can be employed and the $\partial/\partial t$ terms neglected. Then the equations for $\vec{E}^a$ and $\vec{B}^a$ within the aperture are of the same form with:

$$\boxed{\begin{array}{ll} \nabla \cdot \vec{E}^a = 0 & \nabla \cdot \vec{B}^a = 0 \\ \nabla \times \vec{E}^a = 0 & \nabla \times \vec{B}^a = 0 \end{array}}$$

Static Vacuum Maxwell Equations

In general, elements are tuned to limit the strength of nonlinear field terms, so the beam experiences primarily linear applied fields. We will find later that this allows better preservation of beam quality. However, this removal of nonlinear field terms <u>cannot</u> be done absolutely in 3D geometries. There will always be some nonlinear fields in finite 3D structures as a result of the properties of the vacuum Maxwell equations. Also, even in lower-dimensional idealizations of real structures, deviations from ideal symmetry will result from practical concerns and such deviations will produce further nonlinear field terms. As an example of this, 2D iron magnet with infinite pole extent must be truncated leading to nonlinear focusing terms even in 2D:

Cross-Sections of Quadrupole Magnets

(Conte and Mackay, Intro. to the Physics of Particle Accelerators, World Scientific, 1991 pg 59.)

Ideal | Practical

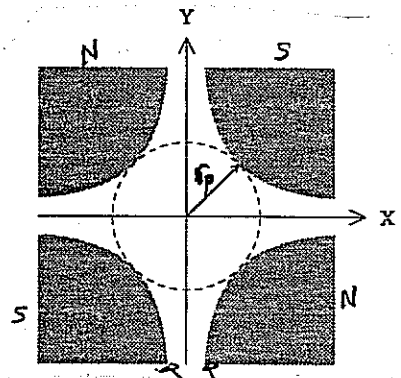

Hyperbolic iron poles : 2D Field Ideal Quadrupole

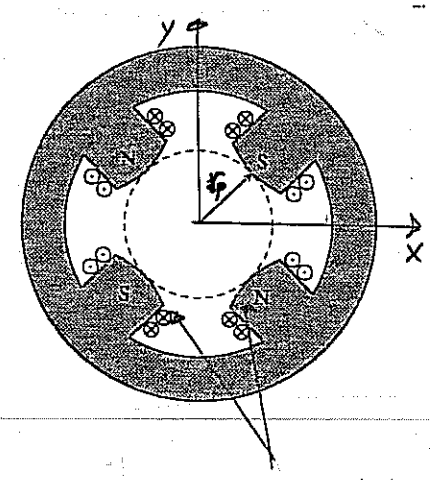

Truncated iron poles : 2D Field Ideal Quadrupole + Error Terms

Magnetic optic and accelerating structures are both extensive topics and it is not possible to cover them in this intro. (survey) class. In the following we will illustrate some simple methods of field error characterization of magnetic optics with transverse field components (dipoles, quadrupoles, sextupoles, ...) This treatment is not comprehensive.

Consider magnetic optics with:

$$\vec{E}^a = 0 \quad \text{and} \quad \vec{B}^a \simeq \vec{B}^a_\perp$$

Electric optics can be treated analogously since the static vacuum Maxwell Equations are the same form for $\vec{E}^a$ and $\vec{B}^a$.

Magnetic Forces

$$\vec{F}_\perp^q \simeq q\beta_b c \cdot \hat{z} \times \vec{B}_\perp^q$$

$$\vec{B}_\perp^q = \hat{x} B_x^q + \hat{y} B_y^q \qquad \perp \text{ Field}$$

$$\boxed{\begin{aligned} F_x^q &\simeq -q\beta_b c \cdot B_y^q \\ F_y^q &\simeq q\beta_b c\, B_x^q \end{aligned}}$$

Field components can be Taylor-series expanded about the element center $\vec{x}_\perp = 0$

$$B_x^q = \underbrace{B_x^q(0)}_{\text{Bend}} + \underbrace{\frac{\partial B_x^q}{\partial y}(0)\, y}_{\substack{\text{Normal}\\ \text{Linear Focus}}} + \underbrace{\frac{\partial B_x^q}{\partial x}(0)\, x}_{\substack{\text{Skew}\\ \text{Linear Focus}}}$$

$$\text{Nonlinear Terms} \left\{ \begin{aligned} &+ \frac{1}{2}\frac{\partial^2 B_x^q}{\partial x^2}(0)\, x^2 + \frac{\partial^2 B_x^q}{\partial x \partial y}(0)\, xy + \frac{1}{2}\frac{\partial^2 B_x^q}{\partial y^2}(0)\, y^2 \\ &+ \cdots\cdots \end{aligned} \right.$$

$$B_y^q = \underbrace{B_y^q(0)}_{\text{Bend}} + \underbrace{\frac{\partial B_y^q}{\partial x}(0)\, x}_{\substack{\text{Normal}\\ \text{Linear Focus}}} + \underbrace{\frac{\partial B_y^q}{\partial y}(0)\, y}_{\substack{\text{Skew}\\ \text{Linear Focus}}}$$

$$\text{Nonlinear Terms} \left\{ \begin{aligned} &+ \frac{1}{2}\frac{\partial^2 B_y^q}{\partial x^2}(0)\, x^2 + \frac{\partial^2 B_y^q}{\partial x \partial y}(0)\, xy + \frac{1}{2}\frac{\partial^2 B_y^q}{\partial y^2}(0)\, y^2 \\ &+ \cdots\cdots \end{aligned} \right.$$

Sources of Undesired Applied Field Components:

1/ Systematic errors or nonideal geometry associated with the intrinsic structure of the magnet.

2/ Random construction errors in individual magnets.

3/ Alignment of magnets giving field projections in unwanted directions

4/ Excitation errors (currents in coils not correct values and/or balanced).

Real 3D magnets can often be modeled for sufficient accuracy by 2D hard-edge equivalent magnets that give same impulse to the beam particles.

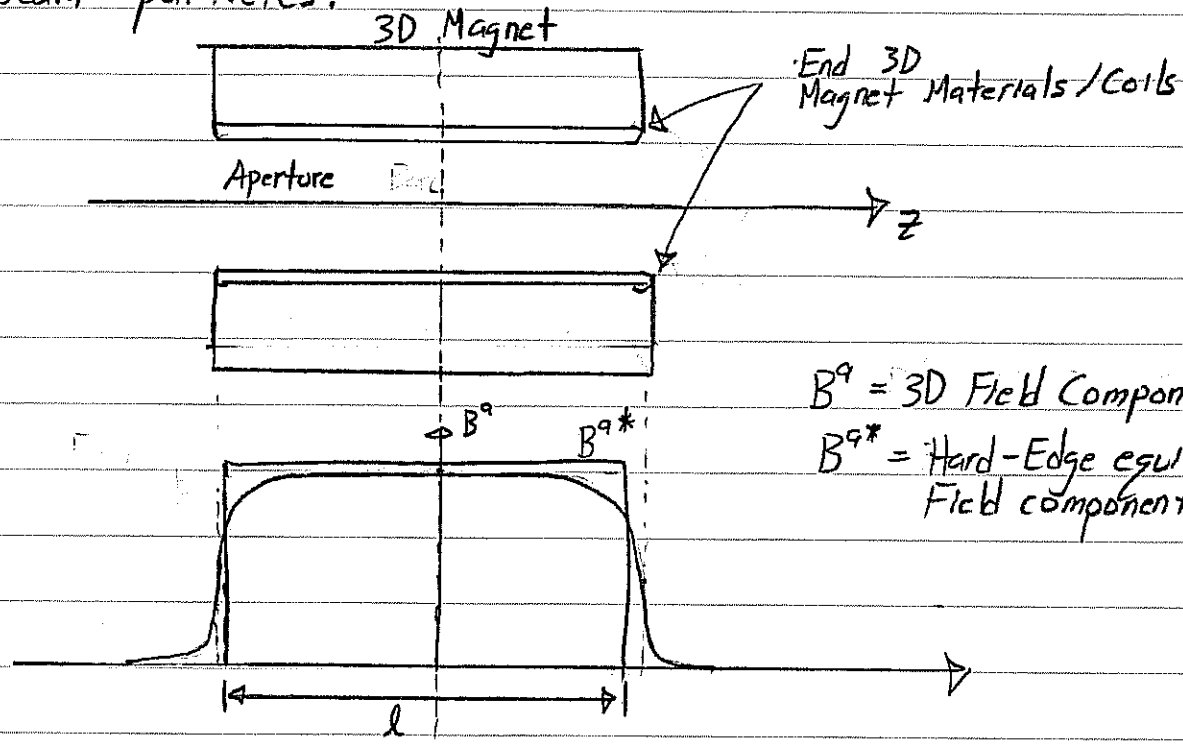

Mid-Plane 2D Structure that generates B^{q*}

ℓ = Hard-Edge length

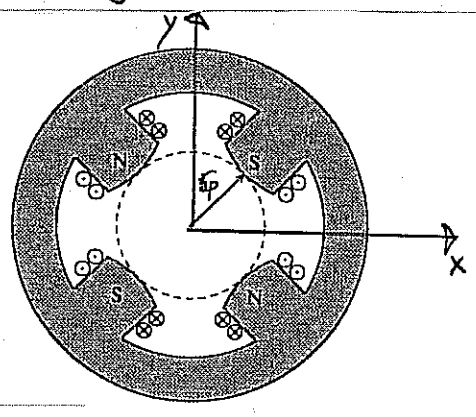

Many perscriptions exist for calculating ℓ and optimal hard-edge models for various purposes. Here we follow, Lund and Bukh, PRSTAB 7 ..... 204801 (2004) Appendix C

A reasonable perscription to calculate ℓ for a physical quadrupole magnet with a linear field gradient G is:

$$\boxed{\begin{aligned} G(z) &\equiv \left.\frac{\partial B_x^a}{\partial y}\right|_{x=y=0} \\ \ell\, G(z=0) &= \int_{-\infty}^{\infty} dz\; G(z) \end{aligned}}$$

ℓ = "effective" magnet length

In many cases it is sufficient to characterize the field errors in 2D hard-edge equivalent as:

$$\boxed{\begin{aligned} B_x(x,y) &= \frac{1}{\ell}\int_{-\infty}^{\infty} dz\; B_x^a(x,y,z) \\ B_y(x,y) &= \frac{1}{\ell}\int_{-\infty}^{\infty} dz\; B_y^a(x,y,z) \end{aligned}}$$

2D Effective Fields 3D Fields

Operating on the vacuum Maxwell equations with $\int_{-\infty}^{\infty}\frac{dz}{\ell}\cdots$ yields the (exact) 2D field equations:

$$\boxed{\begin{aligned} \frac{\partial B_x(x,y)}{\partial x} &= -\frac{\partial B_y(x,y)}{\partial y} \\ \frac{\partial B_x(x,y)}{\partial y} &= \frac{\partial B_y(x,y)}{\partial x} \end{aligned}}$$

These equations can be recognized as the Cauchy-Riemann conditions for a complex field variable

$$\boxed{\underset{\sim}{B} = B_y + i B_x}$$

Here, $i = \sqrt{-1}$

to be an analytical function of the complex variable

$$\boxed{\underset{\sim}{z} = x + iy}$$

$i = \sqrt{-1}$

It follows that $\underset{\sim}{B}(\underset{\sim}{z})$ can be analyzed using the full power of the highly developed theory of analytical functions of a complex variable.

Expand $\underset{\sim}{B}(\underset{\sim}{z})$ as a Laurent series within the vacuum aperture as:

$$\underset{\sim}{B}(\underset{\sim}{z}) = B_y + i B_x = \sum_{n=1}^{\infty} \underset{\sim}{B}_n \left(\underset{\sim}{z} / r_p \right)^{n-1}$$

$\underset{\sim}{B}_n$ = const — complex constants (multipole coefficients) giving the structure of the field.

n = multipole index

r_p = aperture "pipe" radius

The multipole coefficients can be resolved as:

$$\underset{\sim}{B}_n = b_n + i a_n \qquad a_n, b_n \text{ real constants}$$

$b_n \Rightarrow$ "normal" multipoles

$a_n \Rightarrow$ "skew" multipoles (rotated)

Index	Name	Normal Field	
$n=1$	Dipole	$B_x = 0$,	$B_y = b_1$
$n=2$	Quadrupole	$B_x = b_2\, y/r_p$	$B_y = b_2\, x/r_p$
$n=3$	Sextupole	$B_x = -b_3\, 2xy/r_p^2$,	$B_y = b_3\, (x^2-y^2)/r_p^2$
$n=4$	Octupole		
⋮	⋮	⋮	⋮

Higher order multipole field components leading to nonlinear focusing forces decrease rapidly within the aperture. To see this use a polar representation of $\underset{\sim}{z}$ and $\underset{\sim}{B}_n$:

$$\underset{\sim}{z} = x + iy = r e^{i\theta} \qquad r = \sqrt{x^2+y^2}$$
$$\theta = \mathrm{ArcTan}[y, x]$$

similarly:

$$\underset{\sim}{B}_n = |\underset{\sim}{B}_n| \, e^{i\psi}$$

Thus the n-th order multipole term scales as

$$\boxed{\underset{\sim}{B}_n \left(\underset{\sim}{z}/r_p\right)^{n-1} = |\underset{\sim}{B}_n| \left(\frac{r}{r_p}\right)^{n-1} e^{i[(n-1)\theta + \psi]}}$$

- Unless the coefficient $|\underset{\sim}{B}_n|$ is very large, high-order terms will become small rapidly as (r/r_p) decreases

Better linear field quality magnets can be made simply by making the clear bore r_p larger or alternatively smaller beam cross-sections can be employed.

- Larger bore magnets cost more. So design becomes trade-off between cost and performance.

Generally, a practical magnet design will have a "good-field" radius that maximum field errors are specified on. In a good magnet design this can be 70% or more of the clear bore to the begining of magnet material structures.

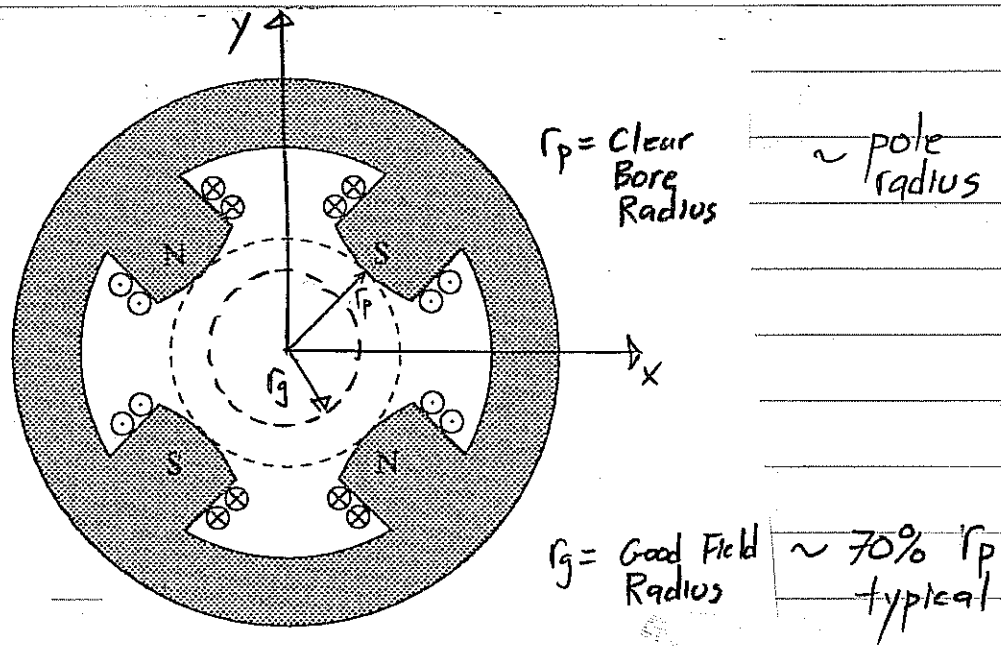

Beam particle orbits are designed to remain within radius r_g.

Field error statements are readily generalized to 3D since

$$\nabla \cdot \vec{B}^q = 0 \qquad \Rightarrow \qquad \nabla^2 \vec{B}^q = 0$$
$$\nabla \times \vec{B}^q = 0$$

each component of $\vec{B}^q$ satisfies a Laplace equation within the vacuum aperture. Therefore, field errors can only decrease when moving deeper within a source free region of 3D space.

S. M. Lund 11/

Example 2D Nonideal Magnets from Permanent Magnet blocks

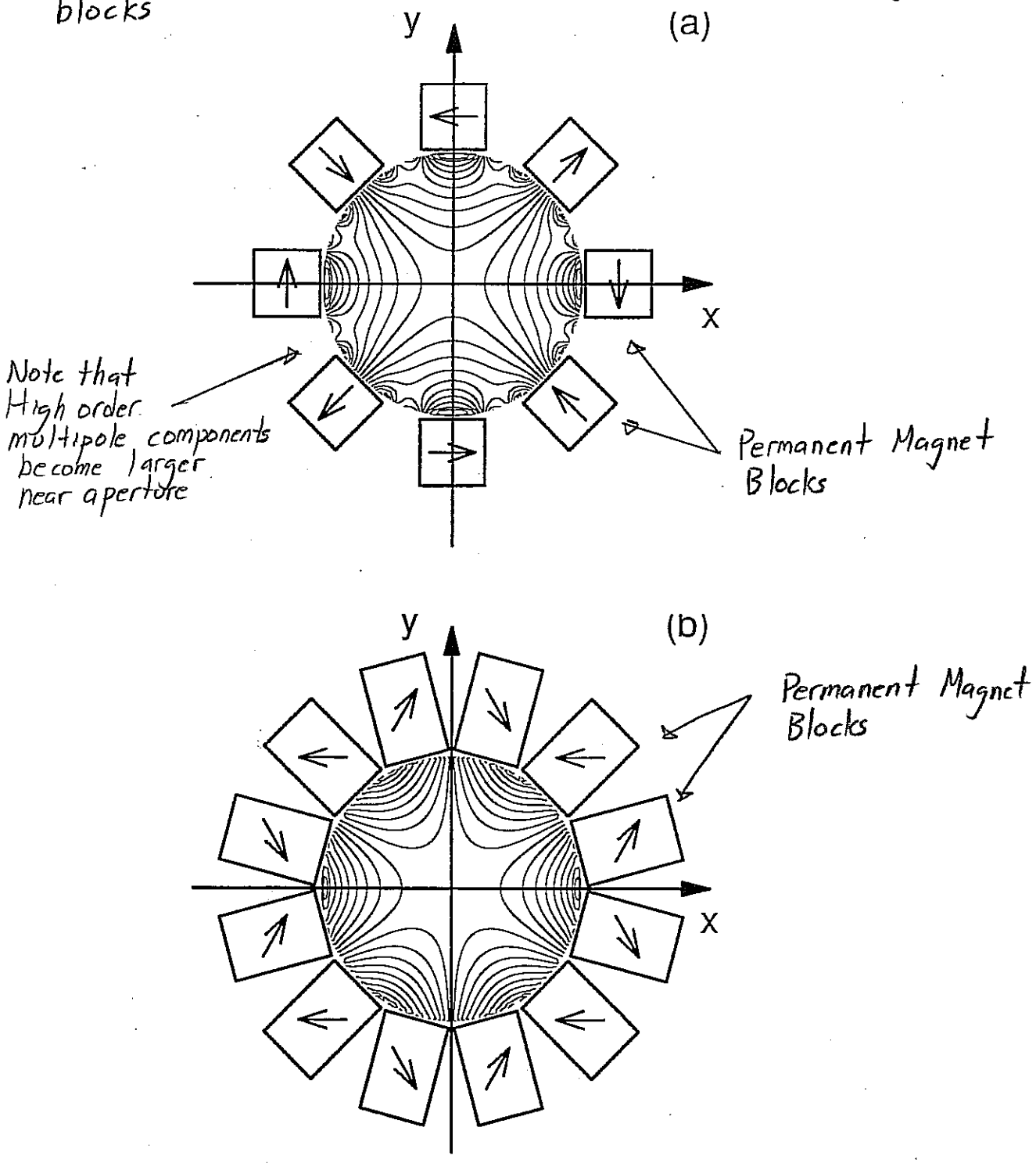

Fig. E1. Cross-sections of a Halbach array quadrupole magnet formed from $M = 8$ square-block magnets (a), and a sextupole magnet formed from $M = 12$ rectangular-block magnets (b).

J.J. Barnard and S.M. Lund
USPAS, June 2006

§4 Transverse Particle Equations of Motion with Nonlinear Applied Fields

In §1 we showed that

$$\boxed{\begin{aligned} x'' + \frac{(\gamma_b\beta_b)'}{(\gamma_b\beta_b)}x' &= \frac{q}{m\gamma_b\beta_b^2c^2}E_x^a - \frac{q}{m\gamma_b\beta_b c}B_y^a + \frac{q}{m\gamma_b\beta_b c}B_z^a y' - \frac{q}{m\gamma_b^3\beta_b^2c^2}\frac{\partial\phi}{\partial x} \\ y'' + \frac{(\gamma_b\beta_b)'}{(\gamma_b\beta_b)}y' &= \frac{q}{m\gamma_b\beta_b^2c^2}E_y^a + \frac{q}{m\gamma_b\beta_b c}B_x^a - \frac{q}{m\gamma_b\beta_b c}B_z^a x' - \frac{q}{m\gamma_b^3\beta_b^2c^2}\frac{\partial\phi}{\partial y} \end{aligned}}$$

for linear applied fields (§2) these equations can be expressed as:

$$\boxed{\begin{aligned} x'' + \frac{(\gamma_b\beta_b)'}{(\gamma_b\beta_b)}x' + \kappa_x x &= \frac{-q}{m\gamma_b^3\beta_b^2c^2}\frac{\partial\phi}{\partial x} \\ y'' + \frac{(\gamma_b\beta_b)'}{(\gamma_b\beta_b)}y' + \kappa_y y &= \frac{-q}{m\gamma_b^3\beta_b^2c^2}\frac{\partial\phi}{\partial y} \end{aligned}}$$

where

$$\kappa_x(s),\ \kappa_y(s)$$

describe the linear applied focusing forces and the equations are implicitly treated in the Larmor frame when $B_z^a \neq 0$.

Lattice designs try to minimize the effect of nonlinear applied fields. However, the 3D Maxwell

equations predict that there will <u>always</u> be some finite nonlinear applied field terms in 3D. Moreover, design idealizations and fabrication and material errors will generate further nonlinear field components in practical devices.

Therefore, nonlinear field effects must be added back into the model when it is necessary to analyze their effects.

There are several approaches to carrying this out:

<u>Approach 1</u> (Explicit 3D)

Simplist – Just employ the explicit 3D applied field components $\vec{E}_\perp^a$, $\vec{B}^a$ in the full equations of motion and avoid using R_x, R_y.

Comments:

- Most easy to apply without unit confusion in simulations where many effects are included.
  - Simplify comparisons to experiments where details matter!

- The accelerating field E_z^a associated with longitudinal electric fields should also be included to calculate $\gamma_b(s)$ and $\beta_b(s)$ for accurate transverse equations of motion.
  - $\perp$ and $\parallel$ dynamics cannot be fully decoupled for high accuracy!

<u>Approach 2</u> (Perturbations about linear)

Exploit the linearity of the Maxwells equation to take

$$\boxed{\begin{aligned} \vec{E}_\perp^{\,q} &= \vec{E}_\perp^{\,q}\Big|_{\text{Linear Focus}} + \delta\vec{E}_\perp^{\,q} \\ \vec{B}^{q} &= \vec{B}^{q}\Big|_{\text{Linear Focus}} + \delta\vec{B}^{q} \end{aligned}}$$

where $\vec{E}_\perp^{\,q}\Big|_{\text{Linear Focus}}$ and $\vec{B}^{q}\Big|_{\text{Linear Focus}}$ are the linear field components included in κ_x, κ_y and then express the equations of motion as:

$$\boxed{\begin{aligned} x'' + \frac{(\gamma_b\beta_b)'}{(\gamma_b\beta_b)}x' + \kappa_x x &= \frac{q}{m\gamma_b\beta_b^2c^2}\delta E_x^q - \frac{q}{m\gamma_b\beta_b c}\delta B_y^q + \frac{q}{m\gamma_b\beta_b c}\delta B_z^q y' \\ &\quad - \frac{q}{m\gamma_b^3\beta_b^2c^2}\frac{\partial\phi}{\partial x} \\ y'' + \frac{(\gamma_b\beta_b)'}{(\gamma_b\beta_b)}y' + \kappa_y y &= \frac{q}{m\gamma_b\beta_b^2c^2}\delta E_y^q + \frac{q}{m\gamma_b\beta_b c}\delta B_x^q - \frac{q}{m\gamma_b\beta_b c}\delta B_z^q x' \\ &\quad - \frac{q}{m\gamma_b^3\beta_b^2c^2}\frac{\partial\phi}{\partial y} \end{aligned}}$$

Comments

- Approach is best suited to non-solenoidal focusing because for solenoidal focusing the form is only valid for $\phi = \phi(r)$ (Axisymmetric beam) and the $\delta\vec{E}_\perp$ and $\delta\vec{B}$ field components would need to be projected into the Larmor frame. This would be more complicated than Approach 1.

- The field components $\delta\vec{E}_\perp^{\,a}$ and $\delta\vec{B}^{\,a}$ will not necessarily satisfy the 3D Maxwell equations <u>by themselves</u>. because $\vec{E}_\perp^{\,a}\big|_{\text{Linear Focus}}$ and $\vec{B}^{\,a}\big|_{\text{Linear Focus}}$ will not, in general, satisfy the 3D Maxwell equations by themselves either.

J.J. Barnard and S.M. Lund
USPAS June 2006

See Reiser §3.8.2 pgs 145–153

§5 Linear Equations of Motion without Space-Charge, Acceleration, and Momentum Spread

Neglect:
- Space charge effects: $\phi \to 0$
- Nonlinear Applied Focusing: $\vec{B}^a, \vec{E}^a$ contain only linear focusing terms
- Acceleration: $\beta_b \gamma_b = \text{const.}$
- Momentum Spread Effects

Then the transverse particle equations of motion can be expressed in the form of Hill's equation:

$$\boxed{x''(s) + \kappa(s)\, x(s) = 0}$$

x = $\perp$ coordinate, possibly formed from various coordinates (even longitudinal coordinates can be cast in this form at some levels of approx.)

s = axial coordinate of ref. particle.

$x' = \dfrac{dx}{ds}$ primes denote derivatives with respect to s.

$\kappa(s)$ = lattice focusing function. (linear fields)

For a periodic lattice:

$$\boxed{\begin{aligned} \kappa(s+L_p) &= \kappa(s) \\ L_p &= \text{Lattice Period.} \end{aligned}}$$

For a ring, one also has the superperiodicity condition:

$$\boxed{\begin{aligned} \kappa(s+C) &= \kappa(s) \quad * \\ C &= N L_p \qquad N = \text{superperiodicity.} \end{aligned}}$$

* This distinction matters when there are random error fields in the ring. (Repeat with super but not lattice period)

Transfer Matrix Form of Solution

The equation of motion is linear and the (unique) solution with

$$\boxed{\begin{aligned} x(s=s_i) &= x(s_i) \\ x'(s=s_i) &= x'(s_i) \end{aligned}}$$ "initial" conditions

can be expressed in matrix form as:

$$\boxed{\begin{pmatrix} x(s) \\ x'(s) \end{pmatrix} \equiv \overline{M}(s|s_i) \begin{pmatrix} x(s_i) \\ x'(s_i) \end{pmatrix} \equiv \begin{pmatrix} C(s|s_i) & S(s|s_i) \\ C'(s|s_i) & S'(s|s_i) \end{pmatrix} \begin{pmatrix} x(s_i) \\ x'(s_i) \end{pmatrix}}$$

where $C(s|s_i)$ and $S(s|s_i)$ are "cosine"-like and "sine"-like principal trajectories satisfying:

$$\boxed{\begin{aligned} &C''(s|s_i) + \kappa(s)\, C(s|s_i) = 0 \,; \quad C(s_i|s_i) = 1 \,, \quad C'(s_i|s_i) = 0 \\ &S''(s|s_i) + \kappa(s)\, S(s|s_i) = 0 \,; \quad S(s_i|s_i) = 0 \,, \quad S'(s_i|s_i) = 1 \end{aligned}}$$

An important property of this linear motion is that the Wronskian is conserved:

$$\boxed{\begin{aligned} W(s|s_i) \equiv \det \overline{M}(s|s_i) &= \det \begin{vmatrix} C(s|s_i) & S(s|s_i) \\ C'(s|s_i) & S'(s|s_i) \end{vmatrix} \\ &= C(s|s_i)\, S'(s|s_i) - C'(s|s_i)\, S(s|s_i) = 1 \end{aligned}}$$

// Proof: (abbreviate notation)

$$\begin{aligned} -S(C'' + \kappa C) &= 0 \\ + \quad C(S'' + \kappa S) &= 0 \end{aligned} \quad \Rightarrow \quad \begin{aligned} CS'' - SC'' + \kappa(\underbrace{CS - SC}_{0}) &= 0 \\ \frac{dW}{ds} &= 0 \end{aligned}$$

$$\Rightarrow \quad W(s) = W(s_i) = C_i S_i' - C_i' S_i = 1 \cdot 1 - 0 \cdot 0 = 1 \quad \checkmark \quad //$$

// Example

For a continuously focused system:

$$\kappa(s) = k_{\beta 0}^2 = \text{const.}$$

$$x'' + k_{\beta 0}^2 x = 0$$

$$C(s|s_i) = \cos[k_{\beta 0}(s-s_i)]$$
$$S(s|s_i) = \frac{\sin[k_{\beta 0}(s-s_i)]}{k_{\beta 0}}$$

$$\begin{pmatrix} x(s) \\ x(s') \end{pmatrix} = \begin{pmatrix} \cos[k_{\beta 0}(s-s_i)] & \frac{\sin[k_{\beta 0}(s-s_i)]}{k_{\beta 0}} \\ -k_{\beta 0}\sin[k_{\beta 0}(s-s_i)] & \cos[k_{\beta 0}(s-s_i)] \end{pmatrix} \begin{pmatrix} x(s_i) \\ x'(s_i) \end{pmatrix}$$

$$\bar{W} = \cos^2[k_{\beta 0}(s-s_i)] + \sin^2[k_{\beta 0}(s-s_i)] = \underline{1} \qquad //$$

Stability

We now examine particle stability. First, $\bar{M}$ must be the <u>same in any period</u> of a periodic lattice:

$$\boxed{\bar{M}(s+L_p|s_i+L_p) = \bar{M}(s|s_i)}$$

For a propogation distance $s-s_i$ satisfying

$$N L_p \leq s-s_i \leq (N+1) L_p$$

with N integer, the advance $\bar{M}(s|s_i)$ can be resolved as:

$$\boxed{\bar{M}(s|s_i) = \overbrace{\bar{M}(s-NL_p|s_i)}^{\text{Residual}}\ \overbrace{\bar{M}(NL_p|s_i)}^{N\text{ period}} = \bar{M}(s-NL_p|s_i)\,\bar{M}(s_i+L_p|s_i)^N}$$

For a particle to have a stable orbit $x(s)$ and $x'(s)$ should remain bounded on propogation through an

For a particle to have a stable orbit $x(s)$ and $x'(s)$ should remain bounded on propogation through an arbitrary number N of lattice periods

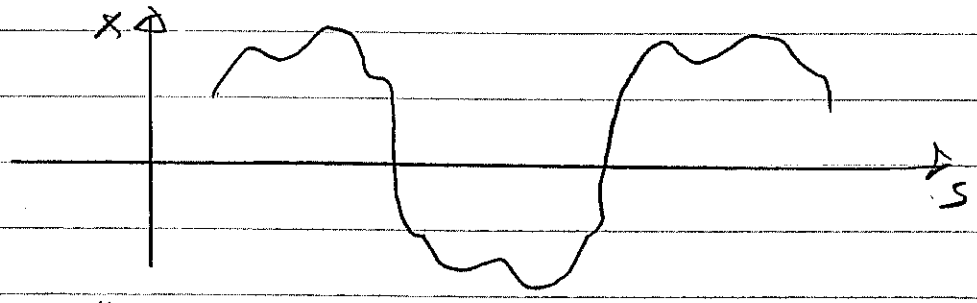

"energetic" particle $\Rightarrow$ $H = \frac{1}{2}x'^2 + \frac{1}{2}k x^2 \sim$ large (but not constant)

Quadratic:

Where: x small x' large
x' small x large

This bounding is equivalent to requiring that the elements of $\overline{M}$ remain bounded on propagation through N lattice periods.

This suggest the <u>stability definition</u>

$$\boxed{\lim_{N\to\infty} \left| \left\{ \overline{M}(s_i + L_p | s_i)^N \right\}_{ij} \right| < \infty}$$

where

$$\overline{A}_{ij} = i,j \text{ component of } \overline{M}$$

To analyze the stability condition – examine the eigenvectors/eigenvalues of $\overline{M}$ for transport through one lattice period:

$$\boxed{\begin{gathered}\overline{M}(s_i+L_p|s_i)\cdot\vec{E}(s_i) = \lambda\vec{E}(s_i)\\ \lambda = \text{eigenvalue}\\ \vec{E}(s_i) = \text{eigenvector}\end{gathered}}$$

Derive the 2 independent eigenvectors/eigenvalues through analysis of the characteristic equation:

Abbreviate:

$$\overline{M}(s_i+L_p|s_i) = \begin{pmatrix} C(s_i+L_p|s_i) & S(s_i+L_p|s_i) \\ C'(s_i+L_p|s_i) & S'(s_i+L_p|s_i)\end{pmatrix} \equiv \begin{pmatrix} C & S \\ C' & S'\end{pmatrix}$$

Nontrivial solutions exist when:

$$\det\begin{vmatrix} C-\lambda & S \\ C' & S'-\lambda\end{vmatrix} = \lambda^2 + (C+S')\lambda + (CS'-C'S) = 0$$

But:

Wronskian Condition: $CS'-CS = W = 1$

Trace Def: $C+S' = \text{Trace}\,\overline{M} \equiv 2\cos\delta_0$

Characteristic eqn:

$$\boxed{\begin{gathered}\lambda^2 - 2\lambda\cos\delta_0 + 1 = 0\\ \lambda = \text{Trace}\,\overline{M}(s_i+L_p|s_i)\end{gathered}}$$

$i = \sqrt{-1}$

Solutions (2):

$$\boxed{\lambda = \cos\delta_0 \pm \sqrt{\cos\delta_0^2 - 1} = \cos\delta_0 \pm i\sin\delta_0}$$

Denote 2 solutions as:

$$\boxed{\begin{array}{l} \lambda_\pm = \cos\delta_0 \pm i \sin\delta_0 = \text{eigenvalues} \\ \vec{E}_\pm = \text{corresponding eigenvectors} \end{array}}$$

Note:
$\lambda_+\lambda_- = 1$
$\lambda_- = \dfrac{1}{\lambda_+}$

Denote an initial condition by

$$\boxed{\vec{X}_i \equiv \begin{pmatrix} x(s_i) \\ x'(s_i) \end{pmatrix}}$$

This initial condition can always be expanded in terms of the eigenvectors as:

$$\boxed{\begin{array}{c} \vec{X}_i = \alpha_+ \vec{E}_+ + \alpha_- \vec{E}_- \\ \alpha_\pm \text{ constants} \end{array}}$$

Then

$$\boxed{\begin{aligned} \overline{M}^N \vec{X}_i &= \alpha_+ \overline{M}^N \vec{E}_+ + \alpha_- \overline{M}^N \vec{E}_- \\ &= \alpha_+ \lambda_+^N \vec{E}_+ + \alpha_- \lambda_-^N \vec{E}_- \end{aligned}}$$

Thus, if $\lambda_\pm^N$ remains bounded the motion is stable. This will always be the case if $|\lambda_+| \le 1$, corresponding to δ_0 real with $|\cos\delta_0| \le 1$, or equivalently

$$\boxed{\begin{array}{c} \frac{1}{2}\left|\text{Trace } \overline{M}(s_i+L_p|s_i)\right| = \frac{1}{2}\left|C(s_i+L_p|s_i) + S'(s_i+L_p|s_i)\right| = |\cos\delta_0| \le 1 \\ \text{For stable motion.} \end{array}}$$

// Example

For continuous focusing:

$$\frac{1}{2}\left|\text{Trace}\left[M(s_i+L_p|s_i)\right]\right| = \left|\cos\left[k_{\beta 0} L_p\right]\right| \le 1$$

Motion is <u>stable</u> for all $k_{\beta 0}$ real. //

Possible Eigenvalue Symmetries for 2x2 Transfer Matrices

a) Stable

Occurs for $0 \leq \delta_0 \leq 180°/\text{period}$

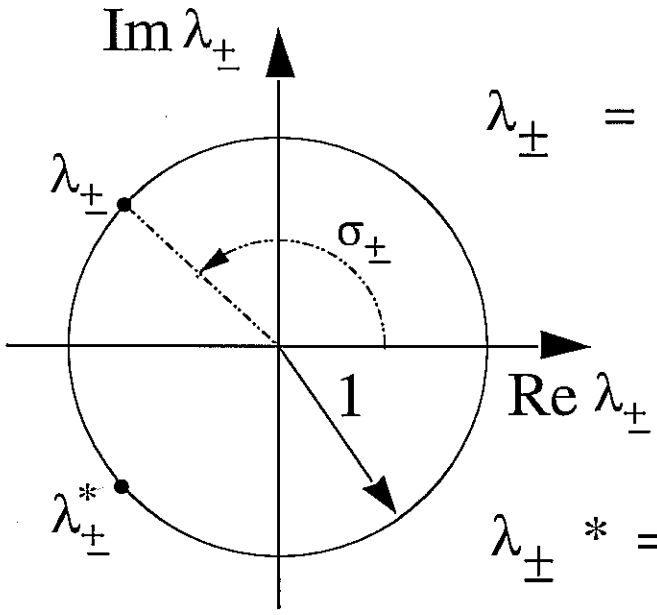

$$\lambda_\pm = e^{i\sigma_\pm}$$

$$\lambda_\pm{}^* = 1/\lambda_\pm = e^{-i\sigma_\pm}$$

b) Unstable, Lattice Resonance

Occurs in bands after focusing strengths are increased past where $\delta_0 = 180°/\text{period}$.

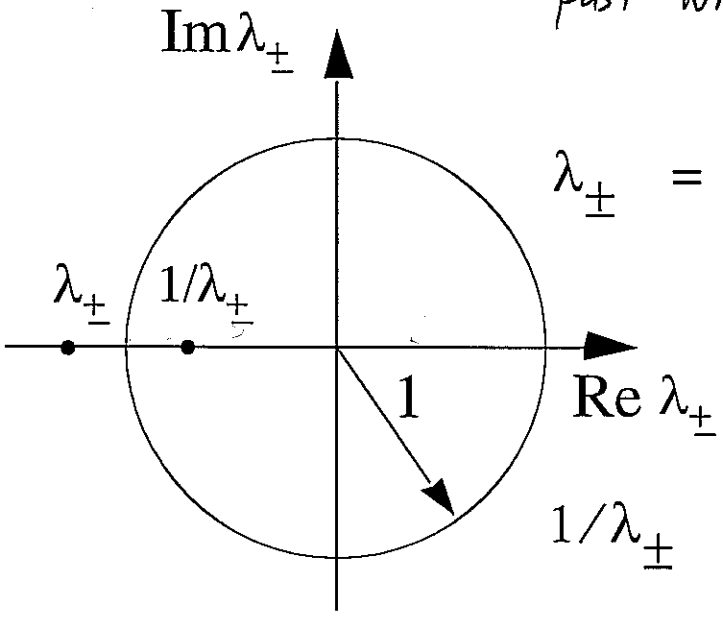

$$\lambda_\pm = \gamma_\pm e^{-i\pi}$$

$$1/\lambda_\pm = (1/\gamma_\pm)e^{-i\pi}$$

For more info see A. Dragt, "Lectures on Nonlinear Orbit Dynamics"
in "Physics of High Energy Accelerators" AIP Conf. Proc. No. 87 (AIP, New York, 1982) p. 147

In a periodic focusing system this condition will place restrictions on the lattice structure that are generally thought of in terms of phase advance limits. Accelerator lattices are almost always tuned for single particle stability. Because even for intense beam machines, when image charges are neglected, the beam centroid obeys single particle equations of motion and instability would result in undesireable, large beam centroid excursions.

- Space charge effects can introduce additional stability constraints on the lattice
  - Envelope modes may be unstable (lowest order collective mode)
  - Higher order space charge modes may be unstable.
- Nonlinear focusing terms in the applied field and machine construction errors etc. may also induce instabilities.

In the Homework problems, a simple example of a stability limit for a thin lens "FODO" periodic focusing channel is analyzed.

Later, we will show that for stable orbits that σ_0 can be interpreted as the phase-advance of single particle oscillations moving in the linear applied field.

J.J. Bernard and S.M. Lund
USPAS June 2006

See: Reiser §3.8.2
pgs 145–153

§6 Floquet's Theorem and the Phase-Amplitude Form of the Particle Orbit

Hill's equation:

$$\boxed{x''(s) + \kappa(s)\, x(s) = 0}$$

For periodic $\kappa(s)$:

$$\boxed{\kappa(s+L_p) = \kappa(s)}$$

Floquet's Theorem:

$x(s)$ has two linearly independent solutions that can be expressed as:

$$x_1(s) = W(s)\, e^{i\mu s}$$

$$x_2(s) = W(s)\, e^{-i\mu s}$$

$$\mu = \frac{1}{2} \mathrm{Tr}\, \bar{M}(s_i+L_p|s_i) = \cos\delta_0 = \text{const}$$

characteristic exponent

where $W(s)$ is a periodic function:

$$W(s+L_p) = W(s)$$

- Strictly speaking, theorem as written only applies when $\bar{M}(s_i+L_p|s_i)$ has non-degenerate eigenvalues. But a similar theorem applies to the degenerate case.
- Similar theorem is also valid for non-periodic $\kappa(s)$.

As a consequence of Floquet's theorem, any stable or nondegenerate unstable solution can be expressed in phase-amplitude form:

Phase-Amplitude Form

$$\boxed{\begin{aligned} x(s) &= A(s)\cdot\cos\psi(s) \qquad & A(s) &= \text{Amplitude} \\ A(s+L_p) &= A(s) \qquad & \psi(s) &= \text{Phase} \end{aligned}}$$

Derive eqns of motion in terms of A, ψ:

$$x = A\cos\psi$$
$$x' = A'\cos\psi - A\psi'\sin\psi$$
$$x'' = A''\cos\psi - 2A'\psi'\sin\psi - A\psi''\sin\psi - A\psi'^2\cos\psi$$

substitute in Hill's equation:

$$\boxed{x'' + \kappa x = \left[A'' + \kappa A - A\psi'^2\right]\cos\psi - \left[2A'\psi' + A\psi''\right]\sin\psi = 0}$$

We are free to introduce a constraint between A and ψ.

- 2 functions A, ψ; residual freedom allows an additional constraint

Take

$$\boxed{2A'\psi' + A\psi'' = 0} \Rightarrow \text{coeff of } \sin\psi = 0$$

Then, since $\cos\psi \neq 0$ for all ψ, the transformed equation of motion then gives:

$$\boxed{A'' + \kappa A - A\psi'^2 = 0} \Rightarrow \text{coeff of } \cos\psi = 0$$

The equation $2A'\psi' + A\psi'' = 0$ (coeff. of $\sin\psi$) can be integrated

$$2A'\psi' + A\psi'' = (A^2\psi')'/A = 0 \qquad A \neq 0$$
$$\Rightarrow (A^2\psi')' = 0$$
$$\Rightarrow \boxed{A^2\psi' = \text{const}}$$

One commonly rescales $A(s)$ such that this constant can be taken to be unity. Take

$$\boxed{\begin{aligned} &A(s) = A_i\, W(s) \quad ; \quad A_i = \text{const} \\ &W^2\psi' \equiv 1 \end{aligned}}$$

Then $W^2\psi' = 1$ can be equivalently expressed as:

$$\boxed{\begin{aligned} &\psi(s) = \psi_i + \int_{s_i}^{s} \frac{d\tilde{s}}{W^2(\tilde{s})} \\ &\psi_i = \text{const} \\ &\quad = \text{Initial phase} \end{aligned}}$$

Using $W^2\psi' = 1$ and $A = A_i W$ in the other equation $A'' + \kappa A - A\psi'^2 = 0$ (coeff of $\cos\psi$) then gives:

$$\boxed{W'' + \kappa W - \frac{1}{W^3} = 0}$$

where W is the periodic solution with period L_p, i.e.,

$$\boxed{W(s + L_p) = W(s)}$$

Summary: Phase Amplitude Form

$$x(s) = A_i\, w(s) \cos \psi(s)$$

where:

$$\begin{cases} w''(s) + \kappa(s)\, w(s) - \dfrac{1}{w^3(s)} = 0 \\ w(s+L_p) = w(s) \end{cases}$$

$$\psi'(s) = \frac{1}{w^2(s)} \quad ; \quad \psi(s) = \psi_i + \int_{s_i}^{s} \frac{d\tilde{s}}{w^2(\tilde{s})}$$

$$\equiv \psi_i + \Delta\psi(s)$$

In this phase-amplitude formulation, the particle trajectory in x-x' phase-space is:

$$x(s) = A_i\, w(s) \cos \psi(s)$$
$$x'(s) = A_i\, w'(s) \cos \psi(s) - \frac{A_i}{w(s)} \sin \psi(s)$$

Here, we have used $\psi' = 1/w^2$. The initial particle coordinates $x(s_i)$ and $x'(s_i)$ at $s = s_i$ are related to the amplitude and phase parameters at $s = s_i$, A_i and ψ_i, by:

$$x(s_i) = A_i\, w_i \cos \psi_i$$
$$x'(s_i) = A_i\, w_i' \cos \psi_i - \frac{A_i}{w_i} \sin \psi_i$$

$$w_i \equiv w(s_i) \quad ; \quad w_i' \equiv w'(s_i)$$

-or-

$$A_i \cos \psi_i = x(s_i)/w_i$$
$$A_i \sin \psi_i = x(s_i)\, w_i' - x'(s_i)\, w_i$$

Some points

1) The sign of $W(s)$ can be taken to be positive definite

$$\boxed{W(s) > 0}$$

"Proof":

Let $W(s)$ be positive at some value of s. Then

$$W'' + \kappa W - \frac{1}{W^3} = 0$$

insures that W can never vanish or change sign since as W becomes small, $W'' \approx 1/W^3 > 0$ can become arbitrarily large, thereby turning W back to the positive direction before W can vanish or reach negative values

- Sign choice removes ambiguity in relating initial conditions $X(s_i)$ and $X'(s_i)$ to A_i and ψ_i

2) $W(s)$ is a unique periodic function.
   - Can be proved using later connections between W and principal orbits.
   - W can be regarded as a special, periodic function characterizing the lattice.

3) The amplitude parameters:

$$W_i = W(s_i)$$
$$W_i' = W'(s_i)$$

depend <u>only</u> on the periodic lattice properties and are <u>independent</u> of the particle initial conditions.

4) The <u>phase advance</u>

$$\Delta\Psi(s) \equiv \int_{s_i}^{s} \frac{d\tilde{s}}{w^2(\tilde{s})}$$

will, in contrast, depend on s_i. However the phase advance through one Lattice period

$$\Delta\Psi(s_i+L_p) = \int_{s_i}^{s_i+L_p} \frac{d\tilde{s}}{w^2(\tilde{s})}$$

will be <u>independent</u> of s_i since w is a periodic function with period L_p.

- Will show that

$$\Delta\Psi(s_i+L_p) = \cos\delta_0$$

is the undepressed particle phase advance.

5) $w(s)$ has dimension [meters$^{1/2}$]

- Inconvenience of this motivate use of an alternative "betatron" function:

$$\beta(s) \equiv w^2(s)$$

with dimension [meters]. (see §8)

6) On the surface, what we have done: Transform a linear Hill's equation to nonlinear equations for w and Ψ via the phase amplitude method seems insane. Why?

- Method will help identify useful invariant (see §7)
- Decoupling of initial conditions enabled by phase-amplitude method will help simplify understanding of bundles of particles.

The principal functions in the transfer matrix analysis of the particle orbit can be expressed in phase amplitude form as:

$$\begin{pmatrix} x(s) \\ x'(s) \end{pmatrix} = \overline{M}(s|s_i) \begin{pmatrix} x(s_i) \\ x'(s_i) \end{pmatrix} = \begin{pmatrix} C(s|s_i) & S(s|s_i) \\ C'(s|s_i) & S'(s|s_i) \end{pmatrix} \begin{pmatrix} x(s_i) \\ x'(s_i) \end{pmatrix}$$

Some algebra identities: (in the problem sets):

$$C(s|s_i) = \frac{W(s)}{W_i} \cos \Delta\Psi(s) - W_i' W(s) \sin \Delta\Psi(s)$$

$$S(s|s_i) = W_i W(s) \sin \Delta\Psi(s)$$

$$C'(s|s_i) = \left(\frac{W'(s)}{W_i} - \frac{W_i'}{W(s)} \right) \cos \Delta\Psi(s) - \left(\frac{1}{W_i W(s)} + W_i' W'(s) \right) \sin \Delta\Psi(s)$$

$$S'(s|s_i) = \frac{W_i}{W(s)} \cos \Delta\Psi(s) + W_i W'(s) \sin \Delta\Psi(s)$$

where $\Delta\Psi(s) \equiv \int_{s_i}^{s} \frac{d\bar{s}}{W^2(\bar{s})}$ $\qquad W_i = W(s=s_i)$, $\quad W_i' = W'(s=s_i)$

Some manipulation (Appendix A) also shows that $W(s)$ is related to the principal orbit functions as:

$$W^2(s) = \beta(s) = \sin\delta_0 \cdot \frac{S(s|s_i)}{S(s_i+L_p|s_i)} + \frac{S(s_i+L_p|s_i)}{\sin\delta_0} \left[C(s|s_i) + \frac{(\cos\delta_0 - C(s_i+L_p|s_i))}{S(s_i+L_p|s_i)} S(s|s_i) \right]^2$$

$$\delta_0 \equiv \int_{s_i}^{s_i+L_p} \frac{d\tilde{s}}{W^2(s)} = \text{phase advance}$$

TOPS. FORM 7527 Made in U.S.A.

This formula for $W^2(s)$ in terms of principal orbits is very useful

- σ_0 (phase advance, see following pages) is generally specified for the lattice.
- Shows that W can be constructed with <u>two</u> principal orbit integrations over <u>one lattice period</u>
  - Integrations can be done numerically for $G'(s|s_i)$ and $S'(s|s_i)$.
  - No rootfinding for appropriate "initial" conditions is needed to construct $W(s)$ periodic
  - s_i can be anywhere in the lattice period and $W(s)$ will be independent of the specific choice of s_i
- The form of W^2 suggests an underlying Courant-Snyder invariant (see Appendix A and §7).
- $W^2 = \beta$ can be used to calculate the maximum beam particle excursions in the absence of space-charge. (see §8)
  - Very useful in machine design
  - Exploits Courant-Snyder Invariant (see §7)

Undepressed Particle Phase Advance

Now we can now connect σ_0 for a stable orbit to the advance in phase Ψ of the orbit through one lattice period:

$$\cos\sigma_0 \equiv \frac{1}{2}\,\mathrm{Trace}\,\overline{M}(s_i+L_p|s_i)$$

$$= \frac{1}{2}\left[C(s_i+L_p|s_i) + S'(s_i+L_p|s_i)\right]$$

$$= \frac{1}{2}\left(\frac{W(s_i+L_p)}{W_i} + \frac{W_i}{W(s_i+L_p)}\right)\cos\Delta\Psi(s_i+L_p)$$

$$+ \frac{1}{2}\left(W_i\,W'(s_i+L_p) - W_i'\,W(s_i+L_p)\right)\sin\Delta\Psi(s_i+L_p)$$

By periodicity:

$$W(s_i+L_p) = W_i \qquad \Rightarrow \qquad \text{coefficient of } \cos\Delta\Psi(s_i+L_p) = 1$$

$$W'(s_i+L_p) = W_i' \qquad \qquad \text{coefficient of } \sin\Delta\Psi(s_i+L_p) = 0$$

$$\boxed{\cos\sigma_0 = \cos\Delta\Psi(s_i+L_p) = \frac{1}{2}\,\mathrm{Trace}\,\overline{M}(s_i+L_p|s_i)}$$

Thus σ_0 is identified as the phase-advance of a stable particle orbit through one lattice period.

$$\boxed{\sigma_0 = \Delta\Psi(s_i+L_p) = \int_{s_i}^{s_i+L_p}\frac{d\bar{s}}{W^2(\bar{s})}}$$

Undepressed Particle Phase Advance.

Note that σ_0 is independent of s_i since $W(s)$ is periodic. The stability criteria $\frac{1}{2}\left|\mathrm{Trace}\,\overline{M}(s_i+L_p|s_i)\right| = |\cos\sigma_0| \le 1$ is now connected to the phase advance of the particle through one period of the focusing lattice.

TOPS FORM 7527 Made in U.S.A.

The phase advance is an extremely useful dimensionless measure to characterize the focusing strength of lattices. Much of conventional accelerator physics centers on focusing strength and suppression of resonance effects. The phase advance is a natural parameter to employ in these situations to present results in a readily interpretable and generalizable manner.

We now present phase advance formulas for σ_0 for 3 classes of periodic lattices with piecewise constant $\kappa_x(s)$ and $\kappa_y(s)$.

a) Continuous Focusing
b) Solenoidal Focusing
c.) Quadrupole Doublet focusing

These formulas are derived from transfer matrix analysis and direct integration of the equations of motion:

1/ Continuous Focusing

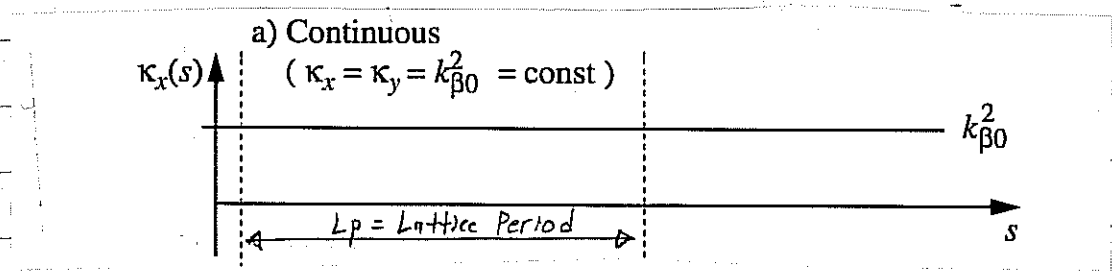

$$\boxed{\sigma_0 = k_{\beta 0} L_p}$$

The "lattice period" here is an arb. length for phase accumulation

S.M. Lund 11/

b) Periodic Solenoidal Focusing

Phase advance must be interpreted in the rotating Larmor frame. (see earlier lectures.)

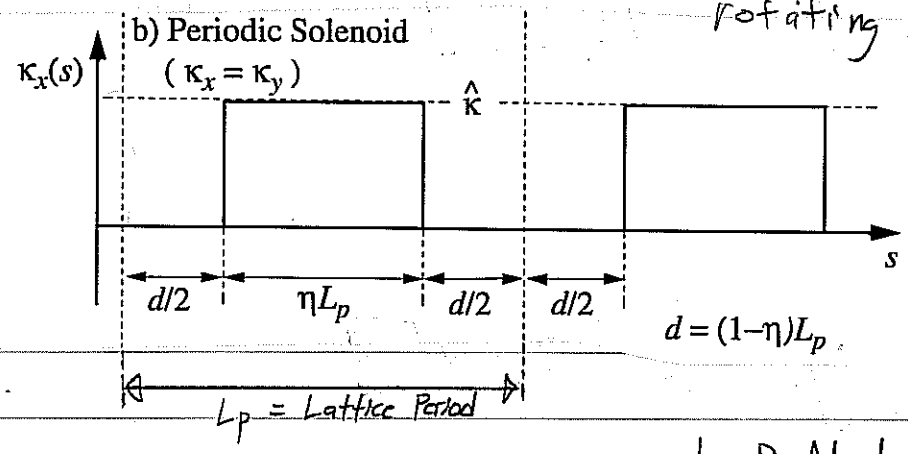

d = Drift length

$\eta \in [0,1]$ = occupancy of solenoid in period.

$$\cos\sigma_0 = \cos(2\Theta) - \frac{1-\eta}{\eta}\Theta\sin(2\Theta)$$

$$\Theta \equiv \sqrt{\hat{\kappa}}\eta L_p/2$$

c) Periodic Quadrupole Doublet Lattice

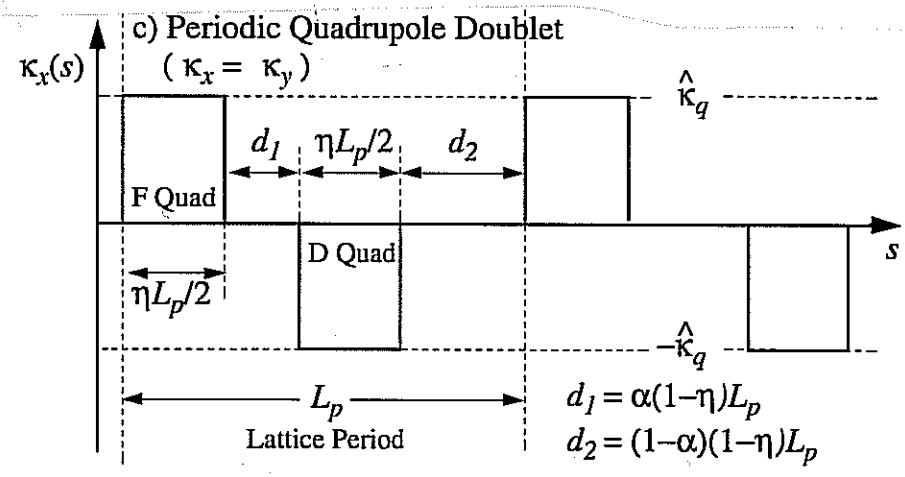

$$\cos\sigma_0 = \cos\Theta\cosh\Theta + \frac{1-\eta}{\eta}\Theta(\cos\Theta\sinh\Theta - \sin\Theta\cosh\Theta) - 2\alpha(1-\alpha)\frac{(1-\eta)^2}{\eta^2}\Theta^2\sin\Theta\sinh\Theta$$

$$\Theta \equiv \sqrt{|\hat{\kappa}_q|}\eta L_p/2$$

d_1, d_2 drift lengths

$\eta \in (0,1]$ = occupancy of quads in period

$\alpha \in [0,1]$ = syncopation parameter

α measures how close focusing (F) and defocusing (D) quadrupoles are to eachother in the lattice.

$$\alpha = 0: \quad d_1 = 0, \quad d_2 = (1-\eta) L_p$$
$$\alpha = 1: \quad d_1 = (1-\eta) L_p, \quad d_2 = 0$$

$$\alpha = \frac{1}{2} \Rightarrow d_1 = d_2 = (1-\eta)\frac{L_p}{2} \equiv \text{"FODO" lattice, with equal drifts.}$$

The range $\alpha \in [\frac{1}{2}, 1]$ can be mapped to $\alpha \in [0, \frac{1}{2}]$ by relabeling lattice quantities. Therefore, take:

$$\alpha \in [0, \tfrac{1}{2}]$$

Thin Lens limit

Convenient to simply understand scaling

$$\kappa_x(s) = \frac{1}{f}\delta(s - s_0)$$

s_0 = optic location
f = const, focal length.

$$\begin{pmatrix} x \\ x' \end{pmatrix}_{s=s_0^+} = \begin{pmatrix} 1 & 0 \\ -\frac{1}{f} & 1 \end{pmatrix} \begin{pmatrix} x \\ x' \end{pmatrix}_{s=s_0^-}$$

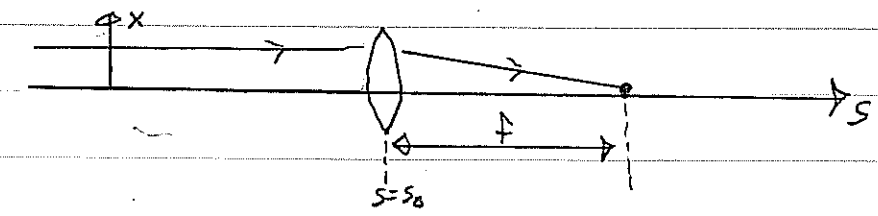

The thinlens limit of "thick" solenoids and quadrupoles can be obtained by taking

Solenoids: $\hat{\kappa} \equiv \frac{1}{\eta f L_p}$; then $\lim_{\eta \to 0}$

Quadrupoles: $\hat{\kappa}_q \equiv \frac{2}{\eta f L_p}$; then $\lim_{\eta \to 0}$

This obtains:

$$\cos\sigma_0 = \begin{cases} 1 - \frac{1}{2}\frac{L_p}{f}, & \text{thin-lens solenoids,} \\ 1 - \frac{\alpha}{2}(1-\alpha)(\frac{L_p}{f})^2, & \text{thin-lens quadrupoles.} \end{cases}$$

This formula can also be derived directly from thin lens transfer matrices:

$$\cos\sigma_0 = \frac{1}{2}\mathrm{Tr}\begin{bmatrix} 1 & L_p \\ 0 & 1 \end{bmatrix}\begin{bmatrix} 1 & 0 \\ -\frac{1}{f} & 1 \end{bmatrix} = 1 - \frac{1}{2}\frac{L_p}{f},$$

Solenoid lattice

$$\cos\sigma_0 = \frac{1}{2}\mathrm{Tr}\begin{bmatrix} 1 & 0 \\ -\frac{1}{f} & 1 \end{bmatrix}\begin{bmatrix} 1 & \alpha L_p \\ 0 & 1 \end{bmatrix}\begin{bmatrix} 1 & 0 \\ \frac{1}{f} & 1 \end{bmatrix} \times \begin{bmatrix} 1 & (1-\alpha)L_p \\ 0 & 1 \end{bmatrix} = 1 - \frac{\alpha}{2}(1-\alpha)\left(\frac{L_p}{f}\right)^2,$$

Quadrupole doublet lattice.

In many cases it is also desireable to have simple formulas for design that relate magnet parameters to σ_0. For example, if the formula for $\cos\sigma_0$ is expanded to leading order in $\theta = \sqrt{|\hat{\kappa}_q|}\,\eta L_p/2$ for quadrupole doublet focusing, we obtain:

$$\cos\sigma_0 = 1 - \frac{(\eta\hat{\kappa}_q L_p^2)^2}{32}\left[\left(1-\frac{2}{3}\eta\right) - 4\left(\alpha - \frac{1}{2}\right)^2(1-\eta)^2\right].$$

where

$$\hat{\kappa}_q = \begin{cases} \dfrac{\hat{G}}{[B\rho]} & ; \text{ Magnetic Quadrupoles} \\ \dfrac{\hat{G}}{\beta_b c\,[B\rho]} & ; \text{ Electric Quadrupoles} \end{cases} \qquad \hat{G} = \text{Field Gradient.}$$

Plot eqn:

For $\sigma_0 = 80^\circ$/period Quadrupole

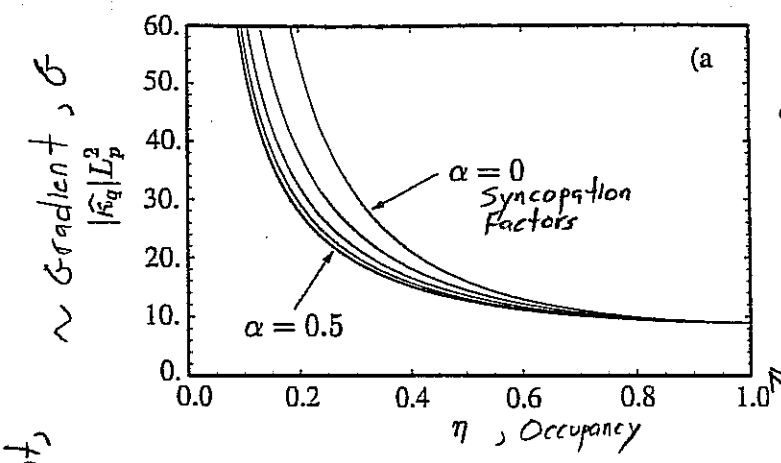

$\alpha = 0, 0.1, 0.2, 0.3, 0.4, 0.5$

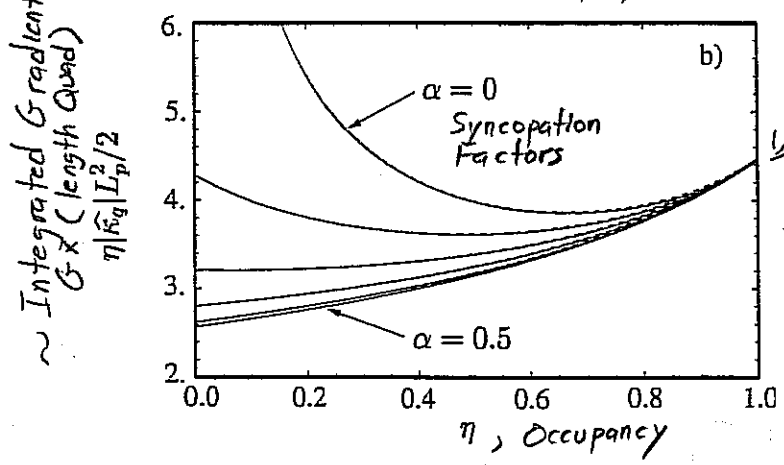

Dashed Curves Exact results (almost overlay)

J.J. Barnard and S.M. Lund
USPAS June 2006

§6 Appendix A: Calculation of W(s) from Principal Orbit Functions

Evaluate transfer matrix elements through one lattice period using:

$$W(s_1+L_p) = W_1$$
$$W'(s_1+L_p) = W_1'$$

and

$$\Delta\Psi(s_1+L_p) = \int_{s_1}^{s_1+L_p} \frac{d\tilde{s}}{W^2(\tilde{s})} = \sigma_0$$

to obtain:

$$C(s_1+L_p|s_1) = \cos\sigma_0 - W_1 W_1' \sin\sigma_0$$
$$S(s_1+L_p|s_1) = W_1^2 \sin\sigma_0$$

$$C'(s_1+L_p|s_1) = -\left(\frac{1}{W_1^2} + W_1 W_1'\right)\sin\sigma_0$$
$$S'(s_1+L_p|s_1) = \cos\sigma_0 + W_1 W_1' \sin\sigma_0$$

giving:

$$\boxed{\begin{aligned} W_1 &= \sqrt{\frac{S(s_1+L_p|s_1)}{\sin\sigma_0}} \\ W_1' &= \frac{\cos\sigma_0 - C(s_1+L_p|s_1)}{\sqrt{S(s_1+L_p|s_1)\sin\sigma_0}} \end{aligned}}$$

or using $\beta = W^2$ and $\beta' = 2WW'$

$$\boxed{\begin{aligned} \beta_1 &= W_1^2 = \frac{S(s_1+L_p|s_1)}{\sin\sigma_0} \\ \beta_1' &= 2W_1 W_1' = \frac{2\left(\cos\sigma_0 - C(s_1+L_p|s_1)\right)}{\sin\sigma_0} \end{aligned}}$$

Next, calculate W from the elements

$$\frac{S'}{W_i W} = \sin \Delta\Psi$$

$$\frac{W_i}{W} C + \frac{W_i'}{W} S' = \cos \Delta\Psi$$

Here $S' \equiv S'(s|s_i)$ etc.

square:

$$\frac{S'^2}{W_i^2 W^2} + \left(\frac{W_i C}{W} + \frac{W_i' S'}{W} \right)^2 = 1$$

- See p 7: This structure, not accidently, has a Courant-Snyder invariant form.

$$\Rightarrow W^2 = \frac{S'^2}{W_i^2} + \left(W_i C + W_i' S' \right)^2$$

Use W_i and W_i' identified and write out:

$$\boxed{W^2(s) = \beta^2(s) = \sin\delta_0 \frac{S'^2(s|s_i)}{S'(s_i+L_p|s_i)} + \frac{S'(s_i+L_p|s_i)}{\sin\delta_0} \left[C(s|s_i) + \frac{(\cos\delta_0 - C(s_i+L_p|s_i))}{S'(s_i+L_p|s_i)} S'(s|s_i) \right]^2}$$

- Formula shows that for given δ_0 (used to specify lattice focus strength) that $W(s)$ is given by two linear principal orbits calculated over one lattice period.
  - Easy to do numerically!

An alternative way to calculate $W(s)$ or $\beta(s)$ is as follows:

$$C(s+L_p|s) = \cos\delta_0 - W(s)W'(s)\sin\delta_0$$
$$S(s+L_p|s) = W^2(s)\sin\delta_0$$

Thus

$$\boxed{W^2(s) = \beta(s) = \frac{S(s+L_p|s)}{\sin\delta_0}}$$

$S(s+L_p|s)$ is M_{12} element of $\overline{M}(s+L_p|s)$

Direct application of this formula requires calculation of $S(s+L_p|s)$ at every value of s desired over the period. The previous method requires <u>one</u> calculation of $C(s|s_i)$ and $S(s|s_i)$ for $s_i \le s \le s_i+L_p$ for any value of s_i. Thus, although the previous formula is simpler to apply in practice. Yet another alternative, is to calculate $W^2(s)$ using Matrix algebra and symmetry:

Advance interval:

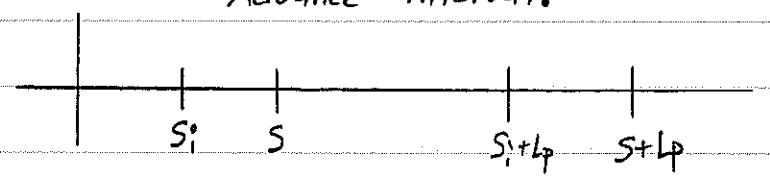

$$\boxed{M_{11}(s+L_p|s) = \sin\delta_0\, W^2(s) = \sin\delta_0\, \beta(s)}$$

Alternative expression of above.

But

$$\overline{M}(s+L_p|s) = \overline{M}(s+L_p|s_i+L_p)\overline{M}(s_i+L_p|s) \quad // I$$
$$= \overline{M}(s|s_i)\underbrace{\overline{M}(s_i+L_p|s)\left[\overline{M}(s|s_i)\right.}_{=\overline{M}(s_i+L_p|s_i)}\left.\overline{M}^{-1}(s|s_i)\right]$$

-or-

$$\boxed{\overline{M}(s+L_p|s) = \overline{M}(s|s_i)\,\overline{M}(s_i+L_p|s_i)\,\overline{M}^{-1}(s|s_i)}$$

Since this uses only elements $\overline{M}(s|s_i)$ for $s_i \le s \le s_i+L_p$ on the RHS, it shows that $\overline{M}(s+L_p|s)$ can be calculated from the evaluation of $\overline{M}(s|s_i)$ over one period with s_i <u>anywhere</u> in the period.
Only the M_{12} element will be needed to calculate $W(s)$.

If we take

$$\overline{M} = \begin{pmatrix} C & S \\ C' & S' \end{pmatrix} \qquad \det \overline{M} = 1$$

(Wronskian condition)

$$\Rightarrow \quad \overline{M}^{-1} = \begin{pmatrix} S' & -C' \\ -S & C \end{pmatrix}$$

using in the eqn above:

$$\overline{M}(s+L_p|s) = \begin{pmatrix} C(s|s_i) & S(s|s_i) \\ C'(s|s_i) & S'(s|s_i) \end{pmatrix} \begin{pmatrix} C(s_i+L_p|s_i) & S(s_i+L_p|s_i) \\ C'(s_i+L_p|s_i) & S'(s_i+L_p|s_i) \end{pmatrix}$$

$$\cdot \begin{pmatrix} S'(s|s_i) & -C'(s|s_i) \\ -S(s|s_i) & C(s|s_i) \end{pmatrix}$$

The $\overline{M}_{12}$ element of this can be explicitly calculated. Using the phase advance definition and the Wronskian, some algebra (see Lund, Chilton, and Lee, "Phys. Rev. Special Topics - Accel. and Beams, 2006) obtains the same formula previously derived.

J.J. Barnard and S.M. Lund
USPAS June 2006

See: Reiser §3.8.2 pgs 145-153

§7 The Courant-Snyder Invariant and Single-Particle Emittance

Constants of the motion simplify interpretation of dynamics in physics.

// Example Review Continuous Focusing System $\leftrightarrow$ simple harmonic oscillator.

$$x'' + k_{\beta 0}^2 x = 0 \quad ; \quad k_{\beta 0}^2 = \text{const.}$$

$$\Rightarrow \boxed{H = \frac{x'^2}{2} + \frac{k_{\beta 0}^2}{2} x^2 = \text{const.}}$$ Conserved Hamiltonian

Particle motion is constrained to move on an ellipse in $x-x'$ phase space with max extents

$$x_{max} \Rightarrow x' = 0 \quad : \quad x_{max_\pm} = \pm\sqrt{2H/k_{\beta 0}^2}$$

$$x'_{max} \Rightarrow x = 0 \quad : \quad x'_{max_\pm} = \pm\sqrt{2H}$$

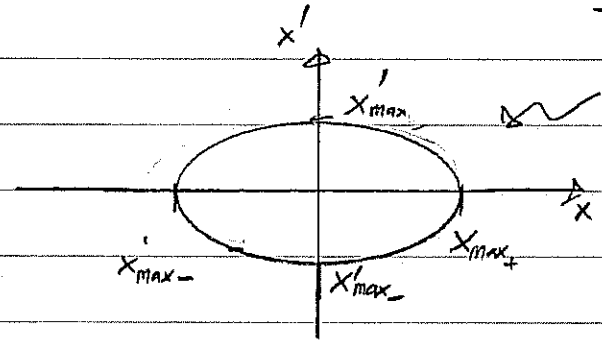

Location of particle on ellipse set by initial conditions. But all initial conditions yield the same shape ellipse thereby simplifying understanding of phase-space evolution. //

Question

For Hill's equation:

$$x''(s) + \kappa(s) x(s) = 0$$

Is there a quadratic invariant that can aid interpretation of the dynamics? Yes! Courant-Snyder Invariant.

TOPS FORM 7527
Made in U.S.A.

Courant-Snyder Invariant

The Courant-Snyder Invariant of Hill's equation is extremely important in accelerator physics.

- Helps interpretation of dynamics
- Named after it's discoverers, Courant and Snyder, who in a seminal (and very elegant!) paper simultaneously developed strong (AG) focusing and constructed/exploited this invariant to understand AG focusing.

  Courant and Snyder, "Theory of the Alternating Gradient Synchrotron" Annals of Physics 3, 1 (1958).

  — Christofolos also understood AG focusing via a more heuristic analysis.

The phase-amplitude method described in §6 makes the construction easy!

$$\boxed{\begin{aligned} x(s) &= A_i \, W(s) \cos \psi(s) \\ x'(s) &= A_i \, w'(s) \cos \psi(s) + \frac{A_i}{W(s)} \sin \psi(s) \end{aligned}}$$

where

$$W'' + \kappa W - \frac{1}{W^3} = 0$$

Re-arrange the phase-amplitude trajectory equations:

$$\frac{x}{w} = A_i \cos\psi$$

$$wx' - w'x = A_i \sin\psi$$

Add the squares to obtain the Courant-Snyder invariant

Courant-Snyder Invariant

$$\boxed{\left(\frac{x}{w}\right)^2 + (wx' - w'x)^2 = A_i^2(\cos^2\psi + \sin^2\psi) = A_i^2 = \text{const}}$$

- Quadratic structure in x, x' defines a rotated ellipse in x-x' phase-space.

- $w^2\left(\frac{x}{w}\right)' = wx' - w'x$, so we can alternatively express the Courant-Snyder invariant as:

$$\left(\frac{x}{w}\right)^2 + \left[w^2\left(\frac{x}{w}\right)'\right]^2 = \text{const.}$$

To better interpret the Courant-Snyder invariant, expand while isolating terms in x^2, xx', and x'^2

$$\left(\frac{1}{w^2} + w'^2\right)x^2 + 2(-ww')xx' + w^2x'^2 = A_i^2 = \text{const.}$$

The coefficients of x^2, xx', and x'^2 are functions of the lattice only and do not involve particle initial conditions. It is conventional to label these coefficients using "Twiss parameter" notation as:

$$\boxed{\begin{aligned} \beta(s) &\equiv w^2(s) \\ \alpha(s) &\equiv -w(s)\,w'(s) \\ \gamma(s) &\equiv \frac{1}{w^2(s)} + w'(s)^2 = \frac{1+\alpha^2(s)}{\beta(s)} \end{aligned}}$$

Then the Courant-Snyder Invariant is expressed as:

$$\boxed{\gamma x^2 + 2\alpha x x' + \beta x'^2 = A_i^2 = \text{const.}}$$

The "area" of this ellipse in xx' phase space is:

$$\boxed{\text{Area} = \int_{\text{ellipse}} dx\,dx' = \frac{\pi A_i^2}{\sqrt{\gamma\beta - \alpha^2}} = \pi A_i^2 \equiv \pi \varepsilon}$$

Analytic Geometry Formula.

where ε is the <u>single particle emittance</u> which corresponds to the phase space area enclosed by the particle orbit <u>divided by π</u>.

// <u>Aside</u> Units

The definition of emittance is not unique. Some prefer to call $\pi\varepsilon$ the emittance. Some write emittance values in units of mm-mrad with a "π" in the units as a reminder, i.e., $\varepsilon = 10\ \pi$-mm-mrad, etc. Use caution to understand the convention used! //

TOPS FORM 7527 Made in U.S.A.

From these identifications:

$$\boxed{\gamma x^2 + 2\alpha x x' + \beta x'^2 = \varepsilon = \text{const.}}$$

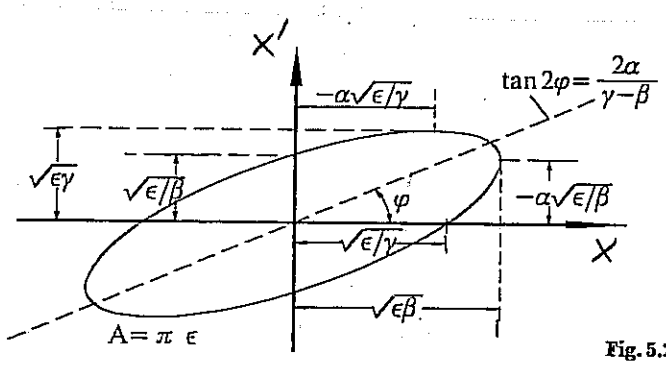

Fig. 5.22. Phase space ellipse

152

From Wiedemann

Properties of Courant-Snyder Invariant

- The ellipse will rotate and change shape as the particle advances through the focusing lattice. But the area of the ellipse will not change. ($\pi\varepsilon = \text{const}$).

- The location of the particle on the ellipse and the size of the ellipse depends on the initial conditions of the particle.

- The orientation of the ellipse is independent of the particle initial conditions. All particles move on nested ellipses.

- The Courant-Snyder invariant is quadratic in the phase-space coordinates, but it is not the transverse particle energy (which is not conserved).

TOPS FORM 7527 Made in U.S.A.

// <u>Example</u> Particle Hamiltonian and energy of a kicked oscillator

$$x'' + \kappa(s)x = 0 \quad ; \quad \kappa(s) \neq \text{const.}$$

$$H = \frac{x'^2}{2} + \frac{\kappa}{2}x^2 \neq \text{const}$$

to see this:

$$\frac{dx}{ds} = \frac{\partial H}{\partial x'} = x'$$

$$\frac{dx'}{ds} = -\frac{\partial H}{\partial x} = -\kappa x$$

$$\frac{dH}{ds} = \frac{\partial H}{\partial s} + \frac{\partial H}{\partial x}\frac{dx}{ds} + \frac{\partial H}{\partial x'}\frac{dx'}{ds} = \frac{\partial H}{\partial s} = \frac{\kappa'}{2}x^2 \neq \text{const.}$$

The energy of a kicked oscillator is not conserved. Do not confuse the energy of an oscillator with the Courant-Snyder invariant. <u>Only</u> in a continuous focusing system (simple harmonic oscillator) will they be simply related:

$$\kappa(x) = k_{\beta 0}^2 = \text{const} \qquad \text{Continuous focusing}$$

$$\Rightarrow H = \frac{x'^2}{2} + \frac{k_{\beta 0}^2}{2}x^2 = \text{const.}$$

$$w'' + k_{\beta 0}^2 w - \frac{1}{w^3} = 0$$

$$\Rightarrow w = \sqrt{\frac{1}{k_{\beta 0}}} = \text{const} \qquad \text{solution.}$$

$$\beta(s) = w^2 = 1/k_{\beta 0} = \text{const}$$

$$\alpha(s) = -ww' = 0$$

$$\gamma(s) = \frac{1}{w^2} + w'^2 = k_{\beta 0} = \text{const.}$$

$$\varepsilon = k_{\beta 0}x^2 + \frac{x'^2}{k_{\beta 0}} = \frac{2}{k_{\beta 0}}\left(\frac{1}{2}x'^2 + \frac{k_{\beta 0}^2}{2}x^2\right) = \text{const.}$$

$$= 2H/k_{\beta 0} = \text{const.}$$

//

TOPS FORM 7507
Made in U.S.A.

Aside: Lattice Maps

The Courant-Snyder invariant helps us understand the phase space evolution of the particles. Knowing how the ellipse transforms (twists and rotates without changing area) is equivalent to knowing the dynamics of a bundle of particles

General s:

$$\gamma x^2 + 2\alpha x x' + \beta x'^2 = \varepsilon$$

Initial $s = s_i$:

$$\gamma_i x_i^2 + 2\alpha_i x_i x_i' + \beta_i x_i'^2 = \varepsilon$$

$$\beta_i \equiv \beta(s_i)$$
$$\alpha_i \equiv \alpha(s_i)$$
$$\gamma_i = \gamma(s_i)$$

Identify coefficients of the transport matrix:

$$\begin{bmatrix} x(s) \\ x'(s) \end{bmatrix} = \begin{bmatrix} C(s|s_i) & S(s|s_i) \\ C'(s|s_i) & S'(s|s_i) \end{bmatrix} \begin{bmatrix} x_i \\ x_i' \end{bmatrix}$$

$$(S'^2\gamma_i - 2S'C'\alpha_i + C'^2\beta_i)x^2 +$$
$$2(-SS'\gamma_i + S'C\alpha_i + SC'\alpha_i - CC'\beta_i)xx' +$$
$$(S^2\gamma_i - 2SC\alpha_i + C^2\beta_i)x'^2 = \varepsilon$$

-or-

$$\begin{bmatrix} \beta \\ \alpha \\ \gamma \end{bmatrix} = \begin{bmatrix} C^2 & -2SC & S^2 \\ -CC' & (S'C+SC') & -SS' \\ C'^2 & -2S'C' & S'^2 \end{bmatrix} \begin{bmatrix} \beta_i \\ \alpha_i \\ \gamma_i \end{bmatrix}$$

TOPS FORM 7527 Made in U.S.A.

Example: Ellipse Maps:

Drift: length s

$$\begin{bmatrix} c & s \\ c' & s' \end{bmatrix} = \begin{bmatrix} 1 & s-s_i \\ 0 & 1 \end{bmatrix}$$

$$\beta = \beta_0 - 2\alpha_i(s-s_i) + \gamma_i(s-s_i)^2$$
$$\alpha = \alpha_i - \gamma_i(s-s_i)$$
$$\gamma = \gamma_i$$

Focusing lense (discreet kick)

$$\begin{bmatrix} c & s \\ c' & s' \end{bmatrix} = \begin{bmatrix} 1 & 0 \\ -1/f & 1 \end{bmatrix}$$

$f > 0$ focusing strength.

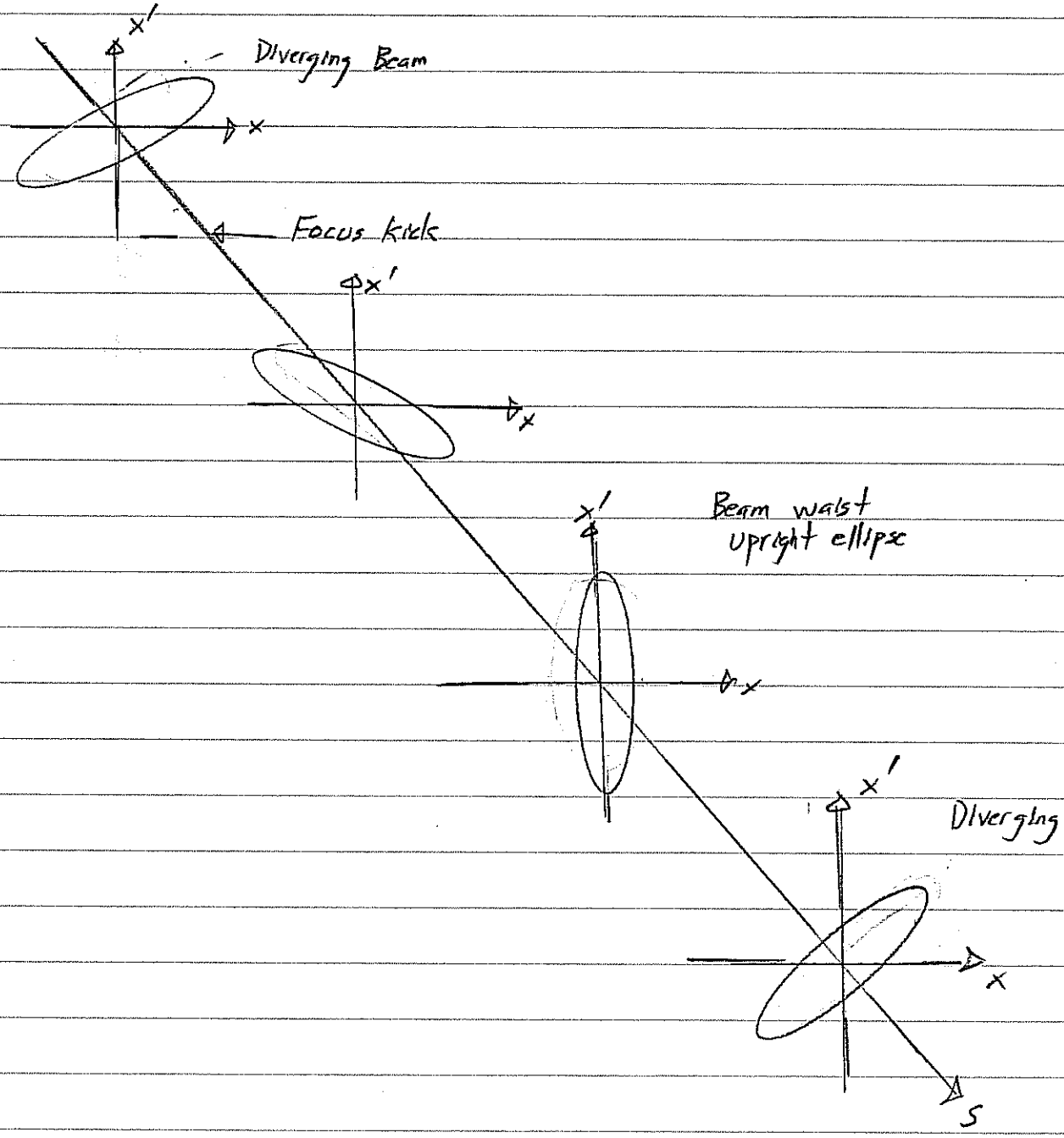

TOPS
FORM 7527
Made in U.S.A.

J.J. Barnard and S.M. Lund
USPAS June 2006

See: Reiser §3.8.2 pgs. 144-153

§8 Betatron Formulation of Particle Orbit

The phase amplitude form we originally chose

$$\boxed{x(s) = A_i\, w(s) \cos \psi(s)}$$

is not a unique choice and w has unusual dimensions of meters$^{1/2}$. Due to this and the utility of the Twiss parameters in describing the Courant-Snyder invariant and the orientation of the phase space ellipse on which the particle moves, it is convenient to take an alternative phase-amplitude representation with:

$$x(s) = \sqrt{\varepsilon}\sqrt{\beta(s)} \cos \psi(s)$$

β-tron function: $\beta(s) \equiv w^2(s)$

emittance: $\varepsilon = A_i^2 = \text{const.}$

phase: $\psi(s) = \psi_i + \int_{s_i}^{s} \frac{d\bar{s}}{\beta(\bar{s})} = \psi_i + \Delta\psi(s)$

Here, $\beta(s) = w^2$ has dimensions of meters.
Note that the initial phase ψ_i will differ from the initial phase in the previous phase-amplitude form $x = A_i\, w \cos(\psi_0 + \Delta\psi)$ since $\sqrt{\varepsilon} > 0$ (we choose not to distinguish the ψ_i for notational simplicity), but the phase advance:

$$\Delta\psi(s) = \int_{s_i}^{s} \frac{d\bar{s}}{w^2(\bar{s})} = \int_{s_i}^{s} \frac{d\bar{s}}{\beta(\bar{s})}$$

is identical in both formulations.

FORM 7527
Made in U.S.A.

In this case the β-tron function satisfies:

$$\boxed{\begin{gathered}\frac{1}{2}\beta(s)\beta''(s) - \frac{1}{4}\beta'^2(s) + \beta^2(s)\kappa(s) = 1 \\ \beta(s+L_p) = \beta(s) \\ \beta(s) > 0.\end{gathered}}$$

From the particle orbit equation

$$x = \sqrt{\varepsilon\beta}\cos\psi,$$

the maximum possible excursion of the particle, $x_m = \mathrm{Max}[|x|]$ occurs where $\cos\psi = \pm 1$ and

$$\boxed{x_m(s) = \sqrt{\varepsilon_m\beta(s)} = \sqrt{\varepsilon_m}\, W(s)}$$

ε_m = max single-particle emittance.

Since all particles move on nested ellipses, the maximum possible excursion of all particles is given by this expression with the maximum single-particle emittance. This excursion is the minimum possible aperture of the accelerator structures to prevent single particle loss. Resonance effects due to nonlinear focusing fields, space-charge, image charges, imperfect vacuum, and finite particle lifetime all influence the practical aperture choice.

TOPS
FORM 7527
Made in U.S.A.

From the equation for w:

$$w''(s) + \kappa(s)\, w(s) - \frac{1}{w^3(s)} = 0$$

$$w(s+L_p) = w(s) \quad ; \quad w(s) > 0$$

we obtain the equation for the maximum envelope of particle orbits $x_m = \sqrt{\varepsilon_m}\, w$

$$\boxed{\begin{gathered} x_m''(s) + \kappa(s)\, x_m(s) - \frac{\varepsilon_m^2}{x_m^3(s)} = 0 \\ x_m(s+L_p) = x_m(s) \\ x_m > 0 \end{gathered}}$$

Note the similarity of this equation to the statistical envelope equations derived in the intro lectures by J.J. Barnard

- When an extra term is added to include linear space-charge forces this equation is the commonly used KV envelope equation.
- Connection will be covered in more detail later.

Comment:

The use of β for this function along with α, β, γ for Twiss parameters does not often result in confusion with relativistic factors (often denoted β, γ rather than β_b and γ_b as used here) because the context usually makes the intent clear. Often relativistic factors are absorbed into definitions of focusing strengths κ too, etc.

J.J. Barnard and S.M. Lund
USPAS, June 2006

See Reiser §5.4.10 pp 437-447

§9 Momentum Spread Effects

Up to this point, we have analyzed particle dynamics with momentum

$$\boxed{p_s = m\gamma_b\beta_b c = \text{const.}}$$

for all particles in a beam slice. In reality, there will be a finite spread of particle momenta in the slice:

$$\boxed{\begin{aligned} p_s &= p_0 + \delta p \\ p_0 &= m\gamma_b\beta_b c = \text{design momentum} \\ \delta p &= \text{"off" momentum} \end{aligned}}$$

Typical values for momentum spread are:

$$\frac{|\delta p|}{p_0} \sim 10^{-2} \text{ to } 10^{-6}$$

in a beam with a single species of particles and a machine with conventional sources and accelerating structures. This spread of momentum can modify particle orbits, particularly in machines with dipole bends where the bending radius of a particle varies strongly with the particle momentum.

To better understand this effect, we analyze the particle equations of motion with leading order dispersive effects:

$$x''(s) + \left[\frac{1}{R(s)^2}\,\frac{1-\delta}{1+\delta} + \frac{\kappa_x(s)}{(1+\delta)^n}\right] x(s) = \frac{\delta}{1+\delta}\cdot\frac{1}{R(s)}$$

$$y''(s) + \frac{\kappa_y(s)}{(1+\delta)^n}\, y(s) = 0$$

where:

$R(s)$ = Local bend radius for design momentum p_0 ($R \to \infty$ in straight sections)

$$\frac{1}{R} = \frac{B_y^a\big|_{dipole}}{[B\rho]} \qquad [B\rho] = p_0/q$$

$\delta \equiv \dfrac{\delta p}{p_0}$ = Fractional momentum error.

$$n = \begin{cases} 1 \; ; & \text{Magnetic Quadrupoles} \\ 2 \; ; & \text{Solenoids, Electric Quadrupoles} \end{cases}$$

Here we have neglected:

- Space charge effects: $\phi \to 0$
- Nonlinear applied focusing: $\vec{E}^a, \vec{B}^a$ contain only linear focusing terms.
- Acceleration: $p_0 = m\gamma_b\beta_b = \text{const.}$

Also, the bends are set from the design particle orbit (see §1)

Terms resulting from the momentum spread can be lumped into two classes, chromatic and dispersive:

<u>Chromatic terms</u>: present in both x- and y-equations resulting from applied focusing fields

$$k_x \cdot x \longrightarrow \frac{k_x x}{(1+\delta)^n}$$

$$k_y \cdot y \longrightarrow \frac{k_y y}{(1+\delta)^n}$$

where $k_{x,y}$ remains defined by the design momentum.

Particle momentum changes vary the focal strength of optics and will thereby modify the phase space trajectory of particles.

- Generally not important (corrections not large) except for very small focal spots when the beam is focused onto a target or when momentum spreads are large.

- Lectures by J.J. Barnard will overview consequences of this effect in final focus optics. We will neglect these terms here.

<u>Dispersive terms</u>: only in the x-equation results from dipole bends in x

Result from particles being bent at different radii when the momentum deviates from the design value. Dispersive terms contain the bend radius R:

$$\frac{1}{R^2(s)}\,\frac{1-\delta}{1+\delta}\,x(s) \quad ; \quad \frac{\delta}{1+\delta}\,\frac{1}{R(s)}$$

Generally, bend radii R are large and δ is small, and we can take to leading order:

$$\left[\frac{1}{R^2}\,\frac{1-\delta}{1+\delta} + k_x\right] x \simeq k_x x$$

$$\frac{\delta}{1+\delta}\,\frac{1}{R} \simeq \frac{\delta}{R}$$

and the equations become:

$$\boxed{\begin{aligned} x''(s) + k_x(s)\,x(s) &= \frac{\delta}{R(s)} \\ y''(s) + k_y(s)\,y(s) &= 0 \end{aligned}}$$

At this level of approx., no change in y-equation

Generally, the x-equation is solved for periodic lattices by exploiting the linear structure of the equation and resolving:

$$\boxed{x = \underset{\text{Particular Sol.}}{x_p} + \underset{\text{Homogeneous sol.}}{x_h}}$$

where

x_h is the general solution to:

$$\boxed{x_h''(s) + K_x(s)\, x_h(s) = 0}$$

and x_p is the <u>periodic solution</u> to:

$$\boxed{\begin{aligned} x_p &= \delta \cdot D \\ D''(s) + K_x(s)\, D(s) &= \frac{1}{R(s)} \\ D(s+L_p) &= D(s) \end{aligned}}$$

This convenient resolution can always be made. D is called the dispersion function and $\delta \cdot D$ measures the offset of the particle orbit with respect to the design orbit.

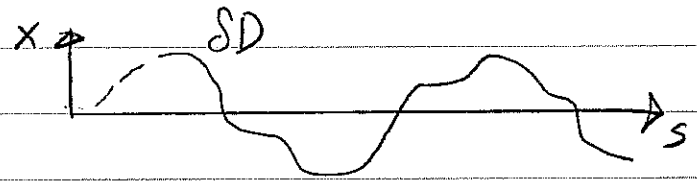

$x = 0 \Rightarrow$ Design orbit.

Bundle of particles $D=0$ | Bundle of particles $D \neq 0$

distribution of δ values

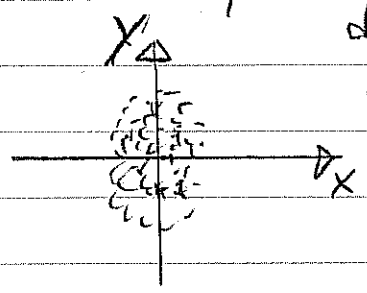

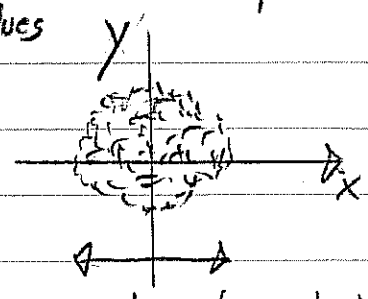

broadens in x

Note: $[D]$ = meters

$\Rightarrow$ $\delta \cdot D$ gives orbit offset in meters.

// Example – Continuous Focusing in a continuous bend.

$$K_x(s) = k_{\beta 0}^2 = \text{const.}$$
$$R(s) = R = \text{const.}$$

$$\Rightarrow \quad D'' + k_{\beta 0}^2 D = \frac{1}{R} \quad \Rightarrow \quad D = \frac{1}{k_{\beta 0}^2 R}$$

In periodic lattices D will oscillate with (approx.) average value:

$$D \sim \frac{L_p^2}{\sigma_0^2 R}$$

//

Many rings are designed to focus the dispersion function to small values in straight sections even though the lattice has strong bends. Quadrupole triplet focusing lattices often are employed for rings since the optics allow enough freedom to do this. This is desireable since it allows smaller beam size at locations where $D \simeq 0$ and these locations can be used to more easily insert and extract (kick) the beam into and out of the ring.

J.J. Barnard and S.M. Lund
USPAS, June 2006

§10 Acceleration and Normalized Emittance

If the beam is accelerated, Hill's equation for the single-particle orbit becomes:

$$\boxed{x''(s) + \underbrace{\frac{(\gamma_b\beta_b)'}{(\gamma_b\beta_b)}}_{\text{Acceleration term}} x'(s) + \kappa_x(s)\, x(s) = \frac{-q}{m\gamma_b^3\beta_b^2c^2}\frac{\partial\phi}{\partial x}}$$

Neglects:

- Nonlinear applied focusing: $\vec{E}^a, \vec{B}^a$ contain only linear focusing terms
- Momentum spread effects.

Also, implicit in this equation, is that any energy variations in $\kappa_x(s)$ are compensated for in focusing optics if the lattice is periodic or otherwise incorporated in the s-dependence.

In typical applications the changes induced by the acceleration term are slow and the fractional energy change induced by individual acceleration cells is small (except possibly near the injector).

The acceleration term

$$\frac{(\gamma_b\beta_b)'}{(\gamma_b\beta_b)} > 0 \quad \Rightarrow \quad \text{damped harmonic oscillator equation in } x.$$

and oscillations in the particle orbit will damp. $\gamma_b\beta_b$ will be a function of s perscribed by the acceleration schedule of the machine – derived

consistently from machine gap structures in the lattice, practical accelerating field breakdown limits. Even with acceleration, we will find that the particle orbit has a Courant-Snyder invariant (normalized emittance) if coordinates are appropriately chosen to compensate for the acceleration induced damping of the particle phase-space area.

Transform:

$$\boxed{\tilde{X} \equiv \sqrt{\gamma_b \beta_b}\, X}$$

"Guess" can be motivated qualitatively based on conjugate variable arguments - see Intro. lecture J.J. Barnard

Then

$$X = \frac{\tilde{X}}{\sqrt{\gamma_b \beta_b}} \quad \Longrightarrow \quad \tilde{X} = \sqrt{\gamma_b \beta_b}\, X$$

$$X' = \frac{\tilde{X}'}{\sqrt{\gamma_b \beta_b}} - \frac{1}{2}\frac{(\gamma_b \beta_b)'}{(\gamma_b \beta_b)^{3/2}}\tilde{X} \qquad \tilde{X}' = \sqrt{\gamma_b \beta_b}\, X' + \frac{1}{2}\frac{(\gamma_b \beta_b)'}{\sqrt{\gamma_b \beta_b}} X$$

$$X'' = \frac{\tilde{X}''}{\sqrt{\gamma_b \beta_b}} - \frac{(\gamma_b \beta_b)'}{(\gamma_b \beta_b)^{3/2}}\tilde{X}' + \frac{3}{4}\frac{(\gamma_b \beta_b)'^2}{(\gamma_b \beta_b)^{5/2}}\tilde{X} - \frac{1}{2}\frac{(\gamma_b \beta_b)''}{(\gamma_b \beta_b)^{3/2}}\tilde{X}$$

substituting these factors, the particle equation of motion with acceleration becomes:

$$\tilde{X}'' + \left[\kappa_x + \frac{1}{4}\frac{(\gamma_b \beta_b)'^2}{(\gamma_b \beta_b)^2} - \frac{1}{2}\frac{(\gamma_b \beta_b)''}{(\gamma_b \beta_b)} \right] \tilde{X} = -\frac{q}{m \gamma_b^2 \beta_b c^2}\frac{\partial \phi}{\partial \tilde{X}}$$

Note factor of $\frac{1}{\gamma_b \beta_b}$ difference from lab frame in the space charge term

To apply this equation to beams with finite space-charge, the Poisson equation must also be transformed:

$$\left(\frac{\partial^2}{\partial x^2}+\frac{\partial^2}{\partial y^2}\right)\phi = -\frac{\rho}{\varepsilon_0}$$

ρ = local charge density.

$$\frac{\partial^2}{\partial x^2} = \left(\frac{\partial \tilde{x}}{\partial x}\frac{\partial}{\partial \tilde{x}}\right)\left(\frac{\partial \tilde{x}}{\partial x}\frac{\partial}{\partial \tilde{x}}\right)$$

$$= \gamma_b\beta_b \frac{\partial^2}{\partial \tilde{x}^2}$$

y-direction transforms the same:

$$\boxed{\left(\frac{\partial^2}{\partial \tilde{x}^2}+\frac{\partial^2}{\partial \tilde{y}^2}\right)\phi = -\frac{\rho}{\gamma_b\beta_b\varepsilon_0}}$$

Denote:

$$\tilde{\phi} \equiv \gamma_b\beta_b\phi$$

$$\Rightarrow \left(\frac{\partial^2}{\partial \tilde{x}^2}+\frac{\partial^2}{\partial \tilde{y}^2}\right)\tilde{\phi} = -\frac{\rho}{\varepsilon_0}$$

In terms of $\tilde{\phi}$ the particle eqn of motion is:

$$\boxed{\tilde{x}'' + \left[\kappa_x + \frac{1}{4}\frac{(\gamma_b\beta_b)'^2}{(\gamma_b\beta_b)^2} - \frac{1}{2}\frac{(\gamma_b\beta_b)''}{(\gamma_b\beta_b)}\right]\tilde{x} = -\frac{q}{m\gamma_b^3\beta_b^2c^2}\frac{\partial\tilde{\phi}}{\partial\tilde{x}}}$$

← Restores the "usual" form of the space-charge term.

The transformed equation can be expressed as

$$\boxed{\begin{aligned} \tilde{x}'' + \tilde{\kappa}_x \tilde{x} &= -\frac{q}{m\gamma_b^3\beta_b^2c^2}\frac{\partial\tilde{\phi}}{\partial\tilde{x}} \\ \tilde{\kappa}_x &\equiv \kappa_x + \frac{1}{4}\frac{(\gamma_b\beta_b)'^2}{(\gamma_b\beta_b)^2} - \frac{1}{2}\frac{(\gamma_b\beta_b)''}{(\gamma_b\beta_b)} \end{aligned}}$$

where $\tilde{\kappa}_x$ is a corrected focusing constant including additional acceleration terms beyond those already contained in κ:

$$\kappa_x = \begin{cases} \pm\kappa_q = \dfrac{qG}{m\gamma_b\beta_b^2c^2} \; ; & G = \text{Electric Quadrupole Gradient} \\ \pm\kappa_q = \dfrac{qG}{m\gamma_b\beta_b c} \; ; & G = \text{Magnetic Quadrupole Gradient} \\ \dfrac{\omega_c^2}{4\gamma_b^2\beta_b^2c^2} = \dfrac{qB_z^a}{4m\gamma_b^2\beta_b^2c^2} \; ; & B_z^a = \text{Solenoidal Magnetic Field.} \end{cases}$$

Note that the transformed equation has the same form as usual Hill's equation with no acceleration when space-charge is neglected ($\tilde{\phi} \to 0$).

$$x'' + \kappa_x x = 0 \quad \underset{\text{same form}}{\Longleftrightarrow} \quad \tilde{x}'' + \tilde{\kappa}_x \tilde{x} = 0$$

Therefore, all previous analysis on Courant-Snyder Invariants in $x-x'$ phase space can be immediately applied to the $\tilde{x}-\tilde{x}'$ phase-space for an accelerating beam.

$\tilde{\phi} \to 0$ Courant-Snyder Invariant

$$\boxed{\begin{gathered}\left(\frac{\tilde{x}}{\tilde{W}_x}\right)^2 + \left(\tilde{W}_x \tilde{x}' - \tilde{W}_x' \tilde{x}\right)^2 = \tilde{\varepsilon}^2 = \text{const} \\ \tilde{W}_x'' + \tilde{K} \tilde{W}_x - \frac{1}{\tilde{W}_x^3} = 0 \\ \tilde{W}_x(s+L_p) = \tilde{W}_x(s)\end{gathered}}$$

where:

$$\boxed{\pi \tilde{\varepsilon} = \text{Area traced by orbit in } \tilde{x}-\tilde{x}' \text{ phase-space} = \text{const.}}$$

It is instructive to relate these acceleration variable "~" emittances to the instantaneous lab-frame $x-x'$ phase-space area.

Phase space areas are related as

$$d\tilde{x} \otimes d\tilde{x}' = |J| \, dx \otimes dx'$$

where J is the Jacobian

$$J = \det \begin{vmatrix} \frac{\partial \tilde{x}}{\partial x} & \frac{\partial \tilde{x}}{\partial x'} \\ \frac{\partial \tilde{x}'}{\partial x} & \frac{\partial \tilde{x}'}{\partial x'} \end{vmatrix} = \det \begin{vmatrix} \sqrt{\gamma_b \beta_b} & 0 \\ \frac{1}{2} \frac{(\gamma_b \beta_b)'}{\sqrt{\gamma_b \beta_b}} & \sqrt{\gamma_b \beta_b} \end{vmatrix}$$

$$= \gamma_b \beta_b$$

Thus:

$$\boxed{d\tilde{x} \otimes d\tilde{x}' = \gamma_b \beta_b \, dx \otimes dx'}$$

Based on this area transform, if we define an (instantaneous) area of the orbit traced in $x - x'$ to be $\pi \cdot \varepsilon$ (regular emittance):

$$\boxed{\begin{aligned} \tilde{\varepsilon} &= \gamma_b \beta_b \, \varepsilon = \text{const.} \\ &\equiv \text{"Normalized" Emittance.} \equiv \varepsilon_n \end{aligned}}$$

The $\gamma_b \beta_b$ factor compensates for the acceleration induced damping of particle oscillations.

J.J. Barnard and S.M. Lund
USPAS, June 2006

§10 Appendix A.

Accelerating Fields and Calculation of $\gamma_b \beta_b$

The equation of motion with acceleration was derived by approximating:

$$\frac{d}{dt}\left(\gamma \frac{dx}{dt}\right) = \frac{q}{m} E_x^q - \frac{q}{m} v_z B_y^q + \frac{q}{m} v_y \overset{\nearrow 0}{B_z^q}$$

Neglect Solenoidal field for simplicity.

using:

$$\frac{d}{dt}\left(\gamma \frac{dx}{dt}\right) \simeq \gamma_b \beta_b^2 c^2 \left(x'' + \frac{(\gamma_b \beta_b)'}{(\gamma_b \beta_b)} x' \right)$$

Changes in $\gamma_b \beta_b$ are calculated from the longitudinal particle equation

$$\frac{d}{dt}\left(\gamma \frac{dz}{dt}\right) = \frac{q}{m} E_z^q + \underbrace{\frac{q}{m} v_x B_y^q - \frac{q}{m} v_y B_x^q}_{\text{Weak change in particle longitudinal energy, neglect.}}$$

with:

1) $$\frac{d}{dt}\left(\gamma \frac{dz}{dt}\right) \simeq c^2 \beta_b (\gamma_b \beta_b)'$$

2) $$\frac{q}{m} E_z^q \simeq -\frac{q}{m} \frac{\partial \phi^q}{\partial z}\bigg|_{r=0}$$

where ϕ^q is the quasi-static approx. accelerating potential from an accelerating "gap" (induction, RF, etc.)
The acceleration also produces $\perp$ focusing fields:

$$E_x^q \simeq E_x^q\bigg|_{\text{Focusing Optics}} - \frac{\partial \phi^q}{\partial x}$$

$\perp$ Focusing from Acceleration

The longitudinal equation then becomes:

$$\beta_b(\gamma_b\beta_b)' \simeq \frac{-q}{mc^2}\frac{\partial\phi^q}{\partial z}\bigg|_{r=0}$$

But:

$$\gamma_b' = \left(\frac{1}{\sqrt{1-\beta_b^2}}\right)' = \gamma_b^3\beta_b\beta_b'$$

$$\Rightarrow \beta_b(\gamma_b\beta_b)' = (1-\gamma_b^2\beta_b^2)\gamma_b\beta_b\beta_b' = \gamma_b^3\beta_b\beta_b' = \gamma_b'$$

and the longitudinal equation can be integrated!

$$\gamma_b' = \frac{-q}{mc^2}\frac{\partial\phi^q}{\partial z}\bigg|_{r=0}$$

$$\Rightarrow \boxed{\gamma_b + \frac{q}{mc^2}\phi^q(r=0,z) = \text{const.}}$$

This result can be used to cast terms occuring in the transverse equation of motion as

$$\boxed{\begin{aligned} x'' + \frac{(\gamma_b\beta_b)'}{(\gamma_b\beta_b)}x' \simeq\ & \frac{q}{m\gamma_b\beta_b^2c^2}E_x^q - \frac{q}{m\gamma_b\beta_b c}B_y^q \\ & - \frac{q}{m\gamma_b\beta_b^2c^2}\frac{\partial\phi^q}{\partial x} \end{aligned}}$$

Applied Focus
Electric Quads etc

Magnetic Focus

Transverse Foc
From Accel. gap.

In the quasi-static approximation, the axisymmetric field of an accelerating gap can be expanded as: (see J.J. Barnard, Intro lectures and Reiser Sec. 3.3):

$$\boxed{\begin{aligned} E_z^a &= -\frac{\partial \phi^a}{\partial z} \\ \phi^a &= V(z) - \frac{1}{4}\frac{\partial^2}{\partial z^2}V(z)\,(x^2+y^2) \\ &\quad + \frac{1}{64}\frac{\partial^4}{\partial z^4}V(z)\,(x^2+y^2)^2 + \cdots\cdots \end{aligned}}$$

where $V(z)$ is the on-axis potential due to gap accelerating structures.

Using these results it is possible to cast certain acceleration terms in more convenient forms – both in the equation for x and the transformed equation for $\tilde{x}$. An example of this can be found in the intro. lectures by J.J. Barnard.

References

The course textbook Reiser provides a solid introduction to many of the topics covered for further reading including more advanced treatments, we suggest the following books:

Floquet's Theorem, Courant-Snyder Invariants, Hill's Equation, Dispersion Function....

* H. Wiedemann, "Particle Accelerator Physics, Basic Principles and Linear Beam Dynamics." Springer Verlag, Berlin, 1993.

* Highly Recommended

Resonances and Solenoidal Focusing

H. Wiedemann, "Particle Accelerator Physics II, Nonlinear and Higher-Order Beam Dynamics." Springer Verlag, Berlin, 1995.

D.A. Edwards and M.J. Syphers, "An Introduction to the Physics of High Energy Accelerators," John Wiley & Sons, Inc., New York, 1993.

Acknowledgement:

The authors wish to acknowledge the role of Guliano Franchetti (GSI) in educating us in many of the methods presented here.

some additional references:

Particle equations of motion with bends and momentum spread:

D.A. Edwards and M.J. Syphers, "An Introduction to the Physics of High Energy Accelerators," John Wiley & Sons, New York, 1993.

Original classic paper on strong alternating gradient focusing

E.D. Courant and H.S. Snyder, "Theory of the Alternating Gradient Synchrotron" Annals of Physics 3, 1 (1958).

More mathematical treatment of transfer maps and stability. A standard, high quality reference

A. Dragt, "Lectures on Nonlinear Orbit Dynamics," in "Physics of High Energy Accelerators," edited by R.A. Carrigan, F.R. Hudson, and M. Month. (AIP Conf. Proc. No. 87. (AIP, New York, 1982) p. 147.

Recent review containing related information on phase advances, orbit stability, etc.

S.M. Lund and B. Bukh, "Stability Properties of the Transverse Envelope Equations Describing Intense Ion Beam Transport," to appear Phys. Rev. Special Topics - Accelerators and Beams, 2004.

Transverse Equilibrium Distribution Functions*

Steven M. Lund
Lawrence Livermore National Laboratory (LLNL)

Steven M. Lund and John J. Barnard
"Beam Physics with Intense Space-Charge"
US Particle Accelerator School
Boston University, Waltham, MA
12-23 June, 2006

* Research supported by the US Dept. of Energy at LBNL and LLNL under contract Nos. DE-AC03-76SF00098 and W-7405-Eng-48

Transverse Equilibrium Distribution Functions: Outline

Vlasov Model
Vlasov Equilibria
The KV Equilibrium Distribution
Continuous Focusing Limit of the KV Equilibrium Distribution
Equilibrium Distributions in Continuous Focusing Channels
Continuous Focusing: The Waterbag Equilibrium Distribution
Continuous Focusing: The Thermal Equilibrium Distribution
Continuous Focusing: Debye Screening in a Thermal Equilibrium Beam
Continuous Focusing: The Density Inversion Theorem
References

Transverse Equilibrium Dist. Functions: Detailed Outline

1) Vlasov Model

- Vlasov-Poisson system
- Review: lattices: continuous, solenoidal, and quadrupole
- Review: Undepressed particle phase advance

2) Vlasov Equilibria

- Equilibrium conditions
- Single particle constants of motion
- Plasma physics approach to beam physics

3) The KV Equilibrium Distribution

- Hill's equation with linear space-charge forces
- Courant-Snyder invariants for a uniform density elliptical beam
- KV envelope equations
- KV equilibrium distribution
- Canonical form of the KV distribution
- Matched envelope structure
- Depressed particle orbits
- rms equivalent beams
- Discussion/Comments on the KV model

Detailed Outline - 2

4) The Continuous Focusing Limit of the KV Equilibrium Distribution

- Wavenumbers of particle oscillations
- Distribution form

5) Continuous Focusing Equilibrium Distributions

- Equilibrium form
- Poisson's equation
- Moments
- Example distributions

6) Continuous Focusing: The Waterbag Equilibrium Distribution

- Distribution form
- Poisson's equation
- Equilibrium properties

7) Continuous Focusing: The Thermal Equilibrium Distribution

- Overview
- Distribution form
- Poisson's equation
- Equilibrium properties

Detailed Outline - 3

8) Continuous Focusing: Debye Screening in a Thermal Equilibrium Beam

Poisson's equation for the perturbed potential due to a test charge

Solution for characteristic Debye screening

9) Continuous Focusing: The Density Inversion Theorem

Relation of density profile to the full distribution function

10) Comments on the plausibility of smooth, non-KV Vlasov equilibria in periodic focusing lattices

Discussion

Appendix A: Self-fields of a Uniform Density Elliptical Beam in Free Space

(separate handwritten notes)

Derivation #1, direct

Derivation #2, simplified

Appendix B: Canonical Transformation of the KV Distribution

(separate handwritten notes)

Canonical transforms

Simplified moment calculations

References

S1: Vlasov Model: Transverse Vlasov model for a coasting, single species beam with electrostatic self-fields propagating in an applied focusing lattice:

$\mathbf{x}_\perp,\ \mathbf{x}'_\perp$ transverse particle coordinate, angle

$q,\ m$ charge, mass

$\gamma_b,\ \beta_b$ axial relativistic factors

$f_\perp(\mathbf{x}_\perp, \mathbf{x}'_\perp, s)$ single particle distribution

$H_\perp(\mathbf{x}_\perp, \mathbf{x}'_\perp, s)$ single particle Hamiltonian

Vlasov Equation (see J.J. Barnard, Introductory Lectures):

$$\frac{d}{ds} f_\perp = \frac{\partial f_\perp}{\partial s} + \frac{d\mathbf{x}_\perp}{ds} \cdot \frac{\partial f_\perp}{\partial \mathbf{x}_\perp} + \frac{d\mathbf{x}'_\perp}{ds} \cdot \frac{\partial f_\perp}{\partial \mathbf{x}'_\perp} = 0$$

Particle Equations of Motion:

$$\frac{d}{ds}\mathbf{x}_\perp = \frac{\partial H_\perp}{\partial \mathbf{x}'_\perp} \qquad \frac{d}{ds}\mathbf{x}'_\perp = -\frac{\partial H_\perp}{\partial \mathbf{x}_\perp}$$

Hamiltonian (see S.M. Lund, lectures on *Transverse Particle Equations of Motion*):

$$H_\perp = \frac{1}{2}\mathbf{x}'^{\,2}_\perp + \frac{1}{2}\kappa_x(s)x^2 + \frac{1}{2}\kappa_y(s)y^2 + \frac{q}{m\gamma_b^3\beta_b^2c^2}\phi$$

Poisson Equation:

$$\left(\frac{\partial^2}{\partial x^2} + \frac{\partial^2}{\partial y^2}\right)\phi = -\frac{q}{\epsilon_0}\int d^2\mathbf{x}'_\perp\ f_\perp$$

+ boundary conditions on ϕ

Hamiltonian expression of the Vlasov equation:

$$\frac{d}{ds}f_\perp = \frac{\partial f_\perp}{\partial s} + \frac{d\mathbf{x}_\perp}{ds}\cdot\frac{\partial f_\perp}{\partial \mathbf{x}_\perp} + \frac{d\mathbf{x}'_\perp}{ds}\cdot\frac{\partial f_\perp}{\partial \mathbf{x}'_\perp} = 0$$

$$= \frac{\partial f_\perp}{\partial s} + \frac{\partial H_\perp}{\partial \mathbf{x}'_\perp}\cdot\frac{\partial f_\perp}{\partial \mathbf{x}_\perp} - \frac{\partial H_\perp}{\partial \mathbf{x}_\perp}\cdot\frac{\partial f_\perp}{\partial \mathbf{x}'_\perp} = 0$$

Using the equations of motion:

$$\frac{d}{ds}\mathbf{x}_\perp = \frac{\partial H_\perp}{\partial \mathbf{x}'_\perp} = \mathbf{x}'_\perp$$

$$\frac{d}{ds}\mathbf{x}'_\perp = -\frac{\partial H_\perp}{\partial \mathbf{x}_\perp} = -\left(\kappa_x x\hat{\mathbf{x}} + \kappa_y y\hat{\mathbf{y}} + \frac{q}{m\gamma_b^3\beta_b^2c^2}\frac{\partial\phi}{\partial \mathbf{x}_\perp}\right)$$

$$\boxed{\frac{\partial f_\perp}{\partial s} + \mathbf{x}'_\perp\cdot\frac{\partial f_\perp}{\partial \mathbf{x}_\perp} - \left(\kappa_x x\hat{\mathbf{x}} + \kappa_y y\hat{\mathbf{y}} + \frac{q}{m\gamma_b^3\beta_b^2c^2}\frac{\partial\phi}{\partial \mathbf{x}_\perp}\right)\cdot\frac{\partial f_\perp}{\partial \mathbf{x}'_\perp} = 0}$$

In formal dynamics, a "Poisson Bracket" notation is frequently employed:

$$\frac{d}{ds}f_\perp = \frac{\partial f_\perp}{\partial s} + \frac{\partial H_\perp}{\partial \mathbf{x}'_\perp}\cdot\frac{\partial f_\perp}{\partial \mathbf{x}_\perp} - \frac{\partial H_\perp}{\partial \mathbf{x}_\perp}\cdot\frac{\partial f_\perp}{\partial \mathbf{x}'_\perp} = 0$$

$$\equiv \frac{\partial f_\perp}{\partial s} + \{H_\perp, f_\perp\} = 0$$

Poisson Bracket

Review: Focusing lattices, continuous and periodic (simple piecewise constant):

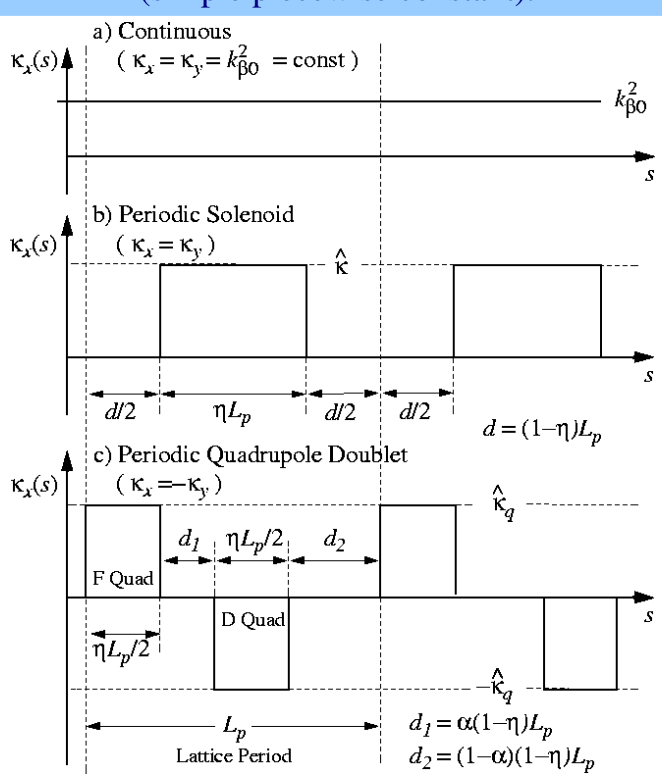

Lattice Period L_p

Occupancy η

$\eta \in [0, 1]$

Solenoid description carried out implicitly in Larmor frame

[see Lund and Bukh, PRST- Accel. and Beams 7, 024801 (2004), Appendix A]

Syncopation Factor α

$$\alpha \in [0, \frac{1}{2}]$$

$$\alpha = \frac{1}{2} \implies FODO$$

Example Hamiltonians:

Continuous focusing $\kappa_x = \kappa_y = k_{\beta 0}^2 = \text{const}$

$$H_\perp = \frac{1}{2}\mathbf{x}_\perp'^{\,2} + \frac{1}{2}k_{\beta 0}^2 \mathbf{x}_\perp^2 + \frac{q}{m\gamma_b^3\beta_b^2 c^2}\phi$$

Solenoidal focusing (in Larmor frame variables) $\kappa_x = \kappa_y = \kappa(s)$

$$H_\perp = \frac{1}{2}\mathbf{x}_\perp'^{\,2} + \frac{1}{2}\kappa \mathbf{x}_\perp^2 + \frac{q}{m\gamma_b^3\beta_b^2 c^2}\phi$$

Quadrupole focusing $\kappa_x = -\kappa_y = \kappa_q(s)$

$$H_\perp = \frac{1}{2}\mathbf{x}_\perp'^{\,2} + \frac{1}{2}\kappa_q x^2 - \frac{1}{2}\kappa_q y^2 + \frac{q}{m\gamma_b^3\beta_b^2 c^2}\phi$$

Review: Undepressed particle phase advance σ_0 is typically employed to characterize the applied focusing strength of periodic lattices:

x-orbit without space-charge satisfies Hill's equation

$$x''(s) + \kappa_x(s)x(s) = 0$$

$$\begin{pmatrix} x(s) \\ x'(s) \end{pmatrix} = \mathbf{M}_x(s \mid s_i) \cdot \begin{pmatrix} x(s_i) \\ x'(s_i) \end{pmatrix}$$

$\mathbf{M}_x =$ 2 x 2 Transfer Matrix from $s = s_i$ to s

Undepressed phase advance

$$\boxed{\cos\sigma_{0x} = \frac{1}{2}\text{Tr}\ \mathbf{M}_x(s_i + L_p|s_i)}$$

Single particle (and centroid) stability requires:

$$\frac{1}{2}\text{Tr}\ \mathbf{M}_x(s_i + L_p|s_i) < 1 \longrightarrow \boxed{\sigma_{0x} < 180^\circ}$$

[Courant and Snyder, Annals of Phys. **3**, 1 (1958)]

Analogous equations hold in the *y*-plane

S2: Vlasov Equilibria: Plasma physics-like approach is to resolve the system into an equilibrium + perturbation and analyze stability

Equilibrium constructed from single-particle constants of motion C_i

$$\boxed{f_\perp = f_\perp(\{C_i\}) \quad \text{equilibrium}}$$

$$\frac{d}{ds} f_\perp(\{C_i\}) = \sum_i \frac{\partial f_\perp}{\partial C_i} \underbrace{\frac{dC_i}{ds}}_{0} = 0$$

Comments:

- Equilibrium is an exact solution to Vlasov's equation that does not change in 4D phase-space as s advances
  - Projections of the distribution can evolve in s in general cases
- Particle conversation constraints are in the presence of (possibly s-varying) applied and space-charge forces
  - Highly non-trivial!
  - Only one exact solution known for s-varying focusing: the KV distribution to be analyzed shortly in this lecture.

// Example: Continuous focusing $f_\perp = f_\perp(H_\perp)$

$$H_\perp = \frac{1}{2}\mathbf{x}_\perp'^{\,2} + \frac{1}{2}k_{\beta 0}^2 \mathbf{x}_\perp^2 + \frac{q}{m\gamma_b^3\beta_b^2 c^2}\phi \qquad \text{no explicit s dependance}$$

$$\frac{df_\perp}{ds} = \frac{\partial f_\perp}{\partial s} + \frac{\partial H_\perp}{\partial \mathbf{x}_\perp'} \cdot \frac{\partial f_\perp}{\partial \mathbf{x}_\perp} - \frac{\partial H_\perp}{\partial \mathbf{x}_\perp} \cdot \frac{\partial f_\perp}{\partial \mathbf{x}_\perp'}$$

$$= \frac{\partial f_\perp}{\partial H_\perp} \underbrace{\frac{\partial H_\perp}{\partial s}}_{0} + \frac{\partial f_\perp}{\partial H_\perp} \underbrace{\left(\frac{\partial H_\perp}{\partial \mathbf{x}_\perp'} \cdot \frac{\partial H_\perp}{\partial \mathbf{x}_\perp} - \frac{\partial H_\perp}{\partial \mathbf{x}_\perp} \cdot \frac{\partial H_\perp}{\partial \mathbf{x}_\perp'} \right)}_{0} = 0$$

Showing that $f_\perp = f_\perp(H_\perp)$ exactly satisfies Vlasov's equation for continuous focusing

//

Typical single particle constants of motion:

Transverse Hamiltonian for continuous focusing:

$$H_\perp = \frac{1}{2}\mathbf{x}_\perp'^{\,2} + \frac{1}{2}k_{\beta 0}^2 \mathbf{x}_\perp^2 + \frac{q}{m\gamma_b^3\beta_b^2 c^2}\phi = \text{const}$$

$$k_{\beta 0}^2 = \text{const}$$

Canonical angular momentum for rotationally invariant systems:

$$P_\theta = xy' - yx' = \text{const}$$

(in Larmor frame variables for solenoidal focusing)

Axial kinetic energy for systems with no acceleration:

$$\mathcal{E} = (\gamma_b - 1)mc^2 = \text{const}$$

More on other classes of constraints later ...

Plasma physics approach to beam physics:

Resolve:

$$f(\mathbf{x}_\perp, \mathbf{x}_\perp', s) = f_\perp(\{C_i\}) + \delta f_\perp(\mathbf{x}_\perp, \mathbf{x}_\perp', s)$$

equilibrium perturbation $f_\perp \gg |\delta f_\perp|$

and carry out equilibrium + stability analysis

Comments:

- Attraction is to parallel the impressive successes of plasma physics
  - Gain insight into preferred state of nature
- Beams are born off a source and may not be close to an equilibrium condition
  - Appropriate single particle constants of the motion unknown for periodic focusing lattices other than the (unphysical) KV distribution
- Intense beam self-fields and finite radial extent vastly complicate equilibrium description and analysis of perturbations
  - It is not clear if smooth Vlasov equilibria exist in periodic focusing
  - Higher model detail vastly complicates picture!
- If system can be tuned to more closely resemble a relaxed, equilibrium, one might expect less deleterious effects based on plasma physics analogies

S3: The KV Equilibrium Distribution

[Kapchinskij and Vladimirskij, Proc. Int. Conf. On High Energy Accel., 1959]

Assume a uniform density elliptical beam in a periodic focusing lattice

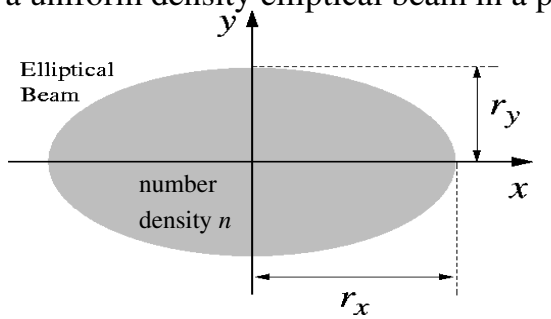

Line-Charge:

$$\lambda = qn(s)\pi r_x(s) r_y(s) = \text{const}$$

Perveance:

$$Q = \frac{q\lambda}{2\pi\epsilon_0 m\gamma_b^3\beta_b^2 c^2} = \text{const}$$

Free-space self field solution within the beam (see Appendix A)

$$\phi = -\frac{\lambda}{2\pi\epsilon_0}\left[\frac{x^2}{(r_x+r_y)r_x} + \frac{y^2}{(r_x+r_y)r_y}\right] + \text{const}$$

Particle equations of motion within the beam (Hill's equation if edge radii given):

$$\boxed{\begin{aligned} x''(s) + \left\{\kappa_x(s) - \frac{2Q}{[r_x(s)+r_y(s)]r_x(s)}\right\}x(s) = 0 \\ y''(s) + \left\{\kappa_y(s) - \frac{2Q}{[r_x(s)+r_y(s)]r_y(s)}\right\}y(s) = 0 \end{aligned}}$$

If we regard the envelope radii as specified functions of s, then these equations of motion are Hill's equations familiar from elementary accelerator physics:

$$\boxed{\begin{aligned} x''(s) + \kappa_x^{\text{eff}}(s)x(s) = 0 \\ y''(s) + \kappa_y^{\text{eff}}(s)y(s) = 0 \\ \kappa_x^{\text{eff}}(s) = \kappa_x(s) - \frac{2Q}{[r_x(s)+r_y(s)]r_x(s)} \\ \kappa_y^{\text{eff}}(s) = \kappa_y(s) - \frac{2Q}{[r_x(s)+r_y(s)]r_y(s)} \end{aligned}}$$

Suggests Procedure:

- Calculate Courant-Snyder invariants under assumptions made
- Construct a distribution function of Courant-Snyder invariants that generates the uniform density elliptical beam projection assumed
  - Nontrivial step: guess and show that it works
- Resulting distribution will be an equilibrium that does not change 4D form as a function of s

Review (1): The Courant-Snyder invariant of Hill's equation

[Courant and Snyder, Annl. Phys. **3**, 1 (1958)]

Hill's equation describes a zero space-charge particle orbit in linear applied focusing fields:

$$\boxed{x''(s) + \kappa(s)x(s) = 0}$$

As a consequence of Floquet's theorem, the solution can be cast in phase-amplitude form:

$$x(s) = A_i w(s) \cos\psi(s)$$

where $w(s)$ is the periodic solution to

$$w''(s) + \kappa(s)w(s) - \frac{1}{w^3(s)} = 0$$

$$w(s + L_p) = w(s) \qquad w(s) > 0$$

$\psi(s)$ is a phase function given by

$$\psi(s) = \psi_i + \int_{s_i}^{s} \frac{d\tilde{s}}{w^2(\tilde{s})}$$

A_i and ψ_i are constants set by initial conditions at $s = s_i$

Review (2): The Courant-Snyder invariant of Hill's equation

From this formulation it follows immediately that

$$x(s) = A_i w(s) \cos\psi(s)$$

$$x'(s) = A_i w'(s) \cos\psi(s) + \frac{A_i}{w(s)} \sin\psi(s)$$

or

$$\frac{x}{w} = A_i \cos\psi$$

$$wx' - w'x = A_i \sin\psi$$

square and add equations to obtain the Courant-Snyder invariant

$$\boxed{\left(\frac{x}{w}\right)^2 + (wx' - w'x)^2 = A_i^2 = \text{const}}$$

- Simplifies interpretation of dynamics
- Extensively used in accelerator physics

Phase-amplitude description of particles evolving within a uniform density beam:

Phase-amplitude form of x-orbit equations:

$$x(s) = A_{xi} w_x(s) \cos\psi_x(s)$$

$$x'(s) = A_{xi} w_x'(s) \cos\psi_x(s) - \frac{A_{xi}}{w_x(s)} \sin\psi_x(s)$$

initial conditions yield:

$$(s = s_i)$$
$$A_{xi} = \text{const}$$
$$\psi_{xi} = \psi_x(s = s_i) = \text{const}$$

where

$$\boxed{\begin{gathered} w_x''(s) + \kappa_x(s) w_x(s) - \frac{2Q}{[r_x(s) + r_y(s)] r_x(s)} w_x(s) - \frac{1}{w_x^3(s)} = 0 \\ w_x(s + L_p) = w_x(s) \qquad\qquad w_x(s) > 0 \\ \psi_x(s) = \psi_{xi} + \int_{s_i}^{s} \frac{d\tilde{s}}{w_x^2(\tilde{s})} \end{gathered}}$$

identifies the Courant-Snyder invariant

$$\boxed{\left(\frac{x}{w_x}\right)^2 + (w_x x' - w_x' x)^2 = A_{xi}^2 = \text{const}}$$

Analogous equations hold for the *y*-plane

The KV envelope equations:

Define *maximum* Courant-Snyder invariants:

$$\varepsilon_x \equiv \text{Max}(A_{xi}^2)$$
$$\varepsilon_y \equiv \text{Max}(A_{yi}^2)$$

These values must correspond to the beam-edge:

$$r_x(s) = \sqrt{\varepsilon_x} w_x(s)$$
$$r_y(s) = \sqrt{\varepsilon_y} w_y(s)$$

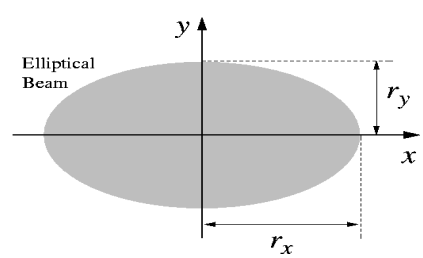

The equations for w_x and w_y can then be rescaled to obtain the familiar KV envelope equations for the matched beam envelope

$$\boxed{\begin{gathered} r_x''(s) + \kappa_x(s) r_x(s) - \frac{2Q}{r_x(s) + r_y(s)} - \frac{\varepsilon_x^2}{r_x^3(s)} = 0 \\ r_y''(s) + \kappa_y(s) r_y(s) - \frac{2Q}{r_x(s) + r_y(s)} - \frac{\varepsilon_y^2}{r_y^3(s)} = 0 \\ r_x(s + L_p) = r_x(s) \qquad\qquad r_x(s) > 0 \\ r_y(s + L_p) = r_y(s) \qquad\qquad r_y(s) > 0 \end{gathered}}$$

Use variable rescalings to denote x- and y-plane Courant-Snyder invariants as:

$$\left(\frac{x}{w_x}\right)^2 + (w_x x' - w_x' x)^2 = A_{xi}^2 = \text{const}$$

$$\boxed{\begin{aligned} \left(\frac{x}{r_x}\right)^2 + \left(\frac{r_x x' - r_x' x}{\varepsilon_x}\right)^2 &= C_x = \text{const} \\ \left(\frac{y}{r_y}\right)^2 + \left(\frac{r_y y' - r_y' y}{\varepsilon_y}\right)^2 &= C_y = \text{const} \end{aligned}}$$

Kapchinskij and Vladimirskij constructed a delta-function distribution of a linear combination of these Courant-Snyder invariants that generates the correct uniform density elliptical beam needed for consistency with the assumptions:

$$f_\perp = \frac{\lambda}{q\pi^2 \varepsilon_x \varepsilon_y} \delta\left[C_x + C_y - 1\right]$$

- Delta function means the sum of the x- and y-invariants is a constant
- Other forms would not generate the needed uniform density elliptical beam projection

The KV equilibrium is constructed from the Courant-Snyder invariants:

KV equilibrium distribution:

$$\boxed{\begin{aligned} f_\perp(\mathbf{x}_\perp, \mathbf{x}_\perp', s) = \frac{\lambda}{q\pi^2 \varepsilon_x \varepsilon_y} \delta \Bigg[&\left(\frac{x}{r_x}\right)^2 + \left(\frac{r_x x' - r_x' x}{\varepsilon_x}\right)^2 + \\ &\left(\frac{y}{r_y}\right)^2 + \left(\frac{r_y y' - r_y' y}{\varepsilon_y}\right)^2 - 1 \Bigg] = \text{const} \\ \delta(x) = &\ \text{Dirac delta function} \end{aligned}}$$

This distribution generates (see proof in Appendix B) the correct uniform density elliptical beam:

$$\boxed{n = \int d^2 x_\perp' \, f_\perp = \begin{cases} \frac{\lambda}{q\pi r_x r_y}, & x^2/r_x^2 + y^2/r_y^2 < 1 \\ 0, & x^2/r_x^2 + y^2/r_y^2 > 1 \end{cases}}$$

Obtaining this form consistent with the assumptions

demonstrates full self-consistency of the KV equilibrium distribution.

- Full 4-D form of the distribution does not evolve in s
- Projections of the distribution can (and generally do!) evolve in s

Comment on notation of integrals:

- 2nd forms useful for systems with azimuthal spatial or annular symmetry

Spatial

$$\int d^2x_\perp \cdots \equiv \int_{-\infty}^{\infty} dx \int_{-\infty}^{\infty} dy \ \cdots$$

$$= \int_0^{\infty} dr\, r \int_{-\pi}^{\pi} d\theta \ \cdots$$

Cylindrical Coordinates:

$$x = r\cos\theta$$

$$y = r\sin\theta$$

Angular

$$\int d^2x'_\perp \cdots \equiv \int_{-\infty}^{\infty} dx' \int_{-\infty}^{\infty} dy' \ \cdots$$

$$= \int_0^{\infty} dr'\, r' \int_{-\pi}^{\pi} d\theta' \ \cdots$$

Angular Cylindrical Coordinates:

$$x' = r'\cos\theta'$$

$$y' = r'\sin\theta'$$

Comment on notation of integrals (continued):

Axisymmetry simplifications

Spatial: for some function $f(\mathbf{x}_\perp^2) = f(r^2)$

$$\int d^2x_\perp\ f(\mathbf{x}_\perp^2) = 2\pi \int_0^{\infty} dr\, r f(r^2)$$

$$= \pi \int_0^{\infty} dr^2\ f(r^2)$$

$$= \pi \int_0^{\infty} dw\ f(w)$$

Cylindrical Coordinates:

$$x = r\cos\theta$$

$$y = r\sin\theta$$

$$w = r^2$$

Angular: for some function $g(\mathbf{x}_\perp'^2) = g(r'^2)$

$$\int d^2x'_\perp\ g(\mathbf{x}_\perp'^2) = 2\pi \int_0^{\infty} dr'\, r' g(r'^2)$$

$$= \pi \int_0^{\infty} dr'^2\ g(r'^2)$$

$$= \pi \int_0^{\infty} du\ g(u)$$

Angular Cylindrical Coordinates:

$$x' = r'\cos\theta'$$

$$y' = r'\sin\theta'$$

$$u = r'^2$$

Moments of the KV distribution can be calculated directly from the distribution to further aid interpretation:

Full 4D average:
$$\langle \cdots \rangle_\perp \equiv \frac{\int d^2x_\perp \int d^2x'_\perp \; \cdots f_\perp}{\int d^2x_\perp \int d^2x'_\perp \; f_\perp}$$

Restricted angle average:
$$\langle \cdots \rangle_{\mathbf{x}'_\perp} \equiv \frac{\int d^2x'_\perp \; \cdots f_\perp}{\int d^2x'_\perp \; f_\perp}$$

Envelope edge radius:
$$r_x = 2\langle x^2 \rangle_\perp^{1/2}$$

rms edge emittance (maximum Courant-Snyder invariant):
$$\varepsilon_x = 4[\langle x^2 \rangle_\perp \langle x'^2 \rangle_\perp - \langle xx' \rangle_\perp^2]^{1/2}$$

Coherent flows (within the beam, zero otherwise):
$$\langle x' \rangle_{\mathbf{x}'_\perp} = r'_x \frac{x}{r_x}$$

Angular spread (x-temperature, within the beam, zero otherwise):
$$T_x \equiv \langle (x' - \langle x' \rangle_{\mathbf{x}'_\perp})^2 \rangle_{\mathbf{x}'_\perp} = \frac{\varepsilon_x^2}{2r_x^2}\left(1 - \frac{x^2}{r_x^2} - \frac{y^2}{r_y^2}\right)$$

Summary of 1st and 2nd order moments of the KV distribution:

Moment	Value
$\int d^2x'_\perp \; x' f_\perp$	$r'_x \frac{x}{r_x} n$
$\int d^2x'_\perp \; y' f_\perp$	$r'_y \frac{y}{r_y} n$
$\int d^2x'_\perp \; x'^2 f_\perp$	$\left[r'^2_x \frac{x^2}{r_x^2} + \frac{\varepsilon_x^2}{2r_x^2}\left(1 - \frac{x^2}{r_x^2} - \frac{y^2}{r_y^2}\right)\right] n$
$\int d^2x'_\perp \; y'^2 f_\perp$	$\left[r'^2_y \frac{y^2}{r_y^2} + \frac{\varepsilon_y^2}{2r_y^2}\left(1 - \frac{x^2}{r_x^2} - \frac{y^2}{r_y^2}\right)\right] n$
$\int d^2x'_\perp \; xx' f_\perp$	$\frac{r'_x}{r_x} x^2 n$
$\int d^2x'_\perp \; yy' f_\perp$	$\frac{r'_y}{r_y} y^2 n$
$\int d^2x'_\perp \; (xy' - yx') f_\perp$	0
$\langle x^2 \rangle_\perp$	$\frac{r_x^2}{4}$
$\langle y^2 \rangle_\perp$	$\frac{r_y^2}{4}$
$\langle x'^2 \rangle_\perp$	$\frac{r'^2_x}{4} + \frac{\varepsilon_x^2}{4r_x^2}$
$\langle y'^2 \rangle_\perp$	$\frac{r'^2_y}{4} + \frac{\varepsilon_y^2}{4r_y^2}$
$\langle xx' \rangle_\perp$	$\frac{r_x r'_x}{4}$
$\langle yy' \rangle_\perp$	$\frac{r_y r'_y}{4}$
$\langle xy' - yx' \rangle_\perp$	0
$16[\langle x^2 \rangle_\perp \langle x'^2 \rangle_\perp - \langle xx' \rangle_\perp^2]$	ε_x^2
$16[\langle y^2 \rangle_\perp \langle y'^2 \rangle_\perp - \langle yy' \rangle_\perp^2]$	ε_y^2

All 1st and 2nd order moments not listed vanish, i.e.,

$$\int d^2x'_\perp \; xy f_\perp = 0$$

$$\langle xy \rangle_\perp = 0$$

Canonical transformation illustrates KV distribution structure:

[Davidson, Physics of Nonneutral Plasmas, Addison-Wesley (1990), and Appendix B]

Phase-space transformation:

$$\boxed{\begin{aligned} X &= \frac{\sqrt{\varepsilon_x}}{r_x} x \\ X' &= \frac{r_x x' - r_x' x}{\sqrt{\varepsilon_x}} \end{aligned}}$$

$$dx\ dy = \frac{r_x r_y}{\sqrt{\varepsilon_x \varepsilon_y}} dX\ dY$$

$$dx'\ dy' = \frac{\sqrt{\varepsilon_x \varepsilon_y}}{r_x r_y} dX'\ dY'$$

$$dx\ dy\ dx'\ dy' = dX\ dY\ dX'\ dY'$$

Courant-Snyder invariants in the presence of beam space-charge are then simply:

$$\boxed{X^2 + X'^2 = \text{const}}$$

and the KV distribution takes the simple, symmetrical form:

$$\boxed{f_\perp(x, y, x', y', s) = f_\perp(X, Y, X', Y') = \frac{\lambda}{q\pi^2 \varepsilon_x \varepsilon_y} \delta \left[\frac{X^2 + X'^2}{\varepsilon_x} + \frac{Y^2 + Y'^2}{\varepsilon_y} - 1 \right]}$$

from which the density and other projections can be more easily (see Appendix B) calculated:

$$n = \int d^2 x'_\perp\ f_\perp = \frac{\lambda}{q\pi r_x r_y} \int_0^\infty dU^2\ \delta \left[U^2 - \left(1 - \frac{x^2}{r_x^2} - \frac{y^2}{r_y^2} \right) \right]$$

$$= \begin{cases} \frac{\lambda}{q\pi r_x r_y}, & x^2/r_x^2 + y^2/r_y^2 < 1 \\ 0, & x^2/r_x^2 + y^2/r_y^2 > 1 \end{cases}$$

KV Envelope equation

The envelope equation reflects low-order force balances

$$r_x'' + \kappa_x r_x - \frac{2Q}{r_x + r_y} - \frac{\varepsilon_x^2}{r_x^3} = 0$$

$$r_y'' + \kappa_y r_y - \frac{2Q}{r_x + r_y} - \frac{\varepsilon_y^2}{r_y^3} = 0$$

	Applied Focusing	Space-Charge Defocusing	Thermal Defocusing
Terms:	Lattice	Perveance	Emittance

Matched Solution

$$r_x(s + L_p) = r_x(s)$$

$$r_y(s + L_p) = r_y(s)$$

- Envelope equation is a projection of the 4D invariant distribution
- Most important basic design equation for transport lattices with high space-charge intensity
  - Simplest consistent design equations incorporating applied focusing, space-charge defocusing, and thermal defocusing forces
  - Starting point of almost all practical machine design!
- Instabilities of envelope equations are well understood and real (to be covered: lectures on *Centroid and Envelope Description of Beams*)
  - Must be avoided for reliable machine operation

The matched solution to the KV envelope equations reflects the symmetry of the focusing lattice and must in general be calculated numerically

$$r_x(s+L_p) = r_x(s)$$
$$r_y(s+L_p) = r_y(s)$$
$$\varepsilon_x = \varepsilon_y$$

Parameters

$L_p = 0.5$ m, $\sigma_0 = 80°$, $\eta = 0.5$

$\varepsilon_x = 50$ mm-mrad

$\sigma/\sigma_0 = 0.2$

Solenoidal Focusing ($Q = 6.6986 \times 10^{-4}$)

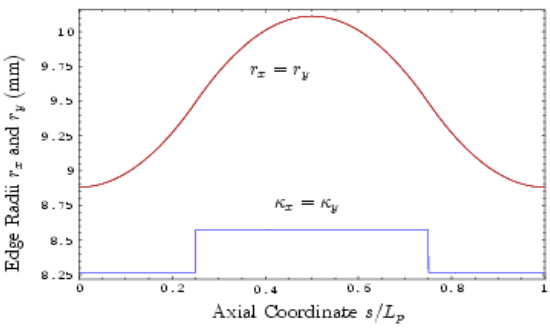

FODO Quadrupole Focusing ($Q = 6.5614 \times 10^{-4}$)

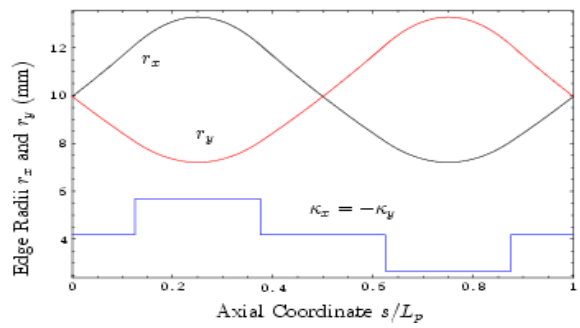

The matched beam is the most radially compact solution to the envelope equations rendering it highly important for beam transport

Beam symmetries of a matched KV equilibrium beam in a periodic FODO transport lattice

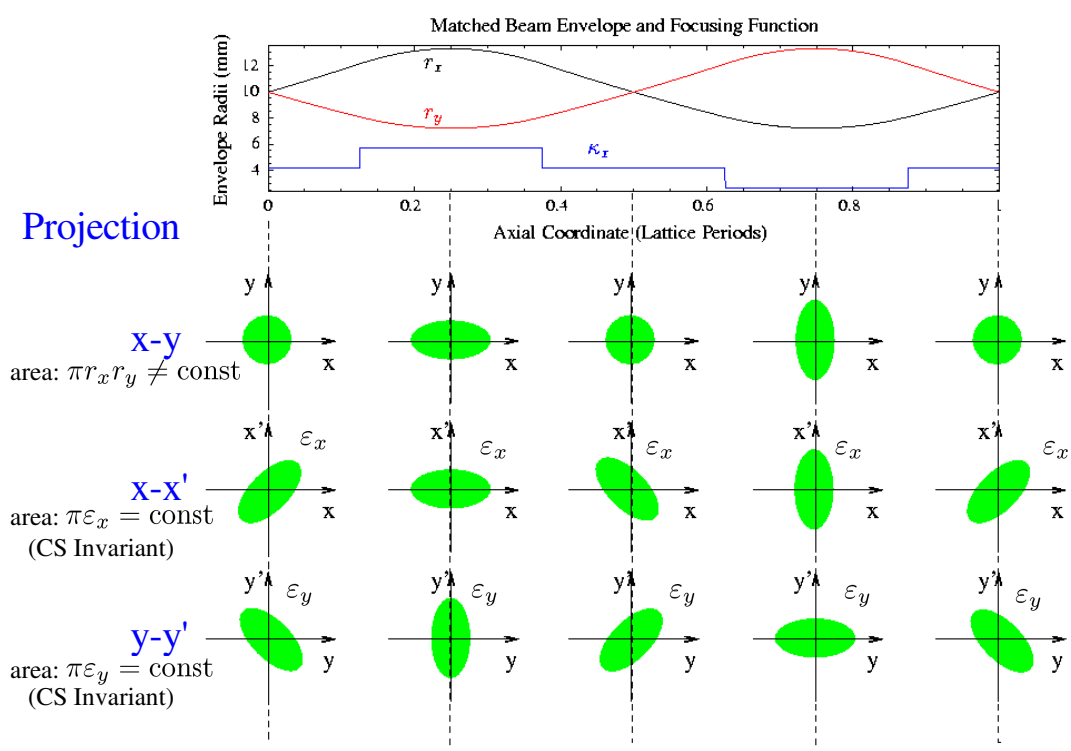

KV model shows that particle orbits in the presence of space-charge can be strongly modified – space charge slows the orbit response:

Matched envelope:

$$r_x''(s) + \kappa_x(s) r_x(s) - \frac{2Q}{r_x(s) + r_y(s)} - \frac{\varepsilon_x^2}{r_x^3(s)} = 0$$

$$r_y''(s) + \kappa_y(s) r_y(s) - \frac{2Q}{r_x(s) + r_y(s)} - \frac{\varepsilon_y^2}{r_y^3(s)} = 0$$

$$r_x(s + L_p) = r_x(s) \qquad r_x(s) > 0$$

$$r_y(s + L_p) = r_y(s) \qquad r_y(s) > 0$$

Equation of motion for x-plane "depressed" orbit in the presence of space-charge:

$$x''(s) + \kappa_x(s) x(s) - \frac{2Q}{[r_x(s) + r_y(s)] r_x(s)} x(s) = 0$$

All particles have the *same value* of depressed phase advance:

$$\sigma_x \equiv \psi_x(s_i + L_p) - \psi_x(s_i) = \varepsilon_x \int_{s_i}^{s_i + L_p} \frac{ds}{r_x^2(s)}$$

Depressed particle x-plane orbits within a matched KV beam in a periodic FODO quadrupole channel for the matched beams previously shown

Solenoidal Focusing (Larmor frame orbit):

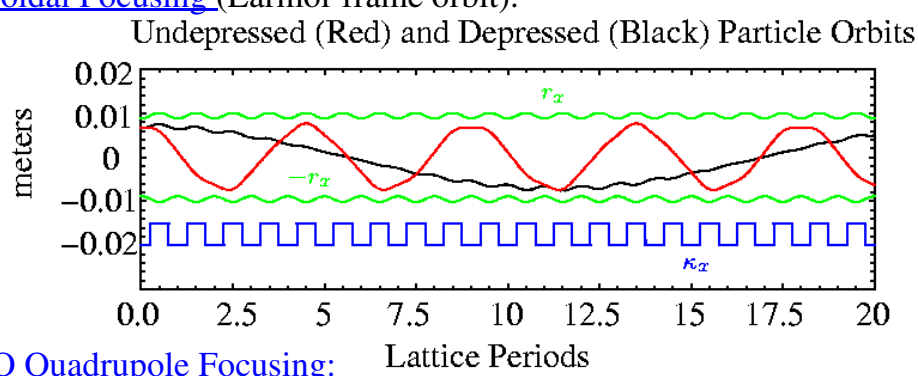

FODO Quadrupole Focusing:

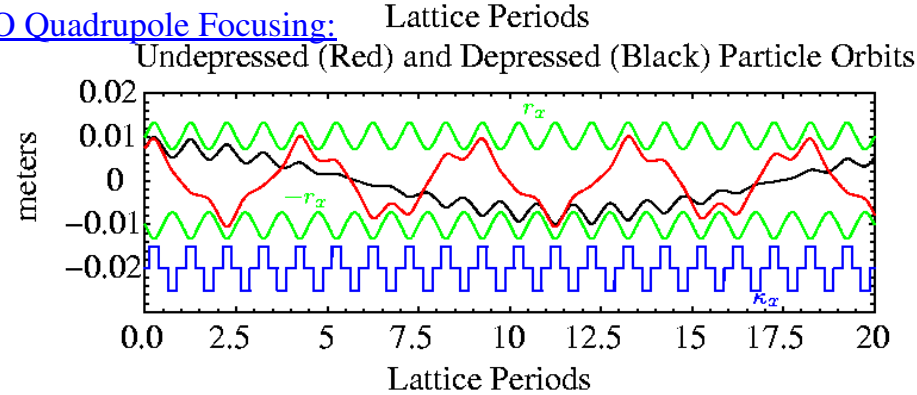

Depressed particle phase advance provides a convenient measure of space-charge strength

For simplicity take (plane symmetry in average focusing and emittance)

$$\sigma_{0x} = \sigma_{0y} \equiv \sigma_0 \qquad\qquad \varepsilon_x = \varepsilon_y \equiv \varepsilon$$

Depressed phase advance within a matched beam

$$\boxed{\sigma = \varepsilon \int_{s_i}^{s_i+L_p} \frac{ds}{r_x^2(s)} = \varepsilon \int_{s_i}^{s_i+L_p} \frac{ds}{r_y^2(s)}}$$

$$\lim_{Q\to 0} \sigma = \sigma_0$$

Normalized space charge strength

$$\boxed{0 \le \sigma/\sigma_0 \le 1}$$

$\sigma/\sigma_0 \to 0$ Cold Beam (space-charge dominated) $\varepsilon \to 0$

$\sigma/\sigma_0 \to 1$ Warm Beam (kinetic dominated) $Q \to 0$

For example matched envelope presented earlier:

Undepressed phase advance: $\sigma_0 = 80^\circ$

Depressed phase advance: $\sigma = 16^\circ \quad \to \sigma/\sigma_0 = 0.2$

repeat periods

4.5

22.5

Periods for 360 degree phase advance

Solenoidal Focusing (Larmor frame orbit):

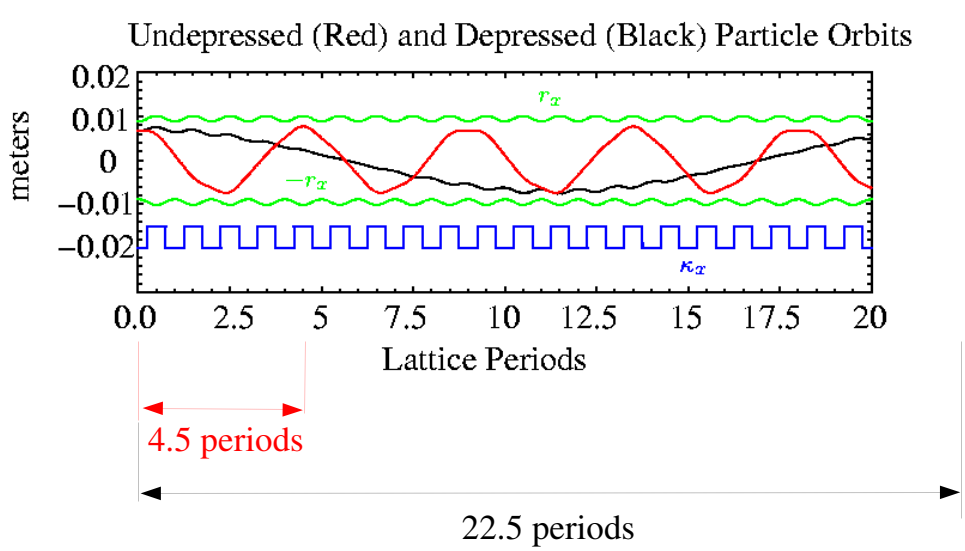

The rms equivalent beam model helps interpret general beam evolution in terms of an "equivalent" local KV distribution

For the same focusing lattice, replace any beam charge $\rho(x,y)$ density by a uniform density KV beam in each axial slice (s) using averages calculated from the actual "real" beam distribution with:

$$\langle \cdots \rangle_\perp \equiv \frac{\int d^2x_\perp \int d^2x'_\perp \; \cdots f_\perp}{\int d^2x_\perp \int d^2x'_\perp \; f_\perp} \qquad f_\perp = \text{ real distribution}$$

rms equivalent beam:

Quantity	KV Equiv.	Calculated from Distribution
Perveance	Q	$= q^2 \int d^2x_\perp \int d^2x'_\perp \; f_\perp \; / [2\pi\epsilon_0\gamma_b^3\beta_b^2c^2]$
x-edge radius	r_x	$= 2\langle x^2\rangle_\perp^{1/2}$
y-edge radius	r_y	$= 2\langle y^2\rangle_\perp^{1/2}$
x-emittance	ε_x	$= 4[\langle x^2\rangle_\perp\langle x'^2\rangle_\perp - \langle xx'\rangle_\perp]^{1/2}$
y-emittance	ε_y	$= 4[\langle y^2\rangle_\perp\langle y'^2\rangle_\perp - \langle yy'\rangle_\perp]^{1/2}$

Comments on rms equivalent beam concept:

- The emittances will generally evolve in s
  - Means that the equivalency must be recalculated in every slice as the emittances evolve
  - For reasons to be analyzed later (lectures on Kinetic Stability of Beams), this evolution is often small
- Concept is highly useful
  - KV equilibrium properties well understood and are approximately correct to model lowest order "real" beam properties

Sacherer expanded the concept of rms equivalency by showing that the equivalency works exactly for beams with elliptic symmetry space-charge [Sacherer, IEEE Trans. Nucl. Sci. 18, 1101 (1971), J.J. Barnard, Intro. Lectures]

For any beam with elliptic symmetry charge density in each transverse slice:

$$\boxed{\rho = \rho\left(\frac{x^2}{r_x^2} + \frac{y^2}{r_y^2}\right)}$$

Based on:

$$\langle x\frac{\partial\phi}{\partial x}\rangle_\perp = -\frac{\lambda}{4\pi\epsilon_0}\frac{r_x}{r_x + r_y}$$

see J.J. Barnard intro. lectures

the KV envelope equations

$$\boxed{\begin{aligned} r_x''(s) + \kappa_x(s) r_x(s) - \frac{2Q}{r_x(s) + r_y(s)} - \frac{\varepsilon_x^2(s)}{r_x^3(s)} &= 0 \\ r_y''(s) + \kappa_y(s) r_y(s) - \frac{2Q}{r_x(s) + r_y(s)} - \frac{\varepsilon_y^2(s)}{r_y^3(s)} &= 0 \end{aligned}}$$

remain valid when (averages taken with the full distribution):

$$Q = \frac{q\lambda}{2\pi\epsilon_0 m\gamma_b^3\beta_b^2 c^2} = \text{const} \qquad \lambda = q\int d^2x_\perp\ \rho\ =\ \text{const}$$

$$r_x = 2\langle x^2\rangle_\perp^{1/2} \qquad \varepsilon_x = 4[\langle x^2\rangle_\perp\langle x'^2\rangle_\perp - \langle xx'\rangle_\perp^2]^{1/2}$$

$$r_y = 2\langle y^2\rangle_\perp^{1/2} \qquad \varepsilon_y = 4[\langle y^2\rangle_\perp\langle y'^2\rangle_\perp - \langle yy'\rangle_\perp^2]^{1/2}$$

The emittances must, in general, evolve in *s* under this model

(see SM Lund lectures on *Transverse Kinetic Stability*)

Further comments on the KV equilibrium: Distribution Structure

Equilibrium distribution:

$$\boxed{f_\perp \sim \delta[\text{Courant-Snyder invariants}]}$$

Forms a highly singular hyper-shell in 4D phase-space

Schematic:

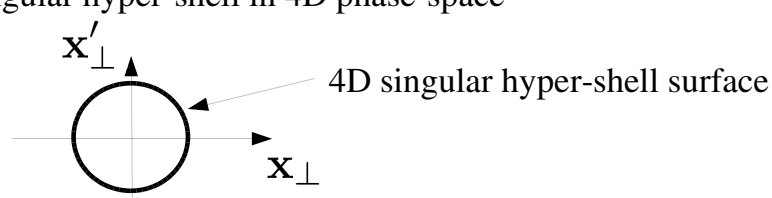

- Singular distribution has large "Free-Energy" to drive many instabilities
  - Low order envelope modes are physical and highly important (see lectures on *Centroid and Envelope Descriptions of Beams*)
- Perturbative analysis shows strong collective instabilities
  - Hofmann, Laslett, Smith, and Haber, Part. Accel. **13**, 145 (1983)
  - Higher order instabilities (collective modes) have unphysical aspects due to (delta-function) structure of distribution and must be applied with care (see lectures on *Kinetic Stability of Beams*)
  - Instabilities can cause problems if the KV distribution is employed as an initial beam state in self-consistent simulations

Preview: lecture on *Centroid and Envelope Descriptions of Beams*

Instability bands of the KV envelope equation are well understood in periodic focusing channels and must be avoided in machine operation

Envelope Mode Instability Growth Rates

Solenoid (η = 0.25) Quadrupole FODO (η = 0.70)

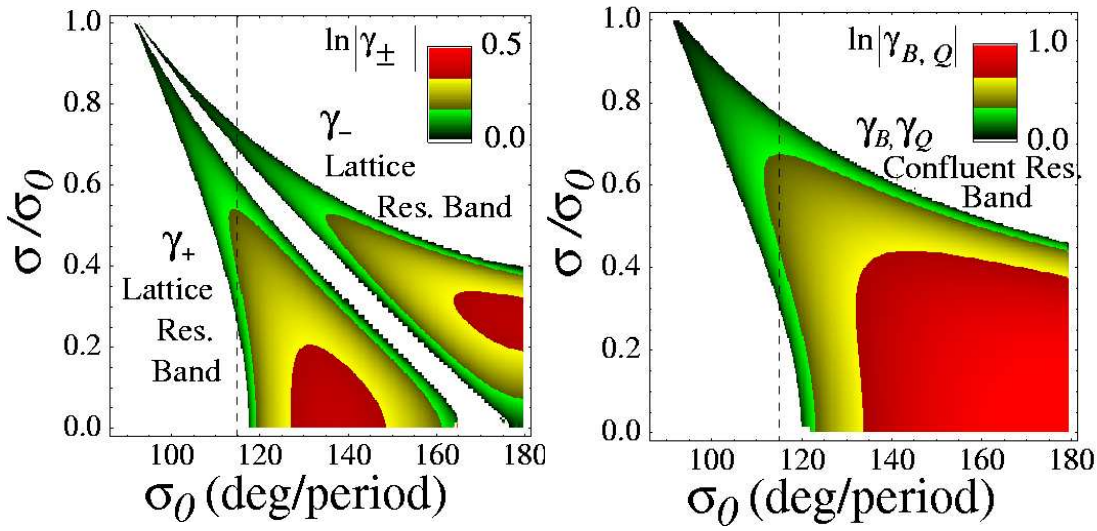

[S.M. Lund and B. Bukh, PRSTAB 024801 (2004)]

Further comments on the KV equilibrium: 2D Projections

All 2D projections of the KV distribution are uniformly filled ellipses

- Not very different from what is often observed in experimental measurements and self-consistent simulations of stable beams with strong space-charge
- Falloff of distribution at "edges" can be rapid, but smooth, for strong space-charge

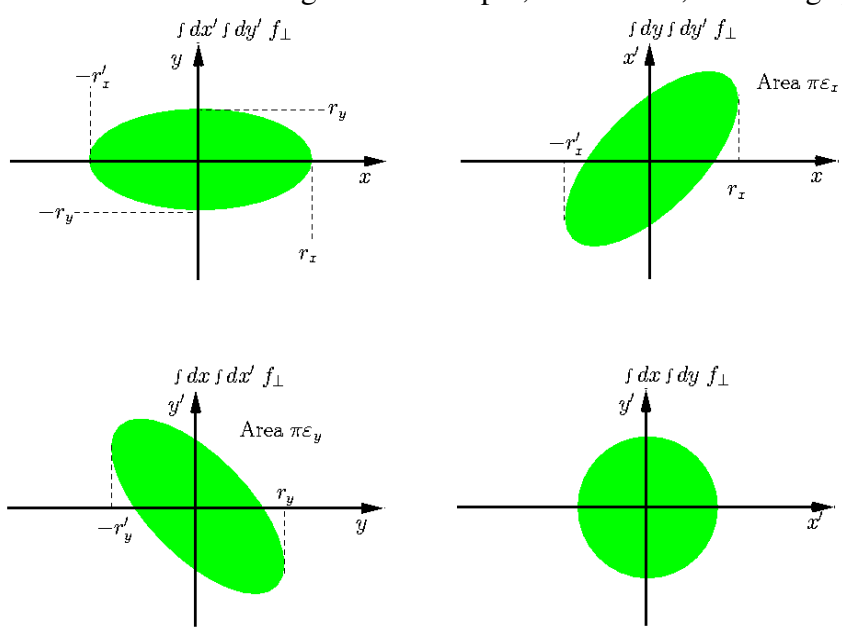

Further comments on the KV equilibrium: Angular Spreads: Coherent and Incoherent

Angular spreads within the beam:

Coherent (flow):

$$\langle x' \rangle_{\mathbf{x}'_\perp} \equiv \frac{\int d^2x'_\perp \; x'_\perp \; f_\perp}{\int d^2x'_\perp \; f_\perp} = r'_x \frac{x}{r_x}$$

Incoherent (temperature):

$$\langle (x' - r'_x x/r_x)^2 \rangle_{\mathbf{x}'_\perp} = \frac{\varepsilon_x^2}{2r_x^2}\left(1 - \frac{x^2}{r_x^2} - \frac{y^2}{r_y^2}\right)$$

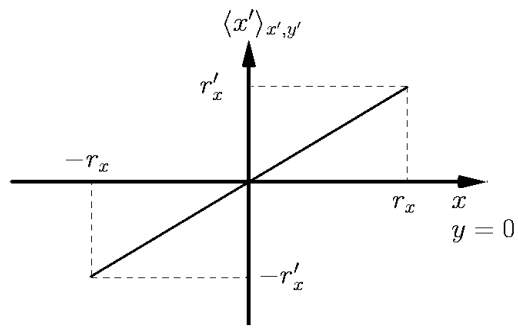

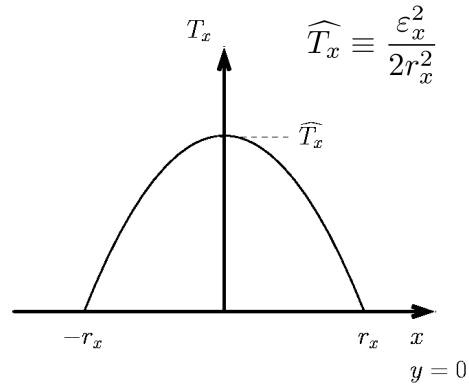

- Coherent flow required for periodic focusing to conserve charge
- Temperature must be zero at the beam edge since the distribution edge is sharp
- Parabolic temperature profile is consistent with linear grad P pressure forces in a fluid model interpretation of the (kinetic) KV distribution

Further comments on the KV equilibrium:

The KV distribution is the *only* known exact equilibrium solution for linear periodic focusing channels that is valid for finite space-charge:

- Low order properties of the distribution are physically appealing
- Illustrates relevant Courant-Snyder invariants in simple form
  - Later arguments demonstrate that these invariants should be a reasonable approximation for beams with strong space charge

Strong Vlasov instabilities associated with the KV model render the distribution inappropriate for use in high levels of detail:

- Instabilities are not all physical and render interpretation of results difficult
  - Difficult to separate physical from nonphysical effects in simulations

Possible Research Problem (unsolved in 40+ years!):

Can a valid Vlasov equilibrium be constructed for a smooth, nonuniform density distribution in a linear, periodic focusing channel?

- Not clear what invariants can be used or if any can exist
  - Nonexistence proof would also be significant
- Lack of a smooth equilibrium would not imply that real machines cannot work!

Because of a lack of theory for a smooth, self-consistent distribution that would be more physically appealing than the KV distribution we will examine smooth distributions in the idealized continuous focusing limit (after an analysis of the continuous limit of the KV theory):

- Allows more classic "plasma physics" like analysis
- Illuminates physics of intense space charge
- Lack of continuous focusing in the laboratory will prevent over generalization of results obtained

S4: Continuous Focusing limit of the KV Equilibrium Distribution

Continuous focusing, symmetric beam

$$\boxed{\begin{aligned} &\kappa_x(s) = \kappa_y(s) = k_{\beta 0}^2 = \text{const} \\ &\varepsilon_x = \varepsilon_y \equiv \varepsilon \\ &r_x = r_y \equiv r_b \end{aligned}}$$

Undepressed betatron wavenumber

envelope equation reduces to

$$r_b'' + k_{\beta 0}^2 r_b - \frac{Q}{r_b} - \frac{\varepsilon^2}{r_b^3} = 0 \longrightarrow \boxed{r_b = \left(\frac{Q + \sqrt{4k_{\beta 0}^2 \varepsilon^2 + Q^2}}{2k_{\beta 0}^2} \right)^{1/2} = \text{const}}$$

Particle orbit in the beam:

$$\mathbf{x}_\perp'' + k_\beta^2 \mathbf{x}_\perp = 0 \qquad k_\beta = \sqrt{k_{\beta 0}^2 - \frac{Q}{r_b^2}} = \text{const}$$

Depressed betatron wavenumber

$$\longrightarrow \boxed{\mathbf{x}_\perp(s) = \mathbf{x}_{\perp i} \cos[k_\beta(s - s_i)] + \frac{\mathbf{x}_{\perp i}'}{k_\beta} \sin[k_\beta(s - s_i)]}$$

Space-charge tune depression (rate of phase advance same everywhere, L_p arb.)

$$\frac{k_\beta}{k_{\beta 0}} = \frac{\sigma}{\sigma_0} = \left(1 - \frac{Q}{k_{\beta 0}^2 r_b^2} \right)^{1/2} \qquad 0 \le \frac{\sigma}{\sigma_0} \le 1$$

$$\varepsilon \to 0 \qquad Q \to 0$$

Continuous Focusing KV Equilibrium – Undepressed and depressed particle orbits

$$k_\beta = \frac{\sigma}{\sigma_0} k_{\beta 0} \qquad \frac{\sigma}{\sigma_0} = 0.2$$

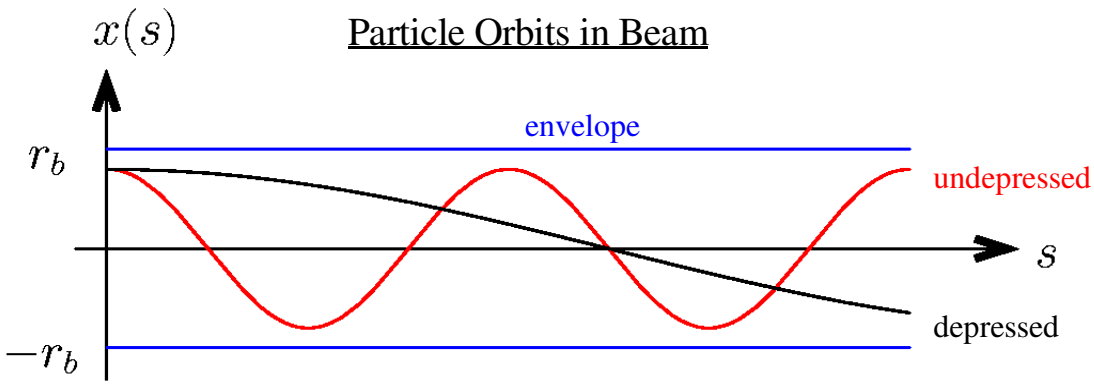

Much simpler in details than the periodic focusing case, but qualitatively similar in that space-charge "depresses" the rate of particle phase advance

Continuous Focusing KV Beam – Equilibrium Distribution Form

Using

$$\lambda = q\pi\hat{n}r_b^2 \qquad \hat{n} = \text{const} \qquad \text{density within the beam}$$

for the beam line charge and

$$\delta(\text{const} \cdot x) = \frac{\delta(x)}{\text{const}}$$

the full elliptic beam KV distribution can be expressed as

$$\boxed{\begin{aligned} f_\perp &= \frac{\lambda}{q\pi^2\varepsilon_x\varepsilon_y}\delta\left[\left(\frac{x}{r_x}\right)^2 + \left(\frac{r_x x' - r_x' x}{\varepsilon_x}\right)^2 + \left(\frac{y}{r_y}\right)^2 + \left(\frac{r_y y' - r_y' y}{\varepsilon_y}\right)^2 - 1\right] \\ &= \frac{\hat{n}}{2\pi}\delta(H_\perp - H_{\perp b}) \end{aligned}}$$

where

$$H_\perp = \frac{1}{2}\mathbf{x}_\perp'^2 + \frac{\varepsilon^2}{2r_b^4}\mathbf{x}_\perp^2 \qquad \text{-- Hamiltonian}$$

$$= \frac{1}{2}\mathbf{x}_\perp'^2 + \frac{1}{2}k_{\beta 0}^2\mathbf{x}_\perp^2 + \frac{q\phi}{m\gamma_b^3\beta_b^2c^2}$$

$$H_{\perp b} \equiv \frac{\varepsilon^2}{2r_b^2} = \text{const} \qquad \text{-- Hamiltonian at beam edge}$$

Equilibrium distribution

$$\boxed{f_\perp(H_\perp) = \frac{\hat{n}}{2\pi}\delta(H_\perp - H_{\perp b})}$$

$$H_{\perp b} = \frac{\varepsilon^2}{2r_b^2} = \text{const}$$

$$\hat{n} = \text{const}$$

then it is straightforward to explicitly calculate (see homework problems)

Density: $$n = \int d^2x'_\perp\, f_\perp = \begin{cases} \hat{n}, & 0 \le r < r_b \\ 0, & r_b < r \end{cases}$$

Temperature: $$T_x = \gamma_b m \beta_b^2 c^2 \frac{\int d^2x'_\perp\, x'^2 f_\perp}{\int d^2x'_\perp\, f_\perp} = \begin{cases} \widehat{T_x}(1 - r^2/r_b^2), & 0 \le r < r_b \\ 0, & r_b < r \end{cases}$$

Density

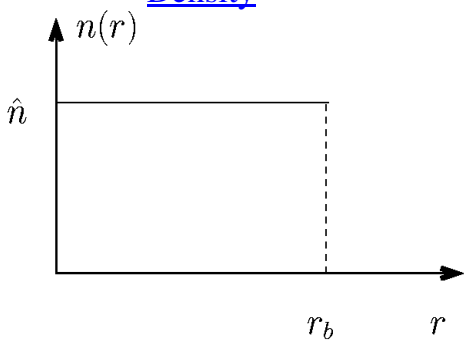

Temperature

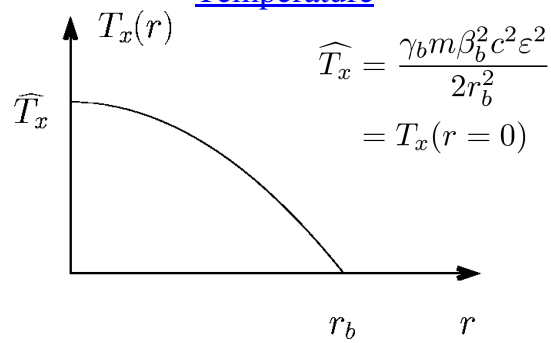

$$\widehat{T_x} = \frac{\gamma_b m \beta_b^2 c^2 \varepsilon^2}{2r_b^2} = T_x(r=0)$$

Continuous Focusing KV Beam – Comments

For continuous focusing, $H_\perp$ is a single particle constant of the motion (see problem sets), so it is not surprising that the KV equilibrium form reduces to a delta function form of $f_\perp(H_\perp)$

- Because of the delta-function distribution form, all particles in the continuous focusing KV beam have the same transverse energy with $H_\perp = H_{\perp b} = \text{const}$

Several textbook treatments of the KV distribution derive continuous focusing versions and then just write down (if at all) the periodic focusing version based on Courant-Snyder invariants. This can create a false impression that the KV distribution is a Hamiltonian-type invariant in the general form.

- For non-continuous focusing channels there is no simple relation between Courant-Snyder type invariants and $H_\perp$

S5: Equilibrium Distributions in Continuous Focusing Channels

Take

$$\boxed{\kappa_x(s) = \kappa_y(s) = k_{\beta 0}^2 = \text{const}}$$

- Real transport channels have s-varying focusing functions
- For a rough correspondence to physical lattices take: $k_{\beta 0} = \sigma_0 / L_p$

A valid family of equilibria can be constructed for any choice of function:

$$\boxed{f_\perp = f_\perp(H_\perp) \geq 0} \qquad H_\perp = \frac{1}{2}\mathbf{x}_\perp'^2 + \frac{1}{2}k_{\beta 0}^2 \mathbf{x}_\perp^2 + \frac{q\phi}{m\gamma_b^3\beta_b^2 c^2}$$

ϕ must be calculated consistently from the nonlinear Poisson equation:

$$\boxed{\left(\frac{\partial^2}{\partial x^2} + \frac{\partial^2}{\partial y^2}\right)\phi = -\frac{q}{\epsilon_0}\int d^2x'_\perp \; f_\perp(H_\perp)}$$

- Solutions generated will be steady-state $(\partial/\partial s = 0)$
- It can be shown that the Poisson equation only has solutions with $(\partial/\partial\theta = 0)$

The Hamiltonian is only equivalent to the Courant-Snyder invariant in continuous focusing. In periodic focusing channels $\kappa_x(s)$ and $\kappa_y(s)$ vary in s and the Hamiltonian is not a constant of the motion.

The axisymmetric Poisson equation simplifies to:

$$\frac{1}{r}\frac{\partial}{\partial r}\left(r\frac{\partial\phi}{\partial r}\right) = -\frac{qn}{\epsilon_0} = -\frac{q}{\epsilon_0}\int d^2x'_\perp \; f_\perp(H_\perp)$$

Introduce a streamfunction

$$\boxed{\psi(r) = \frac{1}{2}k_{\beta 0}^2 r^2 + \frac{q\phi}{m\gamma_b^3\beta_b^2 c^2}} \qquad r = \sqrt{x^2 + y^2}$$

then

$$\boxed{H_\perp = \frac{1}{2}\mathbf{x}_\perp'^2 + \psi}$$

and system axisymmetry can be exploited to calculate the beam density as

$$n(r) = \int d^2x'_\perp \; f_\perp(H_\perp) \; = 2\pi\int_\psi^\infty dH_\perp \; f_\perp(H_\perp)$$

Then the Poisson equation can be recast in terms of the stream function as

$$\boxed{\frac{1}{r}\frac{\partial}{\partial r}\left(r\frac{\partial\psi}{\partial r}\right) = 2k_{\beta 0}^2 - \frac{2\pi q^2}{m\epsilon_0\gamma_b^3\beta_b^2 c^2}\int_{\psi(r)}^\infty dH_\perp \; f_\perp(H_\perp)}$$

To characterize a choice of equilibrium function $f_\perp(H_\perp)$, the (transformed) Poisson equation must be solved

- Equation is, in general, highly nonlinear rendering the procedure difficult

Some general features of equilibria can still be understood in terms of moments

- Apply rms equivalent beam picture

Moment properties of continuous focusing equilibrium distributions

Equilibria satisfy the rms equivalent matched beam envelope equation:

$$\boxed{k_{\beta 0}^2 r_b - \frac{Q}{r_b} - \frac{\varepsilon^2}{r_b^3} = 0}$$

- Describes average radial force balance of particles

where $\langle \cdots \rangle_\perp = \dfrac{\int d^2x_\perp \int d^2x'_\perp \; \cdots f_\perp(H_\perp)}{\int d^2x_\perp \int d^2x'_\perp \; f_\perp(H_\perp)}$

$$Q = \frac{q\lambda}{2\pi\epsilon_0 m\gamma_b^3\beta_b^2c^2} = \text{const} \qquad \lambda = q\int d^2x_\perp \int d^2x'_\perp \; f_\perp(H_\perp)$$

$$r_b^2 = 2\langle r^2\rangle_\perp = \frac{\int_0^\infty dr\; r^3 \int_\psi^\infty dH_\perp \; f_\perp(H_\perp)}{\int_0^\infty dr\; r \int_\psi^\infty dH_\perp \; f_\perp(H_\perp)}$$

$$\varepsilon^2 = 2r_b^2\langle \mathbf{x}_\perp'^2\rangle_\perp = 2r_b^2 \frac{\int_0^\infty dr\; r \int_\psi^\infty dH_\perp \; (H_\perp - \psi) f_\perp(H_\perp)}{\int_0^\infty dr\; r \int_\psi^\infty dH_\perp \; f_\perp(H_\perp)}$$

Parameters used to define

$$f_\perp(H_\perp)$$

should be cast in terms of

$$Q, \quad \varepsilon, \quad r_b$$

for use in accelerator applications. The rms equivalent beam equations can be used to carry out needed parameter eliminations. Such eliminations can be highly nontrivial due to the nonlinear form of the equations.

A kinetic temperature can also be calculated

$$T_x = \langle x'^2 \rangle_{\mathbf{x}'_\perp} \qquad \langle \cdots \rangle_{\mathbf{x}'_\perp} \equiv \frac{\int d^2x'_\perp \; \cdots f_\perp}{\int d^2x'_\perp \; f_\perp}$$

$$\boxed{n(r)T_x(r) = \frac{1}{2}\int d^2x'_\perp \; \mathbf{x}'^2_\perp f_\perp(H_\perp) \; = 2\pi \int_\psi^\infty dH_\perp \; (H_\perp - \psi) f_\perp(H_\perp)}$$

which is also related to the emittance,

$$\langle x'^2 \rangle_\perp = \frac{\int d^2x_\perp \; nT_x}{\int d^2x_\perp n} \qquad \boxed{\varepsilon^2 = 16\langle x^2 \rangle_\perp \langle x'^2 \rangle_\perp = 4r_b^2 \frac{\int d^2x_\perp \; nT}{\int d^2x_\perp \; n}}$$

Choices of continuous focusing equilibrium distributions:

Common choices for $f_\perp(H_\perp)$ analyzed in the literature:

1) KV (already covered)

$$\boxed{f_\perp \propto \delta(H_\perp - H_{\perp b})}$$

$$H_{\perp b} = \text{const}$$

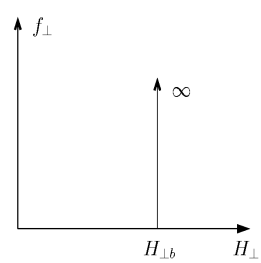

2) Waterbag (to be covered)

[see M. Reiser, *Charged Particle Beams*, (1994)]

$$\boxed{f_\perp \propto \Theta(H_{\perp b} - H_\perp)}$$

$$\Theta(x) = \begin{cases} 0, & x < 0 \\ 1, & 0 < x \end{cases}$$

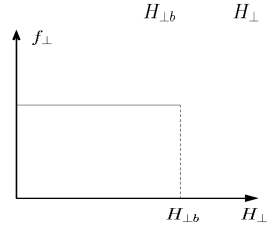

3) Thermal (to be covered)

[see M. Reiser; Davidson, *Noneutral Plasmas*, 1990]

$$\boxed{f_\perp \propto \exp(-H_\perp/T)}$$

$$T = \text{const} > 0$$

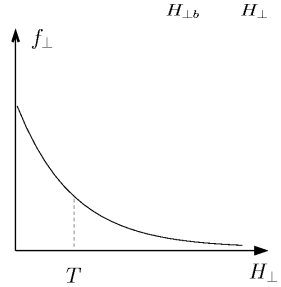

Infinity of choices can be made for an infinity of papers!

- Fortunately, range of behavior can be understood with a few reasonable choices

S6: Continuous Focusing: The Waterbag Equilibrium Distribution:

[see Reiser, Theory and Design of Charged Particle Beams, Wiley (1994)]

Waterbag distribution:

$$f_\perp(H_\perp) = f_0 \Theta(H_b - H_\perp) \qquad f_0 = \text{const}$$

$$H_b = \text{const} \quad \text{Edge Hamiltonian}$$

$$\Theta(x) = \begin{cases} 1, & x > 0 \\ 0, & x < 0 \end{cases}$$

The physical edge radius r_e of the beam will be related to the edge Hamiltonian:

$$H_\perp|_{r=r_e} = H_b$$

Employing the general formulation, the Poisson equation for this choice can be analytically solved simplifying analysis.

Details of Waterbag analysis to be included in later editions of notes.

1) Density profile at fixed line charge and focusing strength

$$Q = 10^{-4} \qquad k_{\beta 0}^2 = \text{const}$$

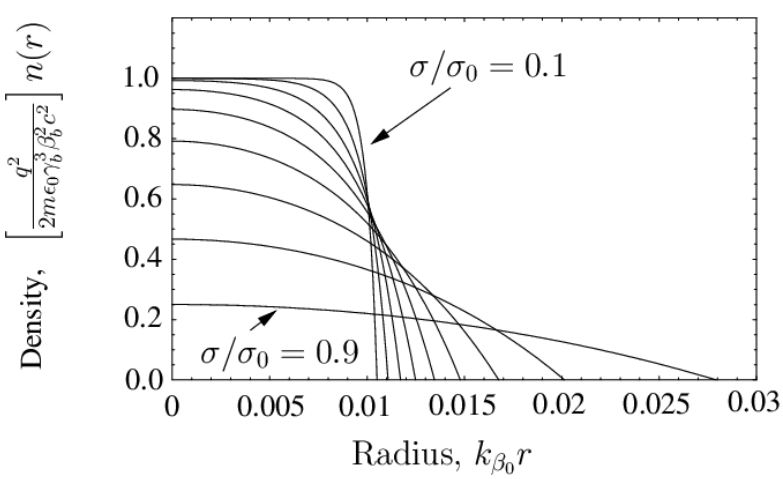

2) Phase-space boundary at fixed line charge and focusing strength

$Q = 10^{-4}$ $\qquad k_{\beta 0}^2 = \text{const}$

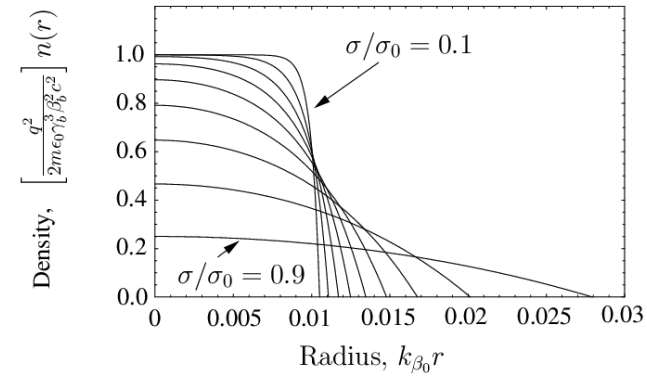

Density Profile

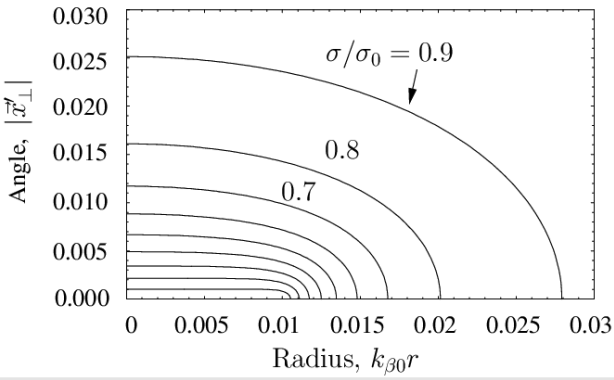

Edge of distribution in phase-space

Scaled parameters for examples

					$Q = 10^{-4}$	
σ/σ_0	s_b	$\frac{k_{\beta 0}^2 r_b^2}{Q}$	$k_0 r_e$	$\frac{r_e}{r_b}$	$\frac{k_0}{k_{\beta 0}}$	$10^3 \times k_{\beta 0}\varepsilon_b$
0.9	0.2502	5.263	1.112	1.217	39.81	0.4737
0.8	0.4666	2.778	1.709	1.208	84.87	0.2222
0.7	0.6477	1.961	2.304	1.197	137.5	0.1373
0.6	0.7916	1.563	2.979	1.183	201.5	0.09375
0.5	0.8968	1.333	3.821	1.166	283.8	0.06667
0.4	0.9626	1.190	4.978	1.144	398.7	0.04762
0.3	0.9928	1.099	6.789	1.118	579.3	0.03297
0.2	0.9997	1.042	10.25	1.085	925.6	0.02083
0.1	1.0000	1.010	20.38	1.046	1938.	0.01010

S7: Continuous Focusing: The Thermal Equilibrium Distribution:

[see Davidson, Physics of Nonneutral Plasma, Addison Wesley (1990) and Reiser, Theory and Design of Charged Particle Beams, Wiley (1994)]

In an infinitely long continuous focusing channel, collisions will eventually relax the beam to thermal equilibrium. The Fokker-Planck equation predicts that the unique Maxwell-Boltzmann distribution describing this limit is:

$$\lim_{s\to\infty} f_\perp \propto \exp\left(-\frac{H_{\rm rest}}{T}\right)$$

$H_{\rm rest} =$ single particle Hamiltonian of beam in rest frame (energy units)

$T = \text{const}$ Thermodynamic temperature (energy units)

Beam propagation time in transport channel is generally short relative to collision time, inhibiting full relaxation

- Collective effects may enhance relaxation rate
  - Wave spectrums likely large for real beams and enhanced by transient and nonequilibrium effects
  - Random errors acting on system may enhance and lock-in phase mixing

Continuous focusing thermal equilibrium distribution

Analysis of the rest frame transformation shows that the 2D Maxwell-Boltzmann distribution (careful on frame for temperature definition!) is:

$$f_\perp(H_\perp) = \frac{m\gamma_b\beta_b^2c^2\hat{n}}{2\pi T}\exp\left(-\frac{m\gamma_b\beta_b^2c^2H_\perp}{T}\right)$$

$$H_\perp = \frac{1}{2}\mathbf{x}_\perp'^2 + \frac{1}{2}k_{\beta 0}^2\mathbf{x}_\perp^2 + \frac{q\phi}{m\gamma_b^3\beta_b^2c^2} = \frac{1}{2}\mathbf{x}_\perp'^2 + \psi$$

$T = \text{const}$ Temperature (energy units, lab frame)

$n(r=0) = \hat{n} = \text{const}$ on-axis density

$\phi(r=0) = 0$ (reference choice)

The density can then be conveniently calculated in terms of a scaled stream function:

$$n(r) = \int d^2x'_\perp\, f_\perp = \hat{n}e^{-\tilde{\psi}}$$

$$\tilde{\psi}(r) \equiv \frac{m\gamma_b\beta_b^2c^2\psi}{T} = \frac{1}{T}\left(\frac{m\gamma_b\beta_b^2c^2k_{\beta 0}^2}{2}r^2 + \frac{q\phi}{\gamma_b^2}\right)$$

and the x- and y-temperatures are equal and spatially uniform with:

$$T_x = \gamma_b m\beta_b^2c^2\frac{\int d^2x'_\perp\, x'^2\, f_\perp}{\int d^2x'_\perp\, f_\perp} = T = \text{const}$$

Scaled Poisson equation for continuous focusing thermal equilibrium

To describe the thermal equilibrium density profile, the Poisson equation must be solved. In terms of the scaled streamfunction:

$$\boxed{\begin{gathered}\frac{1}{\rho}\frac{\partial}{\partial\rho}\left(\rho\frac{\partial\tilde{\psi}}{\partial\rho}\right) = 1 + \Delta - e^{-\tilde{\psi}} \\ \tilde{\psi}(\rho = 0) = 0 \qquad \frac{\partial\tilde{\psi}}{\partial\rho}(\rho = 0) = 0\end{gathered}}$$

Here,

$$\lambda_D = \left(\frac{\epsilon_0 T}{q^2\hat{n}}\right)^{1/2}$$ Debye length formed from the peak, on-axis beam density

$$\rho = \frac{r}{\gamma_b\lambda_D}$$ Scaled radial coordinate in rel. Debye lengths

$$\hat{\omega}_p \equiv \left(\frac{q^2\hat{n}}{\epsilon_0 m}\right)^{1/2}$$ Plasma frequency formed from on-axis beam density $\longrightarrow$ $$\lambda_D = \left(\frac{T}{\hat{\omega}_p^2 m}\right)^{1/2}$$

$$\Delta = \frac{2\gamma_b^3\beta_b^2c^2k_{\beta 0}^2}{\hat{\omega}_p^2} - 1$$ Dimensionless parameter relating the ratio of applied to space-charge defocusing forces

- Equation is highly nonlinear and must, in general, be solved numerically
- Scaled solutions depend only on the single dimensionless parameter Δ

Numerical solution of scaled thermal equilibrium Poisson equation in terms of a normalized density

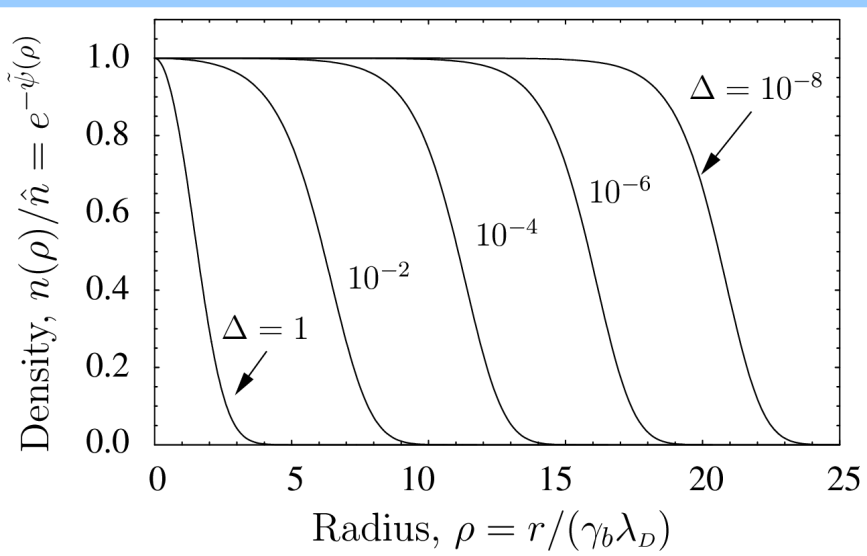

- Equation is highly nonlinear and must, in general, be solved numerically
  - Dependance on Δ is very sensitive
  - For small Δ, the beam is nearly uniform in the core
- Edge fall-off is always in a few Debye lengths when Δ is small
  - Edge becomes very sharp at fixed beam line-charge

Parameters constraints for the thermal equilibrium beam

Parameters employed in $f_\perp(H_\perp)$ to specify the equilibrium are (+ kinematic factors):

$$\hat{n}, \quad T, \quad \Delta$$

Parameters preferred for accelerator applications:

$$k_{\beta 0}, \quad Q, \quad \varepsilon_x = \varepsilon_y = \varepsilon_b$$

Needed constraints can be calculated directly from the equilibrium:

$$\boxed{\begin{aligned} Q &= \left(\frac{T}{\gamma_b m \beta_b^2 c^2}\right) \int_0^\infty d\rho\rho\, e^{-\tilde{\psi}} \\ k_{\beta 0}^2 \varepsilon_b &= 4\left(\frac{T}{\gamma_b m \beta_b^2 c^2}\right)\left[4\left(\frac{T}{\gamma_b m \beta_b^2 c^2}\right) + Q\right] \\ k_{\beta 0}^2 &= \left(\frac{T}{\gamma_b m \beta_b^2 c^2}\right) \frac{1+\Delta}{2(\gamma_b \lambda_D)^2} \end{aligned}}$$

Integral function of Δ only

Also useful,

$$\boxed{r_b^2 = 4\langle x^2 \rangle_\perp = \frac{1}{k_{\beta 0}^2}\left[4\left(\frac{T}{\gamma_b m \beta_b^2 c^2}\right) + Q\right]}$$

These constraints must, in general, be solved numerically

- Useful to probe system sensitivities in relevant parameters

Examples:

1) rms equivalent beam tune depression as a function of Δ

$$\frac{\sigma}{\sigma_0} = \sqrt{1 - \frac{Q}{k_{\beta_0}^2 r_b^2}} = \left\{1 - \frac{[\int_0^\infty d\rho\, \rho e^{-\tilde{\psi}}]^2}{(1+\Delta)\int_0^\infty d\rho\rho^3 e^{-\tilde{\psi}}}\right\}^{1/2}$$

R.H.S function of Δ only

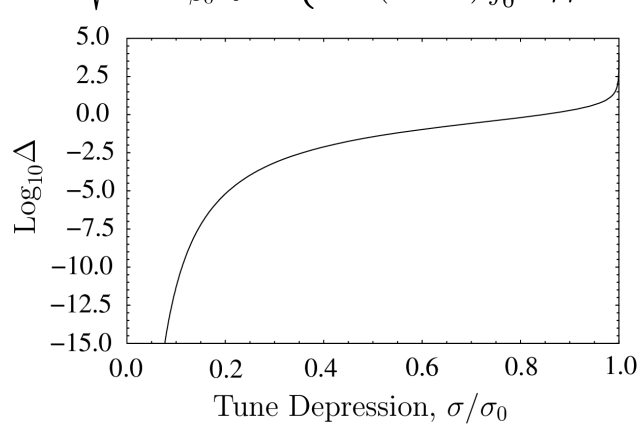

- Small tune depression corresponds to *extremely* small values of Δ
  - Special numerical methods must be employed to calculate

2) Density profile at fixed line charge and focusing strength

$Q = 10^{-4}$ $\qquad k_{\beta 0}^2 = \text{const}$

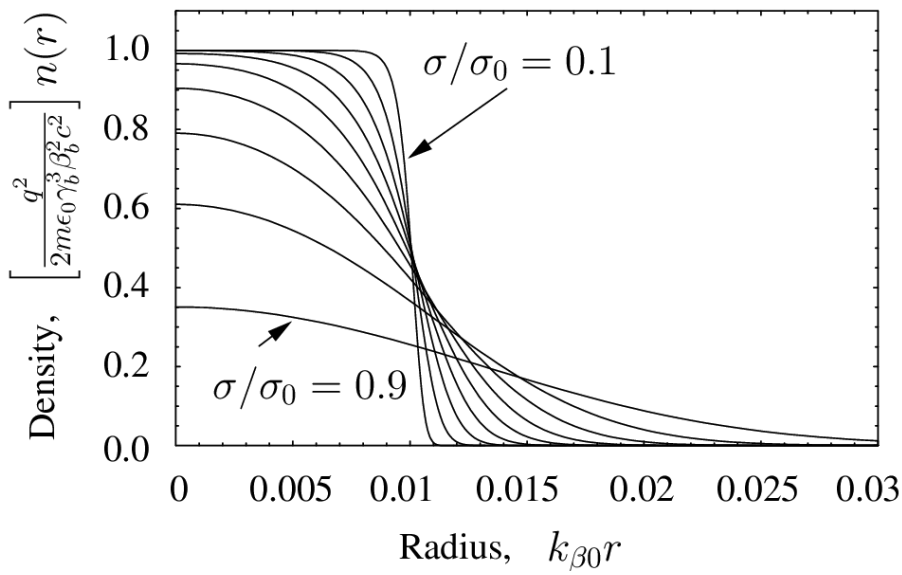

- Density profile changes with scaled T
  - Low values yields a flat-top => $\sigma/\sigma_0 \to 0$
  - High values yield a Gaussian like profile => $\sigma/\sigma_0 \to 1$

3) Distribution contours at fixed line charge and focusing strength

$Q = 10^{-4}$ $\qquad k_{\beta 0}^2 = \text{const}$

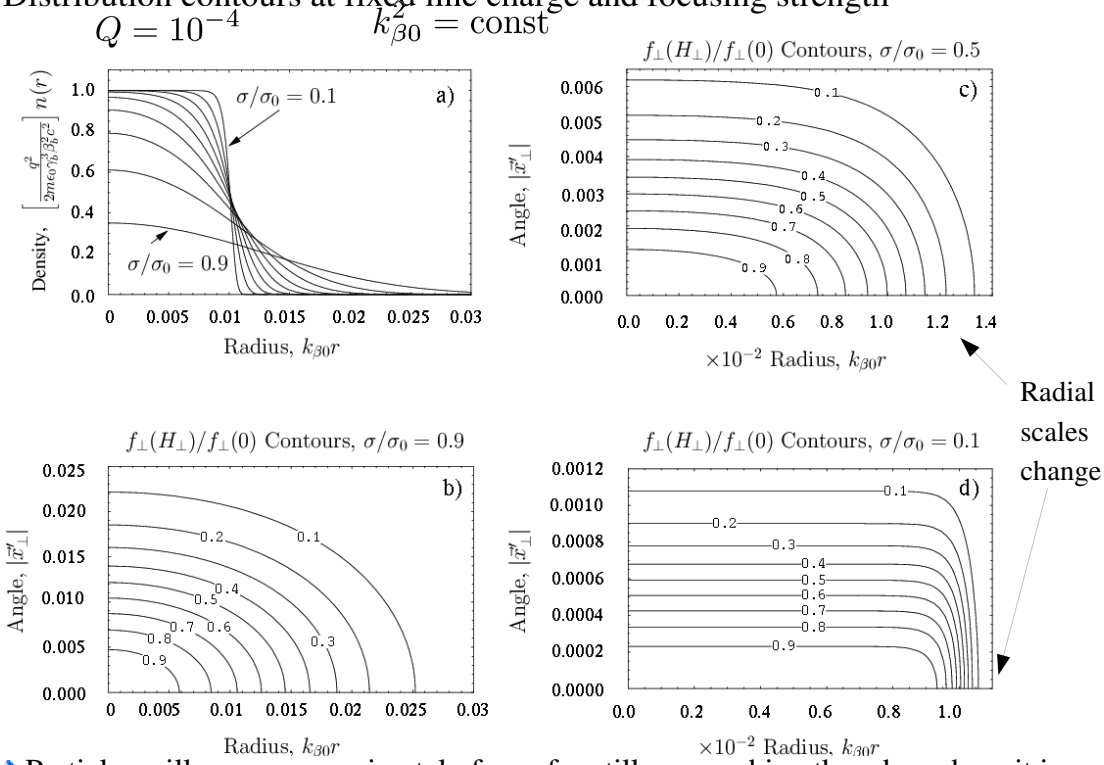

- Particles will move approximately force-free till approaching the edge where it is rapidly bent back (see Debye screening analysis this lecture)

Scaled parameters for examples 2) and 3)

			$Q = 10^{-4}$		
σ/σ_0	Δ	s_b	$k_{\beta 0}\gamma_b\lambda_D$	$\frac{T}{m\gamma_b\beta_b^2c^2}$	$10^3 \times k_{\beta 0}\varepsilon_b$
0.9	1.851	0.3508	12.33	1.065×10^{-4}	0.4737
0.8	6.382×10^{-1}	0.6104	6.034	4.444×10^{-5}	0.2222
0.7	2.649×10^{-1}	0.7906	3.898	2.402×10^{-5}	0.1373
0.6	1.059×10^{-1}	0.9043	2.788	1.406×10^{-5}	0.09375
0.5	3.501×10^{-2}	0.9662	2.077	8.333×10^{-6}	0.06667
0.4	7.684×10^{-3}	0.9924	1.549	4.762×10^{-6}	0.04762
0.3	6.950×10^{-4}	0.9993	1.112	2.473×10^{-6}	0.03297
0.2	6.389×10^{-6}	1.0000	0.7217	1.042×10^{-6}	0.02083
0.1	4.975×10^{-12}	1.0000	0.3553	2.525×10^{-7}	0.01010

Comments on continuous focusing thermal equilibria

From these results it is not surprising that the KV model works well for real beams with strong space-charge (i.e, rms equivalent σ/σ_0 small) since the edges of a smooth thermal distribution become sharp

- Thermal equilibrium likely overestimates the edge with since T = const, whereas a real distribution likely becomes colder near the edge

However, the beam edge contains strong nonlinear terms that will cause deviations from the KV model

- Nonlinear terms can radically change the stability properties (stabilize fictitious higher order KV modes)
- Smooth distributions contain a spectrum of particle oscillation frequencies that are amplitude dependent

S8: Continuous Focusing: Debye Screening in a Thermal Equilibrium Beam

[Davidson, Physics of Nonneutral Plasmas, Addison Wesley (1990)]

We will show that space-charge and the applied focusing forces of the lattice conspire together to Debye screen interactions in the core of a beam with high space-charge intensity

- Will systematically derive the Debye length employed in the intro lectures of J.J. Barnard
- The applied focusing forces are analogous to a stationary neutralizing species in a plasma

// Review:

Free-space field of a "bare" test line-charge λ_t at the origin $r = 0$

$$\rho(r) = \lambda_t \frac{\delta(r)}{2\pi r} \qquad \frac{1}{r}\frac{\partial}{\partial r}\left(r\frac{\partial \phi}{\partial r}\right) = -\frac{\lambda_t}{2\pi\epsilon_0}\frac{\delta(r)}{r}$$

solution (use Gauss' theorem) shows long-range interaction

$$\boxed{\begin{aligned} \phi &= -\frac{\lambda_t}{2\pi\epsilon_0}\ln(r) + \text{const} \\ E_r &= -\frac{\partial \phi}{\partial r} = \frac{\lambda_t}{2\pi\epsilon_0 r} \end{aligned}}$$

//

Place a *small* test line charge at $r = 0$ in a thermal equilibrium beam:

$$\frac{1}{r}\frac{\partial}{\partial r}\left(r\frac{\partial \phi}{\partial r}\right) = -\frac{q}{\epsilon_0}\int d^2x'_\perp\, f_\perp(H_\perp) \;-\; \frac{\lambda_t}{2\pi\epsilon_0}\frac{\delta(r)}{r}$$

Thermal Equilibrium Test Line-Charge

Set:

$$\phi = \phi_0 + \delta\phi$$

$\phi_0 =$ Thermal Equilibrium potential with no test line-charge

$\delta\phi =$ Perturbed potential from test line-charge

Assume thermal equilibrium adapts adiabatically to the test line-charge:

$$n(r) = \int d^2x'_\perp\, f_\perp(H_\perp) = \hat{n}e^{-\tilde{\psi}} \simeq \hat{n}e^{-\tilde{\psi}_0(r)}e^{-q\delta\phi/(\gamma_b^2 T)}$$

$$\simeq \hat{n}e^{-\tilde{\psi}_0(r)}\left(1 - \frac{q\delta\phi}{\gamma_b^2 T}\right) \qquad \left|\frac{q\delta\phi}{\gamma_b^2 T}\right| \ll 1$$

Yields:

$$\frac{1}{r}\frac{\partial}{\partial r}\left(r\frac{\partial \delta\phi}{\partial r}\right) = -\frac{q^2}{\epsilon_0\gamma_b^2 T}\hat{n}e^{-\tilde{\psi}_0(r)} \;-\; \frac{\lambda_t}{2\pi\epsilon_0}\frac{\delta(r)}{r}$$

Assume a relatively cold beam so the density is flat near the test line-charge:

$$\hat{n}e^{-\tilde{\psi}_0(r)} \simeq \hat{n}$$

This gives:

$$\frac{1}{r}\frac{\partial}{\partial r}\left(r\frac{\partial \delta\phi}{\partial r}\right) - \frac{\delta\phi}{\gamma_b^2\lambda_D^2} = -\frac{\lambda_t}{2\pi\epsilon_0}\frac{\delta(r)}{r}$$

$$\lambda_D = \left(\frac{\epsilon_0 T}{q^2\hat{n}}\right)^{1/2} =$$ Debye radius formed from peak, on-axis beam density

Derive a general solution by connecting solution very near the test charge with the general solution for r nonzero:

Near solution: $(r \to 0)$

$$\frac{\delta\phi}{\gamma_b^2\lambda_D^2} \quad \text{Negligible ---> } \quad \frac{1}{r}\frac{\partial}{\partial r}\left(r\frac{\partial \delta\phi}{\partial r}\right) = -\frac{\lambda_t}{2\pi\epsilon_0}\frac{\delta(r)}{r}$$

The free-space solution can be immediately applied:

$$\delta\phi \simeq -\frac{\lambda_t}{2\pi\epsilon_0}\ln(r) + \text{const}$$
$$r \to 0$$

General Exterior Solution: $(r \neq 0)$

The delta-function term vanishes giving:

$$\frac{1}{\rho}\frac{\partial}{\partial \rho}\left(\rho\frac{\partial \delta\phi}{\partial \rho}\right) - \delta\phi = 0 \qquad \rho \equiv \frac{r}{\gamma_b\lambda_D}$$

This is a modified Bessel equation of order 0 with general solution:

$$\delta\phi = C_1 I_0(\rho) + C_2 K_0(\rho)$$

$I_0(x) =$ Modified Bessel Func, 1st kind

$K_0(x) =$ Modified Bessel Func, 2nd kind

$C_1, \quad C_2 = \text{constants}$

Connection and General Solution:

Use limiting forms:

$$\rho \ll 1$$
$$I_0(\rho) \to 1 + \Theta(\rho^2)$$
$$K_0(\rho) \to -[\ln(\rho/2) + 0.5772\cdots + \Theta(\rho^2)]$$

$$\rho \gg 1$$
$$I_0(\rho) \to \frac{e^\rho}{\sqrt{2\pi\rho}}[1 + \Theta(1/\rho)]$$
$$K_0(\rho) \to \sqrt{\frac{\pi}{2\rho}}[1 + \Theta(1/\rho)]$$

Comparison shows that we must choose for connection to the near solution and regularity at infinity:

$$\boxed{\begin{aligned} C_1 &= 0 \\ C_2 &= \frac{\lambda_t}{2\pi\epsilon_0} \end{aligned}}$$

General solution shows Debye screening of test charge in the core of the beam:

$$\boxed{\begin{aligned} \delta\phi &= \frac{\lambda_t}{2\pi\epsilon_0} K_0\left(\frac{r}{\gamma_b\lambda_D}\right) \qquad K_0(x) \quad \text{Order Zero Modified Bessel Function} \\ &\simeq \frac{\lambda_t}{2\sqrt{2\pi}\epsilon_0}\frac{1}{\sqrt{r/(\gamma_b\lambda_D)}} e^{-r/(\gamma_b\lambda_D)} \qquad r \gg \gamma_b\lambda_D \end{aligned}}$$

- Screened interaction does not require overall charge neutrality!
  - Beam particles redistribute to screen bare interaction
  - Beam behaves as a plasma and expect similar collective waves etc.
- Same result for all smooth equilibrium distributions and in 1D, 2D, and 3D
  - Reason why lower dimension models can get the "right" answer for collective interactions in spite of the Coulomb force varying with dimension
- Explains why the radial density profile in the core of space-charge dominated beams are expected to be flat

S9: Continuous Focusing: The Density Inversion Theorem

Shows x and x' dependancies are strongly connected in an equilibrium

For:

$$f_\perp = f_\perp(H_\perp)$$

$$H_\perp = \frac{1}{2}\mathbf{x}_\perp'^2 + \frac{1}{2}k_{\beta 0}^2\mathbf{x}_\perp^2 + \frac{q\phi}{m\gamma_b^3\beta_b^2c^2} = \frac{1}{2}\mathbf{x}_\perp'^2 + \psi(r) \qquad \psi \equiv \frac{1}{2}k_{\beta 0}^2 r^2 + \frac{q\phi}{m\gamma_b^3\beta_b^2c^2}$$

calculate the beam density

$$n(r) = \int d^2x'_\perp\ f_\perp(H_\perp) = 2\pi\int_0^\infty dU\ f_\perp(U+\psi(r))$$

differentiate:

$$\frac{\partial n}{\partial\psi} = 2\pi\int_0^\infty dU\ \frac{\partial}{\partial\psi}f_\perp(U+\psi) = 2\pi\int_0^\infty dU\ \frac{\partial}{\partial U}f_\perp(U+\psi)$$

$$= 2\pi\lim_{U\to\infty} \underbrace{f_\perp(U+\psi)}_{\text{bounded distribution}} \to 0 - 2\pi f_\perp(\psi)$$

$$\boxed{f_\perp(H_\perp) = -\frac{1}{2\pi}\frac{\partial n}{\partial\psi}\bigg|_{\psi=H_\perp} \qquad \psi(r) = \frac{1}{2}k_{\beta 0}^2r^2 + \frac{q\phi(r)}{m\gamma_b^3\beta_b^2c^2}}$$

Assume that $n(r)$ is specified, then the Poisson equation can be integrated:

$$\psi(r) - \frac{q\phi(r=0)}{m\gamma_b^3\beta_b^2c^2} = \frac{1}{2}k_{\beta 0}^2r^2 - \frac{q}{m\gamma_b^3\beta_b^2c^2\epsilon_0}\int_0^r\frac{d\tilde{r}}{\tilde{r}}\int_0^{\tilde{r}}d\tilde{\tilde{r}}\ \tilde{\tilde{r}}\ n(\tilde{\tilde{r}})$$

For $n(r)$ = const $\quad \int_0^r \frac{d\tilde{r}}{\tilde{r}} \int_0^{\tilde{r}} d\tilde{\tilde{r}}\, \tilde{\tilde{r}}\, n(\tilde{\tilde{r}}) \quad \propto r^2$

This suggests that $\psi(r)$ is monotonic in r when $d\,n(r)/dr$ is monotonic. Apply the chain rule:

Density Inversion Theorem

$$\boxed{\begin{aligned} f_\perp(H_\perp) &= -\frac{1}{2\pi}\frac{\partial n}{\partial \psi}\bigg|_{\psi=H_\perp} = -\frac{1}{2\pi}\frac{\partial n(r)/\partial r}{\partial \psi(r)/\partial r}\bigg|_{\psi=H_\perp} \\ \psi(r) &= \frac{1}{2}k_{\beta 0}^2 r^2 + \frac{q\phi}{m\gamma_b^3\beta_b^2 c^2} \end{aligned}}$$

For specified monotonic $n(r)$ the density inversion theorem can be applied with the Poisson equation to calculate the corresponding equilibrium $f_\perp(H_\perp)$

Comments on density inversion theorem:

- Shows that the x and x' dependance of the distribution are *inextricably linked* for an equilibrium distribution function $f_\perp(H_\perp)$
  - Not so surprising -- equilibria are highly constrained
- If $df_\perp(H_\perp)/dH_\perp \le 0$ then the kinetic stability theorem (see Kinetic Stability lectures) shows that the equilibrium is also stable

// Example: Application of the inversion theorem to the KV equilibrium

$$n = \begin{cases} \hat{n}, & 0 \le r < r_b \\ 0, & r_b < r \end{cases} \longrightarrow \frac{\partial n}{\partial r} = -\hat{n}\delta(r - r_b)$$

$$\begin{aligned} \frac{\partial n}{\partial \psi} &= \frac{\partial n/\partial r}{\partial \psi/\partial r} \\ &= -\frac{\hat{n}\delta(r-r_b)}{\partial\psi/\partial r} \\ &= -\frac{\hat{n}\delta(r-r_b)}{\partial\psi/\partial r|_{r=r_b}} \\ &= -\hat{n}\delta(\psi(r) - \psi(r_b)) \end{aligned}$$

property of delta-function:

$$\delta(f(x)) = \sum_i \frac{\delta(x - x_i)}{|df/dx|_{x=x_i}}$$

$$f(x_i) = 0$$

x_i root of f(x)

use: $\psi(r_b) = H_\perp|_{\mathbf{x}'_\perp=0} = H_{\perp b}$

$$\longrightarrow \boxed{f_\perp(H_\perp) = -\frac{1}{2\pi}\frac{\partial n}{\partial \psi}\bigg|_{\psi=H_\perp} = \frac{\hat{n}}{2\pi}\delta(H_\perp - H_{\perp b})}$$

Expected KV form

//

Similar application of derivatives with respect to Courant-Snyder invariants can "derive" the needed form for the KV distribution of an elliptical beam without guessing.

S10: Comments on the plausibility of smooth, Vlasov equilibria in periodic transport channels

The KV and continuous models are the only (or related to simple transforms thereof) known exact beam equilibria. Both suffer from idealizations that render them inappropriate for use as initial distribution functions for modeling of real accelerator systems:

- KV distribution has an unphysical structure giving rise to well known instabilities with unphysical manifestations
- Continuous focusing is inadequate to model real accelerator lattices with periodic or s-varying focusing forces

There is much room for improvement in this area, including study if smooth equilibria exist in periodic focusing and implications if no exact equilibria exist.

Large envelope flutter associated with strong focusing can result in a rapid high-order oscillating force imbalance acting on edge particles of the beam

Temperature Flutter

Elliptical rms Equivalent Beam

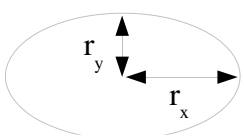

$$\varepsilon_x^2 \propto T_x r_x^2 \simeq \text{const} \implies T_x \propto \frac{1}{r_x^2}$$

Example Systems	$(r_{max}/r_{min})^2$
AG Trans: $\sigma_0 = 60^o$	~ 2.5
AG Trans: $\sigma_0 = 100^o$	~ 4.9
Matching Section	~ 15 Possible

Characteristic Plasma Frequency of Collective Effects

Continuous Focusing Estimate

$$\sigma_{\text{plasma}} \sim \frac{L_p}{r_b}\sqrt{2Q} \qquad \text{Typical: } \sigma_{\text{plasma}} \sim 105^\circ/\text{period}$$

- Temperature asymmetry in beam will rapidly fluctuate with lattice periodicity
  - Converging plane => Warmer
  - Diverging plane => Colder
- Collective plasma wave response slower than lattice frequency
  - Beam edge will not be able to adapt rapidly enough
  - Collective waves will be launched from lack of local force balance near the edge

The continuous focusing equilibrium distribution suggests that varying Debye screening together with envelope flutter would require a rapidly adapting beam edge in a smooth, periodic equilibrium beam distribution

$$f_\perp = \frac{m\gamma_b\beta_b^2c^2\hat{n}}{2\pi T}\exp\left(-\frac{m\gamma_b\beta_b^2c^2H_\perp}{T}\right)$$

Continuous Focusing Thermal Equilibrium Beam

Self Consistent Beam Edge

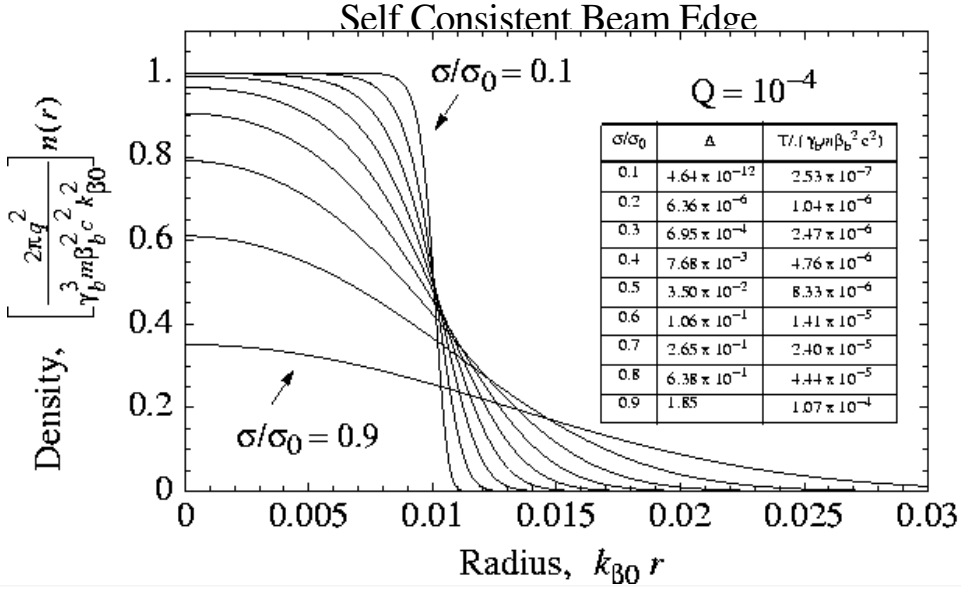

σ/σ_0	Δ	$T/(\gamma_b m\beta_b^2 c^2)$
0.1	4.64×10^{-12}	2.53×10^{-7}
0.2	6.36×10^{-6}	1.04×10^{-6}
0.3	6.95×10^{-4}	2.47×10^{-6}
0.4	7.68×10^{-3}	4.76×10^{-6}
0.5	3.50×10^{-2}	8.33×10^{-6}
0.6	1.06×10^{-1}	1.41×10^{-5}
0.7	2.65×10^{-1}	2.40×10^{-5}
0.8	6.38×10^{-1}	4.44×10^{-5}
0.9	1.85	1.07×10^{-4}

It is clear from these considerations that if smooth "equilibrium" beam distributions exist for periodic focusing, then they are highly nontrivial

Would a nonexistence of an equilibrium distribution be a problem:

- Real beams are born off a source that can be simulated
  - Propagation length can be relatively small in linacs
- Transverse confinement can exist without an equilibrium
  - Particles can turn at large enough radii forming an edge
  - Edge can oscillate from lattice period to lattice period without pumping to large excursions

→ Might not preclude long propagation with preserved statistical beam quality

Even approximate equilibria would help sort out complicated processes:

- Reduce transients and fluctuations can help understand processes in simplest form
  - Allows more "plasma physics" type analysis and advances
- Beams in Vlasov simulations are often observed to "settle down" to a fairly regular state after an initial transient evolution
  - Extreme phase mixing leads to an effective relaxation

These slides will be corrected and expanded for reference and any future editions of the US Particle Accelerator School class:
Beam Physics with Intense Space Charge, by J.J. Barnard and S.M. Lund

Corrections and suggestions are welcome. Contact:

SMLund@lbl.gov

Steven M. Lund
Lawrence Berkeley National Laboratory
BLDG 47 R 0112
1 Cyclotron Road
Berkeley, CA 94720-8201

(510) 486 – 6936

Please do not remove author credits in any redistribuitons of class material.

References: For more information see:

M. Reiser, *Theory and Design of Charged Particle Beams*, Wiley (1994)

R. Davidson, *Theory of Nonneutral Plasmas*, Addison-Wesley (1989)

R. Davidson and H. Qin, Physics of Intense Charged Particle Beams in High Energy Accelerators, World Scientific (2001).

H. Wiedermann, *Particle Accelerator Physics*, Springer-Verlag (1995)

J. Barnard and S. Lund, *Intense Beam Physics*, US Particle Accelerator School Notes, http://uspas.fnal.gov/lect_note.html (2006)

F. Sacherer, *Transverse Space-Charge Effects in Circular Accelerators*, Univ. of California Berkeley, Ph.D Thesis (1968).

S. Lund and B. Bukh, Review Article: *Stability Properties of the Transverse Envelope Equations Describing Intense Beam Transport*, PRST-Accel. and Beams 7, 024801 (2004).

D. Nicholson, *Introduction to Plasma Theory*, Wiley (1983)

I. Kaphinskij and V. Vladimirskij, in *Proc. Of the Int. Conf. On High Energy Accel. and Instrumentation* (CERN Scientific Info. Service, Geneva, 1959) p. 274

J.J. Barnard and S.M. Lund
USPAS June 2006

Appendix A

Self Fields of a Uniform Density Elliptical Beam in Free Space

$$\left(\frac{\partial^2}{\partial x^2}+\frac{\partial^2}{\partial y^2}\right)\phi = \begin{cases} -\dfrac{\lambda}{\pi\varepsilon_0 r_x r_y}\,; & \dfrac{x^2}{r_x^2}+\dfrac{y^2}{r_y^2} < 1 \\ 0\,; & \dfrac{x^2}{r_x^2}+\dfrac{y^2}{r_y^2} > 1 \end{cases}$$

$$\frac{\partial\phi}{\partial r} \sim \frac{\lambda}{2\pi\varepsilon_0 r} \quad \text{as} \quad r \to \infty .$$

The solution to this system to an arb. constant has been formally constructed by Landau & Lifshitz and others (gravitational field analog) as:

$$\phi = -\frac{\lambda}{4\pi\varepsilon_0}\left\{\int_0^{\xi}\frac{ds}{\left[(r_x^2+s)(r_y^2+s)\right]^{1/2}} + \int_{\xi}^{\infty}\frac{ds}{\left[(r_x^2+s)(r_y^2+s)\right]^{1/2}}\left(\frac{x^2}{r_x^2+s}+\frac{y^2}{r_y^2+s}\right)\right\} + \text{const.}$$

where

$$\begin{cases} \xi = 0\,; & \text{when } (x/r_x)^2+(y/r_y)^2 < 1 \\ \xi: \text{ root of } \dfrac{x^2}{r_x^2+\xi}+\dfrac{y^2}{r_y^2+\xi} = 1\,, & \text{when } (x/r_x)^2+(y/r_y)^2 > 1 \end{cases}$$

Trivially for $x=y=0$

$$\phi(x=y=0) = \text{const.}$$

Calculate:

$$\frac{\partial\phi}{\partial x} = -\frac{\lambda}{4\pi\varepsilon_0}\left\{\int_{\xi}^{\infty}\frac{ds}{\left[(r_x^2+s)(r_y^2+s)\right]^{1/2}}\frac{2x}{r_x^2+s} - \frac{1}{\left[(r_x^2+\xi)(r_y^2+\xi)\right]^{1/2}}\left[1-\frac{x^2}{r_x^2+\xi}-\frac{y^2}{r_y^2+\xi}\right]\frac{\partial\xi}{\partial x}\right\}$$

If $\xi \neq 0 \Rightarrow 1 = \dfrac{x^2}{r_x^2+\xi}+\dfrac{y^2}{r_y^2+\xi}$

$\xi = 0 \Rightarrow \dfrac{\partial\xi}{\partial x} = 0$

$\Rightarrow$ 2nd term vanishes

$$\frac{\partial \phi}{\partial x} = -\frac{\lambda}{2\pi\varepsilon_0}\int_\xi^\infty \frac{ds}{[(r_x^2+s)(r_y^2+s)]^{1/2}}\,\frac{x}{r_x^2+s}$$

by symmetry

$$\frac{\partial \phi}{\partial y} = -\frac{\lambda}{2\pi\varepsilon_0}\int_\xi^\infty \frac{ds}{[(r_x^2+s)(r_y^2+s)]^{1/2}}\,\frac{y}{r_y^2+s}$$

Differentiating again and using the chain rule:

$$\left(\frac{\partial^2}{\partial x^2}+\frac{\partial^2}{\partial y^2}\right)\phi = -\frac{\lambda}{2\pi\varepsilon_0}\left\{\int_\xi^\infty \frac{ds}{[(r_x^2+s)(r_y^2+s)]^{1/2}}\left[\frac{1}{r_x^2+s}+\frac{1}{r_y^2+s}\right]\right.$$

$$\left. -\frac{1}{[(r_x^2+\xi)(r_y^2+\xi)]^{1/2}}\left[\frac{x\,\partial\xi/\partial x}{r_x^2+\xi}+\frac{y\,\partial\xi/\partial y}{r_y^2+\xi}\right]\right\}$$

Must show that the r.h.s. reduces to the needed forms for:

<u>case 1</u> exterior ξ satisfies: $\dfrac{x^2}{r_x^2+\xi}+\dfrac{y^2}{r_y^2+\xi}=1$

<u>case 2</u> interior $\xi=0$

<u>case 1</u> (exterior: $x^2/r_x^2+y^2/r_y^2>1$)

Differentiate $\dfrac{x^2}{r_x^2+\xi}+\dfrac{y^2}{r_y^2+\xi}=1$

$$\Rightarrow \frac{\partial\xi}{\partial x} = \frac{2x}{(r_x^2+\xi)\left[\frac{x^2}{(r_x^2+\xi)^2}+\frac{y^2}{(r_y^2+\xi)^2}\right]}$$

$$\frac{\partial\xi}{\partial y} = \frac{2y}{(r_x^2+\xi)\left[\frac{x^2}{(r_x^2+\xi)^2}+\frac{y^2}{(r_y^2+\xi)^2}\right]}$$

$$\Rightarrow \frac{x\,\partial\xi/\partial x}{r_x^2+\xi}+\frac{y\,\partial\xi/\partial y}{r_y^2+\xi} = 2\left[\frac{x^2}{(r_x^2+\xi)^2}+\frac{y^2}{(r_y^2+\xi)^2}\right]\frac{1}{\left[\frac{x^2}{(r_x^2+\xi)^2}+\frac{y^2}{(r_y^2+\xi)^2}\right]}=2$$

Also need Integrals like: $w^2 \equiv s+r_y^2$

$$I_x(\xi) \equiv \int_\xi^\infty \frac{ds}{[(r_x^2+s)(r_y^2+s)]^{1/2}}\,\frac{1}{r_x^2+s} = 2\int_{\sqrt{r_x^2+\xi}}^\infty \frac{dw}{(r_x^2-r_y^2+w^2)^{3/2}}$$

This integral can be done using tables:

$$I_x(\xi) = \frac{2w}{(r_x^2-r_y^2)\sqrt{r_x^2-r_y^2+w^2}}\Bigg|_{w=\sqrt{r_x^2+\xi}}^{w\to\infty} = \frac{2}{r_x^2-r_y^2} - \frac{2\sqrt{r_y^2+\xi}}{(r_x^2-r_y^2)\sqrt{r_x^2+\xi}}$$

Similarly:

$$I_y(\xi) \equiv \int_\xi^\infty \frac{ds}{[(r_x^2+s)(r_y^2+s)]^{1/2}}\frac{1}{(r_y^2+s)} = \frac{2}{r_y^2-r_x^2} - \frac{2\sqrt{r_x^2+\xi}}{(r_y^2-r_x^2)\sqrt{r_y^2+\xi}}$$

$$\int_0^\infty \frac{ds}{[(r_x^2+s)(r_y^2+s)]^{1/2}}\left[\frac{1}{r_x^2+s}+\frac{1}{r_y^2+s}\right] = I_x(\xi)+I_y(\xi)$$

$$= \frac{2}{r_x^2-r_y^2}\left(\frac{\sqrt{r_x^2+\xi}}{\sqrt{r_y^2+\xi}} - \frac{\sqrt{r_y^2+\xi}}{\sqrt{r_x^2+\xi}}\right) = \frac{2}{[(r_x^2+\xi)(r_y^2+\xi)]^{1/2}}$$

Using these results:

$$\left(\frac{\partial^2}{\partial x^2}+\frac{\partial^2}{\partial y^2}\right)\phi = -\frac{\lambda}{2\pi\varepsilon_0}\left\{\frac{2}{[(r_x^2+\xi)(r_y^2+\xi)]^{1/2}} - \frac{2}{[(r_x^2+\xi)(r_y^2+\xi)]^{1/2}}\right\}$$

$$= 0 \quad \text{checks.} \checkmark$$

<u>Case 2</u> (Interior: $x^2/r_x^2 + y^2/r_y^2 < 1$)

$$\xi = 0 \Rightarrow \frac{x\,\partial\xi/\partial x}{r_x^2+\xi} + \frac{y\,\partial\xi/\partial y}{r_y^2+\xi} = 0$$

$$\Rightarrow I_x(\xi=0) = \cancel{I_y(\xi=0)} = \frac{2}{(r_x+r_y)r_x} \quad \text{and} \quad I_y(\xi=0) = \frac{2}{(r_x+r_y)r_y}$$

Using these results:

$$\left(\frac{\partial^2}{\partial x^2}+\frac{\partial^2}{\partial y^2}\right)\phi = -\frac{\lambda}{2\pi\varepsilon_0}\left\{\frac{2}{r_x r_y} - 0\right\} = \frac{-\lambda}{\varepsilon_0\pi r_x r_y} = -\frac{q\hat{n}}{\varepsilon_0} \quad \text{checks} \checkmark$$

Finally, check the limiting form outside the beam for r large $\Rightarrow$ ξ large.

$$-\frac{\partial\phi}{\partial x} = \frac{\lambda}{2\pi\varepsilon_0}\, x\, I_x(\xi) \qquad \lim_{r\to\infty} I_x(\xi) = \frac{1}{\xi} = \frac{1}{r^2}$$

$$-\frac{\partial\phi}{\partial y} = \frac{\lambda}{2\pi\varepsilon_0}\, y\, I_y(\xi) \qquad \lim_{r\to\infty} I_y(\xi) = \frac{1}{\xi} = \frac{1}{r^2}$$

Thus:

$$\lim_{r\to\infty} -\frac{\partial\phi}{\partial x} = \frac{\lambda}{2\pi\varepsilon_0}\frac{x}{r^2} \checkmark$$

$$\lim_{r\to\infty} -\frac{\partial\phi}{\partial y} = \frac{\lambda}{2\pi\varepsilon_0}\frac{y}{r^2} \checkmark$$

These have the correct limiting forms for a line charge at the origin. Completing the verification of the general formula.

In the beam $\left(x^2/r_x^2 + y^2/r_y^2 < 1 \,,\ \xi = 0 \right)$, the formula reduces to:

$$\phi = -\frac{\lambda}{4\pi\varepsilon_0}\left\{ x^2 I_x(\xi=0) + y^2 I_y(\xi=0) \right\} + \text{const.}$$

$$= -\frac{\lambda}{4\pi\varepsilon_0}\left\{ \frac{2x^2}{r_x(r_x+r_y)} + \frac{2y^2}{r_y(r_x+r_y)} \right\} + \text{const.}$$

$$\boxed{\phi = -\frac{\lambda}{2\pi\varepsilon_0}\left\{ \frac{x^2}{r_x(r_x+r_y)} + \frac{y^2}{r_y(r_x+r_y)} \right\} + \text{const.}}$$

The case of an axisymmetric beam with

$$r_x = r_y = r_b$$

is easy to construct explicitly and is included in the homework problems.

There is also an alternative way to do this field calculation, that is less direct but more efficient. We carry out this proof now since steps involved are useful for other purposes.

A density profile with elliptic symmetry can be expressed as:

$$n(x,y) = n\left(\frac{x^2}{r_x^2} + \frac{y^2}{r_y^2}\right)$$

Here we do not assume a specific uniform density profile and we leave $n(x^2/r_x^2 + y^2/r_y^2)$ arbitrary outside of having elliptic symmetry. The solution to the 2D Poisson equation in free-space is

$$\left(\frac{\partial^2}{\partial x^2} + \frac{\partial^2}{\partial y^2}\right)\phi = -\frac{qn}{\varepsilon_0}$$

is then given by

$$\phi = -\frac{q\, r_x r_y}{4\varepsilon_0}\int_0^\infty d\xi\, \frac{\eta(\mathcal{X})}{\sqrt{r_x^2+\xi}\,\sqrt{r_y^2+\xi}}$$

$$\mathcal{X} \equiv \frac{x^2}{r_x^2+\xi} + \frac{y^2}{r_y^2+\xi}$$

where $\eta(\mathcal{X})$ is a function defined such that:

$$n(x,y) = \left.\frac{d\eta(\mathcal{X})}{d\mathcal{X}}\right|_{\xi=0}$$

This choice for $\eta(\mathcal{X})$ can always be made.

We first prove that this solution is valid by direct substitution:

$$\mathcal{X} = \frac{x^2}{r_x^2+\xi} + \frac{y^2}{r_y^2+\xi} \Rightarrow \frac{\partial \mathcal{X}}{\partial x} = \frac{2x}{r_x^2+\xi}\ ;\ \frac{\partial^2 \mathcal{X}}{\partial x^2} = \frac{2}{r_x^2+\xi}$$

$$\frac{\partial \mathcal{X}}{\partial y} = \frac{2y}{r_y^2+\xi}\ ;\ \frac{\partial^2 \mathcal{X}}{\partial y^2} = \frac{2}{r_y^2+\xi}$$

Substitute in Poisson's equation and use the chain rule and results above:

$$\left(\frac{\partial^2}{\partial x^2}+\frac{\partial^2}{\partial y^2}\right)\phi = \frac{-q r_x r_y}{4\varepsilon_0}\int_0^\infty d\xi\, \frac{\left(\frac{d^2\eta}{d\mathcal{X}^2}\right)\left(\frac{4x^2}{(r_x^2+\xi)^2}+\frac{4y^2}{(r_y^2+\xi)^2}\right)+\left(\frac{d\eta}{d\mathcal{X}}\right)\left(\frac{2}{r_x^2+\xi}+\frac{2}{r_y^2+\xi}\right)}{\sqrt{r_x^2+\xi}\sqrt{r_y^2+\xi}}$$

Note: $$d\mathcal{X} = -\left[\frac{x^2}{(r_x^2+\xi)^2}+\frac{y^2}{(r_y^2+\xi)}\right]d\xi$$

so the first integral can be simplified by partial integration:

$$\int_0^\infty d\xi\, \frac{\left(\frac{d^2\eta}{d\mathcal{X}^2}\right)\left(\frac{4x^2}{(r_x^2+\xi)^2}+\frac{4y^2}{(r_y^2+\xi)^2}\right)}{\sqrt{r_x^2+\xi}\sqrt{r_y^2+\xi}} = -4\int_0^\infty d\xi\, \frac{\frac{d^2\eta}{d\mathcal{X}^2}\frac{d\mathcal{X}}{d\xi}}{\sqrt{r_x^2+\xi}\sqrt{r_y^2+\xi}}$$

$$= -4\int_0^\infty d\xi\, \frac{\frac{d}{d\xi}\left(\frac{d\eta}{d\mathcal{X}}\right)}{\sqrt{r_x^2+\xi}\sqrt{r_y^2+\xi}} = -4\int_0^\infty d\xi\, \frac{d}{d\xi}\left[\frac{\frac{d\eta}{d\mathcal{X}}}{\sqrt{r_x^2+\xi}\sqrt{r_y^2+\xi}}\right] + 4\int_0^\infty d\xi\, \frac{d\eta}{d\mathcal{X}}\frac{d}{d\xi}\frac{1}{\sqrt{r_x^2+\xi}\sqrt{r_y^2+\xi}}$$

$$= \left.\frac{-4\frac{d\eta}{d\mathcal{X}}}{\sqrt{r_x^2+\xi}\sqrt{r_y^2+\xi}}\right|_{\xi\to 0}^{\xi\to\infty} - 2\int_0^\infty d\xi\, \frac{\frac{d\eta}{d\mathcal{X}}\left(\frac{1}{r_x^2+\xi}+\frac{1}{r_y^2+\xi}\right)}{\sqrt{r_x^2+\xi}\sqrt{r_y^2+\xi}}$$

$$= \frac{4}{r_x r_y}\left.\frac{d\eta}{d\mathcal{X}}\right|_{\xi=0} - 2\int_0^\infty d\xi\, \frac{\frac{d\eta}{d\mathcal{X}}\left(\frac{1}{r_x^2+\xi}+\frac{1}{r_y^2+\xi}\right)}{\sqrt{r_x^2+\xi}\sqrt{r_y^2+\xi}}$$

term will cancel 2nd Integral

Thus:

$$\left(\frac{\partial^2}{\partial x^2}+\frac{\partial^2}{\partial y^2}\right)\phi = -\frac{q\,\cancel{r_x r_y}}{\cancel{4}\varepsilon_0}\,\frac{\cancel{4}}{\cancel{r_x r_y}}\,\frac{d\eta(\mathcal{X})}{d\mathcal{X}}\bigg|_{\xi=0}$$

But $\left.\dfrac{d\eta(\mathcal{X})}{d\mathcal{X}}\right|_{\xi=0} = n(x,y)$ by definition.

$$\Rightarrow \left(\frac{\partial^2}{\partial x^2}+\frac{\partial^2}{\partial y^2}\right)\phi = -\frac{q\,n(x,y)}{\varepsilon_0}$$ verifying the result.

For a uniform density ellipse we take:

$$\eta(\mathcal{X}) = \frac{\lambda}{q\pi r_x r_y}\begin{cases}\mathcal{X} & ;\ \mathcal{X}<1\\ 1 & ;\ \mathcal{X}>1\end{cases} \Rightarrow \frac{d\eta(\mathcal{X})}{d\mathcal{X}} = \begin{cases}\frac{\lambda}{q\pi r_x r_y} & ;\ \mathcal{X}<1\\ 0 & ;\ \mathcal{X}>1\end{cases}$$

Thus

$$\left.\frac{d\eta(\mathcal{X})}{d\mathcal{X}}\right|_{\xi=0} = \begin{cases}\frac{\lambda}{q\pi r_x r_y} & ;\ \mathcal{X}\big|_{\xi=0}<1\\ 0 & ;\ \mathcal{X}\big|_{\xi=0}\end{cases} = \begin{cases}\frac{\lambda}{q\pi r_x r_y} & ;\ \frac{x^2}{r_x^2}+\frac{y^2}{r_y^2}<1\\ 0 & ;\ \frac{x^2}{r_x^2}+\frac{y^2}{r_y^2}>1\end{cases}$$

$\therefore$ $\left.\dfrac{d\eta(\mathcal{X})}{d\mathcal{X}}\right|_{\xi=0} = n(x,y)$ for a uniform density elliptical beam with radii r_x, r_y and density $\lambda/(q\pi r_x r_y)$

Apply these results to calculate ϕ interior to a uniform density elliptical beam.

$$\phi = -\frac{q\,r_x r_y}{4\varepsilon_0}\int_0^\infty d\xi\,\frac{\eta(\mathcal{X})}{\sqrt{r_x^2+\xi}\,\sqrt{r_y^2+\xi}}$$

$$\mathcal{X} = \frac{x^2}{r_x^2+\xi}+\frac{y^2}{r_y^2+\xi}$$ if $\dfrac{x^2}{r_x^2}+\dfrac{y^2}{r_y^2}<1$, then

$$\mathcal{X} = \frac{x^2}{r_x^2+\xi}+\frac{y^2}{r_y^2+\xi}<1$$ for all $0\le\xi<\infty$

Using this and the result above for $\eta(\mathcal{X})$, ϕ inside the elliptical beam is:

$$\phi = -\frac{q\,r_x r_y}{4\varepsilon_0}\int_0^\infty d\xi\,\frac{\lambda}{q\pi r_x r_y}\left[\frac{x^2}{(r_x^2+\xi)^{3/2}(r_y^2+\xi)^{1/2}}+\frac{y^2}{(r_x^2+\xi)^{1/2}(r_y^2+\xi)^{3/2}}\right]$$

$$\phi = \frac{-\lambda}{4\pi\varepsilon_0}\left\{ x^2 \int_0^\infty d\xi \frac{1}{(r_x^2+\xi)^{3/2}(r_y^2+\xi)^{1/2}} + y^2 \int_0^\infty d\xi \frac{1}{(r_x^2+\xi)^{1/2}(r_y^2+\xi)^{3/2}} \right\}$$

Using Mathematica or Integral tables:

$$\int_0^\infty d\xi \frac{1}{(r_x^2+\xi)^{3/2}(r_y^2+\xi)^{1/2}} = \frac{2}{r_x(r_x+r_y)}$$

$$\int_0^\infty d\xi \frac{1}{(r_x^2+\xi)^{1/2}(r_y^2+\xi)^{3/2}} = \frac{2}{r_y(r_x+r_y)}$$

Hence

$$\underline{\underline{\phi = \frac{-\lambda}{2\pi\varepsilon_0}\left\{ \frac{x^2}{r_x(r_x+r_y)} + \frac{y^2}{r_y(r_x+r_y)} \right\} + \text{const}}}$$

since an overall constant can always be added to ϕ (The integral has a reference choice $\phi(x=y=0)=0$ built in.).

The steps introduced in this proof can also be used to show that:

$$\left\langle x \frac{\partial\phi}{\partial x} \right\rangle_\perp = \frac{-\lambda}{4\pi\varepsilon_0} \frac{r_x}{r_x+r_y}$$

$$\lambda = q\int d^2x\, n$$

$$\left\langle y \frac{\partial\phi}{\partial y} \right\rangle_\perp = \frac{-\lambda}{4\pi\varepsilon_0} \frac{r_y}{r_x+r_y}$$

$$r_x \equiv 2\langle x^2\rangle^{1/2}$$
$$r_y \equiv 2\langle y^2\rangle^{1/2}$$

for <u>any</u> elliptic symmetry density profile $n(x,y) = n(x^2/r_x^2 + y^2/r_y^2)$. In the intro. lectures these results were employed to show that the KV envelope equations with evolving emittances can be applied to elliptic symmetry beams. This result was first demonstrate by Sacherer: [IEEE Trans Nucl. Sci. 18, 1105 (1971)]

J.J. Barnard and S.M. Lund
USPAS June 2006

Appendix B

Canonical Transformation of the KV Distribution

The single-particle equations of motion can be derived from the Hamiltonian: $\left(\frac{d\vec{x}_\perp}{ds} = \frac{\partial H}{\partial \vec{x}_\perp'} , \frac{d\vec{x}_\perp'}{ds} = -\frac{\partial H}{\partial \vec{x}_\perp} \right)$

$$\boxed{\begin{aligned} H_\perp(x,y,x',y',s) = {} & \frac{1}{2}x'^2 + \left[\kappa_x(s) - \frac{2Q}{r_x(s)\left[r_x(s)+r_y(s)\right]} \right]\frac{x^2}{2} \\ & + \frac{1}{2}y'^2 + \left[\kappa_y(s) - \frac{2Q}{r_y(s)\left[r_x(s)+r_y(s)\right]} \right]\frac{y^2}{2} \end{aligned}}$$

Perform a canonical transform to new variables X, Y, X', Y' using the generating function

$$F_2(x,y,X',Y') = \frac{x}{w_x}\left[X' + \frac{x w_x'}{2} \right] + \frac{y}{w_y}\left[Y' + \frac{y w_y'}{2} \right]$$

Then:

$$\boxed{\begin{aligned} X &= \frac{\partial F_2}{\partial X'} = \frac{x}{w_x} \\ Y &= \frac{\partial F_2}{\partial Y'} = \frac{y}{w_y} \end{aligned}}$$

$$x' = \frac{\partial F_2}{\partial x} = \frac{1}{w_x}\left(X' + x w_x' \right)$$

$$y' = \frac{\partial F_2}{\partial y} = \frac{1}{w_y}\left(Y' + y w_y' \right)$$

and solving for X', Y':

$$\boxed{\begin{aligned} X' &= w_x x' - x w_x' \\ Y' &= w_y y' - y w_y' \end{aligned}}$$

Ref:
R.C. Davidson, "Physics of Nonneutral Plasmas" Addison-Wesley, 1990

Comment:
Here, $X' \neq \frac{d}{ds}X$, X' merely denotes the conjugate variable to X. Also, X, X' both have dim. meters$^{1/2}$.

The Courant-Snyder invariants are then simply expressed:

$$\boxed{\begin{aligned} X^2 + X'^2 &= \text{const} \\ Y^2 + Y'^2 &= \text{const} \end{aligned}}$$

One can show from the transformations that:

$$\boxed{\begin{aligned} dx\,dy &= w_x w_y \, dX\,dY \\ dx'dy' &= \frac{dX'dY'}{w_x w_y} \\ dx\,dy\,dx'dy' &= dX\,dY\,dX'dY' \; * \end{aligned}}$$

* Property of canonical transforms in general. — Results from structure of Generating Function

Therefore, the distribution in transformed phase space variables is the same as for the original variables:

$$\boxed{\begin{aligned} f_1(X,Y,X',Y',s) &= f_1(x,y,x',y',s) \\ &= \frac{\lambda}{8\pi^2\varepsilon_x\varepsilon_y}\,\delta\left[\frac{X^2+X'^2}{\varepsilon_x}+\frac{Y^2+Y'^2}{\varepsilon_y}-1\right] \end{aligned}}$$

Now examine the density:

$$n(x,y) = \int dx'dy'\, f_1 = \int \frac{dX'dY'}{w_x w_y} f_1 =$$

$$U_x = X'/\sqrt{\varepsilon_x}, \quad U_y = Y'/\sqrt{\varepsilon_y}$$

$$r_x = \sqrt{\varepsilon_x}\, w_x, \quad r_y = \sqrt{\varepsilon_y}\, w_y \qquad dU_x dU_y = \frac{dX'dY'}{\sqrt{\varepsilon_x\varepsilon_y}}$$

$$\boxed{n = \frac{\lambda}{8\pi^2 r_x r_y}\int dU_x dU_y\, \delta\left[U_x^2+U_y^2-\left(1-\frac{X^2}{\varepsilon_x}-\frac{Y^2}{\varepsilon_y}\right)\right]}$$

Exploit the cylindrical symmetry:

$$U_\perp^2 = U_x^2 + U_y^2$$

$$dU_x dU_y = d\Psi\, U_\perp dU_\perp = d\Psi \frac{dU_\perp^2}{2}$$

$$n(x,y) = \frac{\lambda}{q\pi^2 r_x r_y}\int_0^{2\pi} d\Psi \int_0^\infty \frac{dU_\perp^2}{2}\, \delta\left[U_\perp^2 - \left(1 - \frac{x^2}{r_x^2} - \frac{y^2}{r_y^2}\right)\right]$$

Thus:

$$\boxed{\begin{aligned} n(x,y) &= \frac{\lambda}{q\pi r_x r_y}\int_0^\infty dU_\perp^2\, \delta\left[U_\perp^2 - \left(1 - \frac{x^2}{r_x^2} - \frac{y^2}{r_y^2}\right)\right] \\ &= \begin{cases} \dfrac{\lambda}{q\pi r_x r_y} = \hat{n} & ; \quad \dfrac{x^2}{r_x^2} + \dfrac{y^2}{r_y^2} < 1 \\ 0 & ; \quad \dfrac{x^2}{r_x^2} + \dfrac{y^2}{r_y^2} > 1 \end{cases} \end{aligned}}$$

Showing that the singular KV distribution yields the required uniform density beam of elliptical cross-section.

Note

$$\hat{n} = \frac{\lambda}{q\pi r_x r_y}$$

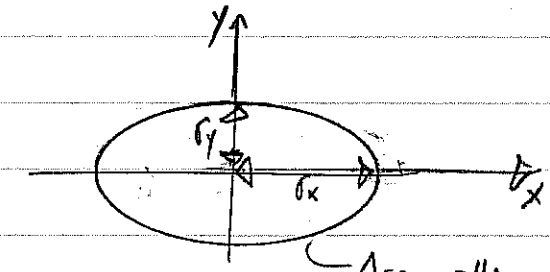

Area ellipse $= \pi r_x r_y$

$\lambda = q\hat{n}\pi r_x r_y$ for uniform density.

An interesting footnote to this appendix is that an infinity of generating functions can be used to transform the KV distribution in standard quadratic form:

$$f_i \sim \delta\left[X'^2 + Y'^2 + X^2 + Y^2 - \text{const}\right]$$

to other sets of variables. This will generate other distributions with KV form for skew coupling and other effects. It would not be logical to label such distributions as "new" as has been done in the literature. However, identifying physically relevant transforms has practical value.

S. M. Lund B5

Inverse transform:

$$x = w_x \bar{X}$$

$$w_x x' = \bar{X}' + x w_x' \quad \Rightarrow \quad x' = \frac{\bar{X}'}{w_x} + w_x' \bar{X}$$

$$\boxed{\begin{aligned} x &= w_x \bar{X} & x' &= \bar{X}'/w_x + w_x' \bar{X} \\ y &= w_y \bar{Y} & y' &= \bar{Y}'/w_y + w_y' \bar{Y} \end{aligned}}$$

Next,

$$\frac{d}{ds}\bar{X} = \frac{x'}{w_x} - \frac{x}{w_x^2} w_x'$$

$$= \frac{\bar{X}'}{w_x^2} + \cancel{\frac{w_x'}{w_x}\bar{X}} - \cancel{\frac{w_x'}{w_x}\bar{X}} = \frac{\bar{X}'}{w_x^2}$$

Thus,

$$\boxed{\begin{aligned} \frac{d}{ds}\bar{X} &= \frac{\bar{X}'}{w_x^2} \\ \frac{d}{ds}\bar{Y} &= \frac{\bar{Y}'}{w_y^2} \end{aligned}}$$

$$\frac{d}{ds}\bar{X}' = \cancel{w_x' x'} + w_x x'' - \cancel{x' w_x'} - x w_x''$$

$$\Rightarrow \boxed{\begin{aligned} x'' &= \frac{\frac{d}{ds}\bar{X}'}{w_x} + w_x'' \bar{X} \\ y'' &= \frac{\frac{d}{ds}\bar{Y}'}{w_y} + w_y'' \bar{Y} \end{aligned}}$$

Apply in Eqn of motion:

$$x'' + \kappa_x x - \frac{2Q x}{(\Gamma_x+\Gamma_y)\Gamma_x} = 0$$

$$\frac{\frac{d}{ds}X'}{W_x} + W_x'' X + \kappa_x W_x X - \frac{2Q W_x X}{(\Gamma_x+\Gamma_y)\Gamma_x} = 0$$

$$\frac{d}{ds}X' + W_x\overbrace{\left(W_x'' + \kappa_x W_x - \frac{2Q W_x}{(\Gamma_x+\Gamma_y)\Gamma_x}\right)}^{= \frac{1}{W_x^3} \text{ from } W_x \text{ eqn}} X = 0$$

$$\boxed{\begin{aligned} &\frac{d}{ds}X' + \frac{1}{W_x^2}X = 0, \qquad \frac{d}{ds}X = \frac{X'}{W_x^2} \\ &\frac{d}{ds}Y' + \frac{1}{W_y^2}Y = 0, \qquad \frac{d}{ds}Y = \frac{Y'}{W_y^2} \end{aligned}}$$

Following Davidson, these eqns can be solved

$$X(s) = X_i \cos\varphi_x(s) + X_i' \sin\varphi_x(s)$$

$$\varphi_x(s) = \int_{s_i}^{s} \frac{d\tilde{s}}{W_x^2(\tilde{s})}$$

This also demonstrates explicitly the C.S. Invariant

$$X^2 + X'^2 = \text{const.}$$

J.J. Barnard and S.M. Lund
US PAS June 2006

Circular Accelerators: Resonance Effects in Rings

A subset of this material is presented by Reiser in §3.8.6 pgs 166-171.

- Overview
- Floquet Coordinates
- Perturbed Hill's equation in Floquet Coordinates
- Sources of and forms of Perturbation Terms.
- Unperturbed solution – relation to a simple harmonic oscillator.
- Perturbative analysis of perturbed Hill's equation and resonances
- Tune restrictions resulting from resonances and machine operating points.
- Effects of Space Charge

Overview

In our treatment of single particle orbits of lattices with s-varying focusing we derived transverse particle equations of motion for a particle subject to linear forces:

$$\boxed{\begin{aligned} x''(s) + \kappa_x(s)\, x(s) &= 0 \\ y''(s) + \kappa_y(s)\, y(s) &= 0 \end{aligned}} \qquad \text{Hill's Equations}$$

Where

$$\kappa_x(s),\ \kappa_y(s)$$

describe the linear applied focusing fields of the lattice. These terms can also include linear space charge forces associated with the self-fields of a uniform density elliptical modeled by the KV distribution.

In analyzing the Hill's equations we employed phase-amplitude methods:

$$\boxed{\begin{aligned} & x = A_{xi}\, W_x(s) \cos \psi_x(s) \\ & W_x''(s) + \kappa_x(s) W_x(s) - \frac{1}{W_x^3(s)} = 0 \ ; \quad \psi_x = \psi_{xi} + \int_{s_i}^{s} \frac{d\tilde{s}}{W_x^2(\tilde{s})} \\ & W_x(s+L_p) = W_x(s) \end{aligned}}$$

This enabled us to simply identify the Courant-Snyder Invariant

$$\boxed{\left(\frac{x}{w_x}\right)^2 + \left(w_x x' - w_x' x\right)^2 = \text{const}}$$

which allowed us to insightfully interpret the dynamics independent of specific particle initial conditions.

We will now show that this formulation can also be exploited to better (analytically!) understand resonant instabilities in periodic focusing lattices. By choosing coordinates such that stable unperturbed orbits governed by Hill's equation

$$\boxed{x''(s) + R_x(s)\,x(s) = 0}$$

are mapped to a continuous oscillator:

$$\boxed{\begin{aligned} \tilde{x}''(\tilde{s}) + \tilde{k}_{\beta 0}^2\,\tilde{x}(\tilde{s}) &= 0 \\ \tilde{k}_{\beta 0}^2 &= \text{const} > 0 \end{aligned}}$$

We will more simply understand the effect of perturbations. (applied field nonlinearities, etc.)

$$\boxed{\begin{aligned} x''(s) + R_x(s)\,x(s) &= P_x(x, y, s, \vec{\delta}) \\ y''(s) + R_y(s)\,y(s) &= P_y(x, y, s, \vec{\delta}) \end{aligned}}$$

Perturbations

Possible vector of other coupled variables

We will restrict analysis in this treatment to:

$$\gamma_b \beta_b = \text{const} \quad : \quad \text{No Acceleration}$$
$$\delta = 0 \quad : \quad \text{No momentum spread}$$
$$\phi = 0 \quad : \quad \text{Neglect space-charge}$$

In order to more simply illustrate procedures. Some comments on the effects of space-charge will be added at the end.

In our analysis we will also take the lattice to be periodic with

$$\boxed{\begin{aligned} P_x(s+L_p) &= P_x(s) \\ L_p &= \text{Lattice Period} \end{aligned}}$$

Ideal linear fields of ring lattice repeat over each element making up the ring.

For a ring we also have the superperiodicity condition

$$\boxed{\begin{aligned} P_x(s+C, \vec{x}_\perp, \vec{\delta}) &= P_x(s, \vec{x}_\perp, \vec{\delta}) \\ C &= \mathcal{N} L_p \\ \mathcal{N} &= \text{"superperiodicity"} \end{aligned}}$$

This applies to <u>random errors</u> in a ring

random error sources:

Fabrication

Alignment ....

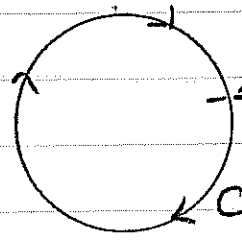

Error

particle encounters same error each lap.

C = Circumfrance. Ring

SIS – 18 Synchrotron
GSI, Germany
18 Tesla–Meter Bending Strength

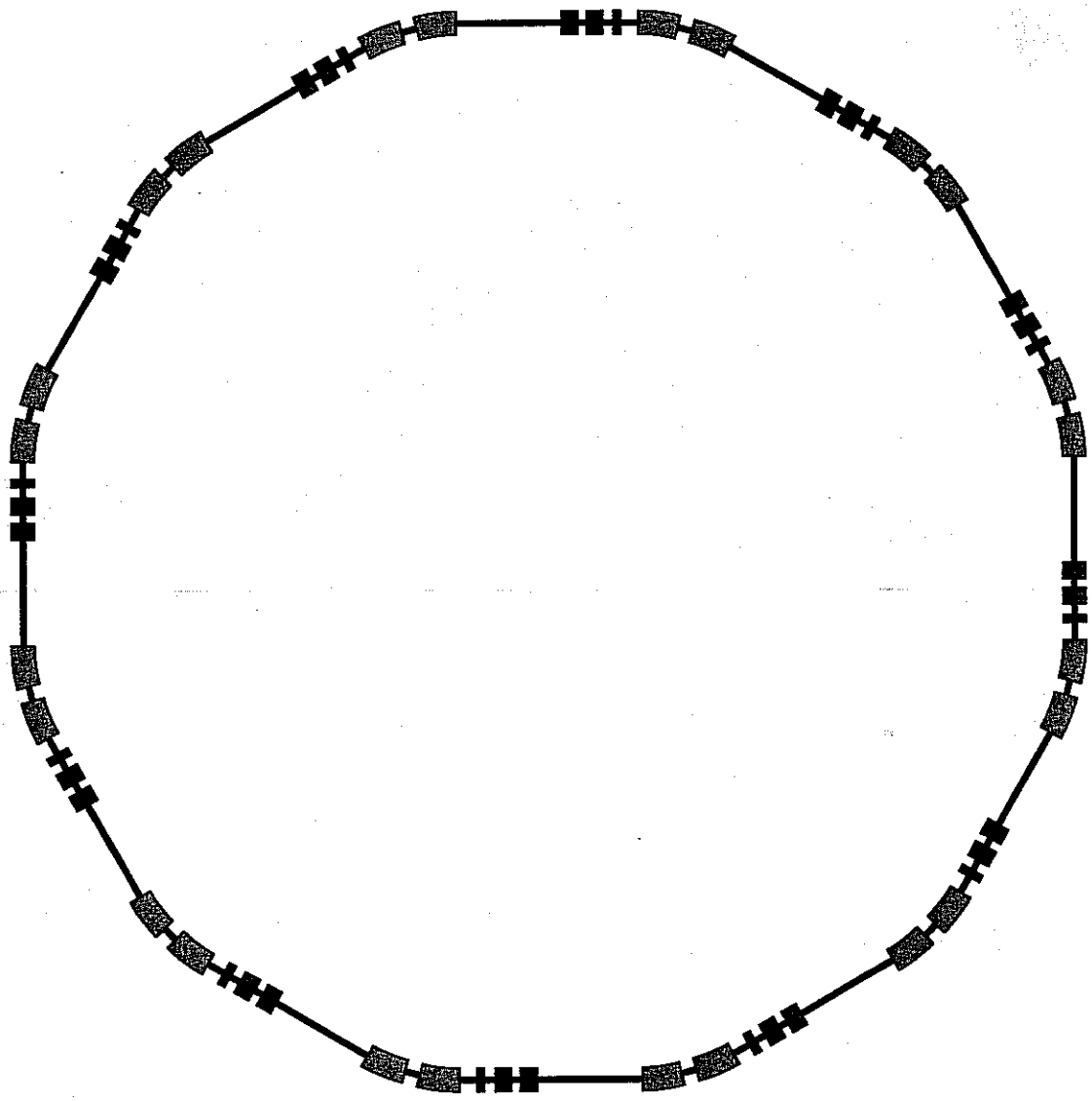

Acceleration Cells
Not Shown

Diplole Bending Magnets

Quadrupole Focusing Magnets (Triplets)

This error condition can also apply to <u>systematic errors</u> that occur each lattice period: by taking $\mathcal{N} = 1$.

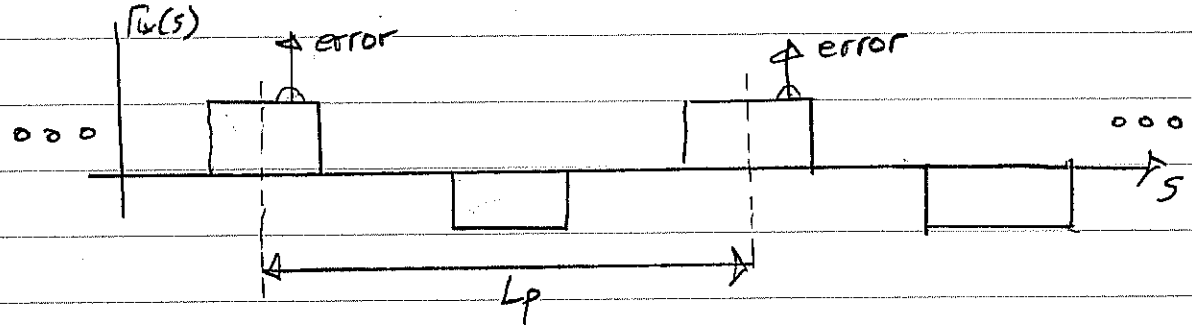

This systematic error condition applies to both ring and linac lattices.

In the following treatment, for simplicity we will (mostly) analyze only the x-orbit and drop subscript x's etc.

Floquet Coordinates -- Connection to a continuous oscillator

Denote: for a stable solution $x(s)$ to Hill's equation:

"Coord" dimensionless $\rightarrow$

$$U \equiv \frac{x(s)}{\sqrt{\beta(s)}} \qquad \beta(s) = W^2(s) = \text{β-tron func. of lattice (periodic)}$$

"Angle" in ring $\rightarrow$

$$\varphi \equiv \frac{1}{\nu_0}\int_{s_i}^{s} \frac{d\tilde{s}}{\beta(\tilde{s})} = \frac{\Delta\Psi(s)}{\nu_0}$$

where the tune "ν_0" is defined by: (we subscript by zero to denote the tune for zero self-field.)

$$\nu_0 \equiv \frac{\Delta\Psi(\mathcal{N} L_p)}{2\pi} \quad ; \quad \mathcal{N} = \text{Superperiodicity } (\mathcal{N} = 1 \text{ for linac})$$

Ψ = phase of x-particle orbit

$\Delta\Psi(s) = \Psi(s) - \Psi(s_i)$

ν_0 = number of undepressed particle oscillations in a ring. (lattice period for linac)

For a linac we take $\mathcal{N} = 1$ and ν_0 is the fraction of an oscillation that the particle advances in a <u>single</u> lattice period.

φ can be interpreted as a normalized angle (measured in particle phase advance) of the particle as it advances around a ring. That is, φ advances by 2π in one particle transit around the ring.

- In a <u>linac</u> φ advances by <u>2π through a lattice period</u>.

Perturbed Hill's Equation in Floquet Coordinates

Take φ to be the independent coordinate and

$$\boxed{U = U(\varphi)}$$

and transform the perturbed Hill's equation

$$\boxed{x'' + K(s)x = P(x,y,s)}$$

← drop additional coupling variables $\vec{\delta}$

to "Floquet" form.

Here $P(x,y,s)$ stands for a perturbation that can represent nonlinear applied fields,

$$U \equiv \frac{x}{\sqrt{\beta}}$$

$$\Rightarrow \quad x = \sqrt{\beta}\, U$$

$$\Rightarrow \quad x' = \frac{\beta' U}{2\sqrt{\beta}} + \sqrt{\beta}\,\frac{dU}{d\varphi}\frac{d\varphi}{ds}$$

Denote

$$\boxed{\dot{U} \equiv \frac{dU}{d\varphi}} \qquad \boxed{\dot{} \equiv \frac{d}{d\varphi}}$$

and note that

$$\boxed{\frac{d\varphi}{ds} = \frac{1}{\nu_0 \beta}} \qquad \varphi = \frac{1}{\nu_0}\int_{s_1}^{s} \frac{d\tilde{s}}{\beta(\tilde{s})}$$

$$\Rightarrow \quad x' = \frac{\beta' U}{2\sqrt{\beta}} + \frac{\dot{U}}{\nu_0\sqrt{\beta}}$$

cancel

$$x'' = \frac{\beta'' U}{2\sqrt{\beta}} - \frac{\beta'^2 U}{4\beta^{3/2}} - \cancel{\frac{\beta'\dot{U}}{2\nu_0\beta^{3/2}}} + \cancel{\frac{\beta'\dot{U}}{2\nu_0\beta^{3/2}}} + \frac{\ddot{U}}{\nu_0^2\beta^{3/2}}$$

Thus

$$\boxed{\begin{aligned} x' &= \frac{\beta' U}{2\sqrt{\beta}} + \frac{\dot{U}}{\nu_0\sqrt{\beta}} \\ x'' &= \frac{\beta'' U}{2\sqrt{\beta}} - \frac{\beta'^2 U}{4\beta^{3/2}} + \frac{\ddot{U}}{\nu_0^2\beta^{3/2}} \end{aligned}}$$

and the perturbed Hill's equation

$$x'' + \kappa x = p$$

becomes:

$$\boxed{\ddot{U} + \nu_0^2\left[\frac{\beta\beta''}{2} - \frac{\beta'^2}{4} + \kappa\beta^2\right]U = \nu_0^2\beta^{3/2}P}$$

But

$$\boxed{\frac{\beta\beta''}{2} - \frac{\beta'^2}{4} + \kappa\beta^2 = 1 \qquad \beta(s+L_p) = \beta(s)}$$

β-tron amplitude eqn
$\beta = w^2$
$\Leftarrow \; w'' + \kappa w - \frac{1}{w^3} = 0$

by definition, so the term in [ ] vanishes and the perturbed equation reduces to:

$$\boxed{\begin{aligned} &\ddot{U} + \nu_0^2 U = \nu_0^2\beta^{3/2}P(x,y,s) \\ &U = U(\varphi) \; ; \qquad \dot{U} \equiv \frac{dU}{d\varphi} \\ &\varphi = \frac{1}{\nu_0}\int_{s_i}^{s}\frac{d\tilde{s}}{\beta(\tilde{s})} \end{aligned}}$$

Here we will take in the perturbations:

$$P(x,y,s) \equiv P(\sqrt{\beta}\,U, y, s(\varphi))$$

Transform other coupled variables similarly.

For $p=0$ (zero perturbation), the equation is just a <u>simple harmonic oscillator</u> equation with solution:

- Transform has mapped the time dependent unperturbed solution of Hill's equation to that of a simple harmonic oscillator.

$$\boxed{U(\varphi) = U_i \cos(\nu_0 \varphi) + \frac{\dot{U}_i}{\nu_0} \sin(\nu_0 \varphi)}$$

where we take U_i and $\dot{U}_i$ to be the particle initial conditions at $s=s_i$ with phase choice $\varphi = 0$ at $s=s_i$ to simplify notation.

The <u>Floquet representation also simplifies the interpretation of the particle dynamics in responce to perturbations</u> due to the simple phase-space form of the unperturbed solution:

$$x = \sqrt{\varepsilon}\sqrt{\beta}\cos\psi \quad ; \quad \psi = \nu_0 \varphi$$

$$U(\varphi) = \frac{x}{\sqrt{\beta}} = \sqrt{\varepsilon}\cos\nu_0\varphi$$

$$\dot{U}(\varphi) = \frac{dU}{d\varphi} = -\nu_0\sqrt{\varepsilon}\sin\nu_0\varphi$$

Thus the Courant-Snyder Invariant and the phase space structure are simply expressed in Floquet Coordinates.

Courant-Snyder Invariant:

$$\boxed{U^2 + \left(\frac{\dot{U}}{\nu_0}\right)^2 = \varepsilon}$$

Equation of a <u>circle</u> rather than a rotated ellipse.

Phase Space ellipse:

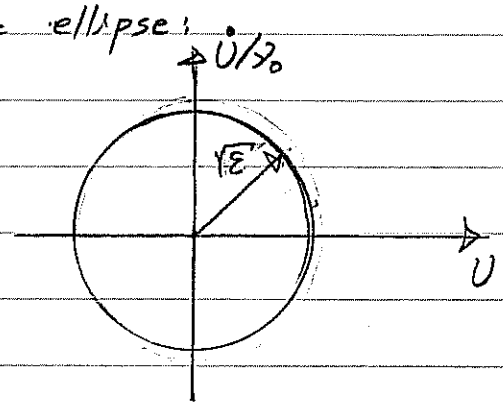

Phase space is a circle for the unperturbed solution to Hill's equation.

Perturbations are more easily understood as distortions on circular phase-space!

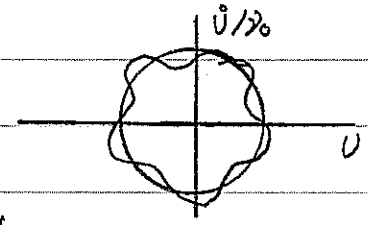

The $u - \dot{u}/\gamma_0$ variables also perserve area measures of phase space (a feature of the transformation being symplectic).

Jacobian

$$\int_{\text{ellipse}} dx \otimes dx' \cdots = \int_{\text{circle}} du \otimes d\dot{u}\ |J| \cdots = \int_{\text{circle}} du \otimes \frac{d\dot{u}}{\gamma_0} \cdots$$

// <u>Proof:</u>

$$x = \sqrt{\beta}\, u$$

$$x' = \frac{\beta'}{2\sqrt{\beta}} u + \sqrt{\beta}\frac{d\varphi}{ds}\dot{u} = \frac{\beta' u}{2\sqrt{\beta}} + \frac{1}{\gamma_0\sqrt{\beta}}\dot{u}$$

$$J = \det\begin{vmatrix} \frac{\partial x}{\partial u} & \frac{\partial x}{\partial \dot{u}} \\ \frac{\partial x'}{\partial u} & \frac{\partial x'}{\partial \dot{u}} \end{vmatrix} = \begin{vmatrix} \sqrt{\beta} & 0 \\ \frac{\beta'}{2\sqrt{\beta}} & \frac{1}{\gamma_0\sqrt{\beta}} \end{vmatrix} = \frac{1}{\gamma_0}$$

//

$$\boxed{dx \otimes dx' = du \otimes \frac{d\dot{u}}{\gamma_0}}$$

We now analyze the effects of perturbations on the dynamics

$$\boxed{\ddot{U} + \nu_0^2 U = \nu_0^2 \beta^{3/2} \underline{P}(x,y,s)} \; *$$

Expand the perturbation in a power series

- Can always be done for all physical applied field perturbations.

$$\underline{P}(x,y,s) = \underline{P}_0(y,s) + \underline{P}_1(y,s)x + \underline{P}_2(y,s)x^2 + \cdots$$

$$= \sum_{n=0}^{\infty} \underline{P}_n(y,s)\, x^n$$

* $\underline{P}$ represents a perturbation due to:
- Systematic or random field errors in magnets etc.
- Alignment error induced field terms etc.

and take

$$x = \sqrt{\beta}\, U$$

to obtain

$$\boxed{\ddot{U} + \nu_0^2 U = \nu_0^2 \sum_{n=0}^{\infty} \beta^{\frac{n+3}{2}} \underline{P}_n(y,s)\, U^n}$$

To more simply illustrate resonances we will take the particle to move in the x-plane only ($y=0$ for all s). If this is not the case the formalism can be generalized by expanding the $\underline{P}_n(y,s)$ in a power series in y and generalizing the notation for the Floquet coordinates to distinguish between the x- and y-planes, etc. The essential character of the more general analysis is illustrated by this simple case.

$$\boxed{y(s) \equiv 0 \quad \text{to simplify picture}}$$

TOPS FORM 7527 Made in U.S.A.

In this special case $(y=0)$ we expand each coefficient in the power series in a Fourier series as:

Here I implicitly assume a ring and keep φ as a 2π "phase" path variable in the ring for both systematic and random errors.

$$P_n(y=0,s)\,\beta^{\frac{n+3}{2}} = \sum_{k=-\infty}^{\infty} C_{n,k}\, e^{ikp\varphi}$$

$$p = \begin{cases} 1 & \text{- A random perturbation (once in ring)} \\ N & \text{- A periodic perturbation (every period)} \end{cases}$$

$$C_{n,k} = \int_{-\pi/p}^{\pi/p} \frac{d\varphi}{2\pi/p}\, P_n(y=0,s)\,\beta(s)^{\frac{n+3}{2}}$$

$$s = s(\varphi) \quad ; \quad \varphi = \int_{s_0}^{s} \frac{d\bar{s}}{\nu_0\,\beta(\bar{s})}$$

Then the perturbed equation of motion becomes:

$$\ddot{U} + \nu_0^2 U = \nu_0^2 \sum_{n=0}^{\infty}\sum_{k=-\infty}^{\infty} C_{n,k}\, e^{ikp\varphi}\, U^n$$

For the case of small amplitude perturbations this equation can be analyzed perturbatively to linear order as:

$$U = U_0 + \delta U \quad ; \quad |U_0| >> |\delta U|$$

where:

Simple Harmonic oscillator →

$$\ddot{U}_0 + \nu_0^2 U_0 = 0$$

put unperturbed solution in perturbation

Simple Harmonic oscillator with driving terms. →

$$\delta\ddot{U} + \nu_0^2\,\delta U \simeq \nu_0^2 \sum_{n=0}^{\infty}\sum_{k=-\infty}^{\infty} C_{n,k}\, e^{ipk\varphi}\, U_0^n$$

FORM 7527
Made in U.S.A.

U_0 represents the unperturbed particle orbit. The general solution to the equation for U_0 can be expressed as:

$$\boxed{\begin{array}{l} U_0 = U_{0i} \cos(\nu_0 \varphi + \psi_i) \\ \\ U_{0i},\ \psi_i \quad \text{initial conditions (constants)} \end{array}}$$

Then,

$$U_0^n = U_{0i}^n \left(\frac{e^{i(\nu_0\varphi + \psi_i)} + e^{-i(\nu_0\varphi+\psi_i)}}{2} \right)^n$$

$$= \frac{U_{0i}^n}{2^n} \sum_{m=0}^{n} \binom{n}{m} e^{i(n-m)(\nu_0\varphi+\psi_i)} e^{-im(\nu_0\varphi+\psi_i)}$$

Here, $\binom{n}{m} \equiv \frac{n!}{m!(n-m)!}$ is a binomial coefficient.

$$= \frac{U_{0i}^n}{2^n} \sum_{m=0}^{n} \binom{n}{m} e^{i(n-2m)\nu_0\varphi} e^{i(n-2m)\psi_i}$$

and the perturbed equation becomes:

$$\boxed{\delta\ddot{U} + \nu_0^2 \delta U \simeq \nu_0^2 \sum_{n=0}^{\infty} \sum_{k=-\infty}^{\infty} \sum_{m=0}^{n} \binom{n}{m} C_{n,k}\, e^{i[(n-2m)\nu_0 + pk]\varphi} \times e^{i(n-2m)\psi_i}}$$

In general, can take $\delta U = \delta U_h + \delta U_p$ where $\delta\ddot{U}_h + \nu_0^2 \delta U_h = 0$ but in this case we can take $\delta U_h = 0$ since this part of the perturbative solution is contained in U_0. Thus <u>only the particular solution</u> need be found. From the properties of a driven harmonic oscillator, we know that no stable solution exists

TOPS FORM 7537 Made in U.S.A.

whenever the the frequency of the driving force equals that of the restoring force (resonant exchange). Thus we have the resonance condition: ← see Homework!

$$\boxed{\begin{array}{l} (n-2m)\,\nu_0 + pk = \pm\nu_0 \\ n = 1, 2, 3, \ldots \quad ; \quad m = 0, 1, 2, \ldots n \\ k = -\infty, \ldots 0, \ldots \infty \\ p = \begin{cases} 1 & \text{A random perturbation (once per ring)} \\ N & \text{A periodic perturbation (every lattice period)} \end{cases} \end{array}}$$

For ν_0 satisfying this condition the perturbation will grow in amplitude. If the growth rate is sufficiently large, such tunes will be unreliable operating points of the machine and the corresponding perturbation must be corrected. Since this is a linear analysis, the perturbations may be analyzed in turn:

Examples:

$n=0$ (Dipole Perturbation)

$n=0 \Rightarrow m=0$ and the resonance condition becomes:

$$\nu_0 = \pm pk \qquad p\cdot k = \text{integer}$$

Therefore:

$$p = \begin{cases} 1; & \text{random pert in ring} \\ N; & \text{Periodic perturbation in lattice.} \end{cases} \qquad \boxed{\begin{array}{l} \nu_0 \neq \text{integer} = |p\cdot k| \\ \quad = p, p+1, \ldots \end{array} \quad \text{for dipole } (n=0) \text{ perturbations}}$$

$p=1$ Note: Random error in ring (once per lap) $\Rightarrow$ $\nu_0 \neq 1, 2, 3, \ldots$

$p=N$: Systematic error (every lattice period) $\nu_0 \neq N, 2N, 3N, \ldots$

Systematic errors less restrictive.

TOPS FORM 7537 Made in U.S.A.

$n=1$ Quadrupole Perturbation

The resonance conditions give: $\Rightarrow$ $n=1$, $m=0,1$

$$\nu_0 + pk = \pm \nu_0 \qquad (n=1, m=0)$$
$$-\nu_0 + pk = \pm \nu_0 \qquad (n=1, m=1)$$

$pk + \nu_0 = \nu_0$ represents a special case that can be eliminated by "renormalizing" the driving force of the oscillator and $pk = 2\nu_0$ implies that:

$p = \begin{cases} 1; & \text{random pert. in ring} \\ N; & \text{periodic pert. in lattice} \end{cases}$

$$\boxed{\nu_0 \neq \text{half-integer} = |pk/2| \quad \text{for quadrupole } (n=1) \text{ perturbations.}}$$

$n=2$ Sextupole Perturbations $\Rightarrow$ $n=3$ $m=0,1,2$

The resonance conditions give:

$$2\nu_0 + pk = \pm \nu_0$$
$$pk = \pm \nu_0$$
$$-2\nu_0 + pk = \pm \nu_0$$

These conditions are equivalent to:

$p = \begin{cases} 1; & \text{random pert. in ring} \\ N; & \text{periodic pert. in lattice} \end{cases}$

$$\boxed{\nu_0 \neq \begin{cases} \text{integer } (pk) \\ \text{half-integer } (pk/2) \\ \text{3rd-integer } (pk/3) \end{cases} \quad \text{for sextupole } (n=3) \text{ perturbations}}$$

The integer and half-integer restrictions were already obtained with respect to the dipole and quadrupole cases. The 3rd integer is a new restriction.

TOPS FORM 7527 Made in U.S.A.

Other cases similar

// Aside Interpretation of low-order resonance conditions:

Dipole Errors

Consider a ring with 1 dipole error along the azimuth of a ring:

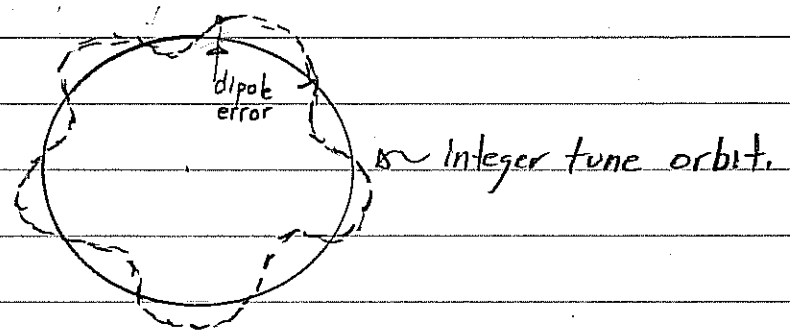

If the particle is oscillating with integer tune, then the particle will experience the error each time with the same phase of oscillation and the particle trajectory will "walk-off" lap-to-lap in phase-space. Since the machine aperture is finite the particle will be lost.

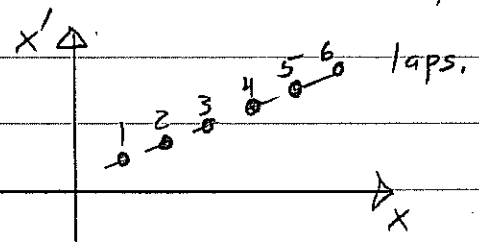

Quadrupole Errors

For a single quadrupole error along the azimuth of a ring, a similiar qualitative argument leads one to conclude that if the particle oscillates with 1/2 integer tune that the orbit can "walk-off" lap-to-lap in phase space patterns as shown here:

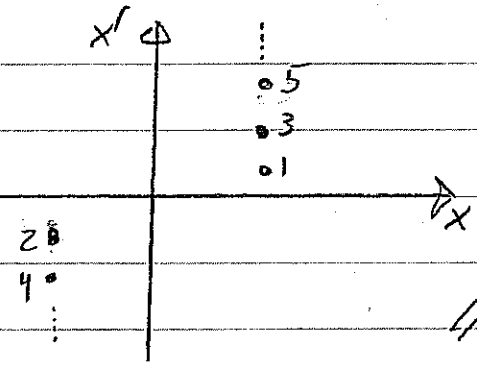

//

The general resonance condition for x-plane motion can be summarized as:

$$\boxed{M \nu_0 = N \qquad M, N \text{ integers of the same sign.}}$$

M = order resonance

Generally <u>higher order numbers are less dangerous.</u>

- Longer coherence path for validity of theory and coefficients generally smaller ∴ Higher order can "wash" out.

In the general case particle motion is not restricted to the x-plane ($y \neq 0$) and a more general resonance analysis shows that:

$$\boxed{\begin{array}{l} M_x \nu_{0x} + M_y \nu_{0y} = N \\ \\ \nu_{0x} = \text{x-plane tune} \\ \nu_{0y} = \text{y-plane tune} \\ \\ M_x, M_y, N \text{ integers of the same sign.} \end{array}}$$

$|M_x| + |M_y|$ = order resonance.

These restrictions are plotted order-by-order in $\nu_x - \nu_y$ plots to find allowed tunes where the machine can safely operate. Generally, lower order resonances are more dangerous, since small effects can invalidate the ideal analysis and "wash out" higher order resonances.

FORM 7527
Made in U.S.A.

Typical tune plots for up to 3rd order resonances:

$\mathcal{N}=1$ Superperiodicity

Machine operating point is chosen to avoid resonance lines.

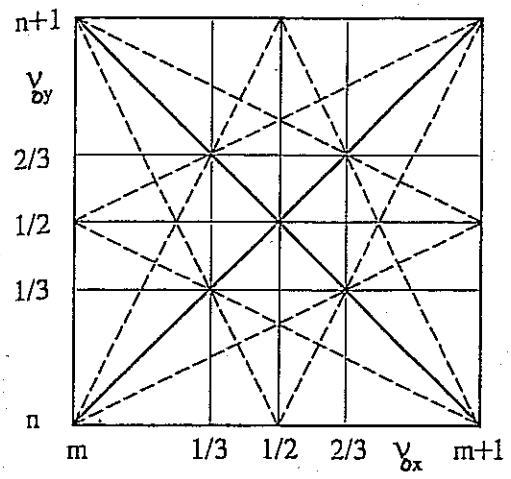

Applicable to field errors from random construction errors.

From Wiedemann

$\mathcal{N}=4$ Superperiodicity

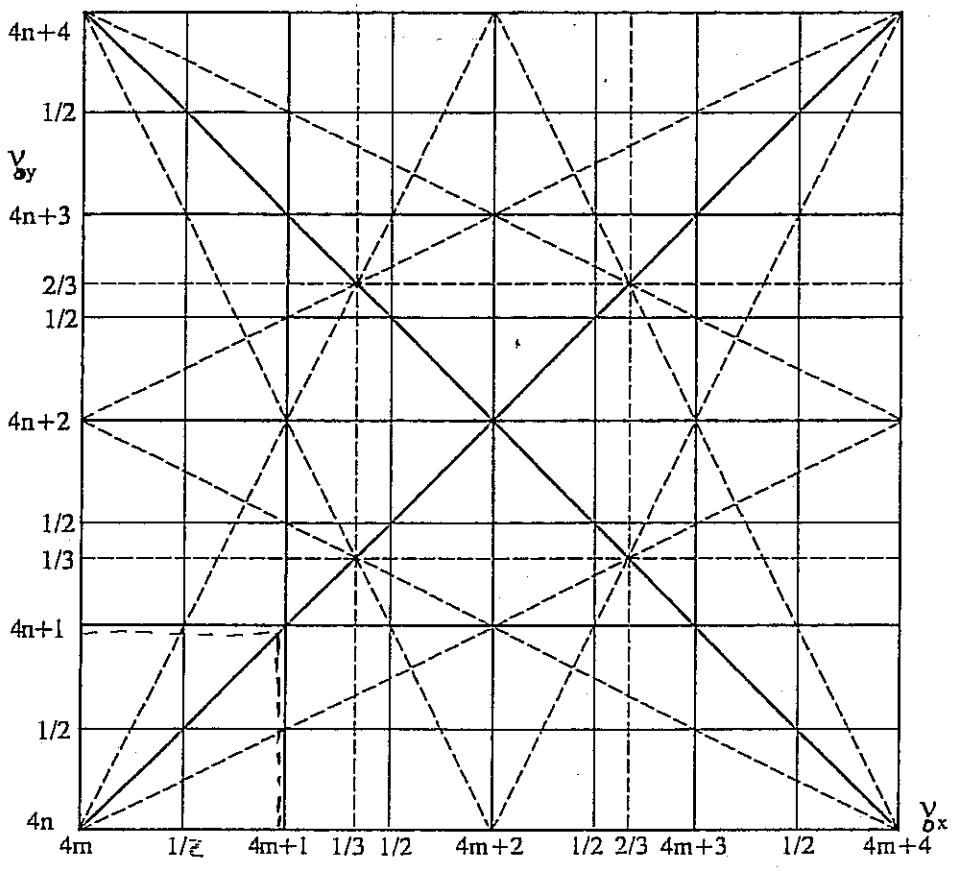

Applicable to systematic lattice field errors in a 4-period ring.

Note lesser density of resonance lines than in the $\mathcal{N}=1$ case.

Distinguishing between field errors from random construction ($p=1$) and systematic errors on the lattice ($p=\mathcal{N}$) is important.

Random errors ($p=1$)

- Errors always present and can give low order resonaces.
- Usually have weak amplitude coefficients and may be corrected.

Systematic errors ($p=\mathcal{N}$)

- Lead to higher order resonaces for large $\mathcal{N}$ and a lower density of resonance lines
  - Large symmetric rings ($\mathcal{N}$ large) have lesser restrictions from systematic errors
  - Practical issues such as construction cost and getting the beam into and out of the ring lead to smaller $\mathcal{N}$
- Amplitude coefficients can be large and the systematic resonances can be strong and thus can be dangerous.

In practice, resonances higher than 3rd order need rarely be considered.

- Effects outside model tend to wash out higher order resonances.

Effects of Space Charge on Resonances

Machine operating points are generally chosen far from low-order resonance lines. Coherent processes that shift tune values towards a low-order resonace are dangerous.

Coherent – same for each particle in distribution.

incoherent – different (random) for each particle in distribution.

Tune shift limits are often called "Laslett Limits" because he first calculated such limits for many processes

- image charges
- image currents
- space charge

⋮

For space-charge, the so-called Laslett limit is taken as:

$$\boxed{\nu_0 - \nu = \Delta\nu < 1/4}$$

ν_0 = tune at zero space charge

ν = KV distribution tune

This is probably over idealized and restrictive but is widely used to set ring current limits.

The Lasleff condition is probably overly restrictive:

- Real space-charge is not coherent like a KV model
  - spectrum of β-tunes.
  - no equilibrium beam and oscillations may crack resonances.
- Simulations indicate that 10's → 100s of laps may pose little problems for strong space charge.
  - Univ. Maryland Ring may soon (~2007+) operate in such regime to test in the lab.

This could be a good research area with new physics.

John Barnard
Steven Lund
USPAS
June 2006

Injectors and longitudinal physics -- I

1. Child-Langmuir Law
   (Reiser 2.5.2, Appendix 1)
2. Pierce electrodes
3. Transients in injectors
4. Injector choices

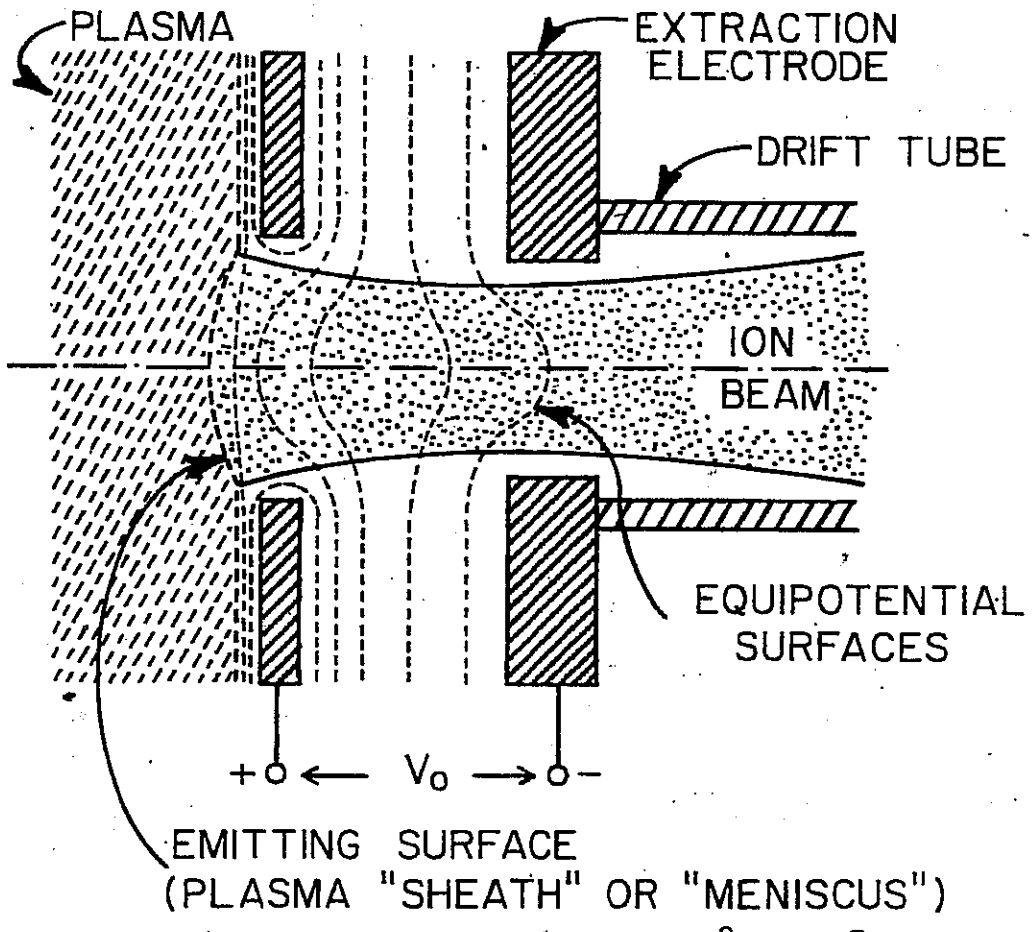

OR "HOT PLATE"

REISER, FIGURE 1.2

- DOPED TUNGSTEN
- ALUMINO-SILICATE

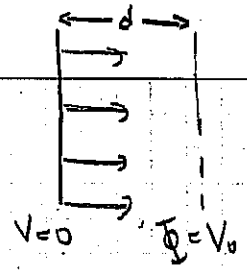

I CHILD-LANGMUIR EMISSION

ASSUME EMISSION IS PLANAR 1-D:

$$J = \rho v_z \qquad (1)$$

$$\frac{1}{2} m v_z^2 = -q\Phi \qquad (2) \Rightarrow v_z = \left(\frac{-2q\Phi}{m}\right)^{1/2}$$

$$\frac{d^2\Phi}{dz^2} = \frac{\rho}{\varepsilon_0} \qquad (3)$$

(NOTE $\Phi = -\phi$ ← ACTUAL E.S. potential)

CONTINUITY EQUATION (1D) $\frac{\partial \rho}{\partial t} + \frac{\partial}{\partial z}\rho v_z = 0$

for time steady emission ρv_z = constant = J

$$\Rightarrow \frac{d^2\Phi}{dz^2} = \frac{J}{\varepsilon_0 v_z} = \frac{J}{\varepsilon_0\left(\frac{-2q\Phi}{m}\right)^{1/2}}$$

MULTIPLYING BY $\frac{d\Phi}{dz}$ AND INTEGRATING:

$$\frac{\Phi'^2}{2} = \frac{J m^{1/2}}{\varepsilon_0 (2q)^{1/2}} 2\Phi^{1/2} + \text{const}$$

Assume $\Phi' = 0$ at $z=0$ (Space-charge limited emission)

$\Phi = 0$ at $z=0 \Rightarrow$ const $= 0$

$$\frac{d\Phi}{dz} = \left(\frac{4J}{\varepsilon_0}\right)^{1/2}\left(\frac{m\Phi}{2q}\right)^{1/4}$$

$$\Rightarrow \frac{4}{3}\Phi^{3/4} = \left(\frac{4J}{\varepsilon_0}\right)^{1/2}\left(\frac{m}{2q}\right)^{1/4} z \Rightarrow \Phi(x) = \left(\frac{3}{4}\right)^{4/3}\left(\frac{4J}{\varepsilon_0}\right)^{2/3}\left(\frac{m}{2q}\right)^{1/3} z^{4/3}$$

If $\Phi = V_0$ at $z = d$ $\Rightarrow$ $\Phi = V_0 \left(\frac{z}{d}\right)^{4/3}$

$$\Rightarrow \quad V_0 = \left(\frac{3}{4}\right)^{4/3} \left(\frac{4J}{\varepsilon_0}\right)^{2/3} \left(\frac{m}{2q}\right)^{1/3} d^{4/3}$$

$$\text{or} \quad J = \frac{4}{9}\varepsilon_0 \left(\frac{2q}{m}\right)^{1/2} \frac{V_0^{3/2}}{d^2}$$

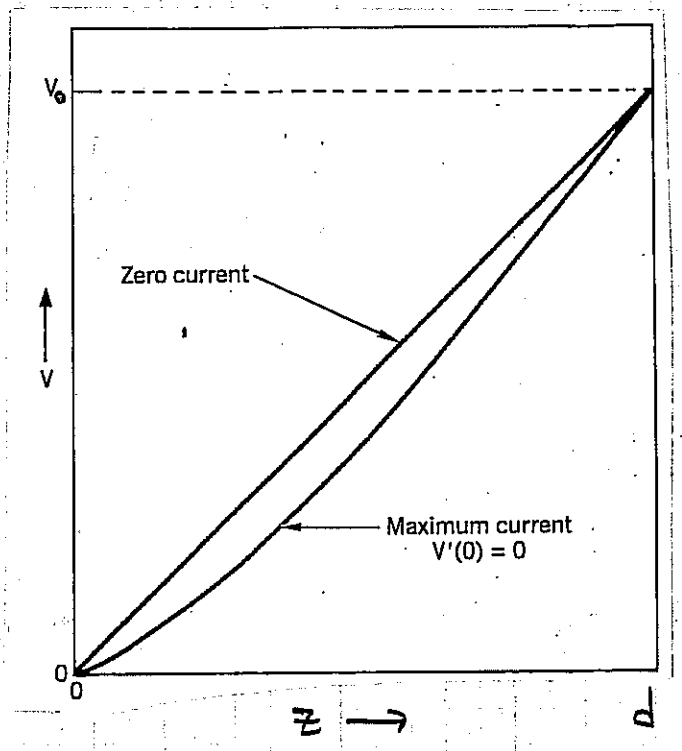

NOTE THAT IF WE MULTIPLY J BY THE BEAM AREA πr_b^2, AND DIVIDE BY $v = \left(\frac{2qV_0}{m}\right)^{1/2}$

$$\Rightarrow \lambda = \frac{4\pi\varepsilon_0 V}{9}\left(\frac{r_b^2}{d^2}\right) \qquad \text{RECALL } Q \equiv \frac{\lambda}{4\pi\varepsilon_0 V} \text{ (NON-RELAT.)}$$

$$\Rightarrow Q = \frac{1}{9}\left(\frac{r_b^2}{d^2}\right) \quad \text{or as a function of } z: \; Q(z) = \frac{1}{9}\left(\frac{r_b^2}{z^2}\right)$$

PERVEANCE

PIERCE COLUMN

$V \sim z^{4/3}$

$E \sim z^{1/3}$

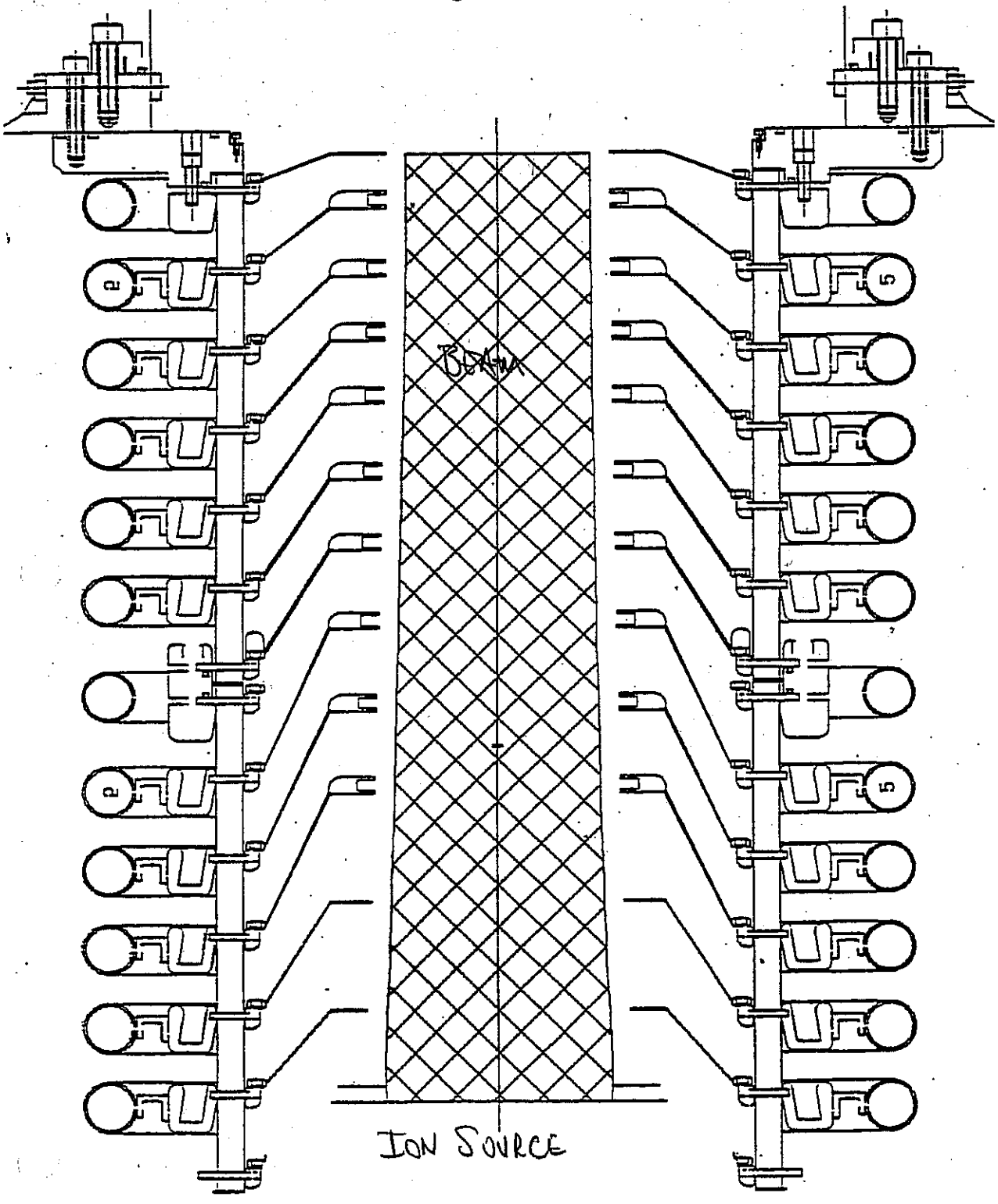

YESTERDAY, WE DERIVED THE PARAXIAL RAY EQUATION FOR PARTICLES IN AXISYMMETRIC SYSTEMS:

$$\underbrace{r'' + \frac{\gamma'}{\beta^2\gamma} r'}_{\text{INERTIAL}} + \underbrace{\frac{\gamma''}{2\beta^2\gamma} r}_{E_r} + \underbrace{\left(\frac{\omega_c}{2\gamma\beta c}\right)^2 r}_{\substack{V_\theta B_z \\ -\text{CENTRIFUGAL}}} - \underbrace{\left(\frac{p_\theta}{\gamma\beta m c}\right)^2 \frac{1}{r^3}}_{\text{CENTRIFUGAL}} - \underbrace{\frac{q}{\gamma^3 m v_z^2} \frac{\lambda(r)}{2\pi\epsilon_0 r}}_{\text{SELF-FIELD}} = 1$$

$$\theta' = \frac{p_\theta}{\gamma m r^2 \beta c} - \frac{\omega_c}{2\gamma\beta c}$$ ← CONSTANCY & DEFINITION OF CANONICAL MOMENTUM

ENVELOPE EQUATION FOR AXISYMMETRIC BEAM

$$r_b'' + \frac{\gamma' r_b'}{\beta^2\gamma} + \frac{\gamma''}{2\beta^2\gamma} r_b + \left(\frac{\omega_c}{2\gamma\beta c}\right)^2 r_b - \frac{4\langle p_\theta\rangle^2}{(\gamma m\beta c)^2 r_b^3} - \frac{\varepsilon_r^2}{r_b^3} - \frac{Q}{r_b} = 0$$

$$\varepsilon_r^2 \equiv 4\left(\langle r^2\rangle\langle r'^2\rangle - \langle r r'\rangle^2 + \langle r^2\rangle\langle r^2\theta'^2\rangle - \langle r^2\theta'\rangle^2\right)$$

RETURNING TO PARAXIAL ENVELOPE EQUATION:

(for $\beta << 1$) $$r_b'' + \frac{\beta'}{\beta} r_b' + \left[\frac{1}{2}\frac{\beta'^2}{\beta^2} + \frac{1}{2}\frac{\beta''}{\beta}\right] r_b - \frac{Q}{r_b} = 0$$

For $r_b'' = \frac{\beta'}{\beta} r_b' = 0$

If $Q = V_0 (z/d)^{4/3}$

$$v = C z^{2/3}$$

$$v' = \frac{2}{3} C z^{-1/3}$$

$$v'' = \frac{-2}{9} C z^{-4/3}$$

$$\Rightarrow \left[\frac{1}{2}\frac{\beta'^2}{\beta^2} + \frac{1}{2}\frac{\beta''}{\beta}\right] r_b^2 = Q$$

$$\left[\frac{2}{9}\frac{1}{z^2} \qquad -\frac{1}{9}\frac{1}{z^2}\right]$$

$$\Rightarrow Q(z) = \frac{1}{9}\frac{r_b^2}{z^2}$$

So Child-Langmuir flow satisfies the PARAXIAL ENVELOPE EQUATION FOR A CONSTANT BEAM RADIUS (AS IT SHOULD!)

PIERCE ELECTRODES: GOING BEYOND PARAXIAL APPROXIMATION

CONSIDER THE CASE A BEAM WHICH FILLS THE LOWER HALF-SPACE.

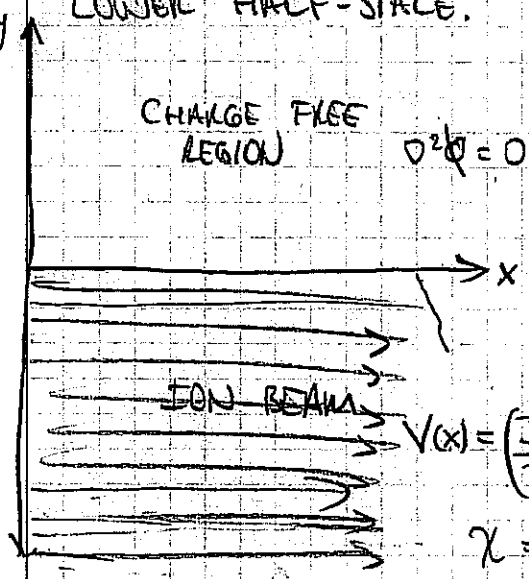

CHARGE FREE REGION $\nabla^2\phi = 0$

$$\frac{\partial^2\phi}{\partial x^2} + \frac{\partial^2\phi}{\partial y^2} = 0$$

$$V(x) = \left(\frac{J}{\chi}\right)^{2/3} x^{4/3}$$

$$\chi = \left(\frac{4\epsilon_0}{9}\right)\sqrt{\frac{2q}{m}}$$

FIND SOLUTION SUCH THAT

$$\frac{\partial\phi}{\partial y}(x, y=0) = 0$$

$$\& \quad \phi(x, y=0) = V(x)$$

PIERCE'S SOLUTION: LET THE POTENTIAL BE THE REAL PART OF

$$\phi + iW = V(x+iy) \equiv V(z) \qquad z \equiv x+iy$$

NOTE THAT FOR ANY $V(z)$ WITH derivatives that exist independent of direction (analytic) the real part of $V(z)$ satisfies Laplace's equation: $\frac{\partial^2 \mathrm{Re}[V]}{\partial x^2} + \frac{\partial^2 \mathrm{Re}[V]}{\partial y^2} = 0$

$$\frac{\partial\phi}{\partial x} = \mathrm{Re}\left[\frac{dV}{dz}\right] \qquad \frac{\partial\phi}{\partial y} = \mathrm{Re}\left[i\frac{dV}{dz}\right]$$

$$\frac{\partial^2\phi}{\partial x^2} = \mathrm{Re}\left[\frac{d^2V}{dz^2}\right] \qquad \frac{\partial^2\phi}{\partial y} = -\mathrm{Re}\left[\frac{d^2V}{dz^2}\right] \Rightarrow \frac{\partial^2\phi}{\partial x^2} + \frac{\partial^2\phi}{\partial y} = \mathrm{Re}\left[\frac{d^2V}{dz^2}\right] - \mathrm{Re}\left[\frac{d^2V}{dz^2}\right] = 0$$

CHOOSE $V(z) = \left(\frac{J}{\chi}\right)^{2/3} (x+iy)^{4/3}$

By construction $\phi(x, y=0) = V(x)$ ✓

$$\phi = \mathrm{Re}\left[\left(\frac{J}{\chi}\right)^{2/3} (x+iy)^{4/3}\right]$$

Let $x+iy = r\exp[i\theta]$
$(x+iy)^{4/3} = r^{4/3}\exp\left[\frac{4i\theta}{3}\right]$

$$= \left(\frac{J}{\chi}\right)^{2/3} (x^2+y^2)^{2/3}\,\mathrm{Re}\left[\exp\left[i\,\frac{4}{3}\tan^{-1}\left(\frac{y}{x}\right)\right]\right]$$

$$\boxed{\phi(x,y) = \left(\frac{J}{\chi}\right)^{2/3} (x^2+y^2)^{2/3} \cos\left[\frac{4}{3}\tan^{-1}\left(\frac{y}{x}\right)\right]}$$

Note that $\phi(x,y) = \phi(x,-y) \Rightarrow \frac{\partial\phi}{\partial y}(x, y=0) = 0$

$\phi = 0$ EQUIPOTENTIAL:

$$\Rightarrow 0 = \cos\left[\frac{4}{3}\tan^{-1}\left(\frac{y}{x}\right)\right]$$

$$\Rightarrow \tan^{-1}\left(\frac{y}{x}\right) = \frac{3}{4}\left(\frac{\pi}{2}\right) = 67.5^\circ$$

FOR A GENERAL EQUIPOTENTIAL PASSING THROUGH X_0:

$$X_0^{4/3} = (x^2+y^2)^{2/3} \cos\left[\frac{4}{3}\tan^{-1}\left(\frac{y}{x}\right)\right]$$

EQUIPOTENTIALS FOR MATCHING TO A PLANAR BOUNDARY

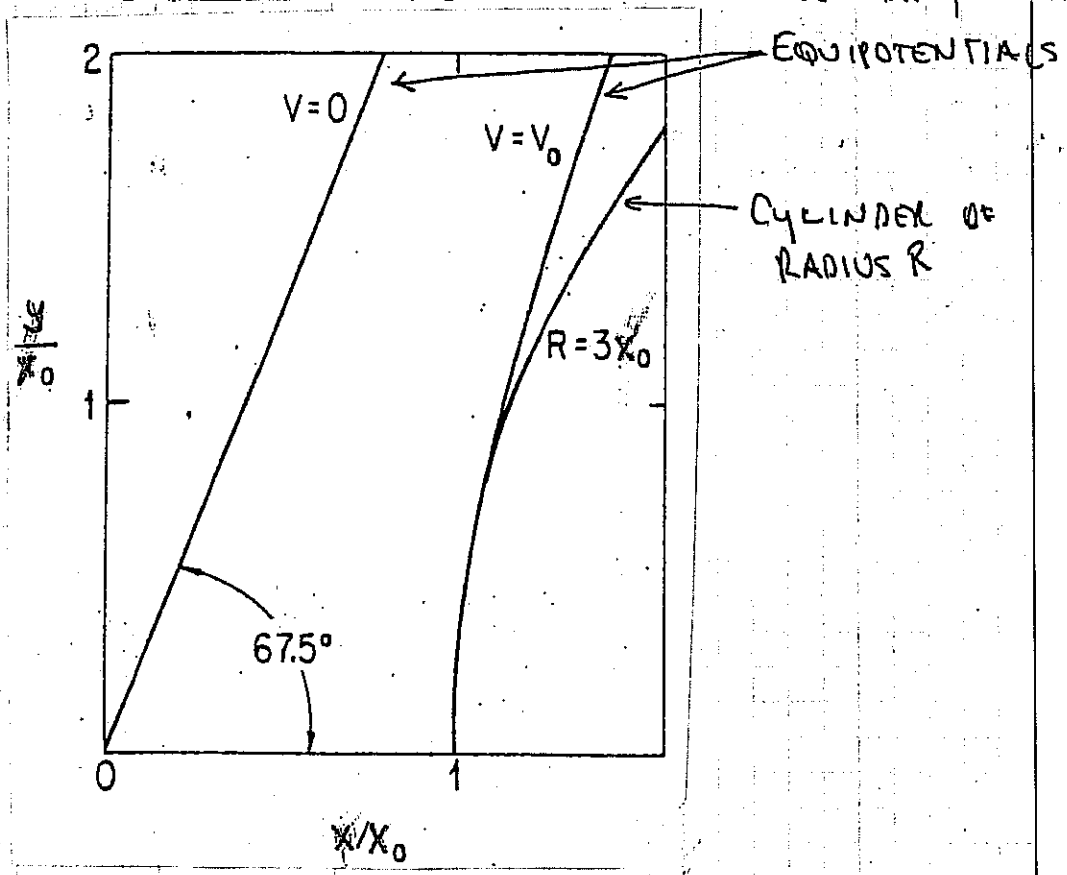

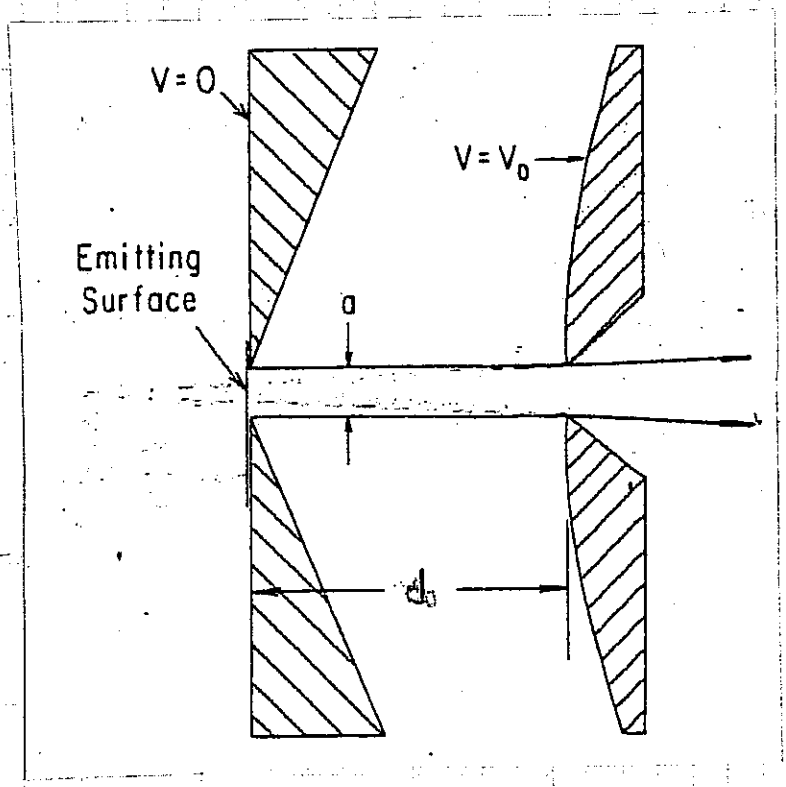

FIGURES FROM "LARGE ION BEAMS, FUNDAMENTALS OF GENERATION AND PROPAGATION" BY A.T. FORRESTER, Wiley, NY, 1988.

ELECTRODES FOR A LONG SLIT ION BEAM SYSTEM

PIERCE ELECTRODES FOR CIRCULAR BEAMS

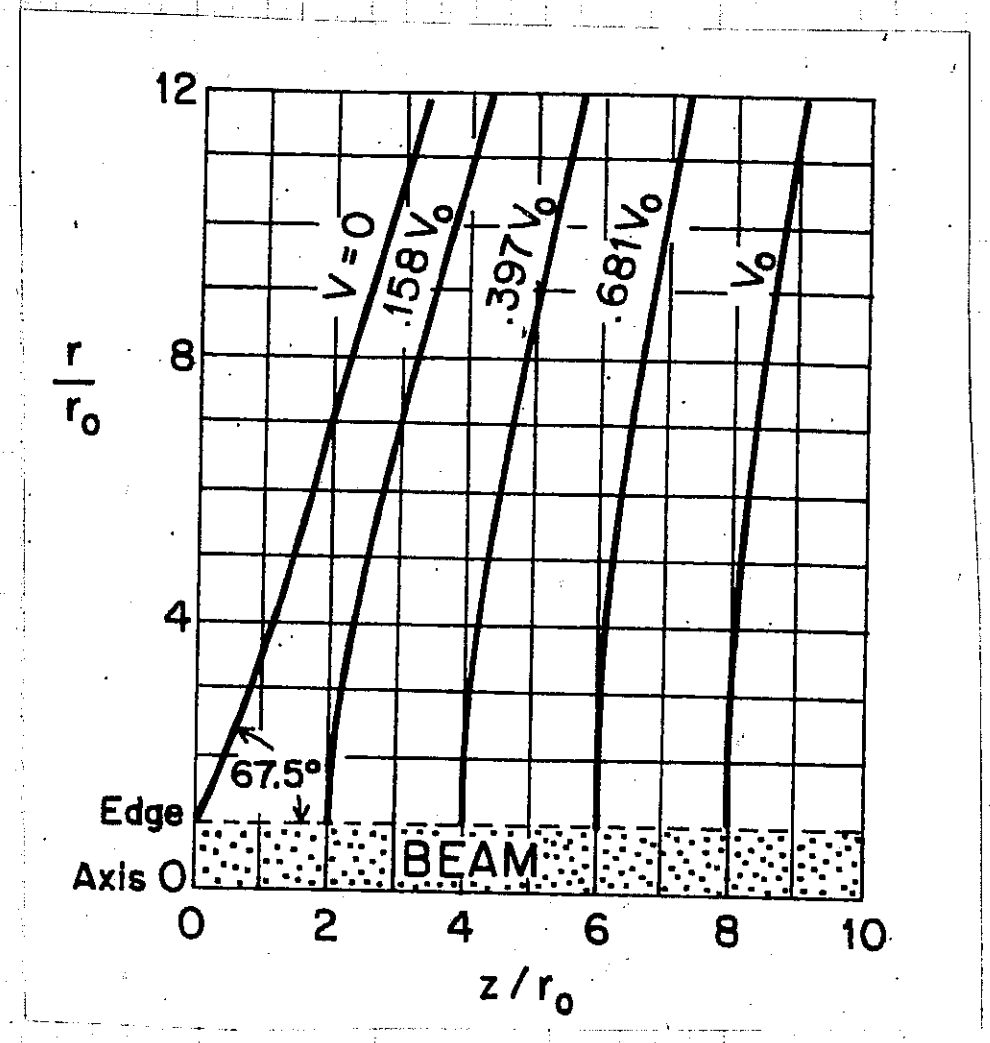

- SOLUTION is similar, but must be done numerically
- $\phi = 0$ is same as planar case

FIGURE FROM A.T. FORRESTER, "LARGE ION BEAMS, ..." Wiley, 1988

TRANSIENTS IN INJECTORS (LAMPEL & TIEFENBACK, APPL. PHYS. LETT, 43, 57, 1983)

DURING TURN-ON THERE IS NO SPACE CHARGE IN FRONT OF BEAM, SO FIELDS MAY NOT BE GIVEN BY CHILD-LANGMUIR LAW. ⇒ CURRENT SPIKES POSSIBLE ⇒ ADVERSE TRANSVERSE COUPLING.

SOLUTION: ADJUST VOLTAGE ON DIODE SUCH THAT C-L EFIELD OCCURS EVERYWHERE THERE IS BEAM.

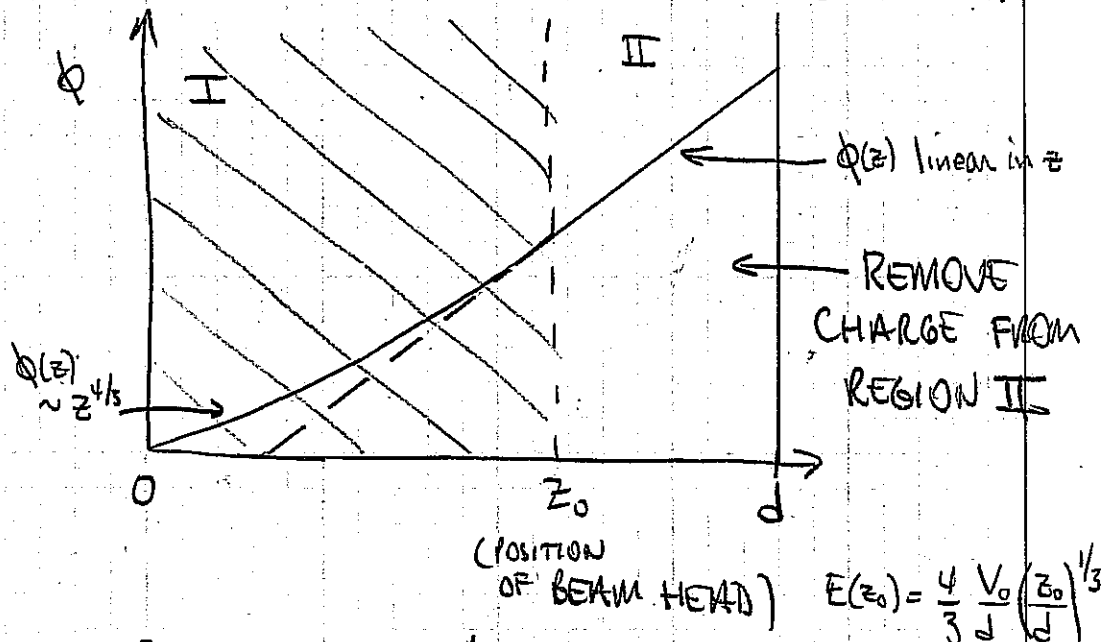

$$E(z_0) = \frac{4}{3}\frac{V_0}{d}\left(\frac{z_0}{d}\right)^{1/3}$$

$$\phi(d) = \int_0^{z_0} E(z)\,dz + \int_{z_0}^{d} E(z)\,dz$$

$$= V_0\left(\frac{z_0}{d}\right)^{4/3} + \frac{4}{3}\frac{V_0}{d}\left(\frac{z_0}{d}\right)^{1/3}(d - z_0)$$

$$= V_0\left[\frac{4}{3}\left(\frac{z_0}{d}\right)^{1/3} - \frac{1}{3}\left(\frac{z_0}{d}\right)^{4/3}\right]$$

(NOTE V_0 IS THE DESIRED STEADY STATE VOLTAGE ACROSS DIODE).

SO IF WE KNOW $z_0(t)$ WE CAN DETERMINE $\Phi(t)$.

$$\frac{1}{2} m \dot{z}_0^2 = q V_0 \left(\frac{z_0}{d}\right)^{4/3}$$

(SINCE BY CONSTRUCTION, HEAD OF BEAM TRAVELS AT CHILD-LANGMUIR VELOCITY LIKE ALL PARTICLES).

$$\dot{z}_0 = \left(\frac{2qV_0}{m}\right)^{1/2} \left(\frac{z_0}{d}\right)^{2/3}$$

$$\frac{dz_0}{z_0^{2/3}} = \left(\frac{2qV_0}{m}\right)^{1/2} \frac{dt}{d^{2/3}}$$

$$\Rightarrow 3 z_0^{1/3} = \left(\frac{2qV_0}{m}\right)^{1/2} \frac{t}{d^{2/3}} \quad \Rightarrow \quad t = \frac{3(z_0 d^2)^{1/3}}{\left(\frac{2qV_0}{m}\right)^{1/2}}$$

Let $\tau = \dfrac{3d}{\left(\frac{2qV_0}{m}\right)^{1/2}}$ = transit time across diode

$$\Rightarrow \frac{t}{\tau} = \left(\frac{z_0}{d}\right)^{1/3}$$

$$\Phi(d, z_0) = V_0 \left[\frac{4}{3}\left(\frac{z_0}{d}\right)^{1/3} - \frac{1}{3}\left(\frac{z_0}{d}\right)^{4/3}\right]$$

$$\Rightarrow \Phi(d,t) = \begin{cases} V_0 \left[\frac{4}{3}\left(\frac{t}{\tau}\right) - \frac{1}{3}\left(\frac{t}{\tau}\right)^4\right] & \text{for } 0 < t < \tau \\ V_0 & \text{for } t > \tau \end{cases}$$

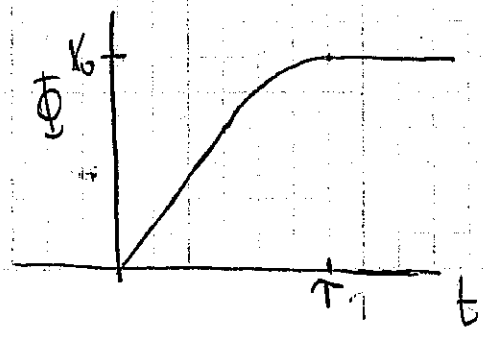

INJECTOR CHOICES (cf. Kuan et al, NIMPRA, 464, 379 (2001))

CHILD-LANGMUIR $\Rightarrow J = \chi \dfrac{V^{3/2}}{d^2}$

where $\chi = \frac{4}{9}\varepsilon_0\left(\frac{2q}{m}\right)^{1/2}$

SOME CONSTRAINTS:

(1) VOLTAGE BREAKDOWN

EMPIRICALLY $V \lesssim \sim 100\,\text{kV} \begin{cases} \left(\dfrac{d}{1\,\text{cm}}\right) & \text{for } d \leq 1\,\text{cm} \\ \left(\dfrac{d}{1\,\text{cm}}\right)^{1/2} & \text{for } d \geq 1\,\text{cm} \end{cases}$

(2) BEAM OPTICS ABERRATIONS: $d \gtrsim \sim 3$ to $4\, r_p$ (TYPICALLY)

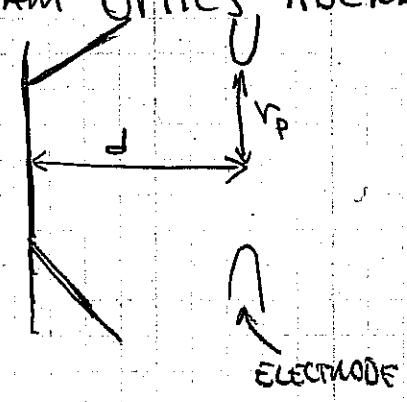

NOTE THAT

$$J \sim \frac{V^{3/2}}{d^2} \sim \begin{cases} V^{-1/2} & d < 1\,\text{cm} \\ V^{-3/2} & d > 1\,\text{cm} \end{cases} \qquad I \sim \pi r_p^2 J \sim \begin{cases} V^{3/2} \end{cases}$$

Thus current density decreases with size and voltage, but I increases.

A_{IV} $V = 24\,S + 7\sqrt{S}$

from A. Fultenc:

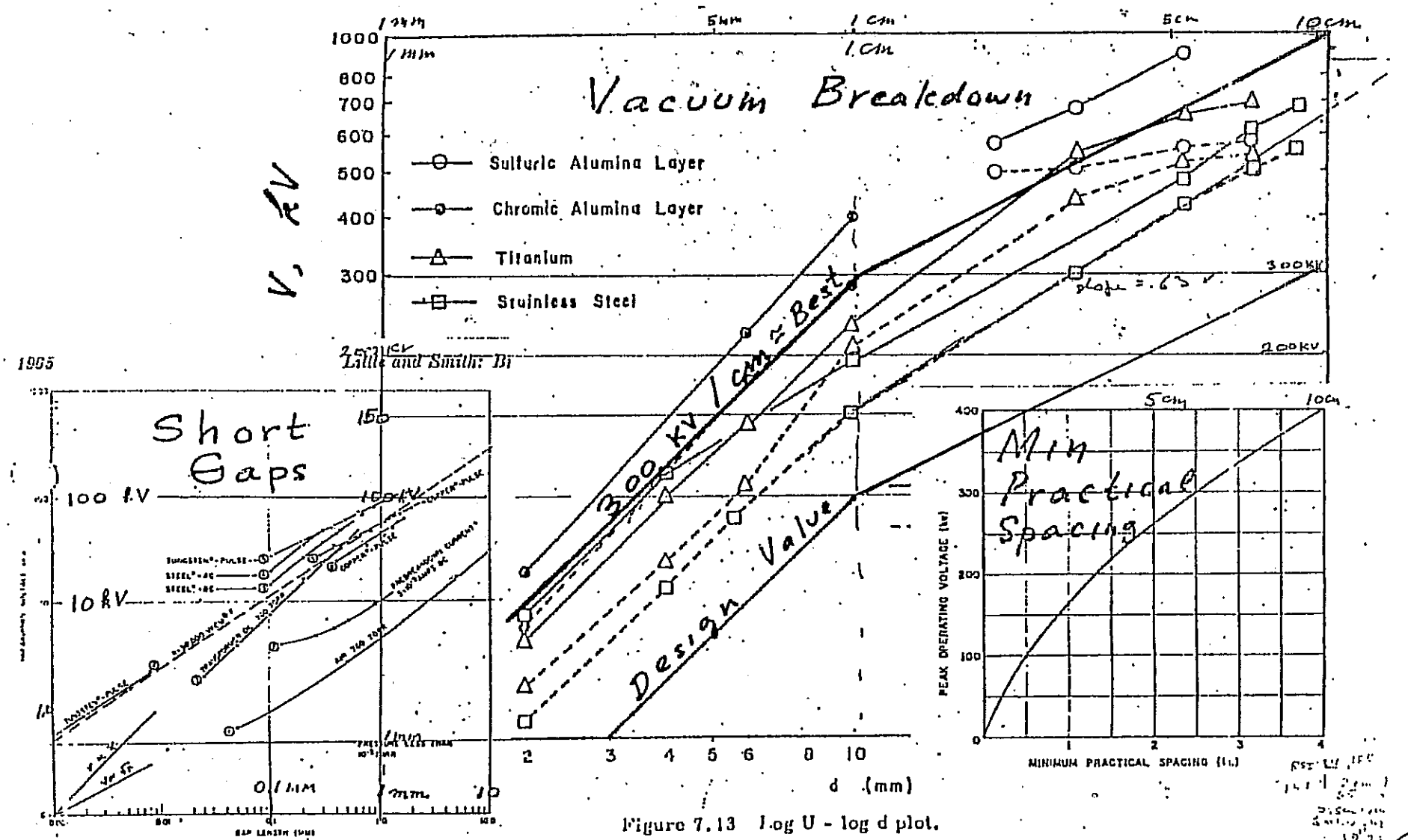

Figure 7.13 Log U - log d plot.

Fig. 1. Breakdown voltage-vs.-gap length for uniform-field and near-uniform-field geometry. Numbers on curves indicate the

MULTIPLE BEAMLET INJECTORS CAN HAVE HIGHER CURRENT DENSITY
DECREASING SIZE OF INJECTOR

traditional design using single large diameter source →

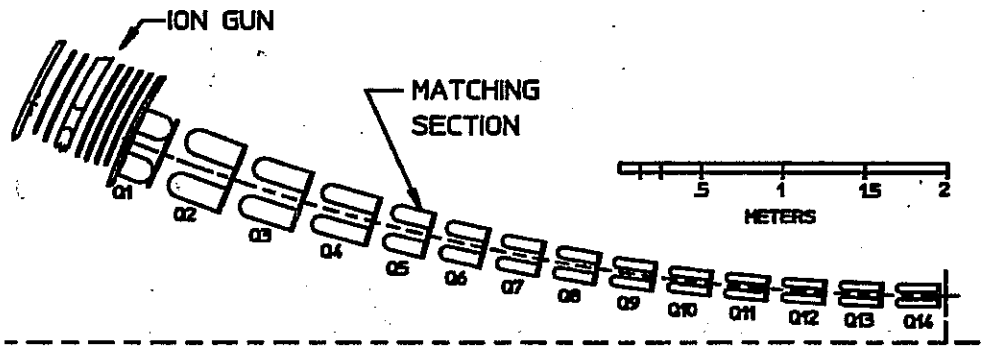

advanced design using multiple beamlets →

Each beamlet carries higher current density; But merging beamlets increases thermal spread.

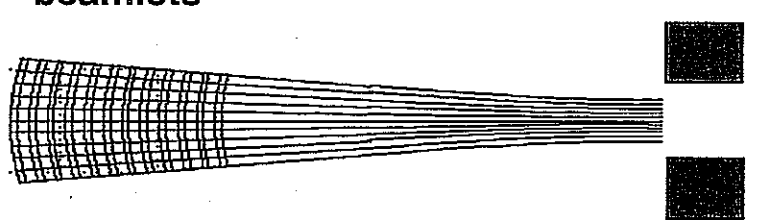

Child-Langmuir $J_{CL} \propto \frac{V^{3/2}}{d^2}$

Breakdown limit $V \propto d^{1.0 \text{ to } 0.5}$

$$J \propto V^{-1/2 \text{ to } -5/2} \propto d^{-1/2 \text{ to } -5/4}$$

Merge and match beamlets into an ESQ channel

Simulations of merging-beamlet injector

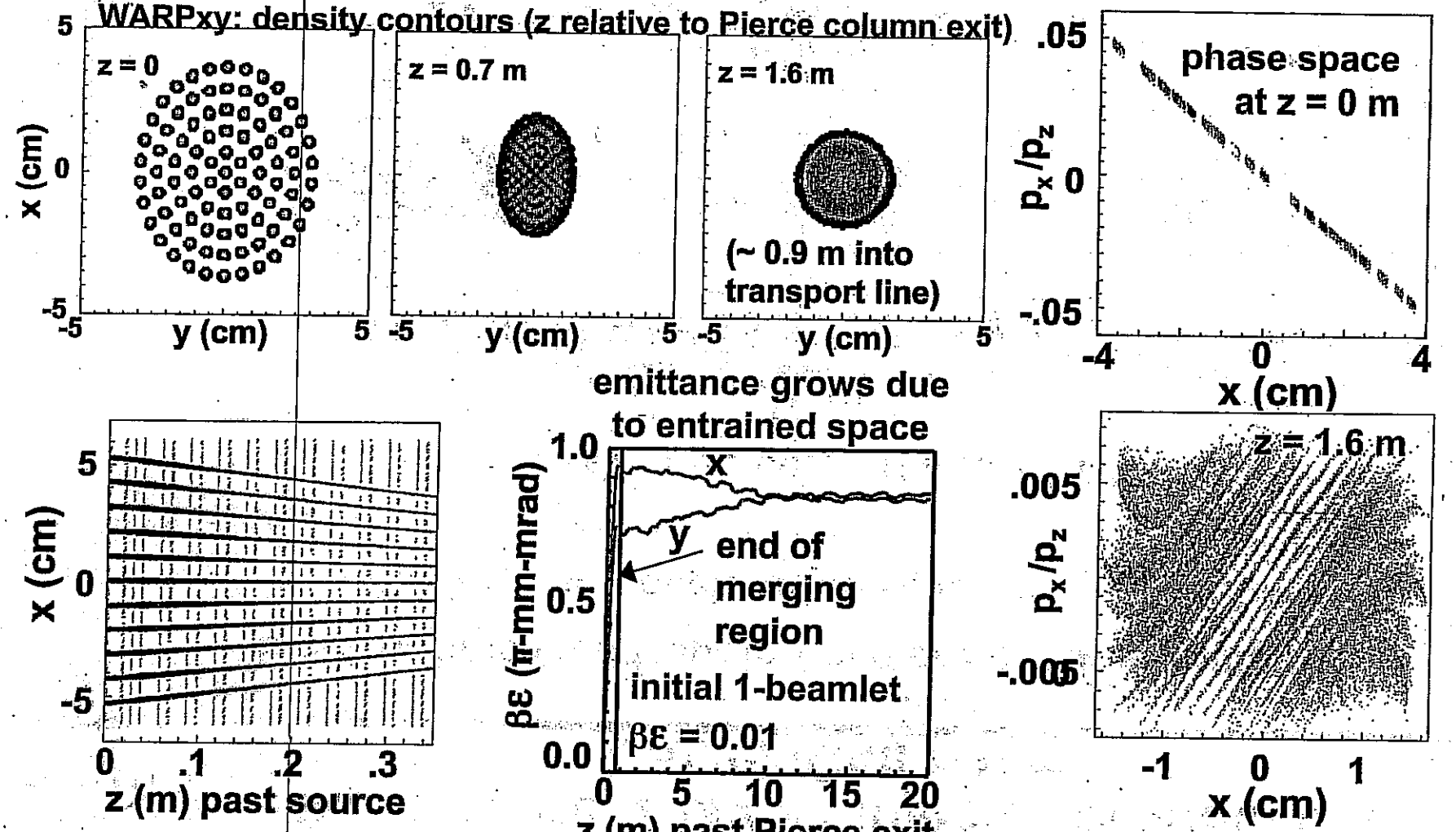

The Heavy Ion Fusion Virtual National Laboratory

from D.L. Grote, E. Henestroza, J.W. Kwan, "Design & Simulation of the Multibeamlet Injector for a High Current Accelerator" Submitted to MSTWG (2002)

0.8 Ampere, 2 MV K^+ Injector produced a λ=0.25μC/m beam

Electrostatic Quadrupole Accelerator for simultaneous focusing and acceleration of ion beams to 2 MV.

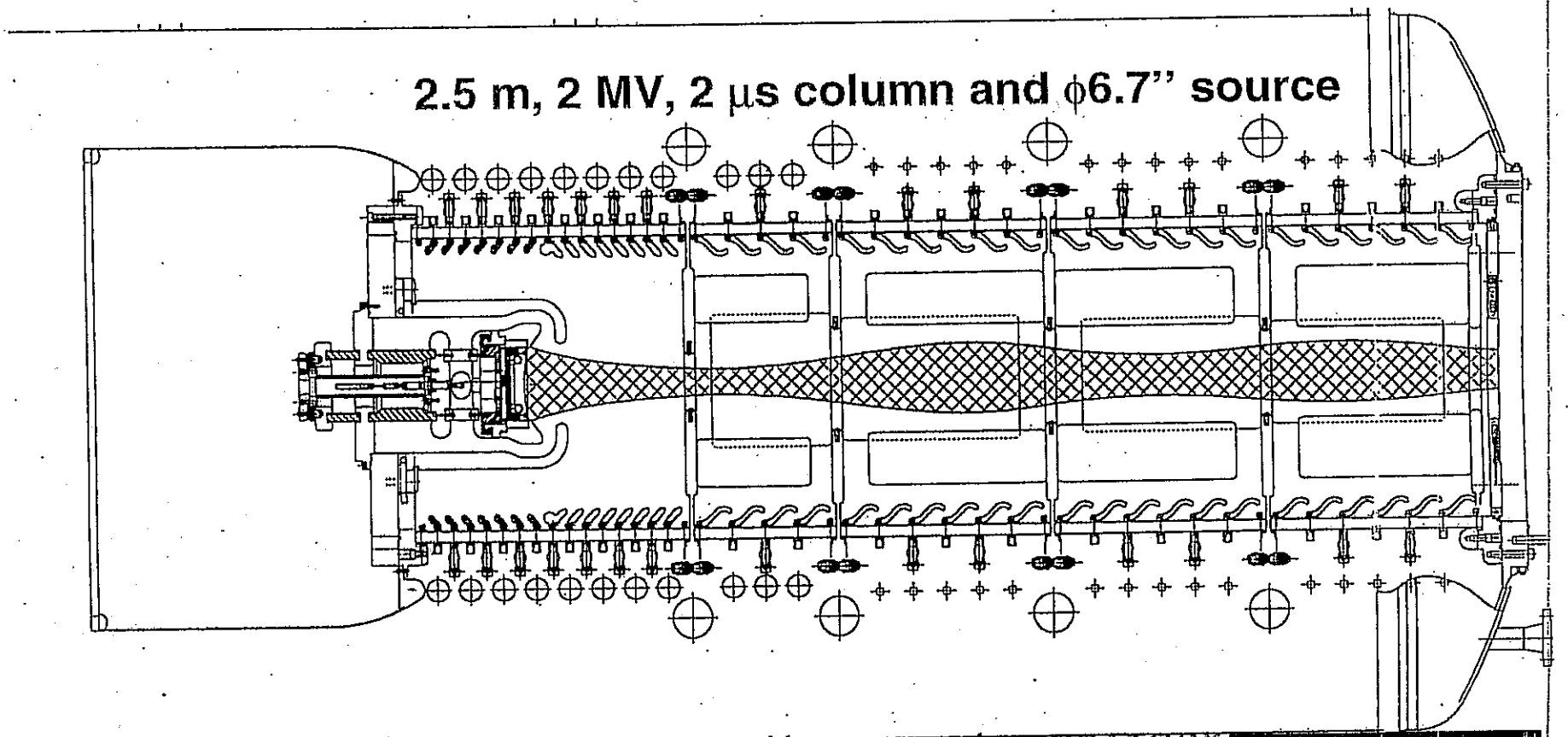

Filmed for ease of reference

SCALING OF BRIGHTNESS IN INJECTORS

$$\epsilon_N = 4\beta\langle x^2\rangle^{1/2}\langle x'^2\rangle^{1/2} = \frac{4}{c}\left(\frac{r_b}{2}\right)\langle v_x^2\rangle^{1/2}$$

$$\frac{1}{2}mv_x^2 = \frac{1}{2}kT$$

$$\epsilon_N = 2r_b\sqrt{\frac{kT}{mc^2}}$$

$$\Rightarrow \quad B = \frac{I}{\epsilon_N^2} = \frac{\pi J}{4(kT/mc^2)} \sim \frac{J}{T}$$

$\Rightarrow$ FOR HIGH BRIGHTNESS & HIGH CURRENT MAY WISH TO ACCELERATE MANY BEAMLETS AND THEN MERGE TO FORM SINGLE BEAM.

National® Brand 42-182 100 SHEETS Made in U.S.A.

MANY ISSUES NOT DISCUSSED HERE!

- SOURCES
- ELECTRON TRAPPING
- CONVERGING BEAMS
- MATCHING TO AN ESQ (e.g.)
- rf
- ...

John Barnard
Steven Lund
USPAS
June 2006

Injectors and longitudinal physics -- II

1. Acceleration - introduction
2. Space charge of short bunches (rf)
3. Space charge of long bunches
4. Longitudinal space charge waves
5. Longitudinal rarefaction waves and bunch ends

ACCELERATION

rf (radio-frequency)

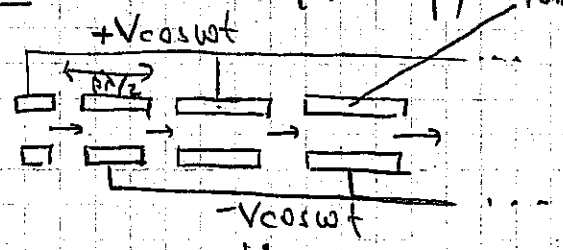

(wideroe linac)
LOW FREQUENCIES (< 100 MHz)

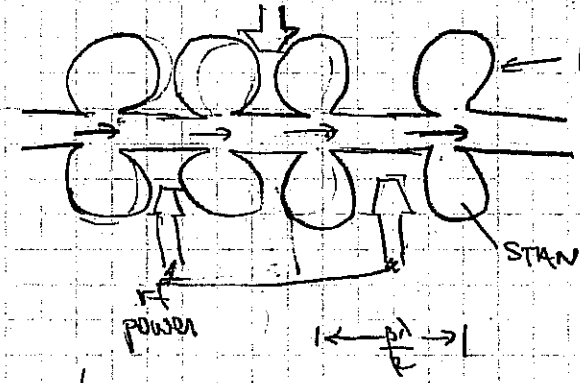

(COUPLED CAVITY LINAC)
$0.4 < \beta < 1.0$

FREQUENCIES ~ 100's MHz – ~ 1 GHz

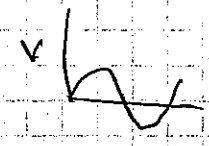

IN EACH GAP $E = E_m \sin \omega t$

Induction acceleration

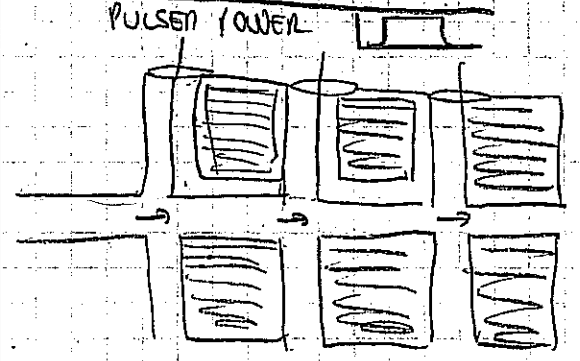

(INDUCTION LINAC)

$\nabla \times E = -\partial B/\partial t$

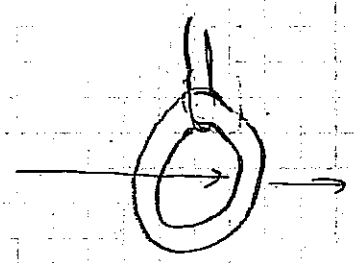

IN EACH GAP $E =$ CONSTANT
(OR SOME PRESCRIBED FUNCTION)

Longitudinal equation of motion

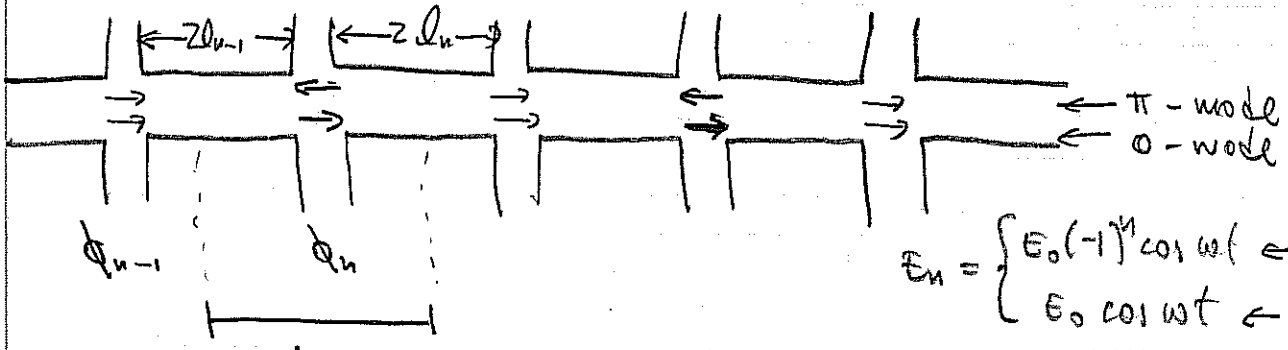

$$E_n = \begin{cases} E_0(-1)^n \cos\omega t & \leftarrow \pi\text{-mode} \\ E_0 \cos\omega t & \leftarrow 0\text{-mode} \end{cases}$$

L_n = center to center distance between drift tubes

$E_z = E_0 \cos(\phi_s)$ ← synchronous particle enters each gap at same phase

RESONANCE CONDITION ON SYNCHRONOUS PARTICLE:

$$\boxed{l_{n-1} = \frac{\beta_s \lambda}{2} \begin{Bmatrix} \frac{1}{2} \\ 1 \end{Bmatrix} \begin{matrix} \pi\text{-mode} \\ 0\text{-mode} \end{matrix} \qquad \lambda = \frac{2\pi}{\omega} c = \text{light travel distance in one} = c\Delta t_{rf} \text{ of oscillation}}$$

(IT TAKES $\begin{Bmatrix} 1/2 \\ 1 \end{Bmatrix}$ OSCILLATION PERIOD TO TRAVEL BETWEEN GAPS).

$\beta_s = \frac{v_s}{c}$ = velocity of synchronous particle

PARTICLE PHASE RELATIVE TO rf at the nth gap:

$$\phi_n = \phi_{n-1} + \omega \frac{2l_{n-1}}{\beta_{n-1} c} + \begin{cases} \pi & \pi\text{-mode} \\ 0 & 0\text{-mode} \end{cases}$$

$$\Delta(\phi - \phi_s)_n = 2\pi \beta_{s,n-1} \left(\frac{1}{\beta_{n-1}} - \frac{1}{\beta_{s,n-1}} \right) \begin{Bmatrix} 1/2 \\ 1 \end{Bmatrix} \begin{matrix} \pi\text{-mode} \\ 0\text{-mode} \end{matrix}$$

$$\cong -2\pi \frac{\delta\beta}{\beta_{s,n}} \begin{Bmatrix} 1/2 \\ 1 \end{Bmatrix}$$

A VELOCITY DIFFERENCE LEADS TO A PHASE DIFFERENCE!!

$$\boxed{\Delta(\phi - \phi_s)_n \cong -2\pi \frac{W_{n-1} - W_{s,n-1}}{mc^2 \gamma_{s,n-1}^3 \beta_{s,n-1}^2} \begin{Bmatrix} 1/2 \\ 1 \end{Bmatrix}}$$

$W = (\gamma - 1) mc^2$

$$\frac{1}{\beta} - \frac{1}{\beta_s} \cong \frac{-\delta\beta}{\beta_s^2}$$

$$\delta W = \gamma_s^3 \beta_s mc^2 \delta\beta$$

SIMILARLY, A PHASE DIFFERENCE PRODUCES AN ENERGY CHANGE (RELATIVE TO SYNCHRONOUS PARTICLE)

$$\boxed{\Delta(W - W_s)_n = q E_0 L_n (\cos\varphi_n - \cos\varphi_{s,n})}$$

$$L_n = \frac{(\beta_{s,n-1} + \beta_{s,n})\lambda}{2} \begin{Bmatrix} 1/2 \\ 1 \end{Bmatrix} =$$ CENTER-TO-CENTER DISTANCE BETWEEN DRIFT SECTION

$$(\Delta W_s = q E_0 L_n \cos\phi_s)$$

CONVERTING TO A CONTINUOUS VARIABLE:

$$\Delta(\phi-\phi_s) \rightarrow \frac{d\Delta\phi}{dn} \qquad \Delta(W-W_s) \rightarrow \frac{d\Delta W}{dn}$$

$$dn = \frac{ds}{\beta_s \lambda} \cdot \left\{ \begin{matrix} 2 \\ 1 \end{matrix} \right\}$$

$$\Rightarrow \boxed{\begin{aligned} \gamma_s^3 \beta_s^3 \frac{d\Delta\phi}{ds} &= -2\pi \frac{\Delta W}{mc^2 \lambda} \\ \frac{d\Delta W}{ds} &= qE_0(\cos\phi - \cos\phi_s) \end{aligned}}$$

$$\frac{d}{ds}\left[\gamma_s^3 \beta_s \frac{d\Delta\phi}{ds}\right] = -2\pi \frac{qE_0}{mc^2\lambda}\left[\cos\phi - \cos\phi_s\right] \qquad \text{(I)}$$

NOW THE SPATIAL SEPARATION IS GIVEN BY:

$$\Delta z \equiv z - z_s = -\frac{\beta_s \lambda}{2\pi}\Delta\phi$$

$\Rightarrow$ ALSO, LET $\cos\phi - \cos\phi_s \simeq -\sin\phi_s \Delta\phi$ $\left[\text{for } \frac{2\pi \Delta z}{\beta\lambda} = \Delta\phi \ll 1\right]$

$$\Rightarrow \frac{d}{ds}\left[\gamma_s^3 \beta_s \frac{d}{ds}\left(\frac{\Delta z}{\beta_s}\right)\right] \cong -\frac{2\pi}{\lambda}\frac{qE_0}{mc^2}\sin\phi_s \frac{\Delta z}{\beta_s}$$

WHEN THE ACCELERATION RATE IS SMALL

$$\Rightarrow \frac{d^2}{ds^2}\Delta z \cong -\frac{2\pi}{\lambda}\frac{qE_0 \sin\phi_s}{\gamma_s^3 \beta_s mc^2}\Delta z$$

$$\equiv -k_{s0}^2 \Delta z \qquad \text{(synchrotron oscillations)}$$

RETURNING TO $\Delta W - \phi$ NOTATION

Let $w = \dfrac{\Delta W}{mc^2}$ $\quad A = \dfrac{2\pi}{\beta_s^3 \gamma_s^3 \lambda}$ $\quad B = \dfrac{qE_0}{mc^2}$

$$\boxed{\begin{aligned} \Rightarrow \quad w' &= B(\cos\phi - \cos\phi_s) \\ \phi' &= -Aw \\ \phi'' &= -AB(\cos\phi - \cos\phi_s) \end{aligned}}$$

MULTIPLYING BY ϕ' AND INTEGRATING:

$$\frac{\phi'^2}{2} = -AB(\sin\phi - \phi\cos\phi_s) + \text{const}$$

USING $\phi' = -Aw$ (& DIVIDING BY A)

$$\Rightarrow \underbrace{\frac{Aw^2}{2}}_{\text{kinetic energy}} + \underbrace{B(\sin\phi - \phi\cos\phi_s)}_{\text{potential energy}} = \text{CONST.}$$

$$\frac{dW_s}{ds} \sim qE_0\cos\phi_s$$

$$V(\phi) = B(\sin\phi - \phi\cos\phi_s)$$

$$\frac{dV}{d\phi} = B(\cos\phi - \cos\phi_s)$$

$$\frac{d^2V}{d\phi^2} = -B\sin\phi$$

$$> 0 \Rightarrow -\pi < \phi_s < 0$$

FOR LONGITUDINAL FOCUSING

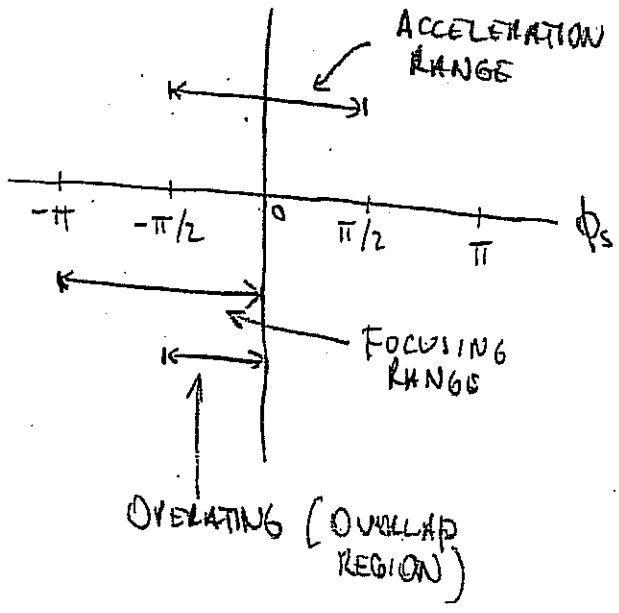

simultaneous acceleration and a potential well when $-\pi/2 \le \phi_s \le 0$. The stable region for the phase motion extends from $\phi_2 < \phi < -\phi_s$, where the lower phase limit ϕ_2 can be obtained numerically by solving for ϕ_2 using $H_\phi(\phi_2) = H_\phi(-\phi_s)$. Figure 6.3 shows longitudinal phase space and the longitudinal potential well. At the potential maximum, where $\phi = -\phi_s$, we

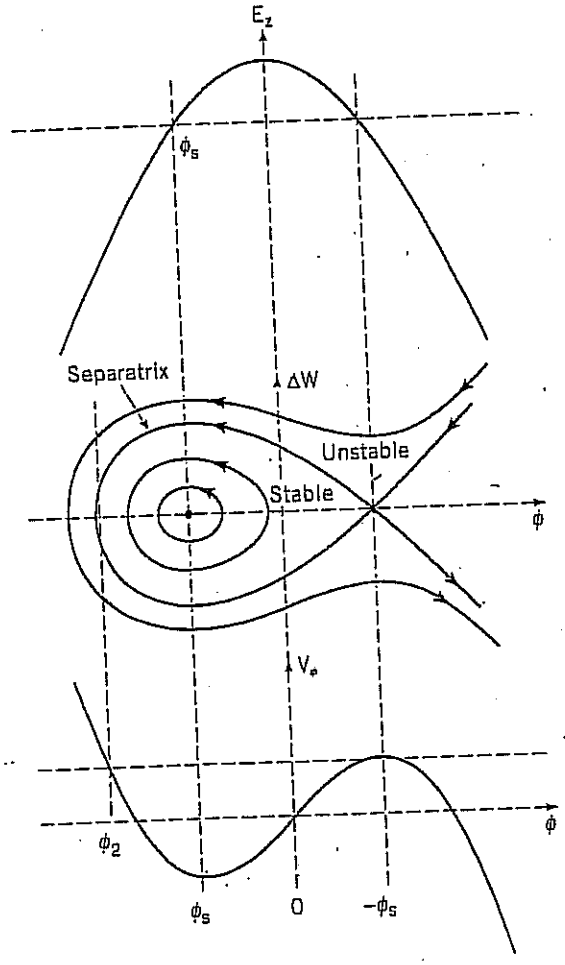

from T. Wangler's "PRINCIPLES of RF LINEAR ACCELERATORS"

Figure 6.3. At the top, the accelerating field is shown as a cosine function of the phase; the synchronous phase ϕ_s is shown as a negative number, which lies earlier than the crest where the field is rising in time. The middle plot shows some longitudinal phase-space trajectories, including the separatrix, the limiting stable trajectory, which passes through the unstable fixed point at $\Delta W = 0$, and $\phi = -\phi_s$. The stable fixed point lies at $\Delta W = 0$ and $\phi = \phi_s$, where the longitudinal potential well has its minimum, as shown in the bottom plot.

SPACE-CHARGE FIELD OF BUNCHED BEAMS

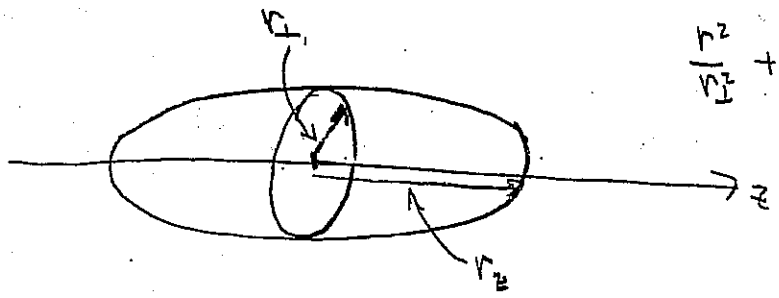

$$\frac{r^2}{r_\perp^2} + \frac{z^2}{r_z^2} = 1$$

BOUNDARY OF ELLIPSOID

THE POTENTIAL OF A UNIFORM DENSITY BUNCH IN FREE SPACE (A MACLAURIN SPHEROID) IS GIVEN BY:

Cf Landau & Lifshitz, Classical Theory of Fields, (p 297)

$$\varphi = \frac{\rho}{4\varepsilon_0}\left(\alpha_\perp r^2 + \alpha_\parallel z^2 - \delta\right)$$

where
$$\alpha_\perp = r_\perp^2 r_z \int_0^\infty \frac{ds}{(r_\perp^2+s)\Delta}$$
$$\alpha_\parallel = r_\perp^2 r_z \int_0^\infty \frac{ds}{(r_z^2+s)\Delta}$$
$$\delta = r_\perp^2 r_z \int_0^\infty \frac{ds}{\Delta}$$
where
$$\Delta^2 = (r_\perp^2+s)^2(r_z^2+s)$$

FOR NON-RELATIVISTIC BEAM:

$$E_z = -\frac{\partial\phi}{\partial z} = f\frac{\rho}{\varepsilon_0} z$$

$$E_r = -\frac{\partial\phi}{\partial r} = \frac{(1-f)}{2}\frac{\rho}{\varepsilon_0} r$$

$$f = f(\alpha) = \begin{cases} \frac{\alpha^2}{1-\alpha^2}\left[\frac{1}{\sqrt{1-\alpha^2}}\tanh^{-1}\sqrt{1-\alpha^2} - 1\right] & \alpha<1 \\ \frac{1}{3} & \alpha=1 \\ \frac{\alpha^2}{\alpha^2-1}\left[1 - \frac{1}{\sqrt{\alpha^2-1}}\tan^{-1}\sqrt{\alpha^2-1}\right] & \alpha>1 \end{cases} \qquad \alpha \equiv \frac{r_\perp}{r_z}$$

FOR RELATIVISTIC BEAM

(cf. LUND & BARNARD PAC97 Conf Proceedings 1997.)

$$\frac{d^2 \underline{x}_\perp}{ds^2} = \frac{F_\perp}{\gamma_s \beta_s^2 mc^2} \qquad \underline{F}_{\perp s} = \frac{-q}{\gamma_s^2}\frac{\partial \phi}{\partial x_\perp} = \frac{q\rho}{2\gamma_s^2 \epsilon_0}\left[1 - f(\alpha)\right] \underline{x}_\perp$$

$$\frac{d^2 \Delta z}{ds^2} = \frac{F_z}{\gamma_s^3 \beta_s^2 mc^2} \qquad F_{zs} = \frac{-q}{\gamma_s^2}\frac{\partial \phi}{\partial z} = \frac{q\rho}{\epsilon_0} f(\alpha)\, \Delta z$$

$$\alpha = \frac{r_\perp}{\gamma r_z} \qquad \left[\alpha = \frac{r_\perp}{(r_z \text{ in comoving frame})}\right]$$

COMBINING FOCUSING + SELF FIELDS

$$\frac{d^2}{ds^2}\Delta z = -k_{s0}^2 \Delta z + \frac{q\rho\, f(\alpha)}{\gamma_s^3 \beta_s^2 mc^2 \epsilon_0}\Delta z \qquad \text{(LINEAR rf)}$$

Total field seen by particle is sum of rf and spacecharge

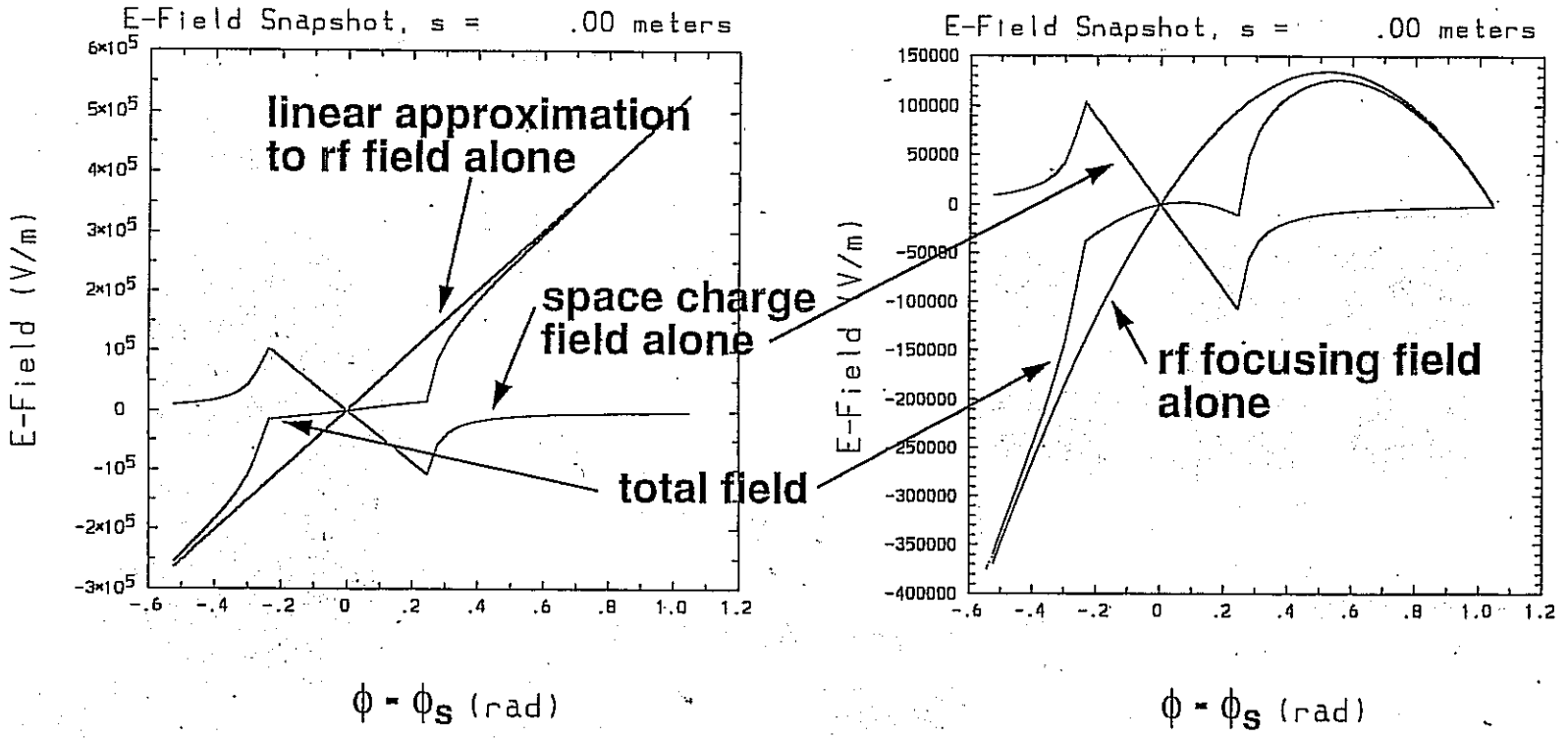

here $\phi - \phi_s = -(2\pi/\beta_s\lambda)\,\Delta z$, where $\beta_s c$ is the longitudinal velocity of the synchronous particle and $\lambda = c/\nu$ is the rf vacuum wavelength

Induction acceleration

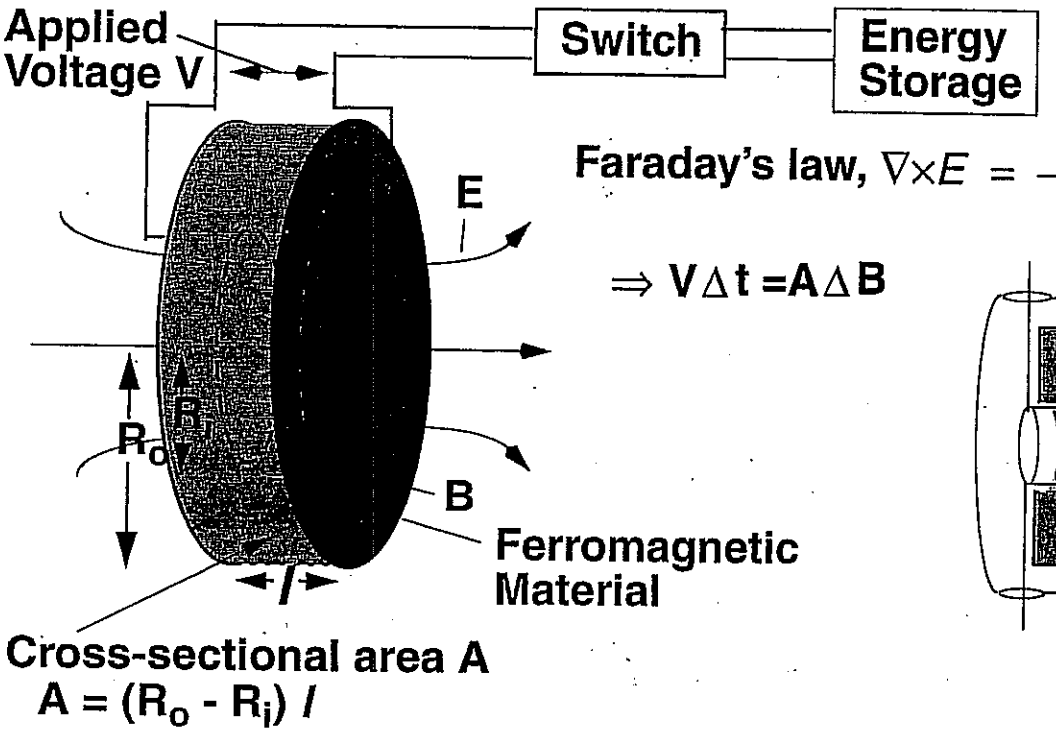

Faraday's law, $\nabla \times E = -\frac{\partial B}{\partial t}$

$\Rightarrow V \Delta t = A \Delta B$

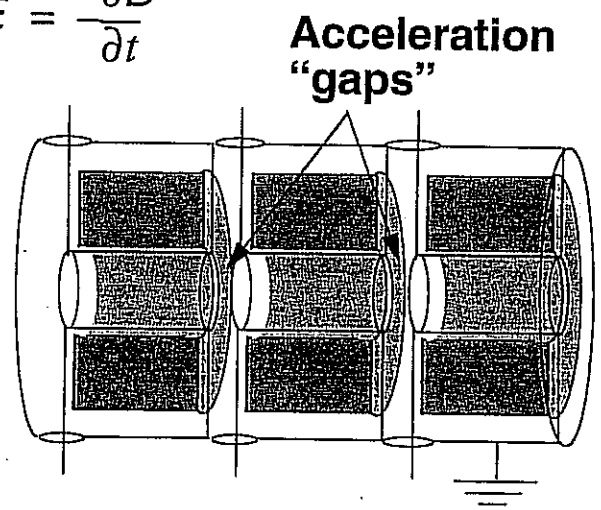

Volt-seconds per m: $(dV/dz)\,\Delta t = (R_o - R_i)\ \Delta B\ f_{radial}\ f_{longit.}$

~1 m ~2.5T ~0.8 ~0.8

$$\boxed{(dV/dz)\,\Delta t <\sim 1.6 \text{ V-s/m}}$$

Several types of waveform are needed to accelerate, compress, and confine the beam

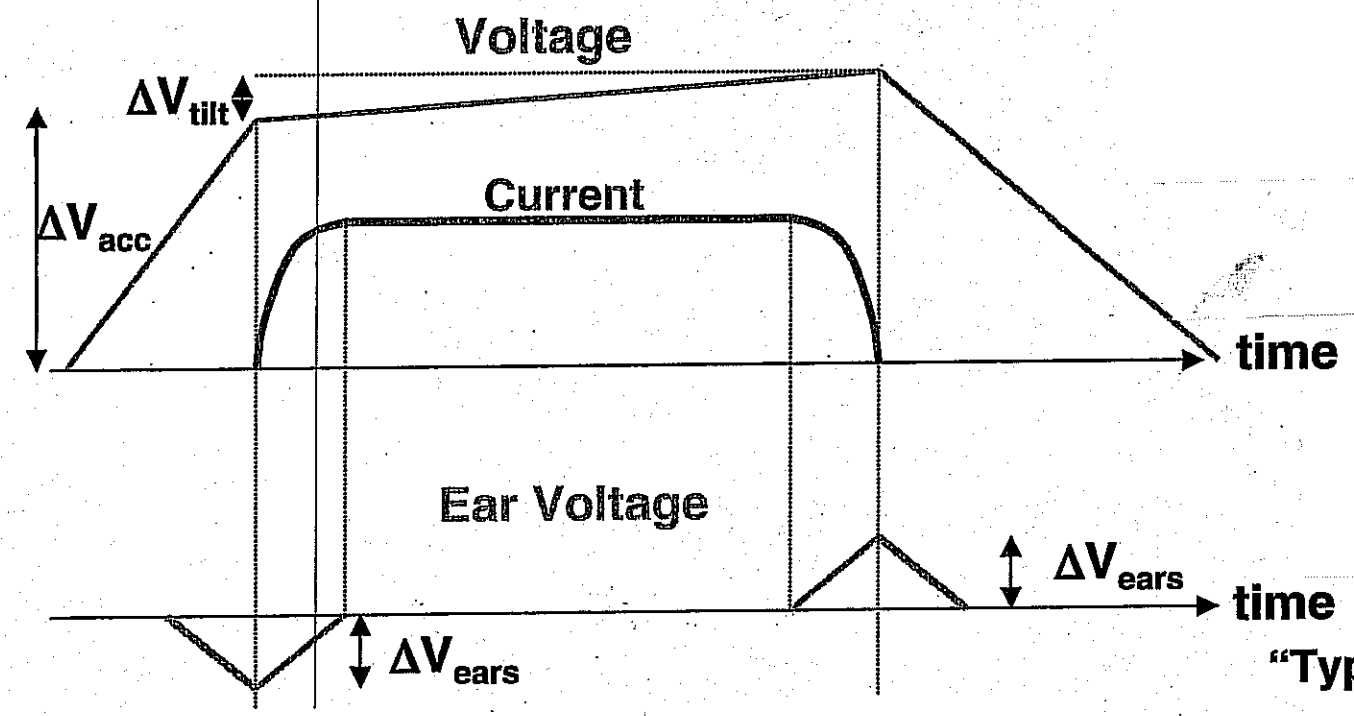

"Typical" numbers:

$\Delta V_{tilt} \sim$ 1 kV
$\Delta V_{ears} \sim$ 14 kV
$\Delta V_{acc} \sim$ 100 kV

COORDINATE SYSTEM

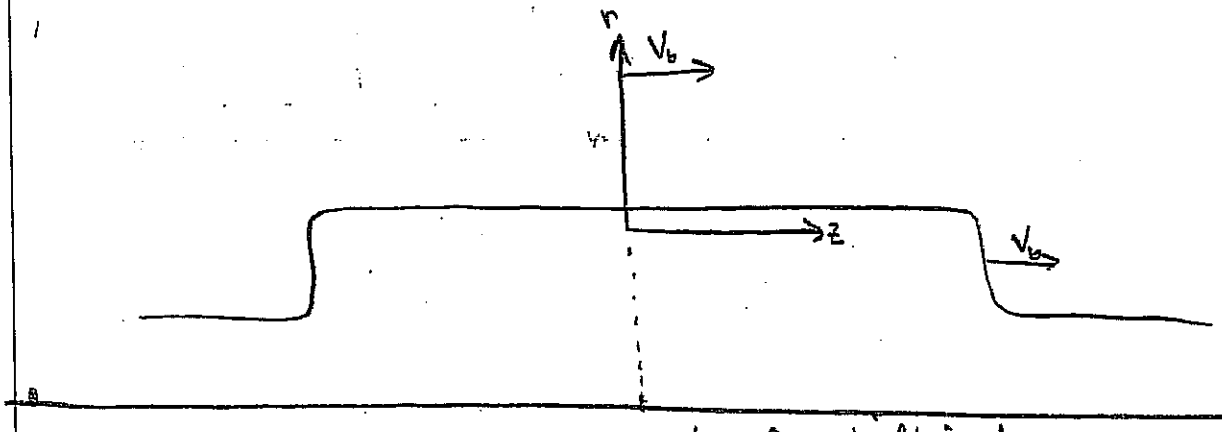

$s = \beta_b c t$ for drifting beam
= position of beam center in lab frame

$s \Longleftrightarrow t$ are related by $\beta_b c$ for drifting beam

z = longitudinal coordinate in beam frame ($z=0$ = beam center)

r = radial coordinate in beam frame (or lab frame).

(This class will assume non-relativistic dynamics)
These are ions with $\beta < 0.2$).

National® Brand 42-182 100 SHEETS Made in U.S.A.

LONGITUDINAL PHYSICS OF LONG PULSES (BUNCH LENGTH >> r_{pipe})

"g-factor" model

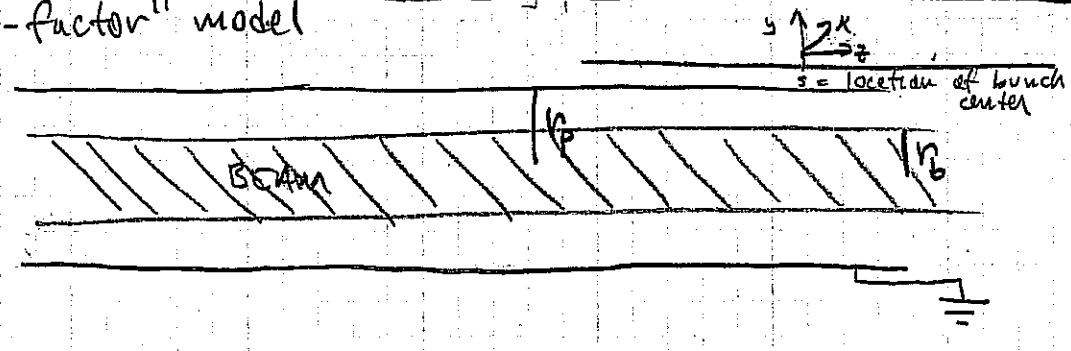

If $\dfrac{\partial^2\varphi}{\partial z^2} << \dfrac{1}{r}\left(\dfrac{\partial}{\partial r} r \dfrac{\partial\varphi}{\partial r}\right) \Rightarrow \dfrac{\partial\varphi}{\partial r} = \dfrac{-\lambda(r)}{2\pi\varepsilon_0 r}$

Let $\rho = \begin{cases} \rho_0 & 0 < r < r_b \\ 0 & r_b < r < r_p \end{cases} \Rightarrow \lambda = \lambda_0 \left(\dfrac{r}{r_b}\right)^2$

$$\varphi = \int \frac{\partial\varphi}{\partial r} dr = \begin{cases} \dfrac{\lambda}{2\pi\varepsilon_0}\left[\dfrac{1}{2}\left(1 - \dfrac{r^2}{r_b^2}\right) + \ln\dfrac{r_p}{r_b}\right] & 0 < r < r_b \\ \dfrac{\lambda}{2\pi\varepsilon_0}\ln\left(\dfrac{r_p}{r}\right) & r_b < r < r_p \end{cases}$$

$$\frac{\partial\phi}{\partial z} = \frac{1}{2\pi\varepsilon_0}\left[\frac{1}{2}\left(1 - \frac{r^2}{r_b^2}\right) + \ln\frac{r_p}{r_b}\right]\frac{d\lambda}{dz} - \frac{1}{2\pi\varepsilon_0}\left[1 - \frac{r^2}{r_b^2}\right]\frac{\lambda}{r_b}\frac{dr_b}{dz}$$

<u>If</u> $\rho = \text{const} \Rightarrow \dfrac{\lambda}{r_b^2} = \text{const} \qquad \dfrac{d\lambda}{dz} = \dfrac{-2\lambda}{r_b}\dfrac{dr_b}{dz}$

[Example of $\rho = \text{const}$.
Magnetic Quad focusing
$\dfrac{\lambda}{4\pi\varepsilon_0 V a} \simeq k_{\rho 0}^2 a$
$\Rightarrow \rho \sim V k_{\rho 0}^2 \simeq \text{const}$]

$$\Rightarrow \frac{\partial\phi}{\partial z} = \frac{1}{2\pi\varepsilon_0}\ln\left(\frac{r_p}{r_b}\right)\frac{\partial\lambda}{\partial z}$$

$$E_z = \frac{-g}{4\pi\varepsilon_0}\frac{\partial\lambda}{\partial z}$$

where $g = 2\ln\left(\dfrac{r_p}{r_b}\right)$

Vlasov - equation for a drifting beam:

$$\frac{\partial f}{\partial s} + x'\frac{\partial f}{\partial x} + x''\frac{\partial f}{\partial x'} + y'\frac{\partial f}{\partial y} + y''\frac{\partial f}{\partial y'} + z'\frac{\partial f}{\partial z} + z''\frac{\partial f}{\partial z'} = 0$$

Let $\tilde{f}(z,z',s) \equiv \iiiint f \, dx \, dx' \, dy \, dy'$

INTEGRATING VLASOV EQUATION: If $z'' \neq f(x,x',y,y')$:

$$\Rightarrow \frac{\partial \tilde{f}}{\partial s} + \iiint x' \underbrace{\int \frac{\partial f}{\partial x} dx}_{= f\Big|_{-\infty}^{\infty} \to 0} dx' \, dy \, dy' + \cdots \quad z'\frac{\partial \tilde{f}}{\partial z} + z''\frac{\partial \tilde{f}}{\partial z'} = 0$$

$$\Rightarrow \boxed{\frac{\partial \tilde{f}}{\partial s} + z'\frac{\partial \tilde{f}}{\partial z} + z''\frac{\partial \tilde{f}}{\partial z'} = 0}$$ 1 D Vlasov

Now let $\lambda \equiv q\int \tilde{f} \, dz'$; $\lambda \overline{z'} = \int \tilde{f} z' \, dz'$; $\lambda \overline{z'^2} \equiv \int \tilde{f} z'^2 \, dz'$

Also, let $\Delta z'^2 \equiv \overline{z'^2} - (\overline{z'})^2$

FLUID EQUATIONS

INTEGRATING 1 D VLASOV OVER z':

$$\boxed{\frac{\partial \lambda}{\partial s} + \frac{\partial}{\partial z}(\lambda \overline{z'}) = 0}$$ (CONTINUITY EQUATION)

MULTIPLYING BY z' & INTEGRATING VLASOV OVER z':

$$\frac{\partial}{\partial s}\lambda \overline{z'} + \frac{\partial}{\partial z}\lambda \overline{z'^2} - \lambda z'' = 0$$

DIVIDING BY λ, USING CONTINUITY EQUATION & DEFINITION OF $\Delta z'^2$:

$$\boxed{\underbrace{\frac{\partial \overline{z'}}{\partial s} + \overline{z'}\frac{\partial}{\partial z}\overline{z'}}_{\text{INERTIAL}} + \underbrace{\frac{1}{\lambda}\frac{\partial}{\partial z}(\lambda \Delta z'^2)}_{\text{PRESSURE TERM}} = \underbrace{z''}_{\text{FORCE}}}$$ (MOMENTUM EQUATION)

COMBINING g-factor model with fluid equations

$$\frac{\partial \lambda}{\partial s} + \frac{\partial}{\partial z}(\lambda \bar{z}') = 0$$

$$\frac{\partial \bar{z}'}{\partial s} + \bar{z}' \frac{\partial \bar{z}'}{\partial z} + \underbrace{\frac{1}{\lambda}\frac{\partial}{\partial z}(\lambda \Delta z'^2)}_{\text{PRESSURE TERM}} = \underbrace{\frac{-qq}{4\pi\epsilon_0 m V_0^2}\frac{\partial \lambda}{\partial z}}_{\text{SPACE CHARGE TERM}}$$

WHEN PRESSURE TERM << SPACE CHARGE TERM,

(& LET $c_s^2 \equiv \frac{qq\lambda_0}{4\pi\epsilon_0 m}$ = "(SPACE CHARGE WAVE SPEED)^2"

$$\Rightarrow \boxed{\begin{aligned} &\frac{\partial \lambda}{\partial s} + \lambda \frac{\partial \bar{z}'}{\partial z} + \bar{z}' \frac{\partial \lambda}{\partial z} = 0 \\ \& \quad &\frac{\partial \bar{z}'}{\partial s} + \bar{z}' \frac{\partial \bar{z}'}{\partial z} + \frac{c_s^2}{\lambda_0 V_0^2}\frac{\partial \lambda}{\partial z} = 0 \end{aligned}} \qquad (g1)$$

LINEARIZING g1

LET $\lambda = \lambda_0 + \lambda_1 \qquad \bar{z}' = \bar{z}_0' + \bar{z}_1'$

EQUILIBRIUM λ_0 = CONSTANT

$\bar{z}_0' = 0$

LINEARIZING

$$\frac{\partial \lambda_1}{\partial s} + \lambda_0 \frac{\partial \bar{z}_1'}{\partial z} = 0 \qquad (g2a)$$

$$\frac{\partial \bar{z}_1'}{\partial s} + \frac{c_s^2}{\lambda_0 V_0^2}\frac{\partial \lambda_1}{\partial z} = 0 \qquad (g2b)$$

TAKING $\frac{\partial}{\partial s}$ of (g2a) & $\frac{\partial}{\partial z}$ of g2b and combining:

$$\Rightarrow \boxed{\frac{\partial^2 \lambda_1}{\partial s^2} - \frac{c_s^2}{V_0^2}\frac{\partial^2 \lambda_1}{\partial z^2} = 0 \quad \Rightarrow \text{WAVE EQUATION}}$$

SOLVING WAVE EQUATION

$$\frac{\partial^2 \lambda_1}{\partial s^2} - \frac{c_s^2}{V_0^2}\frac{\partial^2 \lambda_1}{\partial z^2} = 0$$

Let $\lambda_1 = \tilde{\lambda}_1 \exp\left[\frac{i\omega}{V_0} s \pm ikz\right]$

$$-\frac{\omega^2}{V_0^2} + \frac{k^2 c_s^2}{V_0^2} = 0 \quad \Rightarrow \quad \omega = c_s k$$

$\Rightarrow$ PHASE & GROUP VELOCITY OF WAVES $= c_s$
(in beam frame)

GENERAL SOLUTION

$$\lambda_1 = \lambda_0 f_+[u_+] + \lambda_0 f_-[u_-]$$

where $u_+ = z + \frac{c_s s}{V_0} + C_0$ & $u_- = z - \frac{c_s s}{V_0} + C_0$

& $f_+[u]$ & $f_-[u]$ are any functions of the argument.
& C_0 is an arbitrary constant

$$\overline{z_1'} = \frac{c_s}{V_0}\left[-f_+[u_+] + f_-[u_-]\right]$$

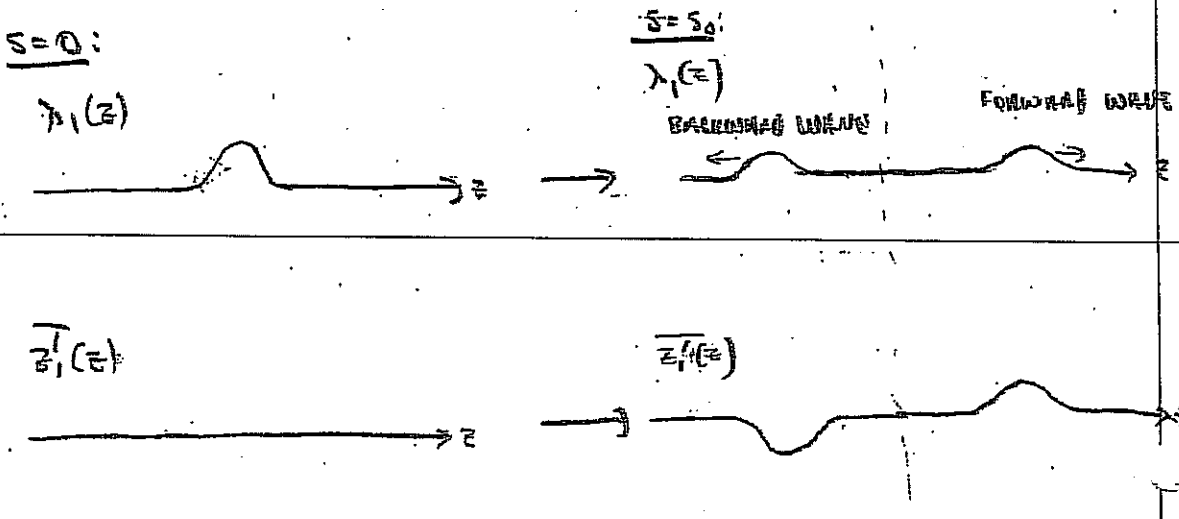

BEAM ENDS & RAREFACTION WAVES

(FALTENS & LEE, J. APP. PHYS. 61, 5219)
(ALSO LANDAU & LIFSHITZ, FLUID MECHANICS)

SUPPOSE YOU START WITH A PULSE THAT ENDS WITH A STEP FUNCTION IN λ. WHAT HAPPENS TO THE END?

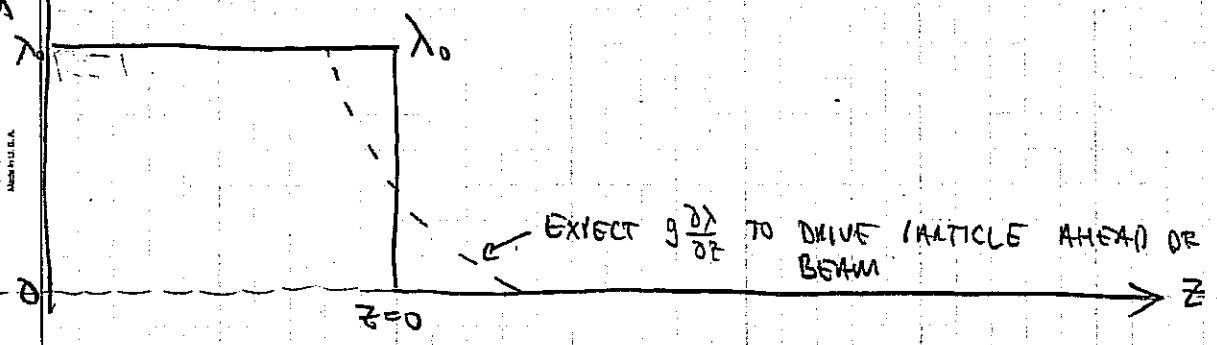

TO ANALYZE: RETURN TO <u>NON-LINEAR</u> FLUID EQUATIONS (SINCE $\delta\lambda \sim \lambda_0$) (g1):

$$\frac{\partial\lambda}{\partial s} + \lambda\frac{\partial\bar{z}'}{\partial z} + \bar{z}'\frac{\partial\lambda}{\partial z} = 0 \qquad \text{(CONTINUITY)}$$

$$\frac{\partial\bar{z}'}{\partial s} + \bar{z}'\frac{\partial\bar{z}'}{\partial z} + \frac{c_s^2}{\lambda_0 v_0^2}\frac{\partial\lambda}{\partial z} = 0 \qquad \text{(MOMENTUM)}$$

1ST IT IS CONVENIENT TO DEFINE:

$$\Lambda \equiv \lambda/\lambda_0$$

$$V \equiv \frac{v_0}{c_s}\bar{z}'$$

$$\zeta \equiv \frac{v_0}{c_s} z$$

$$\left(c_s^2 \equiv \frac{q}{m}\frac{g\lambda_0}{4\pi\varepsilon_0}\right)$$

$$\Rightarrow \quad \frac{\partial\Lambda}{\partial s} + \Lambda\frac{\partial V}{\partial\zeta} + V\frac{\partial\Lambda}{\partial\zeta} = 0 \qquad \text{(CONTINUITY)}$$

$$\frac{\partial V}{\partial s} + V\frac{\partial V}{\partial\zeta} + \frac{\partial\Lambda}{\partial\zeta} = 0 \qquad \text{(MOMENTUM)} \qquad \text{(r1)}$$

TRY A SIMILARITY SOLUTION: $\Lambda = \Lambda(x)$ & $V = V(x)$

WHERE $x = \frac{z}{s} = \left(\frac{V_0 z}{c_s s}\right)$

$$\frac{\partial x}{\partial s} = -\frac{x}{s} \qquad \frac{\partial x}{\partial z} = \frac{x}{z}$$

$$\frac{\partial \Lambda}{\partial s} = -\frac{d\Lambda}{dx}\frac{x}{s} \qquad \frac{\partial \Lambda}{\partial z} = \frac{d\Lambda}{dx}\frac{x}{z} \qquad \frac{\partial V}{\partial s} = -\frac{dV}{dx}\frac{x}{s} \qquad \frac{\partial V}{\partial z} = \frac{dV}{dx}\frac{x}{z}$$

$$\left[-\frac{d\Lambda}{dx}\frac{x}{s} + \Lambda\frac{dV}{dx}\frac{x}{z} + V\frac{d\Lambda}{dx}\frac{x}{z}\right] = 0 \qquad \text{(CONTINUITY)}$$

$$\left[-\frac{dV}{dx}\frac{x}{s} + V\frac{dV}{dx}\frac{x}{z} + \frac{d\Lambda}{dx}\frac{x}{z}\right] = 0 \qquad \text{(momentum)}$$

MULTIPLY BY z/s & gather terms):

$$\Rightarrow \begin{bmatrix} V - x & \Lambda \\ 1 & V - x \end{bmatrix} \begin{bmatrix} d\Lambda/dx \\ dV/dx \end{bmatrix} = 0$$

FOR NON-TRIVIAL SOLUTION DETERMINANT MUST VANISH:

$$\boxed{\Lambda = [V - x]^2}$$

$$\Rightarrow \frac{d\Lambda}{dx} = 2[V - x]\left[\frac{dV}{dx} - 1\right] \quad \& \quad \frac{d\Lambda}{dx} = -[V - x]\frac{dV}{dx}$$

$$\Rightarrow -\frac{dV}{dx} = 2\frac{dV}{dx} - 2 \quad \Rightarrow \quad \frac{dV}{dx} = \frac{2}{3}$$

$$\Rightarrow \boxed{\begin{aligned} V &= \frac{2}{3}x + C \\ \Lambda &= \left[-\frac{1}{3}x + C\right]^2 \end{aligned}}$$

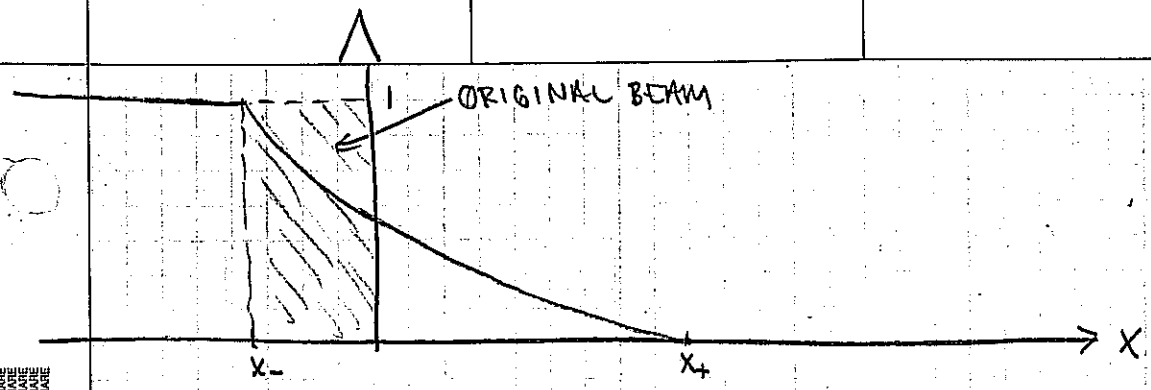

At x_+: $\Lambda = 0 \Rightarrow C = \frac{1}{3}X$ $\qquad x_+ = 3C$

At x_-: $\Lambda = 1 \Rightarrow C = \frac{1}{3}X + 1 \Rightarrow x_- = 3C - 3$

MASS CONSERVATION $\Rightarrow 1(-x_-) = -(3C-3) = \int_{3C-3}^{3C} \left[C - \frac{1}{3}x\right]^2 dx = -3\frac{\left[C - \frac{1}{3}x\right]^3}{3}\Big|_{3C-3}^{3C}$

$-(3C-3) = 1$

$\boxed{C = \frac{2}{3}} \Rightarrow x_- = -1$, $x_+ = 2$

$\Rightarrow$

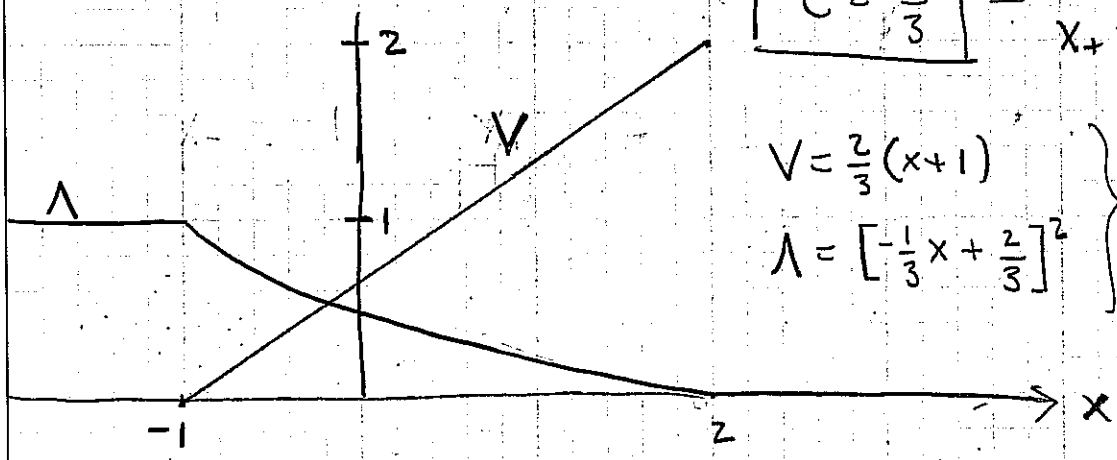

$$\left.\begin{aligned} V &= \frac{2}{3}(x+1) \\ \Lambda &= \left[-\frac{1}{3}x + \frac{2}{3}\right]^2 \end{aligned}\right\} \text{ for } -1 < x < 2$$

RECALL $x = \frac{V_0 z}{C_s S}$ SO $x = 2 \Rightarrow z = 2C_s\left(\frac{S}{V_0}\right)$

$x = -1 \Rightarrow z = -C_s\left(\frac{S}{V_0}\right)$

SO BEAM END EXPANDS AT TWICE SPACE-CHARGE WAVE SPEED & RAREFACTION WAVE PROPAGATES INWARD AT THE SPACE-CHARGE WAVE SPEED.

SNAPSHOTS OF λ/λ_0 VS z AT VARIOUS s

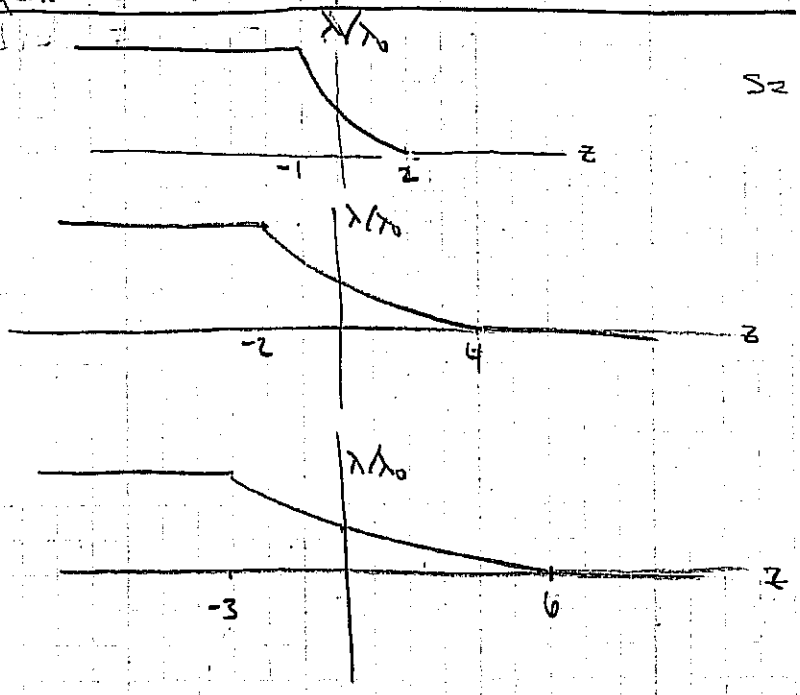

$s = v_0/c_s$

$s = 2v_0/c_s$

$s = 3v_0/c_s$

HOW DOES ONE PREVENT "END EROSION"?

APPLY EAR PULSES AT END OF BEAM:

$$V \sim E_z = \frac{+/-}{4\pi\epsilon_0}\frac{\partial\lambda}{\partial z}$$

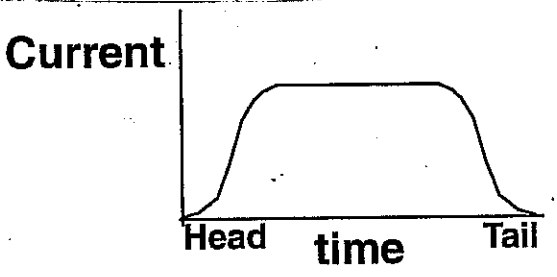

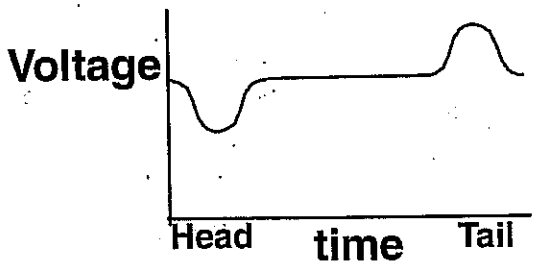

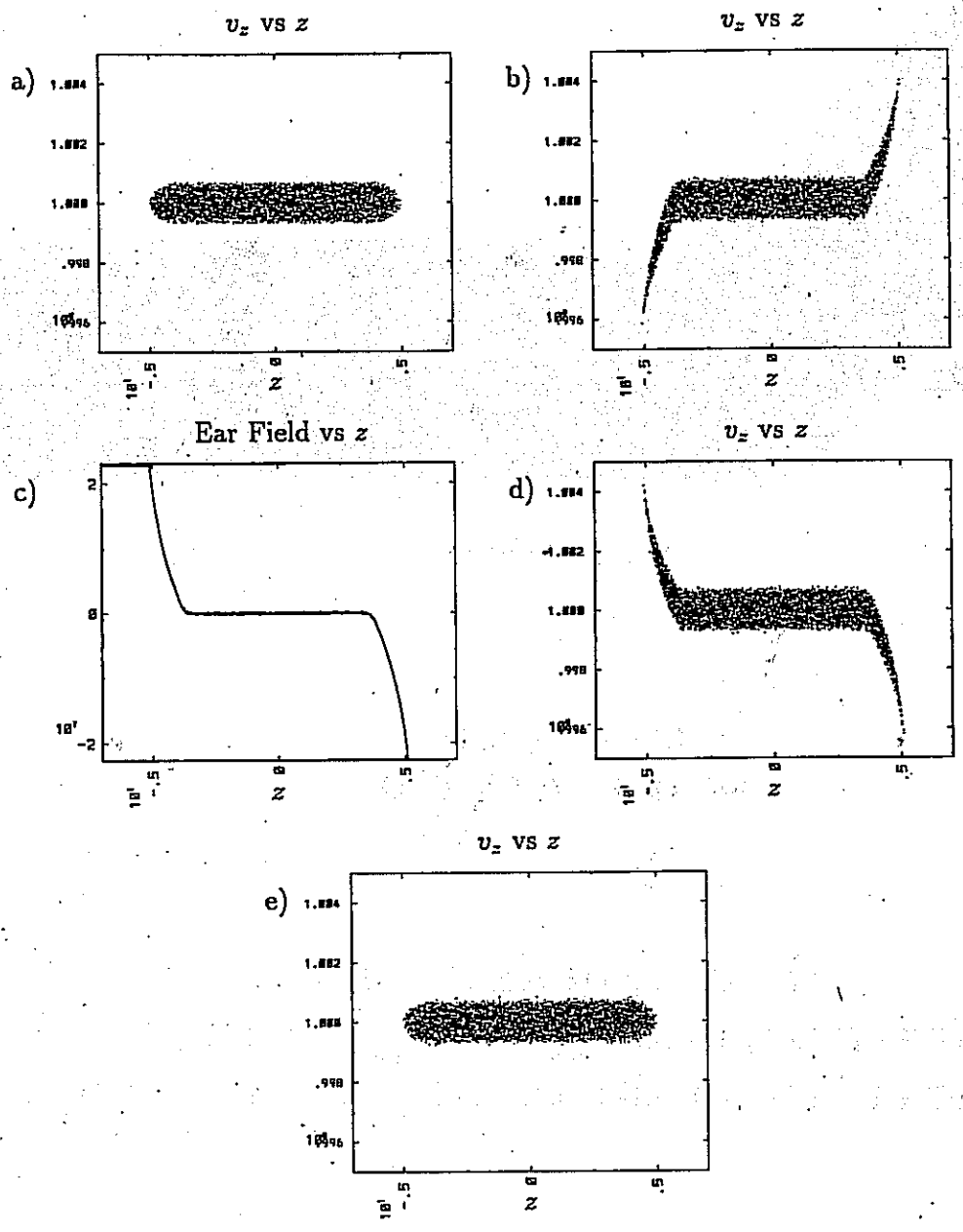

Figure 6.4: One cycle of intermittently-applied ears. (a) Initial phase space (b) Beam expands (c) Ear Field is applied (d) Beam is compressed (e) Beam expands back to its initial state

from D. Callahan Miller
PhD thesis, U.C. Davis, 1994.

John Barnard
Steven Lund
USPAS
June 2006

Injectors and longitudinal physics -- III

1. Longitudinal cooling from acceleration
2. Longitudinal instability
3. Bunch compression
4. Neuffer distribution

LONGITUDINAL COOLING

1. DURING INJECTION BEAM UNDERGOES LARGE LONGITUDINAL EXPANSION
2. $T_{\perp 0} = T_{\parallel 0}$ AT SOURCE, BUT $T_\perp \neq T_\parallel$ AFTER ACCELERATION
3. IMPLICATIONS FOR BEAM STABILITY AND EMITTANCE EVOLUTION

CONSIDER 1D DIODE:

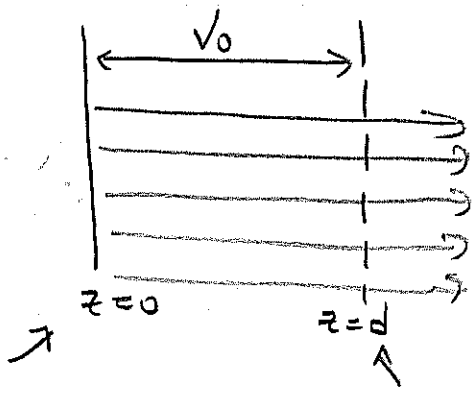

AT SOURCE

$$E_0 = \frac{p_{z0}^2}{2m}$$

$$\Delta E_{\parallel 0} \equiv \frac{\langle p_{z0}^2 \rangle}{2m} = \frac{1}{2} kT_{\parallel 0}$$

AT END OF DIODE

$$E_f = qV_0 + \frac{p_{z0}^2}{2m} = \frac{p_{zf}^2}{2m}$$

$$\Delta E_{\parallel f} = \Delta E_{\parallel 0} \neq \frac{1}{2} kT_f$$

SINCE $E_\parallel = \frac{p_z^2}{2m} \Rightarrow \Delta E_\parallel = \frac{2 p_z \Delta p_z}{2m}$

$$\frac{\Delta E}{E} = \frac{2 \Delta p_z}{p_z}$$

$$\frac{1}{2} kT_f \cong \frac{\Delta p_{zf}^2}{2m} = \left(\frac{p_{zf} \Delta E_f}{2E_f}\right)^2 \frac{1}{2m} = \frac{\Delta E_f^2}{4E_f} = \frac{kT_0}{2}\left[\frac{1}{2}\frac{kT_0}{qV_0}\right]$$

$$\Rightarrow \boxed{kT_f = \frac{1}{2} kT_0 \left[\frac{kT_0}{qV_0}\right]}$$

$$kT_f = \frac{1}{2} kT_0 \underbrace{\left[\frac{kT_0}{qV_0}\right]}_{\ll 1}$$

EXAMPLE $1000°C \Leftrightarrow 0.1\ eV$

FOR $V_0 = 1\ MeV$

$kT_0 = 0.1\ eV$

$kT_f = 5 \times 10^{-9}\ eV$

$\boxed{\text{HOW CAN } kT_f \ll kT_0 \text{ BUT } \Delta E_f = \Delta E_0 ?}$

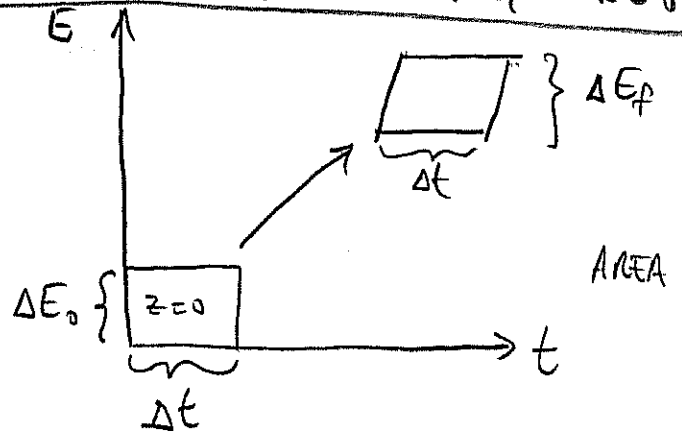

AREA IS CONSERVED

(PULSE DURATION STAYS THE SAME.)

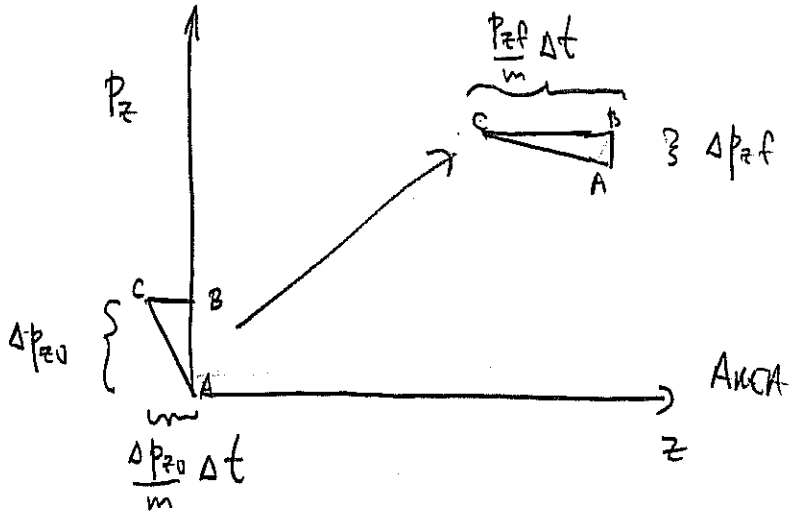

(BUNCH LENGTH GROWS)

AREA IS CONSERVED

$$\frac{1}{2}\frac{\Delta p_{z0}^2}{m}\Delta t = \frac{1}{2}\Delta p_{zf}\left(\frac{p_{zf}}{m}\right)\Delta t$$

$$\Rightarrow \Delta p_{zf} = \frac{\Delta p_{z0}^2}{p_{zf}}$$

$$\Rightarrow kT_f = \frac{1}{2} kT_0 \left(\frac{kT_0}{qV_0}\right)$$

CHANGE IN NOTATION

NOTE: $\overline{z'} \equiv \left\langle \frac{dz}{ds} \right\rangle$; $s \equiv v_0 t$

Let $u = \left\langle \frac{dz}{dt} \right\rangle$; then $u = v_0 \overline{z'}$

= fluid velocity in comoving frame

So

$$\frac{\partial \lambda}{\partial s} + \frac{\partial}{\partial z}(\lambda \overline{z'}) = 0 \quad \Rightarrow \quad \boxed{\frac{\partial \lambda}{\partial t} + \frac{\partial}{\partial z}(\lambda u)}$$

& $$\frac{\partial \overline{z'}}{\partial s} + \overline{z'}\frac{\partial}{\partial z}\overline{z'} + \frac{1}{\lambda}\frac{\partial}{\partial z}(\lambda \Delta z'^2) = \overline{z''}$$

$$\Rightarrow \frac{\partial u}{\partial t} + u\frac{\partial u}{\partial z} + \frac{1}{\lambda}\frac{\partial}{\partial z}\left(\lambda\left[\langle v_z^2\rangle - u^2\right]\right) = \overline{\ddot{z}}$$

Since $p_z = m\int_{-\infty}^{\infty} n\left[v_z^2 - u^2\right] dv_z$ where $n = \frac{\lambda}{\pi r_b^2}$

$$\Rightarrow \boxed{\frac{\partial u}{\partial t} + u\frac{\partial u}{\partial z} + \frac{\pi r_b^2}{m\lambda}\frac{\partial}{\partial z}p_z = \overline{\ddot{z}}}$$

where $\ddot{z} = \frac{d^2 z}{dt^2} = \frac{F_z}{m}$

"LONGITUDINAL" or "RESISTIVE WALL" INSTABILITY

Let us return to the 1-D FLUID EQUATIONS

SEE REISER 6.3.2.
CALLAHAN-MILLER, Ph.D. DISSERTATION, U.C. DAVIS, 1994

$$\frac{\partial \lambda}{\partial t} + \frac{\partial}{\partial z}\lambda u = 0$$

$$\frac{\partial u}{\partial t} + u\frac{\partial u}{\partial z} + \frac{1}{\rho}\frac{\partial p_z}{\partial z} = \frac{-q\,q}{4\pi\epsilon_0 m v_0^2}\frac{\partial \lambda}{\partial z} + \frac{qE_z}{m}$$

IGNORE AGAIN

EXTERNALLY GENERATED

AS BEAM PASSES CONDUCTING SURFACE IMAGE CHARGE AND CURRENT INTERACTS WITH BEAM. HIGHLY GEOMETRY DEPENDENT.

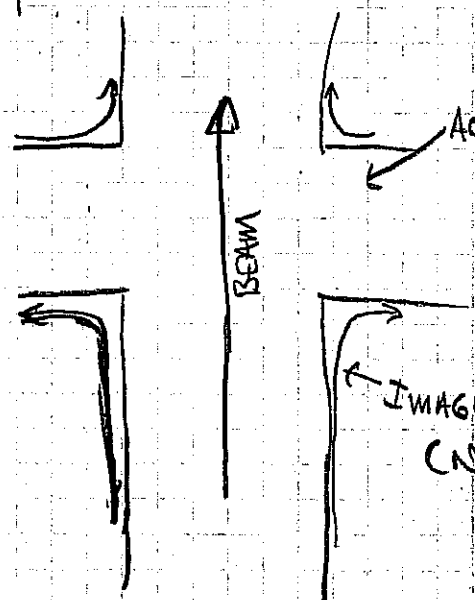

ACCELERATION GAP, PUMPING HOLE, ETC.

IMAGE CHARGES (OF OPPOSITE SIGN) (NEGATIVE CURRENT)

CAN BE CALCULATED APPROXIMATELY USING CIRCUIT MODEL.

RESISTIVITY IN WALL, AND COMPLICATED ELECTRON FLOW PATTERNS CREATE A RETARDING ELECTRIC FIELD ON BEAM.

MODEL OF IMPEDANCE (IN LONG WAVELENGTH REGIME)

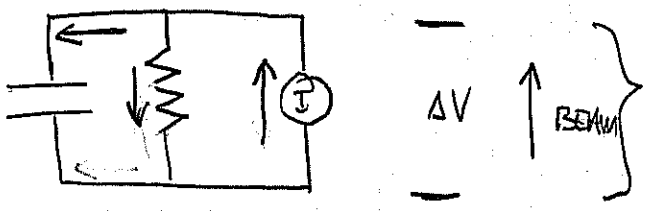

ONE MODULE OF MANY, EACH SEPARATED BY DISTANCE L

$$I = C\frac{d\Delta V}{dt} + \frac{\Delta V}{R} \qquad I = [CL]\frac{d\Delta V/L}{dt} + \frac{\Delta V/L}{R/L}$$

$$E = -\frac{\Delta V}{L} \qquad C^{+} = CL \qquad R^{*} = \frac{R}{L}$$

LET $I = I_0 + I_1 e^{-i\omega t}$ $\qquad E = E_0 + E_1 e^{-i\omega t}$

$$I_1 = i\omega C^{+} E_1 - \frac{E_1}{R^{*}}$$

$$\Rightarrow E_1 = \frac{-R^{*}}{1 - i\omega C^{+} R^{*}} I_1 \qquad Z^{*} \equiv -\frac{E_1}{I_1} = \frac{R^{*}}{1 - i\omega C^{+} R^{*}}$$

RETURNING TO THE 1D FLUID EQUATIONS

$$\frac{\partial \lambda}{\partial t} + \frac{\partial}{\partial z}\lambda v = 0 \qquad \frac{\partial u}{\partial t} + u\frac{\partial u}{\partial z} = \frac{-q g}{4\pi\epsilon_0 m}\frac{\partial \lambda}{\partial z} + \frac{q E_z}{m}$$

Let $\lambda = \lambda_0 + \lambda_1 \exp[i(kz - \omega t)]$

$u = v_0 + u_1 \exp[i(kz - \omega t)]$

$$-i\omega\lambda_1 + ik\lambda_0 u_1 + ikv_0\lambda_1 = 0$$

$$-i\omega u_1 + ikv_0 u_1 + \underbrace{\frac{ikqq\lambda_1}{4\pi\epsilon_0 m i}}_{=\frac{ikc_s^2}{\lambda_0}\lambda_1} + \frac{q}{m}Z^*\underbrace{(\lambda_0 v_1 + v_0\lambda_1)}_{=I_1} = 0$$

$$\begin{bmatrix} \omega - kv_0 & -k\lambda_0 \\ -\frac{c_s^2 k}{\lambda_0} + \frac{iq}{m}Z^* v_0 & \omega - kv_0 + \frac{iq}{m}Z^*\lambda_0 \end{bmatrix} \begin{bmatrix} \lambda_1 \\ u_1 \end{bmatrix} = 0$$

THE DETERMINANT OF THE ABOVE MATRIX MUST VANISH:

$$(\omega - kv_0)^2 + \frac{iq}{m}Z^*\lambda_0(\omega - kv_0) - c_s^2k^2 + \frac{iq}{m}Z^*\lambda_0 v_0 k = 0$$

$$\boxed{(\omega - kv_0)^2 - c_s^2k^2 + \frac{iqZ^*\lambda_0\omega}{m} = 0}$$ (LAB FRAME)

Using a Galileam transformation, in the beam frame:

$\omega' = \omega - kv_0$ ' denotes beam frame

$k' = k$

$$\boxed{\omega'^2 - c_s^2k'^2 + \frac{iqZ^*(\omega')}{m}\lambda_0(\omega' + k'v_0) = 0}$$ (BEAM FRAME)

NOTE $Z^*(\omega') = Z^*(\omega = \omega' + k'v_0)$

National® Brand 42-182 100 SHEETS Made in U.S.A.

CASE I PURE RESISTIVE IMPEDANCE $Z^* = R^*$ (REAL)

$$\omega'^2 = \pm c_s k' \sqrt{1 - iR^* \frac{q\lambda_0}{m} \frac{(\omega' + k'V_0)}{c_s^2 k'^2}}$$

Using $c_s^2 = \frac{gq\lambda_0}{4\pi\epsilon_0 m}$ & $\frac{\omega'}{k'} \sim c_s << V_0$

$$\omega' = \pm c_s k' \sqrt{1 - iR^* \left(\frac{4\pi\epsilon_0}{g}\right) \frac{V_0}{k'}}$$

$$\simeq \pm \left[c_s k' - i \frac{c_s V_0}{2} \left(\frac{4\pi\epsilon_0}{g}\right) R^* \right]$$

Since $\lambda_1, E_1 \sim \exp\left[i(k'z' - \omega' t')\right]$

Choosing "+" (Re $\omega > 0$) $\Rightarrow$ $z' = c_s t$ line of const phase $\Rightarrow$ Forward propagation

(Im $\omega' < 0$) $\Rightarrow$ $\lambda_1 \sim \exp\left[-\frac{c_s V_0}{2}\left(\frac{4\pi\epsilon_0}{g}\right) R^* t\right] \Rightarrow$ DECAYING PERTURBATION

CHOOSING "−"

(Re $\omega' < 0$) $\Rightarrow$ $z' = -c_s t'$ is line of constant phase

$\Rightarrow$ BACKWARD PROPAGATING

$$\Rightarrow \lambda_1 \sim \exp\left[\underbrace{+\frac{c_s V_0}{2}\left(\frac{4\pi\epsilon_0}{g}\right) R^* t}_{G}\right]$$

INSTABILITY!

$$\lambda_1 \simeq \lambda_{10} \exp[G]$$

$$G = \left[\frac{c_s V_0}{2}\left(\frac{4\pi\varepsilon_0}{g}\right) R^* t\right] = \text{LOGARITHMIC GAIN OF INSTABILITY} = \ln\left(\frac{\lambda_{1\,final}}{\lambda_{1\,initial}}\right)$$

$$\text{Now } t_{max} = \begin{cases} \min \begin{cases} l_b / c_s & \text{TRANSIT TIME FOR PERTURBATION TO TRAVEL FROM HEAD TO TAIL} \\ t_{residence} & \text{RESIDENCE TIME WITHIN ACCELERATOR} \end{cases} \end{cases}$$

If upper condition holds

$$G \sim \frac{V_0^2}{2}\left(\frac{4\pi\varepsilon_0}{g}\right) R^* \Delta t$$

If lower condition holds

$$G \sim \sqrt{\lambda}$$

National Brand 42-182. 100 SHEETS Made in U.S.A.

$$I \sim \frac{6\ \text{MJ}}{4\ \text{GeV}\ 200\ \text{ns}} \sim \frac{QV}{V\Delta t}$$

$$\sim 7.5\ \text{kA}$$

EXAMPLE:

FOR MATCHED BEAM IMPEDANCE

$$R^* = \frac{dV/ds}{I} \sim \frac{10^6\ \text{V/m}}{10\ \text{kA}} \sim 100\ \Omega/\text{m}$$

$$V_0 \sim 0.2c$$

$$\Delta t \sim 200\ \text{ns}$$

$$G \sim \frac{V_0^2}{2}\left(\frac{4\pi\varepsilon_0}{g}\right) R^* \Delta t$$

$$\sim 3.6$$

(AN EARLY CONCERN FOR HEAVY ION FUSION).

National® Brand 42-182 100 SHEETS Made in U.S.A.

$R^* = 100\,\Omega/m$

(11)

FOR ALL SIMULATIONS (p 14-15)

$V_b = c/3$

$I = 3\,kA$

$l_b = 10\,m$

$\frac{r_b}{r_p} = 0.4$

$kT_\perp = kT_\parallel = 10\,keV$

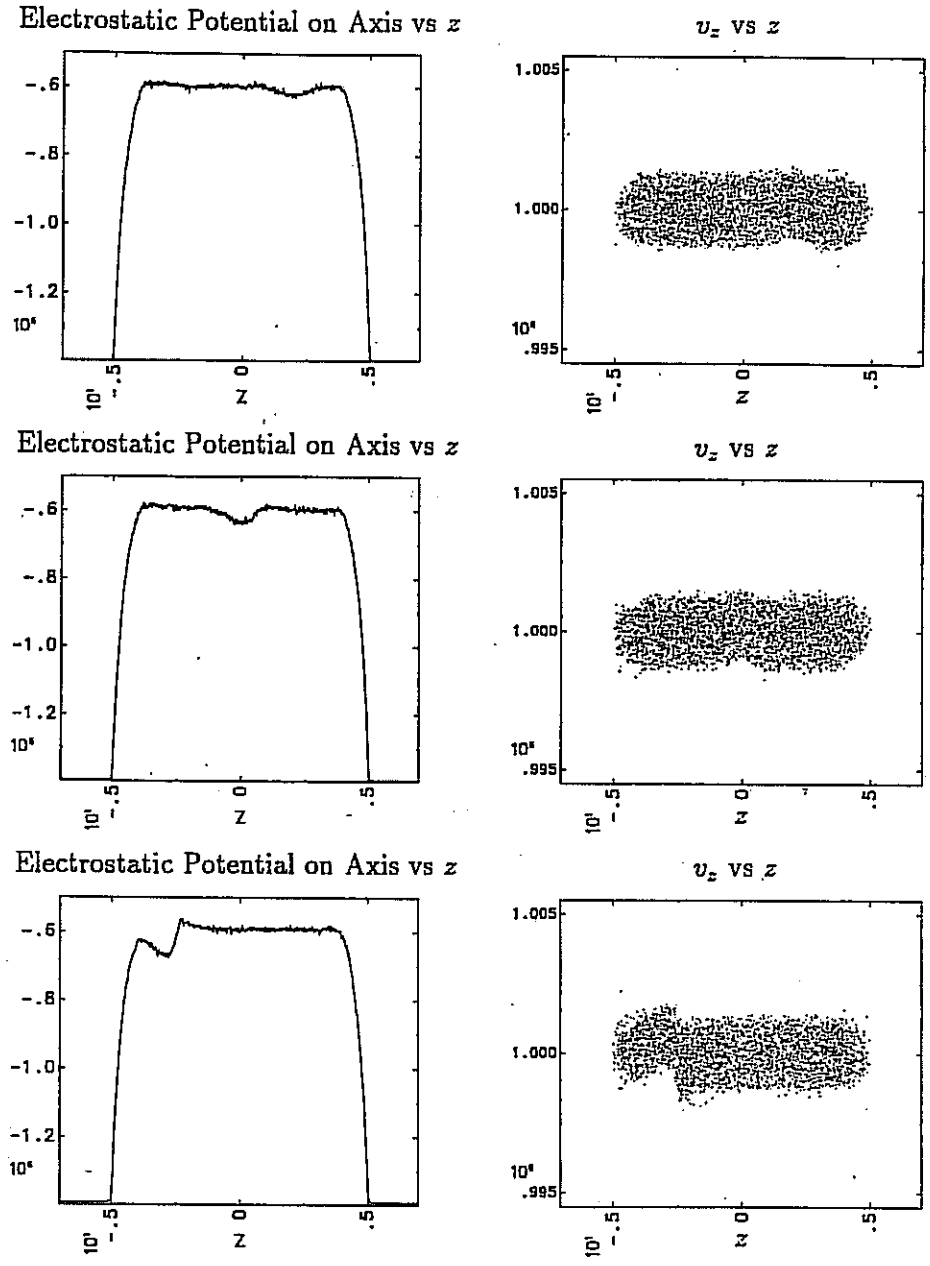

Figure 4.2: A simulation with 100 Ω/m resistance shows moderate growth. (a) 6.6 μs, (b) 10.9 μs, (c) 17.5 μs

from D.A. Callahan Miller, Ph.D. Thesis
U.C. Davis, 1994

$R^* = 100\ \Omega/m$

(21)

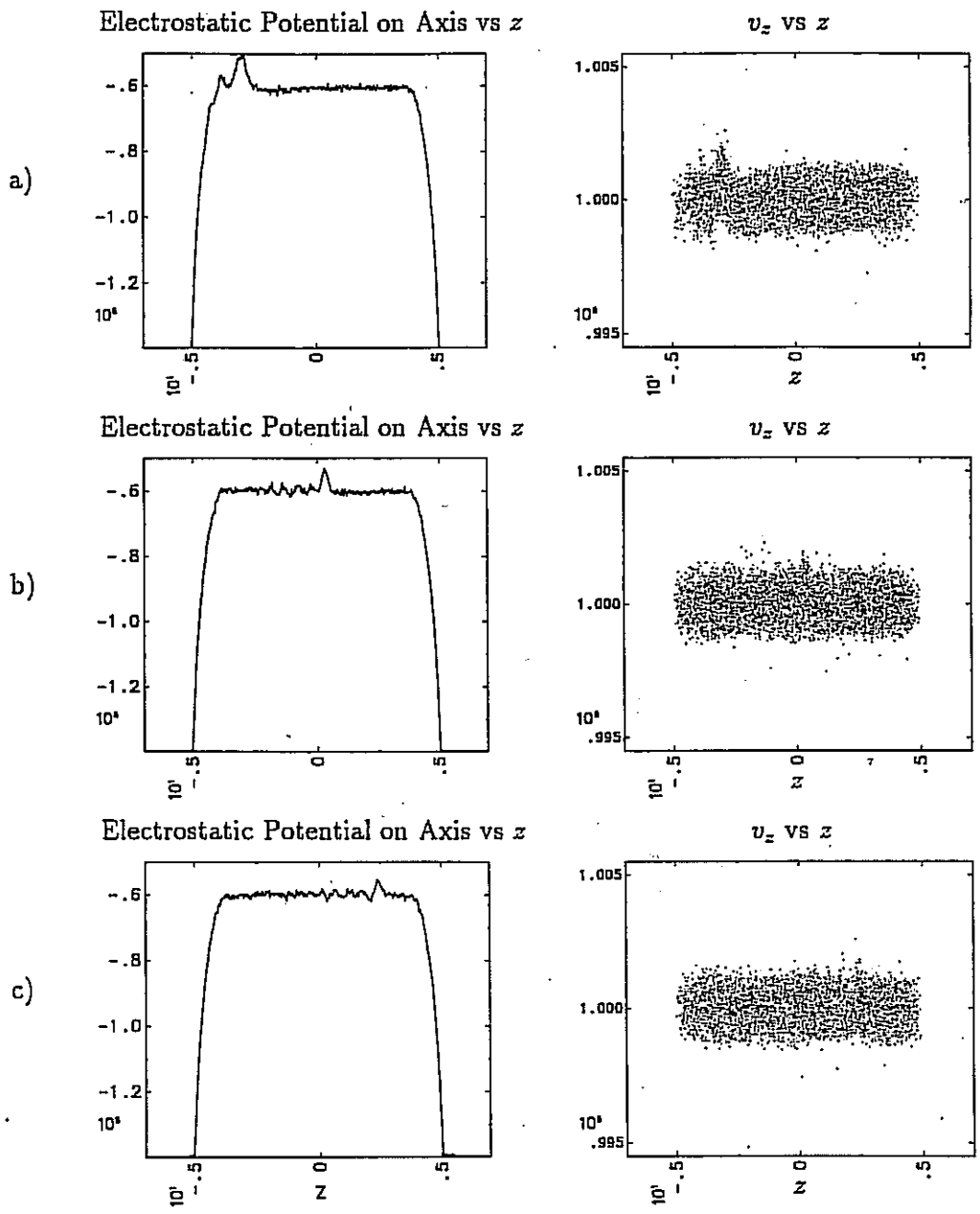

Figure 4.3: The perturbation reflects off the beam end and decays as it travels forward. (a) 28.4 μs, (b) 35.0 μs, (c) 39.4 μs

from D.A. Callahan Miller, Ph.D. Thesis
U.C. Davis, 1994
(FORWARD WAVE)

$R^* = 200\,\Omega/m$

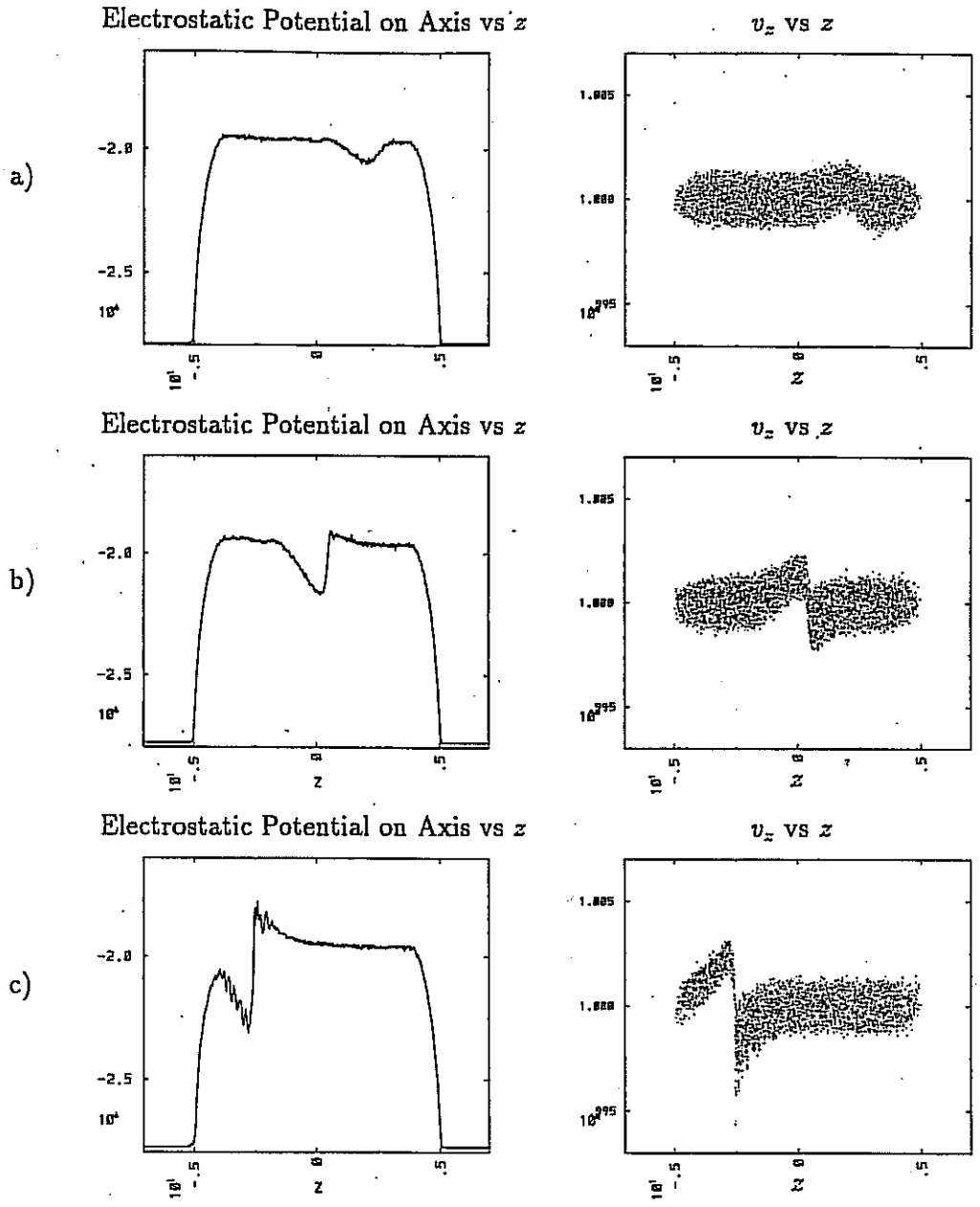

Figure 4.1: A simulation with 200 Ω/m resistance shows large amounts of growth. (a) 6.6 μs, (b) 10.9 μs, (c) 17.5 μs

from D.A. Callahan Miller, Ph.D. Thesis
U.C. Davis, 1994

CASE II RESISTIVE + CAPACITIVE IMPEDANCE

$$Z^* = \frac{R^*}{1 - i\omega C^+ R^*} = \frac{R^* + i\omega C^+ R^{*2}}{1 + \omega^2 C^{+2} R^{*2}}$$

GOING BACK TO PAGE 7:

IN LAB FRAME:

$$(\omega - kv_0)^2 - c_s^2 k^2 + \frac{iq R^* \lambda_0 \omega}{m(1 + \omega^2 C^{+2} R^{*2})} - \frac{q\omega^2 C^+ R^{*2} \lambda_0}{m(1 + \omega^2 C^{+2} R^{*2})} = 0$$

$$(\omega - kv_0)^2 - c_s^2 k^2 - \frac{4\pi\varepsilon_0}{q} \frac{\omega^2 C R^{*2} c_s^2}{(1 + \omega^2 C^2 R^{*2})} + \frac{i 4\pi\varepsilon_0 c_s^2 R_x^* \omega}{q(1 + \omega^2 C^2 R^{*2})}$$

IN BEAM FRAME:

$$\omega'^2 - c_s^2 k^2 - \frac{4\pi\varepsilon_0}{q} \frac{(\omega' + k'v_0)^2 C R^{*2} c_s^2}{(1 + (\omega' + k'v_0)^2 C^2 R^2)} + \frac{i 4\pi\varepsilon_0 c_s^2 R_x^2 (\omega' + k'v_0)}{q(1 + \omega^2 C^2 R^{*2})}$$

So if one takes limit $C \to \infty$ the final two terms tend to zero. Thus Capacitance has reduced the instability growth rate.

$R^*C^* = 2 \times 10^{-8}$ s
$R^* = 100\Omega/m$

(15)

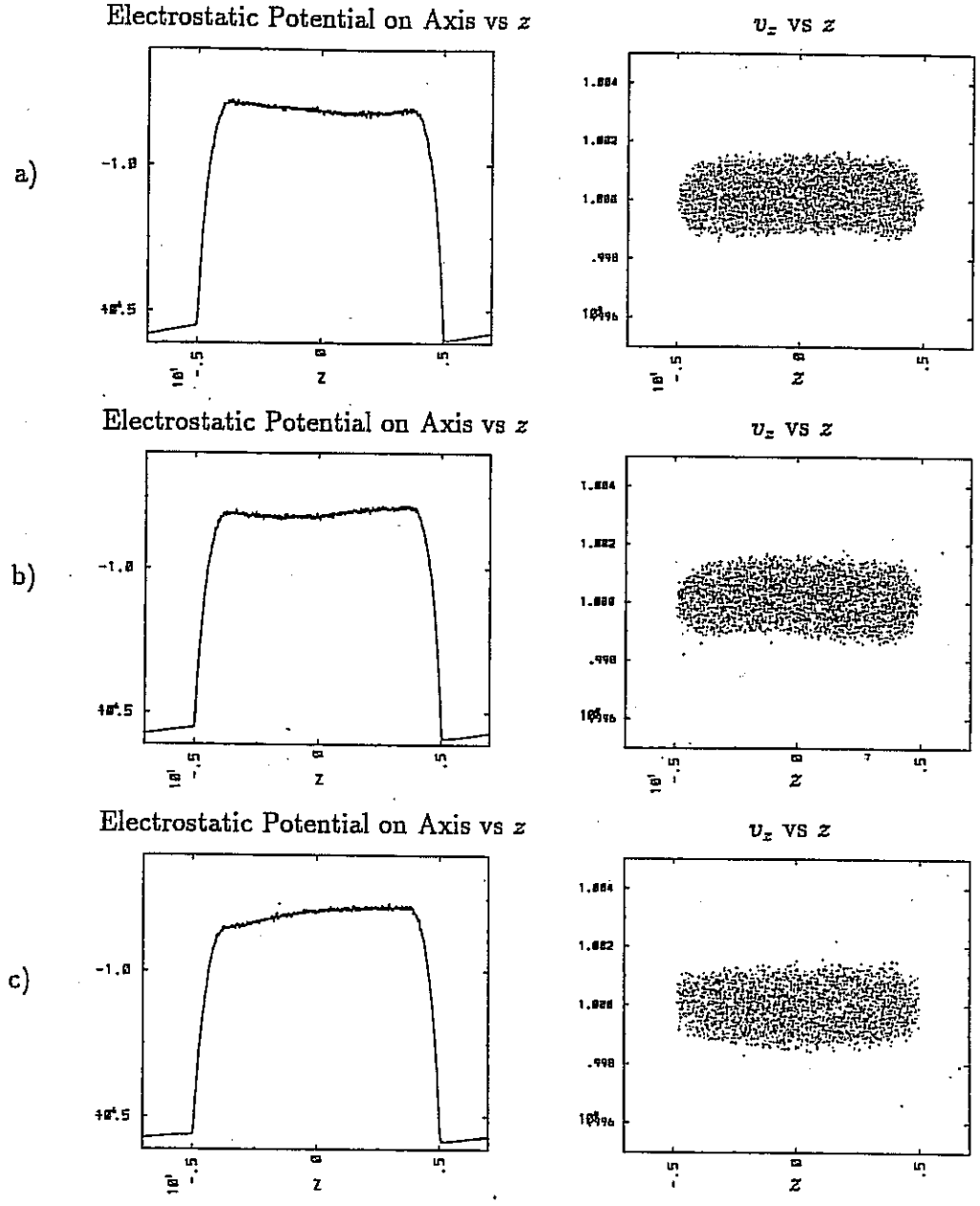

Figure 4.6: When capacitance is added to the system, a larger perturbation is launched, but little growth occurs (a) 6.6 μs, (b) 10.9 μs, (c) 17.5 μs

from D.A. Callahan Miller, Ph.D. Thesis, U.C. Davis, 1994

SUMMARY OF LONGITUDINAL INSTABILITY

"RESISTIVE WALL" OR "LONGITUDINAL" INSTABILITY HAS POTENTIAL TO DEGRADE LONGITUDINAL EMITTANCE IN HIGH CURRENT ACCELERATORS.

HOWEVER, CAPACITANCE (e.g. FROM ACCELERATING GAPS) DECREASES GROWTH CAN MITIGATE INSTABILITY.

NOT DISCUSSED:

1. LONGITUDINAL TEMPERATURE DRIVES INSTABILITY (c.f. REISER 6.3.3)

2. FEEDBACK HAS BEEN PROPOSED TO CONTROL INSTABILITY IF NEEDED

National® Brand 42-182 100 SHEETS Made in U.S.A.

DRIFT COMPRESSION

OBJECTS:

APPLY A HEAD-TO-TAIL VELOCITY TILT TO INCREASE CURRENT BY DECREASING PULSE DURATION

DURING COMPRESSION "EARS" ARE NOT REQUIRED

AT END OF DRIFT COMPRESSION, VELOCITY "TILT" SHOULD BE MINIMIZED, SO THAT CHROMATIC ABERRATIONS IN FINAL FOCUS ARE MINIMIZED.

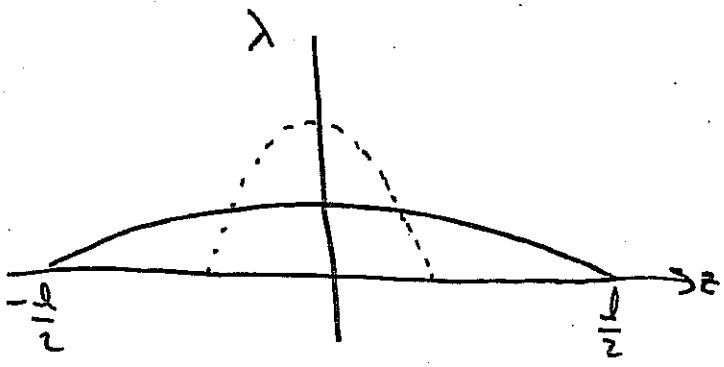

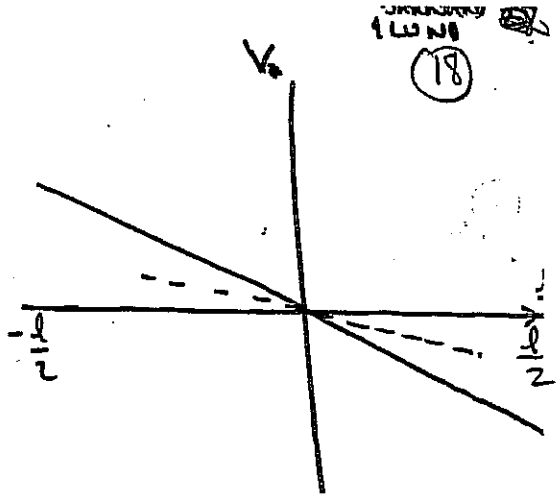

$$\frac{\partial \lambda}{\partial t} + \frac{\partial}{\partial z}\lambda V = 0$$ CONTINUITY EQUATION

$$\frac{\partial v}{\partial t} + v\frac{\partial v}{\partial z} = \frac{-qg}{m\,4\pi\epsilon_0}\frac{\partial \lambda}{\partial z}$$ MOMENTUM EQUATION

LET $\lambda = \lambda_0(t)\left(1 - \frac{4z^2}{l^2(t)}\right)$ ← PARABOLIC LINE CHARGE PROFILE

$V = -\Delta V(t)\,\frac{z}{l(t)}$ ← LINEAR VELOCITY PROFILE

① MASS conservation:

$$Q_c = \int_{-l/2}^{l/2} \lambda\, dz = \lambda_0 \int_{-\frac{l}{2}}^{l/2}\left(1 - \frac{4z^2}{l^2}\right) dz = \frac{2}{3}\lambda_0 l = \text{constant}$$

(but $\lambda_0 = \lambda_0(t)$ & $l = l(t)$)

CALCULATING PARTIAL DERIVATIVES:

$$\frac{\partial \lambda}{\partial t} = \dot{\lambda}_0\left(1-\frac{4z^2}{\ell^2}\right) + 2\lambda_0\left(\frac{4z^2}{\ell^3}\right)\dot{\ell}$$

$$\frac{\partial \lambda}{\partial z} = \frac{-8z}{\ell^2}\lambda_0$$

$$\frac{\partial V}{\partial t} = -\Delta\dot{V}\left(\frac{z}{\ell}\right) + \frac{\Delta V z}{\ell^2}\dot{\ell}$$

$$\frac{\partial V}{\partial z} = -\frac{\Delta V}{\ell}$$

FROM DEFINITION OF ΔV & ℓ:

$$\Delta V = -\dot{\ell}$$

(2) CONTINUITY EQUATION $\Rightarrow \left(1-\frac{4z^2}{\ell^2}\right)\left(\dot{\lambda}_0 - \frac{\Delta V \lambda_0}{\ell}\right) = 0$

(3) MOMENTUM EQUATION $\Rightarrow \left(\frac{z}{\ell}\right)\left[-\Delta\dot{V} + \frac{\dot{\ell}\Delta V}{\ell} + \frac{\Delta V^2}{\ell} + \frac{8qq}{m4\pi\epsilon_0}\frac{\lambda_0}{\ell}\right] = 0$

(1) & (2) $\Rightarrow \frac{\dot{\lambda}_0}{\lambda_0} = \frac{\Delta V}{\ell} = \frac{-\dot{\ell}}{\ell}$ (4)

(3) & (4) $\Rightarrow$

$$\boxed{\ddot{\ell} - \frac{12qq}{4\pi\epsilon_0 m}\frac{Q_c}{\ell^2} = 0}$$

where $Q_c = \frac{2}{3}\lambda_0 \ell = \text{const.}$

$\equiv$ CHARGE IN BUNCH (NOT PERVEANCE)

LONGITUDINAL "ENVELOPE" EQUATION (WITHOUT EMITTANCE)

MULTIPLY BY $\dot{l}$ & INTEGRATE:

$$\frac{\dot{l}^2}{2} + \frac{12qg}{4\pi\epsilon_0 m}\frac{Q_c}{l} = \cancel{\frac{\dot{l}_f^2}{2}} + \frac{12qg}{4\pi\epsilon_0 m}\frac{Q_c}{l_f}$$

$\dot{l}_f^2 \to 0$

HERE SUBSCRIPT "f" = "final"

& SUBSCRIPT "0" = original or initial

$$\Rightarrow \quad \dot{l}_0 = \sqrt{\frac{16qg}{4\pi\epsilon_0 m}\lambda_f\left[1 - \frac{l_f}{l_0}\right]}$$

NOW $Q_F = \dfrac{\lambda_f}{4\pi\epsilon_0 V_f}$ = FINAL PERVEANCE AT CENTER OF PARABOLIC PULSE

(NOTE $Q_c \equiv \frac{2}{3}\lambda_0 l$ = CHARGE

whereas $Q_F \equiv$ PERVEANCE (DIMENSIONLESS)

C = COMPRESSION RATIO $= \dfrac{l_0}{l_f}$

$\dfrac{\Delta V}{V_0}$ = velocity tilt $= \dfrac{|\dot{l}|}{V_0}$

$$\rightarrow \quad \boxed{\frac{\Delta V}{V} = \sqrt{8gQ_f\left[1 - \frac{1}{C}\right]}}$$

for $Q_f = 10^{-4}$
$g = 1.1$
$C = 20$

$$\Rightarrow \quad \frac{\Delta V}{V} = 0.029$$

$$\boxed{\text{DRIFT LENGTH} \cong \frac{l}{\Delta V}V_0 = \frac{l}{\Delta V/V} = 345 \text{ m} \quad \text{for } l = 10 \text{ m}}$$

Vlasov-equation for a drifting beam:

$$\frac{\partial f}{\partial s} + x'\frac{\partial f}{\partial x} + x''\frac{\partial f}{\partial x'} + y'\frac{\partial f}{\partial y} + y''\frac{\partial f}{\partial y'} + z'\frac{\partial f}{\partial z} + z''\frac{\partial f}{\partial z'} = 0$$

Let $\tilde{f}(z,z',s) \equiv \iiiint f \, dx \, dx' \, dy \, dy'$

INTEGRATING VLASOV EQUATION: If $z'' \neq f(x,x',y,y')$:

$$\Rightarrow \frac{\partial \tilde{f}}{\partial s} + \iiint \underbrace{\int \frac{\partial f}{\partial x} dx}_{=\cancel{f}\big|_{-\infty}^{\infty} \to 0} dx' dy dy' + \cdots \quad z'\frac{\partial \tilde{f}}{\partial z} + z''\frac{\partial \tilde{f}}{\partial z'} = 0$$

$$\Rightarrow \boxed{\frac{\partial \tilde{f}}{\partial s} + z'\frac{\partial \tilde{f}}{\partial z} + z''\frac{\partial \tilde{f}}{\partial z'} = 0} \quad \text{1 D Vlasov}$$

Now let $\lambda \equiv q\int \tilde{f}\, dz'$; $\lambda \overline{z'} = \int \tilde{f} z' dz'$; $\lambda \overline{z'^2} \equiv \int \tilde{f} z'^2 dz'$

Also, let $\Delta z'^2 \equiv \overline{z'^2} - (\overline{z'})^2$

FLUID EQUATIONS

INTEGRATING 1D VLASOV OVER z':

$$\boxed{\frac{\partial \lambda}{\partial s} + \frac{\partial}{\partial z}(\lambda \overline{z'}) = 0} \quad \text{(CONTINUITY EQUATION)}$$

MULTIPLYING BY z' & INTEGRATING VLASOV OVER z':

$$\frac{\partial}{\partial s}\lambda\overline{z'} + \frac{\partial}{\partial z}\lambda\overline{z'^2} - \lambda z'' = 0$$

DIVIDING BY λ, USING CONTINUITY EQUATION & DEFINITION OF $\Delta z'^2$:

$$\boxed{\underbrace{\frac{\partial \overline{z'}}{\partial s} + \overline{z'}\frac{\partial}{\partial z}\overline{z'}}_{\text{INERTIAL}} + \underbrace{\frac{1}{\lambda}\frac{\partial}{\partial z}(\lambda \Delta z'^2)}_{\text{PRESSURE TERM}} = \underbrace{\overline{z''}}_{\text{FORCE}}} \quad \text{(MOMENTUM EQUATION)}$$

LONGITUDINAL ENVELOPE EQUATION

$$\frac{\partial \tilde{f}}{\partial s} + z' \frac{\partial \tilde{f}}{\partial z} + z'' \frac{\partial \tilde{f}}{\partial z'} = 0$$

Q_c = total charge in bunch

If $z'' = -K(s) z + \frac{qq}{4\pi\epsilon_0 m v^2}\left(\frac{12 Q_c}{L^3}\right) z$

$$\Rightarrow \frac{\partial}{\partial s}\langle z^2 \rangle = 2\langle z z' \rangle$$

$$\frac{\partial}{\partial s}\langle z z' \rangle = \langle z'^2 \rangle + \frac{qq}{4\pi\epsilon_0 m v^2}\left(\frac{12 Q_c}{L^3}\right)\langle z^2 \rangle - K(s)\langle z^2 \rangle$$

$$\frac{\partial}{\partial s}\langle z'^2 \rangle = 2\left(\frac{qq}{4\pi\epsilon_0 m v^2}\right)\left(\frac{12 Q_c}{L^3}\right)\langle z z' \rangle - 2K(s)\langle z z' \rangle$$

NOTE $\langle z^2 \rangle = \frac{1}{Q_c}\int_{-\infty}^{\infty}\int_{-L/2}^{L/2} z^2 f(z,z')\,dz\,dz' = \frac{1}{20}L^2$

$$\varepsilon_z^2 = 25\left[\langle z^2 \rangle\langle z'^2 \rangle - \langle z z' \rangle^2\right]$$

$$\Rightarrow \frac{d^2 L}{ds^2} = \frac{16\,\varepsilon_z^2}{L^3} + \frac{12\,qq\,Q_c}{4\pi\epsilon_0 m v^2 L^2} - K(s) L$$

Let $r_z = L/2$

$$\Rightarrow \boxed{\frac{d^2 r_z}{ds^2} = \frac{\varepsilon_z^2}{r_z^3} + \frac{3}{2}\frac{qq\,Q_c}{4\pi\epsilon_0 m v^2}\frac{1}{r_z^2} - K(s) r_z}$$

SELF-CONSISTENT LONGITUDINAL DISTRIBUTION:

NEUFFER DISTRIBUTION

D. NEUFFER, PARTICLE ACCELERATORS, Vol 11, p 23 (1980)

RETURNING TO THE 1D VLASOV EQUATION:

$$\frac{\partial f}{\partial s} + z' \frac{\partial f}{\partial z} + z'' \frac{\partial f}{\partial z'} = 0$$

If $z'' = -A \frac{\partial \lambda}{\partial z} - K(s) z$

THEN,

$$f(z, z', s) = \frac{3N}{2\pi \varepsilon_z} \sqrt{1 - \frac{z^2}{r_z^2} - \frac{r_z^2 (z' - r_z' z / r_z)^2}{\varepsilon_z^2}}$$

for $-r_z < z < r_z$

& $\frac{r_z' z}{r_z} - \frac{\varepsilon_z}{r_z}\sqrt{1 - \frac{z^2}{r_z^2}} \leq z' \leq \frac{r_z' z}{r_z} + \frac{\varepsilon_z}{r_z}\sqrt{1 - \frac{z^2}{r_z^2}}$

is a solution to the 1D Vlasov equation.

HERE $\varepsilon_z^2 = 25\left(\langle z^2\rangle\langle z'^2\rangle - \langle z z'\rangle^2\right] =$ CONSTANT

N = total number of particles in bunch

r_z = hard edge of bunch

NOTE THAT $\lambda(z) = \frac{3}{4}\frac{N}{r_z}\left(1 - \frac{z^2}{r_z^2}\right) = \int_{-r_z}^{r_z} f(z, z', s)\, dz'$

$\Rightarrow \frac{\partial \lambda}{\partial z} \propto z \Rightarrow$ LINEAR SPACE CHARGE FIELD

Neuffer Distribution Function

$$f[z,z'] = \frac{3N}{2\pi\varepsilon_z}\sqrt{1-\frac{z^2}{r_z^2}-\frac{r_z^2(z'-r_z'z/r_z)^2}{\varepsilon_z^2}}$$

for:

$$-r_z \le z \le r_z$$

$$\frac{r_z'z}{r_z}-\frac{\varepsilon_z}{r_z}\sqrt{1-\frac{z^2}{r_z^2}} \le z' \le \frac{r_z'z}{r_z}+\frac{\varepsilon_z}{r_z}\sqrt{1-\frac{z^2}{r_z^2}}$$

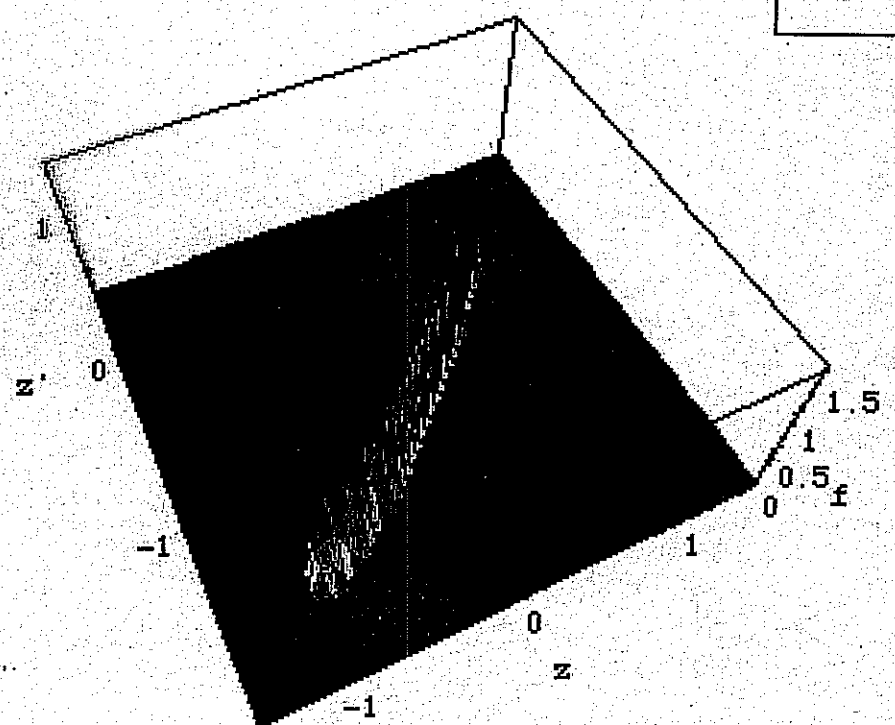

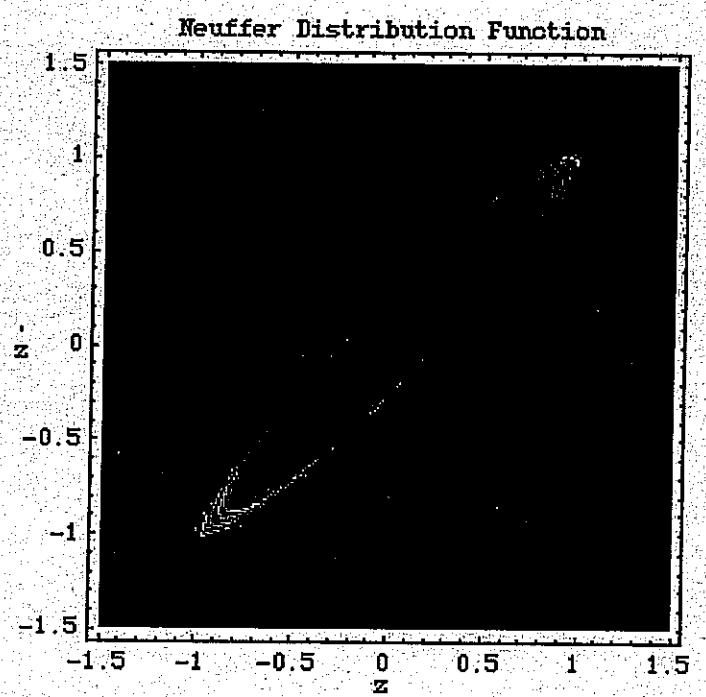

Here $N=r_z=r_z'=1$; $\varepsilon_z=0.3$

NOTE:

- DISTRIBUTION FUNCTION HAS ELLIPTICAL BOUNDARY IN z-z' PHASE SPACE
- $\pi \varepsilon_z$ IS AREA OF ELLIPSE AND IS CONSTANT
- ANALOGOUS TO K-V DISTRIBUTION WITH LINEAR SPACE CHARGE FORCE AND SECOND ORDER ENVELOPE EQUATION TO DESCRIBE THE MOTION OF THE DISTRIBUTION:

$$\frac{d^2 r_z}{ds^2} = \frac{\varepsilon_z^2}{r_z^3} + \frac{3}{2}\frac{AN}{r_z^2} - K(s)\, r_z$$

NOTE ALSO THAT NEUFFER FUNCTION CAN BE USED FOR BUNCHED BEAMS IN WHICH $E_z \propto z$, AS IN A UNIFORM DENSITY ELLIPSOID.

Summary

1D VLASOV EQUATION & g-factor model

$$\frac{\partial \tilde{f}}{\partial s} + z' \frac{\partial \tilde{f}}{\partial z} + z'' \frac{\partial \tilde{f}}{\partial z'} = 0 \qquad z'' = \frac{-g}{4\pi\epsilon_0 m V_z^2} \frac{\partial \lambda}{\partial z}$$

Leads to fluid equations:

$$\frac{\partial \lambda}{\partial s} + \frac{\partial}{\partial z}(\lambda \bar{z}') = 0$$

$$\frac{\partial \bar{z}'}{\partial s} + \bar{z}' \frac{\partial \bar{z}'}{\partial z} + \frac{1}{\lambda}\frac{\partial}{\partial z}(\lambda \Delta z'^2) + \frac{c_s^2}{\lambda_0 V_0^2}\frac{\partial \lambda}{\partial z} = 0$$

$\Rightarrow$ SPACE CHARGE WAVES

↳ LONGITUDINAL OR RESISTIVE WALL INSTABILITY

$\Rightarrow$ SPACE CHARGE RAREFACTION WAVES

$\Rightarrow$ PARABOLIC BUNCH COMPRESSION

VLASOV EQUATION ALSO $\Rightarrow$ ENVELOPE EQUATION

$$\frac{d^2 r_z}{ds^2} = \frac{\varepsilon_z^2}{r_z^3} + \frac{3}{2}\frac{q\,Q_c}{4\pi\epsilon_0 m v^2}\frac{1}{r_z^2} - K(s)\, r_z$$

KINETIC SOLUTION TO VLASOV EQUATION SATISFYING RMS ENVELOPE EQUATION IS "NEUFFER DISTRIBUTION" (ANALOGOUS TO KV).

$$f(z,z') = \frac{3N}{2\pi\varepsilon_z}\sqrt{1 - \frac{z^2}{r_z^2} - \frac{r_z^2\,(z' - r_z' z/r_z)^2}{\varepsilon_z^2}}$$

Transverse Centroid and Envelope Descriptions of Beam Evolution*

Steven M. Lund
Lawrence Livermore National Laboratory (LLNL)

Steven M. Lund and John J. Barnard
"Beam Physics with Intense Space-Charge"
US Particle Accelerator School
Boston University, Waltham, MA
12-23 June, 2006

* Research supported by the US Dept. of Energy at LBNL and LLNL under contract Nos. DE-AC03-76SF00098 and W-7405-Eng-48

Transverse Centroid and Envelope Model: Outline

Overview
Derivation of Centroid and Envelope Equations of Motion
Centroid Equations of Motion
Envelope Equations of Motion
Matched Envelope Solutions
Envelope Perturbations
Envelope Modes in Continuous Focusing
Envelope Modes in Periodic Focusing
Transport Limit Scaling
Centroid and Envelope Descriptions via 1st order Coupled Moment Equations

Comments:

- Some of this material related to J.J. Barnard lectures:
  - Transport limit discussions (Introduction)
  - Transverse envelope modes (Cont. Focusing Envelope Modes and Halo)
  - Longitudinal envelope evolution (Longitudinal Beam Physics III)
  - 3D Envelope Modes in a Bunched Beam (Cont. Focusing Envelope Modes and Halo)
- Specific topics will be covered in more detail here

Transverse Centroid and Envelope Model: Detailed Outline

1) Overview

2) Derivation of Centroid and Envelope Equations of Motion
   - Statistical averages
   - Particle equations of motion
   - Distribution assumptions
   - Self-field calculation
   - Coupled centroid and envelope equations of motion

3) Centroid Equations of Motion
   - Simple limits of centroid equations
   - Effect of image charges
   - Centroid stability

4) Envelope Equations of Motion
   - Properties of terms
   - Matched and mismatched beams
   - Perturbations

5) Matched Envelope Solution
   - Construction of matched solution
   - Examples

Detailed Outline - 2

6) Envelope Perturbations
   - Perturbed equations
   - Driving perturbations and modes

7) Envelope Modes in Continuous Focusing
   - Symmetries
   - Breathing and quadrupole modes

8) Envelope Modes in Periodic Focusing
   - Overview
   - Solenoidal modes
   - Quadrupole modes

9) Transport Limit Scaling Based on Envelope Models (see hand written notes)
   - Simple estimates of matched envelope solutions
   - Ideal current limits

10) Centroid and Envelope Descriptions via 1st Order Coupled Moment Equations (to be covered in future editions)
   - Motivation
   - Example

References

S1: Overview

Analyze transverse centroid and envelope properties of an unbunched $(\partial/\partial z = 0)$ beam

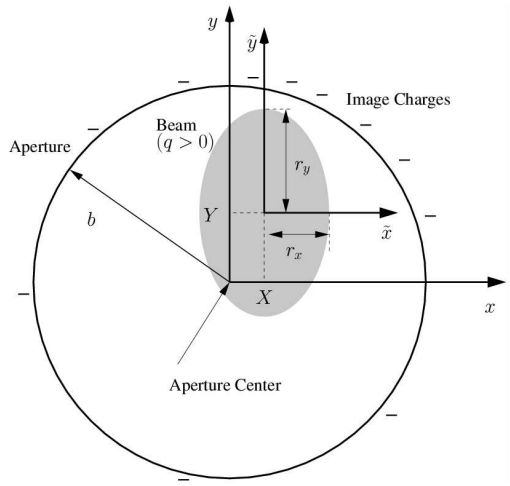

Centroid:

$$X = \langle x \rangle_\perp \qquad Y = \langle y \rangle_\perp$$

x- and y-coordinates of beam center of mass

$$\langle \cdots \rangle_\perp \equiv \frac{\int d^2x_\perp \int d^2x'_\perp \; \cdots f_\perp}{\int d^2x_\perp \int d^2x'_\perp \; f_\perp}$$

Envelope:

$$r_x = 2\sqrt{\langle (x-X)^2 \rangle_\perp} \qquad r_y = 2\sqrt{\langle (y-Y)^2 \rangle_\perp}$$

x- and y-principal axis radii of an elliptical beam envelope

Oscillations in the statistical beam centroid and envelope radii are the *lowest-order* collective responses of the beam

Centroid Oscillations: Associated with errors and are purposefully suppressed to the level possible

- Error Sources:
  - Beam distribution
  - Dipole bending terms from applied field optics
  - Imperfect mechanical alignment
- Exception: When the beam is kicked (insertion or extraction) into our out of a transport channel as is often done in rings

Envelope Oscillations: Can have two components in periodic lattices

Matched Envelope: Periodic flutter synchronized to periodic focusing structure to produce net focusing

Mismatched Envelope: Excursions deviate from matched flutter motion and are seeded/driven by errors

Maximum radial confinement of the maximum beam-edge excursions are desired for economical transport

- Reduces cost by Limiting material volume needed to transport an intense beam

Mismatched beams have larger envelope excursions and have more stability problems since mismatch adds another source of free energy that can drive statistical increases in particle amplitudes (Halo, see J.J. Barnard Lectures on Halo)

Example: FODO Quadrupole Transport Channel

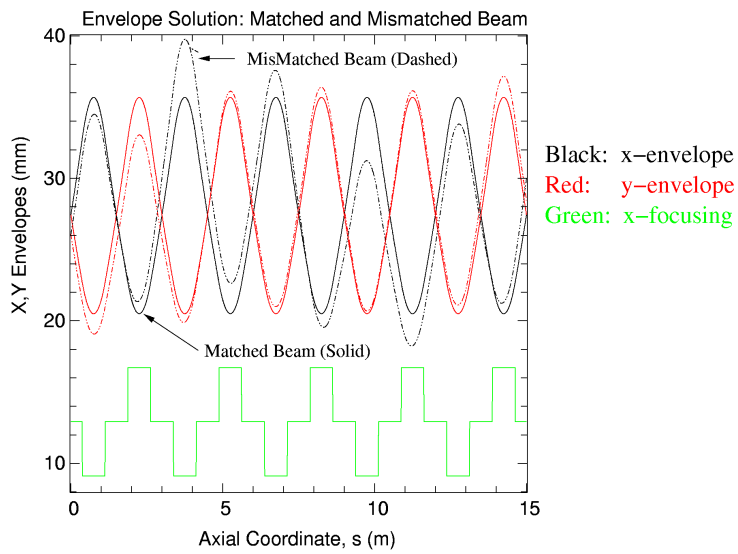

- Larger machine aperture is needed to confine a mismatched beam

Centroid and Envelope oscillations are the *most important collective modes* of an intense beam

- Force balances based on matched beam envelope equation predict scaling of transportable beam parameters
  - Used to design transport lattices
- Instabilities in beam centroid and/or envelope oscillations prevent reliable transport
  - Parameter locations of instability regions should be understood and avoided in machine design

Although it is *necessary* to design to avoid envelope and centroid instabilities, it is not alone *sufficient* for effective machine operation

- Higher-order kinetic and fluid instabilities not expressed in the low-order envelope models can degrade beam quality and control and must also be evaluated
  - To be covered (see S.M. Lund, lectures on *Kinetic Stability*)

S2: Derivation of Transverse Centroid and Envelope Equations of Motion

Analyze centroid and envelope properties of an unbunched $(\partial/\partial z = 0)$ beam

Transverse Statistical Averages:

Let N be the number of particles in a thin axial slice of the beam at axial coordinate s.

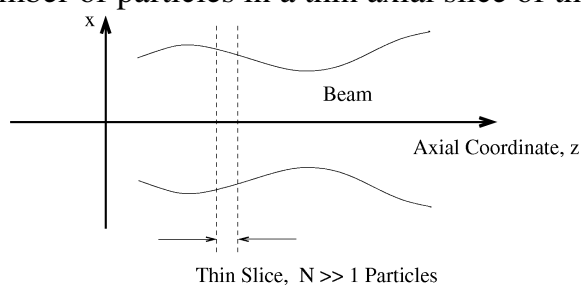

Equivalent averages can be defined in terms of the particles or the transverse Vlasov distribution function:

particles: $$\langle \cdots \rangle_\perp \equiv \frac{1}{N}\sum_{i=1}^{N} \cdots$$

distribution: $$\langle \cdots \rangle_\perp \equiv \frac{\int d^2x_\perp \int d^2x'_\perp \ \cdots f_\perp}{\int d^2x_\perp \int d^2x'_\perp \ f_\perp}$$

- Averages can be generalized to include axial momentum spread

Transverse Particle Equations of Motion

Consistent with earlier analysis, take:

$$x'' + \frac{(\gamma_b\beta_b)'}{(\gamma_b\beta_b)}x' + \kappa_x x = -\frac{q}{m\gamma_b^3\beta_b^2c^2}\frac{\partial\phi}{\partial x}$$

$$y'' + \frac{(\gamma_b\beta_b)'}{(\gamma_b\beta_b)}y' + \kappa_y y = -\frac{q}{m\gamma_b^3\beta_b^2c^2}\frac{\partial\phi}{\partial y}$$

$$\nabla_\perp^2\phi = \left(\frac{\partial^2}{\partial x^2} + \frac{\partial^2}{\partial y^2}\right)\phi = -\frac{\rho}{\epsilon_0}$$

$$\phi|_{\text{aperture}} = 0$$

Assume:

- Unbunched beam
- No axial momentum spread
- Linear applied focusing fields
- Possible acceleration

Various apertures are possible. Some simple examples:

Round Pipe

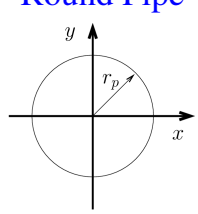

Linac magnetic quadrupoles, acceleration cells, ...

Elliptical Pipe

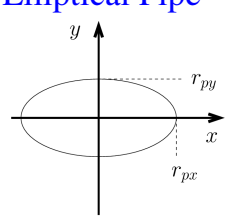

Dispersive rings in drifts, magnetic optics, ...

Hyperbolic Sections

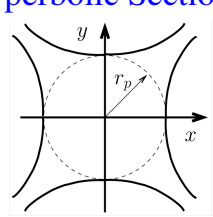

Electric quadrupoles

Review: Focusing lattices we will take in examples: Continuous and piecewise constant periodic solenoid and quadrupole doublet

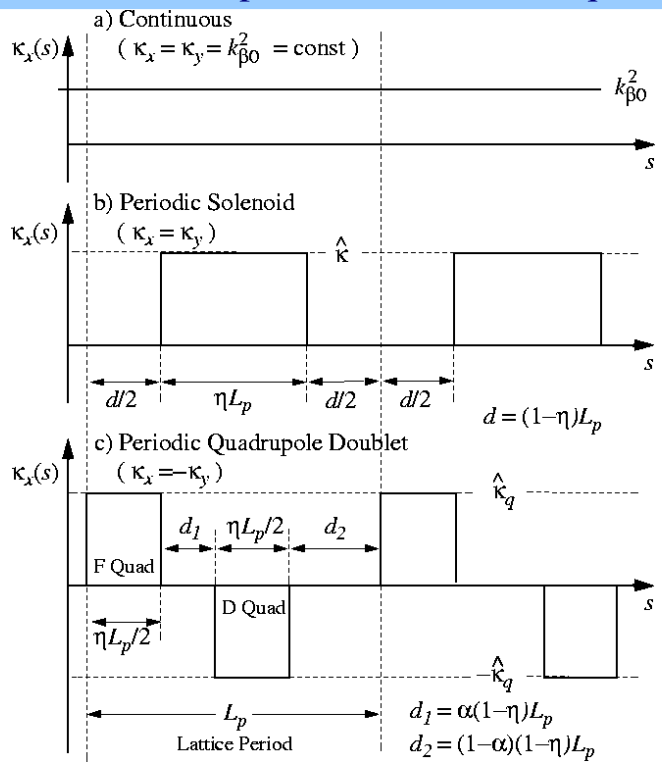

Lattice Period L_p

Occupancy η

$\eta \in [0, 1]$

Solenoid description carried out implicitly in Larmor frame

[see Lund and Bukh, PRST- Accel. and Beams 7, 024801 (2004), Appendix A]

Syncopation Factor α

$$\alpha \in [0, \frac{1}{2}]$$

$$\alpha = \frac{1}{2} \implies FODO$$

Distribution Assumptions

To lowest order, linearly focused intense beams are expected to be nearly uniform in density within the core of the beam out to an edge where the density falls rapidly to zero

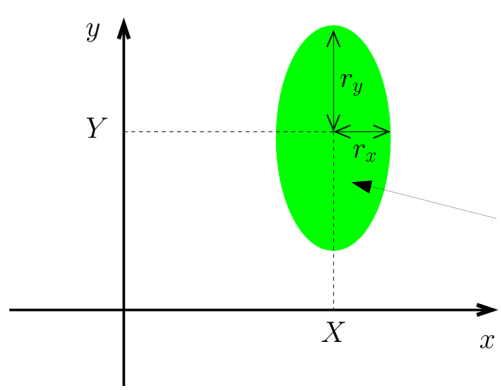

constant density in the beam:

$$\rho = \frac{\lambda}{\pi r_x r_y} = \text{const}$$

$$\rho(x,y) = q \int d^2x'_\perp \; f_\perp \; \simeq \begin{cases} \frac{\lambda}{\pi r_x r_y}, & (x-X)^2/r_x^2 + (y-Y)^2/r_y^2 < 1 \\ 0, & (x-X)^2/r_x^2 + (y-Y)^2/r_y^2 > 1 \end{cases}$$

$$\lambda = q \int d^2x_\perp \int d^2x'_\perp \; f_\perp \; = \int d^2x \; \rho$$

Self-Field Calculation

Temporarily, we will consider an arbitrary beam charge distribution within an arbitrary aperture to formulate the problem.

Electrostatic field of a line charge in free-space

$$\mathbf{E}_\perp = \frac{\lambda_0}{2\pi\epsilon_0}\frac{(\mathbf{x}_\perp - \tilde{\mathbf{x}})}{|\mathbf{x}_\perp - \tilde{\mathbf{x}}|^2}$$

$\lambda_0 =$ line charge

$\mathbf{x}_\perp = \tilde{\mathbf{x}} =$ coordinate of charge

Resolve the field of the beam into direct (free space) and image terms:

$$\mathbf{E}_\perp^s = -\frac{\partial\phi}{\partial\mathbf{x}_\perp} = \mathbf{E}_\perp^d + \mathbf{E}_\perp^i$$

and superimpose free-space solutions for direct and image contributions

Direct Field

$$\mathbf{E}_\perp^d(\mathbf{x}_\perp) = \frac{1}{2\pi\epsilon_0}\int d^2\tilde{x}_\perp \frac{\rho(\tilde{\mathbf{x}}_\perp)(\mathbf{x}_\perp - \tilde{\mathbf{x}}_\perp)}{|\mathbf{x}_\perp - \tilde{\mathbf{x}}_\perp|^2}$$

$\rho(\mathbf{x}) =$ beam charge density

Image Field

$$\mathbf{E}_\perp^i(\mathbf{x}_\perp) = \frac{1}{2\pi\epsilon_0}\int d^2\tilde{x}_\perp \frac{\rho^i(\tilde{\mathbf{x}}_\perp)(\mathbf{x}_\perp - \tilde{\mathbf{x}}_\perp)}{|\mathbf{x}_\perp - \tilde{\mathbf{x}}_\perp|^2}$$

$\rho^i(\mathbf{x}) =$ beam image charge density

Direct Field:

For a uniform density elliptical beam the direct contribution is as calculated for the KV equilibrium, free-space self-field calculation

- see S.M. Lund lectures on *Transverse Beam Equilibria*

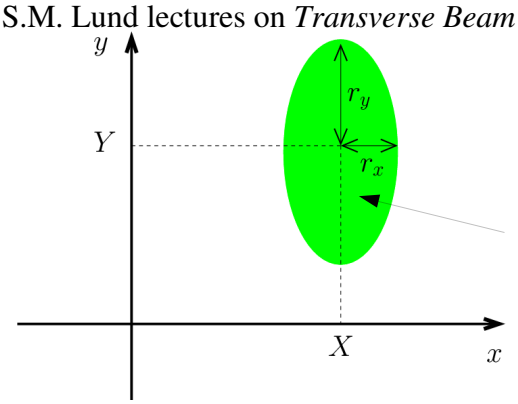

constant density in the beam:

$$\rho = \frac{\lambda}{\pi r_x r_y} = \text{const}$$

$$E_x^d = \frac{\lambda}{\pi\epsilon_0}\frac{x - X}{(r_x + r_y)r_x}$$

$$E_y^d = \frac{\lambda}{\pi\epsilon_0}\frac{y - Y}{(r_x + r_y)r_y}$$

Image Field:

Image structure depends on the aperture. Assume a round pipe for simplicity.

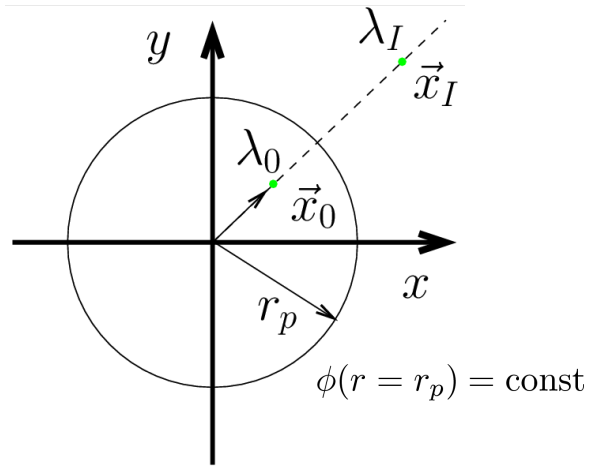

$\lambda_I = -\lambda_0$ image charge

$\mathbf{x}_I = \dfrac{r_p^2}{|\mathbf{x}_0|^2}\mathbf{x}_0$ image location

superimpose all images of beam:

$$\boxed{\mathbf{E}_\perp^i(\mathbf{x}_\perp) = -\frac{1}{2\pi\epsilon_0}\int_{\text{pipe}} d^2\tilde{x}_\perp \, \frac{\rho(\tilde{\mathbf{x}}_\perp)(\mathbf{x}_\perp - r_p^2\tilde{\mathbf{x}}_\perp/|\tilde{\mathbf{x}}_\perp|^2)}{|\mathbf{x}_\perp - r_p^2\tilde{\mathbf{x}}_\perp/|\tilde{\mathbf{x}}_\perp|^2|^2}}$$

- Difficult to calculate even for a uniform density beam

Examine limits of the image field:

1) On-axis line charge: $\rho(\mathbf{x}_\perp) = \lambda\delta(\mathbf{x}_\perp - X\hat{\mathbf{e}}_x)$

$$\boxed{\mathbf{E}_\perp^i(\mathbf{x}_\perp = X\mathbf{e}_x) = \frac{\lambda}{2\pi\epsilon_0(r_p^2/X - X)}\hat{\mathbf{e}}_x}$$

- Generates nonlinear field at position of direct charge

2) Centered, uniform density elliptical beam:

Expand using complex coordinates starting from the general image expression:

$$\underline{E}^i = E_y^i + iE_x^i = \sum_{n=2,4,\cdots}^{\infty} \underline{c}_n \underline{z}^{n-1} \qquad \underline{c}_n = \frac{i}{2\pi\epsilon_0}\int_{\text{pipe}} d^2x_\perp \, \rho(\mathbf{x}_\perp)\frac{(x-iy)^n}{r_p^{2n}}$$

$$\underline{z} = x + iy \qquad = \frac{i\lambda n!}{2\pi\epsilon_0 2^n (n/2+1)!(n/2)!}\left(\frac{r_x^2 - r_y^2}{r_p^4}\right)^{n/2}$$

$$i = \sqrt{-1}$$

The linear (n=2) components of this expansion give:

$$\boxed{E_x^i = \frac{\lambda}{8\pi\epsilon_0}\frac{r_x^2 - r_y^2}{r_p^4}x, \qquad E_y^i = -\frac{\lambda}{8\pi\epsilon_0}\frac{r_x^2 - r_y^2}{r_p^4}y}$$

- Rapidly vanish (higher order terms more rapid) as beam becomes more round

3) Elliptical beam with a small displacement along the x-axis:

$$Y = 0 \qquad |X|/r_p \ll 1$$

Expand using complex coordinates starting from the general image expression:

- Use complex coordinates to simplify calculation

  E.P. Lee, E. Close, and L. Smith, Nuc. Instr. Meth, 1126 (1987)
- Expressions become even more complicated with simultaneous x- and y-displacements and more complicated aperture geometries

$$E_x^i = \frac{\lambda}{2\pi\epsilon_0 r_p^2}\left[f(x-X)+gX\right] + \Theta\left(\frac{X}{r_p}\right)^3$$

$$E_y^i = -\frac{\lambda}{2\pi\epsilon_0 r_p^2} fy + \Theta\left(\frac{X}{r_p}\right)^3$$

$$f = \frac{r_x^2 - r_y^2}{4r_p^2} + \frac{X^2}{r_p^2}\left[1 + \frac{3}{2}\left(\frac{r_x^2 - r_y^2}{r_p^2}\right) + \frac{3}{8}\left(\frac{r_x^2 - r_y^2}{r_p^2}\right)^2\right]$$

$$g = 1 + \frac{r_x^2 - r_y^2}{4r_p^2} + \frac{X^2}{r_p^2}\left[1 + \frac{3}{4}\left(\frac{r_x^2 - r_y^2}{r_p^2}\right) + \frac{1}{8}\left(\frac{r_x^2 - r_y^2}{r_p^2}\right)^2\right]$$

Comments on images:

- Sign is generally such that it will tend to increase beam displacements
  - Also weaker focusing corrections for an elliptical beam
- Can be very difficult to calculate explicitly
  - Even for simple case of circular pipe
  - Special cases of simple geometry formulas can give idea on scaling
  - Generally suppress just by making the beam small relative to characteristic dimensions and keeping the beam near-axis
- Depend strongly on the aperture geometry
  - Generally varies as a function of s in the machine

Round Pipe

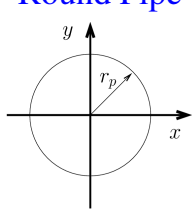

Elliptical Pipe

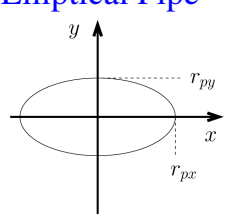

Hyperbolic Sections

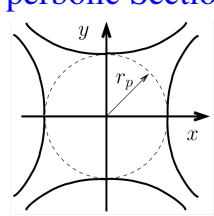

Coupled centroid and envelope equations of motion

Consistent with the assumed structure of the distribution (uniform density elliptical beam), denote:

Beam Centroid:

$$\boxed{\begin{aligned} X &\equiv \langle x \rangle_\perp \\ Y &\equiv \langle y \rangle_\perp \end{aligned}}$$

Coordinates with respect to centroid:

$$\boxed{\begin{aligned} \tilde{x} &\equiv x - X \\ \tilde{y} &\equiv y - Y \end{aligned}}$$

Envelope Edge Radii:

$$\boxed{\begin{aligned} r_x &= 2\sqrt{\langle \tilde{x}^2 \rangle_\perp} \\ r_y &= 2\sqrt{\langle \tilde{y}^2 \rangle_\perp} \end{aligned}}$$

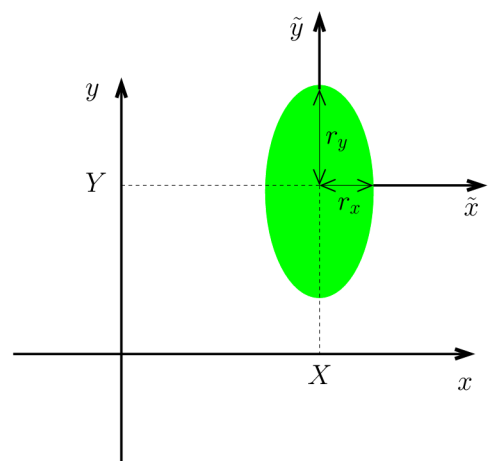

With the assumed uniform elliptical beam, all moments can be calculated in terms of: $X, \quad Y \qquad r_x, \quad r_y$

To derive centroid equations, first use the self-field resolution for a uniform density beam, then the equations of motion for a particle within the beam can be expressed as:

$$x'' + \frac{(\gamma_b\beta_b)'}{(\gamma_b\beta_b)}x' + \kappa_x x - \frac{2Q}{(r_x + r_y)r_x}(x - X) = \frac{q}{m\gamma_b^3\beta_b^2c^2}E_x^i$$

$$y'' + \frac{(\gamma_b\beta_b)'}{(\gamma_b\beta_b)}y' + \kappa_y y - \frac{2Q}{(r_x + r_y)r_y}(y - Y) = \frac{q}{m\gamma_b^3\beta_b^2c^2}E_y^i$$

Direct Terms Image Terms

perveance:

$$Q \equiv \frac{q\lambda}{2\pi\epsilon_0 m\gamma_b^3\beta_b^2c^2}$$

average equations using: $\langle x' \rangle_\perp = \langle x \rangle'_\perp = X'$ etc., to obtain:

Centroid Equations:

$$\boxed{\begin{aligned} X'' + \frac{(\gamma_b\beta_b)'}{(\gamma_b\beta_b)}X' + \kappa_x X &= Q\frac{2\pi\epsilon_0}{\lambda}\langle E_x^i \rangle_\perp \\ Y'' + \frac{(\gamma_b\beta_b)'}{(\gamma_b\beta_b)}Y' + \kappa_y Y &= Q\frac{2\pi\epsilon_0}{\lambda}\langle E_y^i \rangle_\perp \end{aligned}}$$

- $\langle E_x^i \rangle_\perp$ will generally depend on: $X, \quad Y$ and $r_x, \quad r_y$

To derive equations of motion for the envelope radii, first subtract the X centroid equation from the x-particle equation of motion to obtain:

$$\tilde{x} \equiv x - X$$

$$\tilde{x}'' + \frac{(\gamma_b\beta_b)'}{(\gamma_b\beta_b)}\tilde{x}' + \kappa_x\tilde{x} - \frac{2Q\tilde{x}}{(r_x+r_y)r_x} = \frac{q}{m\gamma_b^2\beta_b^2c^2}\left[E_x^i - \langle E_x^i\rangle_\perp\right]$$

Differentiate the equation for the envelope radius:

$$r_x = 2\langle\tilde{x}^2\rangle_\perp^{1/2} \longrightarrow r_x' = \frac{4\langle\tilde{x}\tilde{x}'\rangle_\perp}{r_x}$$

Define (motivated the KV equilibrium results) a statistical rms edge emittance:

$$\varepsilon_x \equiv 4\varepsilon_{x,\mathrm{rms}} = 4\left[\langle\tilde{x}^2\rangle_\perp\langle\tilde{x}'^2\rangle_\perp - \langle\tilde{x}\tilde{x}'\rangle_\perp^2\right]^{1/2}$$

Differentiate the equation for r_x' again and use the emittance definition:

$$r_x'' = 4\frac{\langle\tilde{x}\tilde{x}''\rangle_\perp}{r_x} + \frac{16[\langle\tilde{x}^2\rangle_\perp\langle\tilde{x}'^2\rangle_\perp - \langle\tilde{x}\tilde{x}'\rangle_\perp^2]}{r_x^3}$$

$$= 4\frac{\langle\tilde{x}\tilde{x}''\rangle_\perp}{r_x} + \frac{\varepsilon_x^2}{r_x^3}$$

and then employ the equations of motion to eliminate $\tilde{x}''$ in $\langle\tilde{x}\tilde{x}''\rangle_\perp$ to obtain:

Envelope Equations:

$$\boxed{\begin{aligned} r_x'' + \frac{(\gamma_b\beta_b)'}{(\gamma_b\beta_b)}r_x' + \kappa_x r_x - \frac{2Q}{r_x+r_y} - \frac{\varepsilon_x^2}{r_x^3} &= 4Q\frac{2\pi\epsilon_0}{\lambda}\langle\tilde{x}E_x^i\rangle_\perp \\ r_y'' + \frac{(\gamma_b\beta_b)'}{(\gamma_b\beta_b)}r_x' + \kappa_y r_y - \frac{2Q}{r_x+r_y} - \frac{\varepsilon_y^2}{r_y^3} &= 4Q\frac{2\pi\epsilon_0}{\lambda}\langle\tilde{x}E_x^i\rangle_\perp \end{aligned}}$$

- $\langle\tilde{x}E_x^i\rangle_\perp$ will generally depend on: X, Y and r_x, r_y

Comments on Centroid/Envelope equations:

- Centroid and envelope equations are coupled and must be solved simultaneously
- Image terms contain nonlinear terms that can be difficult to evaluate explicitly
  - Aperture geometry changes image correction
- The formulation is not self-consistent because a charge profile is assumed
  - Uniform density choice motivated by KV results and Debye screening
  - The assumed distribution form not evolving represents a fluid model closure
- Constant (normalized when accelerating) emittances are generally assumed

$$Q = \frac{q\lambda}{2\pi m\epsilon_0\gamma_b^3\beta_b^2c^2}$$

$$\varepsilon_{nx} = \gamma_b\beta_b\varepsilon_x = \mathrm{const}$$

$$\varepsilon_{nx} = \gamma_b\beta_b\varepsilon_x = \mathrm{const}$$

β_b, γ_b, λ specified by "acceleration schedule"

S3: Centroid Equations of Motion

Neglect image charge terms, then the centroid equation of motion becomes:

$$\boxed{X'' + \frac{(\gamma_b\beta_b)'}{(\gamma_b\beta_b)}X' + \kappa_x X = 0}$$

- Usual Hill's equation with additional acceleration term
- Single particle form and usual phase amplitude methods, Courant-Snyder invariants, and stability bounds can be immediately applied

$$\boxed{\sigma_{0x} < 180^\circ}$$ centroid stability, 1st stability condition

Example: FODO channel centroid evolution

Mid-drift launch:

$X(0) = 1$ mm

$X'(0) = 1$ mrad

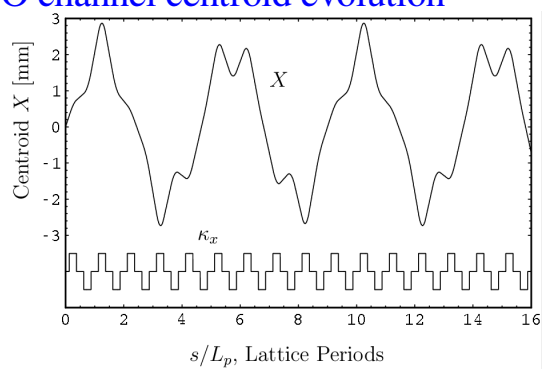

lattice/beam parameters:

$\beta_b = \text{const}$

$\sigma_0 = 80^\circ$

$L_p = 0.5$ m

$\eta = 0.5$

Driving Errors:

The reference orbit is ideally tuned for zero centroid offset. But there will always be driving errors that will cause the centroid oscillations to accumulate with beam propagation distance:

$$\boxed{X'' + \frac{(\gamma_b\beta_b)'}{(\gamma_b\beta_b)}X' + \frac{G_n}{G_0}\kappa_q(s)X = \frac{G_n}{G_0}\kappa_q(s)\Delta_{xn}}$$

$\frac{G_n}{G_0} =$ nth quadrupole gradient error (1 = no error)

$\Delta_{xn} =$ nth quadrupole transverse displacement error

Example: FODO channel centroid with quadrupole displacement errors

$\frac{G_n}{G_0} = 1$

$\Delta_{xn} = [-0.5, 0.5]$ mm (uniform dist)

same lattice as previous

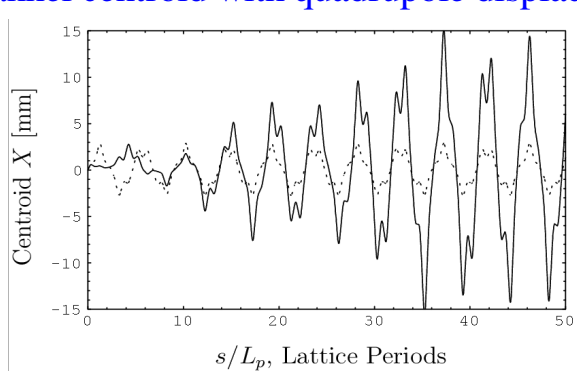

solid – with errors

dashed – no errors

Errors will result in a characteristic random walk increase in oscillation amplitude due to the driving terms.

Control by:

- Synthesize small applied dipole fields to regularly steer the centroid back on-axis
- Fabricate and align focusing elements with higher precision
- Employ a sufficiently large aperture to contain the oscillations and limit detrimental nonlinear image charge effects

Economics dictates the optimal strategy

Image Effects:

Model the beam as a displaced line-charge. Then the equations of motion are modified as:

$$\boxed{X'' + \frac{(\gamma_b\beta_b)'}{(\gamma_b\beta_b)}X' + \kappa_x X = \frac{QX}{r_p^2 - X^2}}$$

$$\frac{QX}{r_p^2 - X^2} \simeq \frac{Q}{r_p^2}X + \frac{Q}{r_p^4}X^3$$

linear correction Nonlinear correction (smaller)

Example: FODO channel centroid with image charge corrections

$r_p = 30$ mm

$Q = 2 \times 10^{-4}$

same lattice as previous

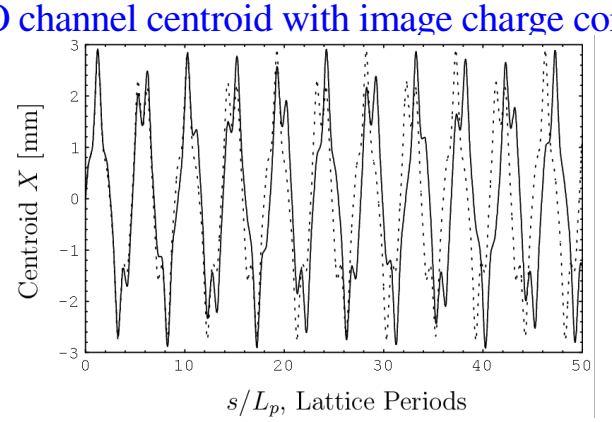

solid – with images

dashed – no images

Main effect appears to be an accumulated phase error of the centroid orbit since, generally the centroid error oscillations are not "matched" orbits. This will complicate extrapolations of errors over many lattice periods

Control by:

- Keeping centroid displacements small by correcting
- Make pipe larger
- Generally less problematic than alignment and excitation errors

General Comments:

- More detailed analyses show that the coupling of the envelope radii to the centroid evolution is often weak
- Fringe fields are more important for accurate calculation of centroid orbits since orbits are not part of a matched lattice
  - Nonideal orbits are poorly tuned to lattice and become more sensitive to the precise phase of impulses
- Over long path lengths many nonlinear terms can influence results
- Lattice errors are not often known so one must often analyze characteristic error distributions to see if centroids measured are consistent with expectations

S4: Envelope Equations of Motion

Overview

- Generally found that couplings to centroid displacements Δ_x Δ_y are weak
  - Centroid ideally zero
- Envelope eqns are most important in designing transverse focusing systems
  - Expresses average radial force balance
  - Unfortunately, can be difficult to analyze analytically for scaling
  - "Systems" codes generally written using envelope equations, stability criteria, and practical engineering constraints
- Instabilities of the envelope equations in periodic focusing lattices must be avoided in machine operation
  - Instabilities are strong and real
  - Represent lowest order "KV" modes of a full kinetic theory
- Previous derivation of envelope equations relied on Courant-Snyder invariants in linear applied and self-fields. Analysis shows that the same force balances result for a uniform elliptical beam with no image couplings.
  - Debye screening arguments suggest assumed uniform density model taken should be a good approximation for intense space-charge

KV/rms Envelope Equations

The envelope equation reflects low-order force balances:

$$r_x'' + \frac{(\gamma_b\beta_b)'}{(\gamma_b\beta_b)} r_x' + \kappa_x r_x - \frac{2Q}{r_x + r_y} - \frac{\varepsilon_x^2}{r_x^3} = 0$$

$$r_y'' + \frac{(\gamma_b\beta_b)'}{(\gamma_b\beta_b)} r_y' + \kappa_y r_y - \frac{2Q}{r_x + r_y} - \frac{\varepsilon_y^2}{r_y^3} = 0$$

	Applied Acceleration	Applied Focusing	Space-Charge Defocusing	Thermal Defocusing
Terms:	Lattice	Lattice	Perveance	Emittance

The "acceleration schedule" specifies both $\gamma_b\beta_b$ and λ
then the equations are integrated with:

$$\gamma_b\beta_b\varepsilon_x = \text{const}$$
$$\gamma_b\beta_b\varepsilon_y = \text{const}$$

normalized emittance conservation

$$Q = \frac{q\lambda}{2\pi\epsilon_0 m\gamma_b^3\beta_b^2c^2}$$

specified perveance

Reminder: It was shown for a coasting beam that the envelope equations remain valid for elliptic charge densities suggesting more general validity [Sacherer, IEEE Trans. Nucl. Sci. 18, 1101 (1971), J.J. Barnard, Intro. Lectures]

For any beam with elliptic symmetry charge density in each transverse slice:

$$\rho = \rho\left(\frac{x^2}{r_x^2} + \frac{y^2}{r_y^2}\right)$$

Based on:

$$\langle x\frac{\partial\phi}{\partial x}\rangle_\perp = -\frac{\lambda}{4\pi\epsilon_0}\frac{r_x}{r_x + r_y}$$

see J.J. Barnard intro. lectures

the KV envelope equations

$$r_x''(s) + \kappa_x(s)r_x(s) - \frac{2Q}{r_x(s) + r_y(s)} - \frac{\varepsilon_x^2(s)}{r_x^3(s)} = 0$$

$$r_y''(s) + \kappa_y(s)r_y(s) - \frac{2Q}{r_x(s) + r_y(s)} - \frac{\varepsilon_y^2(s)}{r_y^3(s)} = 0$$

remain valid when (averages taken with the full distribution):

$$Q = \frac{q\lambda}{2\pi\epsilon_0 m\gamma_b^3\beta_b^2c^2} = \text{const} \qquad \lambda = q\int d^2x_\perp\,\rho = \text{const}$$

$$r_x = 2\langle x^2\rangle_\perp^{1/2} \qquad \varepsilon_x = 4[\langle x^2\rangle_\perp\langle x'^2\rangle_\perp - \langle xx'\rangle_\perp^2]^{1/2}$$

$$r_y = 2\langle y^2\rangle_\perp^{1/2} \qquad \varepsilon_y = 4[\langle y^2\rangle_\perp\langle y'^2\rangle_\perp - \langle yy'\rangle_\perp^2]^{1/2}$$

Properties of Envelope Equation Terms:

Applied Focusing and Acceleration: $\kappa_x r_x \qquad \frac{(\gamma_b\beta_b)'}{(\gamma_b\beta_b)} r_x'$

- Analogous to single particle orbit terms
- Contributions to beam envelope essentially the same as in single particle case
- Have strong s dependance, can be both focusing and defocusing
  - Act only in focusing elements and acceleration gaps

Perveance: $\frac{2Q}{r_x + r_y}$

- Acts continuously in s, always defocusing
- Becomes stronger (relatively to other terms) when the beam expands in cross-sectional area

Emittance: $\frac{\varepsilon_x^2}{r_x^3}$

- Acts continuously in s, always defocusing
- Becomes stronger (relatively to other terms) when the beam becomes small in cross-sectional area
- Scaling makes clear why it is necessary to inhibit emittance growth for applications where small spots are desired on target

As the beam expands, the perveance term will eventually dominate:

[see analytical analysis in: S.M. Lund and B. Bukh, PRSTAB 7, 024801 (2004)]

Free expansion $(\kappa_x = \kappa_y = 0)$

Initial conditions:

Space-Charge Dominated: $\varepsilon_x = 0$

Emittance Dominated: $Q = 0$

Initial Conditions

$$\frac{Q}{r_x(s_i)} = \frac{\varepsilon_x^2}{r_x^3(s_i)}$$

$$r_x'(s_i) = 0$$

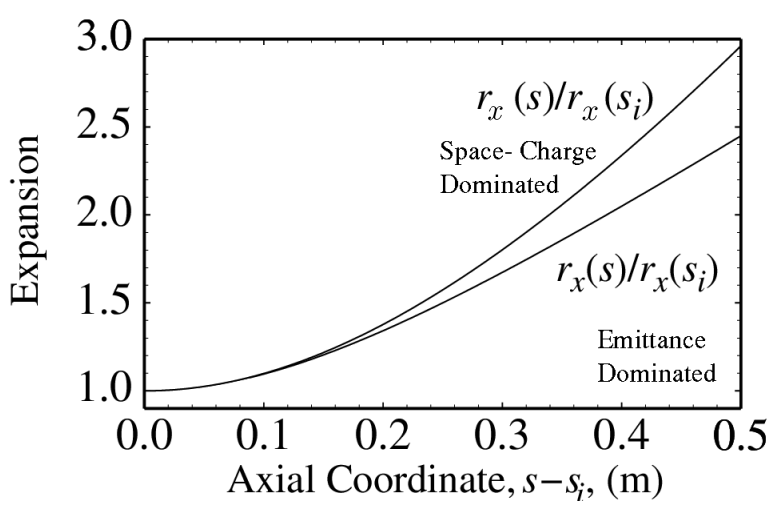

S5: Matched Envelope Solution:

Neglect acceleration $(\gamma_b \beta_b = \text{const})$ or use transformed variables:

$$r_x''(s) + \kappa_x(s) r_x(s) - \frac{2Q}{r_x(s) + r_y(s)} - \frac{\varepsilon_x^2}{r_x^3(s)} = 0$$

$$r_y''(s) + \kappa_y(s) r_y(s) - \frac{2Q}{r_x(s) + r_y(s)} - \frac{\varepsilon_y^2}{r_y^3(s)} = 0$$

$$r_x(s + L_p) = r_x(s) \qquad r_x(s) > 0$$

$$r_y(s + L_p) = r_y(s) \qquad r_y(s) > 0$$

Matching involves finding specific initial conditions for the envelope to have the periodicity of the lattice:

Find Values of:

$$r_x(s_i) \quad r_x'(s_i)$$
$$r_y(s_i) \quad r_y'(s_i)$$

Such That:

$$r_x(s_i + L_p) = r_x(s_i) \qquad r_x'(s_i + L_p) = r_x'(s_i)$$
$$r_y(s_i + L_p) = r_y(s_i) \qquad r_y'(s_i + L_p) = r_y'(s_i)$$

- Typically constructed with numerical root finding from estimated/guessed values
  - Can be difficult in practice for complicated lattices, but well posed
- Recent iterative technique developed to numerically calculate without root finding
  [S.M. Lund, S. Chilton and E.P. Lee, PRSTAB **9**, 064201 (2006)]

Typical Matched vs Mismatched solution for FODO channel:

Matched

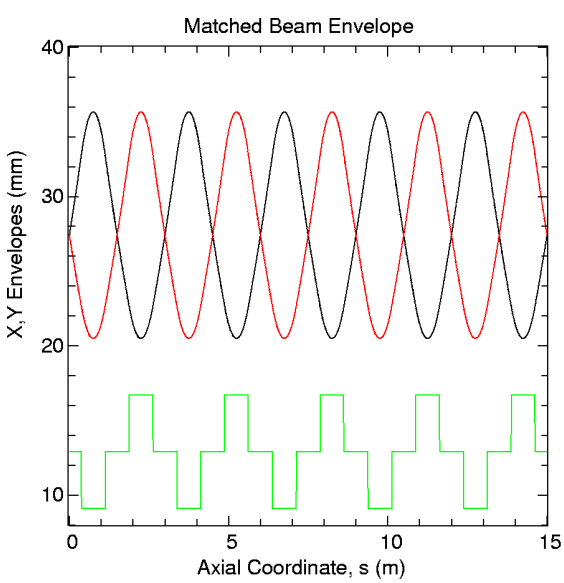

Mismatched

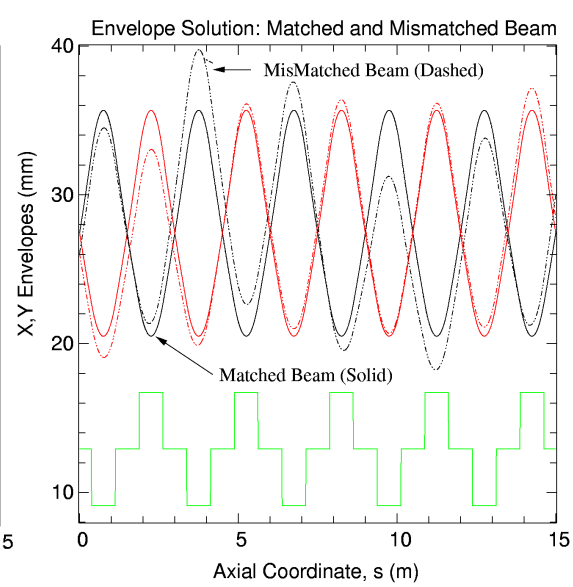

The matched beam is the most radially compact solution to the envelope equations rendering it highly important for beam transport

The matched solution to the KV envelope equations reflects the symmetry of the focusing lattice and must in general be calculated numerically

$$\boxed{\begin{aligned} r_x(s+L_p) &= r_x(s) \\ r_y(s+L_p) &= r_y(s) \\ \varepsilon_x &= \varepsilon_y \end{aligned}}$$

Parameters

$$L_p = 0.5 \text{ m}, \quad \sigma_0 = 80^\circ, \quad \eta = 0.5$$
$$\varepsilon_x = 50 \text{ mm-mrad}$$
$$\sigma/\sigma_0 = 0.2$$

Solenoidal Focusing
$(Q = 6.6986 \times 10^{-4})$

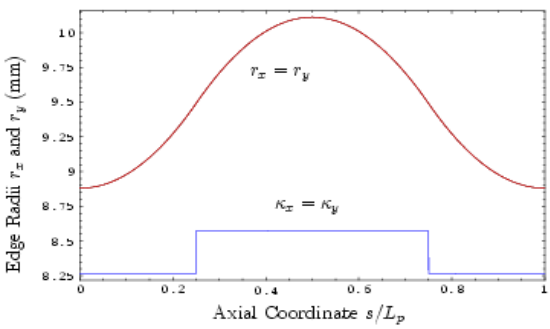

FODO Quadrupole Focusing
$(Q = 6.5614 \times 10^{-4})$

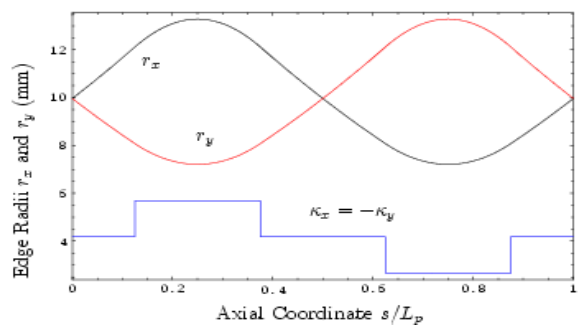

Symmetries of a matched beam are interpreted in terms of a local rms equivalent KV beam and moments/projections of the KV distribution

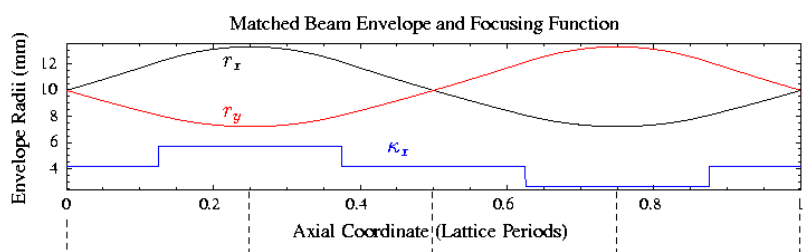

Projection

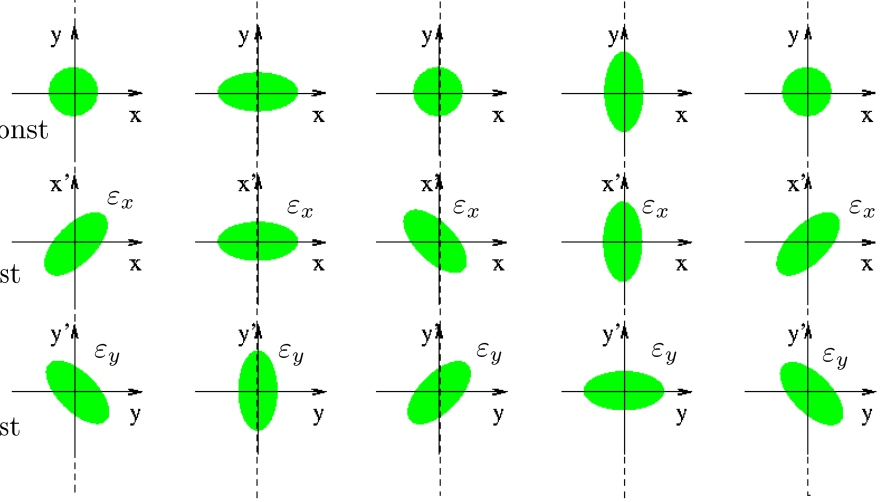

S6: Envelope Perturbations:

In the envelope equations set:

Envelope Perturbations:

$$r_x(s) = r_{xm}(s) + \delta r_x(s)$$
$$r_y(s) = r_{ym}(s) + \delta r_y(s)$$

Matched Envelope — Mismatch Perturbations

$$r_{xm}(s+L_p) = r_{xm}(s) \qquad r_{xm}(s) > 0$$
$$r_{ym}(s+L_p) = r_{ym}(s) \qquad r_{ym}(s) > 0$$

$$r_{xm}(s) \gg |\delta r_{xm}(s)|$$
$$r_{ym}(s) \gg |\delta r_{ym}(s)|$$

Driving Perturbations:

$$\kappa_x(s) \to \kappa_x(s) + \delta\kappa_x(s)$$
$$\kappa_y(s) \to \kappa_y(s) + \delta\kappa_y(s)$$
$$Q \to Q + \delta Q(s)$$
$$\varepsilon_x \to \varepsilon_x + \delta\varepsilon_x(s)$$
$$\varepsilon_y \to \varepsilon_y + \delta\varepsilon_y(s)$$

Amplitudes defined in terms of producing small envelope perturbations with:

$$r_{xm}(s) \gg |\delta r_{xm}(s)|$$
$$r_{ym}(s) \gg |\delta r_{ym}(s)|$$

- Driving terms and distribution errors drive envelope perturbations
  - Arise from many sources: focusing errors, lost particles, emittance growth, ...

The matched solution satisfies:

$$r''_{xm}(s) + \kappa_x(s) r_{xm}(s) - \frac{2Q}{r_{xm}(s) + r_{ym}(s)} - \frac{\varepsilon_x^2}{r_{xm}^3(s)} = 0$$
$$r''_{ym}(s) + \kappa_y(s) r_{ym}(s) - \frac{2Q}{r_{xm}(s) + r_{ym}(s)} - \frac{\varepsilon_y^2}{r_{ym}^3(s)} = 0$$
$$r_{xm}(s+L_p) = r_{xm}(s) \qquad r_{xm}(s) > 0$$
$$r_{ym}(s+L_p) = r_{ym}(s) \qquad r_{ym}(s) > 0$$

Linearized Perturbed Envelope Equations:

$$\delta r_x'' + \kappa_x \delta r_x + \frac{2Q}{(r_{xm}+r_{ym})^2}(\delta r_x + \delta r_y) + \frac{3\varepsilon_x^2}{r_{xm}^4}\delta r_x = -r_{xm}\delta\kappa_x + \frac{2}{r_{xm}+r_{ym}}\delta Q + \frac{2\varepsilon_x^2}{r_{xm}^3}\delta\varepsilon_x$$

$$\delta r_y'' + \kappa_y \delta r_y + \frac{2Q}{(r_{xm}+r_{ym})^2}(\delta r_x + \delta r_y) + \frac{3\varepsilon_y^2}{r_{ym}^4}\delta r_y = -r_{ym}\delta\kappa_y + \frac{2}{r_{xm}+r_{ym}}\delta Q + \frac{2\varepsilon_y^2}{r_{ym}^3}\delta\varepsilon_y$$

Homogeneous Equations:

$$\delta r_x'' + \kappa_x \delta r_x + \frac{2Q}{(r_{xm}+r_{ym})^2}(\delta r_x + \delta r_y) + \frac{3\varepsilon_x^2}{r_{xm}^4}\delta r_x = 0$$

$$\delta r_y'' + \kappa_y \delta r_y + \frac{2Q}{(r_{xm}+r_{ym})^2}(\delta r_x + \delta r_y) + \frac{3\varepsilon_y^2}{r_{ym}^4}\delta r_y = 0$$

Vector Form of the Linearized Perturbed Envelope Equations:

$$\frac{d}{ds}\delta\mathbf{R} + \mathbf{K}\cdot\delta\mathbf{R} = \delta\mathbf{P}$$

$$\delta\mathbf{R} \equiv \begin{pmatrix} \delta r_x \\ \delta r_x' \\ \delta r_y \\ \delta r_y' \end{pmatrix}$$ Coordinate vector

Coefficient matrix

$$\mathbf{K} \equiv \begin{pmatrix} 0 & -1 & 0 & 0 \\ k_{xm} & 0 & k_{0m} & 0 \\ 0 & 0 & 0 & -1 \\ k_{0m} & 0 & k_{ym} & 0 \end{pmatrix}$$

$$k_{0m} = \frac{2Q}{(r_{xm}+r_{ym})^2}$$

$$k_{jm} = \kappa_j + 3\frac{\varepsilon_j^2}{r_{jm}^4} + k_{0m} \qquad j = x,\ y$$

$$\delta\mathbf{P} \equiv \begin{pmatrix} 0 \\ -\delta\kappa_x + 2\frac{\delta Q}{r_{xm}+r_{ym}} + 2\frac{\varepsilon_x\delta\varepsilon_x}{r_{xm}^3} \\ 0 \\ -\delta\kappa_y + 2\frac{\delta Q}{r_{xm}+r_{ym}} + 2\frac{\varepsilon_y\delta\varepsilon_y}{r_{ym}^3} \end{pmatrix}$$ Driving perturbation vector

Expand solution into homogeneous and particular parts:

$$\delta\mathbf{R} = \delta\mathbf{R}_h + \delta\mathbf{R}_p$$

$\delta\mathbf{R}_h =$ homogeneous solution

$\delta\mathbf{R}_p =$ particular solution

$$\frac{d}{ds}\delta\mathbf{R}_h + \mathbf{K}\cdot\delta\mathbf{R}_h = 0 \qquad \frac{d}{ds}\delta\mathbf{R}_p + \mathbf{K}\cdot\delta\mathbf{R}_p = \delta\mathbf{P}$$

Homogeneous Solution:

- Describes normal mode oscillations
- Original analysis by Struckmeier and Reiser [Part. Accel. **14**, 227 (1984)]

Particular Solution:

- Describes action of driving terms
- Characterize in terms of projections on homogeneous response

Homogeneous solution expressible as a map:

$$\delta\vec{R}(s) = \mathbf{M}_e(s|s_i)\cdot\delta\vec{R}(s_i)$$
$$\delta\vec{R}(s) = (\delta r_x, \delta r'_x, \delta r_y, \delta r'_y)$$
$$\mathbf{M}_e(s|s_i) = 4\times 4 \text{ transfer map.}$$

Analogous to the 2x2 analysis of Hill's equation

Eigenvalues and eigenvectors of map through one period describe normal modes and stability properties:

$$\mathbf{M}_e(s_i + L_p|s_i)\cdot\vec{E}_n(s_i) = \lambda_n\vec{E}_n(s_i)$$

Stability

$$\lambda_n = \gamma_n e^{i\sigma_n} \quad \begin{array}{ll} \sigma_n \rightarrow & \text{mode phase advance (real)} \\ \gamma_n \rightarrow & \text{mode growth factor (real)} \end{array}$$

Mode Expansion/Launching

$$\delta\vec{R}(s_i) = \sum_{n=1}^{4}\alpha_n\vec{E}_n(s_i)$$
$$\alpha_n = \text{const}$$

Eigenvalue/Eigenvector Symmetry Classes:

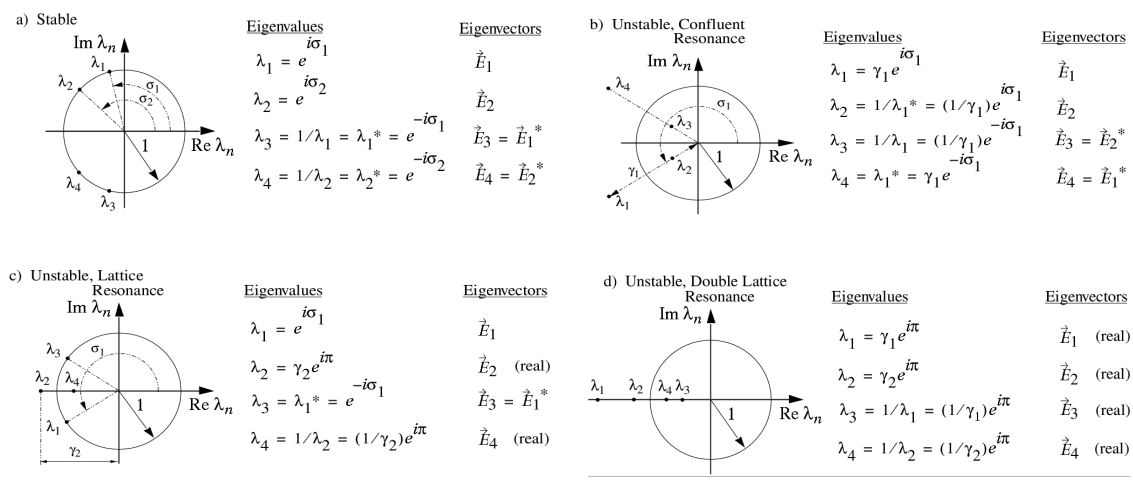

Symmetry classes of eigenvalues/eigenvectors:

- Determine normal mode symmetries
- See A. Dragt, Lectures on Nonlinear Orbit Dynamics, in Physics of High Energy Particle Accelerators, (AIP Conf. Proc. No. 87, 1982, p. 147)

Pure mode launching conditions:

Launching conditions for distinct normal modes corresponding to the eigenvalue classes illustrated:

$$A_\ell = \text{ mode amplitude (real)} \qquad \ell = \text{ mode index}$$
$$\psi_\ell = \text{ mode launch phase (real)}$$

Case	Mode	Launching Condition	Lattice Period Advance
(a) Stable	1 - Stable Osc.	$\delta\mathbf{R}_1 = A_1 e^{i\psi_1}\mathbf{E}_1 + \text{C.C.}$	$\mathbf{M}_e\delta\mathbf{R}_1(\psi_1) = \delta\mathbf{R}_1(\psi_1+\sigma_1)$
	2 - Stable Osc.	$\delta\mathbf{R}_2 = A_2 e^{i\psi_2}\mathbf{E}_2 + \text{C.C.}$	$\mathbf{M}_e\delta\mathbf{R}_2(\psi_2) = \delta\mathbf{R}_2(\psi_2+\sigma_2)$
(b) Unstable	1 - Exp. Growth	$\delta\mathbf{R}_1 = A_1 e^{i\psi_1}\mathbf{E}_1 + \text{C.C.}$	$\mathbf{M}_e\delta\mathbf{R}_1(\psi_1) = \gamma_1\delta\mathbf{R}_1(\psi_1+\sigma_1)$
Confluent Res.	2 - Exp. Damping	$\delta\mathbf{R}_2 = A_2 e^{i\psi_2}\mathbf{E}_2 + \text{C.C.}$	$\mathbf{M}_e\delta\mathbf{R}_2(\psi_2) = (1/\gamma_1)\delta\mathbf{R}_2(\psi_2+\sigma_1)$
(c) Unstable	1 - Stable Osc.	$\delta\mathbf{R}_1 = A_1 e^{i\psi_1}\mathbf{E}_1 + \text{C.C.}$	$\mathbf{M}_e\delta\mathbf{R}_1(\psi_1) = \delta\mathbf{R}_1(\psi_1+\sigma_1)$
Lattice Res.	2 - Exp. Growth	$\delta\mathbf{R}_2 = A_2\mathbf{E}_2$	$\mathbf{M}_e\delta\mathbf{R}_2 = -\gamma_2\delta\mathbf{R}_2$
	3 - Exp. Damping	$\delta\mathbf{R}_3 = A_3\mathbf{E}_4$	$\mathbf{M}_e\delta\mathbf{R}_3 = -(1/\gamma_2)\delta\mathbf{R}_3$
(d) Unstable	1 - Exp. Growth	$\delta\mathbf{R}_1 = A_1\mathbf{E}_1$	$\mathbf{M}_e\delta\mathbf{R}_1 = -\gamma_1\delta\mathbf{R}_1$
Double Lattice	2 - Exp. Growth	$\delta\mathbf{R}_2 = A_2\mathbf{E}_2$	$\mathbf{M}_e\delta\mathbf{R}_2 = -\gamma_2\delta\mathbf{R}_2$
Resonance	3 - Exp. Damping	$\delta\mathbf{R}_3 = A_3\mathbf{E}_3$	$\mathbf{M}_e\delta\mathbf{R}_3 = -(1/\gamma_1)\delta\mathbf{R}_3$
	4 - Exp. Damping	$\delta\mathbf{R}_4 = A_4\mathbf{E}_4$	$\mathbf{M}_e\delta\mathbf{R}_4 = -(1/\gamma_2)\delta\mathbf{R}_4$

$$\delta\vec{R}_\ell \equiv \delta\vec{R}_\ell(s_i), \quad \vec{E}_\ell \equiv \vec{E}_\ell(s_i), \quad \text{and} \quad \mathbf{M}_e \equiv \mathbf{M}_e(s_i+L_p|s_i)$$

$$\delta\mathbf{R}(s) = \begin{cases} A_1[\mathbf{E}_1(s)e^{i\psi_1(s)} + \mathbf{E}_1^*(s)e^{-i\psi_1(s)}] + A_2[\mathbf{E}_2(s)e^{i\psi_2(s)} + \mathbf{E}_2^*(s)e^{-i\psi_2(s)}], & \text{cases (a) and (b)}, \\ A_1[\mathbf{E}_1(s)e^{i\psi_1(s)} + \mathbf{E}_1^*(s)e^{-i\psi_1(s)}] + A_2\mathbf{E}_2(s) + A_3\mathbf{E}_4(s), & \text{case (c)}, \\ A_1\mathbf{E}_1(s) + A_2\mathbf{E}_2(s) + A_3\mathbf{E}_3(s) + A_4\mathbf{E}_4(s), & \text{case (d)}, \end{cases}$$

Decoupled Modes

In a continuous or periodic solenoidal focusing channel

$$\kappa_x(s) = \kappa_y(s) = \kappa(s)$$

with a round matched-beam solution

$$\varepsilon_x = \varepsilon_y = \varepsilon = \text{const}$$
$$r_{xm}(s) = r_{ym}(s) = r_m(s)$$

envelope perturbations are simply decoupled with:

$$\delta r_+(s) = \frac{\delta r_x(s) + \delta r_y(s)}{2} \qquad \text{Breathing Mode}$$
$$\delta r_-(s) = \frac{\delta r_x(s) - \delta r_y(s)}{2} \qquad \text{Quadrupole Mode}$$

$$\delta r_+'' + \kappa\,\delta r_+ + \frac{2Q}{r_m^2}\delta r_+ + \frac{3\varepsilon^2}{r_m^4}\delta r_+ = -r_m\left(\frac{\delta\kappa_x + \delta\kappa_y}{2}\right) + \frac{1}{r_m}\delta Q + \frac{2\varepsilon^2}{r_m^3}\left(\frac{\delta\varepsilon_x + \delta\varepsilon_y}{2}\right)$$
$$\delta r_-'' + \kappa\,\delta r_- + \frac{3\varepsilon^2}{r_m^4}\delta r_- = -r_m\left(\frac{\delta\kappa_x - \delta\kappa_y}{2}\right) + \frac{2\varepsilon^2}{r_m^3}\left(\frac{\delta\varepsilon_x - \delta\varepsilon_y}{2}\right)$$

Decoupled Mode Properties:

Space charge terms ~ Q only directly expressed in equation for $\delta r_+(s)$

- Indirectly present in both equations from matched envelope $r_m(s)$

Homogeneous Solution:

- Restoring term for $\delta r_+(s)$ larger than for $\delta r_-(s)$
  - Breathing mode oscillates faster than quadrupole mode

Particular Solution:

- Misbalances in focusing and emittance driving terms can project onto either mode
  - nonzero perturbed $\kappa_x(s) + \kappa_y(s)$ and $\varepsilon_x(s) + \varepsilon_y(s)$ project onto breathing mode
  - nonzero perturbed $\kappa_x(s) - \kappa_y(s)$ and $\varepsilon_x(s) - \varepsilon_y(s)$ project onto quadrupole mode
- Perveance driving perturbations project only on breathing mode

Previous symmetry classes greatly reduce for decoupled modes:

Previous homogeneous 4x4 solution map:

$$\delta\vec{R}(s) = \mathbf{M}_e(s|s_i) \cdot \delta\vec{R}(s_i)$$
$$\delta\vec{R}(s) = (\delta r_x, \delta r_x', \delta r_y, \delta r_y')$$
$$\mathbf{M}_e(s|s_i) = 4 \times 4 \text{ transfer map.}$$

greatly reduces to two independent 2x2 maps:

$$\boxed{\begin{aligned} &\delta\mathbf{R} \equiv (\delta r_+, \delta r_+', \delta r_-, \delta r_-') \\ &\mathbf{M}_e(s_i + L_p|s_i) = \begin{bmatrix} \mathbf{M}_+(s_i + L_p|s_i) & 0 \\ 0 & \mathbf{M}_-(s_i + L_p|s_i) \end{bmatrix} \end{aligned}}$$

with corresponding eigenvalue problems:

$$\boxed{\mathbf{M}_\pm(s_i + L_p|s_i) \cdot \mathbf{E}_n(s_i) = \lambda_\pm \mathbf{E}_n(s_i)}$$

Many familiar results from analysis of Hills equation can be immediately applied to the decoupled case, for example:

$$\frac{1}{2}|\text{Tr } \mathbf{M}_\pm(s_i + L_p|s_i)| < 1 \quad \longrightarrow \quad \text{mode stability}$$

Eigenvalue symmetries and launching conditions simplify for decoupled modes

Eigenvalue Symmetry 1:

Stable

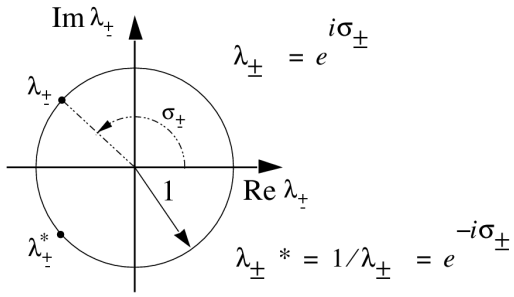

Eigenvalue Symmetry 2:

Unstable, Lattice Resonance

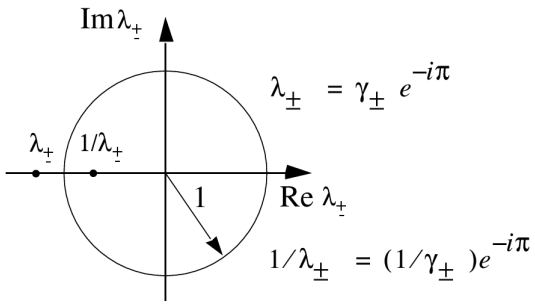

Launching Condition / Projections

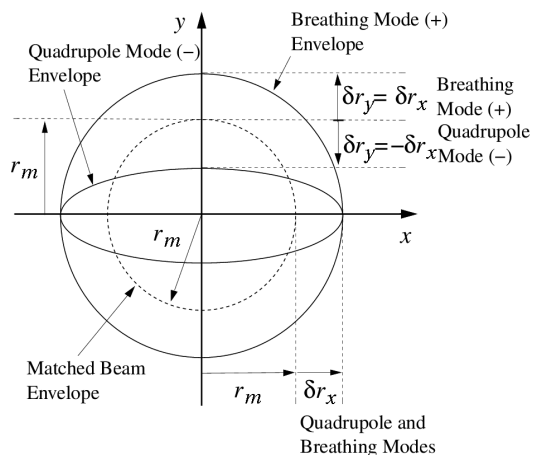

General Mode Limits

Using phase-amplitude analysis can show for any linear focusing lattice:

1) Phase advance of any normal mode satisfies the zero space-charge limit:

$$\boxed{\lim_{Q\to 0} \sigma_\ell = 2\sigma_0}$$

2) Pure normal modes evolve with a quadratic phase-space (Courant-Snyder) invariant in the normal coordinates of the mode

Simply expressed for decoupled modes:

$$\boxed{\left[\frac{\delta r_\pm(s)}{w_\pm(s)}\right]^2 + \left[w'_\pm(s)\delta r_\pm(s) - w_\pm(s)\delta r'_\pm(s)\right]^2 = \text{const}}$$

where

$$w''_+(s) + \kappa(s)\, w_+(s) + \frac{2Q}{r_m^2(s)} w_+(s) + \frac{3\varepsilon^2}{r_m^4(s)} w_+(s) - \frac{1}{w_+^3(s)} = 0$$

$$w''_-(s) + \kappa(s)\, w_-(s) + \frac{3\varepsilon^2}{r_m^4(s)} w_-(s) - \frac{1}{w_-^3(s)} = 0$$

$$w_\pm(s + L_p) = w_\pm(s)$$

Analogous for coupled modes [See Edwards and Teng applies, IEEE Trans Nuc. Sci. **20**, 885 (1973)]

S7: Envelope Modes in Continuous Focusing

Focusing:

$$\kappa_x(s) = \kappa_y(s) = k_{\beta 0}^2 = \left(\frac{\sigma_0}{L_p}\right)^2 = \text{const}$$

Matched beam:

symmetric beam:

$$\varepsilon_x = \varepsilon_y = \varepsilon = \text{const}$$
$$r_{xm}(s) = r_{ym}(s) = r_m(s)$$

match condition:

$$k_{\beta 0}^2 r_m - \frac{Q}{r_m} - \frac{\varepsilon^2}{r_m^3} = 0$$

depressed phase advance:

$$\sigma = \sqrt{\sigma_0^2 - \frac{Q}{(r_m/L_p)^2}} = \frac{\varepsilon L_p}{r_m^2}$$

one parameter needed for scaled solution:

$$\frac{k_{\beta 0}^2 \varepsilon^2}{Q^2} = \frac{\sigma_0^2 \varepsilon^2}{Q^2 L_p^2} = \frac{(\sigma/\sigma_0)^2}{[1-(\sigma/\sigma_0)^2]^2}.$$

Decoupled Modes:

$$\delta r_\pm(s) = \frac{\delta r_x(s) \pm \delta r_y(s)}{2}$$

Envelope equations of motion become:

$$\boxed{\begin{aligned} L_p^2 \frac{d^2}{ds^2}\left(\frac{\delta r_+}{r_m}\right) + \sigma_+^2 \left(\frac{\delta r_+}{r_m}\right) &= -\frac{\sigma_0^2}{2}\left(\frac{\delta\kappa_x}{k_{\beta 0}^2} + \frac{\delta\kappa_y}{k_{\beta 0}^2}\right) + (\sigma_0^2 - \sigma^2)\frac{\delta Q}{Q} + \sigma^2\left(\frac{\delta\varepsilon_x}{\varepsilon} + \frac{\delta\varepsilon_y}{\varepsilon}\right) \\ L_p^2 \frac{d^2}{ds^2}\left(\frac{\delta r_-}{r_m}\right) + \sigma_-^2 \left(\frac{\delta r_-}{r_m}\right) &= -\frac{\sigma_0^2}{2}\left(\frac{\delta\kappa_x}{k_{\beta 0}^2} - \frac{\delta\kappa_y}{k_{\beta 0}^2}\right) + \sigma^2\left(\frac{\delta\varepsilon_x}{\varepsilon} - \frac{\delta\varepsilon_y}{\varepsilon}\right) \end{aligned}}$$

$\sigma_+ \equiv \sqrt{2\sigma_0^2 + 2\sigma^2}$ "breathing" mode phase advance

$\sigma_- \equiv \sqrt{\sigma_0^2 + 3\sigma^2}$ "quadrupole" mode phase advance

Homogeneous Solution (normal modes):

$$\boxed{\delta r_\pm(s) = \delta r_\pm(s_i)\cos\left(\sigma_\pm \frac{s-s_i}{L_p}\right) + \frac{\delta r'_\pm(s_i)}{\sigma_\pm/L_p}\sin\left(\sigma_\pm \frac{s-s_i}{L_p}\right)}$$

Mode Phase Advances

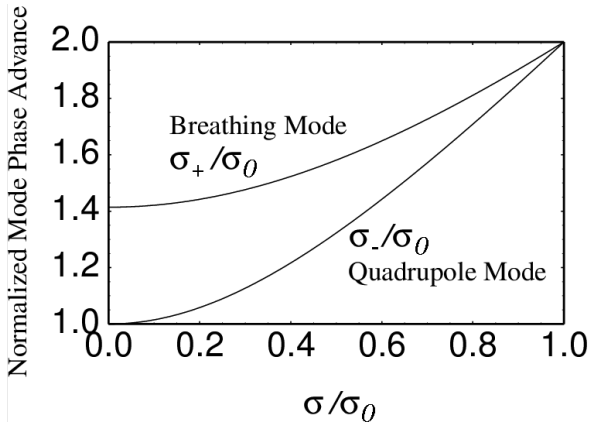

Mode Projections

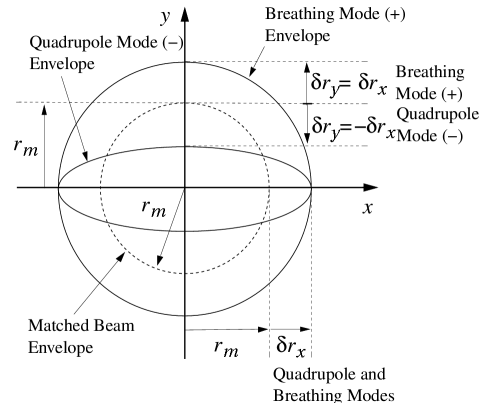

Particular Solution (driving perturbations):

Green's function form of solution:

$$\frac{\delta r_\pm(s)}{r_m} = \frac{1}{L_p^2}\int_{s_i}^{s} d\tilde{s}\; G_\pm(s,\tilde{s})\delta p_\pm(\tilde{s})$$

$$\delta p_+(s) = -\frac{\sigma_0^2}{2}\left[\frac{\delta\kappa_x(s)}{k_{\beta 0}^2} + \frac{\delta\kappa_y(s)}{k_{\beta 0}^2}\right] + (\sigma_0^2 - \sigma^2)\frac{\delta Q(s)}{Q} + \sigma^2\left[\frac{\delta\varepsilon_x(s)}{\varepsilon} + \frac{\delta\varepsilon_y(s)}{\varepsilon}\right]$$

$$\delta p_-(s) = -\frac{\sigma_0^2}{2}\left[\frac{\delta\kappa_x(s)}{k_{\beta 0}^2} - \frac{\delta\kappa_y(s)}{k_{\beta 0}^2}\right] + \sigma^2\left[\frac{\delta\varepsilon_x(s)}{\varepsilon} - \frac{\delta\varepsilon_y(s)}{\varepsilon}\right]$$

$$G_\pm(s,\tilde{s}) = \frac{1}{\sigma_\pm/L_p}\sin\left(\sigma_\pm\frac{s-\tilde{s}}{L_p}\right)$$

Green's function solution is fully general. Insight gained from simplified solutions for specific classes of driving perturbations:

- Adiabatic
- Sudden

covered here

- Ramped
- Harmonic

covered in PRSTAB review article

Continuous Focusing – adiabatic particular solution

For driving perturbations $\delta p_+(s)$ and $\delta p_-(s)$ slow on quadrupole mode wavelength ~ $2\pi L_p/\sigma_-$ the solution is:

$$\frac{\delta r_+(s)}{r_m} = \frac{\delta p_+(s)}{\sigma_+^2}$$

$$= -\left[\frac{1}{2}\frac{1}{1+(\sigma/\sigma_0)^2}\right]\frac{1}{2}\left(\frac{\delta\kappa_x(s)}{k_{\beta 0}^2}+\frac{\delta\kappa_y(s)}{k_{\beta 0}^2}\right) + \left[\frac{1}{2}\frac{1-(\sigma/\sigma_0)^2}{1+(\sigma/\sigma_0)^2}\right]\frac{\delta Q(s)}{Q}$$

$$+\left[\frac{(\sigma/\sigma_0)^2}{1+(\sigma/\sigma_0)^2}\right]\frac{1}{2}\left(\frac{\delta\varepsilon_x(s)}{\varepsilon}+\frac{\delta\varepsilon_y(s)}{\varepsilon}\right)$$

Focusing

Perveance

Emittance

$$\frac{\delta r_-(s)}{r_m} = \frac{\delta p_-(s)}{\sigma_-^2}$$

$$= -\left[\frac{1}{1+3(\sigma/\sigma_0)^2}\right]\frac{1}{2}\left(\frac{\delta\kappa_x(s)}{k_{\beta 0}^2}-\frac{\delta\kappa_y(s)}{k_{\beta 0}^2}\right)$$

$$+\left[\frac{2(\sigma/\sigma_0)^2}{1+3(\sigma/\sigma_0)^2}\right]\frac{1}{2}\left(\frac{\delta\varepsilon_x(s)}{\varepsilon}-\frac{\delta\varepsilon_y(s)}{\varepsilon}\right)$$

Focusing

Emittance

Coefficients of adiabatic terms in square brackets“[ ]”

Continuous Focusing – adiabatic solution coefficients

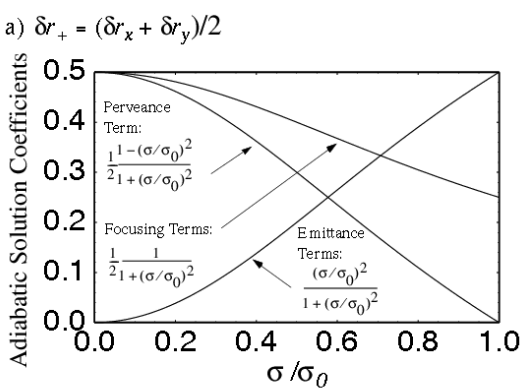

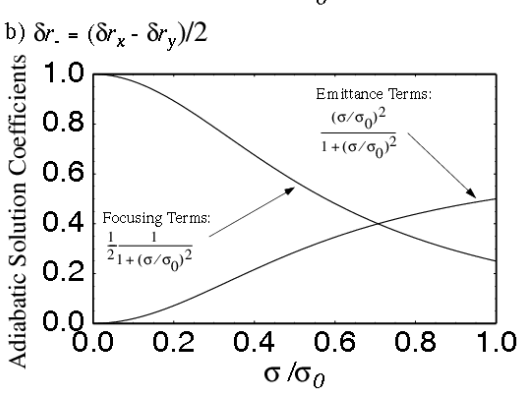

Relative strength of:

- Space-Charge (Perveance)
- Applied Focusing
- Emittance

terms vary with space-charge depression (σ/σ_0) for both breathing and quadrupole modes.

Continuous Focusing – sudden particular solution

For step function driving perturbations of form:

$$\boxed{\delta p_\pm(s) = \widehat{\delta p_\pm}\Theta(s - s_p)} \qquad s = s_p = \text{axial coordinate perturbation applied}$$

with amplitudes:

$$\widehat{\delta p_+} = -\frac{\sigma_0^2}{2}\left[\frac{\widehat{\delta\kappa_x}}{k_{\beta 0}^2} + \frac{\widehat{\delta\kappa_y}}{k_{\beta 0}^2}\right] + (\sigma_0^2 - \sigma^2)\frac{\widehat{\delta Q}}{Q} + \sigma^2\left[\frac{\widehat{\delta\varepsilon_x}}{\varepsilon} + \frac{\widehat{\delta\varepsilon_y}}{\varepsilon}\right] = \text{const}$$

$$\widehat{\delta p_-} = -\frac{\sigma_0^2}{2}\left[\frac{\widehat{\delta\kappa_x}}{k_{\beta 0}^2} - \frac{\widehat{\delta\kappa_y}}{k_{\beta 0}^2}\right] + \sigma^2\left[\frac{\widehat{\delta\varepsilon_x}}{\varepsilon} - \frac{\widehat{\delta\varepsilon_y}}{\varepsilon}\right] = \text{const}$$

The solution is given by the substitution in the expression for the adiabatic solution:

$$\boxed{\delta p_\pm(s) \to \widehat{\delta p_\pm}\left[1 - \cos\left(\sigma_\pm \frac{s - s_p}{L_p}\right)\right]\Theta(s - s_p)}$$

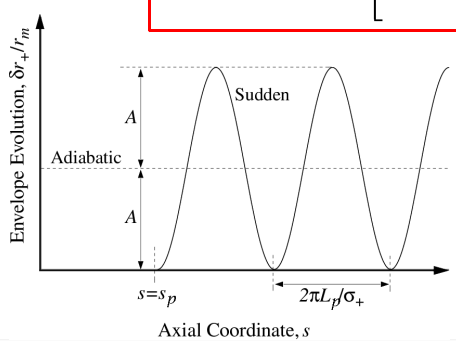

2x Excursion

Adiabatic Excursion

For the same amplitude of total driving perturbations, sudden perturbations result in 2x the envelope excursion that adiabatic perturbations produce.

S8: Envelope Modes in Periodic Focusing Channels

Overview

- Much more complicated the continuous limit results
  - Lattice can couple to oscillations and destabilize the system
  - Broad parametric instability can result
- Instability bands calculated will exclude wide ranges of parameter space from machine operation
  - Exclusion region depends on focusing type

Solenoidal Focusing – Matched Envelope Solution

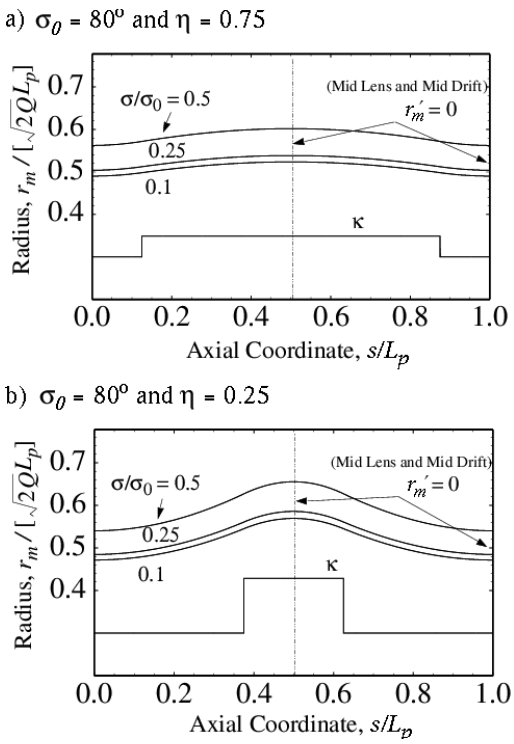

Focusing:

$$\kappa_x(s) = \kappa_y(s) = \kappa(s)$$

$$\kappa(s + L_p) = \kappa(s)$$

Matched Beam:

$$\varepsilon_x = \varepsilon_y = \varepsilon = \text{const}$$
$$r_{xm}(s) = r_{ym}(s) = r_m(s)$$

$$r_m(s + L_p) = r_m(s)$$

Using a transfer matrix approach on undepressed single-particle orbits set the strength of the focusing function for specified undepressed particle phase advance:

Solenoidal Focusing:

$$\cos\sigma_0 = \cos(2\Theta) - \frac{1-\eta}{\eta}\Theta\sin(2\Theta)$$

$$\Theta \equiv \frac{\sqrt{\hat{\kappa}}L_p}{2}$$

Solenoidal Focusing – parametric plots of breathing and quadrupole envelope mode phase advances two values of undepressed phase advance

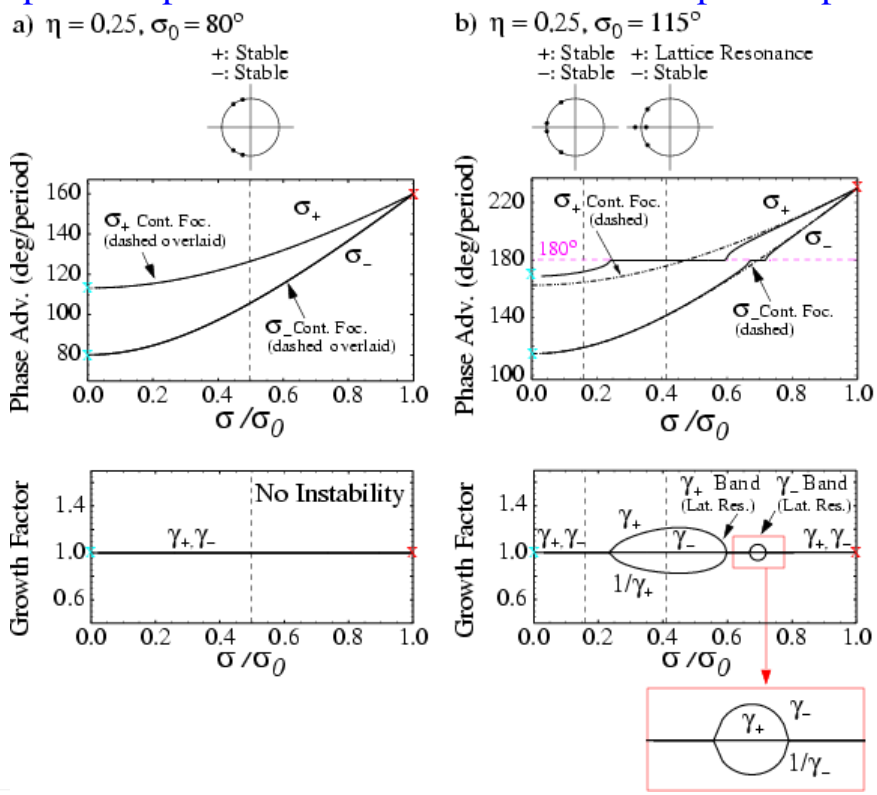

Solenoidal Focusing – mode instability bands become wider and stronger for smaller occupancy

$$\eta = \begin{cases} 0.75 & \text{(Blue)} \\ 0.25 & \text{(Green)} \\ 0.10 & \text{(Red)} \end{cases} \qquad \sigma_0 = 115^\circ$$

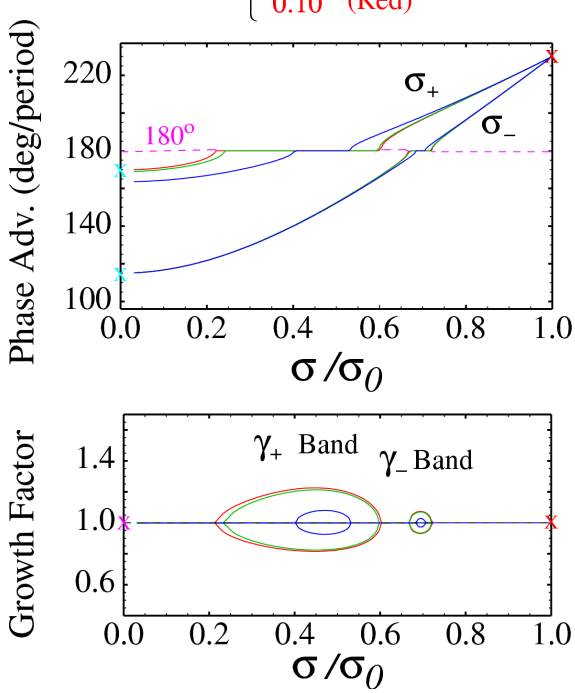

Solenoidal Focusing – broad ranges of parametric instability are found for the breathing and quadrupole bands that must be avoided in machine operation

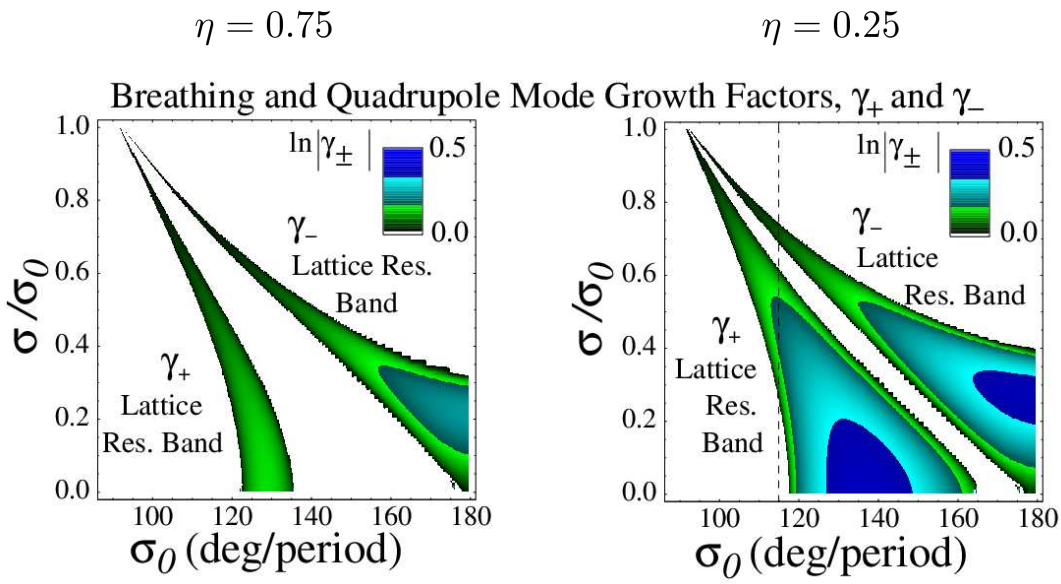

Solenoidal Focusing – parametric mode properties of band oscillations

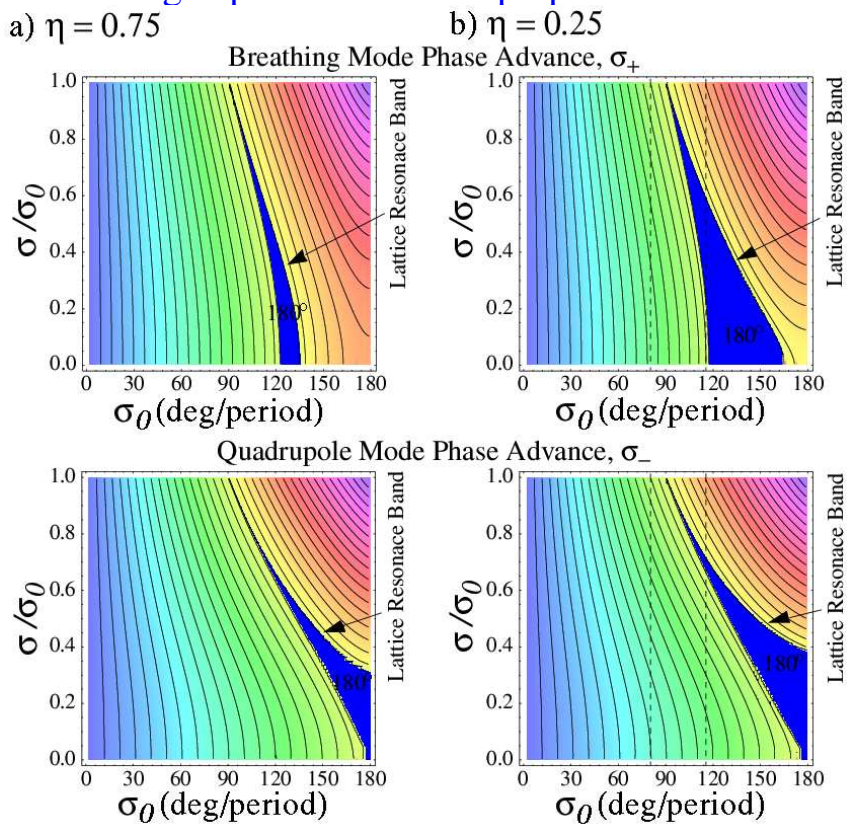

Quadrupole Doublet Focusing – Matched Envelope Solution

FODO and Syncopated Lattices

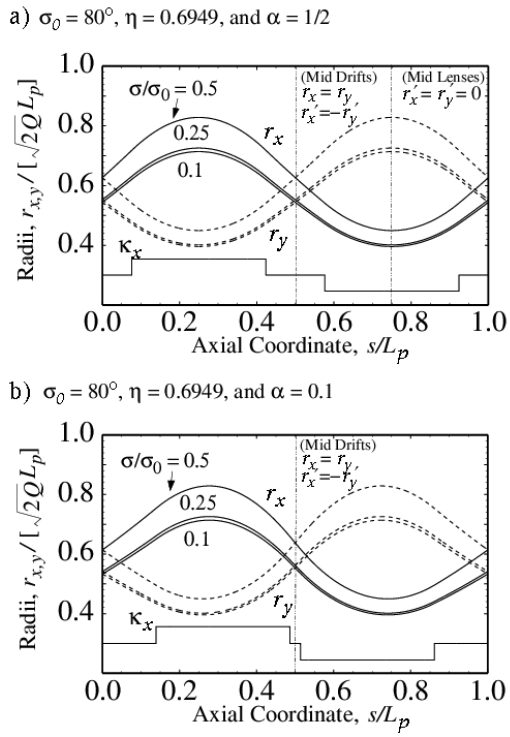

Focusing:

$$\kappa_x(s) = -\kappa_y(s) = \kappa_q(s)$$

$$\kappa_q(s + L_p) = \kappa_q(s)$$

Matched Beam:

$$r_{xm}(s + L_p) = r_{xm}(s)$$
$$r_{ym}(s + L_p) = r_{ym}(s)$$

Using a transfer matrix approach on undepressed single-particle orbits set the strength of the focusing function for specified undepressed particle phase advance:

Quadrupole Focusing:

$$\cos\sigma_0 = \cos\Theta\cosh\Theta + \frac{1-\eta}{\eta}\Theta(\cos\Theta\sinh\Theta - \sin\Theta\cosh\Theta) - 2\alpha(1-\alpha)\frac{(1-\eta)^2}{\eta^2}\Theta^2\sin\Theta\sinh\Theta$$

$$\Theta \equiv \frac{\sqrt{|\widehat{\kappa_q}|}L_p}{2}$$

Quadrupole Focusing – parametric plots of breathing and quadrupole envelope mode phase advances two values of undepressed phase advance

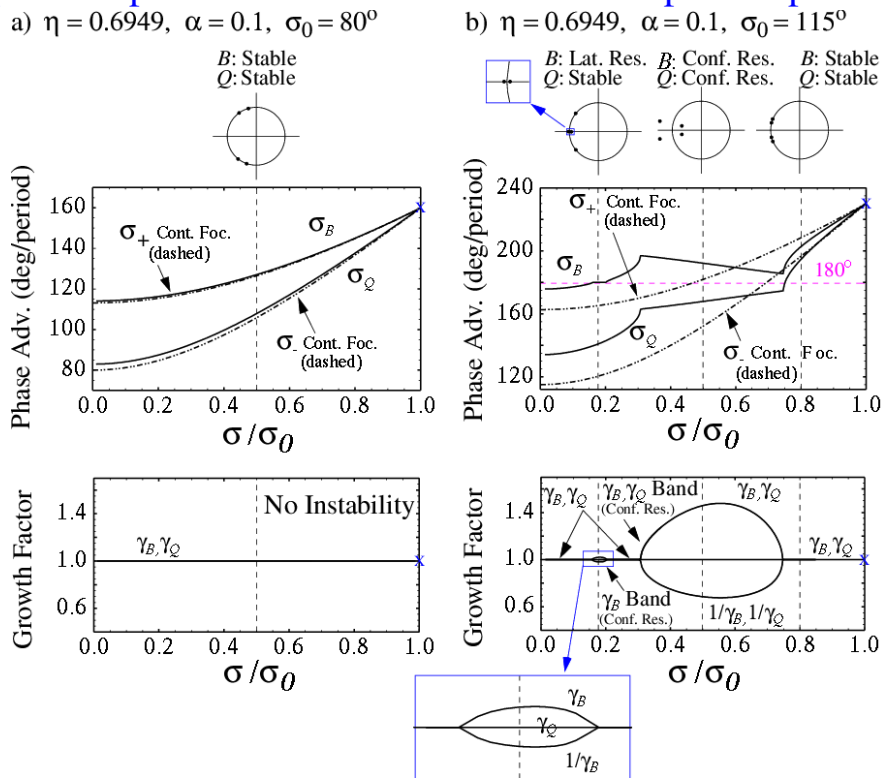

Quadrupole Focusing – mode instability bands vary little/strongly with occupancy for FODO/syncopated lattices

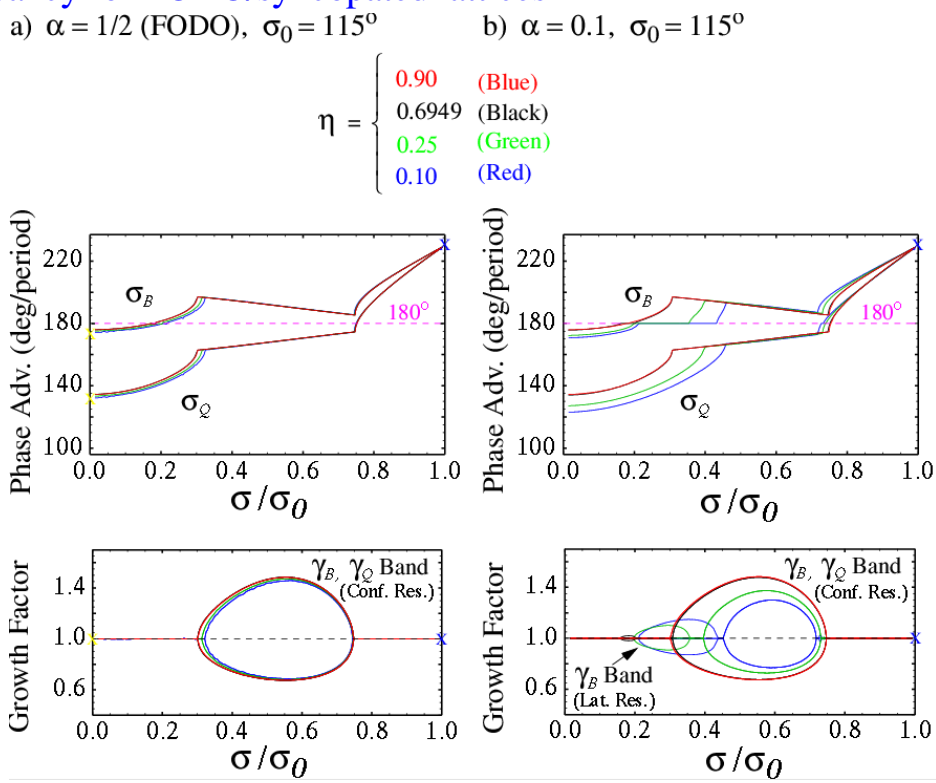

Quadrupole Focusing – broad ranges of parametric instability are found for the breathing and quadrupole bands that must be avoided in machine operation

FODO Lattice
$\eta = 0.6949, \quad \alpha = 1/2$

Syncopated Lattice
$\eta = 0.6949, \quad \alpha = 0.1$

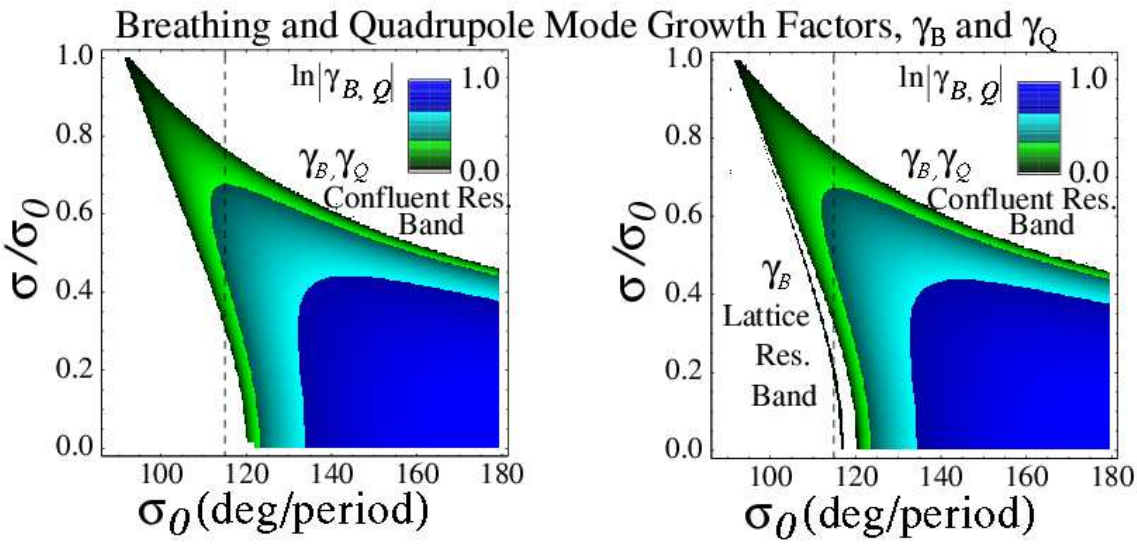

Quadrupole Focusing – parametric mode properties of band oscillations

a) $\eta = 0.6949, \alpha = 1/2$ b) $\eta = 0.6949, \alpha = 0.1$

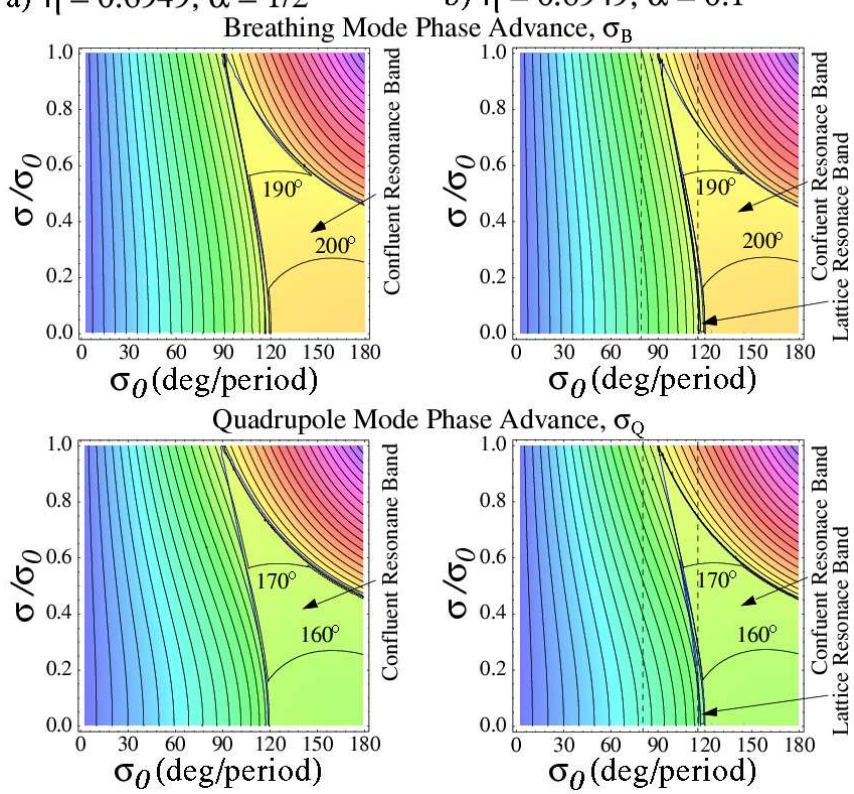

Quadrupole Focusing – mode structure varies strongly with mode phase and the location in the lattice (FODO example)

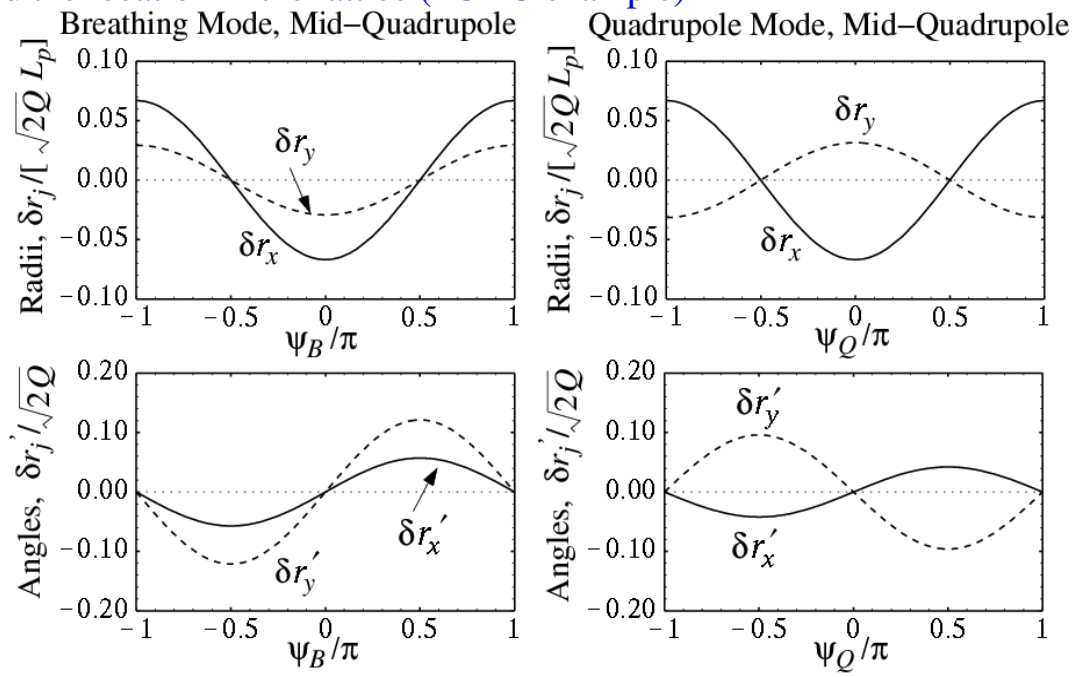

$\delta r_x \neq \delta r_y$

generally not exact

breathing symmetry

$\delta r_x \neq -\delta r_y$

generally not exact

quadrupole symmetry

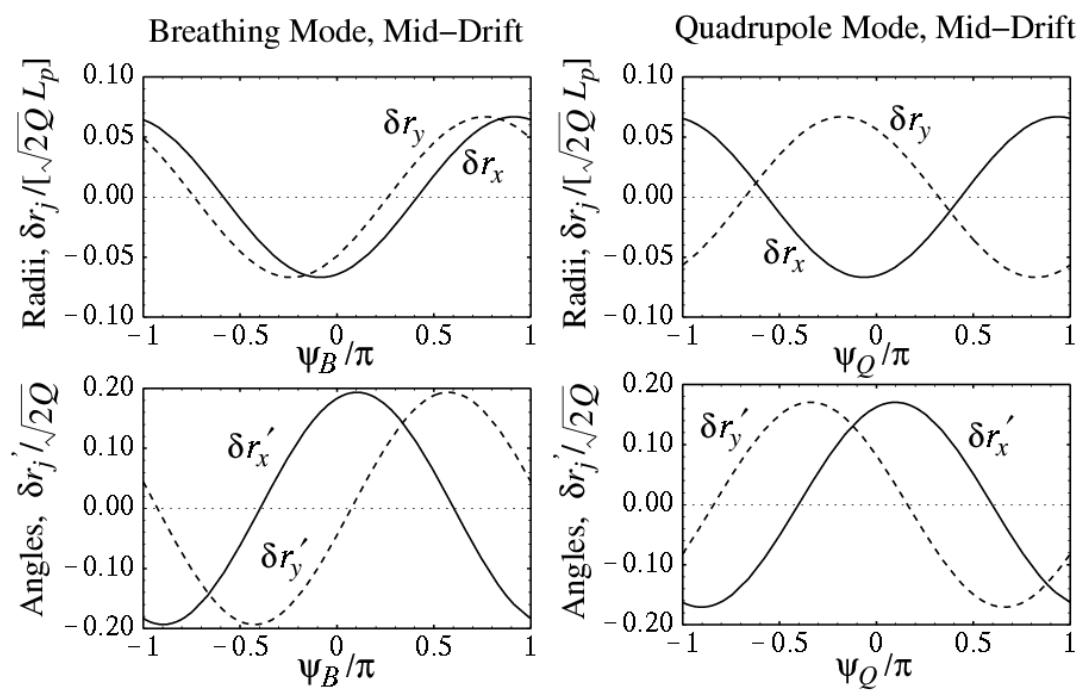

$\delta r_x \neq \delta r_y$

generally not exact

breathing symmetry

$\delta r_x \neq -\delta r_y$

generally not exact

quadrupole symmetry

Summary: Envelope band instabilities and growth rates for periodic solenoidal and quadrupole doublet focusing lattices

Envelope Mode Instability Growth Rates

Solenoid (η = 0.25)

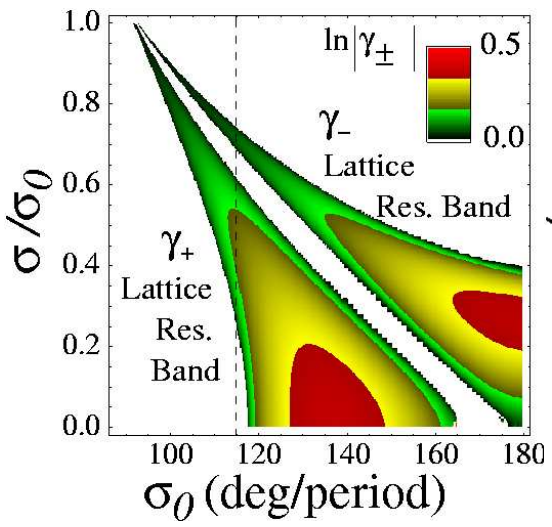

Quadrupole FODO (η = 0.70)

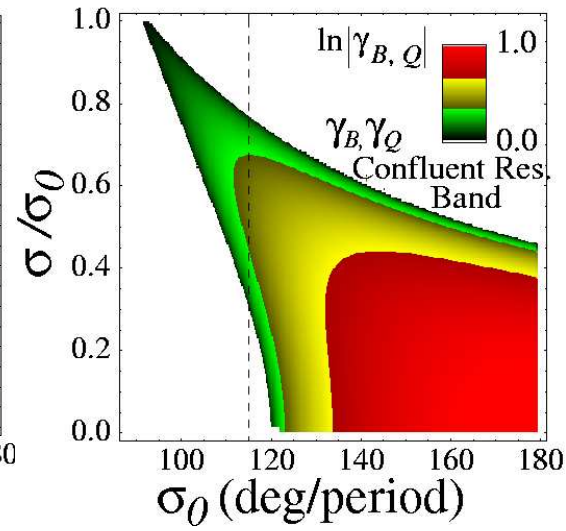

[S.M. Lund and B. Bukh, PRSTAB 024801 (2004)]

S9: Transport Limit Scaling Based on Envelope Models

See Handwritten Notes

S8: Centroid and Envelope Descriptions via 1st Order Coupled Moment Equations

To include in future editions of notes

References: For more information see:

Image charge couplings:

E. P. Lee, E. Close, and L. Smith, Nuc. Inst. And Methods, 1126 (1987)

Seminal work on envelope modes:

J. Struckmeier and M. Reiser, *Theoretical Studies of Envelope Oscillations and Instabilities of Mismatched Intense Charged-Particle Beams in Periodic Focusing Channels*, Part. Accel. **14,** 227 (1984)

M. Reiser, *Theory and Design of Charged Particle Beams* (John Wiley, 1994)

Extensive review on envelope instabilities:

S. M. Lund and B. Bukh, *Stability Properties of the KV Envelope Equations Describing Intense Ion Beam Transport,* PRSTAB **7** 024801 (2004)

KV results:

F. Sacherer, *Transverse Space-Charge Effects in Circular Accelerators*, Univ. of California Berkeley, Ph.D Thesis (1968)

I. Kaphinskij and V. Vladimirskij, in *Proc. Of the Int. Conf. On High Energy Accel. and Instrumentation* (CERN Scientific Info. Service, Geneva, 1959) p. 274

Symmetries and phase-amplitude methods:

A. Dragt, *Lectures on Nonlinear Orbit Dynamics* in *Physics of High Energy Particle Accelerators,* (American Institute of Physics, 1982), AIP Conf. Proc. No. 87, p. 147

E. D. Courant and H. S. Snyder, *Theory of the Alternating-Gradient Synchrotron*, Annals of Physics **3**, 1 (1958)

Analytical analysis of matched envelope solutions and transport scaling:

E. P. Lee, *Precision matched solution of the coupled beam envelope equations for a periodic quadrupole lattice with space-charge*, Phys. Plasmas 9, 4301 (2005).

J.J. Barnard and S.M. Lund
USPAS, June 2006

§9 Transport Limit Scaling Based on the Matched Beam Envelope Equations for Periodic Focusing Channels

The scaling of the maximum beam current, or equivalently, the maximum perveance Q that can be transported at a given energy with a specified focusing technology and lattice is of critical importance in designing optimal transport and acceleration channels. Needed equations can be derived from approximate analytical solutions to the matched beam envelope equations for a given lattice. Alternatively, numerical solutions of the envelope equations can be evaluated. But analytical solutions are preferable to understand scaling and enable rapid evaluation of design tradeoffs.

As a practical matter, equations derived must be applied to regimes where technology is feasible.

- Magnet Field Limits
- Electron breakdown
- Vacuum

⋮

Transport limits are inextricably linked to technology. Moreover, higher order stability constraints etc. must also be respected. Treatments of these topics are beyond the scope of this class. Here we present simplified treatments to highlight issues and methods.

First review an example sketched by J.J. Barnard in the Intro. lectures.

Transport Limits of a Periodic FODO Quadrupole Transport Channel

$$r_{xm}'' + \frac{(\gamma_b\beta_b)'}{(\gamma_b\beta_b)} r_{xm}' + \kappa_x r_{xm} - \frac{2Q}{r_{xm}+r_{ym}} - \frac{\varepsilon_x^2}{r_{xm}^3} = 0$$

$$r_{ym}'' + \frac{(\gamma_b\beta_b)'}{(\gamma_b\beta_b)} r_{ym}' - \kappa_x r_{ym} - \frac{2Q}{r_{xm}+r_{ym}} - \frac{\varepsilon_y^2}{r_{ym}^3} = 0$$

$$r_{xm}(s+L_p) = r_{xm}(s) \quad ; \quad r_{ym}(s+L_p) = r_{ym}(s)$$

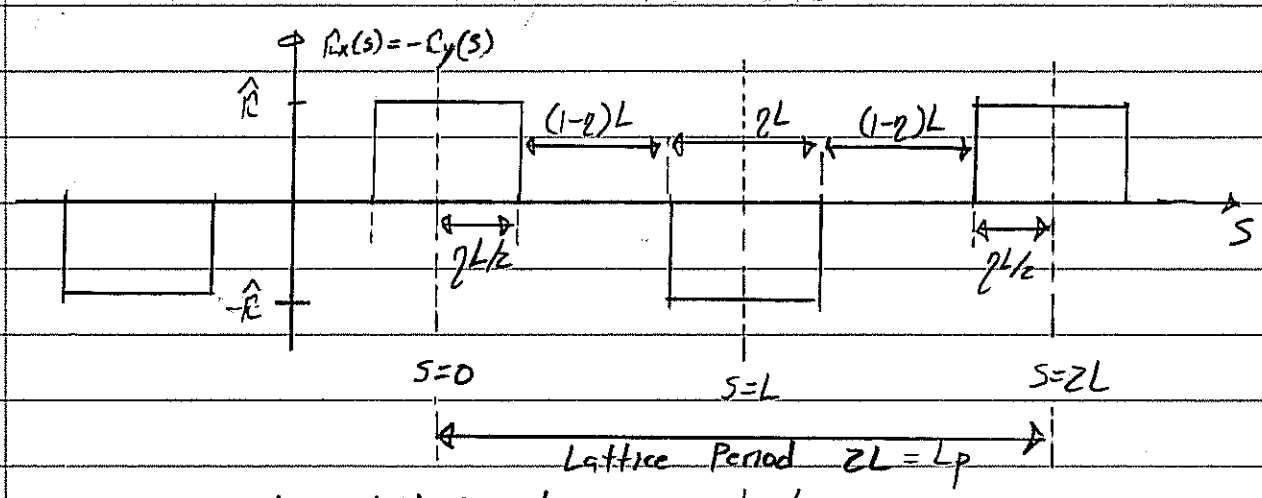

L = Half-Period $\quad L = L_p/2$

η = Quadrupole "occupancy" $\quad 0 < \eta \le 1$

$\hat{\kappa}$ = Focus strength $\quad \hat{\kappa} = \begin{cases} \dfrac{qE_y'(s)}{m\gamma_b\beta_b^2c^2} \; ; \text{ Electric} \\ \dfrac{qB_y'(s)}{m\gamma_b\beta_b c} \; ; \text{ Magnetic} \end{cases}$

Expand $\kappa_x(s)$ as a Fourier Series:

$$\boxed{\begin{aligned} \kappa_x(s) &= \sum_{n=1}^{\infty} \kappa_n \cos\left(\frac{n\pi s}{L}\right) \\ \kappa_n &= \frac{1}{L}\int_0^{2L} \kappa_x(s)\cos\left(\frac{n\pi s}{L}\right) = \frac{2\hat{\kappa}}{n\pi}\left[1-(-1)^n\right]\sin\left(\frac{n\pi\eta}{2}\right) \end{aligned}}$$

And expand the periodic matched beam envelope by:

$$r_{xm} = r_b\left[1 + \Delta\cos\left(\frac{\pi s}{L}\right)\right] + \sum_{n=2}^{\infty}\Delta_{xn}\cos\left(\frac{n\pi s}{L}\right)$$

$$r_{ym} = r_b\left[1 - \Delta\cos\left(\frac{\pi s}{L}\right)\right] + \sum_{n=2}^{\infty}\Delta_{yn}\cos\left(\frac{n\pi s}{L}\right)$$

r_b = const = avg. beam radius.
$|\Delta|$ = const $\ll 1$
$\Delta_{\substack{x\\y}n}$ constants with $|\Delta_{\substack{x\\y}n}| \ll |\Delta|$

Take:

- $(\gamma_b\beta_b)' = 0 \Rightarrow$ coasting beam
- $\varepsilon_x = \varepsilon_y = \varepsilon \Rightarrow$ isotropic beam

and insert these expansions in the envelope equations.

Neglect:

- All terms $\mathcal{O}(\Delta^2)$ and higher
- Fast oscillation terms $\sim \cos\left(\frac{n\pi s}{L}\right)$ with $n \geq 2$.

to obtain two independent constraint equations:

Avg (const): $$\frac{2\Delta\hat{\kappa}}{\pi} r_b \sin\left(\frac{\pi\eta}{2L}\right) - \frac{Q}{r_b} - \frac{\varepsilon^2}{r_b^3} = 0$$

Fundamental $\propto \cos\left(\frac{\pi s}{L}\right)$: $$-\Delta\left(\frac{\pi}{L}\right)^2 r_b + \frac{4\hat{\kappa} r_b}{\pi}\sin\left(\frac{\pi\eta}{2L}\right) + \frac{3\Delta\varepsilon^2}{r_b^3} = 0$$

These equations can be solved to express the maximum beam edge excursion as

$$\boxed{\mathrm{Max}[r_{xm}] = \mathrm{Max}[r_{ym}] \simeq r_b(1+|\Delta|) = r_b\left\{1 + \frac{4|\hat{\kappa}|L^2}{\pi^3}\frac{\sin\left(\frac{\pi\eta}{2L}\right)}{\left(1-\frac{3L^2\varepsilon^2}{\pi^2 r_b^4}\right)}\right\}}$$

and the beam Perveance as:

$$\boxed{Q = \frac{2}{\pi^2}\left[\frac{\sin\left(\frac{\pi\eta}{2L}\right)}{\left(\frac{\pi\eta}{2L}\right)}\right]^2 \frac{\eta^2\hat{\kappa}^2L^2r_b^2}{\left(1-\frac{3L^2\varepsilon^2}{\pi^2r_b^4}\right)} - \frac{\varepsilon^2}{r_b^2}}$$

<u>Design Strategy:</u>

1) Choose a lattice period $2L$, quadrupole occupancy η, and clear machine "pipe" radius r_p consistent with focusing technology employed.
2) Choose the largest possible focus strength $\hat{\kappa}$ (quadrupole current or voltage excitation) for beam energy with undepressed particle phase advance:

$$\boxed{\sigma_0 \lesssim 80^\circ / \text{period}. \quad \text{"Tietenback Limit"}}$$

- Larger phase advances correspond to stronger focus and smaller beam cross-sectional area for given values of Q, ε.

- Weaker phase advance suppresses various particle, envelope, and collective instabilities for reliable transport: [Ref: M.G. Tietenback, "Space-Charge Limits on the Transport of Ion Beams," U.C. Berkeley Ph.d Thesis, 1986 LBL-22465

3) Choose a suitable beam-edge to aperture clearance factor:

$$\boxed{\begin{aligned} r_p &= \mathrm{Max}[r_{xm}] + \Delta_p \\ \Delta_p &= \text{Clearance.} \end{aligned}}$$

to allow for misalignments, limit scraping of halo particles outside the beam core, reduce image charges, gas propagation times from the aperture to the beam, and other nonideal effects.

4) Evaluate choices made using higher-order theory, numerical simulations etc.. Iterate choices made to reoptimize when evaluating cost.

Effective application of this formulation requires extensive practical knowledge:

- Nonideal effects: collective instabilities, halo, electron and gas interactions (species contamination), ...
- Technology limits: Voltage breakdown, vacuum, superconducting magnets, ...

In practice, for intense beam transport, the emittance terms $\varepsilon_x, \varepsilon_y$ can often be neglected for the purpose of obtaining simpler scaling relations that are more easily understood.

$$\lim_{\varepsilon_x \to 0} \delta_x = 0$$

$$\lim_{\varepsilon_y \to 0} \delta_y = 0$$

$\Rightarrow$ Full space charge depression

In this limit $Q \to Q_{max}$, the maximum transportable perveance.

For our previous example for FODO quadrupoles, the $\varepsilon \to 0$ limit obtains:

$$\lim_{\varepsilon \to 0} \mathrm{Max}[r_{xm}] = r_b \left\{ 1 + \frac{4|\hat{k}| L^2}{\pi^3} \sin\left(\frac{\pi}{2}\eta\right) \right\}$$

$$\lim_{\varepsilon \to 0} Q = Q_{max} = \frac{2}{\pi^2} \left[\frac{\sin\left(\frac{\pi}{2}\eta\right)^2}{\left(\frac{\pi}{2}\eta\right)} \right] \eta^2 \hat{k}^2 L^2 r_b^2$$

Unfortunately, the method introduced before are inadequate for lattices with lesser degrees of symmetry such as syncopated quadrupole doublet lattices. However, methods introduced by Lee [E. P. Lee, Physics of Plasmas 9, 4301 (2002)], can be applied in this situation and also obtain more accurate results. It is beyond the scope of this class to carry out derivations with these methods, but we summarize results derived.

Quadrupole Doublet Lattice

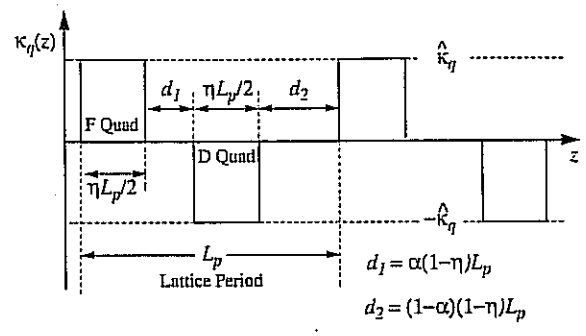

Denote:

Avg Radius: $\overline{r_m} = \int_0^{L_p} \frac{ds}{L_p} r_{xm}(s) = \int_0^{L_p} \frac{ds}{L_p} r_{ym}(s)$

Max Excursion in period: $\mathrm{Max}[r_m] \equiv \mathrm{Max}[r_{xm}, r_{ym}]$

Phase Advance

$$\cos\sigma_0 = 1 - \frac{(\eta\widehat{\kappa_q}L_p^2)^2}{32}\left[\left(1-\frac{2}{3}\eta\right) - 4\left(\alpha-\frac{1}{2}\right)^2(1-\eta)^2\right].$$

For $\sigma_0 = 80^\circ$

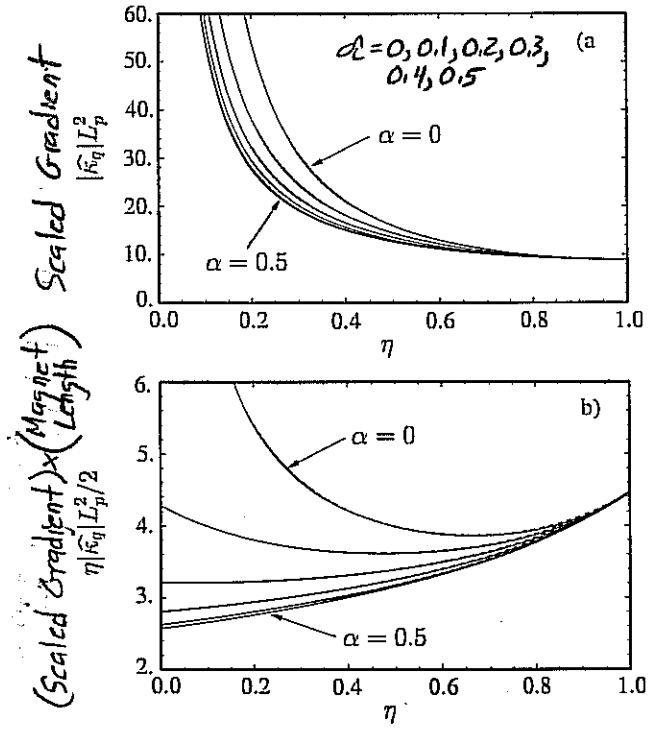

Envelope Flutter

$$\frac{\mathrm{Max}[r_m]}{\overline{r_m}} - 1 = \frac{(1-\cos\sigma_0)^{1/2}(1-\eta/2)[1-4(\alpha-1/2)^2(1-\eta)^2]}{2^{3/2}\left[(1-2\eta/3)-4(\alpha-1/2)^2(1-\eta)^2\right]^{1/2}}.$$

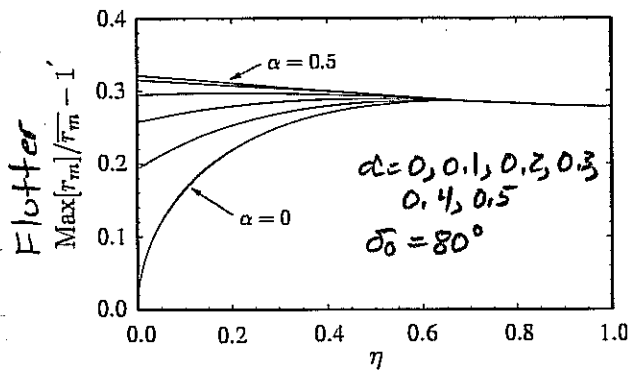

Relations Connecting Max Transportable Perveance Qmax and Lattice Parameters

$$Q_{\max} = \frac{(1-\cos\sigma_0)^{1/2}}{2^{3/2}} \frac{\eta[(1-2\eta/3) - 4(\alpha-1/2)^2(1-\eta)^2]^{1/2}}{(\mathrm{Max}[r_m]/\overline{r_m})^2} |\widehat{\kappa_q}| \,\mathrm{Max}[r_m]^2$$
$$= \frac{(1-\cos\sigma_0)^{1/2}}{2^{3/2}} \frac{\eta[(1-2\eta/3) - 4(\alpha-1/2)^2(1-\eta)^2]^{1/2}}{\left\{1 + \frac{(1-\cos\sigma_0)^{1/2}(1-\eta/2)[1-4(\alpha-1/2)^2(1-\eta)^2]}{2^{3/2}[(1-2\eta/3)-4(\alpha-1/2)^2(1-\eta)^2]^{1/2}}\right\}^2} |\widehat{\kappa_q}| \,\mathrm{Max}[r_m]^2.$$

$$\frac{\mathrm{Max}[r_m]}{L_p} = \sqrt{\frac{Q_{\max}}{2(1-\cos\sigma_0)}} \left(\frac{\mathrm{Max}[r_m]}{\overline{r_m}}\right)$$
$$= \sqrt{\frac{Q_{\max}}{2(1-\cos\sigma_0)}} \left\{1 + \frac{(1-\cos\sigma_0)^{1/2}(1-\eta/2)[1-4(\alpha-1/2)^2(1-\eta)^2]}{2^{3/2}\,[(1-2\eta/3)-4(\alpha-1/2)^2(1-\eta)^2]^{1/2}}\right\},$$

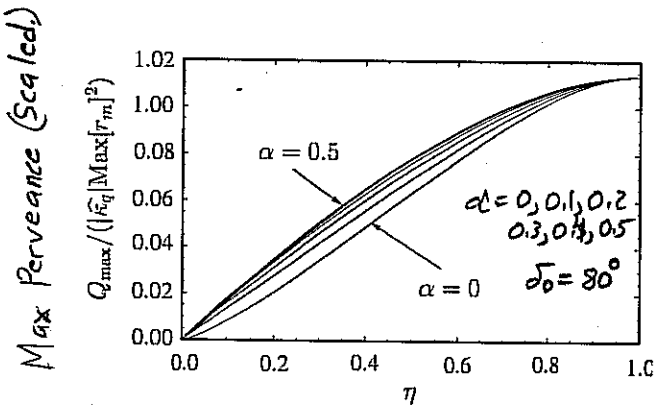

Derivation and aplication of scaling relations can be complicated. They are often applied in systems codes to generate plots that can be interpreted more readily.

John Barnard
Steven Lund
USPAS
June 2006

Mismatched Beams and Beam Halo

Envelope modes of beams in continuous focusing

Envelope modes of bunched beams in continuous focusing

Halos from mismatched beams

SMOOTH FOCUSING ENVELOPE MODES

If $\frac{d}{ds}\gamma\beta = 0$ & $K(s) = k_{\beta 0}^2 =$ constant & $\epsilon_x = \epsilon_y$

$$\Rightarrow \quad r_x'' + k_{\beta 0}^2 r_x - \frac{2Q}{r_x + r_y} - \frac{\epsilon^2}{r_x^3} = 0$$

$$r_y'' + k_{\beta 0}^2 r_y - \frac{2Q}{r_x + r_y} - \frac{\epsilon^2}{r_y^3} = 0 \qquad (S1)$$

THE EQUILIBRIUM OCCURS WHEN $r_x'' = r_y'' = 0$ & $r_x = r_y = r_b$

$$\Rightarrow \quad k_{\beta 0}^2 r_b - \frac{Q}{r_b} - \frac{\epsilon^2}{r_b^3} = 0$$

THIS IS EASILY SOLVED FOR r_b:

$$r_b = \frac{Q^{1/2}}{k_{\beta 0}}\left[\frac{1}{2} + \frac{1}{2}\sqrt{1 + 4k_{\beta 0}^2\epsilon^2/Q^2}\right]^{1/2} \rightarrow \begin{cases} \dfrac{Q^{1/2}}{k_{\beta 0}}; & 2\dfrac{k_{\beta 0}\epsilon}{Q} \ll 1 \\[2ex] \dfrac{\epsilon^{1/2}}{k_{\beta 0}^{1/2}}; & 2\dfrac{k_{\beta 0}\epsilon}{Q} \gg 1 \end{cases}$$

Let $\quad r_x = r_b + \xi(s)$

$\quad\quad r_y = r_b + \eta(s)$

LINEARIZING (S1)

$$(S1) \Rightarrow 0 = \xi'' + k_{\beta 0}^2 (r_b + \xi) - \frac{2Q}{2r_b}\left(1 - \frac{\xi}{2r_b} - \frac{\eta}{2r_b}\right) - \frac{\epsilon^2}{r_b^3}\left(1 - \frac{3\xi}{r_b}\right)$$

$$\& \quad 0 = \eta'' + k_{\beta 0}^2 (r_b + \eta) - \frac{2Q}{2r_b}\left(1 - \frac{\xi}{2r_b} - \frac{\eta}{2r_b}\right) - \frac{\epsilon^2}{r_b^3}\left(1 - \frac{3\eta}{r_b}\right)$$

SUBTRACTING THE EQUILIBRIUM:

$$\xi'' + \left(k_{\beta 0}^2 + \frac{Q}{2r_b^2} + \frac{3\epsilon^2}{r_b^4}\right)\xi + \frac{Q}{2r_b^2}\eta = 0$$

$$\eta'' + \left(k_{\beta 0}^2 + \frac{Q}{2r_b^2} + \frac{3\epsilon^2}{r_b^4}\right)\eta + \frac{Q}{2r_b^2}\xi = 0$$

USING $\quad k_\beta^2 = k_{\beta 0}^2 - \frac{Q}{r_b^2} = \frac{\epsilon^2}{r_b^4}$

$$\Rightarrow \quad \xi'' + \left(\tfrac{3}{2}k_{\beta 0}^2 + \tfrac{5}{2}k_\beta^2\right)\xi + \left(\tfrac{1}{2}k_{\beta 0}^2 - \tfrac{1}{2}k_\beta^2\right)\eta = 0 \qquad (A)$$

$$\eta'' + \left(\tfrac{3}{2}k_{\beta 0}^2 + \tfrac{5}{2}k_\beta^2\right)\eta + \left(\tfrac{1}{2}k_{\beta 0}^2 - \tfrac{1}{2}k_\beta^2\right)\xi = 0 \qquad (B)$$

LET $\varphi_1 = \xi - \eta$ SUBTRACTING (B) FROM (A):

$$\varphi_1'' + k_1^2 \varphi_1 = 0$$

where $k_1^2 = \left(\tfrac{3}{2}k_{\beta 0}^2 + \tfrac{5}{2}k_\beta^2 - \tfrac{1}{2}k_{\beta 0}^2 + \tfrac{1}{2}k_\beta^2\right) = k_{\beta 0}^2 + 3k_\beta^2$

LET $\varphi_2 = \xi + \eta$ ADDING (A) & (B):

$$\varphi_2'' + k_2^2 \varphi_2 = 0$$

where $k_2^2 = \left(\tfrac{3}{2}k_{\beta 0}^2 + \tfrac{5}{2}k_\beta^2 + \tfrac{1}{2}k_{\beta 0}^2 - \tfrac{1}{2}k_\beta^2\right) = 2k_{\beta 0}^2 + 2k_\beta^2$

THE SOLUTIONS ARE:

$$\mathcal{J}_1 \sim e^{ik_1 s} \Rightarrow \xi \,\&\, \eta \sim e^{ik_1 s}$$

EQUATIONS (A) & (B) CAN BE WRITTEN (when $\xi, \eta \sim e^{ik_1 s}$ is substituted into DE's)

$$\begin{pmatrix} 1 & 1 \\ 1 & 1 \end{pmatrix}\begin{pmatrix} \xi \\ \eta \end{pmatrix} = 0 \Rightarrow \xi = -\eta \Rightarrow \text{"QUADRUPOLE MODE"}$$

FOR $\mathcal{J}_2 \sim e^{ik_2 s}$ THE MATRIX EQUATION BECOMES

$$\begin{pmatrix} -1 & 1 \\ 1 & -1 \end{pmatrix}\begin{pmatrix} \xi \\ \eta \end{pmatrix} = 0 \Rightarrow \xi = \eta \Rightarrow \text{"BREATHING MODE"}$$

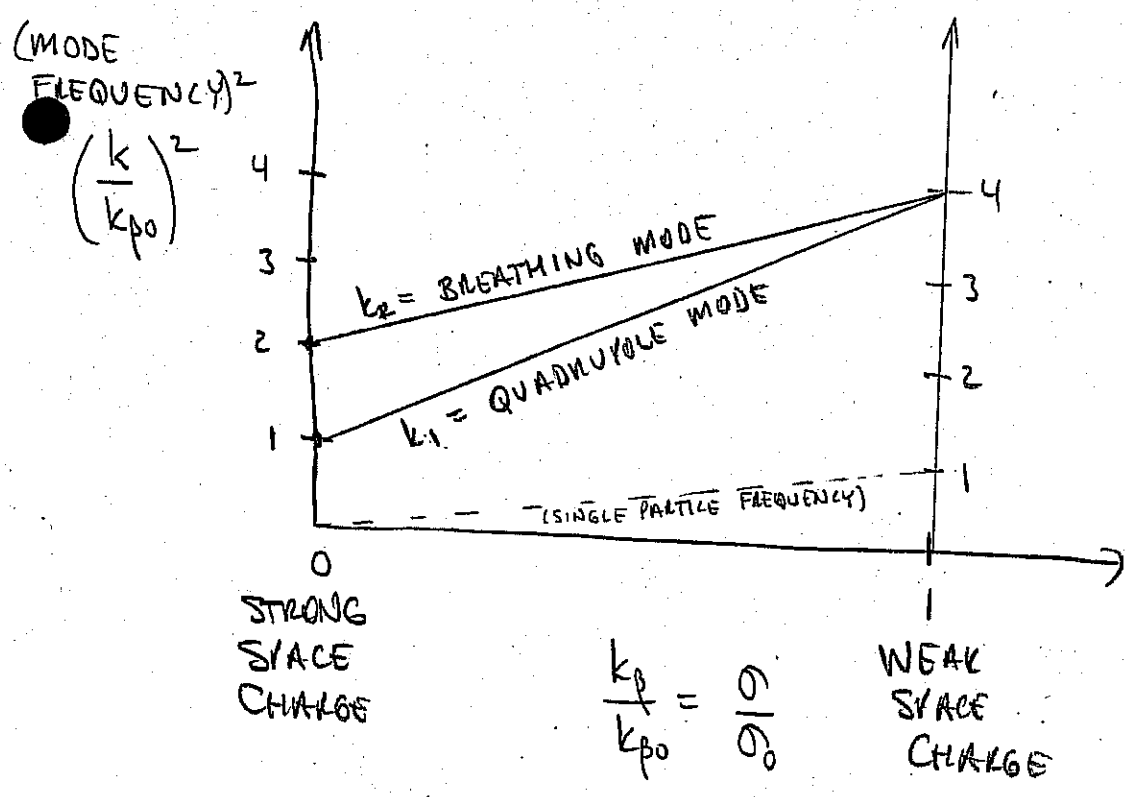

$$k_1^2 = k_{p0}^2 + 3k_p^2 \qquad k_2^2 = 2k_{p0}^2 + 2k_p^2 \quad \leftarrow \text{MODE FREQUENCY}$$

$$k_p^2 = k_{p0}^2 - \frac{Q}{r_b^2} \quad \leftarrow \text{SINGLE PARTICLE FREQUENCY}$$

Smooth focusing: breathing mode and quadrupole mode

Breathing mode:

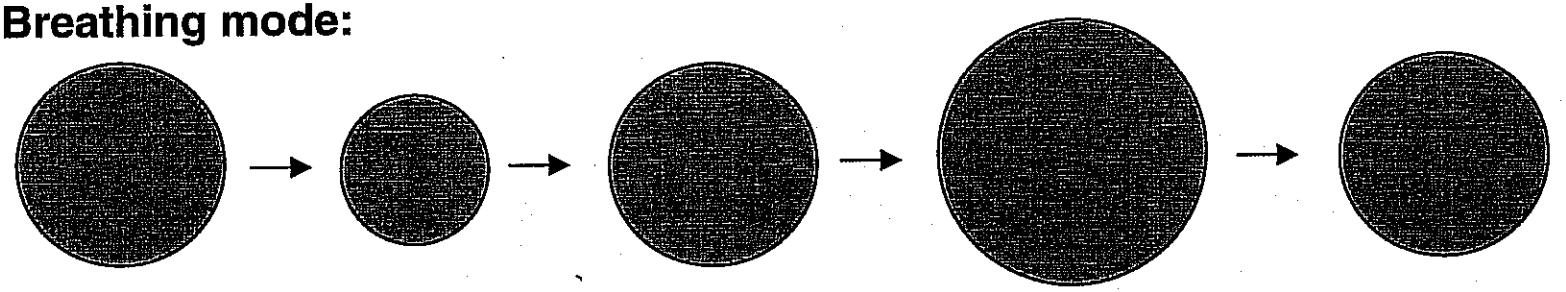

Quadrupole mode:

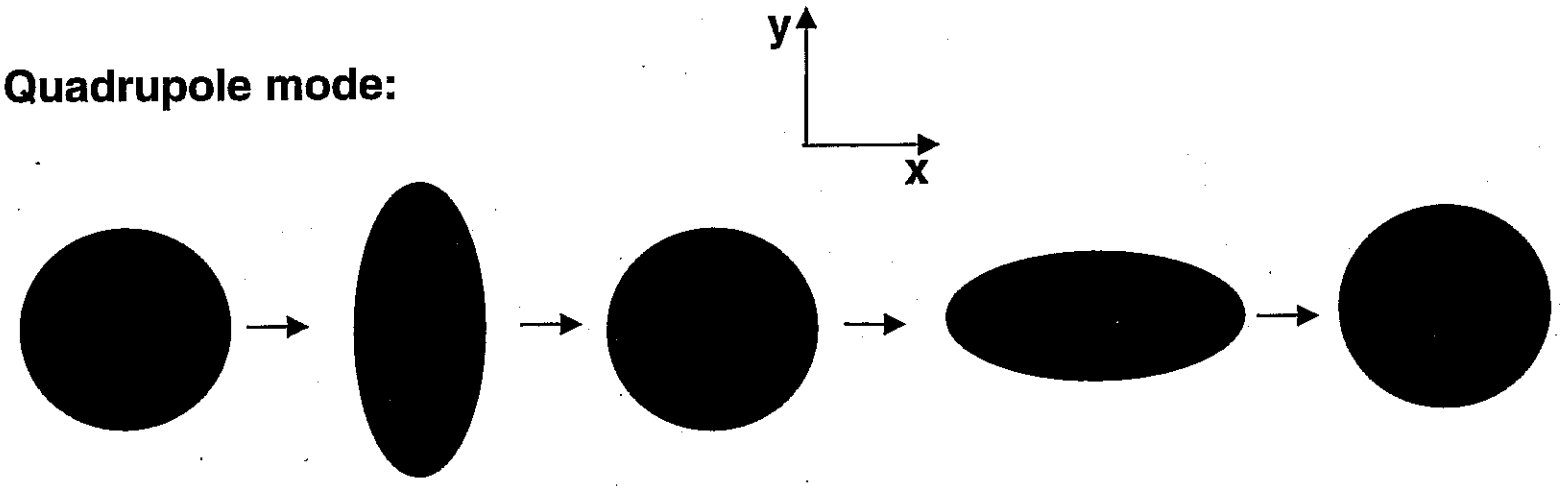

Note that in the quadrupole mode the beam area is nearly constant, whereas in the breathing mode, density increases increasing restoring force; hence breathing mode has the higher frequency of the two modes.

BAHNAD 5

JOHN BARNARD
& STEVEN LUND
USPAS
JANUARY 2004

II ENVELOPE MODES OF BUNCHED BEAMS

IN CONTINUOUS FOCUSING CHANNELS

Total field seen by particle is sum of rf and spacecharge

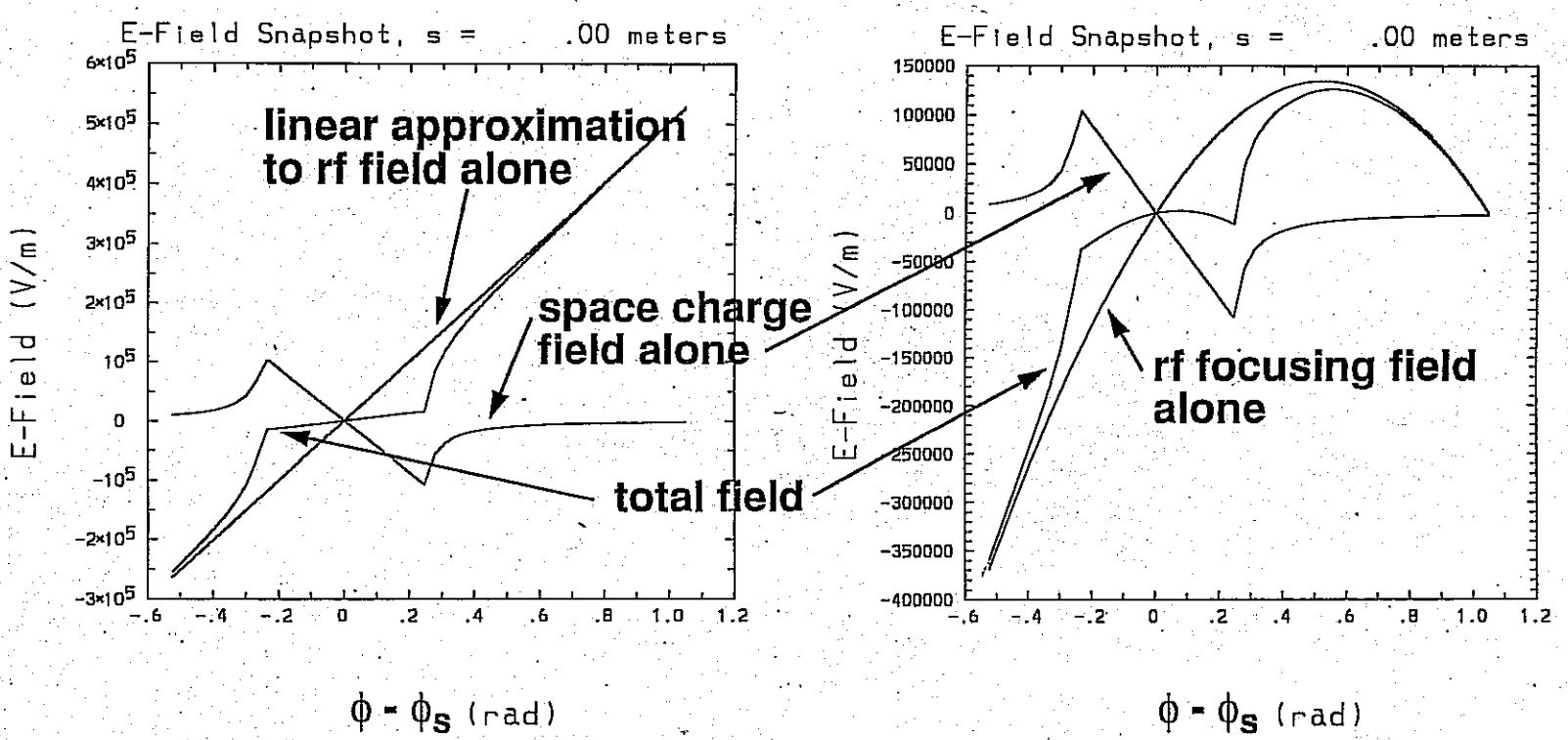

here $\phi - \phi_s = -(2\pi/\beta_s\lambda)\,\Delta z$, where $\beta_s c$ is the longitudinal velocity of the synchronous particle and $\lambda = c/\nu$ is the rf vacuum wavelength

SPACE-CHARGE FIELD OF BUNCHED BEAMS

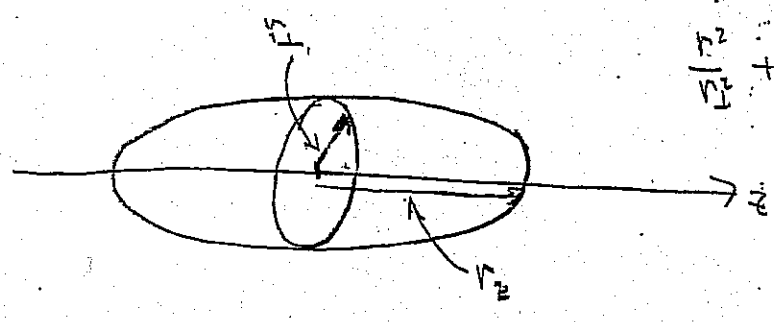

$$\frac{r^2}{r_\perp^2} + \frac{z^2}{r_z^2} = 1$$

BOUNDARY OF ELLIPSOID

THE POTENTIAL OF A UNIFORM DENSITY BUNCH IN FREE SPACE (A MACLAURIN SPHEROID) IS GIVEN BY:

Cf. Landau & Lifshitz, Classical Theory of Fields, p 297)

$$\varphi = \frac{\rho}{4\epsilon_0}\left(\alpha_\perp r^2 + \alpha_\parallel z^2 - \delta\right)$$

where $\alpha_\perp = r_\perp^2 r_z \int_0^\infty \frac{ds}{(r_\perp^2+s)\Delta}$

$$\alpha_\parallel = r_\perp^2 r_z \int_0^\infty \frac{ds}{(r_z^2+s)\Delta}$$

$$\delta = r_\perp^2 r_z \int_0^\infty \frac{ds}{\Delta}$$

where $\Delta^2 = (r_\perp^2+s)^2(r_z^2+s)$

FOR NON-RELATIVISTIC BEAM:

$$E_z = -\frac{\partial\phi}{\partial z} = f\frac{\rho}{\epsilon_0} z$$

$$E_r = -\frac{\partial\phi}{\partial r} = \frac{(1-f)}{2}\frac{\rho}{\epsilon_0} r$$

$$f = f(\alpha) = \begin{cases} \frac{\alpha^2}{1-\alpha^2}\left[\frac{1}{\sqrt{1-\alpha^2}}\tanh^{-1}\sqrt{1-\alpha^2} - 1\right] & \alpha < 1 \\ \frac{1}{3} & \alpha = 1 \\ \frac{\alpha^2}{\alpha^2-1}\left[1 - \frac{1}{\sqrt{\alpha^2-1}}\tan^{-1}\sqrt{\alpha^2-1}\right] & \alpha > 1 \end{cases} \qquad \alpha \equiv \frac{r_\perp}{r_z}$$

FOR RELATIVISTIC BEAM

(cf. LUND & BARNARD 1997)
PAC97 Conf. Proceedings, Vancouver

$$\frac{d^2 \underline{x}_\perp}{ds^2} = \frac{F_\perp}{\gamma_s \beta_s^2 mc^2} \qquad \underline{F}_{\perp s} = \frac{-q}{\gamma_s^2}\frac{\partial \phi}{\partial \underline{x}_\perp} = \frac{q\rho}{2\gamma_s^2 \epsilon_0}\left[1 - f(\alpha)\right]\underline{x}_\perp$$

$$\frac{d^2 \Delta z}{ds^2} = \frac{F_z}{\gamma_s^3 \beta_s^2 mc^2} \qquad F_{zs} = \frac{-q}{\gamma_s^2}\frac{\partial \phi}{\partial z} = \frac{q\rho}{\epsilon_0} f(\alpha)\,\Delta z$$

$$\alpha = \frac{r_\perp}{\gamma v_z} \qquad \left[\alpha = \frac{r_\perp}{(v_z \text{ in comoving frame})}\right]$$

COMBINING FOCUSING + SELF FIELDS

$$\frac{d^2}{ds^2}\Delta z = -k_{s0}^2 \Delta z + \frac{q\rho\, f(\alpha)}{\gamma_s^3 \beta_s^2 mc^2 \epsilon_0}\Delta z \qquad \text{(LINEAR PF)}$$

Envelope Equations for an Unaccelerated Ellipsoidal Beam Bunch with Uniform Space-Charge

$$\boxed{\begin{aligned} &\frac{d^2 r_\perp}{ds^2} + k_{\beta 0}^2 r_\perp - \frac{K_{3D}[1 - f(\alpha)]}{2 r_\perp r_z} - \frac{\epsilon_x^2}{r_\perp^3} = 0 \\ &\frac{d^2 r_z}{ds^2} + f_{nl}(\zeta)\, k_{s0}^2 r_z - \frac{K_{3D} f(\alpha)}{r_\perp^2} - \frac{\epsilon_z^2}{r_z^3} = 0 \end{aligned}}$$

$f_{nl}(\zeta) = (15/\zeta^5)[(3 - \zeta^2)\sin\zeta - 3\zeta\cos\zeta]$ Let $\zeta = (2\pi/\beta_s\lambda) r_z$

$k_{\beta 0}^2$	Undepressed Transverse Betatron Wavenumber-Squared
k_{s0}^2	Undepressed Longitudinal Synchrotron Wavenumber-Squared
$K_{3D} = 3qI\lambda/4\pi\epsilon_0\gamma_s^3\beta_s^3 mc^3$	3D Space-Charge Parameter (dimension of length)
$\epsilon_x^2 = 25[\langle x^2\rangle\langle x'^2\rangle - \langle xx'\rangle^2]$	3D Bunched Beam Transverse Emittance-Squared
$\epsilon_z^2 = 25[\langle \Delta z^2\rangle\langle \Delta z'^2\rangle - \langle \Delta z \Delta z'\rangle^2]$	3D Bunched Beam Longitudinal Emittance-Squared
f_{nl}	Accounts for Nonlinear rf Focusing, $f_{nl}(\zeta) \to 1$ when $\zeta \to 0$

- Envelope equations couple the transverse and longitudinal single-particle motion
- Bunch acceleration results in additional terms
- Linear rf envelope equations presented in Wangler, "Intro. to Linear Accelerators"

$\lambda \equiv \frac{2\pi c}{\omega}$ = rf vacuum wavelength

$I \equiv \frac{qNc}{\lambda}$ = average current

Envelope Equations will be used to:

- Calculate equilibrium values of the envelope widths r_z and $r_\perp$
- Calculate properties of mismatch eigenmodes
  - Mode wavenumber
  - Relative amplitude of transverse and longitudinal mismatch

Perturbed Envelope Equations
Yield Linear Eigenmode for a Mismatched Ellipsoidal Beam Bunch

Assume small-amplitude perturbations ($|\delta r_\perp|/r_{\perp 0} \ll 1$ and $|\delta r_z|/r_{z0} \ll 1$):

$$\boxed{\begin{aligned} r_\perp &= r_{\perp 0} + \delta r_\perp \exp(iks) \\ r_z &= r_{z0} + \delta r_z \exp(iks) \end{aligned}}$$

SEE
BARNARD & LUND
LUND & BARNARD
PAC 97, VANCOUVER
CONF. PROCEEDINGS

To obtain coupled linear mode equations:

$$\boxed{\begin{pmatrix} -k^2 + K_{11} & K_{12} \\ K_{21} & -k^2 + K_{22} \end{pmatrix} \begin{pmatrix} \delta r_\perp / r_{\perp 0} \\ \delta r_z / r_{z0} \end{pmatrix} = 0}$$

$$K_{11} = 4k_\beta^2 - \frac{K_{3D}}{r_{\perp 0}^2 r_{z0}} \left[1 - f(\alpha) - \frac{\alpha}{2} \frac{df(\alpha)}{d\alpha} \right]_{r_\perp = r_{\perp 0}, r_z = r_{z0}}$$

$$K_{22} = 4k_{s0}^2 \left[f_{nl}(\zeta) + \frac{\zeta}{4} \frac{df_{nl}(\zeta)}{d\zeta} \right]_{r_\perp = r_{\perp 0}, r_z = r_{z0}} - \frac{3K_{3D}}{r_{\perp 0}^2 r_{z0}} \left[f(\alpha) - \frac{\alpha}{3} \frac{df(\alpha)}{d\alpha} \right]_{r_\perp = r_{\perp 0}, r_z = r_{z0}}$$

$$K_{12} = \frac{K_{3D}}{2 r_{\perp 0}^2 r_{z0}} \left[1 - f(\alpha) - \alpha \frac{df(\alpha)}{d\alpha} \right]_{r_\perp = r_{\perp 0}, r_z = r_{z0}}$$

$$K_{21} = \frac{K_{3D}}{r_{\perp 0}^2 r_{z0}} \left[2f(\alpha) - \alpha \frac{df(\alpha)}{d\alpha} \right]_{r_\perp = r_{\perp 0}, r_z = r_{z0}}$$

Solution of the quartic dispersion relation characterizes the envelope mismatch modes

Spatial Frequencies:

High Frequency Mode : $$k^2 = k_H^2 = \frac{1}{2}(K_{11} + K_{22}) + \frac{1}{2}\sqrt{(K_{11} - K_{22})^2 + 4K_{12}K_{21}}$$

Low Frequency Mode : $$k^2 = k_L^2 = \frac{1}{2}(K_{11} + K_{22}) - \frac{1}{2}\sqrt{(K_{11} - K_{22})^2 + 4K_{12}K_{21}}$$

Relative Amplitude of Transverse and Longitudinal Oscillations:

$$\frac{\delta r_\perp / r_{\perp 0}}{\delta r_z / r_{z0}} = \frac{K_{12}}{k^2 - K_{11}}$$

BARNARD 21

(=)

Envelope equations yield equilibrium beam parameters and eigenfrequencies and modes of mismatched beam

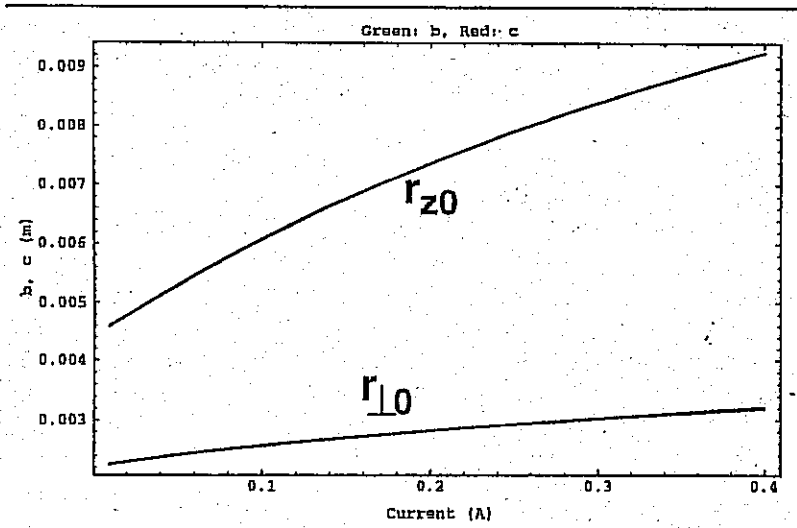

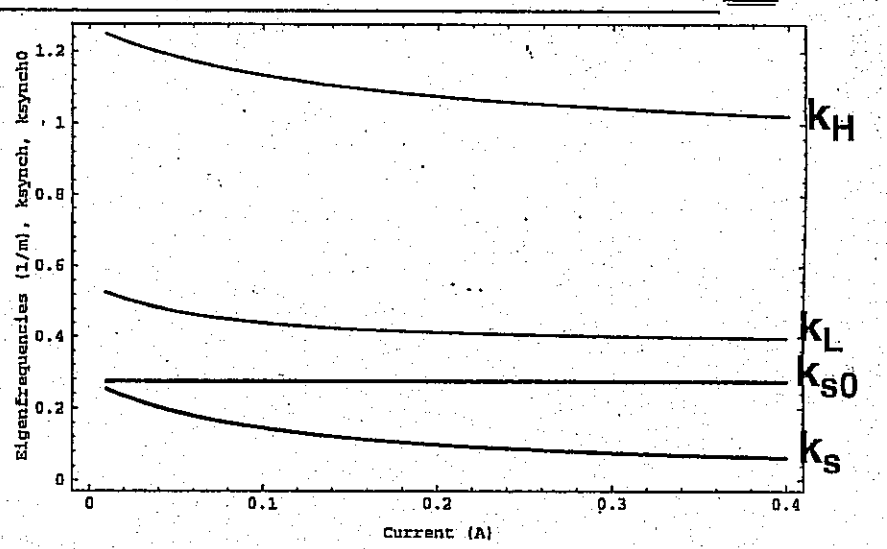

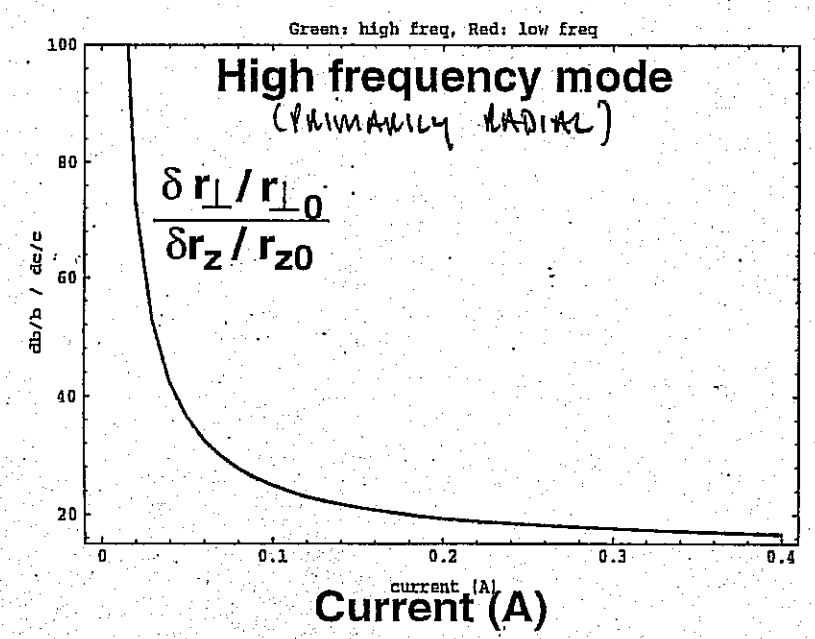

← INCREASING σ/σ_0

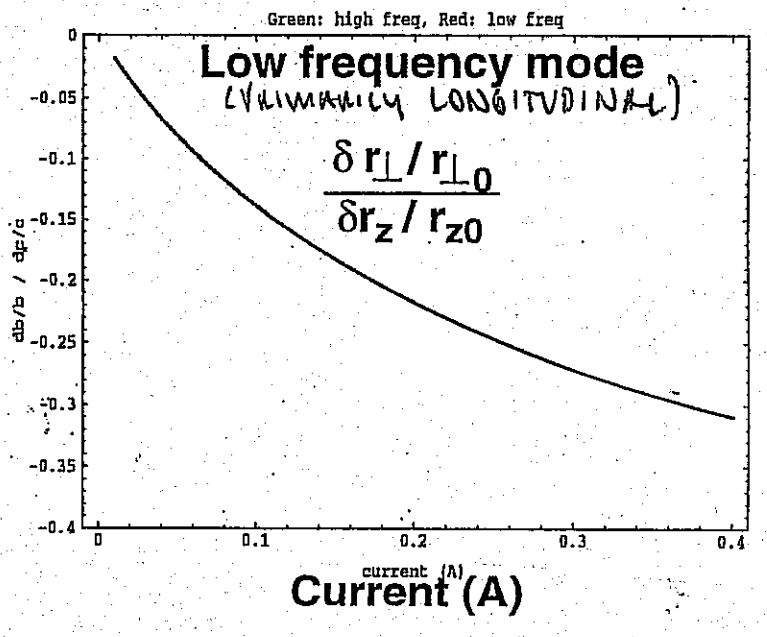

JOHN BARNARD
& STEVEN LUNO
USPAS JANUARY 2004

III HALOS

1. WHAT IS HALO? WHY DO WE CARE?

2. QUALITATIVE PICTURE OF HALO FORMATION:
   MISMATCHES RESONANTLY DRIVE PARTICLES TO LARGE AMPLITUDE

3. CORE/PARTICLE MODELS

4. AMPLITUDE/PHASE ANALYSIS

FROM
"BEAM LOSS & BEAM HALO STUDIES"
ROBERT RYNE, 1995

FULLY SELF-CONSISTENT PIC CODE RESULTS

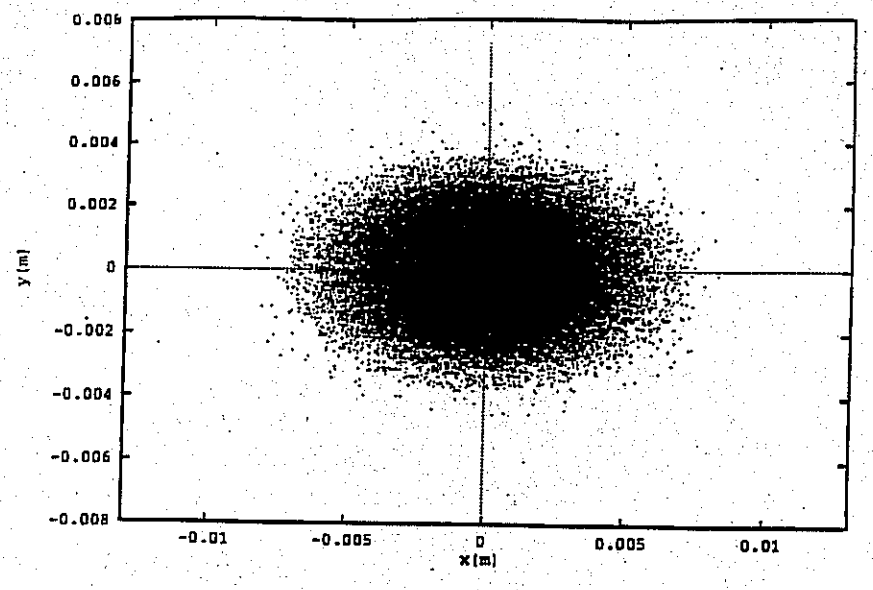

MATCHED BEAM

Figure 5: Beam halo after 22 focusing periods in a FODO channel. The initial distribution is an *rms* matched Gaussian beam. ($\sigma_0 = 70\,\mathrm{deg}$, $\sigma = 35\,\mathrm{deg}$)

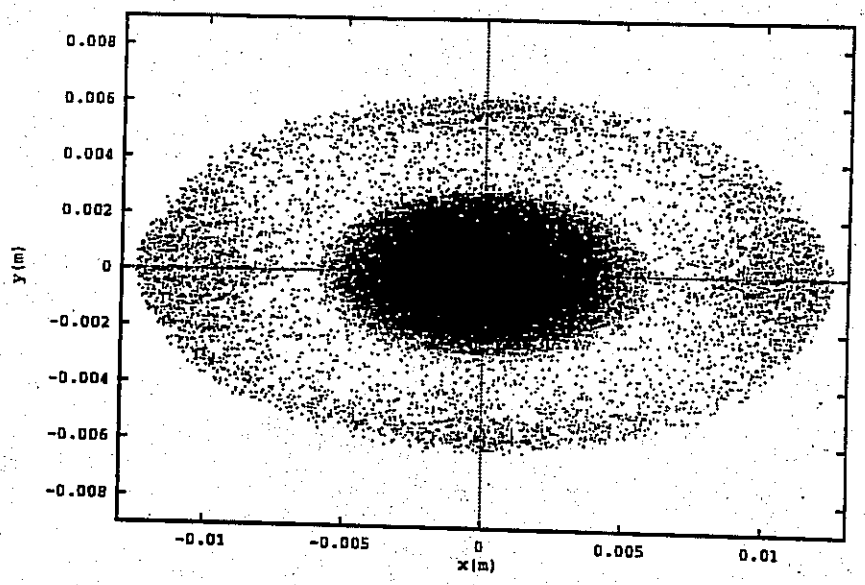

MISMATCHED BEAM

Figure 6: Beam halo after 22 focusing periods in a FODO channel. The initial distribution is an *rms* mismatched Gaussian beam. ($\sigma_0 = 70\,\mathrm{deg}$, $\sigma = 35\,\mathrm{deg}$)

WHY DO WE CARE?

1). BEAM LOSS OF HIGH ENERGY PARTICLES

⇒ ACCELERATOR ACTIVATION

EXAMPLE: FOR THE 1 GeV, 100 mA ACCELERATOR PRODUCTION OF TRITIUM (APT) PARAMETERS

1 nA/m OF BEAM LOSS ALLOWED FOR "HANDS ON" MAINTENANCE (FOR $E \gtrsim 1$ GeV)

$\left(\frac{1\,nA}{m} m \times 1000\,m \Rightarrow 10^{-6}\,A \text{ loss allowed} \right)$

$\Rightarrow \frac{10^{-6}\,A}{0.1\,A} \Rightarrow 10^{-5}$ fractional beam loss allowed!!

2). BEAM LOSS ON WALLS

⇒ ELECTRON / GAS EMISSION FROM WALLS

FOR LONG PULSE OR DC MACHINES, OR STORAGE RINGS, WHERE ELECTRONS CAN BE DRAWN INTO BEAM AND ACCUMULATION ⇒ INSTABILITIES AND NON-LINEAR FIELDS COULD DESTROY BEAM EMITTANCE OR EVEN DISRUPT BEAM.

3). INCREASE IN EMITTANCE

MAY REDUCE FOCUSABILITY FOR APPLICATIONS REQUIRING A SMALL BEAM SPOT.

WHAT IS THE BASIC PHYSICS?

RECALL DISPERSION RELATION FOR ENVELOPE MODES:

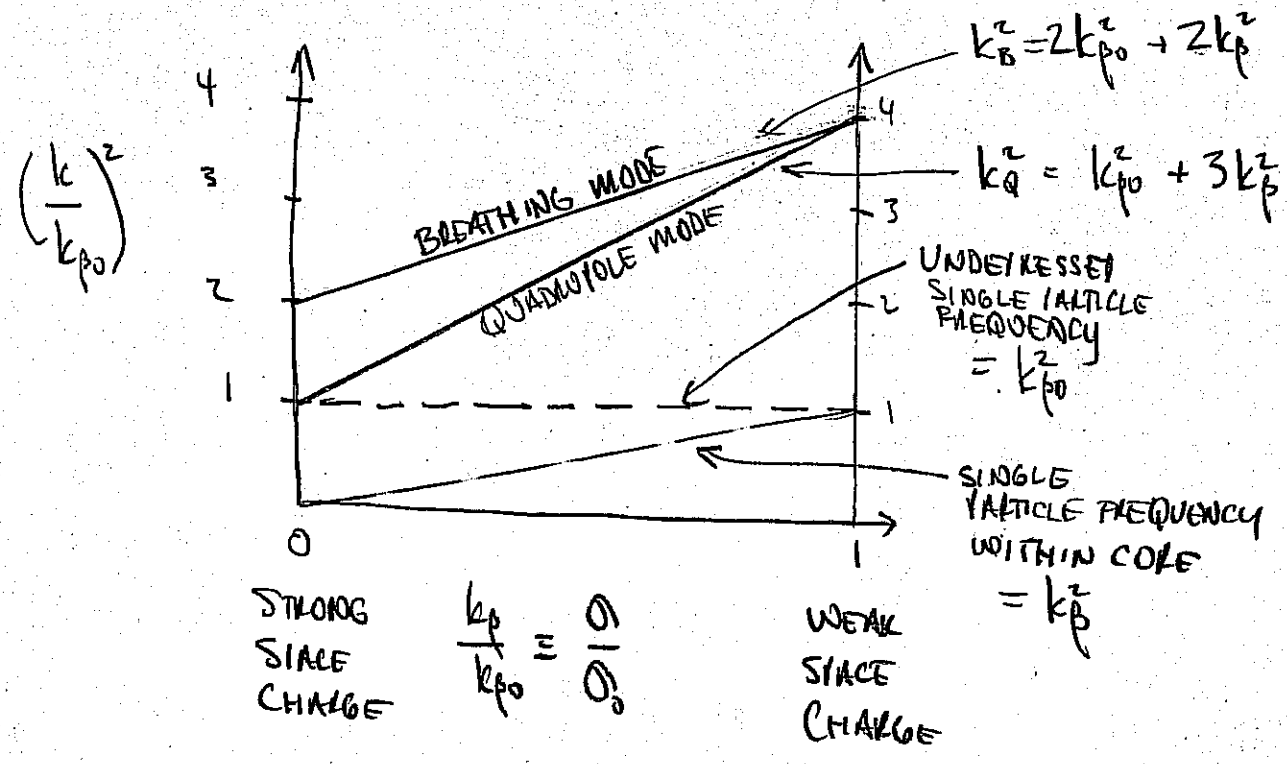

CONSIDER DIAGRAM FOR $\frac{k_B}{2}$ AND $\frac{k_Q}{2}$:

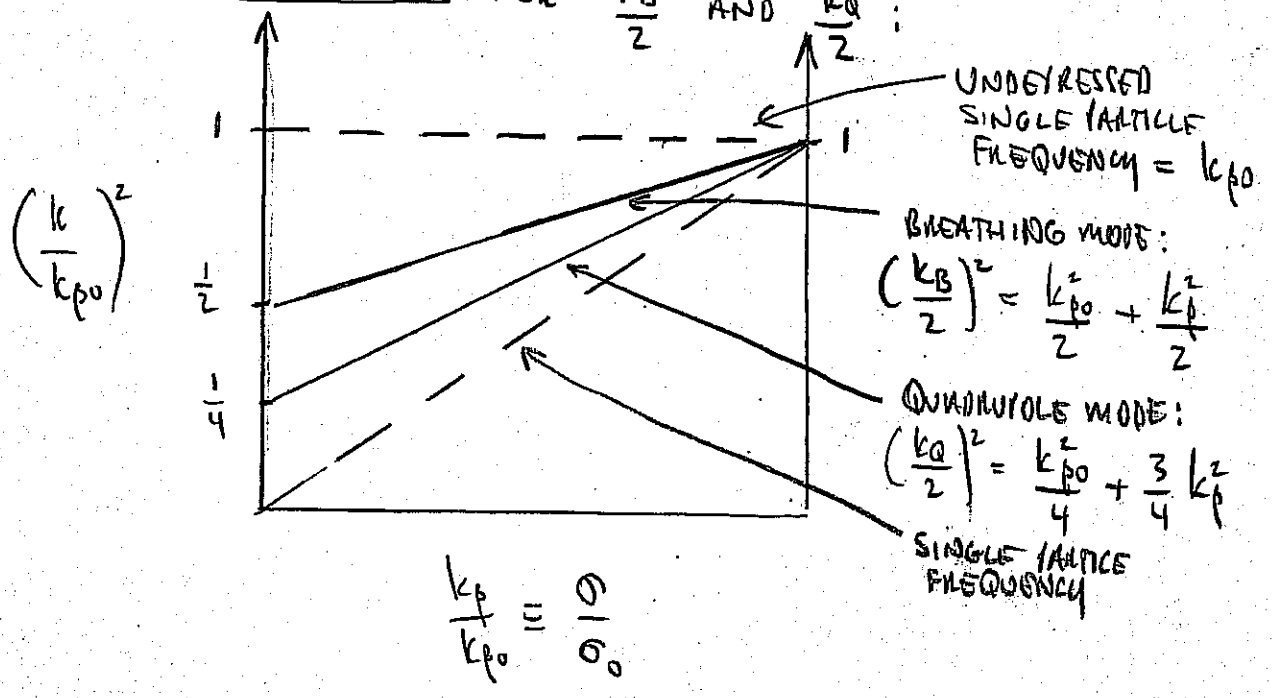

PARTICLES IN ORBITS FAR FROM CORE OSCILLATE AT FREQUENCY k_{p0}, WHEREAS THOSE WITHIN CORE OSCILLATE AT FREQUENCY k_p.

AT INTERMEDIATE RADII, PARTICLE FREQUENCY = ENVELOPE FREQUENCY / 2

$\Rightarrow$ POSSIBILITY OF RESONANCE

$\Rightarrow$ MISMATCHES (EXCITATION OF ENVELOPE MODES) TOGETHER WITH COMMENSURATE PARTICLE FREQUENCY AND ENVELOPE HALF-FREQUENCY ARE THE SOURCE OF HALO.

SUGGESTS USING A <u>CORE / TEST PARTICLE</u> MODE TO EXPLORE THESE EFFECTS (O'CONNEL, WANGLER, JAMESON, RYNE, ...)

ASSUME KV ENVELOPE, OSCILLATING AT A MODE FREQUENCY.

USE KNOWN ANALYTIC FORMULAS INTERIOR AND EXTERIOR TO BEAM.

FOR EXAMPLE, FOR CIRCULAR BEAM

$$x'' = \begin{cases} -\left[k_{\beta 0}^2 - \dfrac{Q}{r_b^2}\right] x & \text{for } r < r_b \\ -\left[k_{\beta 0}^2 - \dfrac{Q}{r^2}\right] x & \text{for } r > r_b \end{cases}$$

Similarly for y.

$$r_b = r_{b0} + \delta r_b \cos(k_B s + \phi)$$

BREATHING MODE k_B

DISTRIBUTE TEST PARTICLES IN PHASE SPACE AND FOLLOW EVOLUTION OF ORBITS. ALLOWS PHYSICS STUDIES, WHICH CAN BE FOLLOWED UP WITH SELF-CONSISTENT PIC RUNS.

NOTE THAT THE SAME TYPE OF RESONANCES OCCUR LONGITUDINALLY, IN BUNCHED BEAMS.

BETATRON FREQUENCY → SYNCHROTRON FREQUENCY

$k_{\beta 0} \rightarrow k_{s0}$

$k_\beta \rightarrow k_s$ (DEPRESSED) SYNCHROTRON FREQUENCY)

BREATHING MODE $k_B \rightarrow k_L$ LOW FREQUENCY MODE

RESONANCE CONDITION

$$k_\beta < \frac{k_B}{2} < k_{\beta 0} \quad \longrightarrow \quad k_s < \frac{k_L}{2} < k_{s0}$$

ADDITIONAL COMPLICATION:

INTRINSIC NON-LINEARITY OF rf BUCKET

FROM Tom Wangler
Los Alamos National Lab

Stroboscopic Map (The Peanut Diagram)

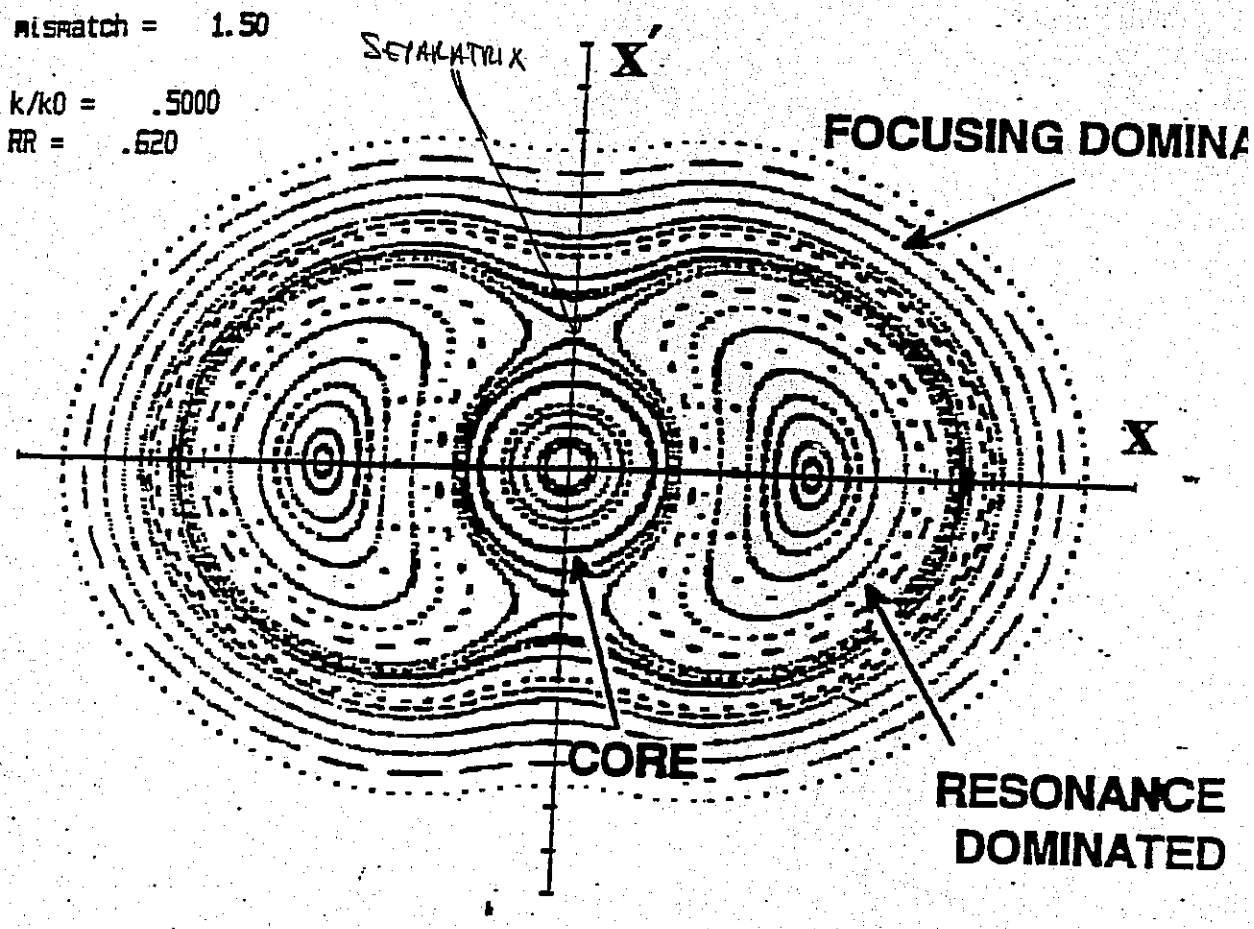

- Accumulate Many Snapshots of Phase Space Taken at Minimum Amplitude of Core Oscillation. (OR ANY PARTICULAR PHASE)
- Follow an Array of Particles to Obtain a "Trajectory Field".
- Regular Trajectories Appear as Smooth Curves.
- Chaotic Trajectories Appear as Stochastic Scatter.
- INITIAL POSITIONS OF PARTICLES IN PHASE SPACE WERE EQUALLY SPACED ALONG X & X' AXES.

Orbits of resonant particles have amplitudes which are highly varying compared to non-resonant particles

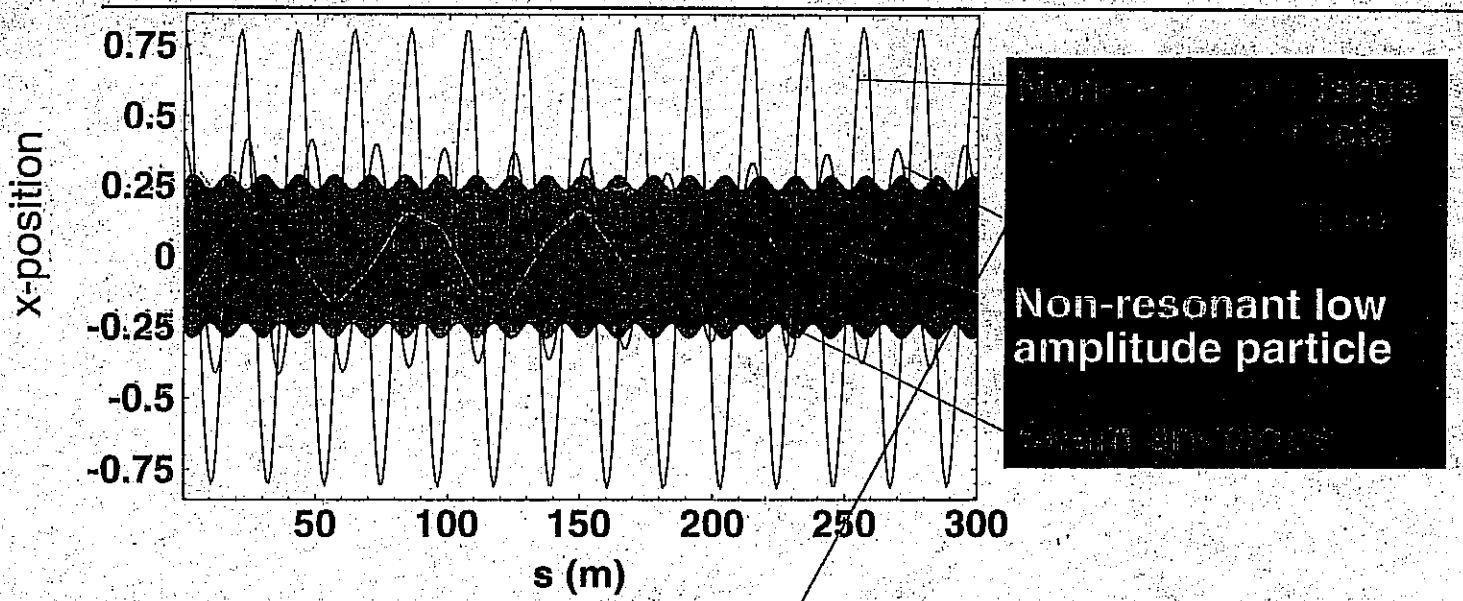

Oscillation frequency

$< k_{\beta 0}$ UNDEFINED BETATRON (PARTICLE OUTSIDE CORE)

$\sim k_{env}/2$ BREATHING MODE/2

$\approx k_B/2$

$\sim k_\beta$ DEPRESSED BETATRON (PARTICLE IN CORE)

$k_{[redacted]}$ – BREATHING MODE

Poincare plot strobes phase space each envelope oscillation

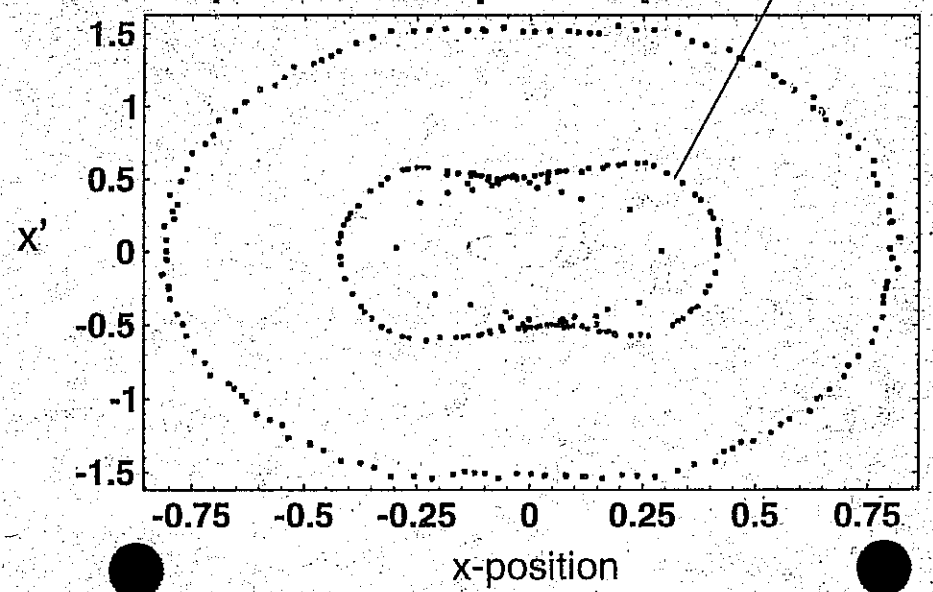

Note that resonant particle undergoes 11 oscillation periods, half of the 22 periods of the envelope. (The two non-resonant particles undergo 14 and 5 oscillation periods.)

Non-resonant large and small amplitude particles have regular orbits whereas resonant particles have varying amplitudes

Changing Poincare phase rotates diagram as expected

$k_L s = 0$

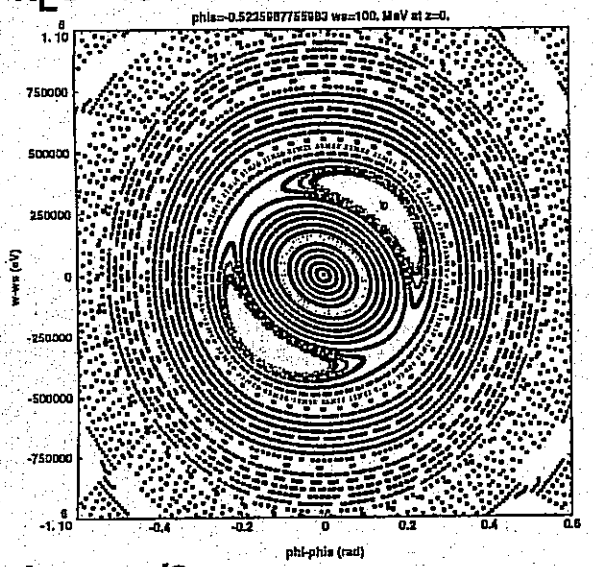

$k_L s = \pi/6$

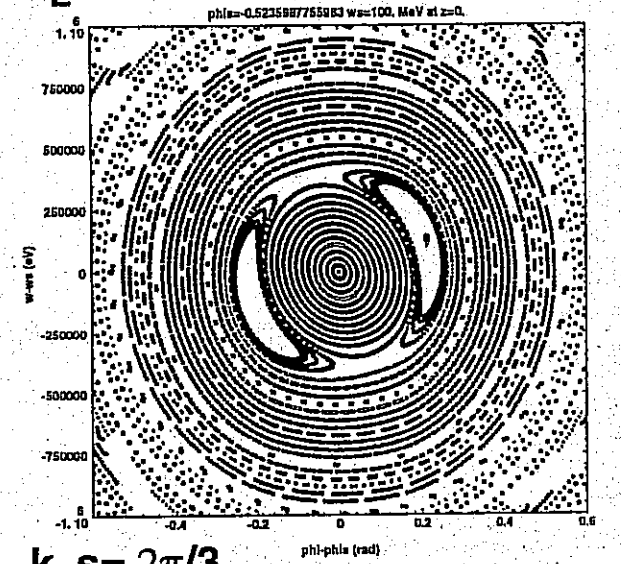

$k_L s = \pi/3$

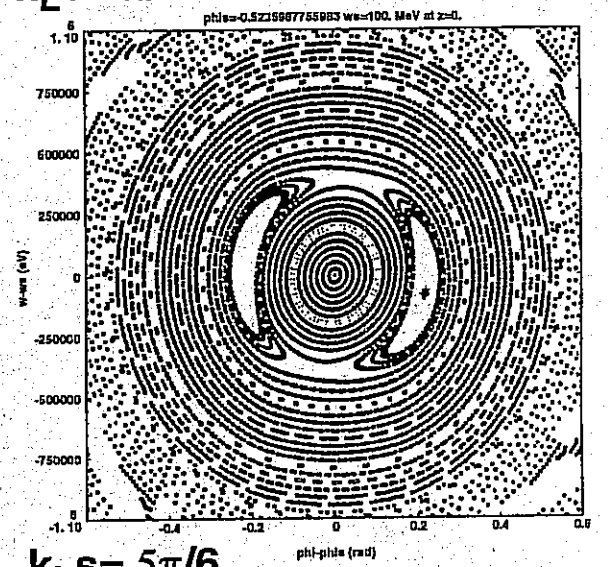

$k_L s = \pi/2$

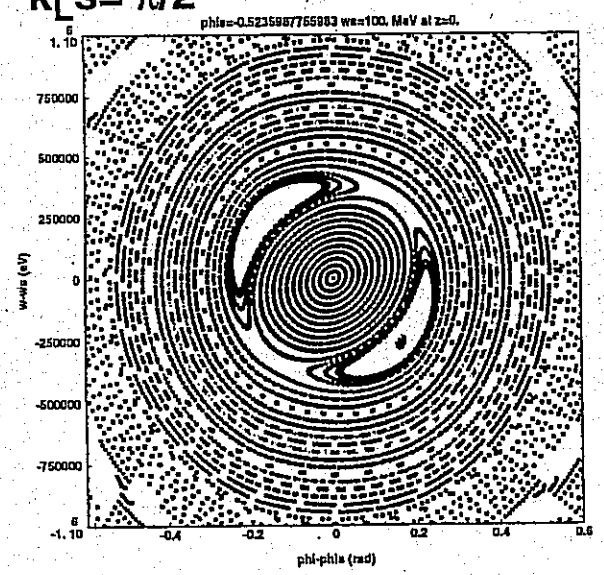

$k_L s = 2\pi/3$

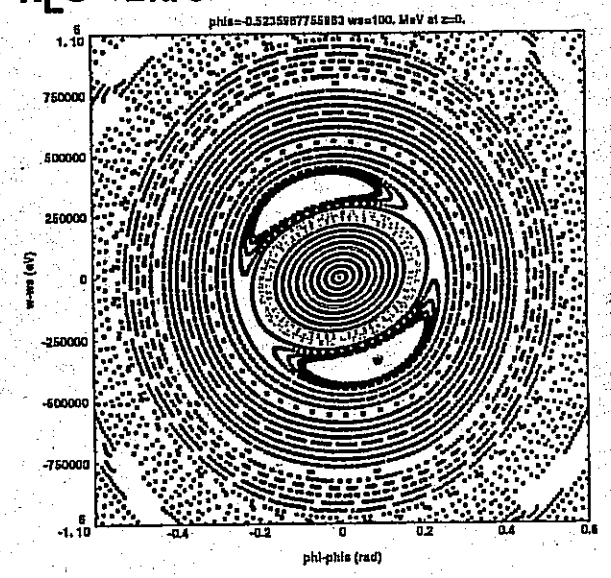

$k_L s = 5\pi/6$

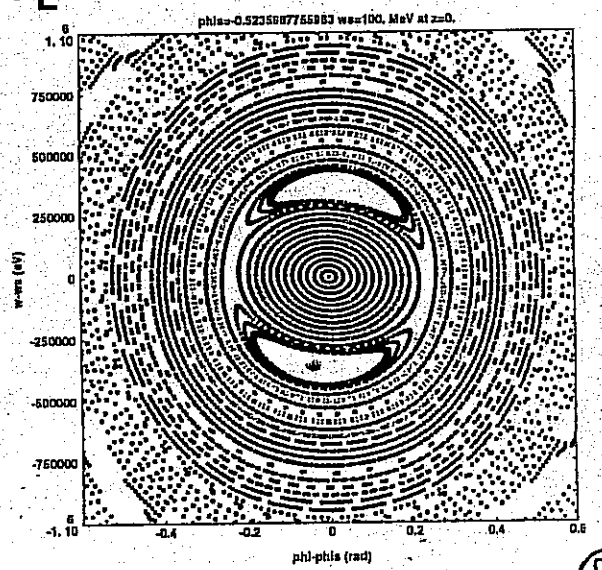

(CHANGING $k_L s$ by π ROTATES POINCARE PLOT BY π.)

$k_b^2/k_0^2 = 3 + \eta^2$ for the spherical bunch.

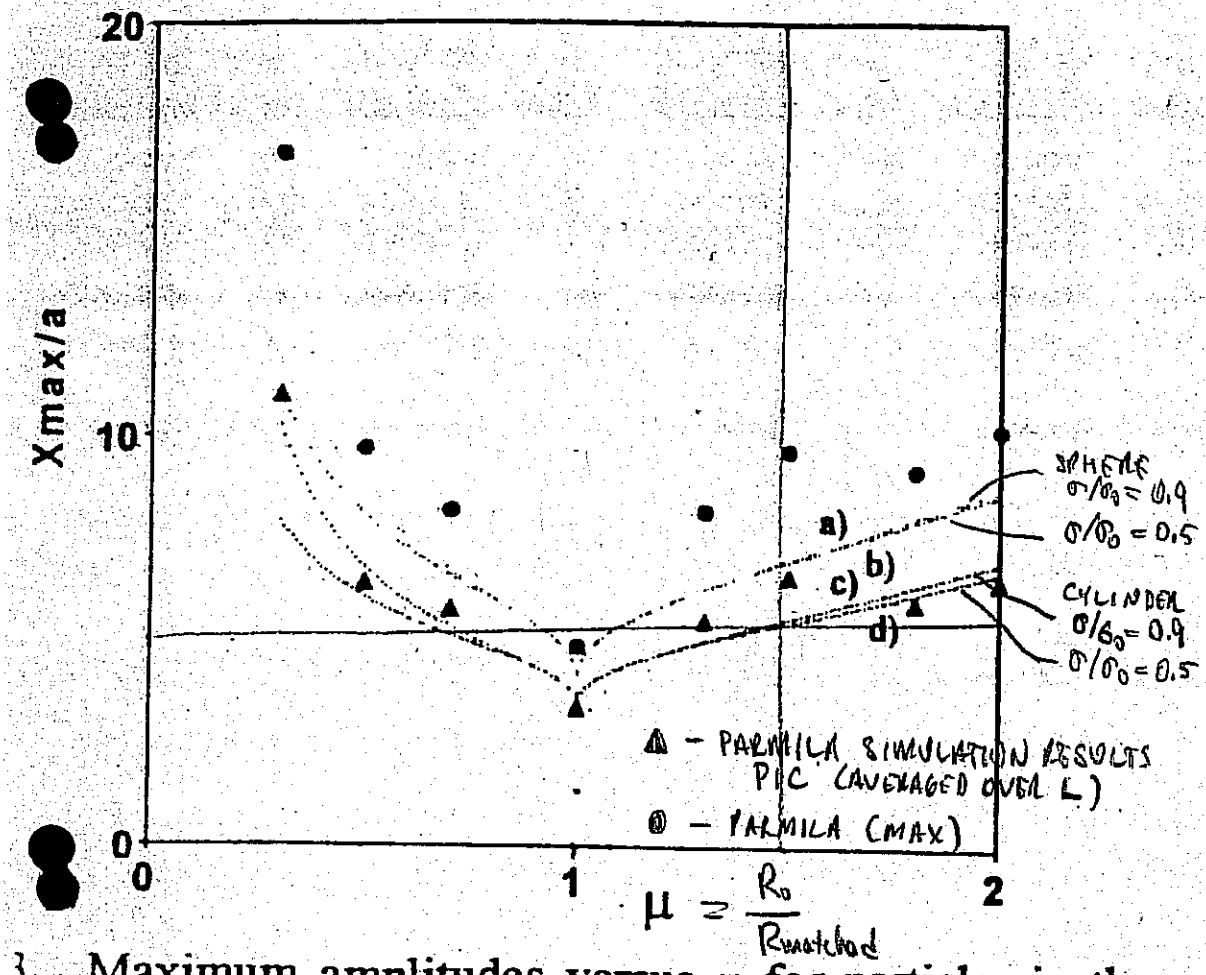

3. Maximum amplitudes versus μ for particles in the nance regions for the cylinder, and sphere models: a) re, η = 0.9, b) sphere, η = 0.5, c) cylinder, η = 0.9, and d) nder, η = 0.5. The triangles represent the smoothed MILA simulation results for comparison with the els, and the dots represent the maximum amplitudes ding quadrupole flutter.

a real linac, additional effects that are not included in the cle-core model, must be accounted for, such as beam-ope flutter associated with a quadrupole focusing system, eration, and the influence of other modes of the ha hed beam. We have conducted a test of the predictions e particle-core model, by carrying out PARMILA ations, using an r-z space-charge mesh with individual

note that t
mesh to ens
simulations

Work du
that beam
the new li
mainly resp
models to n
formed. Th
and one fo
limited to a
the strengt
predictions
bounds of t
a linac. Sin
produce sn
consistent v
that the brea
the halo. To
as well as
keeping ε s
can contrib
beam-resid
However, th
than beam n

The author
Gluckstern a

* Work supp

FROM WANGLER et al
XVIII Int'l LINAC CONF.
GENEVA, SWITZERLAND,
AUG. 26-30, 1996

WANGLER'S CORE/TEST PARTICLE RESULTS

$$\frac{X_{max}}{\langle x^2 \rangle^{1/2}} = A + B|\ln \mu|$$

$$\mu = \left(\frac{r_{bi}}{r_{bo}}\right) = \frac{\text{INITIAL BEAM RADIUS}}{\text{MATCHED BEAM RADIUS}}$$

FOR

	σ/σ_0	A	B
CYLINDER	0.5	3.97	3.83
CYLINDER	0.9	3.91	4.25
SPHERE	0.5	4.87	5.30
SPHERE	0.9	4.81	5.56

Numerical Validation of 1D particle-core model

- Maximum beam size in large scale simulations found to be in excellent agreement with "peanut diagram" of particle-core model

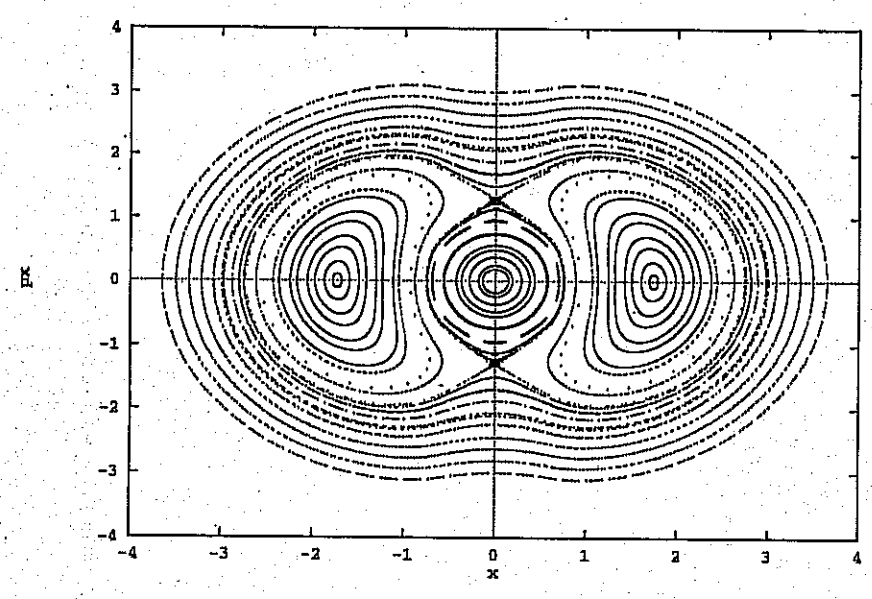

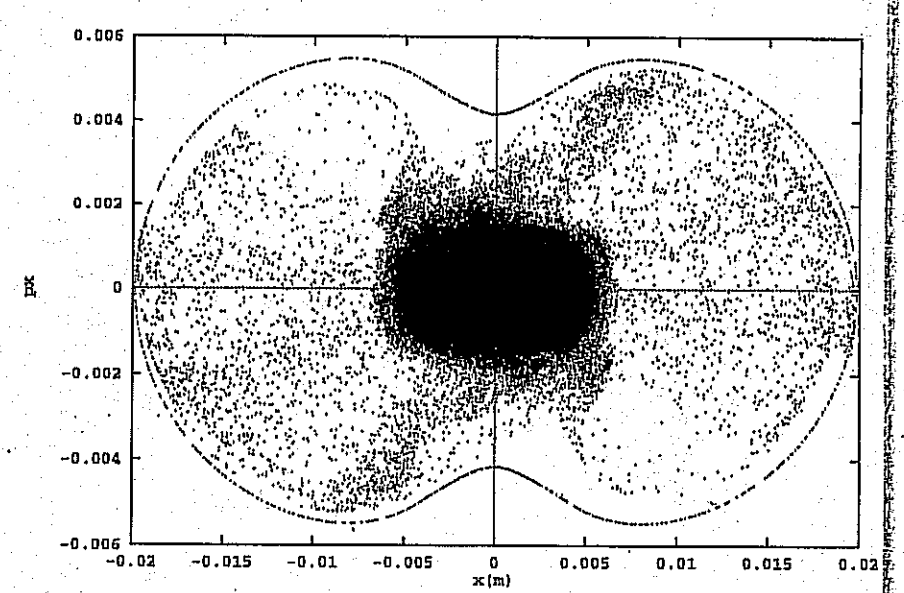

25

Longitudinal Particle-Core Model w/ RF Nonlinearity

- Core-Test-Particle (CTP) code exhibits asymmetry in peanut diagram also observed in simulations with HALO3D PIC code
- 200 mA simulation:

CTP test particles

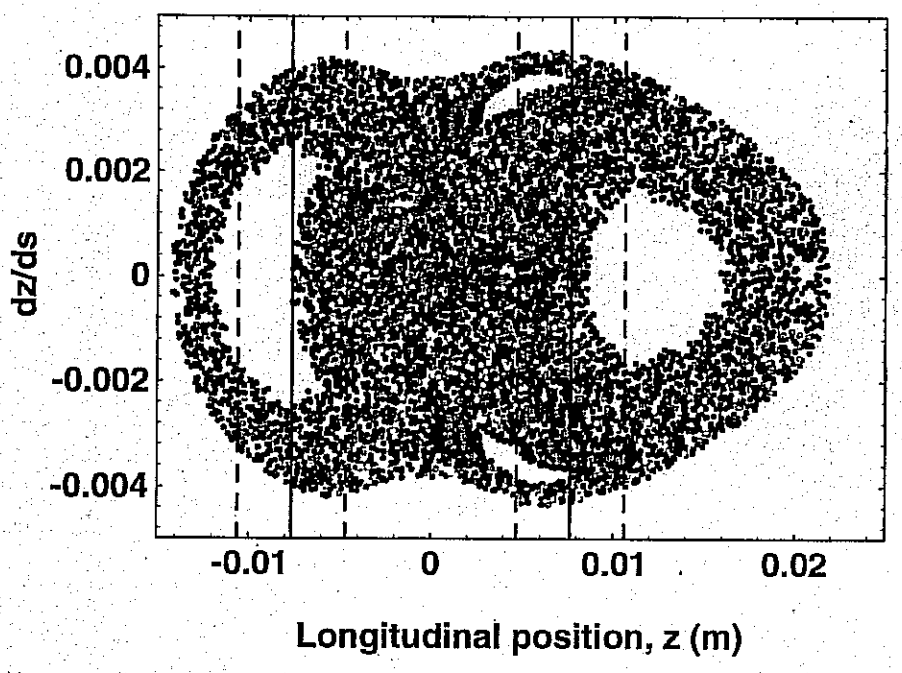

HALO3D beam particles

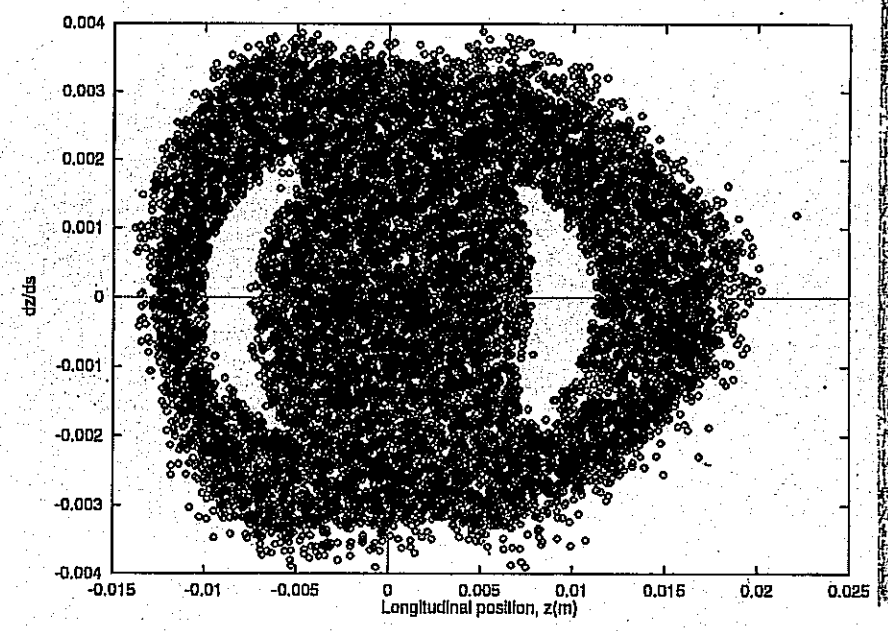

92

Longitudinal Particle-Core Model w/ RF Nonlinearity

- Absence of $k_L/2$ resonance (and associated halo) predicted by CTP analysis confirmed in HALO3D simulations
- 5 mA simulation:

CTP test particles

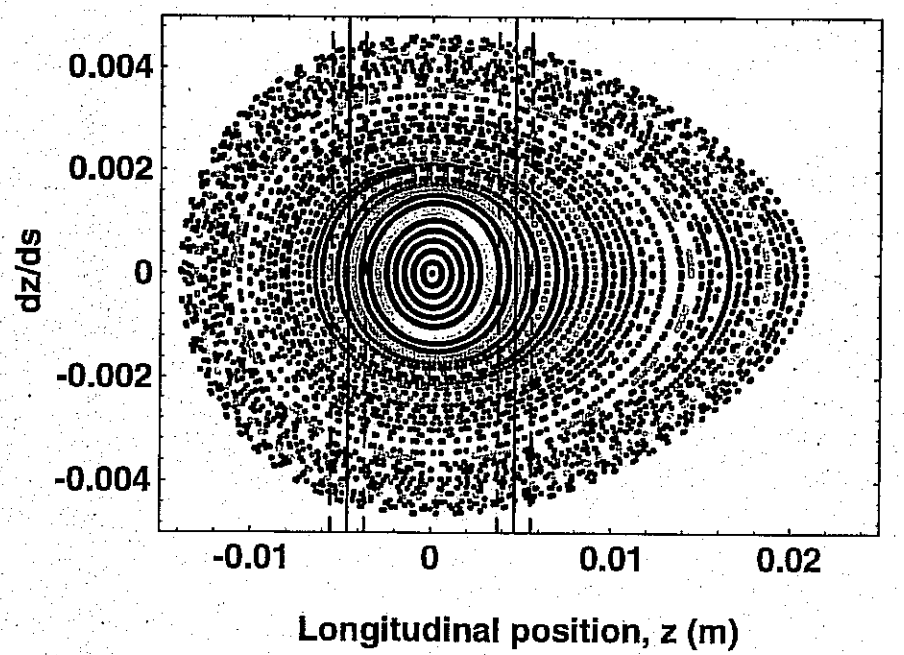

HALO3D test particles

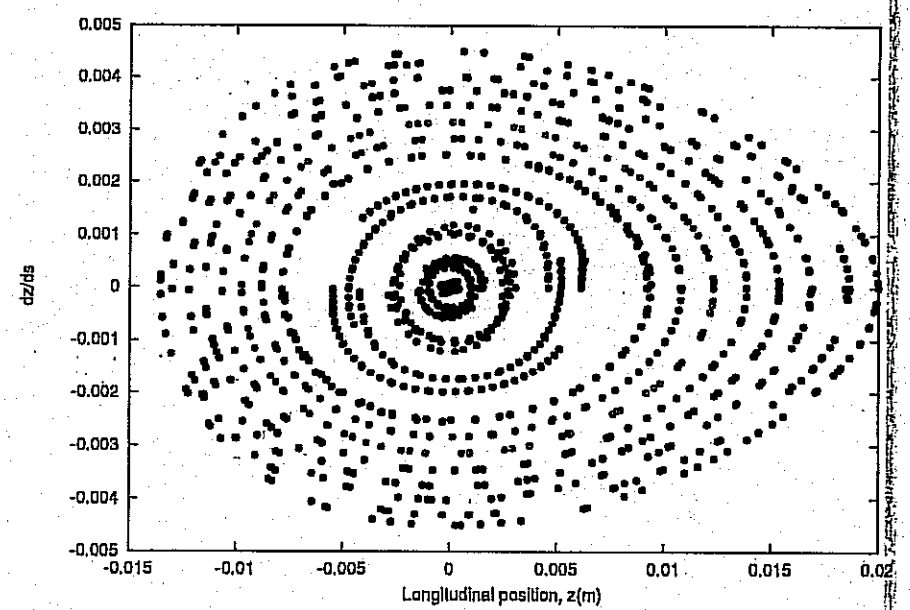

Model w/out RF Nonlinearity

- $k_L/2$ resonance present in 5 mA CTP run when nonlinearity is turned off. Also observed in HALO3D.

CTP test particles

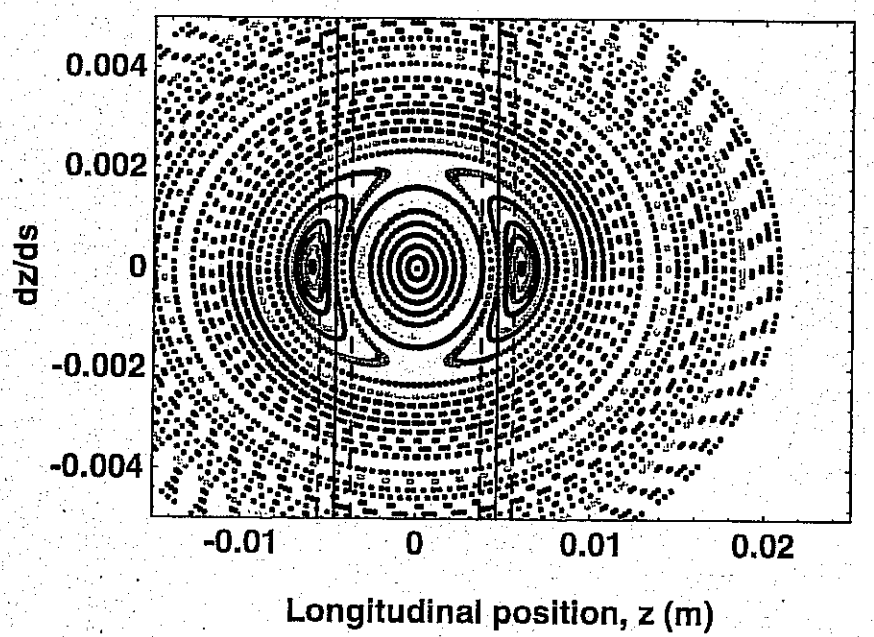

HALO3D test particles

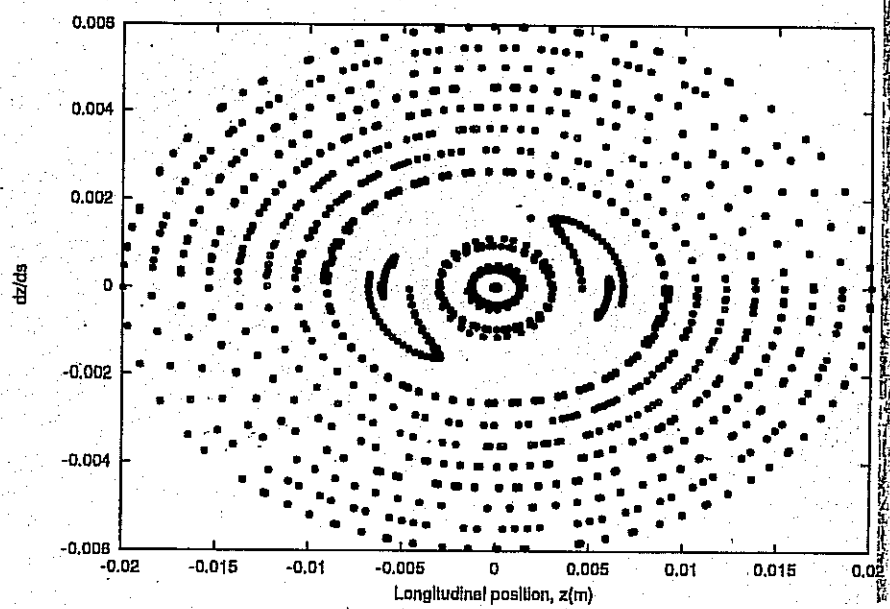

(13)

Numerically determined frequency and amplitude of particle oscillations: non-linear rf focusing

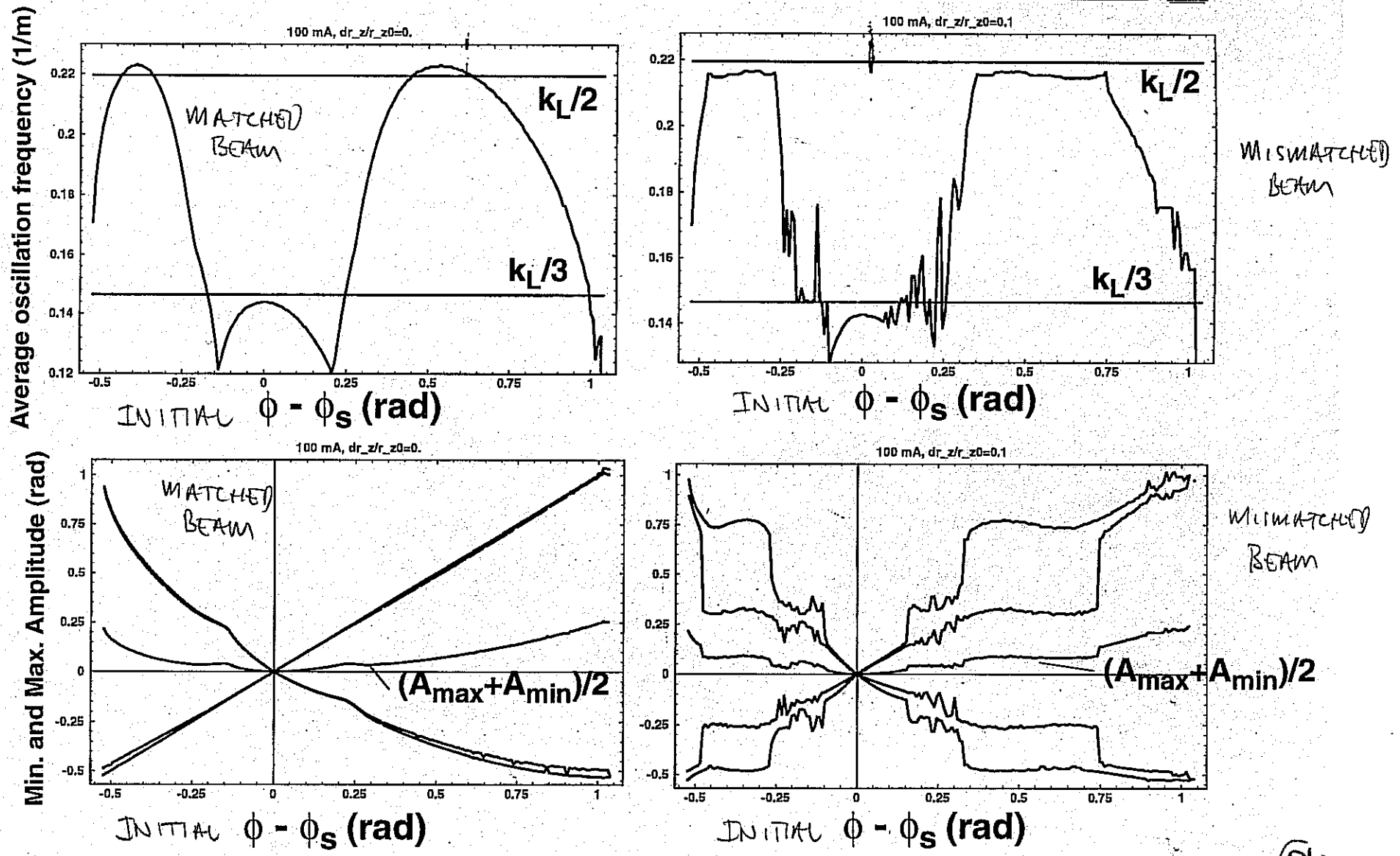

For non-linear rf, $k_L/2$ resonance occurs only over a range of current

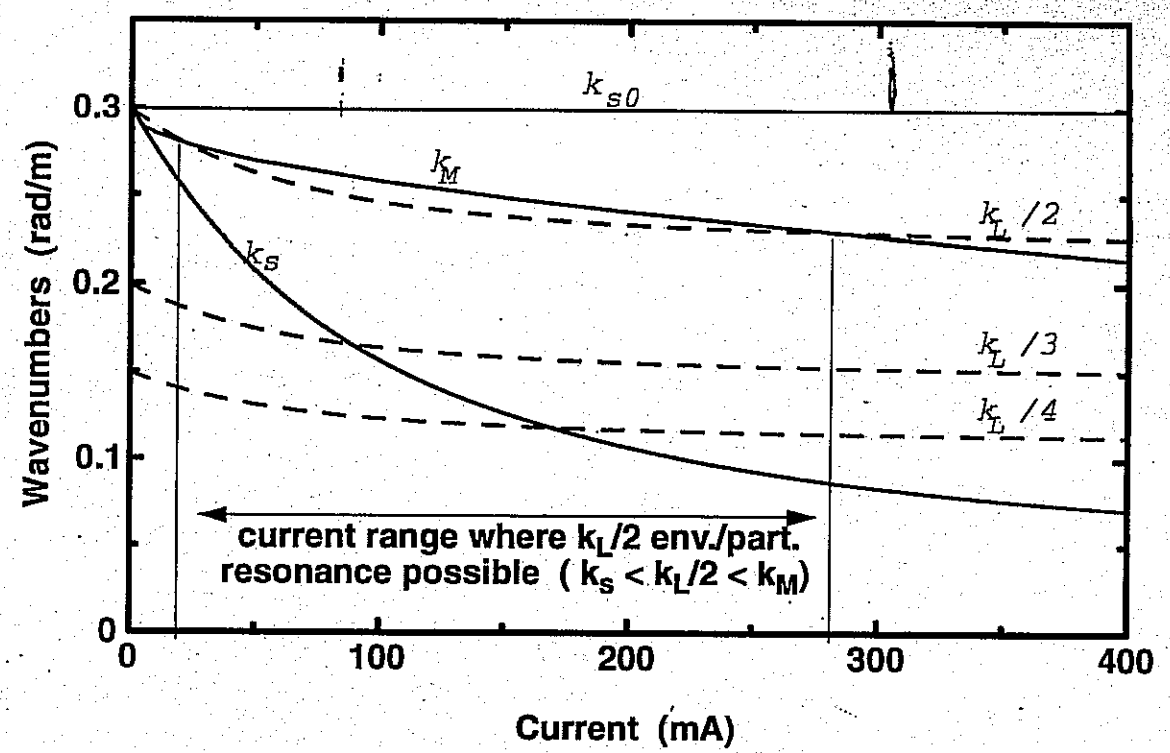

k_{s0} = single particle frequency

k_s = space-charge depressed synchrotron frequency

k_M = maximum particle oscillation frequency

k_L = longitudinal envelope oscillation frequency

AMPLITUDE PHASE ANALYSIS

GLUCKSTERN, PHYS. REV. LETTERS 73, 1247 1994

$$x'' + k_{\beta 0}^2 x = \begin{cases} \dfrac{Q}{r_b^2} x & \text{for } r < r_b \\ \dfrac{Q}{r^2} x & \text{for } r > r_b \end{cases}$$

Assume $r_b = r_{b0} + \epsilon \cos(k_B s)$

$$x'' + k_\beta^2 x = \overbrace{-\frac{Q}{r_{b0}^2} x \left(1 - \frac{r_{b0}^2}{r^2}\right) \Theta(r - r_{b0})}^{\text{EXTERIOR}} + \overbrace{\frac{2\epsilon Q}{r_{b0}^2} x \cos k_B s\, \Theta(r_{b0} - r)}^{\text{INTERIOR}}$$

$$\Theta(x) = \begin{cases} 1 & x > 0 \\ 0 & x < 0 \end{cases}$$

NON-LINEAR TERM MAKES AMPLITUDE DEPENDENT FREQUENCY

ARISING SOLEY FROM ENVELOPE PERTURBATION; ALLOWS TRANSFER FROM CORE

$$k_\beta^2 = k_{\beta 0}^2 - \frac{Q}{r_{b0}^2}$$

GLUCKSTERN TREATED GENERAL CASE OF ARBITRARY ANGULAR MOMENTUM. FOR ILLUSTRATION HERE I SET ANG. MOM = 0. $\Rightarrow x = r$

USE PHASE AMPLITUDE METHOD

$$\frac{x}{r_{b0}} \equiv A(s) \sin \psi(s) \qquad \psi \equiv k_\beta s + \alpha(s)$$

$$\frac{x'}{r_{b0}} \equiv k_\beta A(s) \cos \psi(s)$$

Oscillation AT DEFLECTED PHASE ADVANCE

SLOWLY CHANGING PHASE

Let $x'' + k_\beta^2 x = f(x, s)$

$$= f(A, \psi, k_B s)$$

NOTE
$$\left.\begin{aligned} \frac{x'}{r_{b0}} &= A' \sin\psi + (k_\beta + \alpha') A \cos\psi \\ &= k_\beta A \cos\psi \end{aligned}\right\} \Rightarrow A' \sin\psi + \alpha' A \cos\psi = 0$$

$\frac{d}{ds}A$ & $\frac{d}{ds}\alpha$ CAN BE EXPRESSED IN TERMS OF f

$$x'' = k_p r_{bo} A' \cos\psi - k_p r_{bo} A \sin\psi \overbrace{(k_p + \alpha')}^{\psi'}$$

$$+ k_p^2 x = k_p^2 r_{bo} A \sin\psi$$

$$x'' + k_p^2 x = k_p r_{bo} A' \cos\psi - k_p r_{bo} A \sin\psi\, \alpha' = f(x, s)$$

ALSO $$A' \sin\psi + A \cos\psi\, \alpha' = 0$$

$$\begin{bmatrix} k_p r_{bo} \cos\psi & -k_p r_{bo} \sin\psi \\ \sin\psi & A\cos\psi \end{bmatrix} \begin{bmatrix} A' \\ \alpha' \end{bmatrix} = \begin{bmatrix} f \\ 0 \end{bmatrix}$$

INVERTING MATRIX:

$$\begin{bmatrix} A' \\ \alpha' \end{bmatrix} = \frac{1}{A k_p r_{bo}} \begin{bmatrix} A\cos\psi & k_p r_{bo} \sin\psi \\ -\sin\psi & k_p r_{bo} \cos\psi \end{bmatrix} \begin{bmatrix} f \\ 0 \end{bmatrix}$$

$$A' = \frac{\cos\psi}{k_p r_{bo}} f$$

$$\alpha' = \frac{-\sin\psi}{k_p r_{bo} A} f$$

National® Brand 42-182 100 SHEETS Made in U.S.A.

USING THESE DEFINITIONS THE EQUATION OF MOTION CAN BE EXPRESSED AS:

$$A' = \frac{1}{k_p r_{b0}} f(A, \psi, k_B s) \cos\psi$$

$$\alpha' = \frac{-1}{k_p A r_{b0}} f(A, \psi, k_B s) \sin\psi$$

At resonance we expect $2k_p - k_B \sim 0$,

so define $\Psi = 2\psi - k_B s = (2k_p - k_B)s + 2\alpha$

$$\Rightarrow \Psi' = (2k_p - k_B) + 2\alpha'$$

ELIMINATE $k_B s$ in $f(A, \psi, k_B s)$ using

$$k_B s = 2\psi - \Psi$$

AVERAGE OVER ALL NON-RESONANT FREQUENCY COMPONENTS, FOR RESONANT PARTICLE EQUATIONS OF MOTION:

$$A_r' = \frac{1}{k_p r_{b0}} \int_{-\pi}^{\pi} \frac{d\psi}{2\pi} f(A_r, \Psi_r, \psi) \cos\psi$$

$$\alpha_r' = \frac{-1}{r_{b0} k_p A_r} \int_{-\pi}^{\pi} \frac{d\psi}{2\pi} f(A_r, \Psi_r, \psi) \sin\psi$$

A_r & $\Psi_r = (2k_p - k_B)s + 2\alpha$ are held fixed during integration.

THE RESULT IS

$$A_r' = F_1(A_r, \Psi_r)$$

$$\Psi_r' = (2k_\beta - k_\delta) + 2F_2(A_r, \Psi_r)$$ where F_1 & F_2 are explicit functions of A_r & Ψ_r

Let $w = A_r^2$

$$w' = 2A_r A_r' = 2A_r F_1(A_r, \Psi_r) = 2w^{1/2} F_1(w^{1/2}, \Psi_r)$$

$$\Psi' = (2k_\beta - k_\delta) + 2F_2(A_r, \Psi_r)$$

w & Ψ are conjugate variables, and the resonant particle equation of motion can be derived from an s-independent Hamiltonian H as:

$$w' = \frac{\partial H}{\partial \Psi} \qquad \Psi' = -\frac{\partial H}{\partial w}$$

GLUCKSTERN FOUND A CONSTANT OF THE MOTION $H_r(w, \Psi)$ which satisfies Hamilton's EQUATIONS.

RESONANT PARTICLE WOULD STAY ON LINES OF CONSTANT H.

GLUCKSTERN'S SIMPLIFIED EXAMPLE

$$x'' + k_\beta^2 x = -\frac{Q}{r_{b0}^4} x^3 + \frac{\varepsilon Q}{r_{b0}^2} x \cos k_B s$$

NON-LINEAR FORCE

OSCILLATING CORE

THIS example:

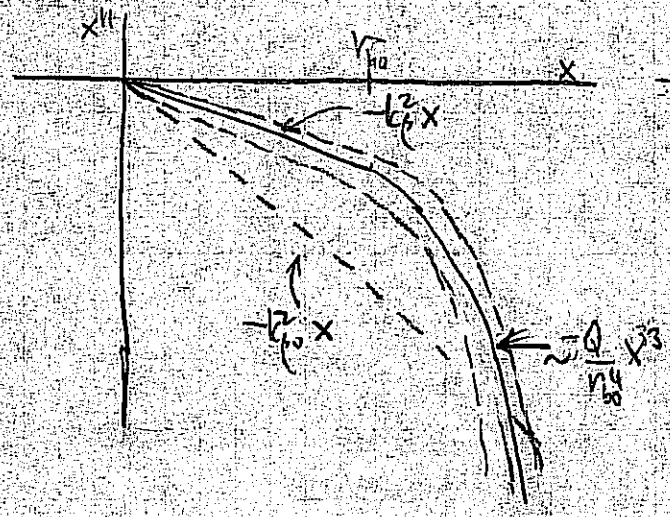

ACTUAL MODEL OF BREATHING BEAM

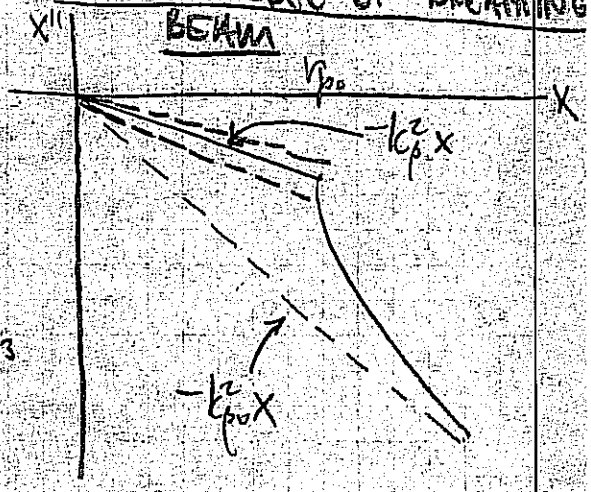

$$x'' + k_\beta^2 x = \frac{-Q}{r_{bo}^4} x^3 + \frac{2\epsilon Q}{r_{bo}^2} x \cos k_B s$$

$$\equiv f(x, s)$$

$$= \frac{-Q}{r_{bo}} A^3 \sin^3\psi + \frac{2\epsilon Q}{r_{bo}} A \sin\psi \cos k_B s$$

$$\left(\text{where } \frac{x}{r_{bo}} \equiv A \sin\psi \;\; \& \;\; \frac{x'}{r_{bo}} \equiv k_\beta A \cos\psi\right)$$

$$\Rightarrow A' = \frac{\cos\psi}{k_\beta r_{bo}} f = \frac{-Q}{k_\beta r_{bo}^2} A^3 \sin^3\psi \cos\psi + \frac{\epsilon Q}{k_\beta r_{bo}^2} A \sin 2\psi \cos k_B s$$

$$\alpha' = \frac{-\sin\psi}{k_\beta r_{bo} A} f = \frac{Q}{k_\beta r_{bo}^2} A^2 \sin^4\psi + \frac{2\epsilon Q}{k_\beta r_{bo}^2} \sin^2\psi \cos k_B s$$

Using $\Psi \equiv 2\psi - k_\beta s \Rightarrow \cos k_B s = \cos[2\psi - \Psi]$

$$= \cos[2\psi]\cos[\Psi] + \sin[2\psi]\sin[\Psi]$$

<u>TRIG IDENTITIES:</u>

$$\sin 2\psi \cos k_B s = \frac{1}{2}\sin\Psi - \frac{1}{2}\cos 4\psi \sin\Psi + \frac{1}{2}\sin 4\psi \cos\Psi$$

$$\sin^4\psi = \frac{3}{8} - \frac{1}{2}\cos 2\psi - \frac{1}{8}\cos 4\psi$$

$$\sin^2\psi \cos k_B s = \cos\Psi\left[-\frac{1}{4} + \frac{1}{2}\cos 2\psi - \frac{1}{4}\cos 4\psi\right] + \sin\Psi\left[\frac{1}{2}\sin 2\psi - \frac{1}{4}\sin 4\psi\right]$$

$$\sin^3\psi \cos\psi = \frac{1}{4}\sin 2\psi - \frac{1}{8}\sin 4\psi$$

$$\Rightarrow \quad A_r' = \frac{\epsilon Q}{2k_p r_{b0}^2} A_r \sin \Psi_r$$

$$\Psi_r' = (2k_p - k_B) + 2\alpha_r'$$

$$= (2k_p - k_B) + \frac{3Q}{4k_p r_{b0}^2} A_r^2 + \frac{\epsilon Q}{k_p r_{b0}^2} \cos \Psi$$

DEFINE $\omega = A_r^2$

$$\omega' = 2 A_r A_r' = \frac{\epsilon Q}{k_p r_{b0}^2} \omega \sin \Psi_r$$

$$\Psi_r' = (2k_p - k_B) + \frac{3Q}{4k_p r_{b0}^2} \omega + \frac{\epsilon Q}{k_p r_{b0}^2} \cos \Psi$$

A Hamiltonian can be found satisfying Hamilton's equations:

$$H = (2k_p - k_B)\omega + \frac{3}{8} \frac{Q}{k_p r_{b0}^2} \omega^2 + \frac{\epsilon Q}{k_p r_{b0}^2} \omega \cos \Psi$$

THIS CAN BE EXPRESSED AS:

$$\epsilon \cos \Psi = \Delta - \frac{3}{8} \omega - \frac{C}{\omega}$$

where C is determined by initial conditions and:

$$\Delta = k_p (k_B - 2k_p) r_{b0}^2 / Q$$

(NOTE: $k_B^2 = 4k_p^2 + 2Q/r_{b0}^2$ for breathing mode).

cos pz], (2.5)

:]. (2.6)

oscillatory terms
number $2q - p$

(2.7)

os Ψ, (2.8)

of this resonant
al of the motion

, (2.9)

and where the
he initial values
ipe equation we
breathing mode,

, (2.10)

d by the space

Guided by the parametrization of the x and
separately, the amplitude-phase parametrizati
two-dimensional oscillation is written as

$$s = \frac{w^2 + L^2}{2w} - \frac{w^2 - L^2}{2w} \cos(2qz + \gamma).$$

Here w and γ are slowly varying amplitude
parameters which would be constant if the rig
Eq. (2.11) vanished. We now write

$$s' = q\,\frac{w^2 - L^2}{w} \sin(2qz + \gamma)$$

and use Eq. (2.11) and the required connectio
w' and γ' implied by Eq. (2.13) to obtain explic
sions for w' and γ'. We then average over osci

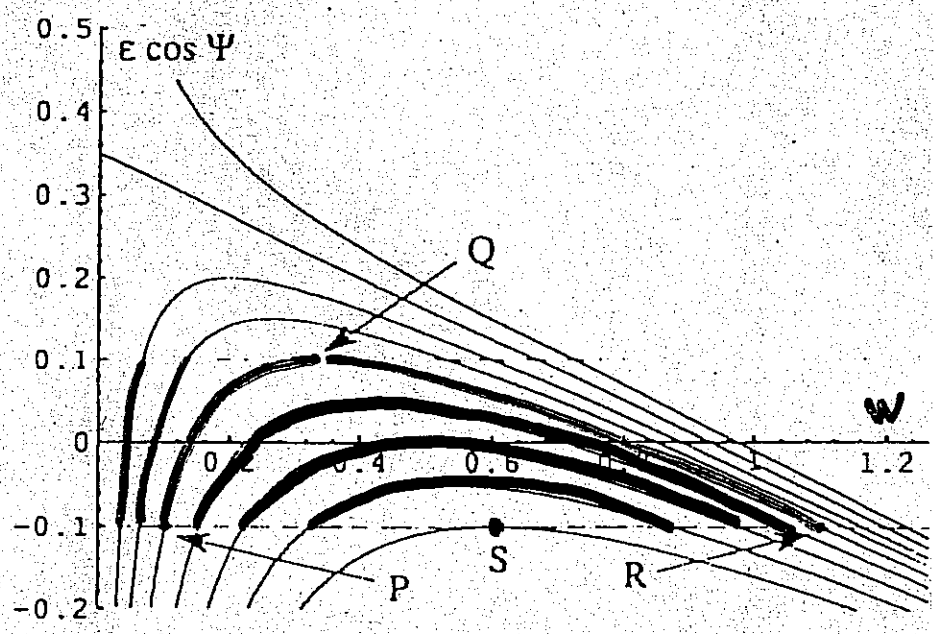

FIG. 1. Plot of $\epsilon \cos\Psi$ vs w for the simplified n
$\Delta = 0.35$.

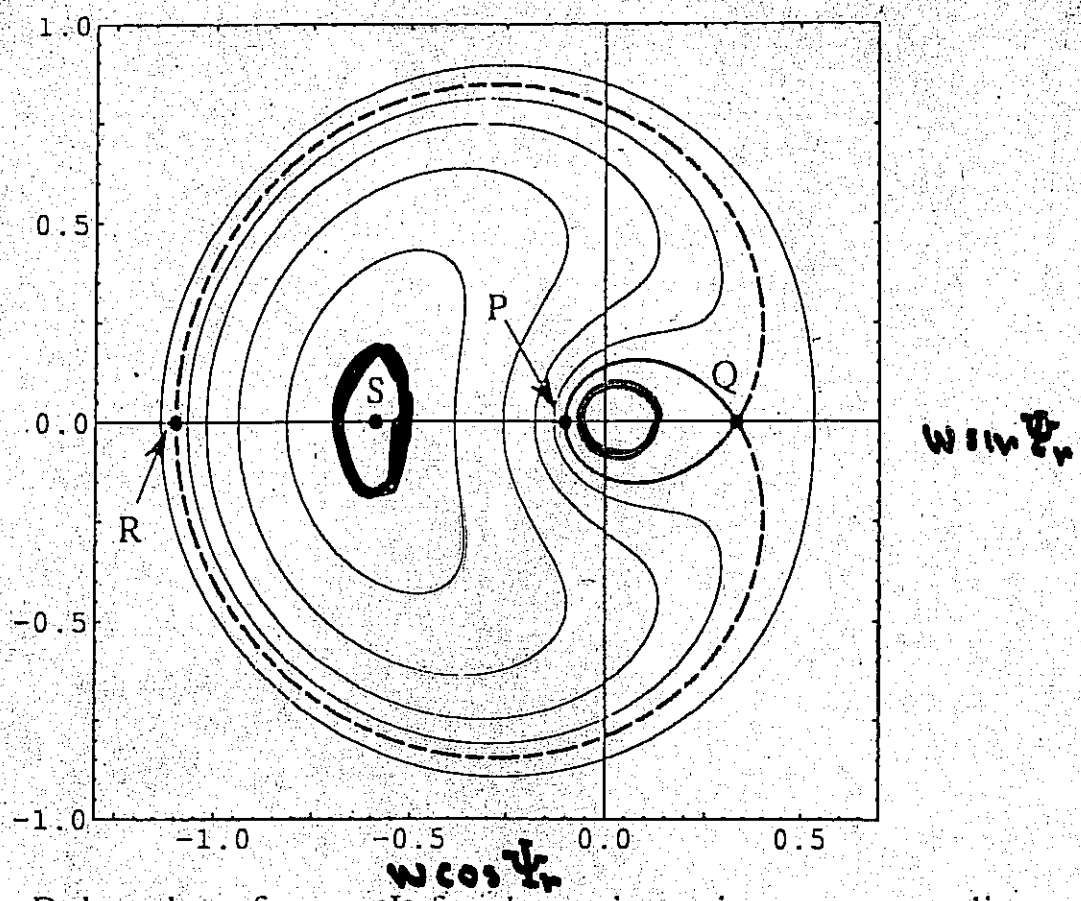

FIG. 2. Polar plot of w vs Ψ for the trajectories corresponding to the parametric resonance using $\Delta = 0.35$, $\epsilon = 0.1$, and the simplified model.

all wave numbers except $2q - p$, being careful to include the step functions as we obtain these averages. The final equations for w' and Ψ' [$\Psi = (2q - p)z + \gamma$] are similar to Eqs. (2.7) and (2.8) and again lead to an integral of the motion, which now is

$$g(1 - h)\epsilon \cos\Psi = f\Delta - t - C, \qquad (2.14)$$

where $f(w) = (w^2 + L^2)/2w$, $g(w) = (w^2 - L^2)/2w$.

Here

^{2} (2.15)

Also

$\overline{f}\Big)$

(2.16)

The arc-
quadrant.
ependence
ession for
Eq. (2.6)

fect when
rough the
$\Delta = 0.35$
ery similar
Fig. 4 for
model in
cale for w
ming with
en by the

am.—The
to

where $\delta = \epsilon^2 - (1/2)^2$ and $\Omega = (1/2)$

Therefore the distribution in L for a K-V beam is unif
from $L = -1/2$ to $L = 1/2$ and vanishes for $|L| > 1/$

IV. Implications of the model.—Since the breat
K-V beam is a solution of the Vlasov equation, parti
within the core will continue to remain there, ever
the presence of the resonant interaction. If howe

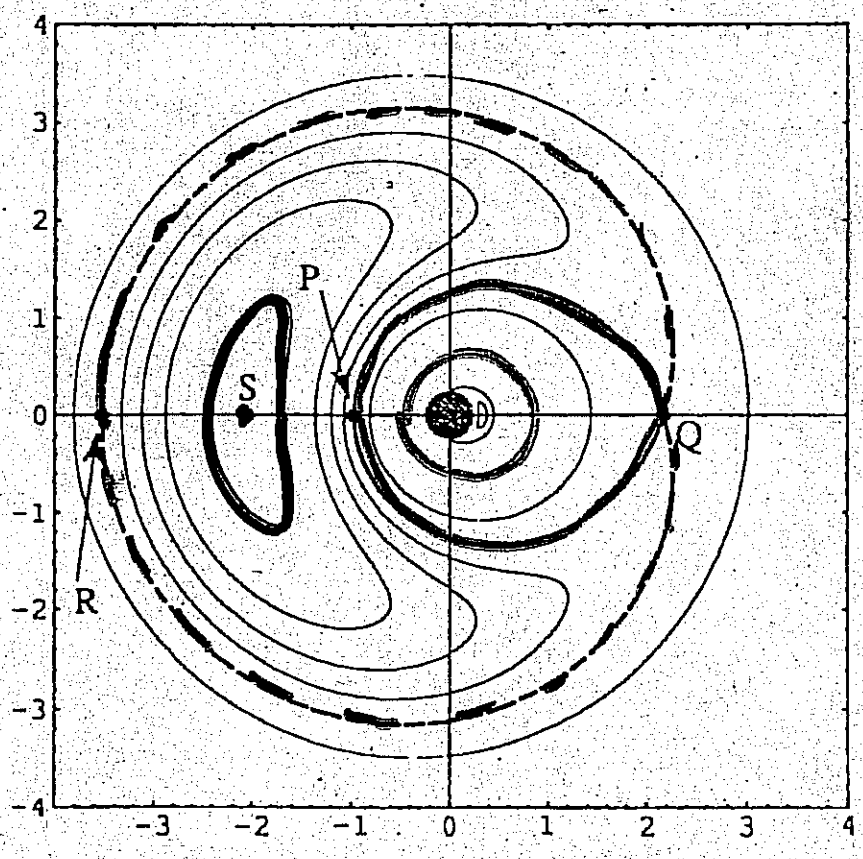

FIG. 4. Polar plot of w vs Ψ for the trajectories correspon
to the parametric resonance using $\Delta = 0.35$, $L = 0$, $\epsilon =$
and the exact model.

Bob Gluckstern
Univ. of Maryland.

$$x = \pm 3^{1/2} r_0 \left[\frac{\sin\xi_0 + \xi_0 \cos\xi_0}{\xi_0 + \xi_0 \cos\xi_0}\right]^2$$

$$x' = \pm 3^{1/2} r_0 k_0 \left[\frac{\cos\xi_0}{\xi_0 + \xi_0 \cos\xi_0}\right]^2$$

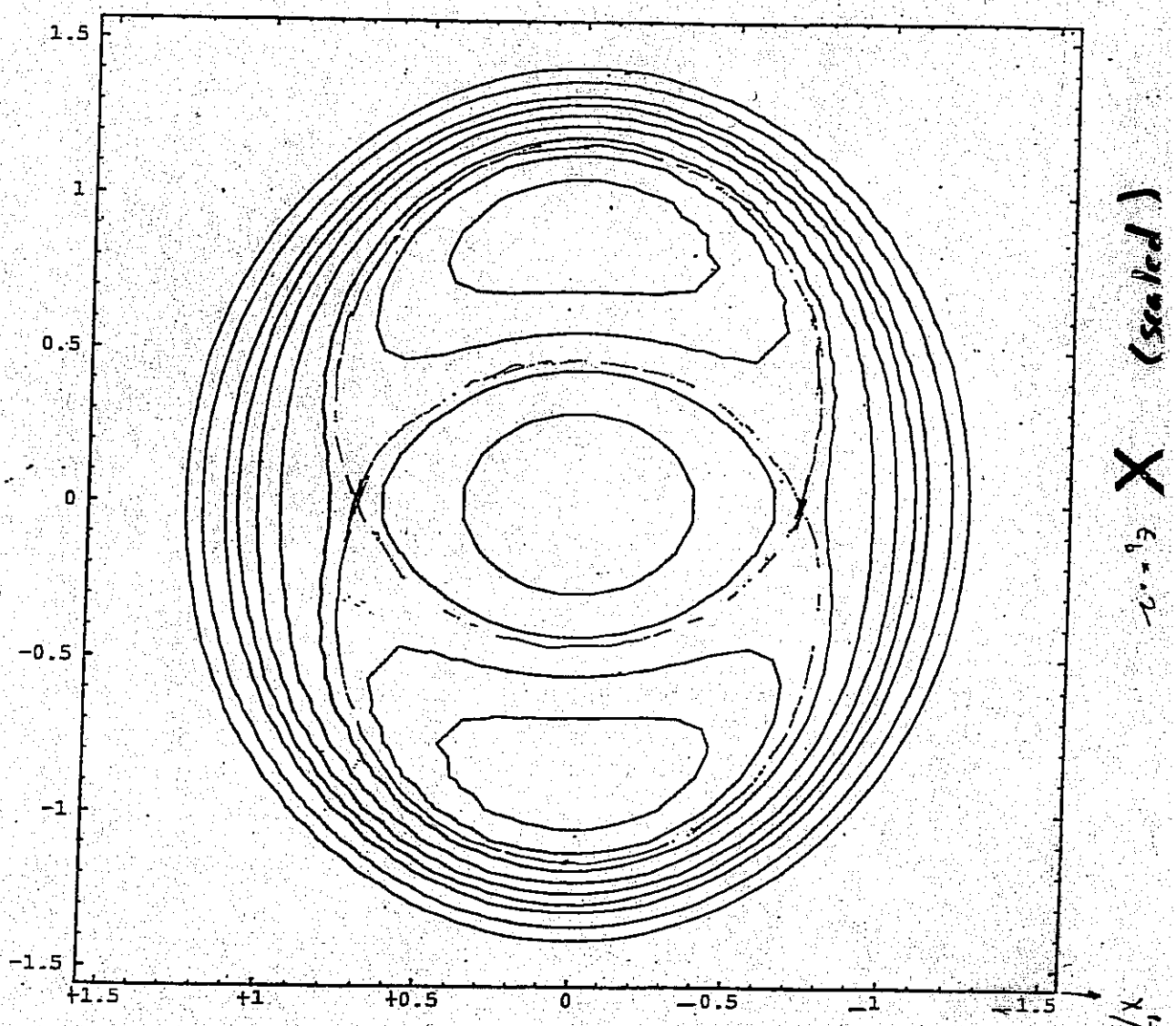

Fig 3.

FROM Tom Wangler
Los Alamos National Lab

Stroboscopic Map (The Peanut Diagram)

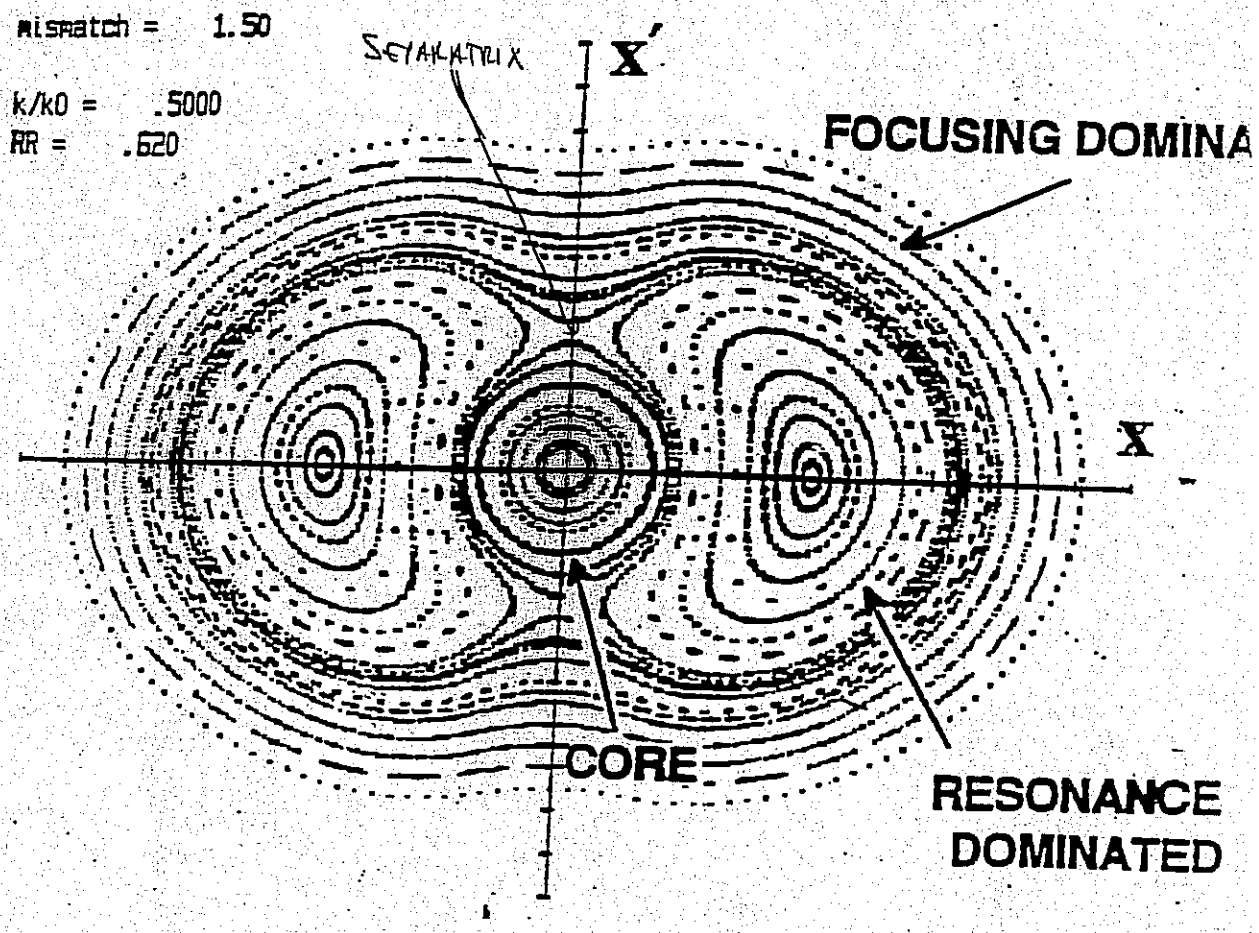

- Accumulate **Many Snapshots of Phase Space Taken at Minimum Amplitude of Core Oscillation.** (OR ANY PARTICULAR PHASE)
- Follow an Array of Particles to Obtain a "Trajectory Field".
- Regular Trajectories Appear as Smooth Curves.
- Chaotic Trajectories Appear as Stochastic Scatter.
- INITIAL POSITIONS OF PARTICLES IN PHASE SPACE WERE EQUALLY SPACED ALONG X & X' AXES.

Analytic Model for Halo Formation in High Current Ion Linacs

Robert L. Gluckstern
Physics Department, University of Maryland, College Park, Maryland 20742
(Received 8 March 1994)

We construct an azimuthally symmetric 2D model for halo formation in high current ion linacs. The driving term, a "breathing" oscillation caused by a transverse mismatch along the linac, leads to growth of ion amplitudes in the core through the parametric resonance. As the ion amplitude grows, its wave number increases, enhancing the resonance. This leads to the formation of a halo surrounding the core. We explore the dependence of this mechanism on the tune depression and the size of the mismatch. The model agrees well with simulations at Los Alamos, but does not yet include the effects of chaos observed in the simulations as the tune depression becomes severe.

PACS numbers: 41.85.−p, 29.17.+w, 29.27.Bd

I. Introduction.—High current, high duty factor ion linacs have become increasingly attractive in recent years. Among possible applications are heavy ion drivers for thermonuclear energy production, production of tritium, transmutation of radioactive wastes, and production of radioactive isotopes for medical use.

Obviously, it is desirable to accelerate the maximum possible current in such linacs. Much work has been done to explore the optimum transverse phase space distribution in such beams. In particular, the Kapchinsky-Vladimirsky (K-V) distribution [1] is simplest to analyze, since this projection into real space has a uniform density and therefore linear space charge forces. The stability of the K-V distribution has been analyzed and approximately confirmed by numerical simulations. Nevertheless it appears that, particularly at high currents, the K-V and other equilibrium distributions evolve to ones with rounded edges and tails. In many cases involving high peak current, the distribution spins off a cluster of particles in the form of a halo surrounding a dense core. This halo is seen in simulations as well as in actual linacs, such as LAMPF [2]. And efforts to remove the halo by collimation have been largely unsuccessful since the halos almost always regenerate.

It is clear that the halos will produce unacceptably high levels of radioactivity in high current, high duty factor linacs. For this reason considerable effort has recently been devoted to exploring their detailed structure and understanding the mechanism or mechanisms by which the halos are produced [3–6]. What has been learned is that halos are most likely to be produced at transition locations, such as where there are discontinuities in frequency, structure geometry, transverse focusing pattern, accelerating gradient and phase, etc.

In the present paper, we propose an analytic model for halo formation which appears to reproduce the main features seen in simulations and in actual linacs. In particular we consider a circular cw beam with a K-V core distribution and explore the motion of individual ions passing through the core. Since energy transfer between ions and the core can take place only if the core has a time dependent behavior, we consider the driving mechanism to be a "breathing" oscillation of the core. We then explore the resonant (parametric) interaction between the breathing core and the ions oscillating about and through the core. Of particular importance is the dependence of the frequency of each oscillating ion on its amplitude, which is related to the fraction of the oscillation for which the ion is within the core.

In spite of the fact that the actual distribution will have nonlinear fields, the use of a K-V distribution for the analysis leads us to a very likely mechanism for the development of the halo. In particular, the results provide an explanation for the low density region around the core which is surrounded by a somewhat higher density halo ring. This explanation will probably still apply for other self-consistent distributions.

II. Model.—We consider an azimuthally symmetric K-V core of radius a for which the equation of motion of an ion is

$$x'' + k^2 x = x \begin{Bmatrix} \kappa/a^2, & r \le a \\ \kappa/r^2, & r \ge a \end{Bmatrix}, \tag{2.1}$$

where the prime stands for d/dz, and k is the wave number of the transverse motion in the absence of space charge. The perveance of the beam, $\kappa = eI/2\pi\epsilon_0 m v^3$, is a dimensionless parameter proportional to the current I, where e, m, and v are the charge, mass, and ion velocity, and ϵ_0 is the permittivity of free space. The equation for y is identical to Eq. (2.1).

We now assume a core oscillation of wave number p of the form $a \to a(1 - \epsilon \cos pz)$ and expand a^{-2} in Eq. (2.1) to first order in ϵ, the relative oscillation amplitude. After some algebra, Eq. (2.1) can be written as

$$x'' + q^2 x = -\frac{\kappa}{a^2} x\left(1 - \frac{a^2}{r^2}\right)\Theta(r-a) + \frac{2\epsilon\kappa}{a^2} x \cos pz\, \Theta(a-r), \tag{2.2}$$

where $\Theta(u) = 1,0$ for $u > 0, u < 0$ and where $q = \sqrt{k^2 - \kappa/a^2}$ is the wave number of oscillations within the core.

© 1994 The American Physical Society

With the radial forces of Eq. (2.2), we see that the angular momentum $Lqa^2 = xy' - x'y = r^2\theta'$ is constant. The equation for radial motion then becomes

$$r'' + q^2\left(r - \frac{L^2a^4}{r^3}\right) = -\frac{\kappa}{a^2}r\left(1 - \frac{a^2}{r^2}\right)\Theta(r-a) + 2\frac{\epsilon\kappa}{a^2}r\cos pz\,\Theta(a-r). \tag{2.3}$$

The first term on the right makes the oscillation wave number depend on amplitude and the second allows for energy transfer between the core and the oscillating ion.

In order to understand the role of the different terms in Eq. (2.3), we construct a simplified model by setting $L = 0$ and invoking a pendulum model for the first term on the right side of Eq. (2.3) by replacing $r(1 - a^2/r^2)\Theta(r-a)$ by r^3/a^2, corresponding to the cubic nonlinear term for a pendulum. (However, its sign is opposite from the conventional pendulum since, in our model, the wave number *increases* with increasing amplitude.) In addition, we extend the driving term to all values of r. The simplified equation for x is therefore

$$x'' + q^2x = -\frac{\kappa}{a^2}\frac{x^3}{a^2} + 2\frac{\epsilon\kappa}{a^2}x\cos pz. \tag{2.4}$$

We now use the phase-amplitude method by writing $x/a = A\sin\psi$, $x'/a = qA\cos\psi$, where $\psi = qz + \alpha$, implying $A'\sin\psi + A\alpha'\cos\psi = 0$. Here A and α are taken to be the slowly varying amplitude and phase parameters of the ion oscillation. Substituting into Eq. (2.4) and solving for A' and α' we obtain

$$A' = -\frac{\kappa A}{qa^4}[A^2\sin^3\psi\cos\psi - \epsilon a^2\sin 2\psi\cos pz], \tag{2.5}$$

$$\alpha' = \frac{\kappa}{qa^4}[A^2\sin^4\psi - 2\epsilon a^2\sin^2\psi\cos pz]. \tag{2.6}$$

We now average over all rapidly varying oscillatory terms with the exception of the one with wave number $2q - p$ (the parametric resonance) and obtain

$$A' = \frac{\epsilon\kappa}{2qa^2}A\sin\Psi, \tag{2.7}$$

$$\Psi' = (2q - p) + \frac{3\kappa}{4qa^4}A^2 + \frac{\epsilon\kappa}{qa^2}\cos\Psi, \tag{2.8}$$

where $\Psi = (2q - p)z + 2\alpha$ is the phase of this resonant interaction. One then finds that an integral of the motion exists, enabling us to write [7]

$$\epsilon\cos\Psi = \Delta - \frac{3}{8}w - \frac{C}{w}, \tag{2.9}$$

where $w = A^2/a^2$, $\Delta = q(p - 2q)a^2/\kappa$, and where the integration constant C is determined by the initial values of w and 2α. By resorting to the envelope equation we can show that $p^2 = 4q^2 + 2\kappa/a^2$ for the breathing mode, so that

$$\Delta = \frac{1}{1 + \sqrt{(1 + k^2/q^2)/2}}, \tag{2.10}$$

where q/k is the tune depression caused by the space charge. In Fig. 1 we plot $\epsilon\cos\Psi$ vs w for $q/k = 0.412$, $\Delta = 0.35$, and various values of C. For $\epsilon = 0.1$, the polar plot of w vs Ψ is shown in Fig. 2. It is clear that Q is an unstable fixed point and that the origin and S are stable fixed points. Figure 2 is equivalent to a "second order stroboscopic plot" for integral values of $pz/2\pi$, and contains the main features of the resonant interaction. Specifically, all trajectories starting within the inner separatrix (thick solid curve) bounded by P and Q oscillate in stable orbits while any trajectory starting just outside will travel along the outer separatrix (thick dashed curve). For these particles, as the amplitude of motion grows the true oscillation wave number increases, enhancing the resonant term and *locking in* to the resonance. And the presence of a thin distribution of trajectories near the outer separatrix has the appearance of a halo in $x - y$ space at the radius corresponding to R in Figs. 1 and 2.

We now drop the simplified model and return to Eq. (2.3). Although the algebra is far more complicated we eventually obtain a more accurate version of Eq. (2.9) with a very similar set of curves to those in Figs. 1 and 2. First we rewrite Eq. (2.3) for the variable $s = r^2/a^2$, obtaining

$$s'' - \frac{(s')^2}{2s} + 2q^2\left(s - \frac{L^2}{s}\right) = -\frac{2\kappa}{a^2}(s-1)\Theta(s-1) + 4\frac{\epsilon\kappa}{a^2}s\cos pz\,\Theta(1-s). \tag{2.11}$$

Guided by the parametrization of the x and y motions separately, the amplitude-phase parametrization of the two-dimensional oscillation is written as

$$s = \frac{w^2 + L^2}{2w} - \frac{w^2 - L^2}{2w}\cos(2qz + \gamma). \tag{2.12}$$

Here w and γ are slowly varying amplitude and phase parameters which would be constant if the right side of Eq. (2.11) vanished. We now write

$$s' = q\frac{w^2 - L^2}{w}\sin(2qz + \gamma) \tag{2.13}$$

and use Eq. (2.11) and the required connection between w' and γ' implied by Eq. (2.13) to obtain explicit expressions for w' and γ'. We then average over oscillations at

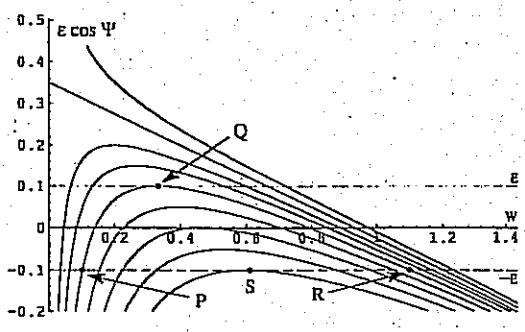

FIG. 1. Plot of $\epsilon\cos\Psi$ vs w for the simplified model with $\Delta = 0.35$.

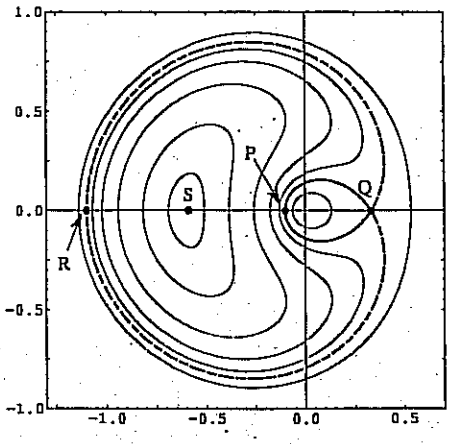

FIG. 2. Polar plot of w vs Ψ for the trajectories corresponding to the parametric resonance using $\Delta = 0.35$, $\epsilon = 0.1$, and the simplified model.

all wave numbers except $2q - p$, being careful to include the step functions as we obtain these averages. The final equations for w' and Ψ' [$\Psi = (2q - p)z + \gamma$] are similar to Eqs. (2.7) and (2.8) and again lead to an integral of the motion, which now is

$$g(1 - h)\epsilon\cos\Psi = f\Delta - t - C, \qquad (2.14)$$

where $f(w) = (w^2 + L^2)/2w$, $g(w) = (w^2 - L^2)/2w$. Here

$$\pi h(w) = \tan^{-1}[\ell/(1 - f)] + \ell(1 - f)/2g^2 \qquad (2.15)$$

for $w \geq 1$ and $\ell(w) = \sqrt{(w - 1)(w - L^2)/w}$. Also

$$t(w) = \frac{1}{\pi}\int_1^w \frac{dw}{wg}\left[(g^2 - f)\tan^{-1}\left(\frac{\ell}{1 - f}\right) + f\ell + L\tan^{-1}\left(\frac{2L\ell}{f - L^2}\right)\right], \qquad (2.16)$$

for $w \geq 1$, and $h(w) = t(w) = 0$ for $w \leq 1$. The arctangents are taken to be in the first or second quadrant. The term in $b(w)$ comes from the amplitude dependence of the ion wave number. A more accurate expression for $b(w)$ can be obtained, if necessary, by solving Eq. (2.6) with $\epsilon = 0$.

Since the resonance will have its greatest effect when $L = 0$, corresponding to ion orbits which pass through the core center, we present a plot of $\epsilon\cos\Psi$ vs w for $\Delta = 0.35$ and $L = 0$ in Fig. 3. The pattern of curves is very similar to that in Fig. 1, and the w, Ψ polar plot in Fig. 4 for $\epsilon = 0.1$ has the same topology as for the simple model in Fig. 2, as is also the case for $L \neq 0$. But the scale for w is about 7 times larger, corresponding to a detuning with amplitude about 7 times smaller than that given by the 3/8 factor in Eq. (2.14).

III. Distribution of L in a symmetric K-V beam.—The distribution in L for a K-V beam is proportional to

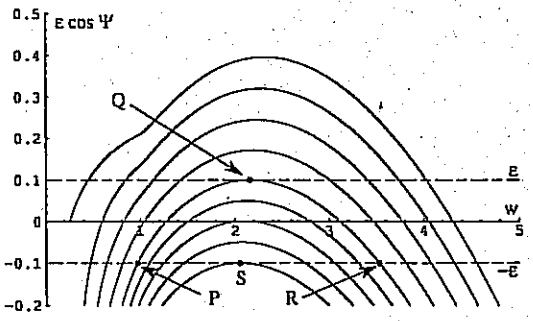

FIG. 3. Plot of $\epsilon\cos\Psi$ vs w for the exact model with $\Delta = 0.35$, $L = 0$.

$$f(L) \sim \int\int\int\int dx\,dy\,dx'\,dy'\,\delta\Big(x^2 + y^2 + \frac{(x')^2}{q^2} + \frac{(y')^2}{q^2} - a^2\Big)\delta(x'y - xy' - Lqa^2). \qquad (3.1)$$

We first do 45° rotations from the x/a, y'/qa space to the u, u' space and from the y/a, x'/qa space to the v, v' space and follow this by integrating over the polar angles in the uv' and vu' spaces. This leads to

$$f(L) \sim \int_0^\infty ds \int_0^\infty dt\,\delta(s + t - 1)\delta\Big(\frac{s - t}{2} - L\Big) = \begin{cases} 1, & 2|L| < 1 \\ 0, & 2|L| > 1 \end{cases}, \qquad (3.2)$$

where $s = u^2 + (v')^2$ and $t = v^2 + (u')^2$ are both positive. Therefore the distribution in L for a K-V beam is uniform from $L = -1/2$ to $L = 1/2$ and vanishes for $|L| > 1/2$.

IV. Implications of the model.—Since the breathing K-V beam is a solution of the Vlasov equation, particles within the core will continue to remain there, even in the presence of the resonant interaction. If however,

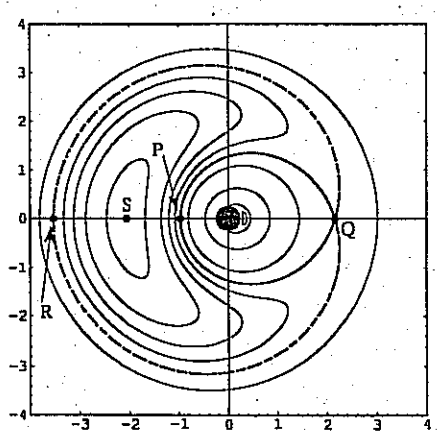

FIG. 4. Polar plot of w vs Ψ for the trajectories corresponding to the parametric resonance using $\Delta = 0.35$, $L = 0$, $\epsilon = 0.1$, and the exact model.

some other mechanism moves the particle outside the core, particularly to an oscillation amplitude exceeding that corresponding to the points P or Q in the figures, a halo will develop at a radius corresponding to point R in the figures. The most likely mechanism to do this is an instability associated with a nonlinear density perturbation. In addition, simulations show that chaotic motion develops near point Q in the figures for a large amplitude breathing mode at high current, enabling particles in the core to populate the halo.

V. Summary and discussion.—We considered a symmetric K-V beam undergoing a breathing mode and found that the parametric resonance ($2q = p$) is a vehicle for particles to leave the core of the beam and perform excursions to large amplitude, forming a distribution in real space in the form of a halo. In this calculation, we neglected the effect of high frequency terms, and the effect of other possible resonances and driving oscillations. Thus our model, which successfully describes a mechanism by which halos can and probably do form, is only an approximation to a much more complicated situation.

We have compared our predictions with some preliminary simulations performed for $L = 0$ by Wangler [8], and find that, for tune depressions from $q/k = 1$ to 0.6, the topology of the stroboscopic plot resembles Figs. 2 and 4 very closely. For tune depressions below 0.6, the stroboscopic plot shows the onset of chaotic behavior in an ever widening band near the inner separatrix as the tune depression deepens. Particles inside but near to the inner separatrix are then able to move outside the inner separatrix and participate more easily in the development of the halo.

Wangler's simulations using a K-V beam [8] confirm that core ions always remain within the inner separatrix. It is quite possible for core ions to lie outside the equivalent inner separatrix for nonuniform equilibrium charge density distributions. We therefore expect the halo mechanisms in the present model to apply to non-K-V beams as well. Lagniel's simulations [6] give similar results, showing the onset of chaos for high space charge as well as the similarity with the three-body astronomical problem.

Our present model is unable to describe either diffusion or chaos in the w, Ψ phase space. If we were to try to do so we would have to include the neglected high frequency terms, as well as resonances other than the one corresponding to the parametric resonance. Integrals of the motion corresponding to Eq. (2.14) would no longer be valid. Descriptions of the growth of halos including the effects of chaos and diffusion will require further analysis and/or extensive numerical simulations.

The author would like to thank Alex Dragt, Bob Jameson, Pierre Lapostolle, Ron Ruth, Rob, Ryne, Fred Skiff, and Tom Wangler for several helpful comments. He is also indebted to Dan Abell for performing the calculations leading to Figs. 1–4.

[1] See I.M. Kapchinsky, *Theory of Resonance Linear Accelerators* (Harford Academic Press, New York, 1985), p. 247ff.

[2] R.A. Jameson, Los Alamos Report No. LA-UR-93-1209 (unpublished). Jameson describes the early observations of emittance growth and halo production, with particular reference to LAMPF simulations and observations.

[3] M. Reiser, in Proceedings of the 1991 Particle Accelerator Conference, San Francisco, California, (unpublished), p. 2497.

[4] A. Cucchetti, M. Reiser, and T. Wangler, in Proceedings of the 1991 Particle Accelerator Conference (Ref. [3]), p. 251.

[5] J.S. O'Connell, T.P. Wangler, R.S. Mills, and K.R. Crandall, in Proceedings of the 1993 Particle Accelerator Conference, Washington, D.C. (unpublished), p. 3657.

[6] J.M. Lagniel, Nucl. Instrum. Methods Phys. Res., Sect. A 345, 46 (1994).

[7] This result can also be obtained using a contact transformation, followed by neglecting rapidly oscillating terms. In fact, the transformed Hamiltonian in the canonical variables w and Ψ is $H = (\kappa/qa^2)[w\epsilon\cos\Psi - \Delta w + 3w^2/8]$.

[8] Tom Wangler (private communication).

Transverse Kinetic Stability*

Steven M. Lund
Lawrence Livermore National Laboratory (LLNL)

Steven M. Lund and John J. Barnard
"Beam Physics with Intense Space-Charge"
US Particle Accelerator School
Boston University, Waltham, MA
12-23 June, 2006

* Research supported by the US Dept. of Energy at LBNL and LLNL under contract Nos. DE-AC03-76SF00098 and W-7405-Eng-48

Transverse Kinetic Stability: Outline

Overview: Machine Operating Points
Overview: Collective Modes and Transverse Kinetic Stability
Linearized Vlasov Equation
Collective Modes on a KV Equilibrium Beam
Global Conservation Constraints
Kinetic Stability Theorem
rms Emittance Growth and Nonlinear Fields
rms Emittance Growth and Nonlinear Space-Charge Fields
Uniform Density Beams and Extreme Energy States
Collective Relaxation and rms Emittance Growth
Phase Mixing and Landau Damping in Beams
References

Transverse Kinetic Stability: Detailed Outline

1) Overview: Machine Operating Points

Notions of beam stability
Tiefenback experimental results for quadrupole transport

2) Overview: Collective Modes and Transverse Kinetic Stability

Possibility of collective internal modes
Vlasov model review
Plasma physics approach to beam physics

3) The Linearized Vlasov Equation

Equilibrium and perturbations
Linear Vlasov equation
Method of Characteristics
Discussion

4) Collective Modes on a KV Equilibrium Beam

KV equilibrium
Linearized equations of motion
Solution of equations
Mode properties
Physical mode components based on fluid model
Periodic focusing results

Detailed Outline - 2

5) Global Conservation Constraints

Conserved quantities
Implications

6) Kinetic Stability Theorem

Effective free energy
Perturbation bound

7) rms Emittance Growth and Nonlinear Forces

Equations of motion
Coupling of nonlinear forces to rms emittance evolution

8) rms Emittance Growth and Nonlinear Space-Charge Forces

Self-field energy
rms equivalent beam forms
Wangler's theorem

Detailed Outline - 3

9) Uniform Density Beams and Extreme Energy States
- Variational formulation
- Self-field energy minimization

10) Collective Relaxation and rms Emittance Growth
- Conservation constraints
- Relaxation processes
- Emittance growth bounds from space-charge nonuniformities

11) Phase Mixing and Landau Damping in Beams

References

S1: Overview: Machine Operating Points

Good transport of a single component beam with intense space-charge described by a Vlasov-Poisson type model requires:

Lowest Order:

1. Stable single-particle centroid

Next Order:

2. Stable rms envelope

Higher Order:

3. "Stable" Vlasov description

Transport of a relatively smooth initial beam distribution can fail or become "unstable" within the Vlasov model for several reasons:

- Collective modes internal to beam become unstable and grow
  - Large amplitudes can lead to statistical (rms) beam emittance growth
- Excessive halo generated
  - Increased statistical beam emittance and particle losses
- Combined processes above

Transport limits in periodic (FODO) quadrupole lattices that result from higher order processes have been measured in the SBTE experiment. These results have only a limited theoretical understanding in 20+ years

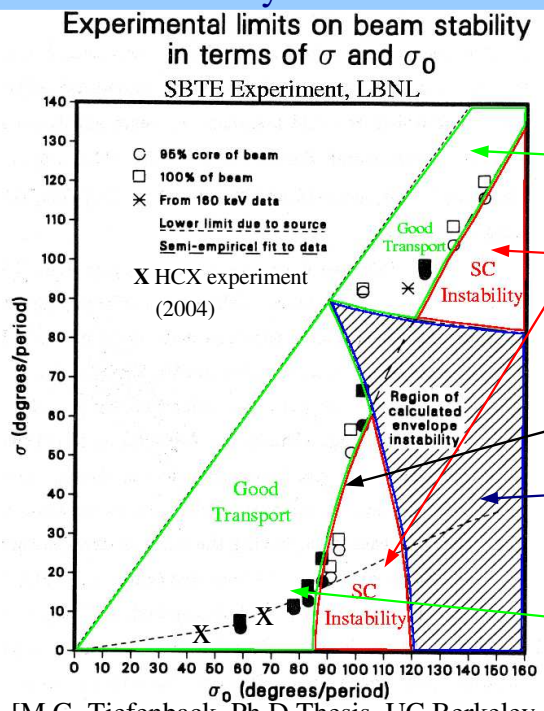

Limits defined with respect to reasonable (smooth) initial distributions

Low Space-Charge Intensity Transport

Emittance Blow Up (Unexplained)
-- Not Practical for Applications

Empirical fit to higher-order stability boundary

$$\sigma_0^2 - \sigma^2 = \frac{1}{2}(120^\circ)^2$$

Envelope Instability
– Not Practical for Applications

High Space-Charge Intensity Transport
- Valid for Practical Applications

[M.G. Tiefenback, Ph.D Thesis, UC Berkeley (1986)]

Summary of beam stability with intense space-charge in a quadrupole transport lattice: centroid, envelope, and theory boundary based on higher order emittance growth/particle losses

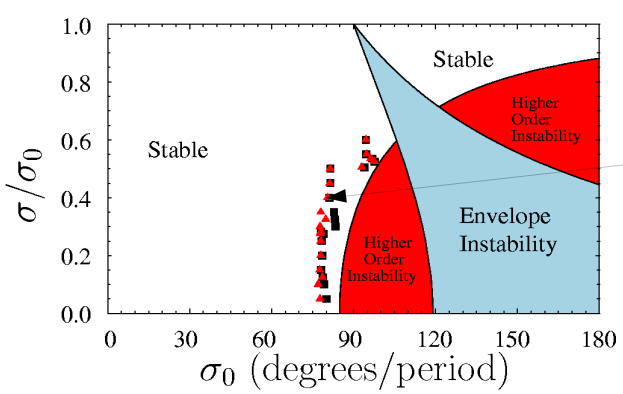

Theory stability boundary points

New theory analyzes processes relating to AG transport limits without equilibria

- Suggests near core, chaotic halo resonances can drive strong emittance growth and particle losses
- Results checked with fully self-consistent simulations

Analogous results (with less "instability") exist for solenoidal transport

[Lund and Chawla, NIMA 561 203 (2006)]

S2: Overview:
Collective Modes and Transverse Kinetic Stability

In discussion of transverse beam physics we have focused on:

Equilibrium

- Used to estimate balance of space-charge and focusing forces
  - KV model for periodic focusing
  - Continuous focusing equilibria for qualitative guide on space-charge effects such as Debye screening and nonlinear equilibrium self-field effects

Centroid/Envelope Modes and Stability

- Lowest order collective oscillations of the beam
  - Analyzed assuming fixed internal form of the distribution
- Model only exactly correct for KV equilibrium distribution
  - Should hold in a leading-order sense for a wide variety of real beams
- Predictions of instability regions are well verified by experiment
  - Significantly restricts allowed system parameters for periodic focusing lattices

Example – Envelope Modes on a Round, Continuously Focused Beam

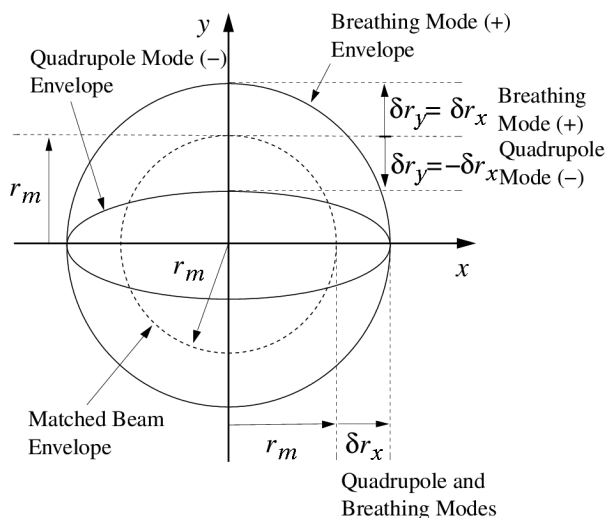

The analog of these modes in a periodic focusing lattice can be destabilized

- Constrains system parameters to avoid band (parametric) regions of instability

Reminder (lecture on *Centroid and Envelope Descriptions of Beams*): Instability bands of the KV envelope equation are well understood in periodic focusing channels

Envelope Mode Instability Growth Rates

Solenoid (η = 0.25) Quadrupole FODO (η = 0.70)

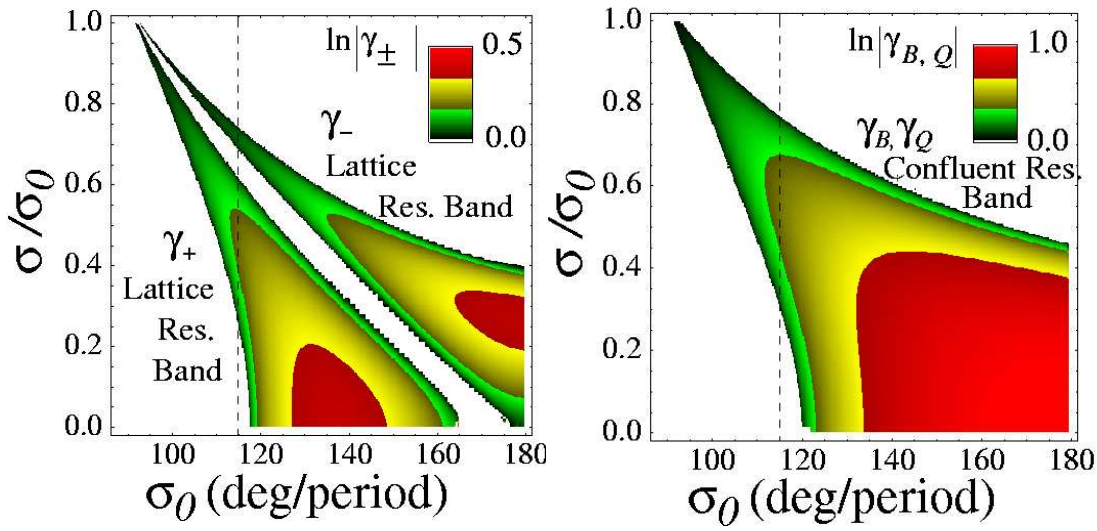

[S.M. Lund and B. Bukh, PRSTAB 024801 (2004)]

More instabilities are possible than can be described by statistical (moment/envelope) equations. Look at a more complete, Vlasov based kinetic theory including self-consistent space-charge:

Higher-order Collective (internal) Mode Stability

- Perturbations will generally drive nonlinear space-charge forces
- Evolution of such perturbations can change the beam rms emittance
- Many possible internal modes of oscillation should be possible
  - Frequencies can differ significantly from envelope modes
  - Creates more possibilities for resonant exchanges with a periodic focusing lattice and various beam characteristic responses opening many possibilities for system destabilization

KV Envelope Mode (breathing) Higher Order Mode

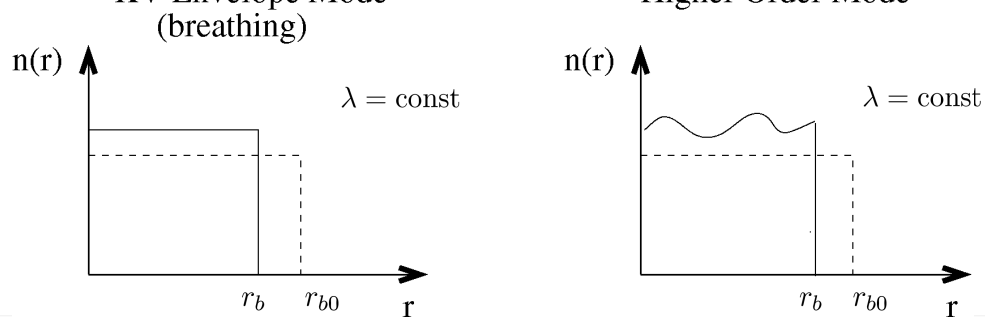

Plasma physics approach to beam physics:

Resolve:

$$f(\mathbf{x}_\perp, \mathbf{x}'_\perp, s) = f_\perp(\{C_i\}) + \delta f_\perp(\mathbf{x}_\perp, \mathbf{x}'_\perp, s)$$

equilibrium perturbation $f_\perp \gg \delta f_\perp$

and carry out equilibrium + stability analysis

Comments:

- Attraction is to parallel the impressive successes of plasma physics
  - Gain insight into preferred state of nature
- Beams are born off a source and may not be close to an equilibrium condition
  - Appropriate single particle constants of the motion unknown for periodic focusing lattices other than the KV distribution
- Intense beam self-fields and finite radial extent vastly complicate equilibrium description and analysis of perturbations

Review: Vlasov Model: Transverse Vlasov model for a coasting, single species beam with electrostatic self-fields propagating in an applied focusing lattice:

$\mathbf{x}_\perp, \mathbf{x}'_\perp$ transverse particle coordinate, angle

q, m charge, mass

γ_b, β_b axial relativistic factors

$f_\perp(\mathbf{x}_\perp, \mathbf{x}'_\perp, s)$ single particle distribution

$H_\perp(\mathbf{x}_\perp, \mathbf{x}'_\perp, s)$ single particle Hamiltonian

Vlasov Equation (see J.J. Barnard, Introductory Lectures):

$$\frac{d}{ds} f_\perp = \frac{\partial f_\perp}{\partial s} + \frac{d\mathbf{x}_\perp}{ds} \cdot \frac{\partial f_\perp}{\partial \mathbf{x}_\perp} + \frac{d\mathbf{x}'_\perp}{ds} \cdot \frac{\partial f_\perp}{\partial \mathbf{x}'_\perp} = 0$$

Particle Equations of Motion:

$$\frac{d}{ds}\mathbf{x}_\perp = \frac{\partial H_\perp}{\partial \mathbf{x}'_\perp} \qquad \frac{d}{ds}\mathbf{x}'_\perp = -\frac{\partial H_\perp}{\partial \mathbf{x}_\perp}$$

Hamiltonian (see S.M. Lund, lectures on *Transverse Particle Equations of Motion*):

$$H_\perp = \frac{1}{2}\mathbf{x}'^{\,2}_\perp + \frac{1}{2}\kappa_x(s)x^2 + \frac{1}{2}\kappa_y(s)y^2 + \frac{q}{m\gamma_b^3\beta_b^2c^2}\phi$$

Poisson Equation:

$$\left(\frac{\partial^2}{\partial x^2} + \frac{\partial^2}{\partial y^2}\right)\phi = -\frac{q}{\epsilon_0}\int d^2\mathbf{x}'_\perp \; f_\perp$$

+ boundary conditions on ϕ

Review: Focusing lattices, continuous and periodic (simple piecewise constant):

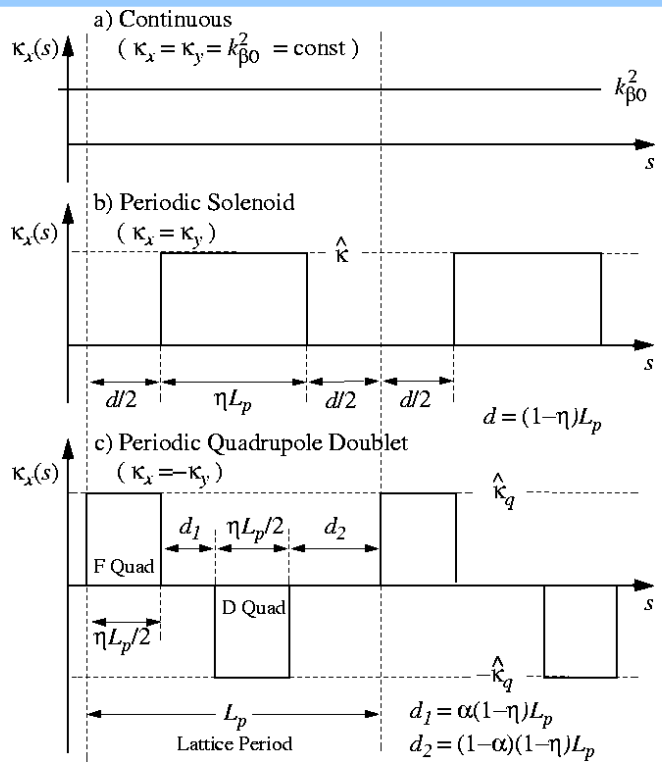

Lattice Period L_p

Occupancy η

$\eta \in [0, 1]$

Solenoid description carried out implicitly in Larmor frame

[see Lund and Bukh, PRST- Accel. and Beams 7, 024801 (2004), Appendix A]

Syncopation Factor α

$$\alpha \in [0, \frac{1}{2}]$$

$$\alpha = \frac{1}{2} \implies FODO$$

Continuous Focusing: $\kappa_x = \kappa_y = k_{\beta 0}^2 = \text{const}$

$$\boxed{H_\perp = \frac{1}{2}\mathbf{x}_\perp'^{\,2} + \frac{1}{2}k_{\beta 0}^2 \mathbf{x}_\perp^2 + \frac{q}{m\gamma_b^3\beta_b^2 c^2}\phi}$$

Solenoidal Focusing (in Larmor frame variables): $\kappa_x = \kappa_y = \kappa(s)$

$$H_\perp = \frac{1}{2}\mathbf{x}_\perp'^{\,2} + \frac{1}{2}\kappa \mathbf{x}_\perp^2 + \frac{q}{m\gamma_b^3\beta_b^2 c^2}\phi$$

Quadrupole Focusing: $\kappa_x = -\kappa_y = \kappa_q(s)$

$$H_\perp = \frac{1}{2}\mathbf{x}_\perp'^{\,2} + \frac{1}{2}\kappa_q x^2 - \frac{1}{2}\kappa_q y^2 + \frac{q}{m\gamma_b^3\beta_b^2 c^2}\phi$$

We will concentrate on the continuous focusing model in these lectures

- Kinetic theory is notoriously complicated even in this (simple) case
- By analogy with envelope mode results expect that kinetic theory of periodic focusing systems to have more instabilities
- As in equilibrium analysis the continuous model can give simplified insight on a range of relevant kinetic stability considerations

S3: Linearized Vlasov Equation

Because of the complexity of kinetic theory, we will limit discussion to a simple continuous focusing model Vlasov-Poisson system for a coasting beam within a round pipe

$$\frac{df_\perp}{ds} = \left\{ \frac{\partial}{\partial s} + \mathbf{x}'_\perp \cdot \frac{\partial}{\partial \mathbf{x}_\perp} - \left(k_{\beta 0}^2 \mathbf{x}_\perp + \frac{q}{m\gamma_b^3\beta_b^2c^2}\frac{\partial \phi}{\partial \mathbf{x}_\perp} \right) \cdot \frac{\partial}{\partial \mathbf{x}'_\perp} \right\} f_\perp(\mathbf{x}_\perp, \mathbf{x}'_\perp, s) = 0$$

$$\nabla_\perp^2 \phi(\mathbf{x}_\perp, s) = -\frac{q}{\epsilon_0} \int d^2x'_\perp \; f_\perp(\mathbf{x}_\perp, \mathbf{x}_\perp, s)$$

$$\phi(|\mathbf{x}_\perp| = r_p, s) = \text{const}$$

Then expand the distribution and field as:

$$\begin{aligned} f_\perp &= f_0(H_0) + \delta f_\perp \\ \phi &= \phi_0 + \delta\phi \end{aligned}$$

equilibrium perturbation

At present, there is *no assumption* that the perturbations are small.

The equilibrium satisfies:

(see S.M. Lund, lectures on *Transverse Equilibrium Distributions*)

$$H_0 = \frac{1}{2}\mathbf{x}'^{\,2}_\perp + \frac{1}{2}k_{\beta 0}^2 \mathbf{x}_\perp^2 + \frac{q}{m\gamma_b^3\beta_b^2c^2}\phi_0$$

$$f_0(H_0) = \text{ any non-negative function}$$

$$\frac{1}{r}\frac{\partial}{\partial r}\left(r \frac{\partial \phi_0}{\partial r} \right) = -\frac{q}{\epsilon_0} \int d^2x'_\perp \; f_0(H_0)$$

The unperturbed distribution must then satisfy the equilibrium Vlasov equation:

$$\left\{ \frac{\partial}{\partial s} + \mathbf{x}'_\perp \cdot \frac{\partial}{\partial \mathbf{x}_\perp} - \left(k_{\beta 0}^2 \mathbf{x}_\perp + \frac{q}{m\gamma_b^3\beta_b^2c^2}\frac{\partial \phi_0}{\partial \mathbf{x}_\perp} \right) \cdot \frac{\partial}{\partial \mathbf{x}'_\perp} \right\} f_0(H_0) = 0$$

Because the Poisson equation is linear:

$$\nabla_\perp^2 \delta\phi(\mathbf{x}_\perp, s) = -\frac{q}{\epsilon_0} \int d^2x'_\perp \; \delta f_\perp(\mathbf{x}_\perp, \mathbf{x}_\perp, s)$$

$$\delta\phi(|\mathbf{x}_\perp| = r_p, s) = \text{const}$$

Insert the perturbations in Vlasov's equation and expand terms:

$$\left\{\frac{\partial}{\partial s}+\mathbf{x}'_\perp\cdot\frac{\partial}{\partial \mathbf{x}_\perp}-\left(k_{\beta 0}^2\mathbf{x}_\perp+\frac{q}{m\gamma_b^3\beta_b^2c^2}\frac{\partial\phi_0}{\partial\mathbf{x}_\perp}\right)\cdot\frac{\partial}{\partial\mathbf{x}'_\perp}\right\}f_0(H_0)$$

equilibrium term

$$+\left\{\frac{\partial}{\partial s}+\mathbf{x}'_\perp\cdot\frac{\partial}{\partial \mathbf{x}_\perp}-\left(k_{\beta 0}^2\mathbf{x}_\perp+\frac{q}{m\gamma_b^3\beta_b^2c^2}\frac{\partial\phi_0}{\partial\mathbf{x}_\perp}\right)\cdot\frac{\partial}{\partial\mathbf{x}'_\perp}\right\}\delta f_\perp$$

equilibrium characteristics of perturbed distribution

$$=\frac{q}{m\gamma_b^3\beta_b^2c^2}\frac{\partial\delta\phi}{\partial\mathbf{x}_\perp}\cdot\frac{\partial}{\partial\mathbf{x}'_\perp}f_0(H_0)+\frac{q}{m\gamma_b^3\beta_b^2c^2}\frac{\partial\delta\phi}{\partial\mathbf{x}_\perp}\cdot\frac{\partial}{\partial\mathbf{x}'_\perp}\delta f_\perp$$

perturbed field linear correction term

nonlinear term

Take the perturbations to be small-amplitude:

$$\boxed{\begin{aligned} f_0(H_0) &\gg \delta f_\perp \\ \phi_0 &\gg \delta\phi \end{aligned}}$$

<--- follows automatically from distribution/Poisson eq

and neglect the nonlinear terms to obtain the linearized Vlasov-Poisson system:

$$\left\{\frac{\partial}{\partial s}+\mathbf{x}'_\perp\cdot\frac{\partial}{\partial \mathbf{x}_\perp}-\left(k_{\beta 0}^2\mathbf{x}_\perp+\frac{q}{m\gamma_b^3\beta_b^2c^2}\frac{\partial\phi_0}{\partial\mathbf{x}_\perp}\right)\cdot\frac{\partial}{\partial\mathbf{x}'_\perp}\right\}\delta f_\perp(\mathbf{x}_\perp,\mathbf{x}'_\perp,s)$$

$$=\frac{q}{m\gamma_b^3\beta_b^2c^2}\frac{\partial\delta\phi(\mathbf{x}_\perp,s)}{\partial\mathbf{x}_\perp}\cdot\frac{\partial}{\partial\mathbf{x}'_\perp}f_0(H_0)$$

$$\nabla_\perp^2\delta\phi(\mathbf{x}_\perp,s)=-\frac{q}{\epsilon_0}\int d^2x'_\perp\;\delta f_\perp(\mathbf{x}_\perp,\mathbf{x}_\perp,s)\qquad \delta\phi(|\mathbf{x}_\perp|=r_p,s)=\text{const}$$

Solution of the Linearized Vlasov Equation, the method of characteristics

The linearized Vlasov equation is a integral-partial differential equation system

- Highly nontrivial to solve
- Method of characteristics can be employed to simplify analysis due to the structure of the equation

Note that the equilibrium Vlasov equation is:

$$\left\{\frac{\partial}{\partial s}+\mathbf{x}'_\perp\cdot\frac{\partial}{\partial \mathbf{x}_\perp}-\left(k_{\beta 0}^2\mathbf{x}_\perp+\frac{q}{m\gamma_b^3\beta_b^2c^2}\frac{\partial\phi_0}{\partial\mathbf{x}_\perp}\right)\cdot\frac{\partial}{\partial\mathbf{x}'_\perp}\right\}f_0=0$$

$$\left.\frac{d}{ds}\right|_{\text{eq. orbit}}f_0=0$$

Interpret:

$$\left\{\frac{\partial}{\partial s}+\mathbf{x}'_\perp\cdot\frac{\partial}{\partial \mathbf{x}_\perp}-\left(k_{\beta 0}^2\mathbf{x}_\perp+\frac{q}{m\gamma_b^3\beta_b^2c^2}\frac{\partial\phi_0}{\partial\mathbf{x}_\perp}\right)\cdot\frac{\partial}{\partial\mathbf{x}'_\perp}\right\}=\left.\frac{d}{ds}\right|_{\text{eq. orbit}}$$

as a total derivative evaluated along an equilibrium particle orbit. This suggests employing the method of characteristics.

Method of Characteristics:

Equilibrium orbit:

$$\boxed{\begin{aligned} \frac{d}{d\tilde{s}}\mathbf{x}_\perp(\tilde{s}) &= \mathbf{x}'_\perp(\tilde{s}) \\ \frac{d}{d\tilde{s}}\mathbf{x}'_\perp(\tilde{s}) &= -k_{\beta 0}^2\mathbf{x}_\perp(\tilde{s}) - \frac{q}{m\gamma_b^3\beta_b^2c^2}\frac{\partial\phi_0(\mathbf{x}_\perp(\tilde{s}))}{\partial\mathbf{x}_\perp(\tilde{s})} \end{aligned}}$$

"Initial" conditions of characteristic orbit:

$$\boxed{\begin{aligned} \mathbf{x}_\perp(\tilde{s}=s) &= \mathbf{x}_\perp \\ \mathbf{x}'_\perp(\tilde{s}=s) &= \mathbf{x}'_\perp \end{aligned}}$$

Then the linearized Vlasov equation can be expressed as:

$$\frac{d}{d\tilde{s}}\delta f_\perp(\mathbf{x}_\perp(\tilde{s}),\mathbf{x}'_\perp(\tilde{s}),\tilde{s}) = \frac{q}{m\gamma_b^3\beta_b^2c^2}\frac{\partial\delta\phi(\mathbf{x}_\perp(\tilde{s}))}{\partial\mathbf{x}_\perp(\tilde{s})}\cdot\frac{\partial}{\partial\mathbf{x}'_\perp}f_0(H_0(\mathbf{x}_\perp(\tilde{s}),\mathbf{x}'_\perp(\tilde{s})))$$

This is a total derivative and can be integrated:

- To analyze instabilities assume growing perturbations that grow in s
- Neglect initial conditions at $\tilde{s}\to-\infty$ and integrate

$$\boxed{\begin{aligned} \delta f_\perp(\mathbf{x}_\perp,\mathbf{x}'_\perp,s) &= \frac{q}{m\gamma_b^3\beta_b^2c^2}\int_{-\infty}^{s}d\tilde{s}\,\frac{\partial\delta\phi(\mathbf{x}_\perp(\tilde{s}))}{\partial\mathbf{x}_\perp(\tilde{s})}\cdot\frac{\partial}{\partial\mathbf{x}'_\perp}f_0(H_0(\mathbf{x}_\perp(\tilde{s}),\mathbf{x}'_\perp(\tilde{s}))) \\ \nabla_\perp^2\delta\phi(\mathbf{x}_\perp,s) &= -\frac{q}{\epsilon_0}\int d^2x'_\perp\;\delta f_\perp(\mathbf{x}_\perp,\mathbf{x}_\perp,s) \\ \delta\phi(|\mathbf{x}_\perp|=r_p,s) &= \text{const} \end{aligned}}$$

Gives the self-consistent evolution of the perturbations

- Similar statement for nonlinear perturbations (Homework problem)

Effectively restates the Poisson equation as a differential-integral equation that is solved to understand the evolution of perturbations

- Simpler to work with but still *very* complicated

S4: Collective Modes on a KV Equilibrium Beam

Unfortunately, calculation of normal modes is generally complicated even in continuous focusing. Nevertheless, the normal modes of the KV distribution can be analytically calculated and give insight on the expected collective response of a beam with intense space-charge.

Review: Continuous Focusing KV Equilibrium

$$\boxed{f_\perp(H_\perp) = \frac{\hat{n}}{2\pi}\delta\left(H_\perp - \frac{\varepsilon^2}{2r_b^2}\right)}$$

$$r_b = \left(\frac{Q + \sqrt{4k_{\beta 0}^2\varepsilon^2 + Q^2}}{2k_{\beta 0}^2}\right)^{1/2} = \text{const}$$

$k_{\beta 0} =$ Undepressed betatron wavenumber

$r_b =$ Beam edge radius

$\hat{n} =$ Beam number density

$Q =$ Dimensionless perveance

$\varepsilon =$ rms edge emittance

Further comments on the KV equilibrium: Distribution Structure

Equilibrium distribution:

$$\boxed{f_\perp \sim \delta[\text{Courant-Snyder invariants}]}$$

Forms a highly singular hyper-shell in 4D phase-space

Schematic:

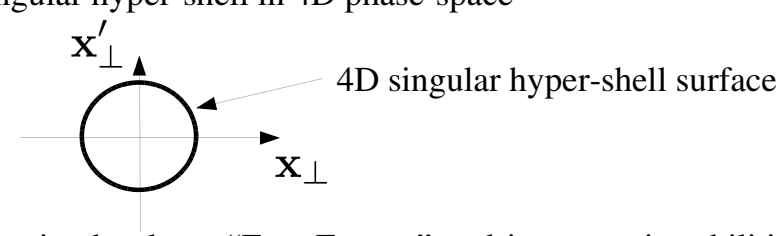

- Singular distribution has large "Free-Energy" to drive many instabilities
  - Low order envelope modes are physical and highly important (see lectures on *Centroid and Envelope Descriptions of Beams*)
- Perturbative analysis shows strong collective instabilities
  - Hofmann, Laslett, Smith, and Haber, Part. Accel. **13**, 145 (1983)
  - Higher order instabilities (collective modes) have unphysical aspects due to (delta-function) structure of distribution and must be applied with care (see lectures on *Kinetic Stability of Beams*)
  - Instabilities can cause problems if the KV distribution is employed as an initial beam state in self-consistent simulations

A full kinetic stability analysis of the KV equilibrium distribution is complicated and uncovers many strong instabilities

[I. Hofmann, J.L. Laslett, L. Smith, and I. Haber, Particle Accel. 13, 145 (1983); R. Gluckstern, Proc. 1970 Proton Linac Conf., Batavia 811 (1971)]

Expand Vlasov's equation to linear order with:

$$f_\perp \to f_\perp(\text{ C.S. Invariant}) \;+\; \delta f_\perp$$

$f_\perp(\text{C.S. Invariant})$ = equilibrium

$\delta f_\perp$ = perturbation

Solve the Poisson equation:

$$\nabla_\perp^2 \delta\phi = -\frac{q}{\epsilon_0}\int d^2x'\; \delta f_\perp$$

using truncated polynomials for $\delta\phi$ internal to the beam to represent a "normal mode"

$$\delta\phi = \sum_{m=0}^{n} A_m^{(0)}(s) x^{n-m} y^m + \sum_{m=0}^{n-2} A_m^{(1)}(s) x^{n-m-2} y^m + \cdots$$

$n = 2, 3, 4, \cdots$ order or mode

m can be restricted to <u>even</u> or <u>odd</u> terms

- Truncated polynomials can meet all boundary conditions
- Eigenvalues of a Floquet form transfer matrix analyzed for stability properties
  - Lowest order results reproduce KV envelope instabilities
  - Higher order results manifest many strong instabilities

Higher order kinetic instabilities of the KV equilibrium are strong and cover a wide parameter range for periodic focusing lattices

<u>Example: FODO Quadrupole Stability</u>

4th order even mode

[Hofmann et. al, Particle Accel. **13**, 145 (1983)]

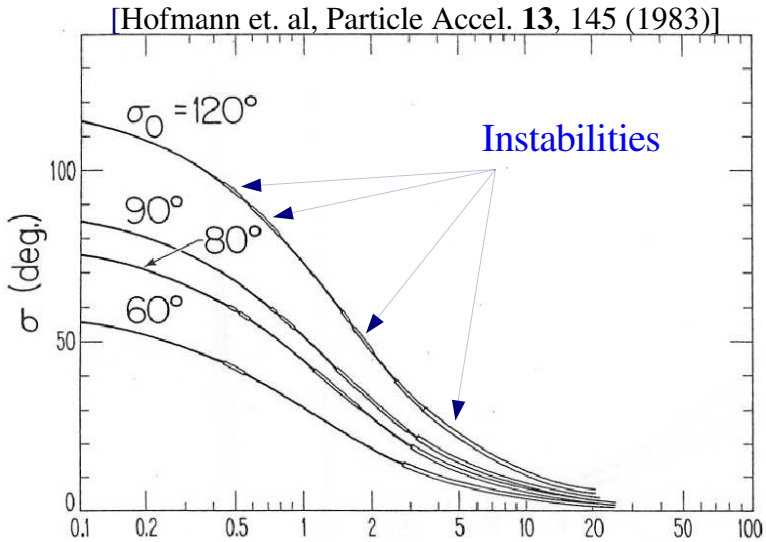

$\sigma/\sigma_0 \to 1$ (undepressed) --> (space-charge parameter) increasing space-charge --> $\sigma/\sigma_0 \to 0$ (fully depressed)

The continuous focusing limit can be analyzed to better understand properties of internal modes on a KV beam (1)

[S. Lund and R. Davidson, Physics of Plasmas **5**, 3028 (1998): see Appendix B, C]

Continuous focusing, symmetric beam:

$$\kappa_x(s) = \kappa_y(s) = k_{\beta 0}^2 = \text{const} \qquad \varepsilon_x = \varepsilon_y \equiv \varepsilon \qquad r_x = r_y \equiv r_b$$

Mode eigenfunction (2 n "order"):

$$\delta\phi_n = \begin{cases} \frac{A_n}{2}\left[P_{n-1}\left(1-2\frac{r^2}{r_b^2}\right) + P_n\left(1-2\frac{r^2}{r_b^2}\right)\right], & 0 \le r \le r_b \\ 0, & r_b < r \end{cases}$$

$$A_n = \text{const} \qquad P_n(x) = \text{n}^{\text{th}} \text{ order Legendre polynomial}$$

Potential

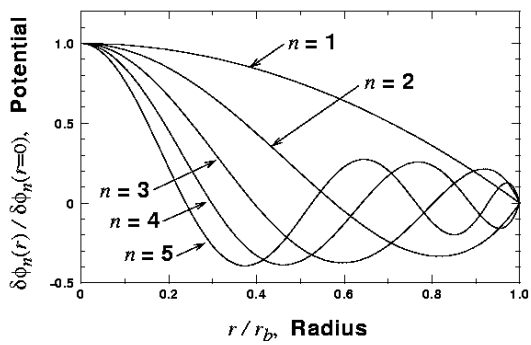

Density ($\delta n_n = \epsilon_0 \nabla_\perp^2 \delta\phi_n / q$)

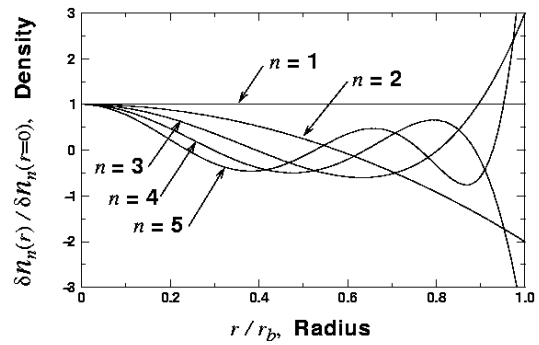

The continuous focusing limit can be analyzed to better understand properties of internal modes on a KV beam (2)

Mode dispersion relation for e^{-iks} variations:

$$2n + \frac{1-\sigma/\sigma_0}{(\sigma/\sigma_0)^2}\left[B_{n-1}\left(\frac{k/k_{\beta 0}}{\sigma/\sigma_0}\right) - B_n\left(\frac{k/k_{\beta 0}}{\sigma/\sigma_0}\right)\right] = 0$$

where: $$B_n(\alpha) \equiv \begin{cases} 1, & n = 0 \\ \frac{(\alpha/2)^2-0^2}{(\alpha/2)^2-1^2}\frac{(\alpha/2)^2-2^2}{(\alpha/2)^2-3^2}\cdots\frac{(\alpha/2)^2-(n-1)^2}{(\alpha/2)^2-n^2} & n = 1,3,5,\cdots \\ \frac{(\alpha/2)^2-1^2}{(\alpha/2)^2-2^2}\frac{(\alpha/2)^2-3^3}{(\alpha/2)^2-4^2}\cdots\frac{(\alpha/2)^2-(n-1)^2}{(\alpha/2)^2-n^2} & n = 2,4,6,\cdots \end{cases}$$

- Eigenfunction structure suggestive of wave perturbations often observed internal to the beam in simulations for a variety of beam distributions
- n distinct branches for 2n order (real coefficient) polynomial dispersion relation
- Some range of σ/σ_0 will be unstable for all n > 1
  - Instability exists for some n for $\sigma/\sigma_0 < 0.3985$
  - Growth rates are strong

Continuous focusing limit dispersion relation results for KV beam stability

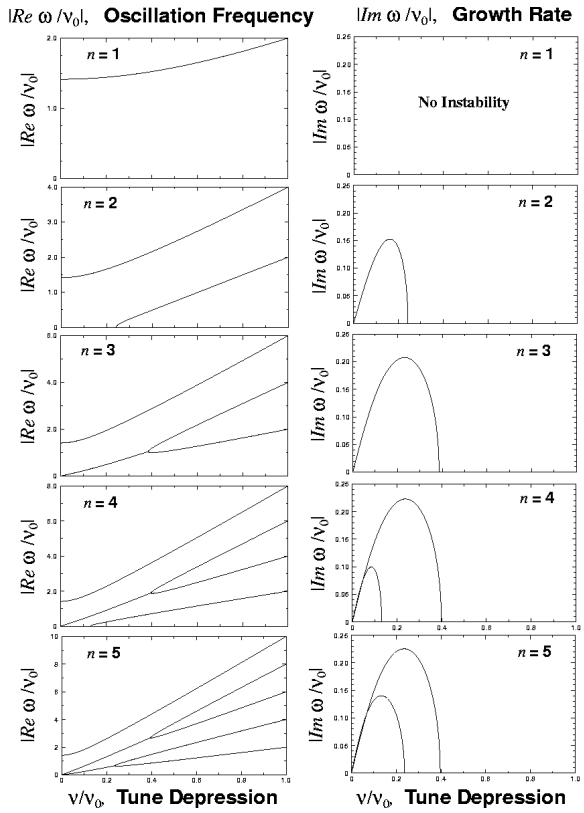

Notation Change:

$$k/k_{\beta 0} \equiv \omega/\nu_0$$

$$\sigma/\sigma_0 \equiv \nu/\nu_0$$

[S. Lund and R. Davidson, Physics of Plasmas **5**, 3028 (1998): see Appendix B, C]

For continuous focusing, fluid theory shows that at least some branches of the KV dispersion relation are physical

[S. Lund and R. Davidson, Physics of Plasmas **5**, 3028 (1998)]

Fluid theory:

- KV equilibrium distribution is reasonable in fluid theory
  - No singularities
  - Flat density and parabolic radial temperature profiles
- Theory truncated by assuming zero heat flow

Mode eigenfunctions:

Exactly the same as derived under kinetic theory!

Mode dispersion relation:

$$\boxed{\frac{k}{k_{\beta 0}} = \sqrt{2 + 2\left(\frac{\sigma}{\sigma_0}\right)^2 (2n^2 - 1)}}$$

- Single, stable branch
  - Agrees well with high frequency branch from kinetic theory

Results show that aspects of higher-order KV internal modes are physical!

Continuous focusing limit dispersion relation results for KV beam stability

n = 1, envelope mode curves overlap

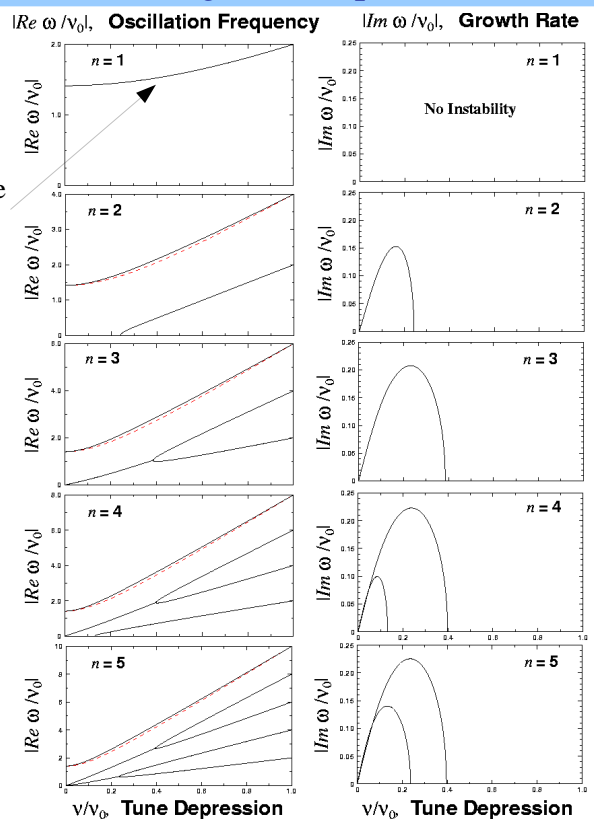

Notation Change:

$$k/k_{\beta 0} \equiv \omega/\nu_0$$

$$\sigma/\sigma_0 \equiv \nu/\nu_0$$

Red: Fluid Theory

(no instability)

Black: Kinetic Theory

(unstable branches)

[S. Lund and R. Davidson, Physics of Plasmas **5**, 3028 (1998)]

S5: Global Conservation Constraints

Apply for any initial distribution, equilibrium or not.

- Strongly constrain nonlinear evolution of the system.
- Valid even with a beam pipe provided that particles are not lost from the system and that symmetries are respected.
- Useful to bound perturbations, but yields no information on evolution timescales.

1) Generalized Entropy

$$U_G = \int d^2x_\perp \int d^2x'_\perp \; G(f_\perp) \; = \text{const}$$

$$G(f_\perp) = \text{Any diffrentiable functions satisfying } G(f_\perp \to 0) = 0$$

- Applies to all Vlasov evolutions.

// Examples

Line-charge: $G(f_\perp) = q f_\perp$ → $\lambda = q \int d^2x \int d^2x' \; f_\perp \; = \text{const}$

Entropy: $G(f_\perp) = -\dfrac{f_\perp}{A} \ln\left(\dfrac{f_\perp}{f_0}\right)$ $A,\ f_0$ constants

→ $\mathcal{S} = -\int \dfrac{d^2x}{A} \int d^2x' \; f_\perp \ln\left(\dfrac{f_\perp}{f_0}\right) \; = \text{const}$ //

2) Transverse Energy in continuous focusing

$$\boxed{U_{\mathcal{E}} = \int d^2x'_\perp \int d^2x_\perp \left\{ \frac{1}{2}\mathbf{x}'^2_\perp + \frac{1}{2}k^2_{\beta 0}\mathbf{x}^2_\perp \right\} f_\perp + \int d^2x_\perp \frac{\epsilon_0 |\nabla_\perp \phi|^2}{2m\gamma_b^3\beta_b^2c^2} = \text{const}}$$

Here,

$$\int d^2x'_\perp \int d^2x_\perp \frac{1}{2}\mathbf{x}'^2_\perp f_\perp \quad \sim \text{Kinetic Energy}$$

$$\int d^2x'_\perp \int d^2x_\perp \frac{1}{2}k^2_{\beta 0}\mathbf{x}^2_\perp f_\perp \quad \sim \text{Potential Energy of applied focusing forces}$$

$$\int d^2x_\perp \frac{\epsilon_0 |\nabla_\perp \phi|^2}{2m\gamma_b^3\beta_b^2c^2} \quad \sim \text{Self-Field Energy}$$

- Does not hold when focusing forces vary in s
  - Can still be approximately valid for rms matched beams where energy will regularly pump into and out of the beam
- Self field energy term diverges in radially unbounded systems (no aperture)
  - Still useful if an appropriate infinite constant is subtracted (to regularize)

Comments on system energy form:

$$U_{\mathcal{E}} = \int d^2x'_\perp \int d^2x_\perp \left\{ \frac{1}{2}\mathbf{x}'^2_\perp + \frac{1}{2}k^2_{\beta 0}\mathbf{x}^2_\perp \right\} f_\perp + \int d^2x_\perp \frac{\epsilon_0 |\nabla_\perp \phi|^2}{2m\gamma_b^3\beta_b^2c^2} = \text{const}$$

Analyze the energy term:

zero for grounded aperture in finite system

$$\int d^2x_\perp \frac{\epsilon_0 |\nabla_\perp \phi|^2}{2} = \cancel{\int d^2x_\perp \frac{1}{2}\nabla_\perp \cdot (\phi \nabla_\perp \phi)} - \int d^2x_\perp \frac{1}{2}\phi \nabla^2_\perp \phi$$

or infinite constant in free space

Employ the Poisson equation:

$$\nabla^2_\perp \phi = -\frac{q}{\epsilon_0}\int d^2x'_\perp f_\perp$$

Giving:

$$\longrightarrow \int d^2x_\perp \frac{\epsilon_0 |\nabla_\perp \phi|^2}{2} = \int d^2x_\perp \int d^2x'_\perp \frac{q}{2\epsilon_0}\phi f_\perp$$

$$\boxed{U_{\mathcal{E}} = \int d^2x'_\perp \int d^2x_\perp \left\{ \frac{1}{2}\mathbf{x}'^2_\perp + \frac{1}{2}k^2_{\beta 0}\mathbf{x}^2_\perp + \frac{1}{2}\frac{q\phi}{m\gamma_b^3\beta_b^2c^2} \right\} f_\perp = \text{const}}$$

symmetry factor

- Note the relation to the system Hamiltonian with a symmetry factor to not double count particle contributions

$$H_\perp = \frac{1}{2}\mathbf{x}'^{\,2}_\perp + \frac{1}{2}k^2_{\beta 0}\mathbf{x}^2_\perp + \frac{q}{m\gamma_b^3\beta_b^2c^2}\phi$$

Comments on self-field energy divergences:

In unbounded (free space) systems, far from the beam the field must look like a line charge:

$$-\frac{\partial \phi}{\partial r} \sim \frac{\lambda}{2\pi\epsilon_0 r} \qquad r > r_{\text{large}}$$

Resolve the total field energy into a finite (near) term and a divergent term:

$$\int d^2x_\perp \, \frac{\epsilon_0 |\nabla_\perp \phi|^2}{2} = \int_{r \le r_{\text{large}}} d^2x_\perp \, \frac{\epsilon_0 |\nabla_\perp \phi|^2}{2} + \frac{\lambda^2}{4\pi\epsilon_0} \int_{r_{\text{large}}}^{\infty} dr \frac{1}{r}$$

total — finite term — lograthmically divergent term

- This divergence can be subtracted out to thereby regularized the system energy
  - Renders energy constraint useful for application to equilibria in radially unbounded systems such as thermal equilibrium

3) Angular Momentum

$$\boxed{U_\theta = \int d^2x_\perp \int d^2x'_\perp \, (yx' - x'y) f_\perp \; = \text{const}}$$

- Focusing and beam pipe (if present) must be axisymmetric
  - Useful for solenoidal magnetic focusing
  - Does not apply to alternating gradient quadrupole focusing since such systems do not have the required axisymmetry

4) Axial Momentum

$$\boxed{U_z = \int d^2x_\perp \int d^2x'_\perp \, m\gamma_b\beta_b c \, f_\perp \; = \text{const}}$$

- Trivial here, but useful when models are generalized for coasting beams with axial momentum spread

Comments on applications of the global conservation constraints:

Global invariants strongly constrain the nonlinear evolution of the system

- Only evolutions consistent with Vlasov's equation are physical
- Constraints consistent with the model can bound kinematically accessible evolutions

Application of the invariants does not require (difficult to derive) normal mode descriptions

- But cannot, by itself, provide information on evolution timescales

Use of global constraints to bound perturbations has appeal since distributions in real machines may be far from an equilibrium. Used to:

- Derive sufficient conditions for stability
- Bound particle losses [O'Neil, Phys. Fluids **23**, 2216 (1980)]
- Bound changes of system moments (for example the rms emittance) under assumed relaxation processes
- Application does not require (difficult to derive) normal mode descriptions

S6: Kinetic Stability Theorem for continuous focusing equilibria

[Fowler, J. Math Phys. **4,** 559 (1963); Gardner, Phys. Fluids **6**, 839 (1963); R. Davidson, Physics of Nonneutral Plasmas, Addison-Wesley (1990)]

Resolve:

$$f_\perp = f_0(H_0) + \delta f_\perp$$

$f_0(H_0) =$ Equilibrium (subscript 0) distribution

$\delta f_\perp =$ Perturbation about equilibrium

Employ generalized entropy and transverse energy global constraints:

$$U_G = \int d^2x_\perp \int d^2x'_\perp \; G(f_\perp) \; = \text{const}$$

$$U_\mathcal{E} = \int d^2x'_\perp \int d^2x_\perp \; \left\{ \frac{1}{2}\mathbf{x}'^2_\perp + \frac{1}{2}k^2_{\beta 0}\mathbf{x}^2_\perp \right\} f_\perp \; + \; \int d^2x_\perp \; \frac{\epsilon_0 |\nabla_\perp \phi|^2}{2m\gamma_b^3\beta_b^2c^2} \; = \text{const}$$

Apply to equilibrium and full distribution to form an effective "free-energy":

$$\Delta U_G = U_G - U_{G0} = \text{const} \qquad \Delta U_\mathcal{E} = U_\mathcal{E} - U_{\mathcal{E}0} = \text{const}$$

$$\begin{aligned} F &= \Delta U_\mathcal{E} - \Delta U_G \\ &= \int d^2x'_\perp \int d^2x_\perp \; \left\{ \frac{1}{2}\mathbf{x}'^2_\perp + \frac{1}{2}k^2_{\beta 0}\mathbf{x}^2_\perp \right\} \delta f_\perp \; + \; \int d^2x_\perp \; \frac{\epsilon_0 |\nabla_\perp \phi|^2}{2m\gamma_b^3\beta_b^2c^2} \\ &\quad + \int d^2x_\perp \int d^2x'_\perp \; [G(f_\perp) - G(f_0)] \; = \text{const} \end{aligned}$$

The perturbed potential satisfies:

$$\delta\phi \equiv \phi - \phi_0 \qquad \nabla_\perp^2 \delta\phi = -\frac{q}{\epsilon_0}\int d^2x'_\perp\ \delta f_\perp$$

Take $|\delta f_\perp| \ll f_0$ and Taylor expand to 2nd order

$$G(f_0 + \delta f_\perp) = G(f_0) + \frac{dG(f_0)}{df_0}\delta f_\perp + \frac{d^2G(f_0)}{df_0^2}\frac{(\delta f_\perp)^2}{2} + \Theta(\delta^3)$$

Without loss of generality, choose:

$$\frac{dG(f_0)}{df_0}\delta f_\perp = -H_0 = -\left(\frac{1}{2}\mathbf{x}_\perp'^2 + \frac{1}{2}k_{\beta 0}^2\mathbf{x}_\perp^2 + \frac{q\phi}{m\gamma_b^2\beta_b^2c^2}\right)$$

Then

$$\frac{d^2G(f_0)}{df_0^2} = -\frac{\partial H_0}{\partial f_0} = \frac{-1}{\partial f_0(H_0)/\partial H_0}$$

Some algebra (few lines using partial integration) yields:

$$\boxed{F = \int d^2x_\perp\ \left\{\frac{\epsilon_0|\nabla_\perp\delta\phi|^2}{2m\gamma_b^3\beta_b^2c^2} - \int d^2x'_\perp\ \frac{(\delta f_\perp)^2}{\partial f_0(H_0)/\partial H_0}\right\} + \Theta(\delta^3) = \text{const}}$$

- If $\partial f_0(H_0)/\partial H_0 < 0$ then F is a sum of two positive definite terms and perturbations are bounded by F = const.

$$F = \int d^2x_\perp\ \left\{\frac{|\nabla_\perp\delta\phi|^2}{2m\gamma_b^3\beta_b^2c^2} - \int d^2x'_\perp\ \frac{(\delta f_\perp)^2}{\partial f_0(H_0)/\partial H_0}\right\} = \text{const}$$

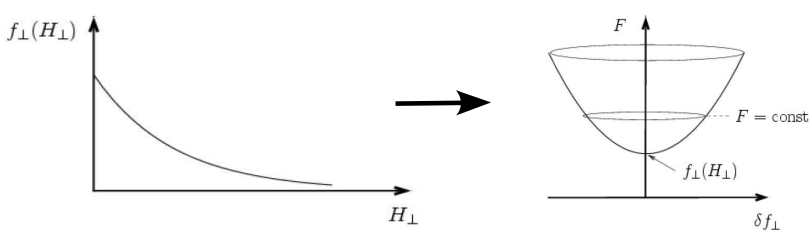

Value of F set by initial perturbations and concavity bounds excursions

Drop zero subscripts in stability statement:

Kinetic Stability Theorem

If $f_\perp(H_\perp)$ is a monotonic decreasing function of $H_\perp$ with $\partial f_\perp(H_\perp)/\partial H_\perp < 0$ then the equilibrium defined by $f_\perp(H_\perp)$ is stable to arbitrary small-amplitude perturbations.

- Is a sufficient condition for stability
  - Equilibria that violate may or may not be stable
- Mean value theorem can be used to generalize conclusions for arbitrary amplitude
  - R. Davidson proof

// Example Applications of Kinetic Stability Theorem

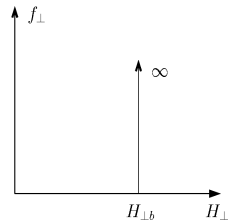

KV Equilibrium:

$$f_\perp(H_\perp) = \frac{\hat{n}}{2\pi}\delta(H_\perp - H_{\perp b})$$

$\partial f_\perp / \partial H_\perp$ changes sign

inconclusive stability by theorem

- Full normal mode analysis in Kinetic theory shows strong instabilities when space-charge becomes strong
- Not surprising, delta function represents a highly inverted population in phase-space with "free-energy" to drive instabilities

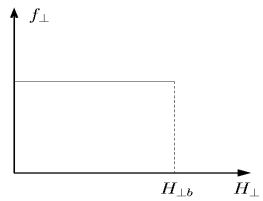

Waterbag Equilibrium:

$$f_\perp(H_\perp) = f_0\Theta(H_{\perp b} - H_\perp)$$

$$\partial f_\perp / \partial H_\perp = f_0\delta(H_\perp - H_{\perp b}) \leq 0$$

monotonic decreasing, stable by theorem

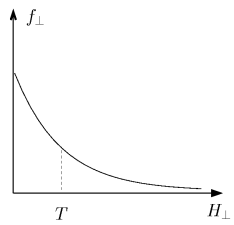

Thermal Equilibrium:

$$f_\perp(H_\perp) = f_0 \exp(-\beta H_\perp),$$

$$\partial f_\perp / \partial H_\perp = -f_0 \exp(-\beta H_\perp) \leq 0$$

monotonic decreasing, stable by theorem //

S7: rms Emittance Growth and Nonlinear Forces

Fundamental theme of beam physics is to minimize statistical beam emittance growth in transport to preserve focusability on target

Return to the full transverse beam model with:

$$x'' + \kappa_x x = -\frac{q}{m\gamma_b^3\beta_b^2c^2}\frac{\partial\phi}{\partial x} \quad + \quad \text{Applied Nonlinear Field Terms}$$

and express as:

$$x''(s) + \kappa_x(s)x(s) = f_x^L(s)x(s) + F_x^{NL}(x,y,s)$$

$f_x^L(s) =$ Linear Space-Charge Coefficient

$F_x^{NL}(x,y,s) =$ Nonlinear Forces + Linear Skew Coupled Forces (Applied and Space-Charge)

// Examples:

$$f_x^L(s) = \frac{Q}{r_b(s)}$$

Self-field forces within an axisymmetric (mismatched) KV beam core in a continuous focusing model

$$F_x^{NL}(x,y,s) = \text{Im}\left[\underline{b}_3\left(\frac{x+iy}{r_p}\right)^2\right]$$

Electric (with normal and skew components) sextupole optic based on multipole expansions (see lectures on *Particle Equations of Motion*) //

From the definition of the statistical (rms) emittance:

$$\varepsilon_x \equiv 4[\langle x^2\rangle_\perp \langle x'^2\rangle_\perp - \langle xx'\rangle_\perp^2]^{1/2}$$

Differentiate the squared emittance and apply the chain rule:

$$\begin{aligned}\frac{d}{ds}\varepsilon_x^2 &\equiv 32[\langle xx'\rangle_\perp \langle x'^2\rangle_\perp + \langle x^2\rangle_\perp \langle x'x''\rangle_\perp - \langle xx'\rangle_\perp \langle x'^2\rangle_\perp - \langle xx'\rangle_\perp \langle xx''\rangle_\perp] \\ &= 32[\langle x^2\rangle_\perp \langle x'x''\rangle_\perp - \langle xx'\rangle_\perp \langle xx''\rangle_\perp]\end{aligned}$$

Insert the equations of motion:

$$x'' + \kappa_x x = f_x^L x + F_x^{NL}$$

The linear terms cancel to show *for any beam distribution* that:

$$\boxed{\frac{d}{ds}\varepsilon_x^2 = 32\left[\langle x^2\rangle_\perp \langle x' F_x^{NL}\rangle_\perp - \langle xx'\rangle_\perp \langle x F_x^{NL}\rangle_\perp\right]}$$

Implications of:

$$\boxed{\frac{d}{ds}\varepsilon_x^2 = 32\left[\langle x^2\rangle_\perp \langle x' F_x^{NL}\rangle_\perp - \langle xx'\rangle_\perp \langle x F_x^{NL}\rangle_\perp\right]}$$

- Emittance evolution/growth is driven by nonlinear or skew coupling forces
  - Nonlinear terms can result from applied or space-charge fields
  - More detailed analysis shows that skew coupled forces cause x-y plane transfer oscillations but there is still a 4D quadratic invariant
- Minimize nonlinear forces to preserve emittance and maintain focusability

If the beam is accelerating, the equations of motion become:

$$x'' + \frac{(\gamma_b\beta_b)'}{(\gamma_b\beta_b)}x' + \kappa_x x = f_x^L x + F_x^{NL}$$

and this result can be generalized (see homework problems) using the normalized emittance:

$$\boxed{\begin{aligned}\varepsilon_{nx} &\equiv \gamma_b\beta_b\varepsilon_x \\ \frac{d}{ds}\varepsilon_{nx}^2 &= 32(\gamma_b\beta_b)^2\left[\langle x^2\rangle_\perp \langle x' F_x^{NL}\rangle_\perp - \langle xx'\rangle_\perp \langle x F_x^{NL}\rangle_\perp\right]\end{aligned}}$$

S8: rms Emittance Growth and Nonlinear Space-Charge Forces

[Wangler et. al, IEEE Trans. Nuc. Sci. 32, 2196 (1985), Reiser, *Charged Particle Beams*, (1994)]

In continuous focusing all nonlinear force terms are from space-charge, giving:

$$\boxed{\frac{d}{ds}\varepsilon_x^2 = -\frac{32q}{m\gamma_b^3\beta_b^2c^2}\left[\langle x^2\rangle_\perp\langle x'\frac{\partial\phi}{\partial x}\rangle_\perp - \langle xx'\rangle_\perp\langle x\frac{\partial\phi}{\partial x}\rangle_\perp\right]}$$

For any axisymmetric beam it can be shown that:

$$\langle x\frac{\partial\phi}{\partial x}\rangle_\perp = \frac{1}{2}\langle\frac{\partial\phi}{\partial r}\rangle_\perp = -\frac{\lambda}{8\pi\epsilon_0}$$

$$\langle x'\frac{\partial\phi}{\partial x}\rangle_\perp = \frac{1}{2}\langle r'\frac{\partial\phi}{\partial x}\rangle_\perp = \frac{1}{8\pi\epsilon_0\lambda}\frac{dW}{ds}$$

$$W = \frac{\epsilon_0}{2}\int d^2x\,|\nabla_\perp\phi|^2$$

$=$ self-field energy (per unit axial length)

For any axisymmetric beam it can also be shown that:

$$\langle xx'\rangle_\perp = \frac{1}{2}\langle rr'\rangle_\perp = -\frac{\langle x^2\rangle_\perp}{\lambda^2}\frac{dW_u}{ds}$$

$W_u =$ W for an rms equivalent uniform density beam

These results give (Wangler, Lapostolle):

$$\boxed{\frac{d}{ds}\varepsilon_x^2 = -4Q\langle x^2\rangle_\perp\frac{d}{ds}\left(\frac{W-W_u}{\lambda^2}\right)}$$

$$\boxed{\frac{d}{ds}\varepsilon_x^2 = -8Q\langle x^2\rangle_\perp\frac{d}{ds}\left(\frac{W-W_u}{\lambda^2}\right)}$$

- Applies to both radially bounded and radially infinite systems
- Result does not require an equilibrium for validity – only axisymmetry
- For a beam with s-variation, this result suggests that *only* the (mismatched) KV equilibrium can subsequently evolve with no change in rms emittance
- Result can be partially generalizable [J. Struckmeier and I. Hofmann, Part. Accel. **39**, 219 (1992)] to an unbunched elliptical beam
  - Result may have implications to existence/nonexistence of nonuniform density Vlasov equilibria in periodic focusing channels

If the rms beam radius does not change much in the beam evolution:

$$r_b^2 = 2\langle x^2\rangle_\perp \simeq \text{const}$$

Then the equation can be integrated to show that:

$$\Delta_{fi}(\varepsilon_x^2) = -4Qr_b^2\Delta_{fi}\left(\frac{W-W_u}{\lambda^2}\right)$$

$$\Delta_{fi}(\cdots) \equiv \text{Final State Value} - \text{Initial State Value}$$

S9: Uniform Density Beams and Extreme Energy States

Construct minima of the self-field energy per unit axial length:

$$\boxed{W = \frac{\epsilon_0}{2}\int d^2x_\perp\ |\nabla_\perp\phi|^2}$$

subject to: $\lambda = \text{const}$ ... fixed line-charge

$r_b = \sqrt{2\langle r^2\rangle_\perp} = \text{const}$ ... fixed rms equivalent beam radius

Using the method of Lagrange multipliers, vary (Helmholtz free energy):

$$F = W - \mu(\lambda/q)\langle r^2\rangle_\perp = \int d^2x_\perp\ \left\{\epsilon_0\frac{|\nabla_\perp\phi|^2}{2} - \mu r^2 n\right\} \qquad \mu = \text{const}$$

and require that variations satisfy the Poisson equation and conserve charge

$$\nabla_\perp^2\delta\phi = -\frac{q}{\epsilon_0}\delta n \qquad \delta\phi|_{\text{boundary}} = 0 \qquad \int d^2x_\perp\ \delta n\ = 0$$

Then variations terminate at 2nd order giving:

$$\delta F = -\int d^2x_\perp\ \left\{\mu r^2 + \text{const}\right\}\delta n + \epsilon_0\int d^2x_\perp \nabla_\perp\phi\cdot\nabla_\perp\delta\phi + \frac{\epsilon_0}{2}\int d^2x_\perp|\nabla_\perp\delta\phi|^2$$

Integrating the 2nd term by parts and employing the Poisson equation then gives:

$$\boxed{\delta F = \int d^2x_\perp\ \left\{q\phi - \mu r^2 - \text{const}\right\}\delta n\ +\ \frac{\epsilon_0}{2}\int d^2x_\perp|\nabla_\perp\delta\phi|^2}$$

For an extremum, the first order term must vanish, giving within the beam:

$$q\phi = \mu r^2 + \text{const}$$

From the Poisson equation, this can only be consistent with a uniform density axisymmetric beam. The 2nd order term is positive definite, immediately implying that this extremum is a global *minimum* of F

Result:

At fixed line charge and rms radius, a uniform density beam minimizes the electrostatic self-field energy

At fixed line charge and rms radius, a uniform density beam minimizes the electrostatic self-field energy

This result, combined with Wangler's Theorem:

$$\boxed{\frac{d}{ds}\varepsilon_x^2 = -Q\langle x^2\rangle_\perp \frac{d}{ds}\left(\frac{W - W_u}{\lambda^2}\right)}$$

shows that:

- Self-field energy drives emittance evolution
  - Nonuniform density => more uniform density <=> local emittance growth
  - Uniform density => more nonuniform density <=> local emittance reduction
- Try to maintain density uniformity to preserve beam emittance
- Results can be partially generalized to 2D elliptical beams

  [J. Struckmeier and I. Hofmann, Part Accel. **39**, 219 (1992)]

S10: Collective Relaxation and rms Emittance Growth

The space-charge profile of intense beams can be born highly nonuniform out of nonideal (real) injectors or become nonuniform due to a variety of (error) processes. Also, low-order envelope matching of the beam may be incorrect due to focusing and/or distribution errors.

How much emittance growth and changes in other characteristic parameters may be induced by relaxation of characteristic perturbations?

- Employ Global Conservation Constraints of system to bound possible changes
- Assume full relaxation to a final, uniform density state for simplicity

What is the mechanism for the assumed relaxation?

- Collective modes launched by errors will have a broad spectrum
  - Phase mixing can smooth nonuniformities – mode frequencies incommensurate
- Nonlinear interactions, Landau damping, interaction with external errors, ...
- Certain errors more/less likely to relax:
  - Internal wave perturbations expected to relax due to many interactions
  - Envelope mismatch will not (coherent mode) unless amplitudes are very large producing copious halo and nonlinear interactions

Example: Relaxation of nonlinear space-charge waves

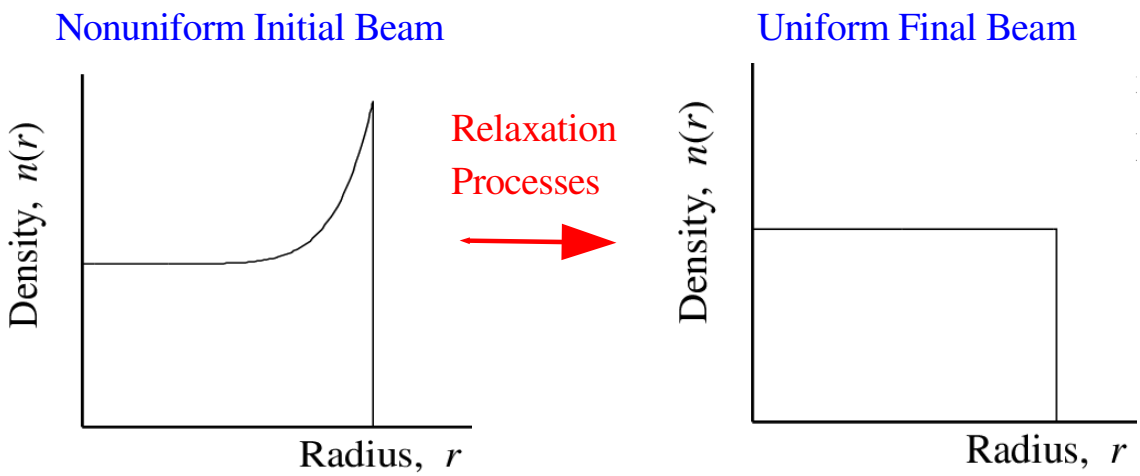

Reference: High resolution self-consistent PIC simulations shown in class

- Continuous focusing and a more realistic FODO transport lattice
  - Relaxation more complete in real lattice due to a richer frequency spectrum
- Relaxations surprisingly rapid: few undepressed betatron wavelengths

Initial Nonuniform Beam Parameterization

$$n(r) = \begin{cases} \hat{n}\left[1 + \frac{1-h}{h}\left(\frac{r}{r_b}\right)^p\right], & 0 \le r \le r_b \\ 0, & r_b < r \le r_p \end{cases}$$

$h =$ hollowing parameter

$p =$ radial power

$$\lambda = \int d^2x_\perp \, n = \pi q \hat{n} r_b^2 \left[\frac{(ph+2)}{(p+2)h}\right]$$

$$R = 2\langle x^2\rangle_\perp^{1/2} = \sqrt{\frac{(p+2)(ph+4)}{(p+4)(ph+2)}}\, r_b$$

Hollowed Initial Density

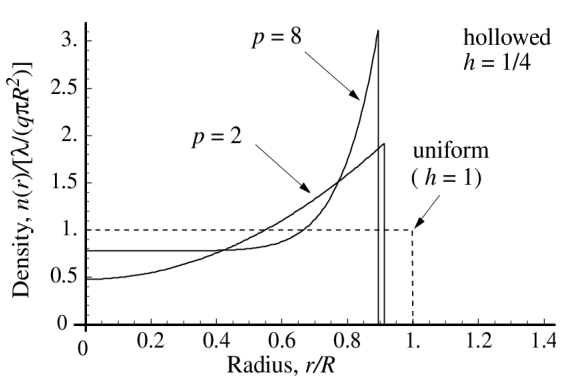

Peaked Initial Density

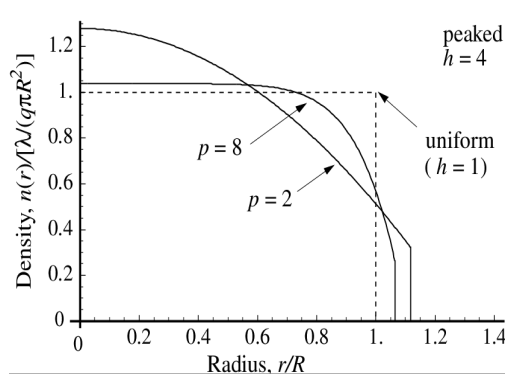

- Analogous definitions are made for the radial temperature profile of the beam

Example Simulations, Initial Nonuniform Beam

$\sigma/\sigma_0 = 0.2$ Initial density: h=1/4, p=8 Initial Temp: h = infinity, p=2

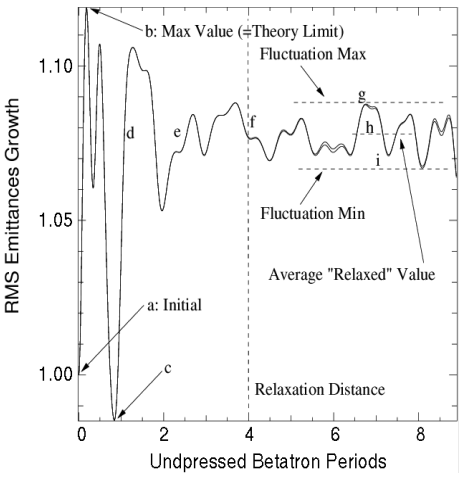

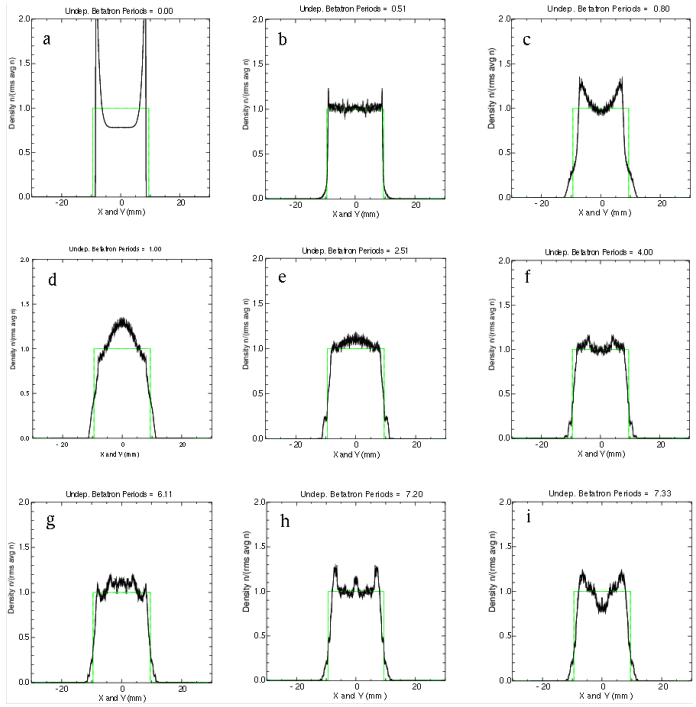

[Lund, Grote, and Davidson, Nuc. Instr. Meth. A 544, 472 (2005)]

Initial beam					Relaxed and transient beam		
σ_i/σ_0	Density		Temperature		Emittance growth		Undep. betatron periods to relax
	h	p	h	p	Theory	Simulation	
0.1	0.25	4	1	arb.	1.57	1.42 (1.57, 1.31–1.52)	3.5
			∞	2		1.45 (1.57, 1.38–1.52)	3.0
			0.5			1.41 (1.57, 1.30–1.52)	3.0
	0.25	8	1	arb.	1.43	1.33 (1.43, 1.28–1.38)	3.5
			∞	2		1.35 (1.43, 1.30–1.40)	4.5
			0.5			1.32 (1.43, 1.26–1.38)	4.0
0.20	0.25	4	1	arb.	1.17	1.11 (1.16, 1.09–1.13)	4.5
			∞	2		1.12 (1.16, 1.10–1.13)	3.0
			0.5			1.11 (1.16, 1.09–1.13)	4.0
	0.25	8	1	arb.	1.12	1.08 (1.12, 1.06–1.09)	5.5
			∞	2		1.08 (1.12, 1.07–1.09)	4.0
			0.5			1.08 (1.12, 1.06–1.09)	4.5

Theory estimates made from global conservation constraints work well but what if the beam relaxed to a smooth thermal equilibrium profile instead?

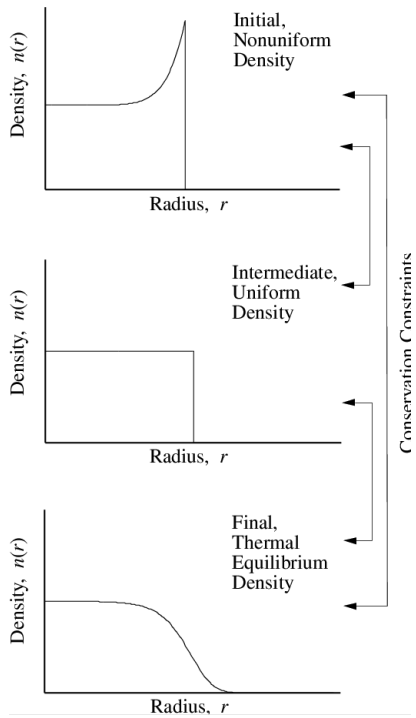

Lund, Barnard, and Miller, PAC 1995, p. 3278

Essentially no rms changes in 2nd step!

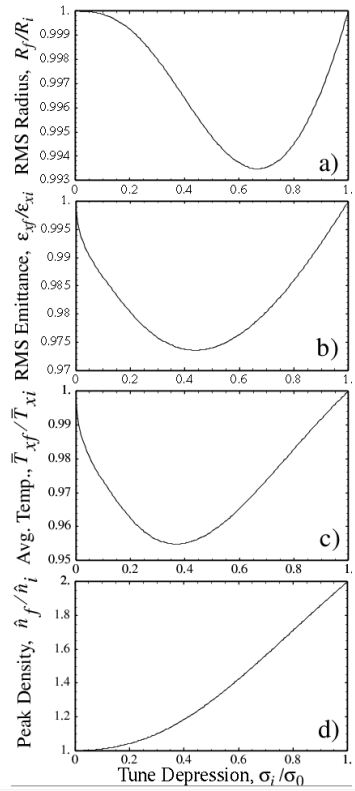

S11: Phase Mixing and Landau Damping in Beams

To be covered in future editions of notes

These slides will be corrected and expanded for reference and any future editions of the US Particle Accelerator School class:
Beam Physics with Intense Space Charge, by J.J. Barnard and S.M. Lund

Corrections and suggestions are welcome. Contact:

SMLund@lbl.gov

Steven M. Lund
Lawrence Berkeley National Laboratory
BLDG 47 R 0112
1 Cyclotron Road
Berkeley, CA 94720-8201

(510) 486 – 6936

Please do not remove author credits in any redistributions of class material.

References: For more information see:

M. Reiser, *Theory and Design of Charged Particle Beams*, Wiley (1994)

R. Davidson, *Theory of Nonneutral Plasmas*, Addison-Wesley (1989)

R. Davidson and H. Qin, Physics of Intense Charged Particle Beams in High Energy Accelerators, World Scientific (2001)

F. Sacherer, *Transverse Space-Charge Effects in Circular Accelerators*, Univ. of California Berkeley, Ph.D Thesis (1968)

S. Lund and B. Bukh, Review Article: *Stability Properties of the Transverse Envelope Equations Describing Intense Beam Transport*, PRST-Accel. and Beams 7, 024801 (2004)

S. Lund and R. Davidson, *Warm Fluid Description of Intense Beam Equilibrium and Electrostatic Stability Properties*, Phys. Plasmas 5, 3028 (1998)

D. Nicholson, *Introduction to Plasma Theory*, Wiley (1983)

John Barnard
Steven Lund
USPAS
June 2006

Intrabeam collisions, gas and electron effects in intense beams

1. Beam/beam coulomb collisions
2. Beam/gas scattering
3. Charge changing processes
4. Gas pressure instability
5. Electron cloud processes
6. Electron-ion instability

Gas and electron effects

-Effects are quite different depending on q, m of species being accelerated

-Circular accelerators vs. Linacs
($t_{residence}$ ~ ms to days vs. 10's of μs)

-Long pulse vs. short pulse
(t_{pulse} ~ 10's of μs vs. 10's of ns)

+ Heavy ion	Residual gas molecule	e^- electron

Processes:

1. Coulomb collisons (intra-beam)

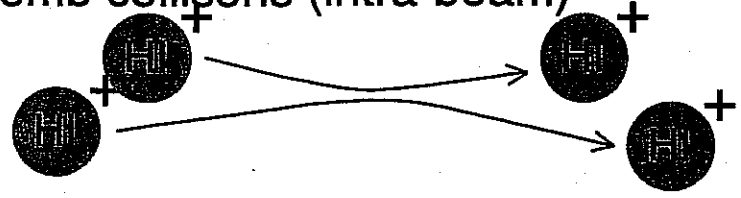

2. Coulomb collisions with residual gas

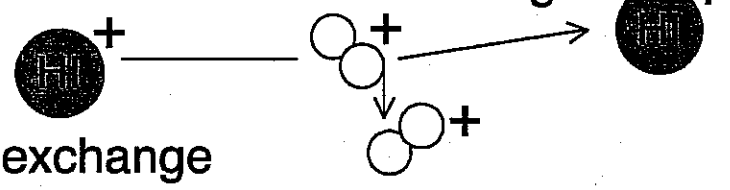

3. Charge exchange

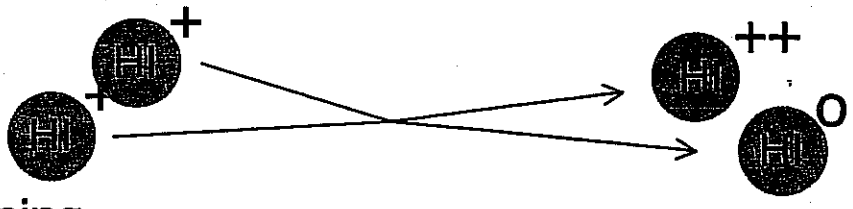

4. Stripping

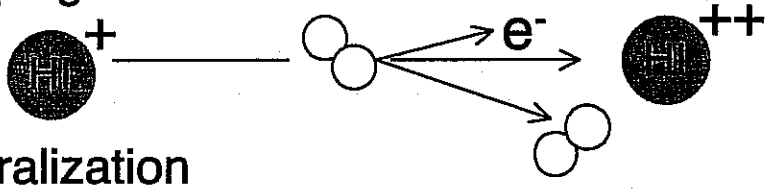

5. Neutralization

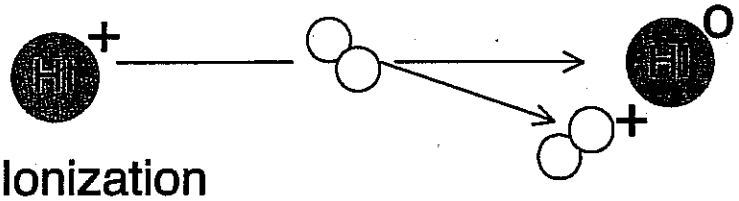

6. Gas Ionization

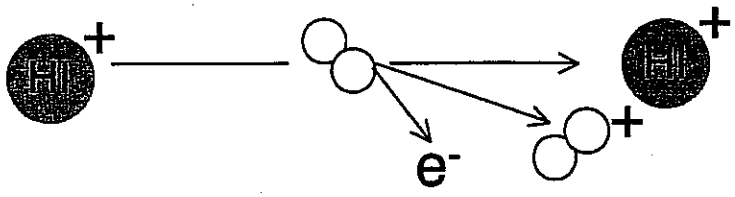

7. Wall interactions

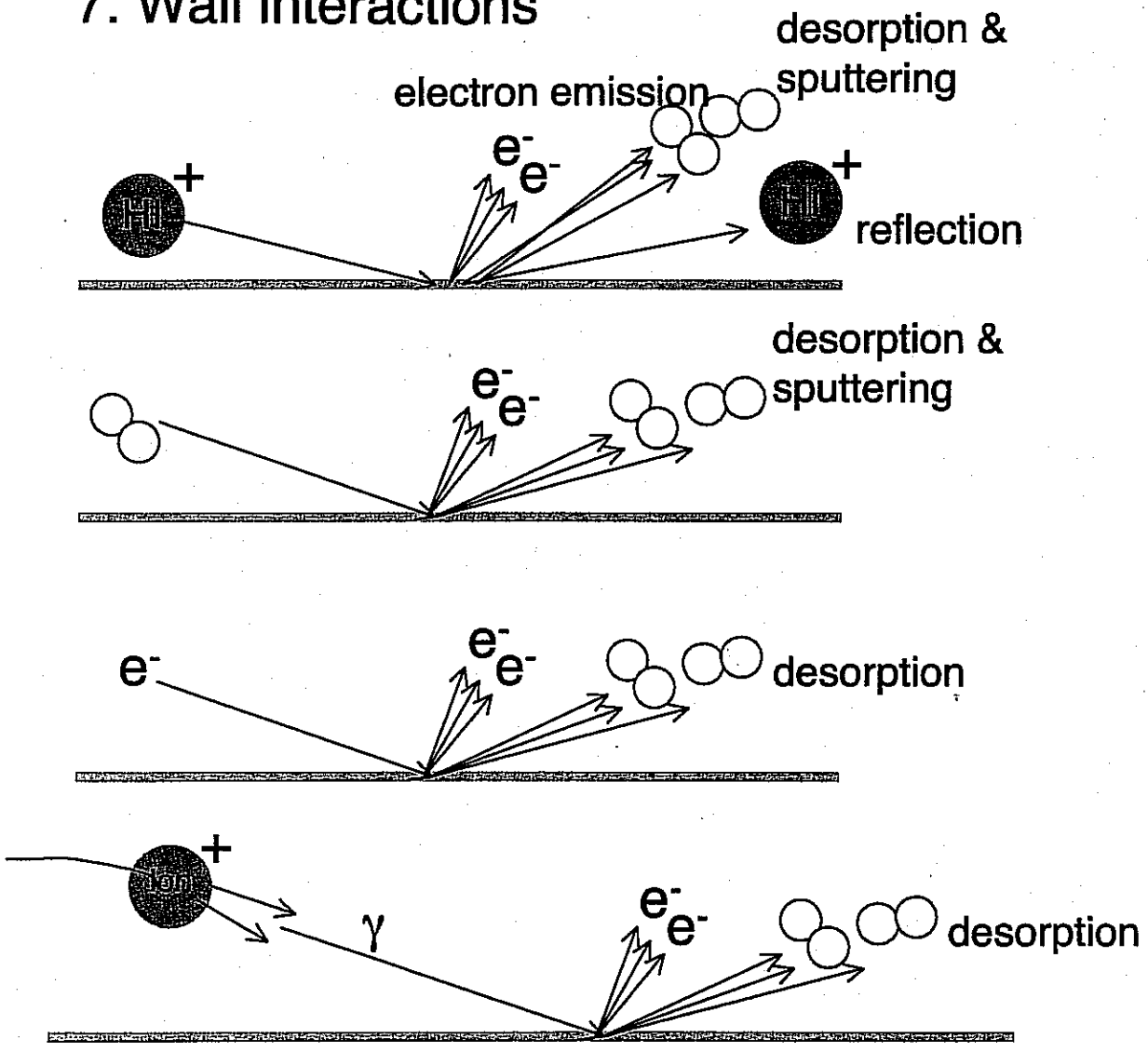

γ	synchrotron photon

1. COLLISIONS WITHIN BEAM REISER 6.4

CONSIDER EFFECTS OF COULOMB COLLISIONS IN A CONTINUOUS BEAM PROPAGATING THROUGH A SMOOTH FOCUSING CHANNEL WITH $T_{\perp 0} \neq T_{\parallel 0}$

(IF $T_{\perp 0} = T_{\parallel 0} \Rightarrow$ BEAM ALREADY RELAXED).

FROM ICHIMARU & ROSENBLUTH, PHYS FLUIDS 13, 2778, (1970):

$$\frac{dT_\perp}{dt} = -\frac{1}{2}\frac{dT_\parallel}{dt} = \frac{-(T_\perp - T_\parallel)}{\tau}$$

(SINCE $T_x = T_y = T_\perp$, $T_\parallel$ CHANGES AT TWICE THE RATE OF $T_\perp$)
(SINCE $2k_B T_\perp + k_B T_\parallel = \text{const}$)

τ = RELAXATION TIME

$$= \frac{15\,(k_B T_{eff}/mc^2)^{3/2}(4\pi\epsilon_0)^2 m^2 c^3}{8\pi^{1/2} q^4 \ln\Lambda\, n} = \left(\frac{15\,\pi^{1/2}}{8\ln\Lambda}\right)\nu_c^{-1}$$

COULOMB COLLISION APPROXIMATE RATE FOR LARGE ANGLES (PAGE 9 OF INTRODUCTION NOTES)

$$\ln\Lambda = \begin{cases} \ln \dfrac{(\epsilon_0 k T_{eff})^{3/2} 12\pi}{q^3 n^{1/2}} & \text{for } \lambda_D < r_b \\[2ex] \ln \dfrac{12\pi\epsilon_0 k T_{eff} r_b}{q^2} & \text{for } \lambda_D > r_b \end{cases}$$

$$T_{eff} = T_\perp \left[\frac{15}{4}\int_{-1}^{1} \frac{\mu^2(1-\mu^2)\,d\mu}{\left[(1-\mu^2) + \mu^2 (T_\parallel/T_\perp)\right]^{3/2}}\right]^{-2/3}$$

T_{eff} is an appropriate average of $T_\perp$ & $T_\parallel$

$\frac{T_{eff}}{T_\perp}$

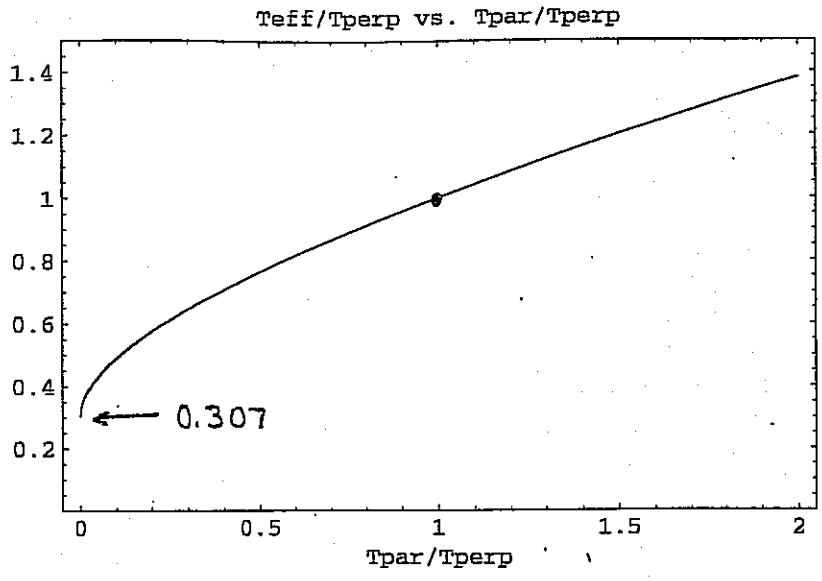

FOR $T_\parallel = 0$

$$T_\perp = \frac{2}{3} T_{\perp 0}\left(1 + \frac{1}{2} e^{-3t/\tau_{\text{eff}}}\right), \tag{6.156a}$$

(APPROXIMATE SOLUTIONS)

$$T_\parallel = \frac{2}{3} T_{\perp 0}\left(1 - e^{-3t/\tau_{\text{eff}}}\right), \tag{6.156b}$$

$\tau_{eff} = 0.42\,\tau_{eq}$

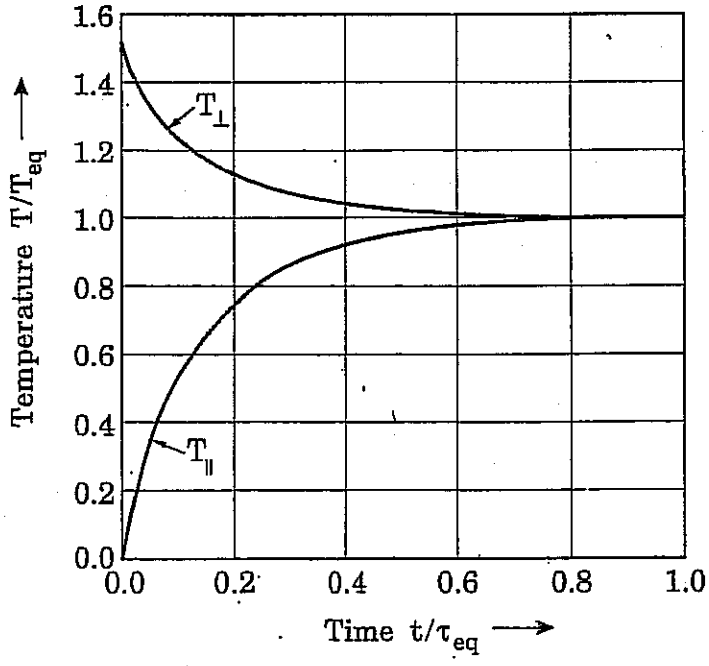

FROM REISER p.527

$\tau_{eq} = \tau(T_{eq})$

BOERSCH EFFECT

AREN'T COLLISIONS NEGLIGIBLE? (NOT ALWAYS)

PUTTING IN NUMBERS:

FOR IONS:

$$\tau_{eff} = 4.3 \cdot 10^{-4}\,s \; \frac{(A^{1/2})}{Z^4} \left(\frac{kT_{eff}}{1\,eV}\right)^{3/2} \left(\frac{15}{\ln\Lambda}\right)\left(\frac{10^{10}\,cm^{-3}}{n}\right)$$

$$\ln\Lambda = \ln\left[\frac{1.5 \cdot 10^5\,(kT/1\,eV)^{3/2}}{Z^3\,(n/10^{10}\,cm^{-3})}\right]$$

EXAMPLE: 2 MeV INJECTOR

$\tau_{eff} \simeq 8.8 \cdot 10^{-4}\,s$ for $A = 39$, $Z = 1$, $n = 10^{10}\,cm^{-3}$, $kT_{eff} = 0.3\,eV$, $\ln\Lambda = 8.5$

$$t_{transit} \simeq \frac{2d}{V} \simeq \frac{2\,(2m)}{(.01)\,3 \cdot 10^8} = 1.3\,\mu s$$

So $\tau_{eff} >> t_{transit}$ $\Rightarrow$ collisions are rare BUT

$$T_{\substack{accel\\cool}} = \frac{1}{2}\left(\frac{kT_0}{qV}\right) kT_0 = 2.5 \cdot 10^{-9}\,eV \quad \text{for } \begin{matrix} kT_0 = 0.1\,eV \\ qV = 2\,MeV \end{matrix}$$

$$T_{\parallel\,collisions} \simeq \frac{2}{3} T_{\perp 0}\left(1 - \exp\left(-3t/\tau_{eff}\right)\right) \simeq 2T_{\perp 0}\left(\frac{t_{transit}}{\tau_{eff}}\right) = .006\,eV \quad \text{for } T_{\perp 0} = 1\,eV$$

SO T_H FROM "BOERSCH EFFECT"

$\gg$ $T_{\parallel}$ FROM LONGITUDINAL COOLING

100 SHEETS
U.S.A.

COULOMB COLLISIONS IN RESIDUAL GAS (REISER 6.4.3)

JACKSON CHAPTER 13

(RUTHERFORD SCATTERING)

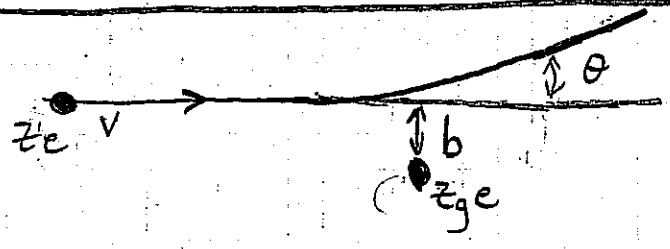

$$\frac{dp_x}{dt} = \frac{z z_g e^2}{4\pi\epsilon_0 r^2}\frac{b}{r} \Longrightarrow \Delta p = \int_{-\infty}^{\infty} \frac{dp_x}{dt}\frac{dt}{dz}\,dz$$

$$= \frac{z z_g e^2 b}{4\pi\epsilon_0 v}\underbrace{\int_{-\infty}^{\infty}\frac{dz}{(z^2+b^2)^{3/2}}}_{2/b^2}$$

$$= \frac{2 z z_g e^2}{4\pi\epsilon_0 v b}$$

$$\Delta p\,\theta \cong \frac{\Delta p}{p} = \frac{2 z z_g e^2}{4\pi\epsilon_0 p v b} \Rightarrow \frac{db}{d\theta} \sim \frac{1}{\theta^2}$$

DIFFERENTIAL CROSS SECTION FOR SCATTERING WITH IMPACT PARAMETER b INTO SOLID ANGLE $d\Omega$ AT ANGLE θ SATISFIES

$$\underbrace{2\pi b\,db}_{\text{AREA}} = \frac{d\sigma}{d\Omega}\underbrace{2\pi\sin\theta\,d\theta}_{\text{SOLID ANGLE}}$$

$$\Rightarrow \frac{d\sigma}{d\Omega} = \frac{b}{\sin\theta}\left|\frac{db}{d\theta}\right| = \left(\frac{2 z z_g e^2}{4\pi\epsilon_0 p v}\right)^2 \frac{1}{\theta^4}$$

ELECTRON SCREENING PUTS CUTOFF AT SMALL θ (LARGE b) SO BETTER TO USE

$$\frac{d\sigma}{d\Omega} = \left(\frac{2 z z_g e^2}{4\pi\epsilon_0 p v}\right)^2 \frac{1}{(\theta^2+\theta_{min}^2)^2}$$

AVERAGE ANGLE SQUARED FOR A SINGLE SCATTERING IS:

$$\bar{\theta}^2 = \frac{\int \theta^2 \frac{d\sigma}{d\Omega} 2\pi \sin\theta \, d\theta}{\int \frac{d\sigma}{d\Omega} 2\pi \sin\theta \, d\theta} \cong \frac{\int_0^{\theta_{max}} \frac{\theta^3}{(\theta^2+\theta_{min}^2)^2} d\theta}{\int_0^{\theta_{max}} \frac{\theta}{(\theta^2+\theta_{min}^2)^2} d\theta}$$

$$\cong 2\theta_{min}^2 \ln\left(\frac{\theta_{max}}{\theta_{min}}\right)$$

ASSUMES $\theta_{max}^2 \gg \theta_{min}^2$

& $\ln\left(\frac{\theta_{max}}{\theta_{min}}\right) \gg 1$

MULTIPLE COLLISIONS

AFTER TRAVERSING DISTANCE s, AND UNDERGOING N_s COLLISIONS, THE MEAN SQUARE ANGLE $\overline{\Theta^2}$ $\left[\sigma_s = \pi\left(\frac{2Z_g e^2}{4\pi\epsilon_0 pv}\right)^2 \frac{1}{\theta_{min}^2}\right]$

$$\overline{\Theta^2} = N_s \bar{\theta}^2 = n_g \sigma_s s \bar{\theta}^2$$

$$= 16\pi n_g \left(\frac{Z Z_g e^2}{4\pi\epsilon_0 m c^2 \gamma p^2}\right)^2 \ln\left(\frac{\theta_{max}}{\theta_{min}}\right) s$$

JACKSON ARGUES θ_{max} ARISES FROM DISTRIBUTED NATURE OF NUCLEUS (NOT POINT CHARGE) AND θ_{min} ARISES FROM SCREENING OF ELECTRONS OR UNCERTAINTY PRINCIPLE

$$\ln\frac{\theta_{max}}{\theta_{min}} \simeq \ln\left(204 Z_g^{-1/3}\right)$$

$$\Delta\langle x'^2\rangle = \frac{1}{2}\overline{\Theta^2}$$ [since $\Delta\langle x'^2\rangle + \Delta\langle y'^2\rangle = \Delta\overline{\Theta^2}$]

$$\epsilon = 4\sqrt{\langle x^2\rangle\langle x'^2\rangle - \langle xx'\rangle^2}$$

FOR A MATCHED BEAM

$$k_p^2\langle x^2\rangle = \langle x'^2\rangle$$ where k_p = depressed betatron wavenumber

$$\Rightarrow \quad \epsilon = \frac{4\langle x'^2\rangle}{k_p}$$

$$\Delta\epsilon = \frac{4\,\Delta\langle x'^2\rangle}{k_p} = \frac{2\,\overline{\Theta^2}}{k_p}$$

$$\Rightarrow \boxed{\frac{d\epsilon}{ds} = \frac{32\pi}{k_p} n_g \left(\frac{Z Z_g e^2}{4\pi\epsilon_0 mc^2\gamma\beta^2}\right)^2 \ln\left(204 Z_g^{-1/3}\right)}$$

IN TERMS OF NORMALIZED EMITTANCE:

$$\boxed{\frac{d\epsilon_N}{ds} = \frac{32\pi}{k_p} n_g \left(\frac{Z Z_g e^2}{4\pi\epsilon_0 mc^2}\right)^2 \frac{1}{\gamma\beta^3} \ln\left(204 Z_g^{-1/3}\right)}$$

<u>Example:</u> $n_g = 10^{-7}$ torr $= 3.5\cdot 10^{9}\ \mathrm{cm}^{-3} = 3.5\cdot 10^{15}\ \mathrm{m}^{-3}$

$k_{p0} = 2.5\ \mathrm{m}^{-1}$ $\quad k_p = 0.25\ \mathrm{m}^{-1}$

$Z_g = 7$, $Z = 19$, $A = 39$, $\beta = 0.01$, $\epsilon_N = 1\cdot 10^{-6}$ m-rad

$\Rightarrow \frac{d\epsilon_N}{ds} = 3.7\cdot 10^{-11}\ \mathrm{m}^{-1}$ $\Rightarrow$ Need 27 km to equal original emittance!

(But more important for rings & low mass!)

PRESSURE "BUMPS" AND BEAM LOSS FROM CHARGE CHANGING COLLISIONS

REFERENCE: WORKSHOP ON BEAM INDUCED PRESSURE RISE IN RINGS, BNL, Dec. 2003.

σ_s = STRIPPING CROSS SECTION

σ_{ce} = CHARGE EXCHANGE CROSS SECTION

σ_i = IONIZATION CROSS SECTION

V_{cm} = mean ion velocity in ion beam frame

(1) BEAM LOSS

$$\frac{dn_b}{dt} = -\sigma_s V_i n_b \bar{n} - \sigma_{ce} V_{cm} n_b^2 - \left.\frac{\partial n_b}{\partial t}\right|_{HALO}$$

(2) GAS EVOLUTION

$\bar{n}$ = average gas density

$$\frac{d}{dt}\bar{n} = \underbrace{\eta_G \sigma_i V_i n_b \bar{n}}_{\text{IONIZATION}} \left(\frac{V_{beam}}{V_{pipe}}\right) + \underbrace{\eta_{HI} \sigma_s V_i n_b \bar{n}}_{\text{STRIPPING}} \left(\frac{V_{beam}}{V_{pipe}}\right) + \underbrace{\eta_{HI} \sigma_{ce} V_{cm} n_b^2}_{\text{CHARGE EXCHANGE}} \left(\frac{V_{beam}}{V_{pipe}}\right) + \underbrace{q}_{\text{OUTGASSING}} - \underbrace{(S/A_p)\bar{n}}_{\text{PUMPING}}$$

VOLUME OF BEAM

VOLUME OF PIPE

S = Effective linear pumping rate $[m^3 s^{-1}/m]$ $\qquad A_p = \pi r_p^2$ = AREA OF PIPE

q = OUTGASSING rate $= \frac{2\pi r_p Q}{\pi r_p^2} = \frac{2Q}{r_p}$; $\quad Q = \frac{\#}{m^2 s}$

η_G = GAS MOLECULES DESORBED PER INCIDENT RESIDUAL GAS ION

η_{HI} = GAS MOLECULES DESORBED PER INCIDENT IONIZATION STRIKING WALL

$\left(V_{beam}/V_{pipe} \rightarrow \left(\frac{n_b}{n_{pipe}}\right) \nu_{rep} \Delta t_{beam} \text{ for a rep rated linac} \right)$

If we take $n_b \simeq$ constant

then we may express gas evolution equation as:

$$\frac{d\bar{n}}{dt} = \frac{\bar{n}}{\tau} + q_{eff}$$

with solution:

$$\bar{n} = (\bar{n}_0 + \tau q_{eff}) \exp[t/\tau] - \tau q_{eff}$$

HERE $$\tau = \frac{1}{(\eta_g \sigma_i + \eta_{HI} \sigma_s)\left(\frac{V_{beam}}{V_{pipe}}\right) n_b V_i - S/A_p}$$

$$q_{eff} = q + \eta_{HI} \sigma_{CE} V_{cm} n_b^2 \left(\frac{V_{beam}}{V_{pipe}}\right)$$

<u>EQUILIBRIUM</u> REACHED IF $\tau < 0$ (i.e. pumping exceeds desorption).

$$\Rightarrow \bar{n} = -\tau q_{eff} = \frac{q + \eta_{HI} \sigma_{CE} V_{cm} n_b^2 (V_{beam}/V_{pipe})}{S/A_p - (\eta_g \sigma_i + \eta_{HI} \sigma_s)\left(\frac{V_{beam}}{V_{pipe}}\right) n_b V_i}$$

<u>INSTABILITY</u> IF $$n_b V_i \geq \frac{\frac{S}{A_p}\left(\frac{V_{pipe}}{V_{beam}}\right)}{\eta_g \sigma_i + \eta_{HI} \sigma_s}$$

Instability first observed on the ISR proton storage ring, limiting current in mng, in 1970's.

If $l_{beam} = l_{pipe}$

INSTABILITY CRITERION MAY BE WRITTEN

$$I > \frac{ZeS}{\eta_g \sigma_i + \eta_{HI} \sigma_s}$$

<u>EXAMPLE:</u> If $S = 100\ \ell\, s^{-1} m^{-1} = 0.1\ m^3 s^{-1} m^{-1}$

ISR

$\eta_g = 4$

$\sigma_i = 10^{-22}\ m^2 = 10^{-16}\ cm^2$; $\sigma_s = 0$

$Z = 1$ (protons)

$\Rightarrow I \leq 40$ Amperes

(PRESSURE RUNAWAYS WERE OBSERVED ON the ISR AT 14-18A, (BENVENUTI et al, IEEE Trans. on Nuc. Sci. NS-24, 1773, 1977)

SEE "BEAM INDUCED PRESSURE RISE IN RINGS"
13th ICFA BEAM DYNAMICS MINI WORKSHOP, BNL, Dec. 9-12, 2003.
WEBSITE: http://www.c-ad.bnl.gov/icfa

"ELECTRON CLOUD EFFECTS"

REFERENCE: CERN e-CLOUD WORKSHOP
http://wwwslap.cern.ch/collective/ecloud02/
→ proceedings.html

BASIC IDEA

IN ION storage rings or collider rings:

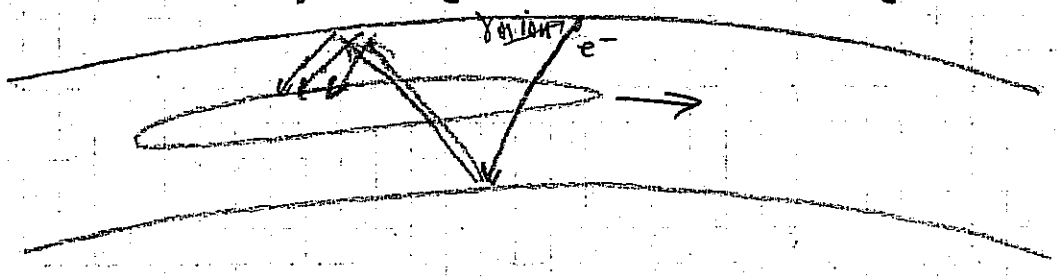

ELECTRONS ARE ATTRACTED TO POSITIVE POTENTIAL OF BEAM & ACCUMULATE

SOME SYMPTOMS:

1. BEAM LOSS & pressure rise
2. HIGH FREQUENCY CENTROID oscillations

SOME ACCELERATORS WHICH SHOW EVIDENCE OF e^- EFFECTS

1. LANL PSR
2. CERN PS & SPS
3. BNL RHIC

COULD LIMIT PLANNED / UNDER CONSTRUCTION:

1. SNS ACCUMULATOR RING
2. LHC

cf. "Electron-cloud effects in HIGH INTENSITY PROTON ACCELERATORS" J. Wei & R. Macek, CERN

BEAM INDUCED MULTIPACTING

a). MULTI-BUNCH

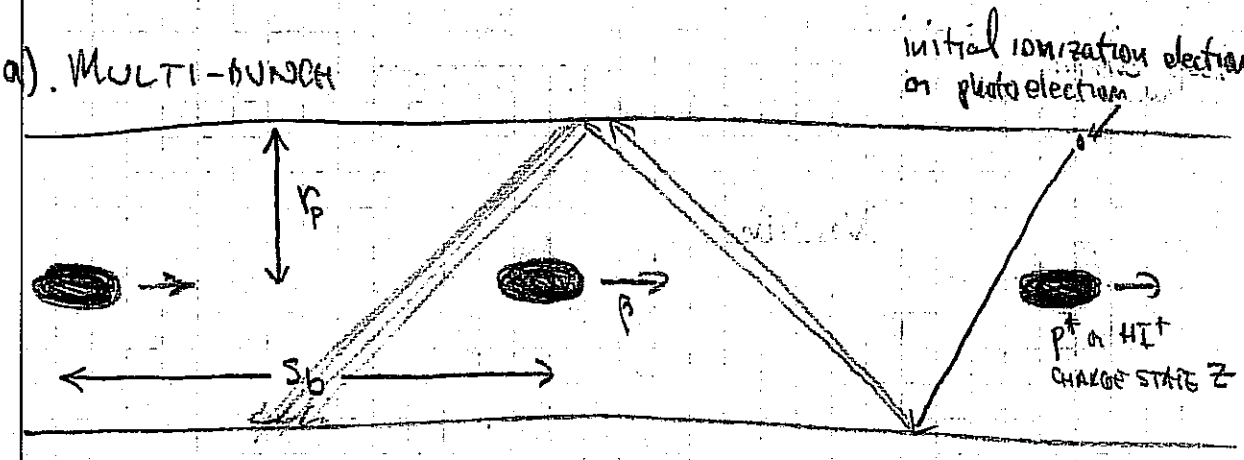

USING COULOMB COLLISION FORMULA FROM PAGE 9:

$$\Delta p_x \cong \frac{2 Z N_b e^2}{4\pi\epsilon_0 v r_p}$$

N_b = Number of ions of charge Z in bunch

$$\Delta E_e = m_e c^2\left[\sqrt{\frac{\Delta p_x^2}{m^2c^2}+1} - 1\right] = m_e c^2\left[\sqrt{\left(\frac{2 r_e Z N_b}{\beta r_p}\right)^2 + 1} - 1\right]$$

$$\cong 2 r_e^2 m_e c^2 \frac{Z^2 N_b^2}{\beta^2 r_p^2}$$

for $\Delta E_e \ll m_e c^2$ $\left(\text{or } \frac{2 r_e Z N_b}{\beta r_p} \ll 1\right)$

$$\left(\text{where } r_e = \frac{e^2}{4\pi\epsilon_0 m_e c^2} \simeq 2.8 \times 10^{-15}\,\text{m}\right)$$

DEFINE A MULTIPACTING PARAMETER $\mathcal{J}_m$

$$\mathcal{J}_m = \frac{\text{TIME FOR ELECTRON TO CROSS PIPE}}{\text{TIME BETWEEN BUNCHES}} = \frac{2 r_p}{s_b}\frac{\beta}{\beta_e}$$

$$\cong \frac{\beta^2 r_p^2}{Z N_b r_e s_b}$$

RESONANCE CONDITION:

$$\mathcal{J}_m = 1$$

s_b = distance between bunches

b). SINGLE-BUNCH BEAM-INDUCED MULTIPACTING

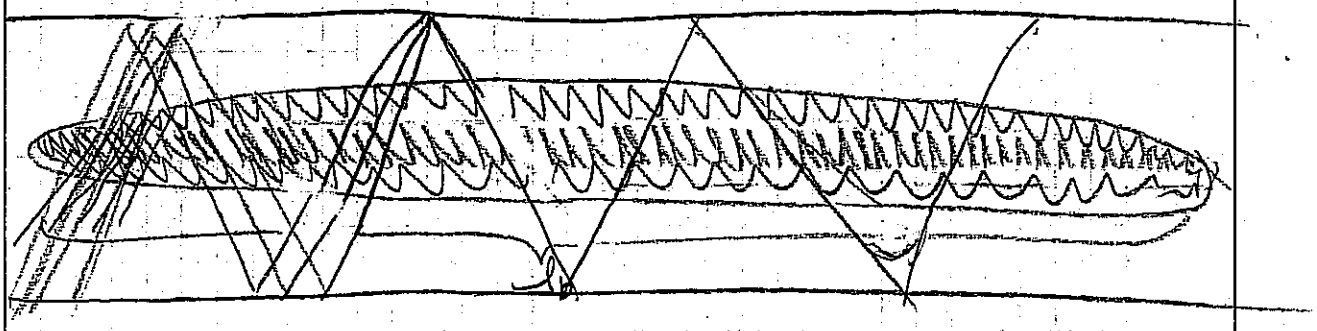

$$\zeta_s = \frac{r_p\,\beta}{l_b\,\beta_e} = \frac{\text{time for electrons to cross pipe}}{\text{passage time for half of the bunch}}$$

Recall:

$$\varphi = \begin{cases} \frac{\lambda}{2\pi\epsilon_0}\left[\frac{1}{2}\left(1-\frac{r^2}{r_b^2}\right)+\ln\frac{r_p}{r_b}\right] & 0<r<r_b \\ \frac{\lambda}{2\pi\epsilon_0}\left[\ln\frac{r_p}{r}\right] & r_b<r<r_p \end{cases}$$

$$\frac{1}{2}m_e v_e^2 + q\varphi \simeq \text{const} \simeq 0$$

$$\beta_e \sim \frac{1}{2}\sqrt{\frac{2q\varphi}{m_e c^2}} \sim \sqrt{\frac{N_0 Z e^2}{l_b\, 4\pi\epsilon_0 m_e c^2}} \sim \sqrt{\frac{Z r_e N_0}{l_b 4\pi\epsilon_0}}$$

(AVERAGE e^- VELOCITY)

$$\Rightarrow \zeta_s = \frac{\beta r_p}{\sqrt{r_e l_b N_0 Z}}$$

THE ENERGY GAIN OF THE ELECTRON, RELIES ON THE DENSITY CHANGING OVER THE COURSE OF THE BUNCH.

$$\Delta E_e \sim \frac{m_e c^2}{2}\left[\frac{Z r_e N_0(s)}{l_b}\right] - \frac{m_e c^2}{2}\left[\frac{Z r_e N_0(s+\Delta s)}{l_b}\right]$$

$$\sim \frac{m_e c^2}{2}\left(\frac{\partial N_0}{\partial z}\Delta z\right)\left(\frac{Z r_e}{l_b}\right)$$

$$\Delta E_e \sim \frac{m_e c^2}{2}\left(\frac{\partial N_0}{\partial z}\Delta z\right)\left(\frac{Z r_e}{l_b}\right)$$

$$\Delta z = \frac{r_p}{\gamma_e}\beta\epsilon = \beta r_p\sqrt{\frac{l_b}{Z r_e N_0}}\,; \qquad \frac{\partial N_0}{\partial z} \sim \frac{N_0}{l_b}$$

So $\Delta E_e \approx m_e c^2\left(\frac{Z N_0 r_e}{l_b^3}\right)^{1/2}\beta r_p$

$\xi \leq 1 \Rightarrow$ Electron build up possible within bunch

WHAT IS STEADY STATE ELECTRON DENSITY?

Electrons can build up until E_r at pipe ~ 0.

$$\Rightarrow \lambda_e = \lambda_J$$

$$\pi r_p^2 n_e = \pi r_b^2 Z n_i$$

$$n_e = \left(\frac{r_b}{r_p}\right)^2 Z n_i$$

ELECTRON - ION INSTABILITY

(SEE ALSO R.C. DAVIDSON & H. QIN, Physics of Intense Charged Particle Beams in High Energy Accelerators, p 503 FOR KINETIC TREATMENT).

CONSIDER A UNIFORM DISTRIBUTION OF ELECTRONS (AT REST) WHICH HAS THE SAME RADIUS (OR SLIGHTLY SMALLER RADIUS) AS A UNIFORM DENSITY ION BEAM, THAT IS MOVING AT VELOCITY V_z (OUT OF THE PLANE OF THE PAPER).

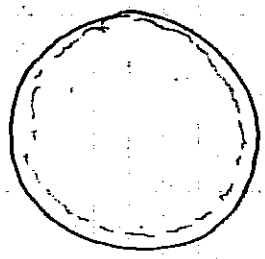

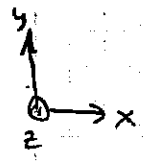

$$E_x = \frac{\lambda_i(r)(x-x_i)}{2\pi\epsilon_0 r_0 r} = \frac{\rho_i}{2\epsilon_0}(x-x_i)$$

THE EQUATION OF MOTION FOR THE CENTROID OF THE ELECTRONS IS OBTAINED FROM

$$m_e\ddot{x} = \frac{-e\rho_i}{2\epsilon_0}(x-x_i) + \frac{e\rho_e}{2\epsilon_0}(x-x_e)$$

or

$$\frac{d^2x_e}{dt^2} = -\frac{\omega_{pi}^2}{2}\left(\frac{m_i}{q}\frac{e}{m_e}\right)(x_e - x_i)$$

here $\omega_{pi}^2 = \dfrac{q^2 n_i}{\epsilon_0 m_i} = \dfrac{q\rho_i}{\epsilon_0 m_i}$

(THE CENTER OF oscillation for the electrons is the center of the ion beam).

x_e = centroid of electron beam

x_i = centroid of ion beam

THE EQUATION OF MOTION FOR THE CENTROID OF THE IONS IS GIVEN BY

$$\frac{d^2 x_i}{dt^2} = -\omega_{po}^2 x_i - \left[\frac{m_e N_e}{m_i N_i}\right]\left(\frac{\omega_{pi}^2}{2}\frac{m_i}{q}\frac{e}{m_e}\right)(x_i - x_e)$$

THE TOTAL MOMENTUM KICK TO EACH SPECIES MUST BE EQUAL & OPPOSITE

$$\Rightarrow \frac{d^2 x_i}{dt^2} = -\omega_{po}^2 x_i - f\,\frac{\omega_{pi}^2}{2}(x_i - x_e)$$

HERE $f \equiv \dfrac{e N_e}{q N_i}$ = fractional neutralization

Now $\dfrac{d}{dt}$ = total derivative $= \dfrac{\partial}{\partial t} + v_z \dfrac{\partial}{\partial z}$

$\Rightarrow$ THE ION & ELECTRON EQUATIONS MAY BE WRITTEN

$$\left(\frac{\partial}{\partial t} + v_z \frac{\partial}{\partial z}\right)^2 x_i = -\omega_{po}^2 x_i - f\,\frac{\omega_{pi}^2}{2}(x_i - x_e)$$

$$\frac{\partial^2}{\partial t^2} x_e = -\frac{\omega_{pi}^2}{2}\left(\frac{m_i}{q}\frac{e}{m_e}\right)(x_e - x_i)$$

National® Brand 42-182 100 SHEETS Made in U.S.A.

Now let $x_e = x_e \exp[i(\omega t - kz)]$; $\quad x_i = x_i \exp[i(\omega t - kz)]$

$$\Rightarrow (-\omega^2 + 2\omega k v_z - k^2 v_z^2)\, x_i = -\omega_{p0}^2 x_i - f\frac{\omega_{pi}^2}{2}(x_i - x_e)$$

$$-\omega^2 x_e = -\frac{\omega_{pi}^2}{2}\left(\frac{m_i}{m_e}\frac{e}{q}\right)(x_e - x_i)$$

$$\Rightarrow \left[(\omega - kv_z)^2 - \omega_{p0}^2 - f\frac{\omega_{pi}^2}{2}\right] x_i = -\frac{f\omega_{pi}^2}{2} x_e$$

$$\left[\omega^2 - \frac{\omega_{pi}^2}{2}\left(\frac{m_i}{m_e}\frac{e}{q}\right)\right] x_e = -\frac{\omega_{pi}^2}{2}\left(\frac{m_i}{m_e}\frac{e}{q}\right) x_i$$

Multiplying the above equations and dividing by $x_e x_i$, yields the dispersion relation:

$$\underbrace{\left[(\omega - kv_z)^2 - \omega_{p0}^2 - f\frac{\omega_{pi}^2}{2}\right]}_{\text{ION BETATRON FREQUENCY (INCREASED BY SPACE CHARGE OF ELECTRONS)}}\underbrace{\left[\omega^2 - \frac{\omega_{pi}^2}{2}\left(\frac{m_i}{m_e}\frac{e}{q}\right)\right]}_{\text{ELECTRON OSCILLATING IN POTENTIAL WELL OF ION}} = \underbrace{+\frac{f\omega_{pi}^4}{4}\left(\frac{m_i}{m_e}\frac{e}{q}\right)}_{\text{COUPLING}}$$

So a beam with high spatial frequency undergoing betatron oscillations in the comoving frame, $kv_z - \omega \cong \sqrt{\omega_{p0}^2 + \frac{f\omega_{pi}^2}{2}}$ will resonate with electrons oscillating in the ion well if

$$\omega \cong \frac{\omega_{pi}}{\sqrt{2}}\sqrt{\frac{m_i e}{m_e q}}$$

Giving rise to instability!

FROM DAVIDSON & QIN (22)
PHYSICS OF INTENSE CHARGED PARTICLE BEAMS, 2001.

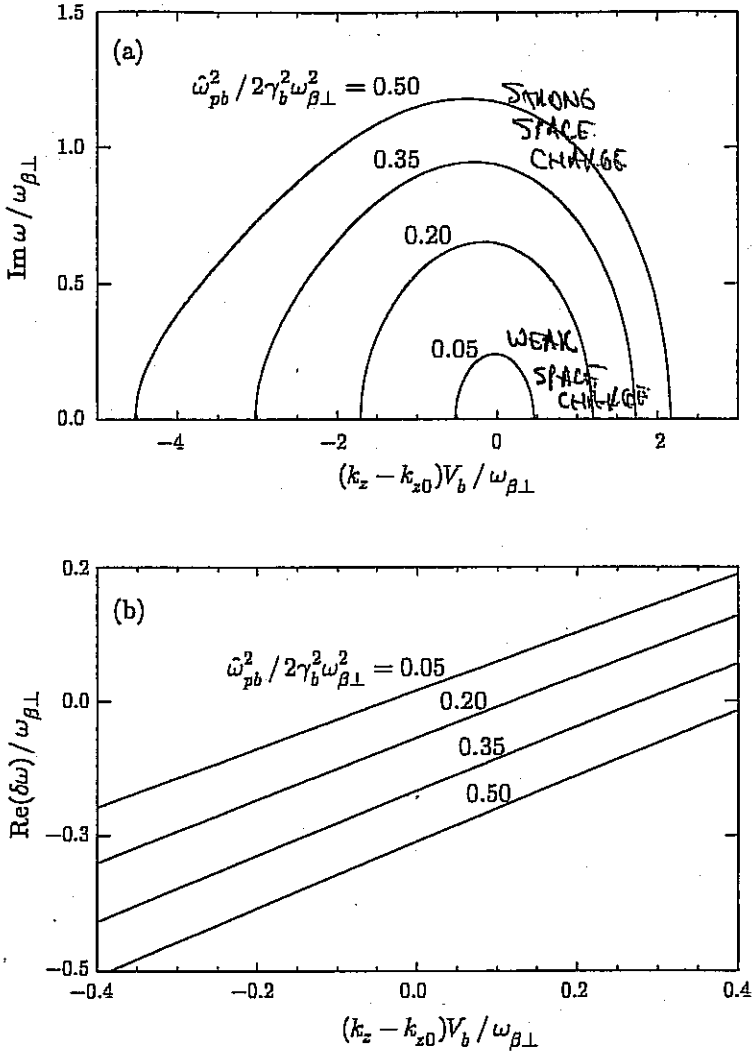

$\omega_{\beta\perp}^2 \equiv \omega_{\beta 0}^2$

$\frac{\hat{\omega}_{pb}^2}{2V_p^2\omega_{\beta\perp}^2} = \left(1 - \frac{\sigma^2}{\sigma_0^2}\right)$

Figure 10.11. Plots of (a) normalized growth rate ($Im\omega/\omega_{\beta\perp}$), and (b) normalized real frequency $(Re\omega - \omega_e)/\omega_{\beta b}$ versus shifted axial wavenumber $(k_z - k_{z0})V_b/\omega_{\beta\perp}$ obtained from the dispersion relation (10.103) for the unstable branch with positive real frequency. System parameters correspond to $v_{T\|b} = 0 = v_{T\|e}$, $m_b/m_e = 1836$ (protons), $(\gamma_b - 1)m_bc^2 = 800$ MeV, $r_b/r_w = 0.5$, and $f = 0.1$. Curves are shown for several values of normalized beam intensity $\hat{\omega}_{pb}^2/2\gamma_b^2\omega_{\beta\perp}^2$ ranging from 0.05 to 0.5.

$k_{z0} V_z = \omega \mp \sqrt{\omega_{\beta 0}^2 + f\omega_p^2/2}$; $\omega = \frac{\omega_{pi}}{2}\sqrt{\frac{m_i e}{m_e q}}$

FROM DAVIDSON & QIN, 2001 (23)

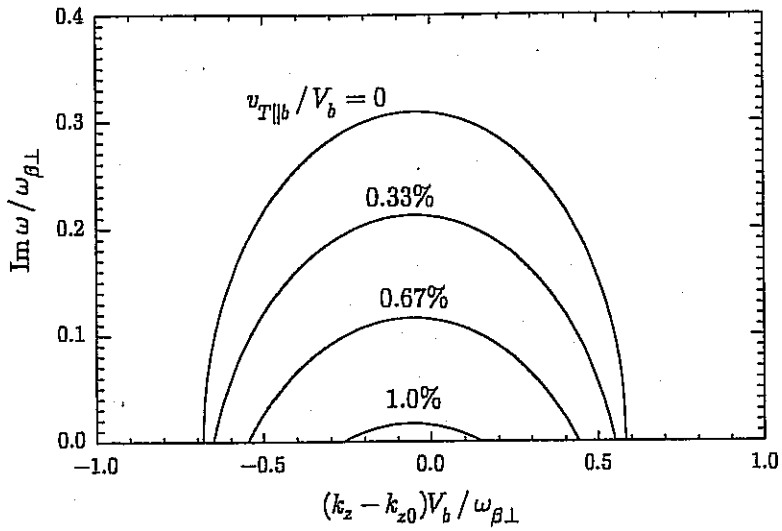

Figure 10.12. Plot of normalized growth rate ($Im\omega/\omega_{\beta\perp}$), and normalized real frequency $(Re\omega - \omega_e)/\omega_{\beta\perp}$ versus positive real frequency. System parameters correspond to $\hat{\omega}_{pb}^2/2\gamma_b^2\omega_{\beta\perp}^2 = 0.07$, $v_{T\|e} = v_{T\|b}$, $m_b/m_e = 1836$ (protons), $(\gamma_b - 1)m_bc^2 = 800$ MeV, $r_b/r_w = 0.5$, and $f = 0.1$. Curves are shown for several values of normalized ion thermal spread $v_{T\|b}/V_b$ ranging from 0 to 0.01.

velocity V_b [Eq. (10.105)], it is expected that Landau damping by parallel ion kinetic effects can have a strong stabilizing influence at modest values of $v_{T\|b}/V_b$. That this is indeed the case is evident from Fig. 10.12, which shows a substantial reduction in maximum growth rate and eradication of the instability over the instability bandwidth as $v_{T\|b}/V_b$ is increased from 0 to 0.01.

We now make use of the nonlinear particle perturbative simulation method [60, 61] described in Sec. 8.5 to illustrate several important properties of the two-stream instability in intense beam systems (Sec. 10.4.2).

PREVENTIVE MEASURES (from J. Weid & L. Maccek, CERN electron cloud workshop 2003).

- SUPPRESS ELECTRON GENERATION
  - SURFACE TREATMENT OF THE VACUUM PIPE
  - KICKER MAGNETS IN GAPS
  - VACUUM PORTS SCREENED TO REDUCE E-field
  - CLEARING ELECTRODES
  - HIGH VACUUM
  - SOLENOIDS - TO REDUCE MULTIPACTING

National® Brand 42-182 100 SHEETS Made in U.S.A.

SUMMARY OF ELECTRON, GAS, PRESSURE, & SCATTERING EFFECTS

1. COULOMB COLLISIONS WITHIN BEAM CAN TRANSFER ENERGY FROM ⊥ TO ∥ AND PROVIDE LOWER LIMIT ON $T_{\parallel}$, HIGHER THAN FROM ACCELERATIVE COOLING.

2. COULOMB INTERACTIONS WITH RESIDUAL GAS NUCLEI PROVIDE A SOURCE OF EMITTANCE GROWTH (BUT NOT IMPORTANT FOR HIGHER MASS AND LINAC RESIDENCE TIMES).

3. PRESSURE INSTABILITY FROM DESORPTION OF RESIDUAL GAS BY STRIKED BEAM IONS HITTING WALL OR BEAM-IONIZED RESIDUAL GAS ATOMS, FORCED TO WALL BY E-field of BEAM. LIMITS CURRENT IN RINGS OR HIGH REP RATE LINAC.

4. ELECTRONS CAN CASCADE AND REACH A "QUASI" EQUILIBRIUM POPULATION OF SIMILAR LINE CHARGE TO THE ION BEAM. ELECTRON-ION TWO STREAM INSTABILITY IS UNSTABLE, AND CAN LEAD TO TRANSVERSE INSTABILITY, SIMILAR TO WHAT IS OBSERVED IN SOME PROTON RINGS.

National® Brand 42-182 100 SHEETS Made in U.S.A.

John Barnard
Steven Lund
USPAS
June 2006

An application of intense beams

1. Heavy-ion fusion
   A. Requirements
   B. Targets for ICF
   C. Accelerator
   D. Drift compression
   E. Final focus
   F. Experiments

Inertial Fusion Energy (IFE) power plants of the future will consist of four parts

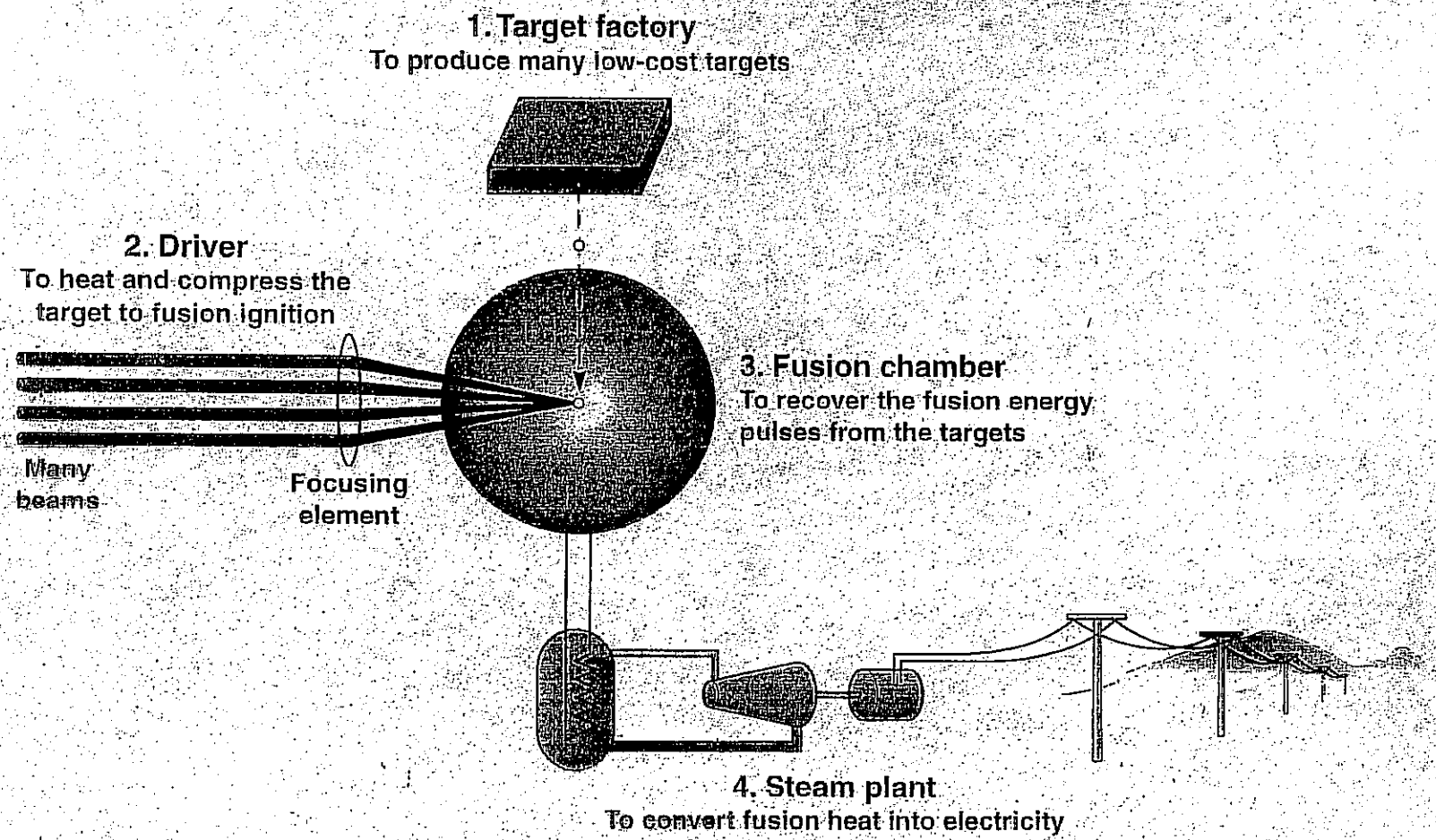

A power-plant driver would fire about five targets per second to produce as much electricity as today's 1000-megawatt power plant

05-00-0896-0609
2RWM/mcm

3/26/96

2

Heavy Ion Fusion provides an attractive approach to long term energy production

Fusion offers an inexaustible, long term solution to the problem of future energy supplies free from long-lived radioactive by-products and greenhouse CO_2.

Inertial Confinement Fusion (ICF) uses laser or particle beams to implode a target, raising the temperature and density of the fuel, creating the conditions necessary for the following reaction:

$$D + T \rightarrow n\ (14.06\ MeV) + He^4\ (3.52\ MeV)\ .$$

Heavy ion accelerators are a strong candidate for inertial fusion *energy production* (IFE) because of:

- High efficiency
- High repetition rate
- Survivability of final lens
- Favorable target illumination geometry

Focusability at the target is key scientific issue

Conditions of beam at target are set by hohlraum and implosion physics

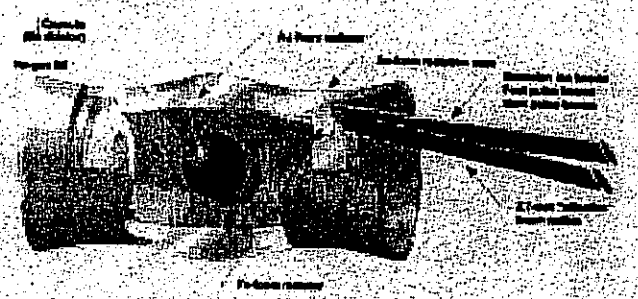

Energy in pulse: ~ 3 to 6 MJ

Duration of main pulse: ~ 8 to 10 ns

Duration of foot pulse: ~ 30 ns

Spot radius: ~ 1.5 to 3 mm

Transverse and longitudinal compression are required to meet target specifications.

Length of beam just outside of injector ~25-50 m

At target ~ 0.5 - 1 m

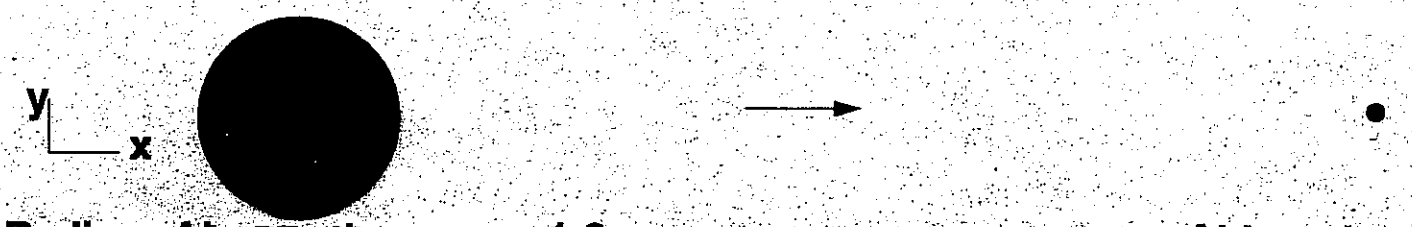

Radius of beam at source ~ 1-3 cm

At target ~ 1.5-3 mm

Compression factors of 10 to 50 in both longitudinal and transverse directions are required.

A "DISTRIBUTED RADIATOR" TARGET PRODUCES HIGH GAIN IN RADIATION–HYDRODYNAMIC SIMULATIONS

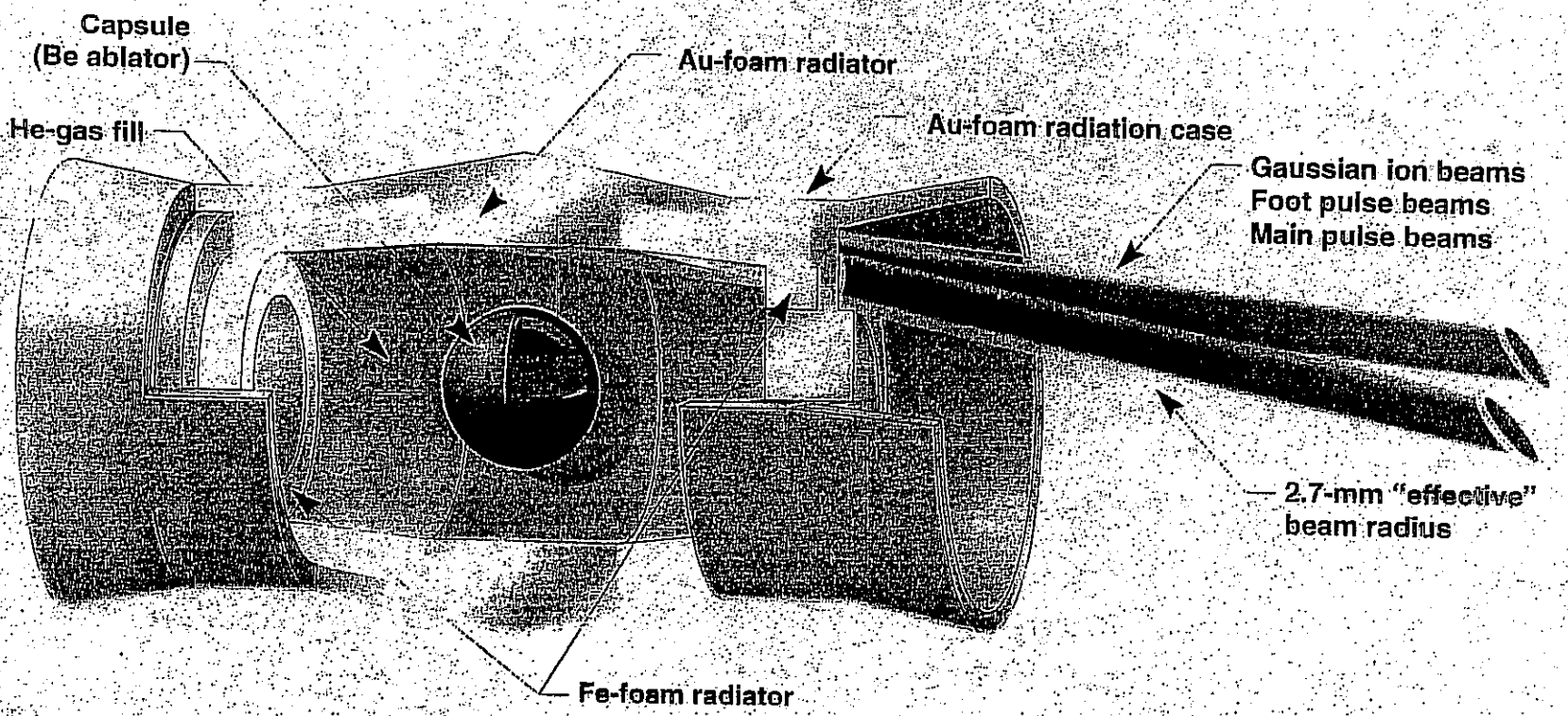

05-00-0998-1862A
sjOLrld

9/10/98

The two principal approaches to ICF are direct drive and indirect drive

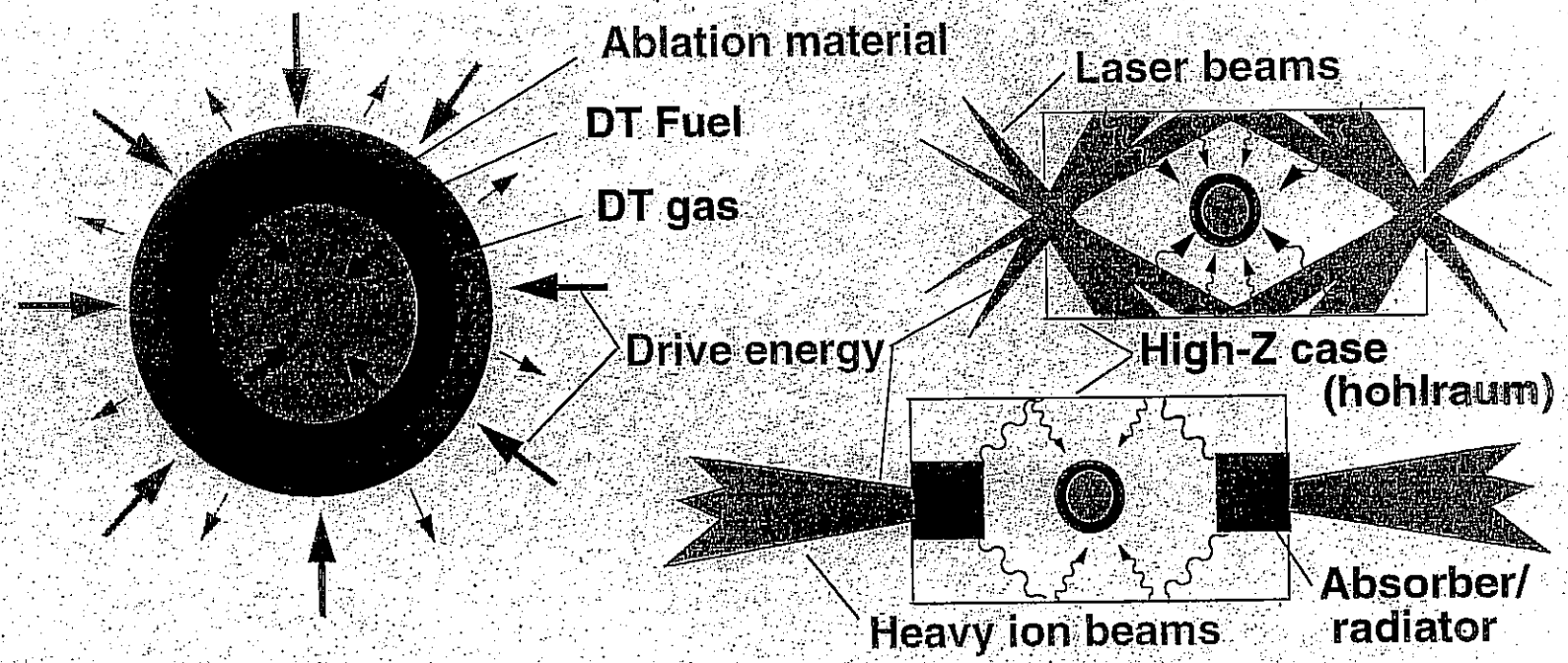

Direct drive:

Advantage:

- Higher coupling efficiency (with potential for higher gain)

Indirect drive:

Advantages:

- Relaxed beam uniformity (reduced hydro instability)
- Significant commonality for lasers and ion beams
- Significant simplification of chamber geometry

National Ignition Facility has 192 beams of 40-cm aperture arranged in four beam clusters

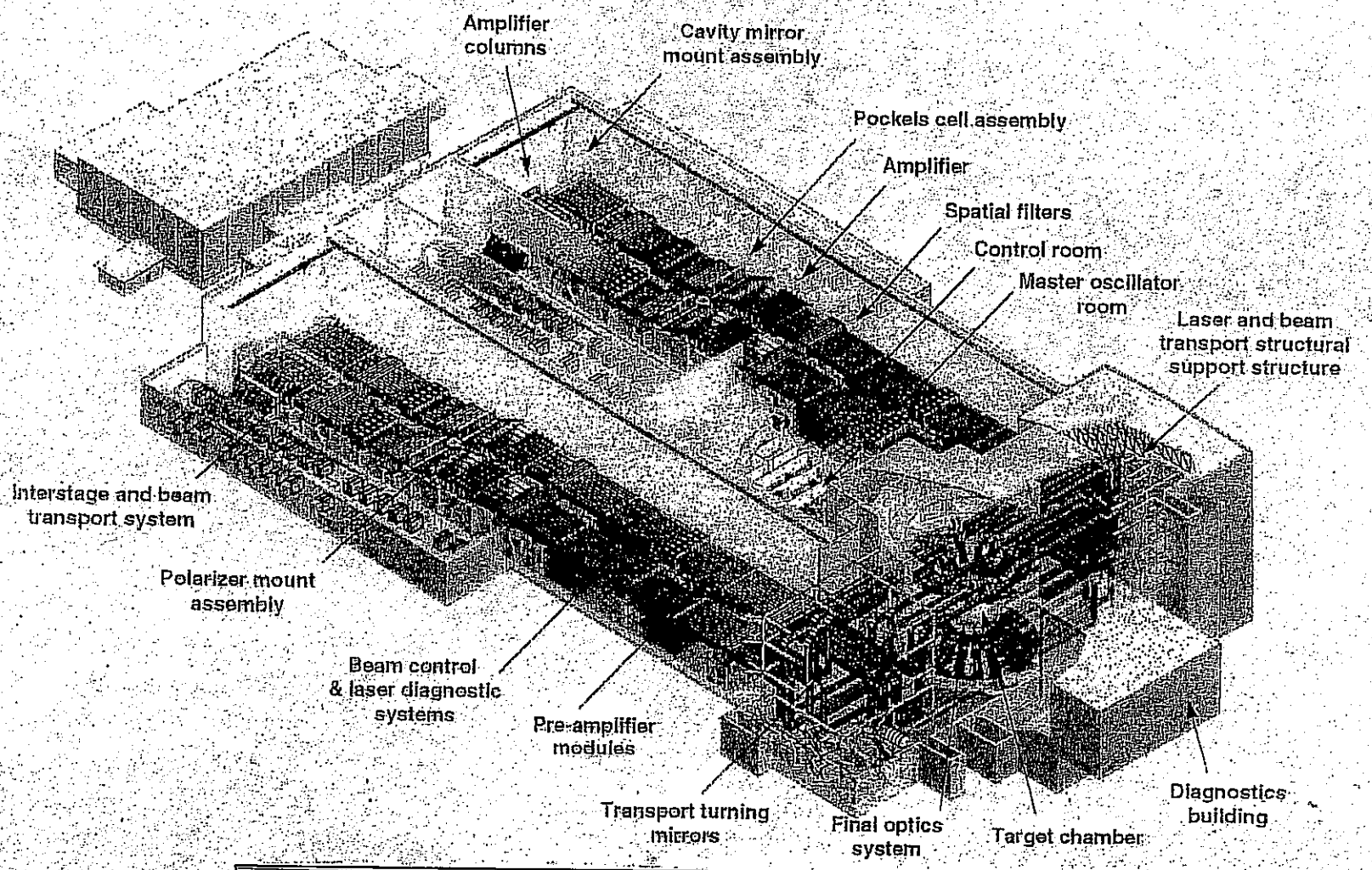

NIF illustrates many of the features of IFE development and will play a critical role in addressing IFE feasibility

40-00-0996-2100YA
03GAD/gbh

5/1/98
BMC/jco

7

Ion current profile and radiation temperature

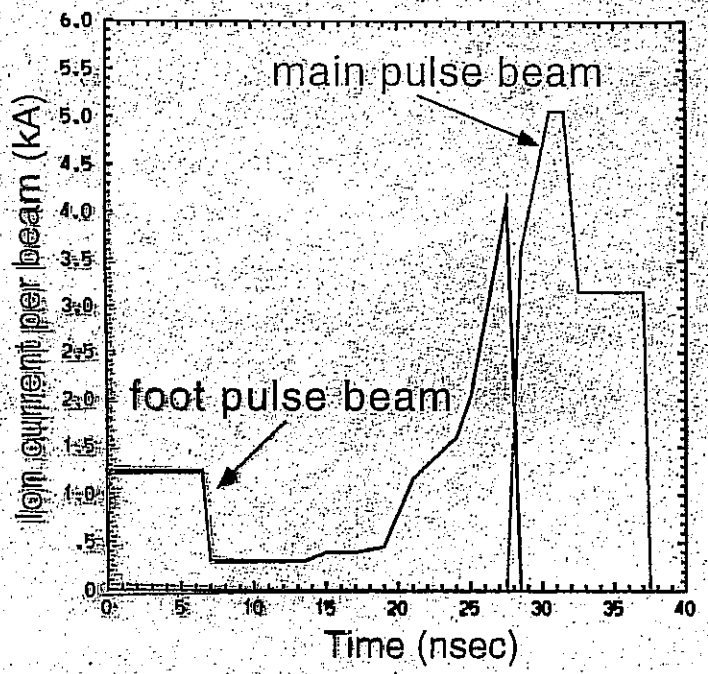

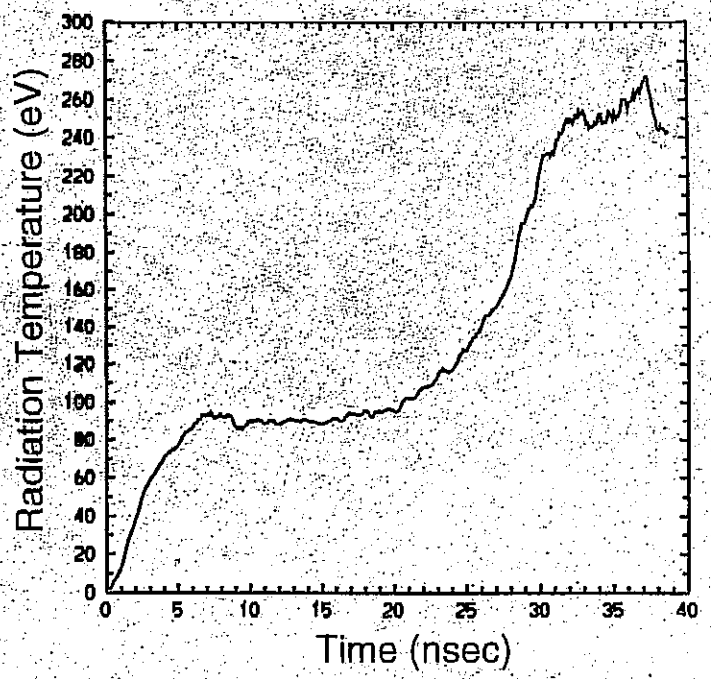

Current assumes 16 beams in foot pulse
32 beams in main pulse

Callahan 11/97

Overlapping Gaussian, elliptical beams are focused at the end of the target

Each beam is an ellipse

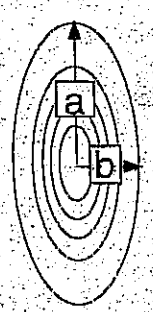

8 beams overlap in the foot pulse

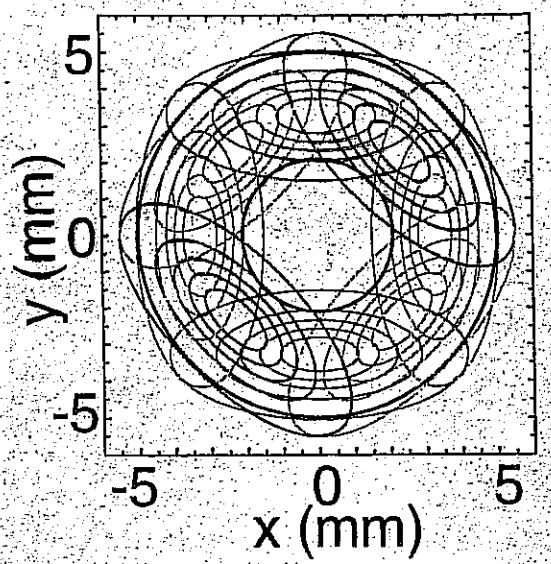

Sum of 8 foot pulse beams

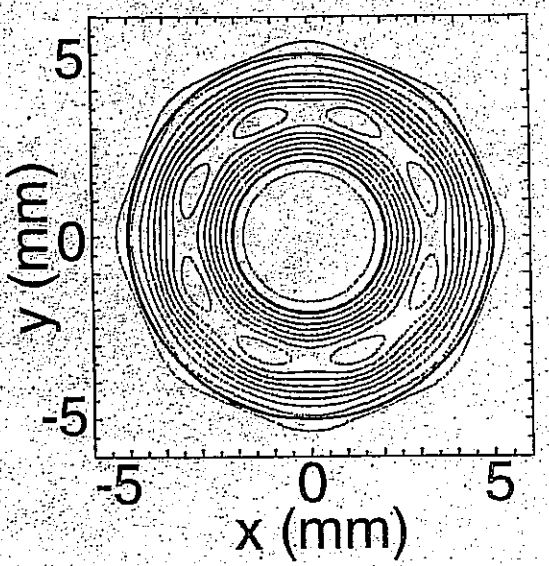

a = 4.15 mm
b = 1.8 mm
effective r=2.7 mm
95% of charge inside

Azimuthal asymmetry:
foot pulse: -1.6% in m=8
main pulse: 0.06% in m=16

Callahan 8/97

Why Heavy Ions?

Target requires:

3.5 - 6 MJ in ~ 10 ns ⇒ ~ 500 TW = I · V

Range ~ 0.02 - .2 g/cm²

qV = kinetic energy

I = current

Range requirement → Higher mass ⇔ higher kinetic energy

Power Requirement → Current ∝ $\frac{1}{\text{kinetic energy}}$

Higher mass requires lower current (easier to focus).

5

Heavier Ions ⇒ Higher Kinetic Energy

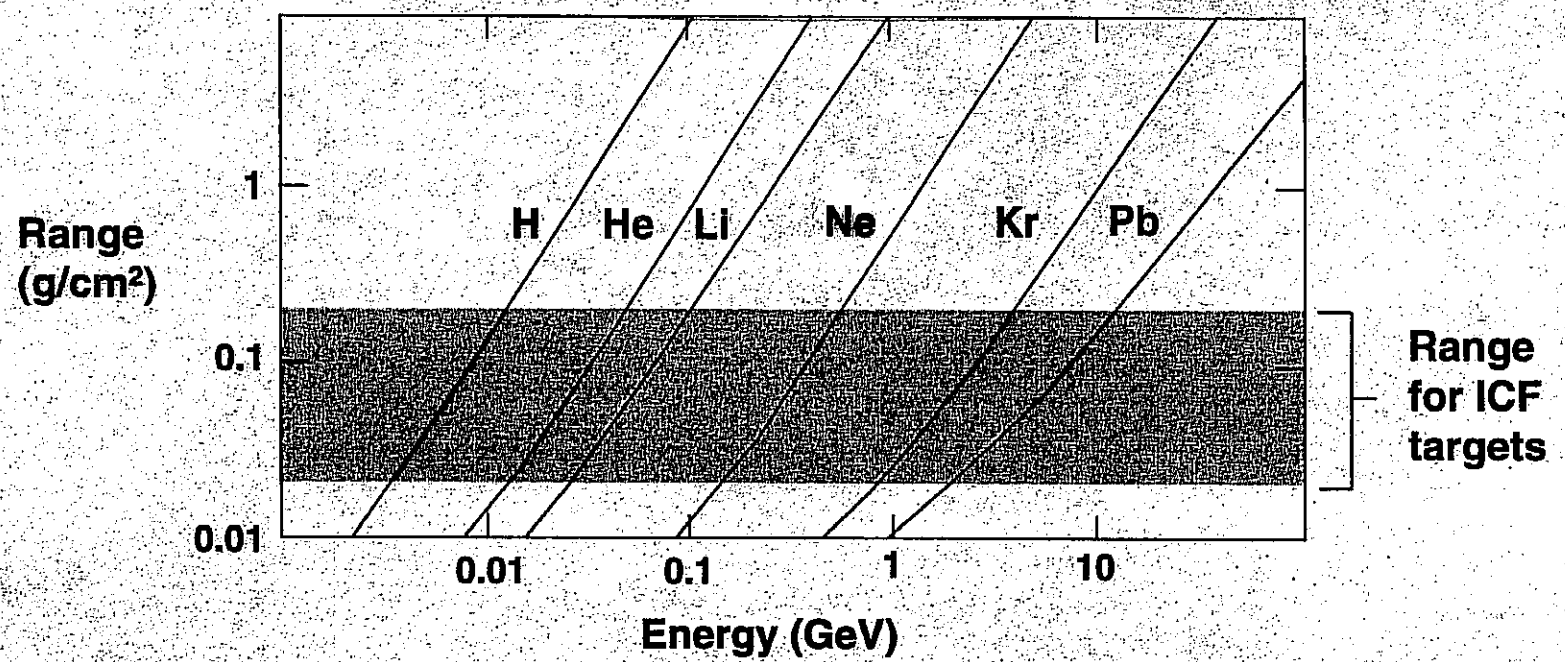

Targets require high power (kinetic energy x current).

- Light Ion Fusion requires high-current, unconventional accelerators (Sandia 1970s).
- Heavy Ion Fusion requires lower currents enabling the use of more conventional high energy accelerators (Maschke ~ 1974).

There are two principle methods of acceleration

1. r.f. acceleration
(Approach in Europe and Japan)

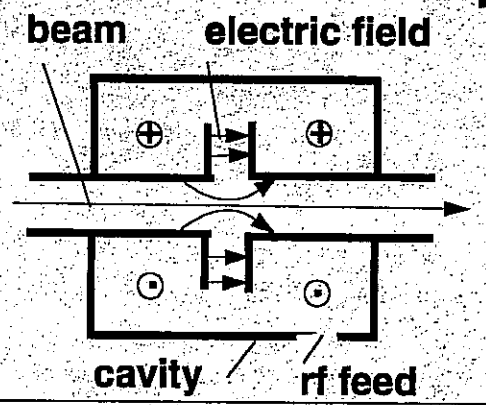

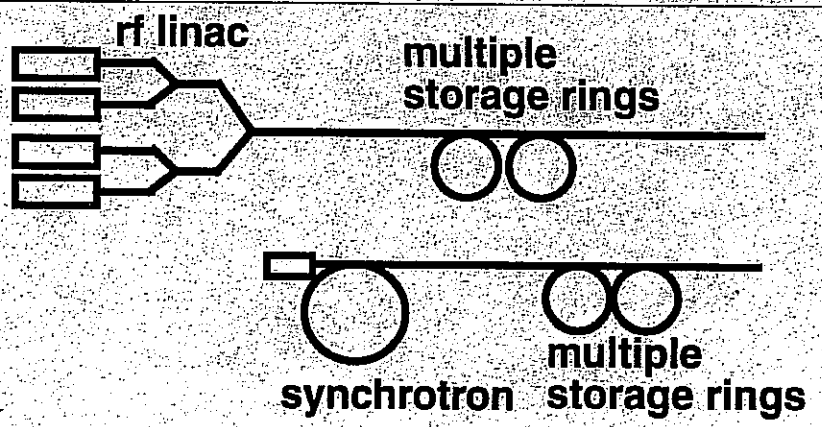

2. Induction acceleration
(U.S. approach)

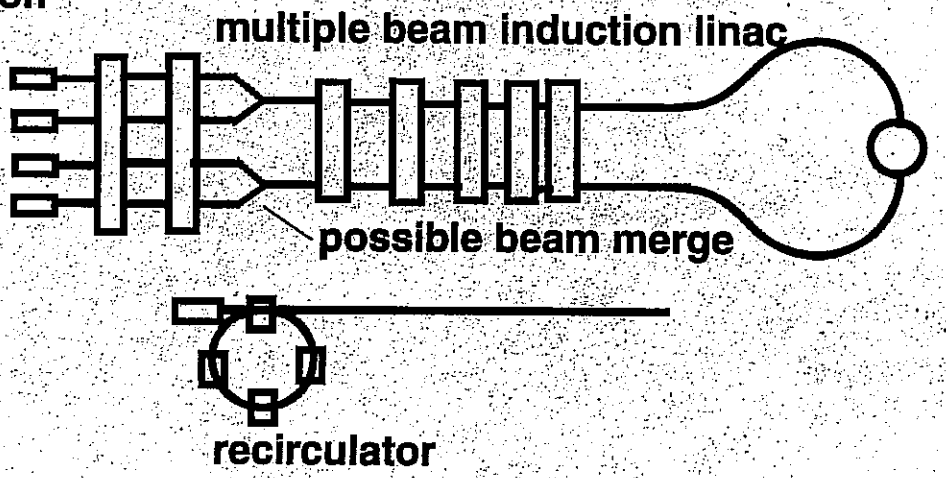

Induction acceleration for HIF consists of several subsystems and a variety of beam manipulations

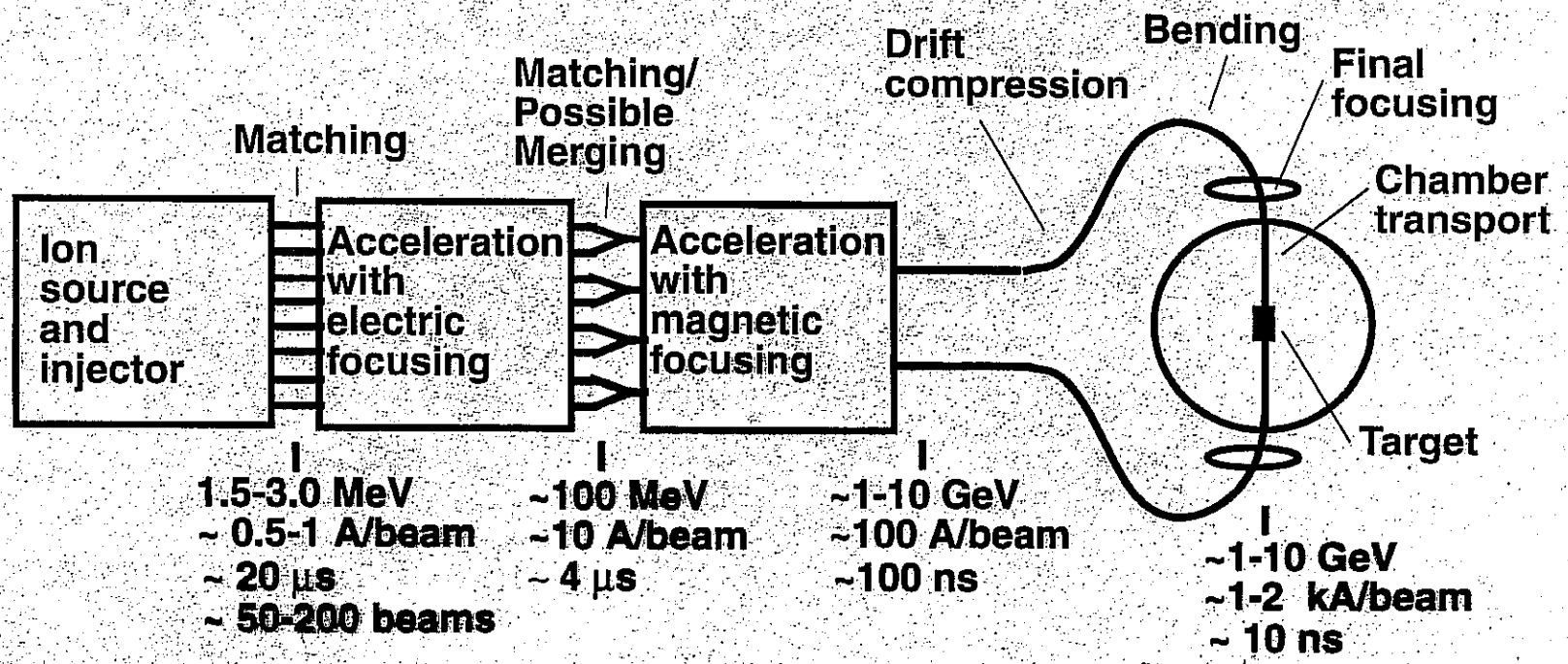

A Robust Point Design study established a baseline for a multiple-beam quadrupole induction linac HIF driver

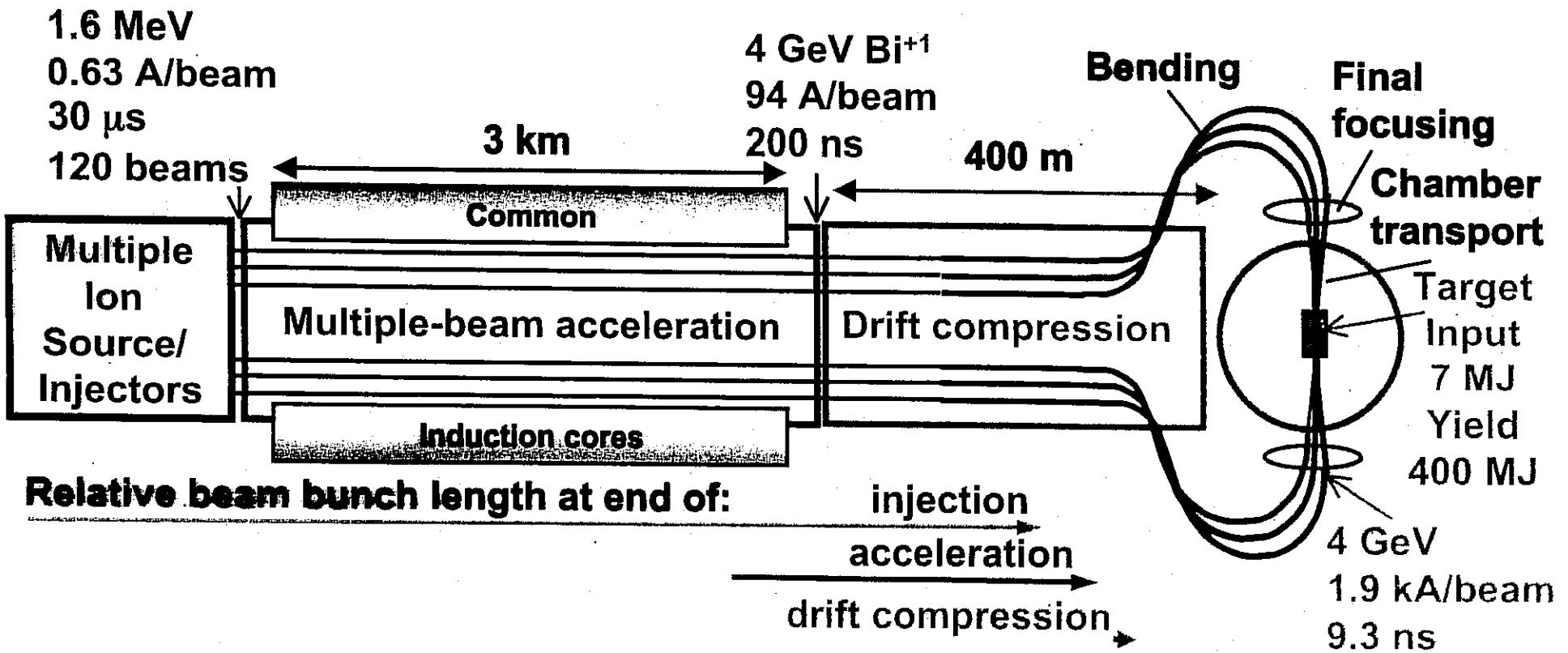

Major components of an induction linac

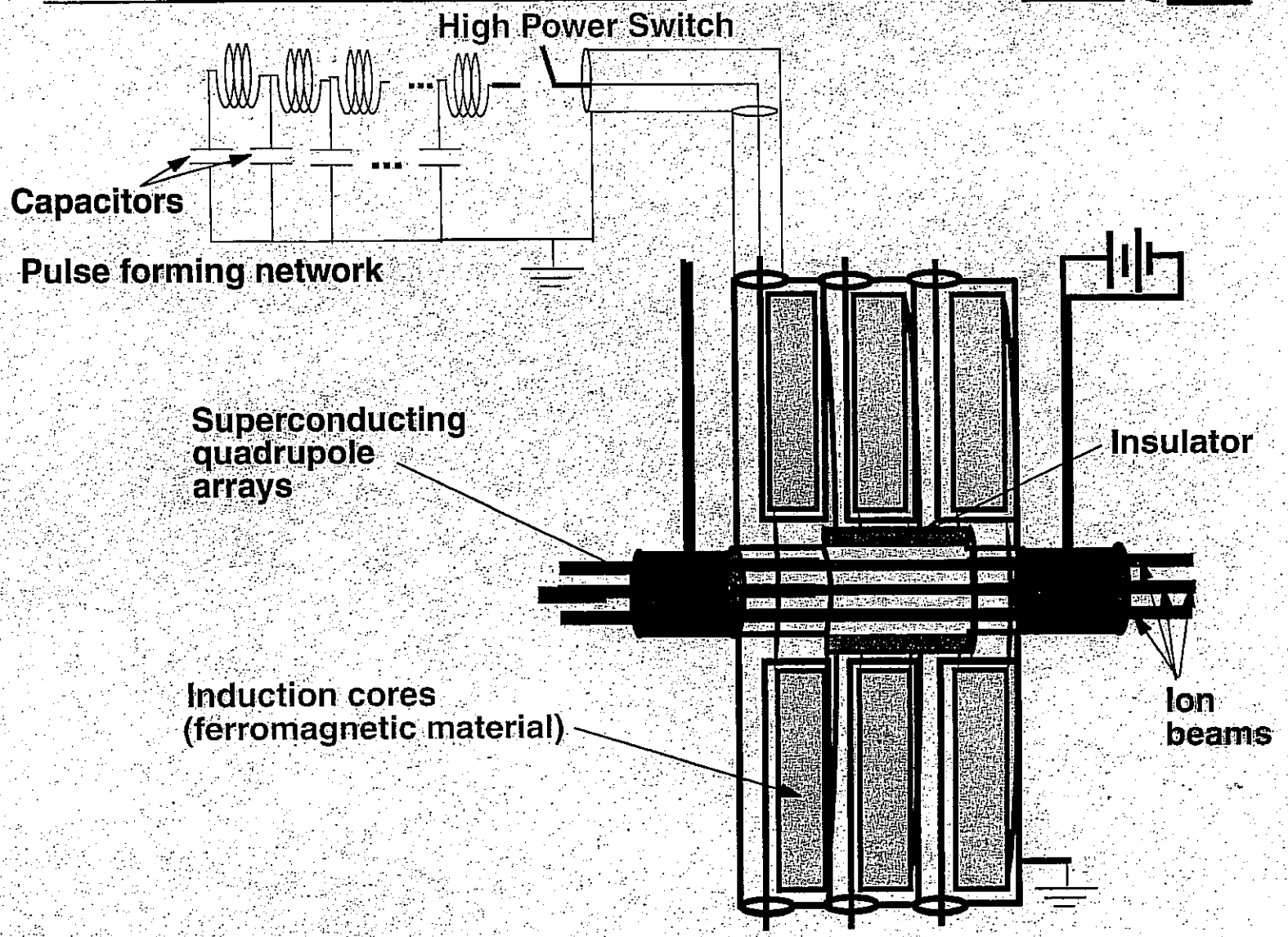

An Induction Core

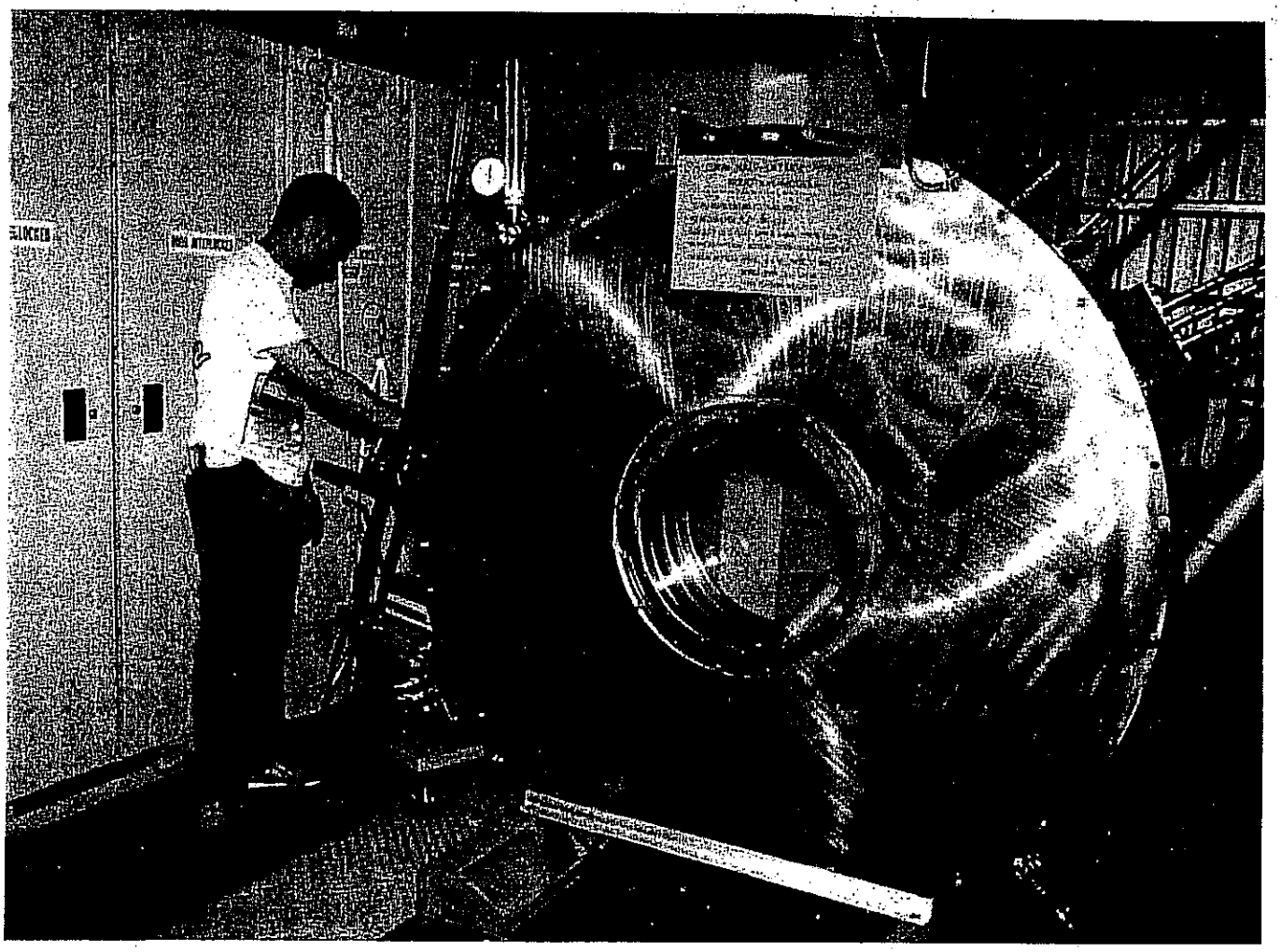

An array of small beamlets increases the total beam current through the core

From class:

$$\frac{Q}{a} = \left(\frac{Q_0^2}{4L^2}\right) a$$

$$Q_0 \cong \frac{4L^2}{C_0 \zeta} \frac{B'}{}$$

$$I \sim \beta^3 Q$$

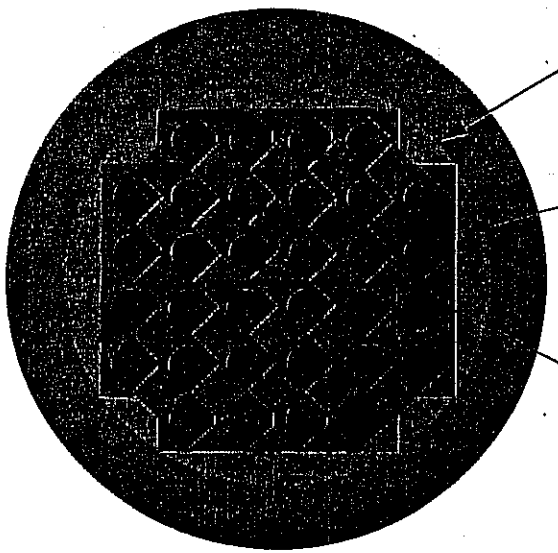

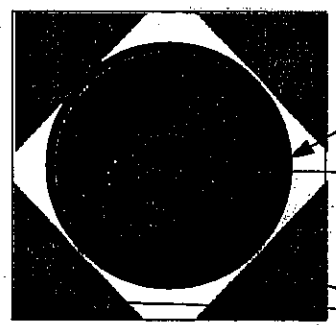

Current per beam = $I_b \sim a^2 B \beta^2/r_p$

$r_p \sim a$ (until misalignments require minimum size--better: $r_p = c_1 a + c_2$)

so $I_b \sim a$; N_b = number of beams in array $\sim R^2_{core} / a^2$

Total current through core = $I_{tot} = N_b I_b \sim R^2_{core} / a$ (until misalignments dominate scaling)

A Typical driver has about 2000 individual modules

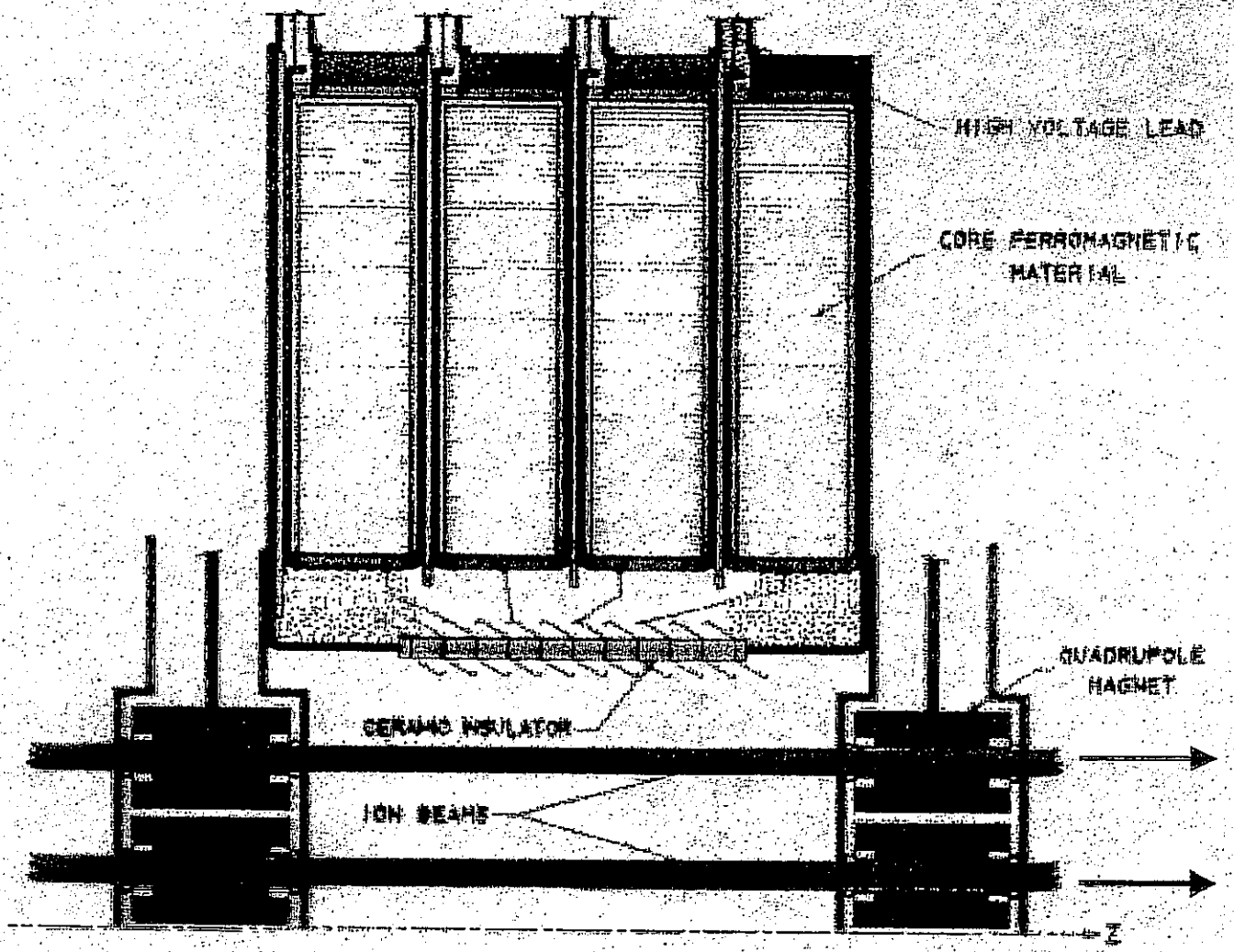

In an induction linac, certain limits constrain design

Phase advance per lattice period $\sigma_0 < \sim 85^o$ **(to avoid envelope/lattice instabilities** & emittance growth).

Space charge is limited by external focusing $K < (\sigma_0 a/2L)^2$ **where K is the perveance (proportional to line charge density over beam Voltage), a is the average beam radius and L is the half-lattice period.**

Velocity tilt $\Delta v/v < \sim$ 0.3 for electrostatic quads **(larger for magnetic quads) to avoid mismatches at head and tail of beam, and to ensure tail radius within pipe and head σ_0 within limit)**

Volt-seconds per meter $(dV/ds)\, l/v_0$ <~ 1.5-2.0 V-s/m **(for "reasonable" core sizes)**

Voltage gradient dV/ds < ~ 1-2 MV/m **(to avoid breakdown in gaps)**

Sources of non-linearity and mismatch are well defined

Sources of non-linearities

- External focusing magnets
- Space-charge
- Multiple-beam effects

Sources of mismatch

- Accelerator imperfections
  - Quad strength and placement errors
  - Acceleration waveform errors
  - Bend strength errors
- Velocity tilt

Simulations give reliable and definitive tolerances on each source

Several potential instabilities have been investigated in HIF drivers

Temperature anisotropy instability

After acceleration $T_{||} << T_{\perp}$, internal beam modes are unstable; saturation occurs when $T_{||} \sim T_{\perp}/3$

Longitudinal resistive instability

Module impedance interacts with beam, amplifying space-charge waves that are backward propagating in beam frame

Beam break-up (BBU) instability

High frequency waves in induction module cavities interact transversely with beam

Beam-plasma instability

Beam interacts with residual gas in target chamber

All of these instabilities have known analytic linear growth rates, which constrain the accelerator design (to ensure minimal growth or benign saturation).

M. de Hoon studied a final current pulse that is flat with parabolic ends using the HERMES code

15 ns final pulse duration

The initial tilt on the beam is about 4% (compare to ~30% at the beginning of the accelerator)

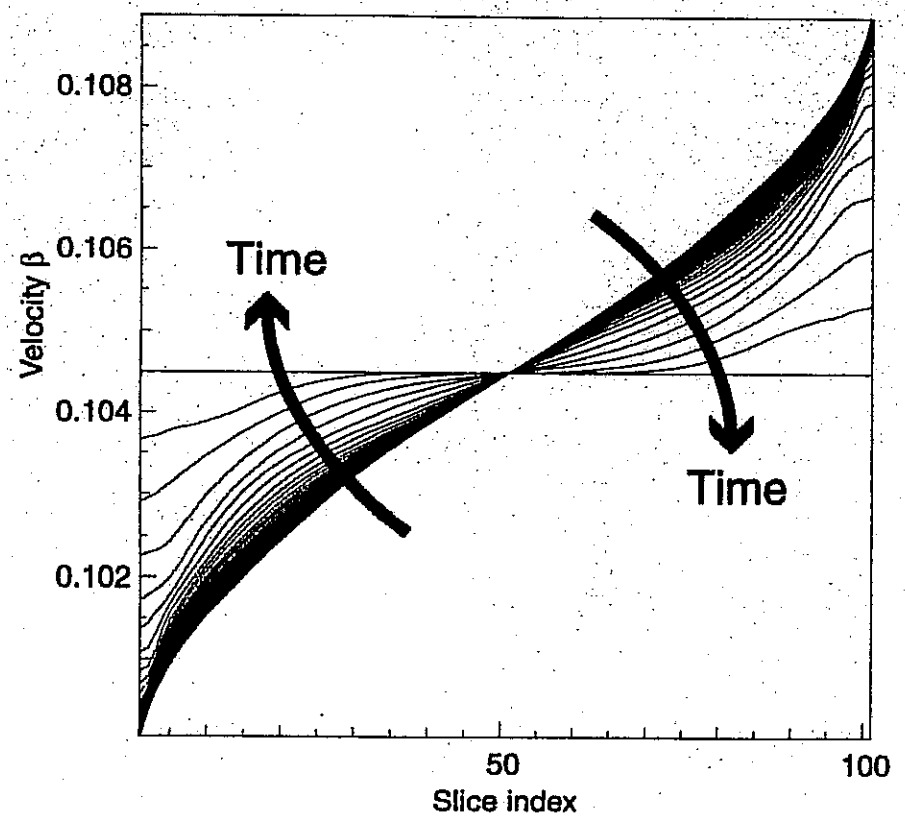

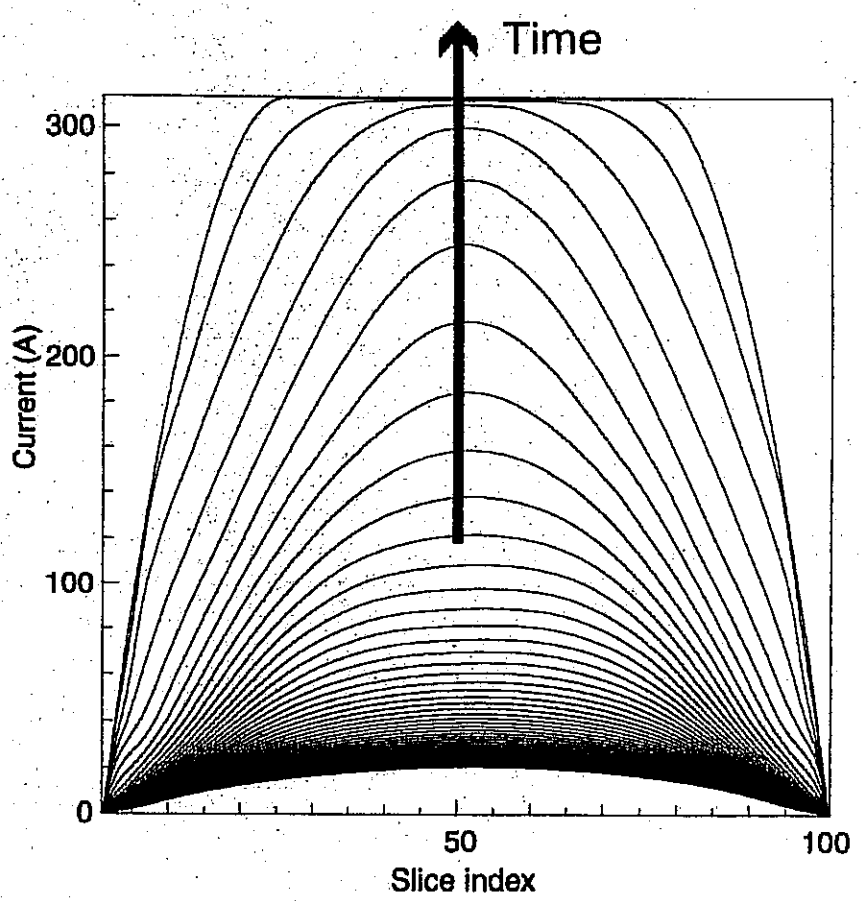

Although the final beam profile is flat, it is parabolic for most of the drift compression

Drift compression section is designed by running code first backwards from target, then forwards after rematching

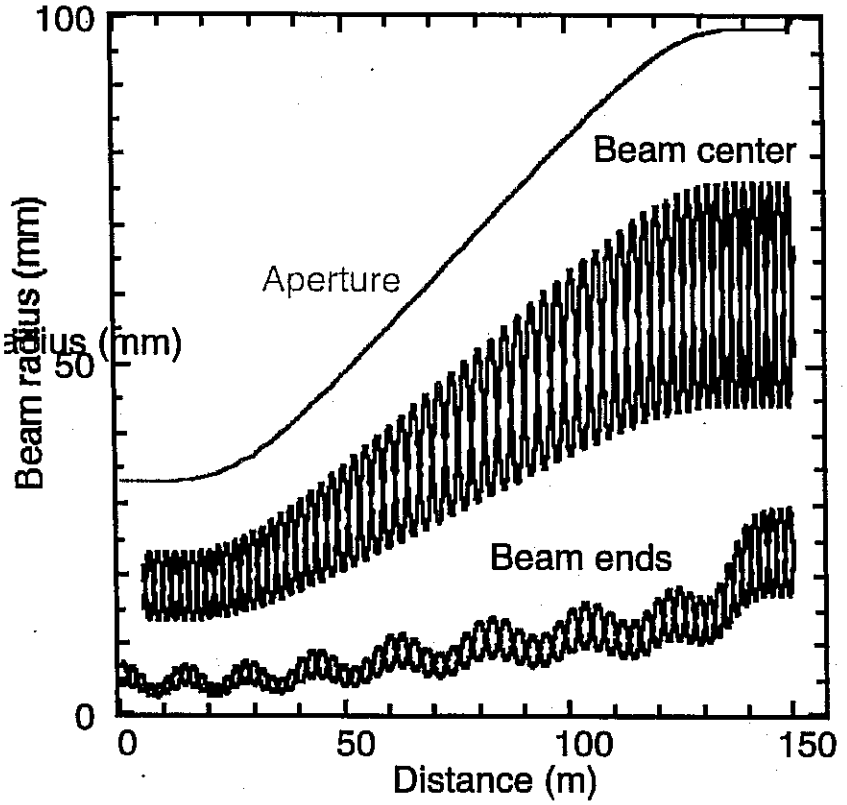

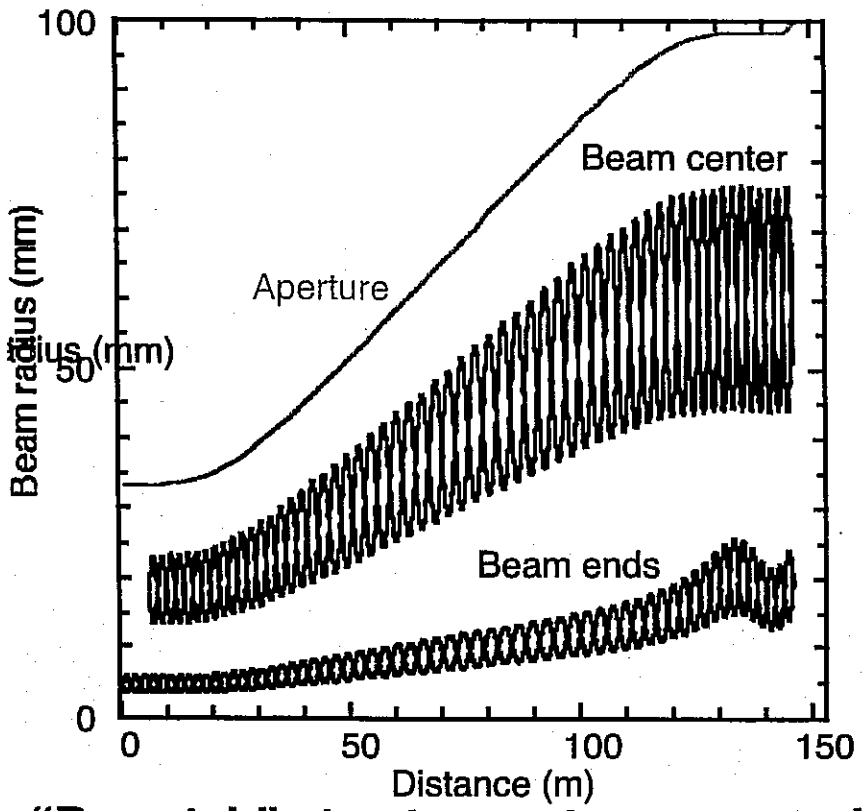

Begin with a desired 20ns, constant-energy pulse at end of compression, track backwards, design lattice for central slice; beam end becomes mismatched early on

"Rematch" at entrance to compression section, by adjusting a,a',b,b'; then track forward

A solenoid focus option leads to a low V, high current modular driver with advantageous development path

Pulse energy ~ 6.7 MJ

V~ 200-300 MV: T~ 2.5 GeV Xe^{+8} ions or T ~ 200 MeV for Ne^{+1}

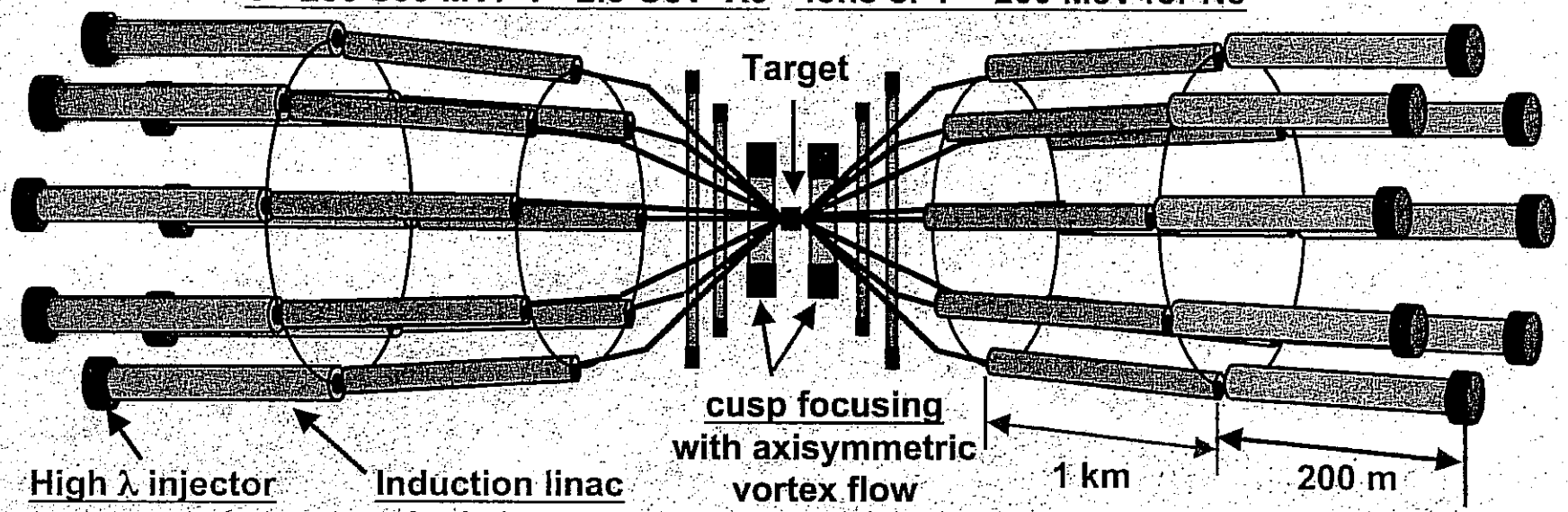

High λ injector

Merging beamlet source/injector

or

accel/decel injector

Induction linac

single beams

r_p ~ 15 cm

B_s ~ 9T

I ~ 6.7 kA

T ~ 2.5 GeV

Δt ~ 100 ns

double pulsed for foot and main pulses

cusp focusing

with axisymmetric vortex flow

or

adiabatic plasma lense assisted pinch with cross-jet flow. liquid walls

Neutralized drift compression

Δv/v ~ 0.01

(no space charge stagnation)

Summary of Current Limits From Different Focusing Methods

Einzel Lens

$$Q_{max} \cong \frac{3\pi^2}{\gamma}\left(\frac{q\phi_0}{m v_0^2}\right)^2\left(\frac{r_b}{L}\right)^2$$

Solenoids

$$Q_{max} = \left(\frac{\omega_c r_b}{2\gamma\beta c}\right)^2$$

Quadrupole Focusing

$$Q_{max} \cong \frac{\eta\phi_0}{2\pi}\left(\frac{\sin\frac{\eta\pi}{2}}{\frac{\eta\pi}{2}}\right)\left[\frac{B r_b}{[B\rho]}\left[\frac{r_b}{r_p}\right] \quad \frac{2qV_q}{\gamma m v_z^2}\left[\frac{r_b^2}{r_p^2}\right]\right]$$

MAGNETIC

Electric

For Non-Relativistic Beams

$$\lambda_{max} \propto \frac{Q_0^2}{V} \qquad \lambda_{max} \propto \frac{q}{m} B^2 r_p^2 \qquad \lambda_{max} \propto \begin{cases} B, V^{1/2} r_p \\ V_q \end{cases}$$

Note
Q_0 = Voltage between Einzel lenses
V_q = Voltage on a quad relative to ground
V = particle energy / q

The HYLIFE-II Ion beam-driven power plant is shown with a two-end target, illustrated from two sides and a linear heavy-ion induction driver

The liquid wall protection including beam ports is provided by pumping molten salt (Flibe) through the chamber

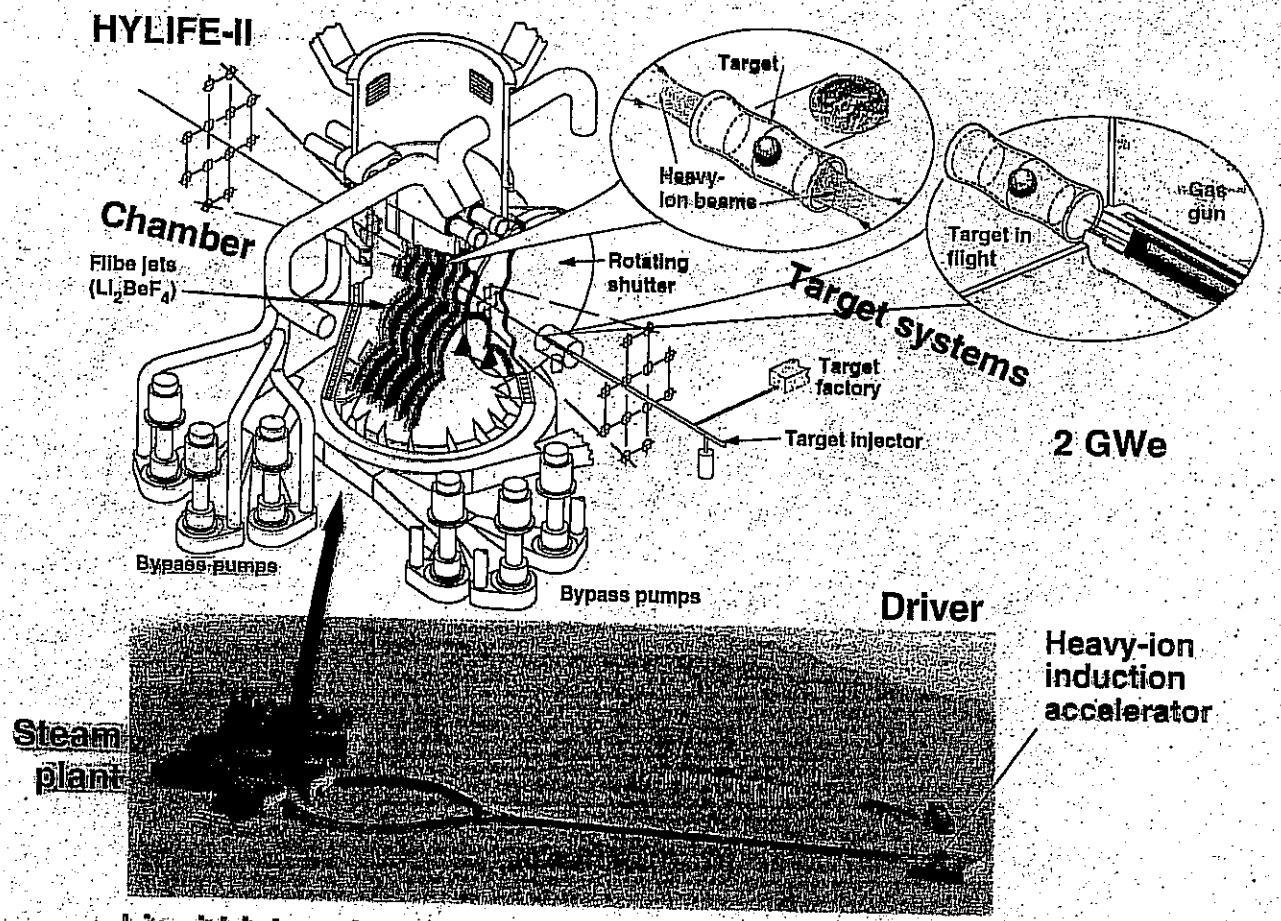

Liquid-jet protected fusion chambers for long lifetime, low cost, and low environmental impact

05-00-1194-3846U
16RWM/gbh

10/7/98

The First Wall Protected by Neutron-thick Molten Salt FLiBe,

FLiBe is a low Z salt ⇒ low activation ⇒ Green fusion energy

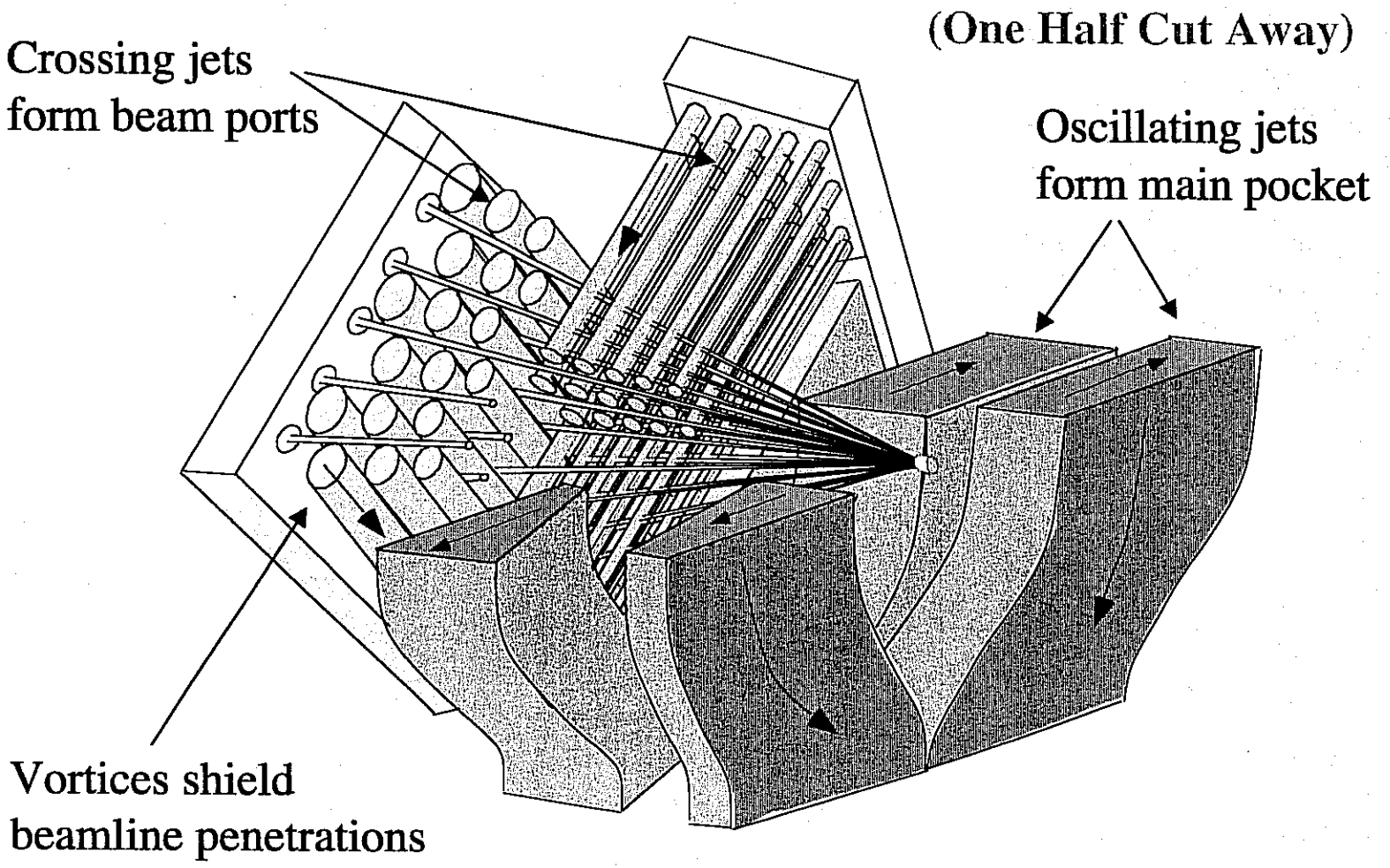

A number of final focus options are being considered for HIF applications

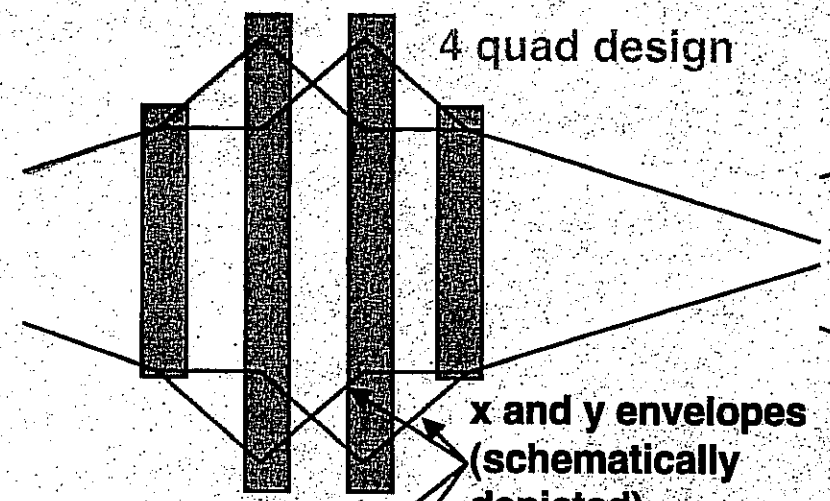

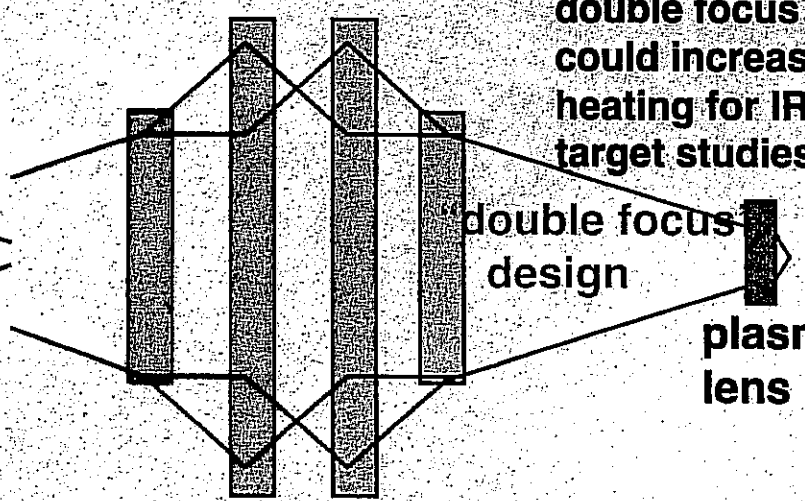

double focus design could increase spot heating for IRE target studies

x and y envelopes (schematically depicted)

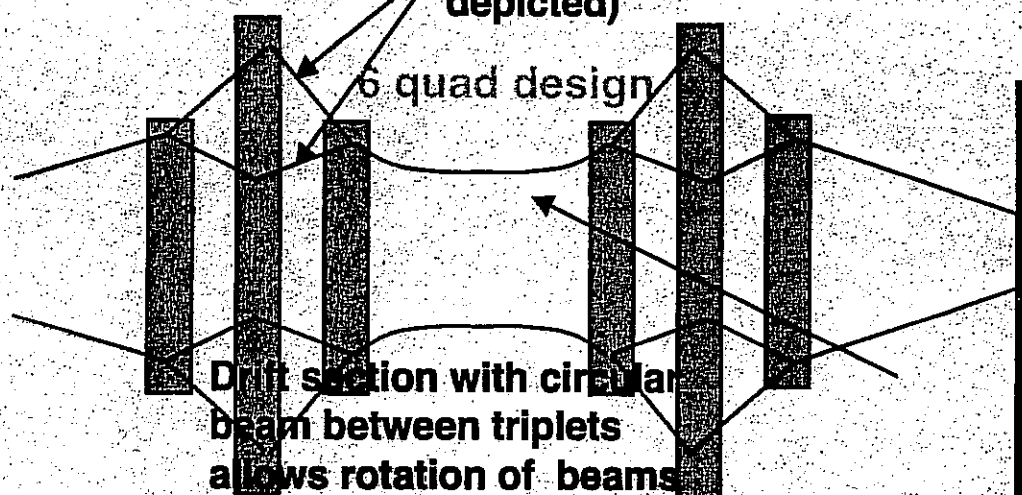

Drift section with circular beam between triplets allows rotation of beams or insertion of bend

Solenoid or cusp focusing is being considered for modular drivers:

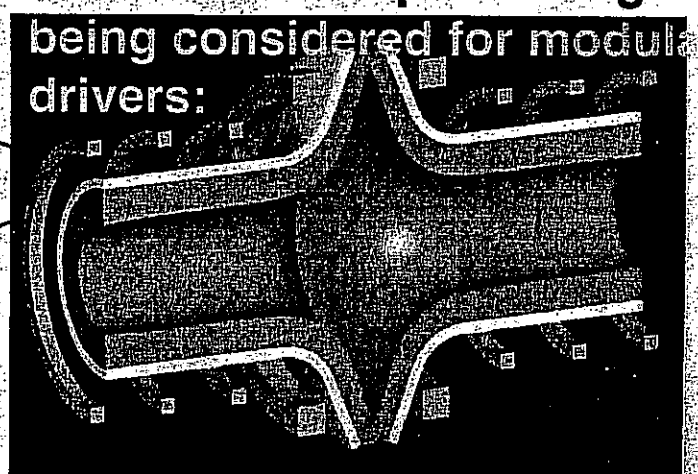

ESTIMATING SPOT SIZE

$$r_x'' + \frac{(\gamma_b \beta_b)'}{\gamma_b \beta_b} r_x + K_x r_x - \frac{2Q}{r_x + r_y} - \frac{\epsilon_x^2}{r_x^3} = 0$$

$$r_y'' + \frac{(\gamma_b \beta_b)'}{\gamma_b \beta_b} r_y + K_y r_y - \frac{2Q}{r_x + r_y} - \frac{\epsilon_y^2}{r_y^3} = 0$$

IN CHAMBER: NO EXTERNAL FOCUSING, NO ACCELERATION AND BEAM IS OFTEN CIRCULAR (BY DESIGN)

$$\Rightarrow K_x = K_y = (\gamma_b \beta_b)' = 0 \quad \& \quad r_x = r_y = r_b$$

$\Rightarrow$ ENVELOPE EQUATION IS:

$$r_b'' = \frac{Q}{r_b} + \frac{\epsilon^2}{r_b^3}$$

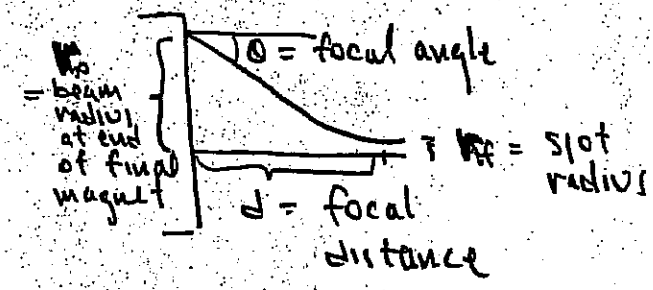

MULTIPLYING BY r_b' & INTEGRATING $\Rightarrow$

$$\frac{r_{bf}'^2}{2} - \frac{r_{bo}'^2}{2} = Q \ln \frac{r_{bf}}{r_{bo}} + \frac{\epsilon^2}{2 r_{bo}^2} - \frac{\epsilon^2}{2 r_{bf}^2}$$

Now $r_{bo}' \cong \theta$ $\quad r_{bf}$ = spot radius $\quad r_{bf} << r_{bo}$

$r_{bf}' = 0 \quad r_{bo} \cong d\theta$

$$\Rightarrow \boxed{\theta^2 \cong 2Q \ln\left(\frac{\theta d}{r_{bf}}\right) + \frac{\epsilon^2}{r_{bf}^2}}$$

FOR EMITTANCE DOMINATED SPOT: $r_{bf} = \frac{\epsilon}{\theta}$

"CHROMATIC ABERRATIONS" TEND TO BROADEN SPOT

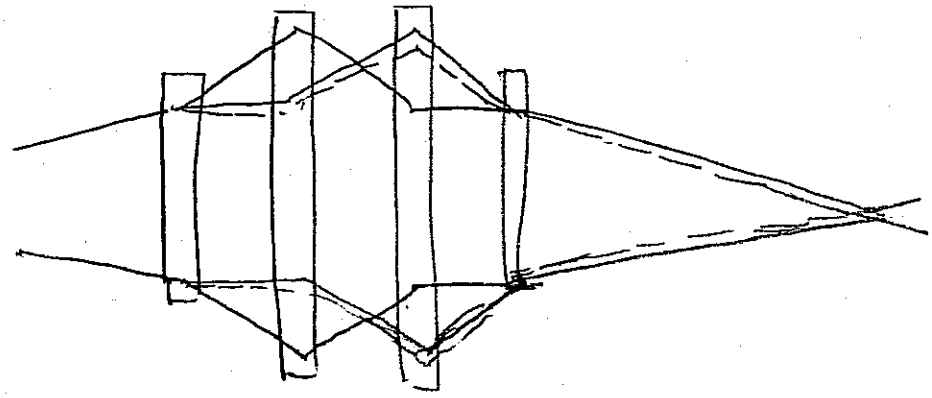

SINCE QUADRUPOLE MAGNET FOCUSING $\propto \frac{1}{V_z}$

(i.e. $x'' = \frac{qB'}{\gamma m v_z} x$) A SPREAD IN LONGITUDINAL VELOCITY GIVES RISE TO A BROADENING OF FINAL SPOT.

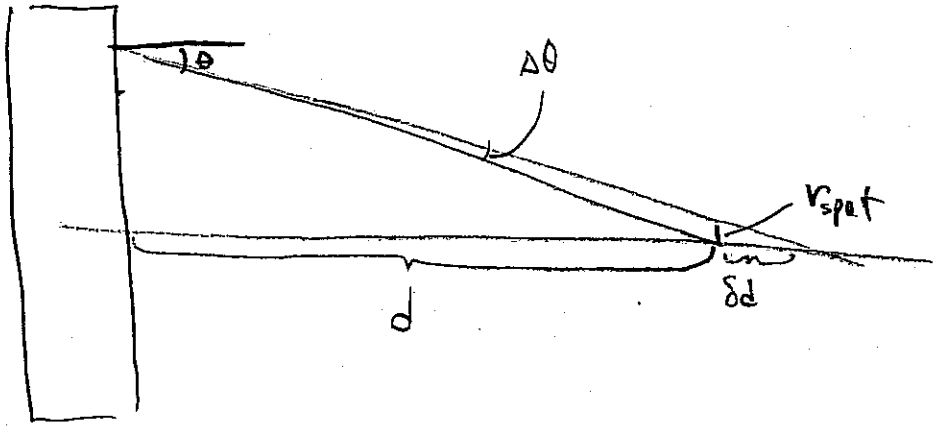

$$r_{spot} = \theta\,\delta d$$
$$= \theta \frac{dd}{d\theta} \frac{d\theta}{dp} \delta p$$
$$= \alpha\, \theta d \left(\frac{\delta p}{p}\right)$$

α = some constant depending on focal system

<u>HEURISTICALLY</u> THE CONTRIBUTION FROM CHROMATIC ABERRATIONS CAN BE WRITTEN

$$r_{chrom}^2 = \alpha^2 J^2 \left(\frac{\delta\gamma}{\gamma}\right)^2 \theta^2$$

where α depends on system, typically 4-8

$$r_{tot}^2 = r_{bf}^2 + r_{chrom}^2$$

DETAILED SIMULATIONS OR MOMENT CODE RESULTS REQUIRED TO FIX α.

We constructed moment models to study chromatic effects (through 2nd order) in final focus system

$$\frac{dp_x}{dt} = q(E_x + v_z B_y - v_y B_z)$$

Expand through 2nd order in x', y', $k_{\beta 0}x$, $k_{\beta 0}y$, $\delta p/p$

$$x'' + \left(\frac{1}{\gamma v_{z0}}\frac{d}{dz}(\gamma v_z)\right)x' = \frac{qB'}{\gamma m v_{z0}}x\left(1-\frac{\delta p}{p}\right) + \frac{q\lambda}{4\pi\varepsilon_0 m v_{z0}^2}\frac{(x-\bar{x})(1-\frac{2\delta p}{p})}{(\Delta x^2 + [\Delta x^2 \Delta y^2]^{1/2})}$$

The equation of motions can be written (where $\delta = \delta p/p$**) :**

$$\boxed{x'' = K_{xx}x + K_{xx1}x\delta \qquad y'' = K_{yy}y + K_{yy1}y\delta}$$

Here:

$$K_{xx} = \frac{B'}{[B\rho]_0} + \frac{Q}{2(\Delta x^2 + [\Delta x^2 \Delta y^2]^{1/2})} \qquad K_{yy} = \frac{-B'}{[B\rho]_0} + \frac{Q}{2(\Delta y^2 + [\Delta x^2 \Delta y^2]^{1/2})}$$

$$K_{xx1} = -\left[\frac{B'}{[B\rho]_0} + \frac{2Q}{2(\Delta x^2 + [\Delta x^2 \Delta y^2]^{1/2})}\right] \qquad K_{yy1} = -\left[\frac{-B'}{[B\rho]_0} + \frac{2Q}{2(\Delta y^2 + [\Delta x^2 \Delta y^2]^{1/2})}\right]$$

B' = **quadrupole gradient;** $[B\rho]$ = **Ion rigidity** $= p/q$; Q = **perveance** $= \frac{q\lambda}{2\pi\varepsilon_0 \gamma_0^3 m v_{z0}^2}$

We take averages of 2nd, 3rd,... order quantities, forming infinite set of 1st order ode's

$$\frac{d}{ds}\langle x^2\rangle = 2\langle xx'\rangle$$

$$\frac{d}{ds}\langle xx'\rangle = \langle x'^2\rangle + \langle xx''\rangle$$

$$= \langle x'^2\rangle + K_{xx}\langle x^2\rangle + \underline{K_{xx1}\langle x^2\delta\rangle}$$

$$\frac{d}{ds}\langle x'^2\rangle = 2\langle x'x''\rangle$$

$$= 2K_{xx}\langle xx'\rangle + \underline{2K_{xx1}\langle xx'\delta\rangle}$$

$$\frac{d}{ds}\langle x^2\delta\rangle = 2\langle xx'\delta\rangle$$

$$\frac{d}{ds}\langle xx'\delta\rangle = \langle x'^2\delta\rangle + \langle xx''\delta\rangle$$

$$= \langle x'^2\delta\rangle + K_{xx}\langle x^2\delta\rangle + \underline{K_{xx1}\langle x^2\delta^2\rangle}$$

$$\frac{d}{ds}\langle x'^2\delta\rangle = 2\langle x'x''\delta\rangle$$

$$= 2K_{xx}\langle xx'\delta\rangle + \underline{2K_{xx1}\langle xx'\delta^2\rangle}$$

...

$$\frac{d}{ds}\langle x^2\delta^n\rangle = 2\langle xx'\delta^n\rangle$$

$$\frac{d}{ds}\langle xx'\delta^n\rangle = \langle x'^2\delta^n\rangle + \langle xx''\delta^n\rangle$$

$$= \langle x'^2\delta^n\rangle + K_{xx}\langle x^2\delta^n\rangle + \underline{K_{xx1}\langle x^2\delta^{n+1}\rangle}$$

$$\frac{d}{ds}\langle x'^2\delta^n\rangle = 2\langle x'x''\delta^n\rangle$$

$$= 2K_{xx}\langle xx'\delta^n\rangle + \underline{2K_{xx1}\langle xx'\delta^{n+1}\rangle}$$

$\underline{\quad\quad}$ => term higher order by one

Infinite set of equations can be truncated, but are reliable over only finite distances

Two equivalent methods of truncation have been employed:

1. $\langle x^2\delta^2\rangle \sim \langle x^2\rangle\langle\delta^2\rangle$ and $\langle xx'\delta^2\rangle \sim \langle xx'\rangle\langle\delta^2\rangle$; or
2. Noticing that $\frac{1}{1+\delta} = 1-\delta+\delta^2+\ldots$ and $\frac{1}{1-\delta} = 1+\delta+\delta^2+\ldots$ thus,

$\frac{1}{1-\delta} - \frac{1}{1+\delta} = 2\delta + 2\delta^3 + \ldots$ also $\frac{\delta}{1+\delta} = 1 - \frac{1}{1+\delta}$

so that we may, to good approximation, write

$$\frac{d}{ds}\langle x^2\rangle = 2\langle xx'\rangle \qquad \frac{d}{ds}\langle xx'\rangle = \langle x'^2\rangle + K_{xx}\langle x^2\rangle + \frac{K_{xx1}}{2}\left[\left\langle\frac{x^2}{1-\delta}\right\rangle - \left\langle\frac{x^2}{1+\delta}\right\rangle\right] + O\left(x^2\delta^3\right)$$

$$\frac{d}{ds}\langle x'^2\rangle = 2K_{xx}\langle xx'\rangle + K_{xx1}\left[\left\langle\frac{xx'}{1-\delta}\right\rangle - \left\langle\frac{xx'}{1+\delta}\right\rangle\right] + O(xx'\delta^3)$$

$$\frac{d}{ds}\left\langle\frac{xx'}{1+\delta}\right\rangle = \left\langle\frac{x'^2}{1+\delta}\right\rangle + K_{xx}\left\langle\frac{x^2}{1+\delta}\right\rangle - K_{xx1}\left\langle\frac{x^2}{1+\delta}\right\rangle + K_{xx1}\langle x^2\rangle \qquad \frac{d}{ds}\left\langle\frac{x^2}{1+\delta}\right\rangle = 2\left\langle\frac{xx'}{1+\delta}\right\rangle$$

$$\frac{d}{ds}\left\langle\frac{x'^2}{1+\delta}\right\rangle = 2K_{xx}\left\langle\frac{xx'}{1+\delta}\right\rangle + 2K_{xx1}\langle xx'\rangle - 2K_{xx1}\left\langle\frac{xx'}{1+\delta}\right\rangle$$

Truncated set of equations forms closed set.

both methods give nearly identical results for $\langle\delta^2\rangle$ in the regime of interest; similar equations for $\langle x^2/(1-\delta)\rangle$, $\langle xx'/(1-\delta)\rangle$, $\langle x'^2/(1-\delta)\rangle$, and the same set for y; 18 equations total.

Comparison of moment equations with Particle-in-Cell (WARP[1]) simulations (1% velocity spread)

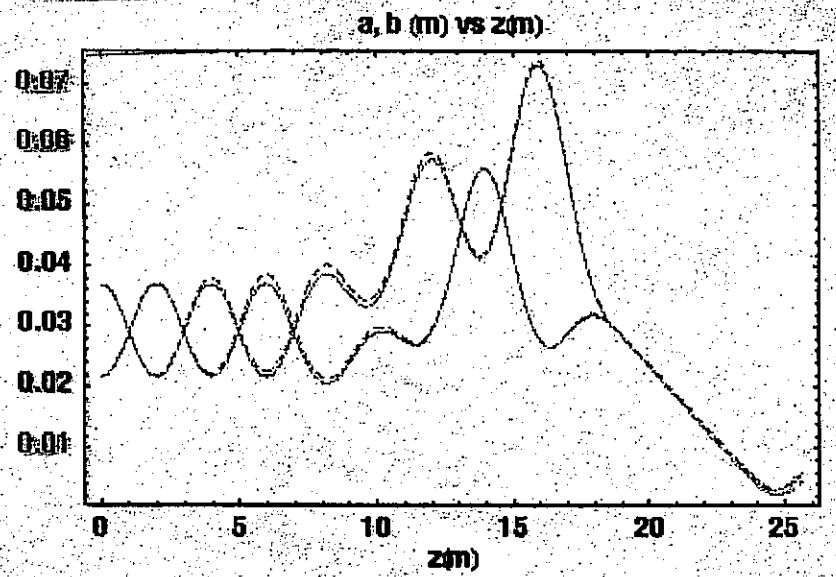

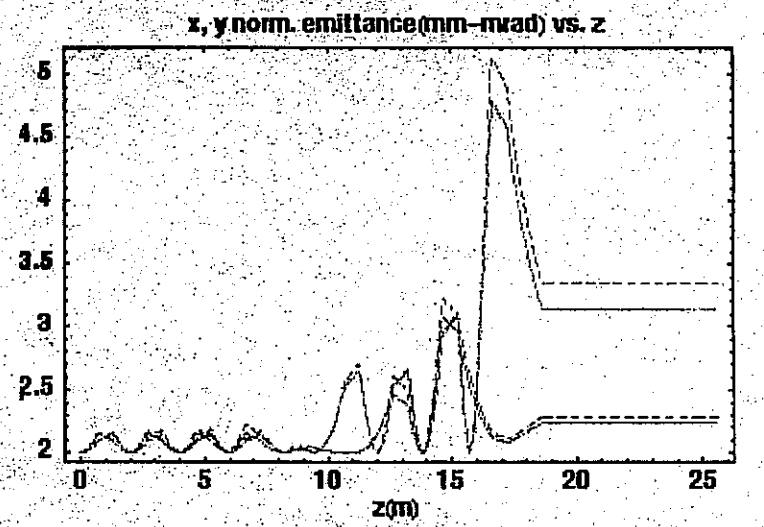

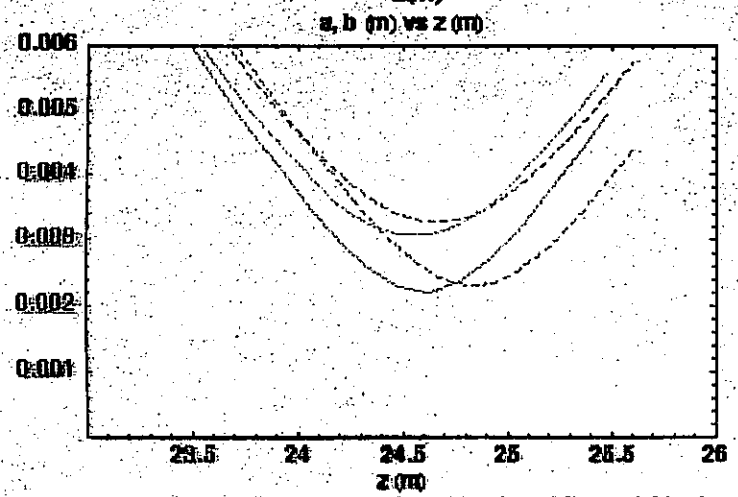

Particle simulations:
Dashed, red (x) and blue (y)
Initial distribution: KV

Moment calculations:
Solid, magenta (x), and aqua (y)

Comparison of moment equations with PIC simulations (WARP) -- no velocity spread

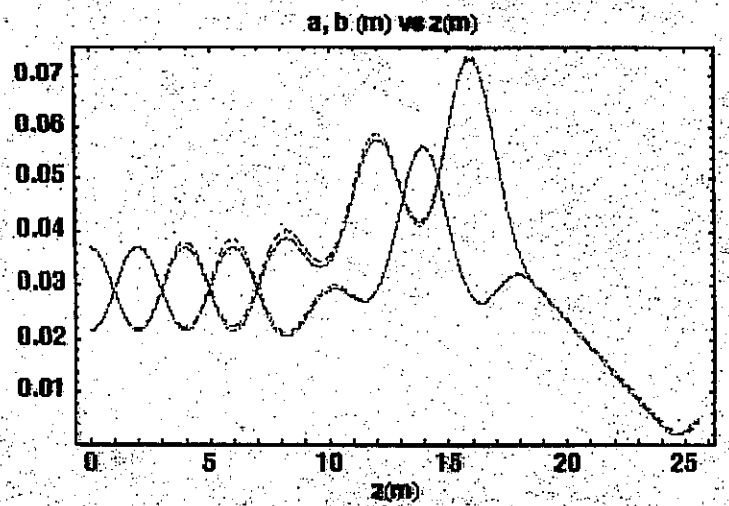

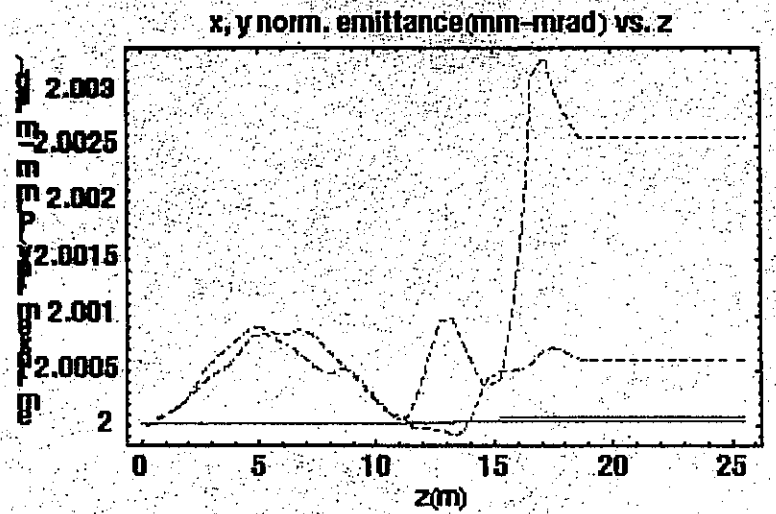

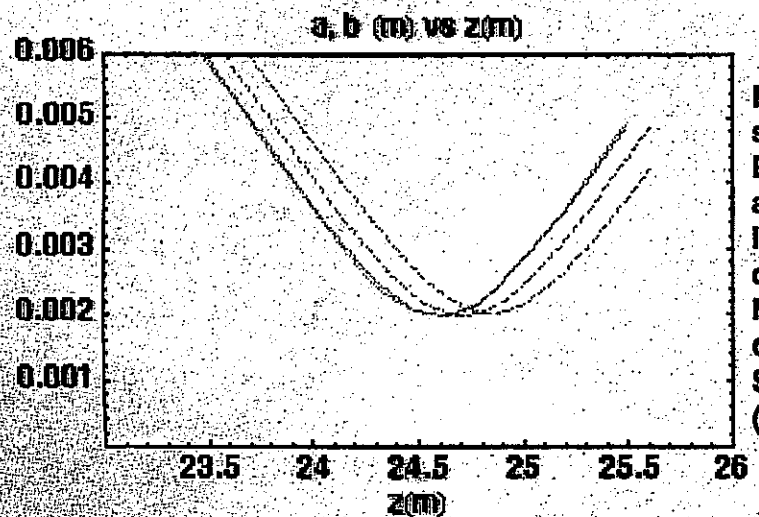

Particle simulations: Dashed, red (x) and blue (y)
Initial distribution: KV
Moment calculations: Solid, magenta (x), and aqua (y)

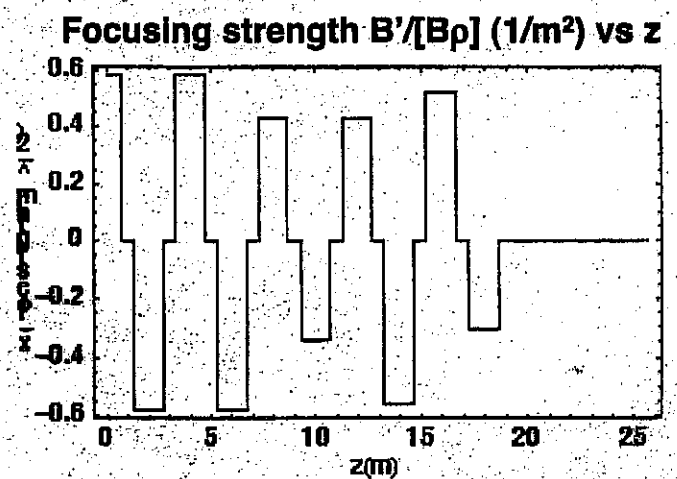

BEAM PHYSICS RESEARCH AT LLNL/LBNL/PPPL (THE HEAVY ION FUSION SCIENCE VIRTUAL NATIONAL LAB) FOCUSES ON TWO MAIN EXPERIMENTS:

1. "HIGH BEAM BRIGHTNESS" ON THE HIGH CURRENT EXPERIMENT (HCX)
   - ELECTRON CLOUD
   - MAXIMUM TRANSPORTABLE CURRENT

2. NEUTRALIZED DRIFT COMPRESSION AND FOCUSING EXPERIMENTS (NDCX-1)
   - NEUTRALIZED DRIFT COMPRESSION
   - NEUTRALIZED FINAL FOCUS
   - PULSE LINE ION ACCELERATOR

The High Current Experiment (HCX) is exploring beam transport limits

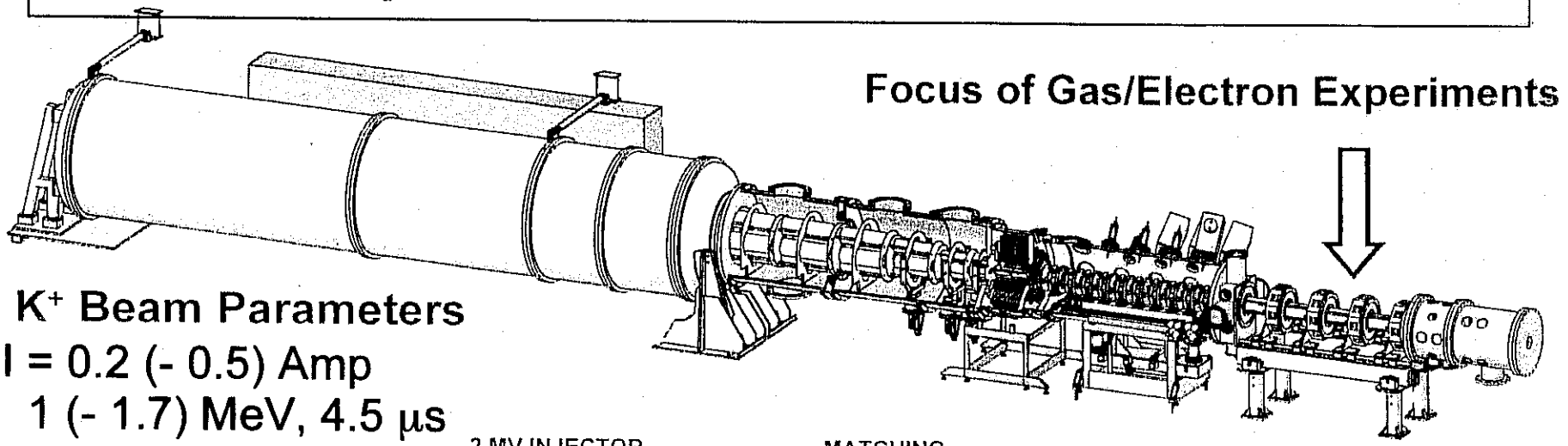

K^+ Beam Parameters
I = 0.2 (- 0.5) Amp
1 (- 1.7) MeV, 4.5 μs

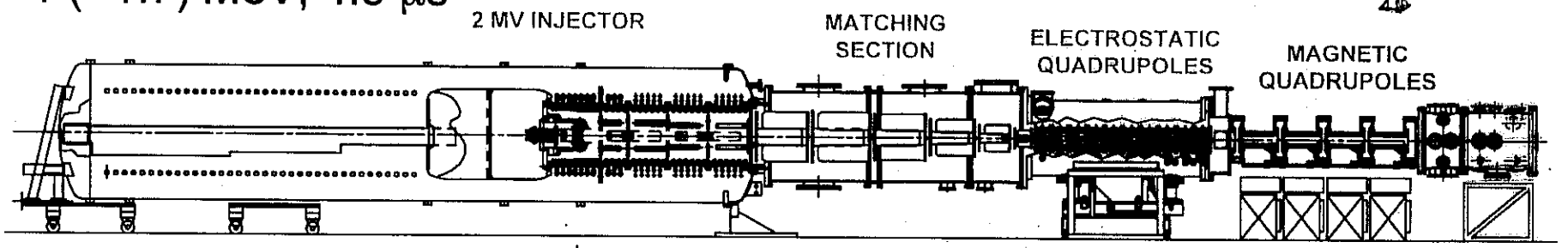

4 magnetic quadrupoles; many diagnostics

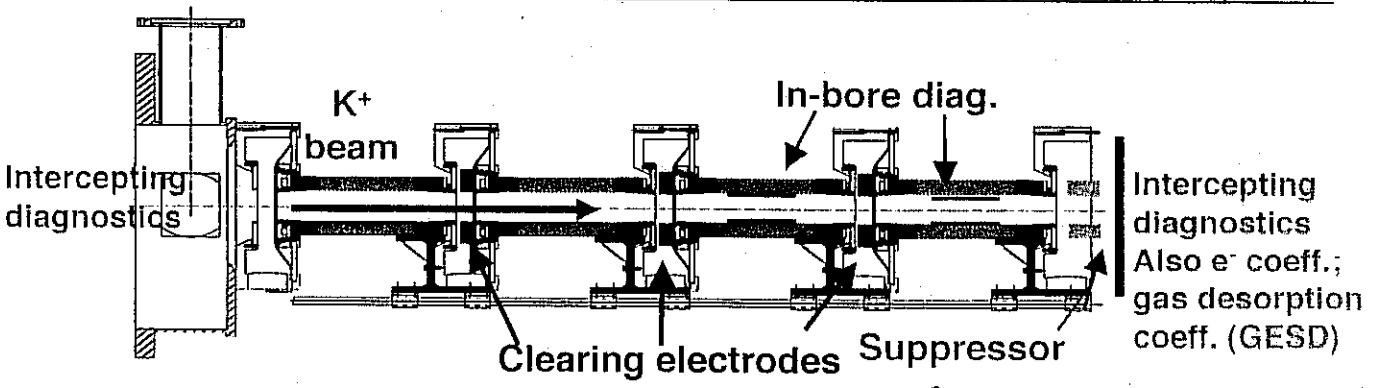

Neutralized Transport Experiment investigated physics of neutralized focusing

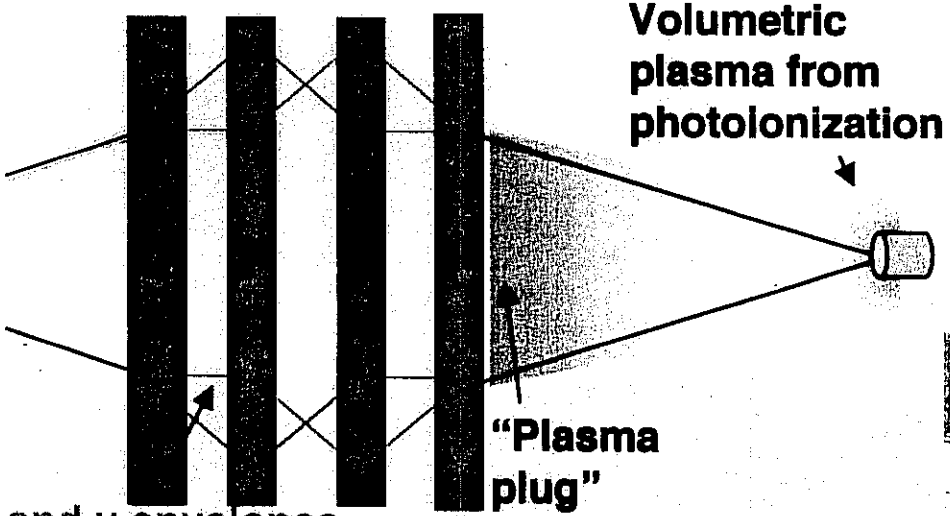

x and y envelopes (schematically depicted)

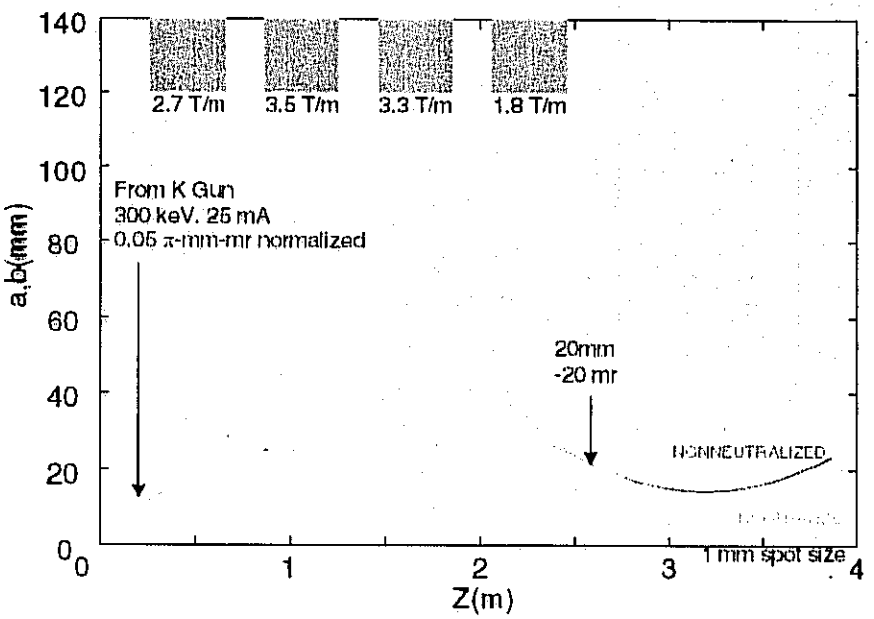

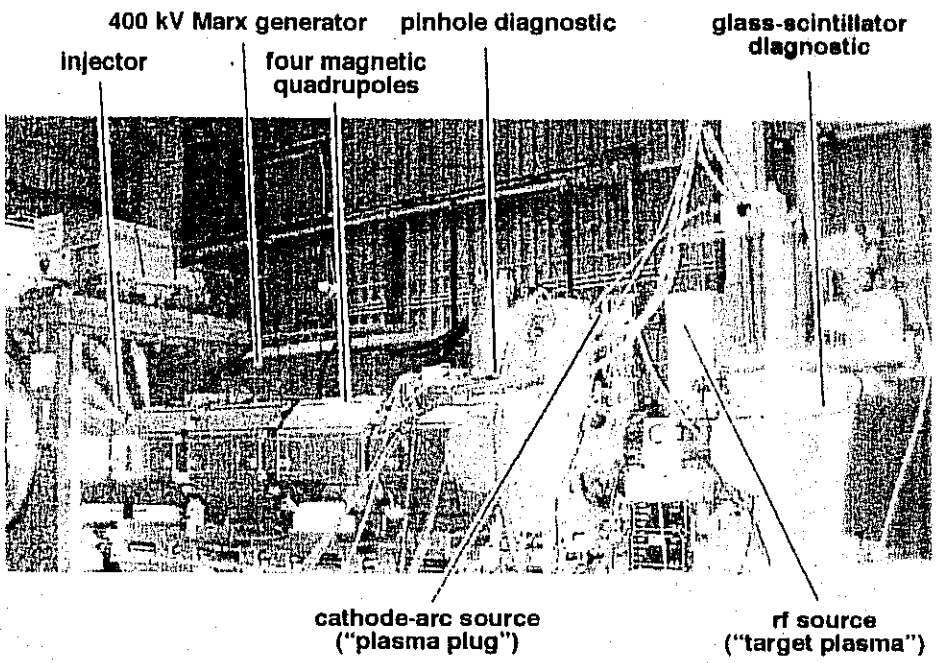

300 keV K+ ions at 25 mA

2004

Measurements on the Neutralized Transport Experiment (NTX) demonstrate achievement of smaller transverse spot size using volumetric plasma

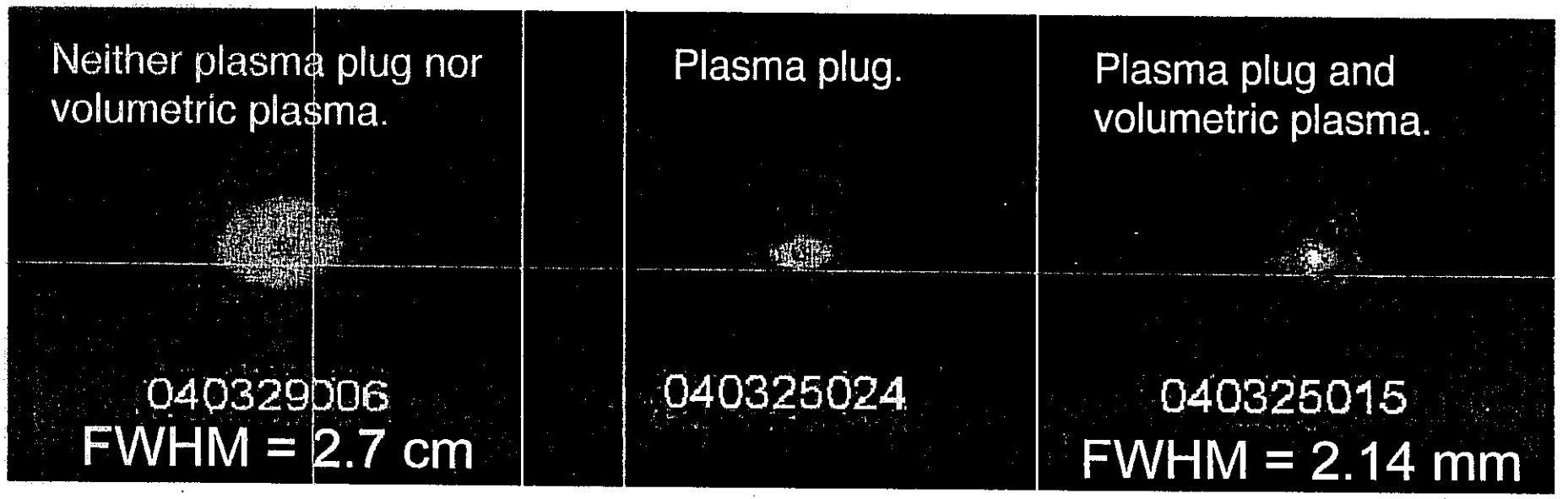

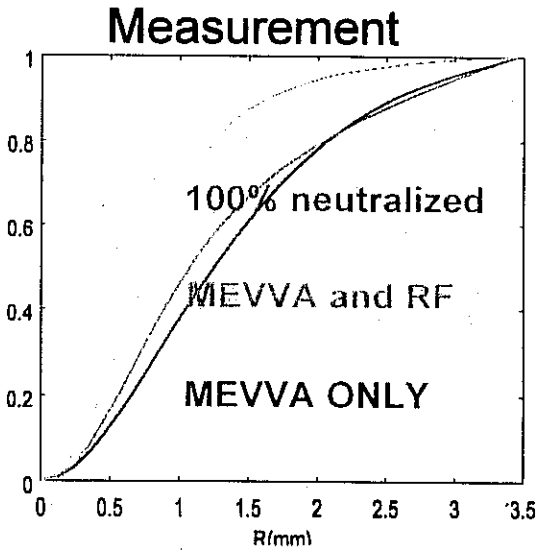

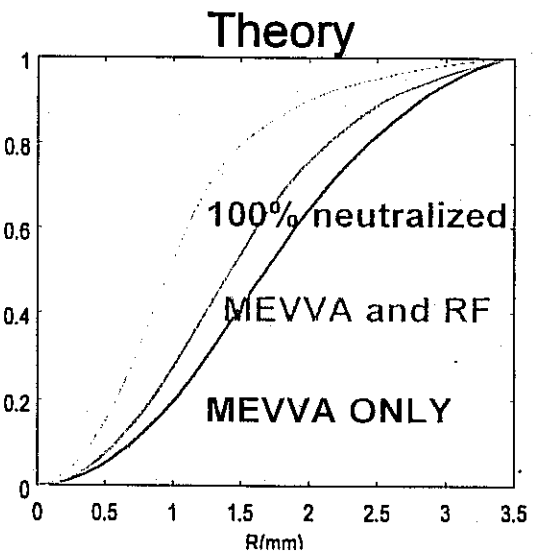

Neutralized drift compression experiment (NDCX) - 300 keV K+ ions at 25 mA

Tiltcore waveform

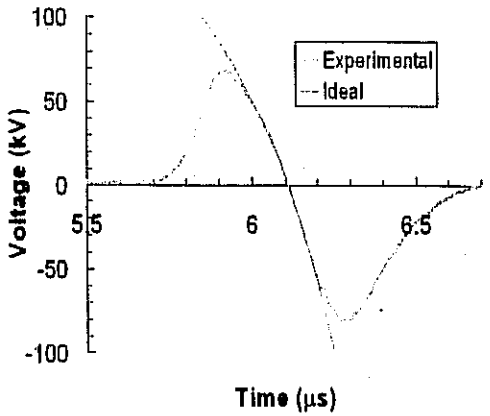

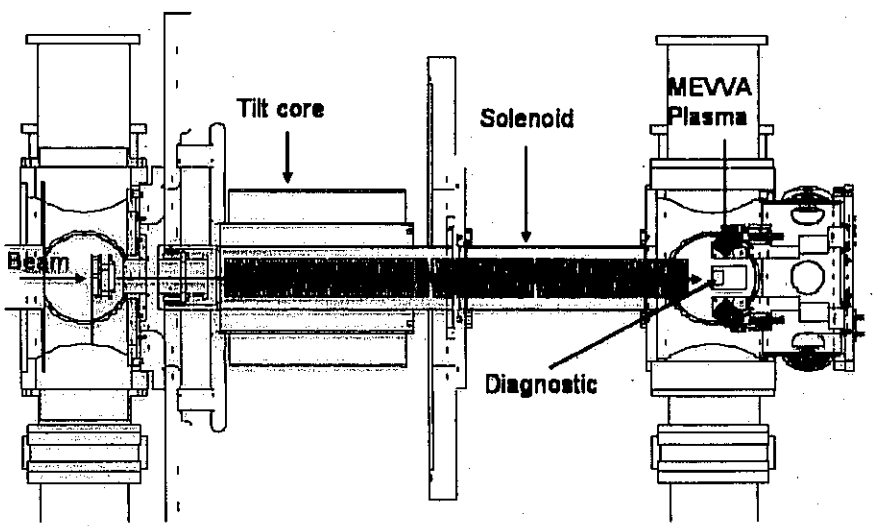

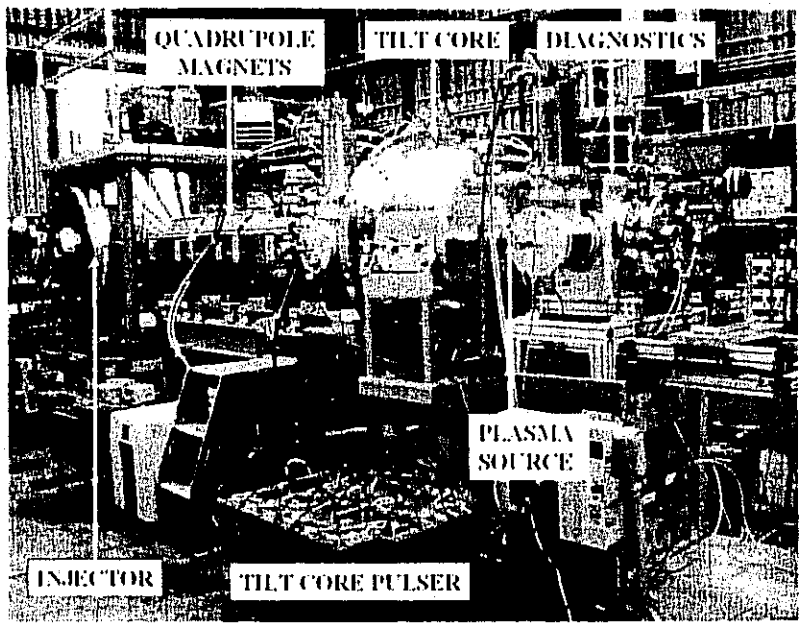

50 Fold Beam compression achieved in neutralized drift compression experiment

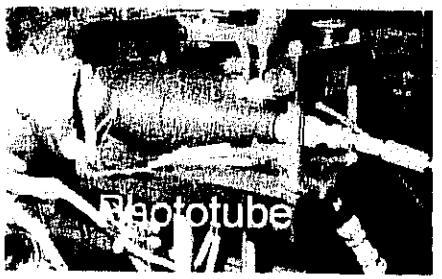

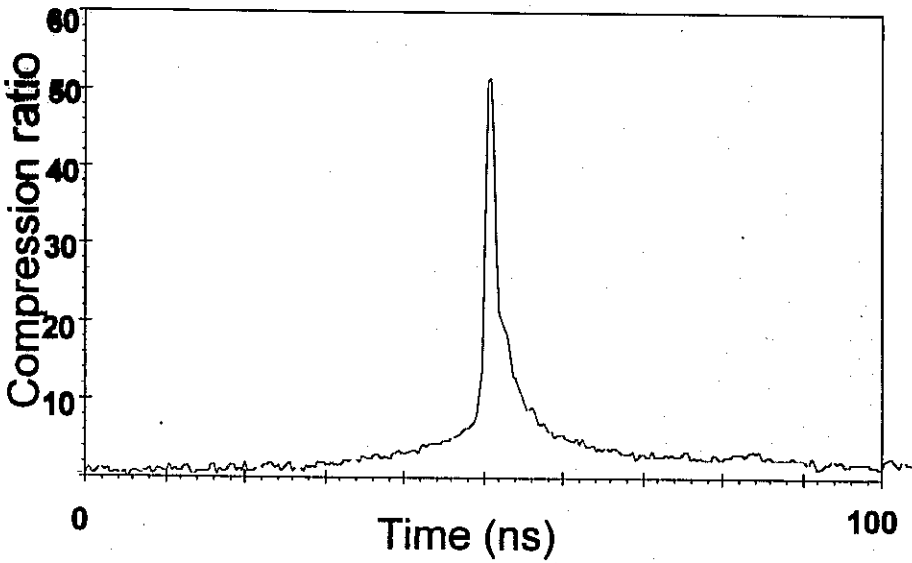

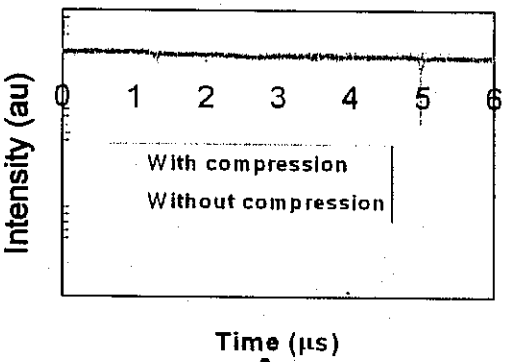

Optical data

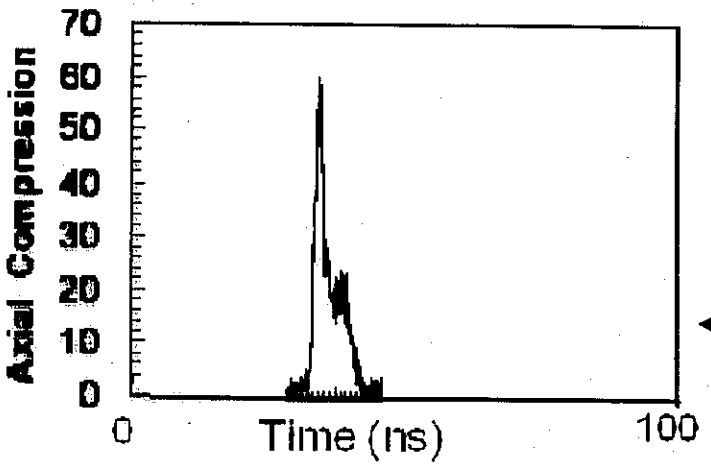

LSP simulation

Corroborating data from Faraday cup

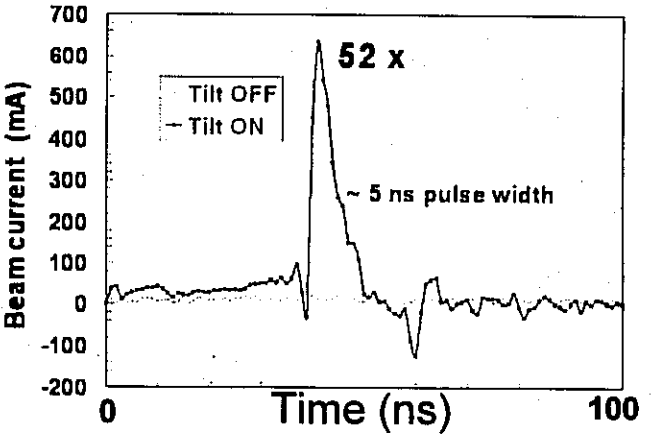

P.K. Roy et al, PRL, **95**, 234801, 2 Dec. 2005

NDCX-I: A series of experiments towards HEDP (NDCX-II)

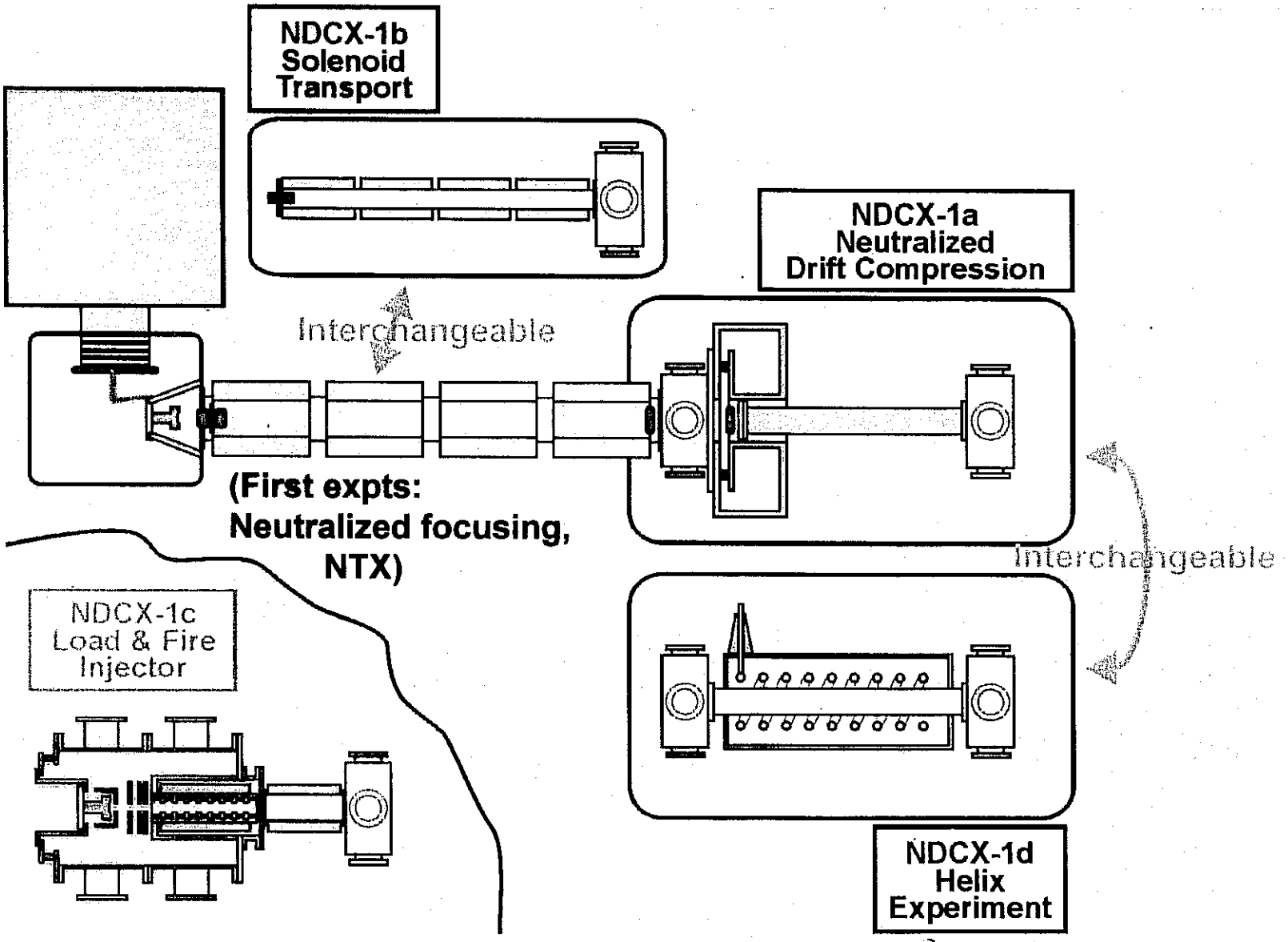

Artist's Conception of an HIF Power Plant on a few km^2 site

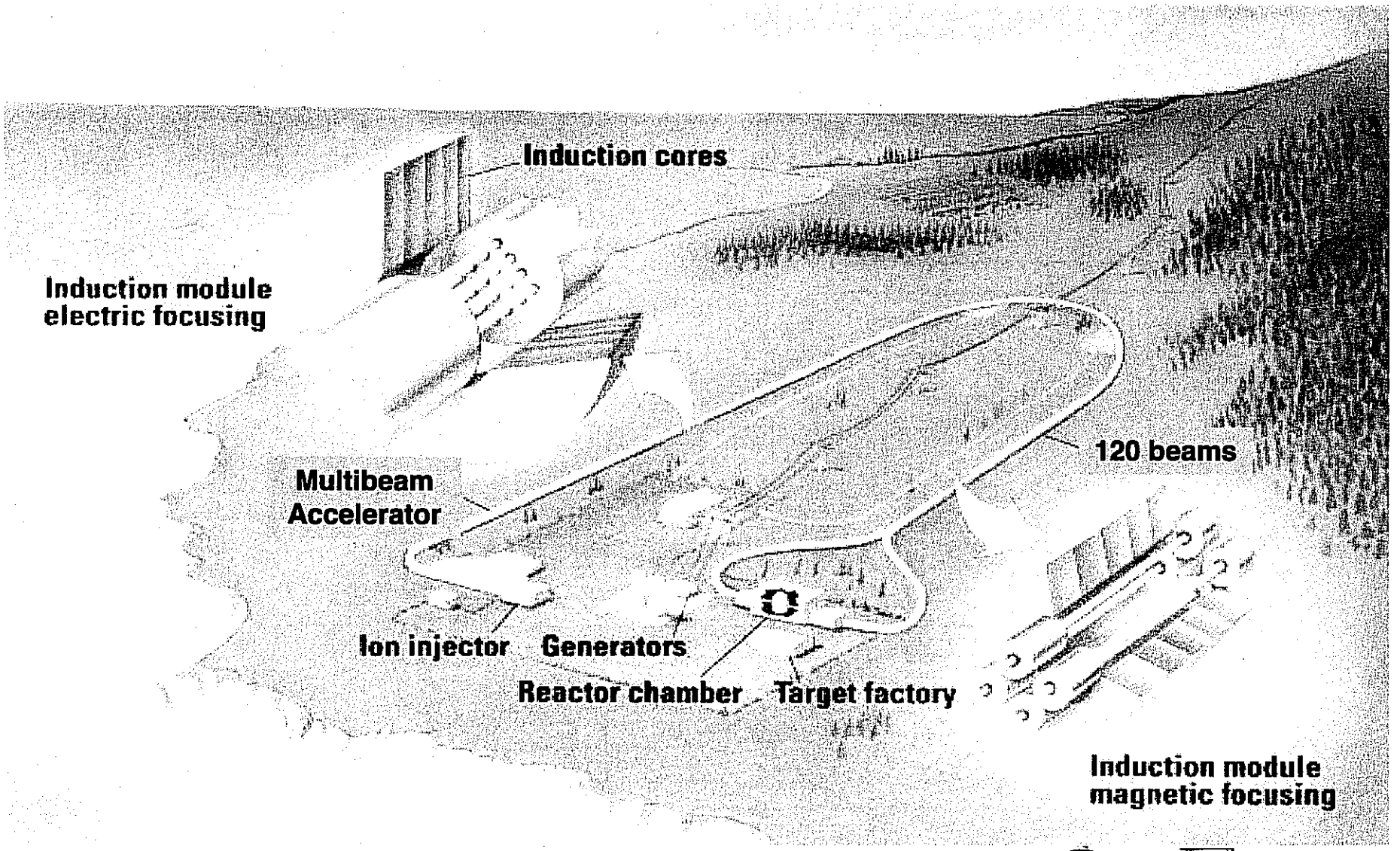

Computation Lecture #1

June 12, 2006

Computation for Intense Beams

USPAS - "Boston"

Rami Kishek,

University of Maryland

Rm. 206

ramiak@umd.edu

Displaying these Slides Major Team Effort

Thanks to:

- My wife: sent copies from home
- John Barnard: using memory stick
- Diktys Stratakis: Used laptop
- Christos Papadopoulos: Using Laptop
- Steve Lund: Using Notes

Suggested Bible

Charles K. Birdsall and A. Bruce Langdon, Plasma Physics via Computer Simulation, (McGraw Hill 1985). *Chaps. 1 and 2 suffice.*

All you need to know about beams …

Maxwell's Equations:

$$\vec{\nabla} \times \vec{E} = -\frac{\partial \vec{B}}{\partial t} \qquad \vec{\nabla} \bullet \vec{E} = \frac{\rho}{\varepsilon_o}$$

$$\vec{\nabla} \times \vec{B} = \frac{1}{c^2}\frac{\partial \vec{E}}{\partial t} + \mu_o \vec{J} \qquad \vec{\nabla} \bullet \vec{B} = 0$$

Lorentz Force Law:

$$\vec{F} = \frac{d}{dt}\left(\gamma m \vec{v}\right) = q\left(\vec{E} + \vec{v} \times \vec{B}\right)$$

Some simple cases don't need simulation

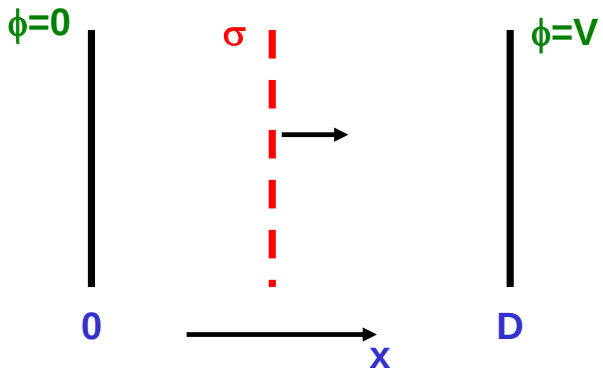

σ is surface charge density

Theoretical Approach (this course, Reiser's book)

Simplify problem sufficiently to solve, e.g.:

- Single particle wandering through known lattice

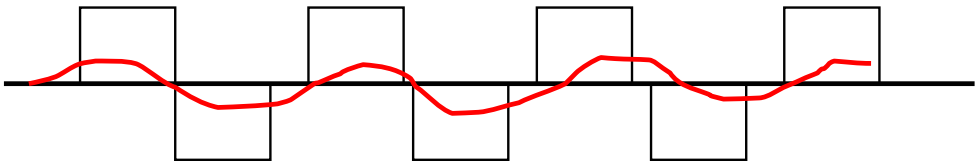

- "Cylinder" beam with uniform density distribution

Even "analytical" cases like this often require computers to solve (numerical integration).

Problem 1: Real Beams are not K-V

Experiment (100 mA) (top) [Bernal]

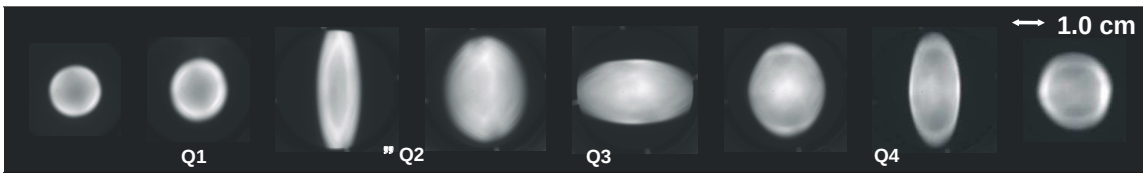

WARP Simulation (below) [Kishek]

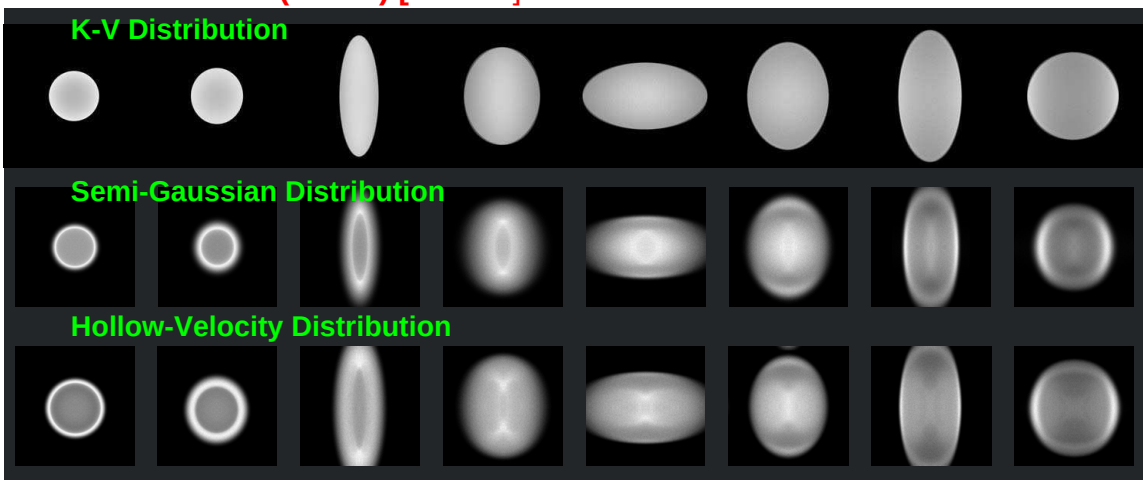

Problem 2: Real Accelerators are Very Complex

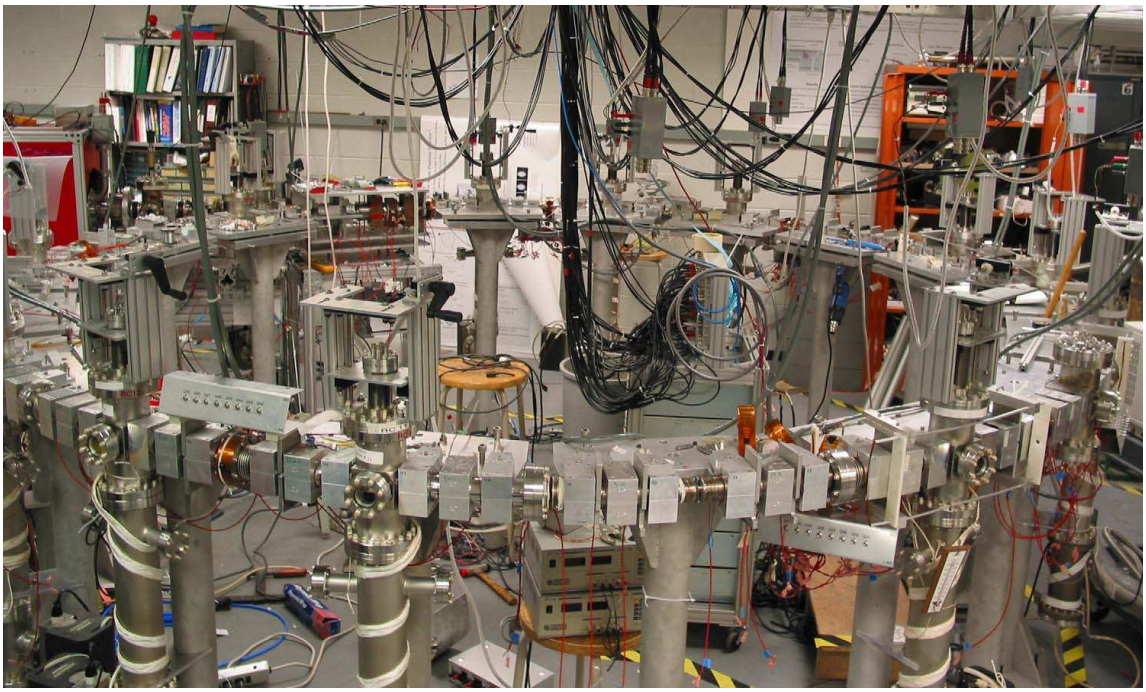

The University of Maryland Electron Ring (UMER)

Problem 3: Realistic Geometries May be Difficult

Electron Gun

Grid

Problem 4: Real Accelerators are Expensive

Computation has Many Advantages:

1. Verification of simpler analytic models.
   Layers of complexity can be added or removed at will from the computer model.

2. Understanding and interpreting experimental results.
   Simulation is much easier (and cheaper) to set up and perform than experiment.

3. To facilitate design of large, expensive accelerators.
   The computer model can be used to study the physics of a large accelerator well before such an accelerator can be constructed.

Simulation

Central issue: What happens to charged particles in an environment of electric and magnetic fields?

For real beams:

- Self-Fields linear only for uniform beam density
- Emittance conserved only for linear fields
- Envelope equation valid only if emittance conserved.

In general, evolution of beam size, emittance, and particle trajectories can be complicated and difficult to predict analytically.

Simulation: Applying physical laws (approximately) to model reality on a computer

Where Does Simulation Fit in?

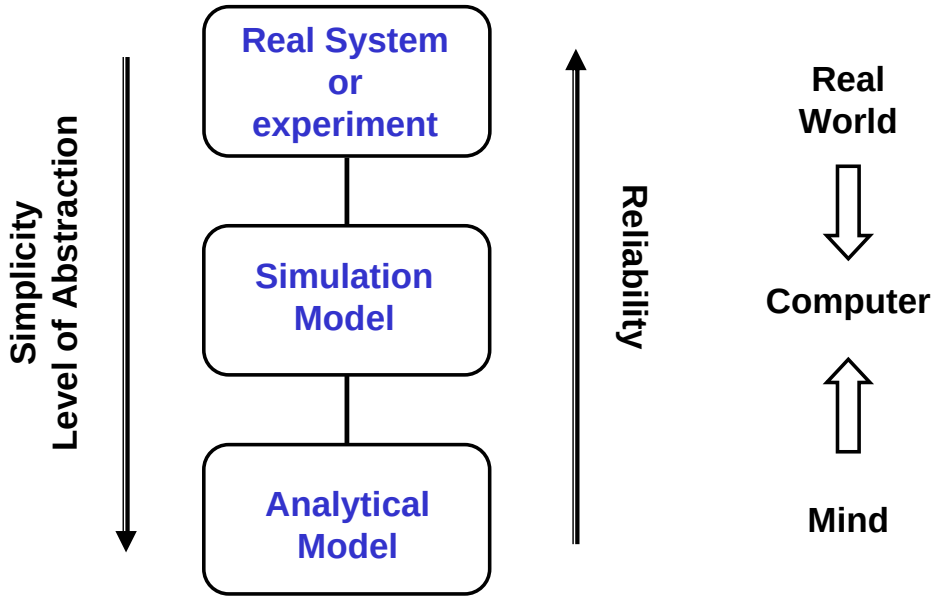

Particle Simulations

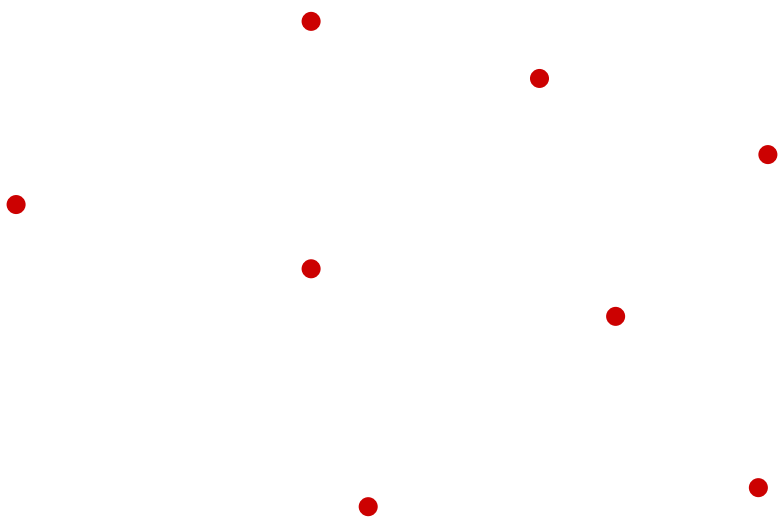

Galaxies face similar issue-how to model 10^{11} stars?

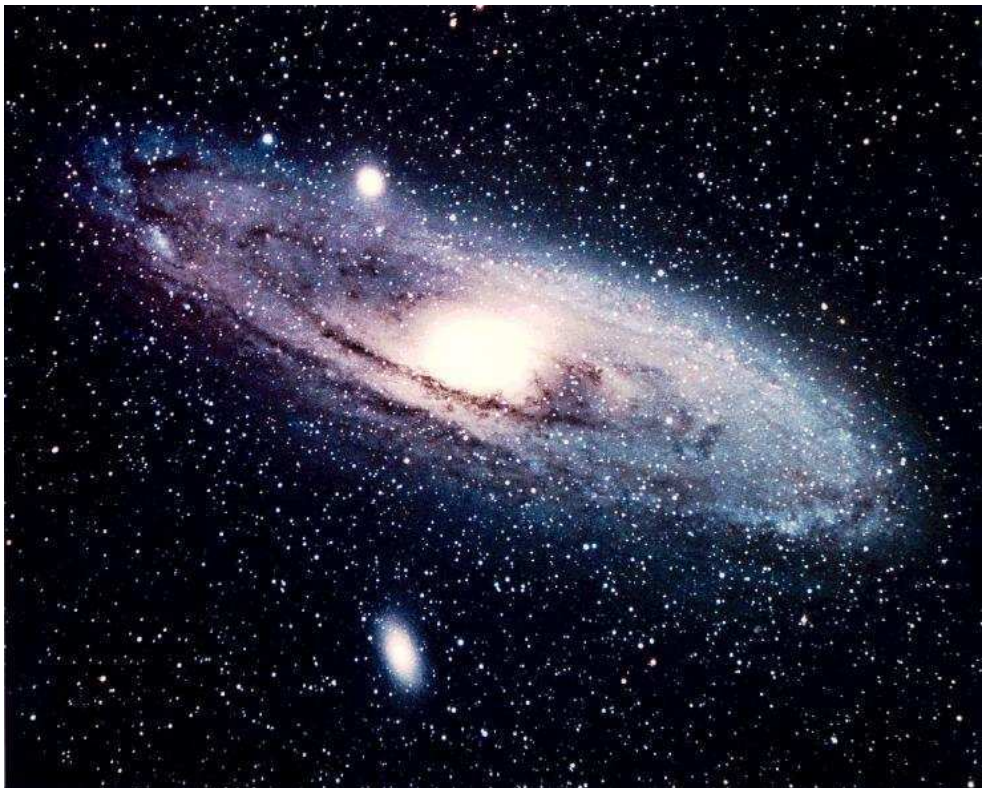

Coulomb's Law

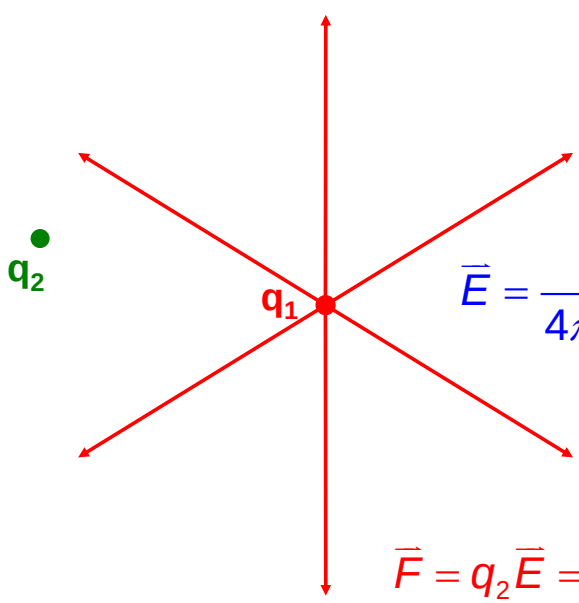

$$\vec{E} = \frac{q_1}{4\pi\varepsilon_o r^2}\hat{r}$$ (Gauss' Law)

$$\vec{F} = q_2\vec{E} = \frac{q_2 q_1}{4\pi\varepsilon_o r^2}\hat{r}$$ (Lorentz Force)

Gravity – same form, different sign

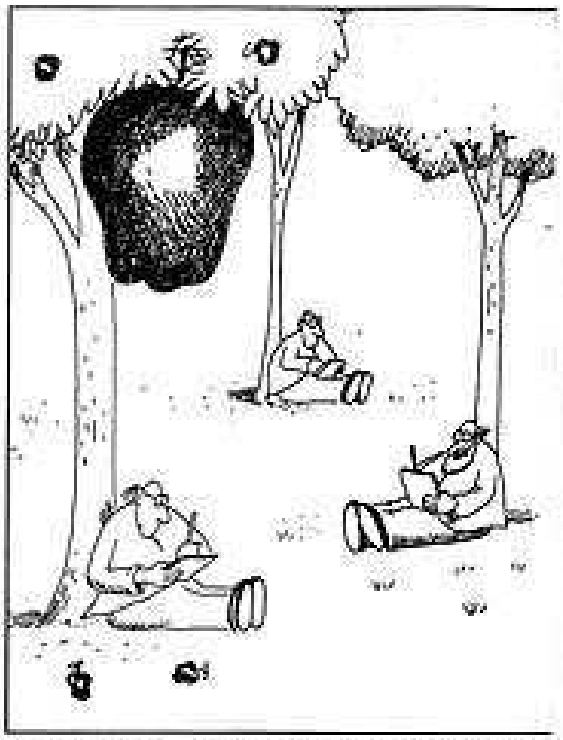

"Nothing yet. ...How about you, Newton?"

$$\vec{g} = -\frac{GM}{r^2}\hat{r}$$

$$\vec{F} = m\vec{g} = -\frac{GmM}{r^2}\hat{r}$$

Classification of Computing Methods

Lund Notes - classify by the way the beam is represented:

- Particle Methods
- Distribution Methods
- Moment Methods

Approach

- Start with simplest brute force approach
- Find out problems with that approach
- Add some sophistication
- Find out problems

Each technique has its own strengths and weaknesses

Need to be aware of the boutique of available computational methods

Rami: Classification by Physical Laws (Loose)

Maxwell's Equations:

$$\vec{\nabla} \times \vec{E} = -\frac{\partial \vec{B}}{\partial t} \qquad \vec{\nabla} \bullet \vec{E} = \frac{\rho}{\varepsilon_o}$$

$$\vec{\nabla} \times \vec{B} = \frac{1}{c^2}\frac{\partial \vec{E}}{\partial t} + \mu_o \vec{J} \qquad \vec{\nabla} \bullet \vec{B} = 0$$

Lorentz Force Law:

$$\vec{F} = \frac{d}{dt}\left(\gamma m \vec{v}\right) = q\left(\vec{E} + \vec{v} \times \vec{B}\right)$$

Specific Needs Behind Computing

- **Field Solvers**: Calculating the electromagnetic fields affecting the particles.
- **Particle Trackers**: Calculating particle trajectories in those fields.
- Calculating electric and magnetic fields generated by those particles. Self-Consistency → **Particle-in-cell (PIC) Codes**.

In most realistic situations, these factors are difficult to derive analytically.

Analytical models typically employ drastic simplification, which may or may not result in correct predictions.

Types of Accelerator Codes

Field Solvers

Static
- *Poisson*
- *COULOMB*

Eigenmode
- *YAP*

Time Domain
- *MAFIA*
- *AMOS*
- *GDFIDL*
- *Maxwell*

Other
- *SuperFISH*

Magnet Design
- *MAGPC*
- *Maxwell 3D*

Particle-in-Cell

Electrostatic
- *pdp1 / pdc2 / etc.*
- ***WARP***

Electromagnetic
- *MAGIC / SOS*
- *OOPIC*
- *ARGUS*
- *VORPAL*

Gun Codes

E-Gun

Particle Trackers

Transfer Maps
- *MaryLie*

Matrices
- *MAD / DIMAD*
- *TRANSPORT*

Multi-Particle
- *PARMELLA/ILLA*
- *COZY*

Other
- *SIMION*

Envelope

TRACE
PBOLab
EMATCH

Other Approaches

Plasma Codes

Fluid model
Vlasov-Poisson model -
δf Methods
Green's Function model

Other Accelerator Codes

Mechanical: structural / thermal / vacuum (*ProE*)
Radiation
Optics; FELs
Controls (*LabView; EPICS*)
Data Processing
Systems

Hybrid Codes

Particle-core model:
Envelope or PIC model for beam bulk (core);
Tracking of halo particles.

PIC + map codes:
use PIC for self-fields;
transfer maps for external

Fluid + Envelope: (*CIRCE*)
Fluid for longitudinal;
Envelope for transverse

A Few Notes of Caution

- Successful codes are usually tremendous projects
- You really don't want to develop a new code if an existing one contains suitable approximations
- Sometimes a "less accurate" approximation can work better than more sophisticated models
- GIGO: The results you get are (at best) as good as the input you put in

Multiparticle Model

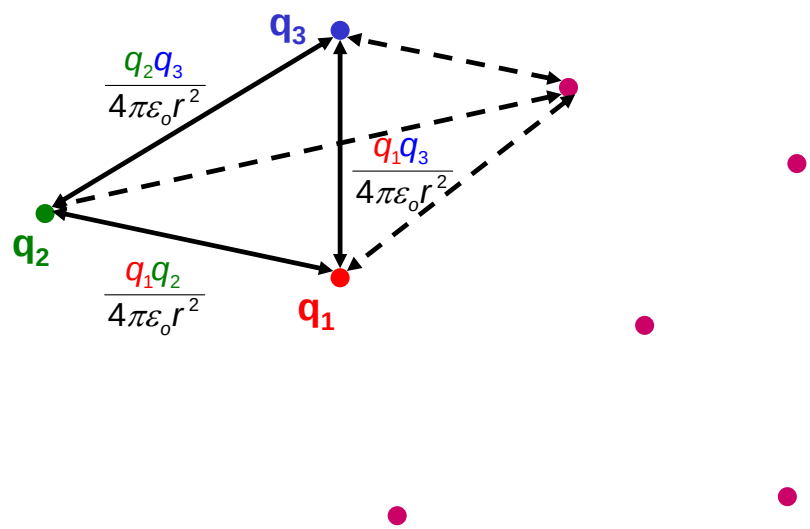

Number of Interactions ~ N_p^2

N-Body Problem

- Typical beam contains ~ 10^9 particles.
- Typical galaxy contains ~ 10^{11} stars.
- Laboratory plasmas may contain 10^{12} - 10^{15} cm^{-3} and inertial fusion plasmas up to ~ 10^{22} cm^{-3}.
- Even with 10^9 particles, calculation of particle-particle interaction for every particle implies 10^{18} calculations to determine the forces.
- ***Once particles are advanced, forces change, and all 10^{18} interactions have to be recalculated.***

How Do We Simplify?

Approximation #1: Macroparticles

- Instead of accounting for every particle, take a statistical sample of particles → **Macroparticles**.
- A macroparticle is a special particle which carries the weight of a large number of particles when used to calculate the fields exerted on other particles.
- In response to a given field, the macroparticle moves as if it were a regular test particle.
- E.g, 10^9 particles → 10^5 particles.
  Still have to deal with 10^{10} calculations.

Number of calculations ~ n_p^2.

Notes on Sampling

For Approximation to be valid, need to ensure:

- Number of macroparticles should be sufficiently large to give good statistics.
- Average behavior and distribution of macroparticles should resemble that of real beam.

Observation

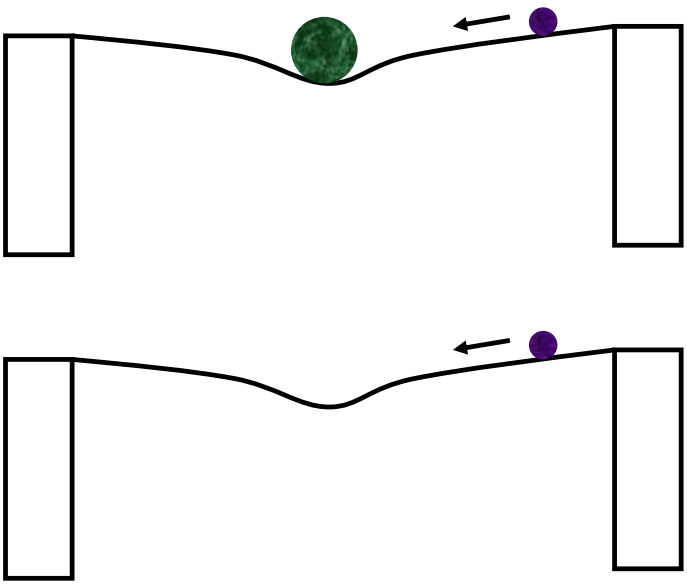

Approximation #2: Fields not Forces

- Do not deal with every possible interaction.
- Instead, use the concept of fields or potentials:
  i. Interpolate particle positions onto grid to determine charge density.
  ii. Calculate Fields as in previous lecture.
  iii. Interpolate fields to position of each particle to determine force.

Total number of calculations ~ n_p

- In addition, have to do field calculation which for a 2D FFT ~ $n_x^2 \log n_x$

How (When) is This Possible?

Reiser Sec. 4.1
Birdsall Chap 1

Grid method ignores close-collisions (interactions between particles within same cell).

This is justified in reality when large number of particles

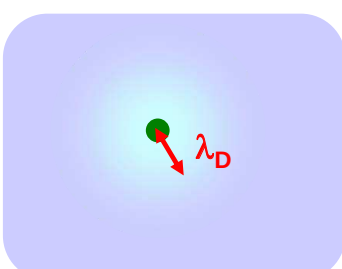

Uniform distribution of particles confined by external field $\phi(r) = \phi_e(r) + \phi_s(r)$

Boltzmann distribution:

$$\rho(r) = en(r)\,exp\left(\frac{e\phi(r)}{k_B T}\right) \approx \frac{e^2 n(r)}{k_B T}\phi_s(r)$$

Solve for Potential from Poisson Equation:

$$\nabla^2\phi = \frac{1}{r^2}\frac{d}{dr}\left(r^2\frac{d\phi_s}{dr}\right) = -\frac{\rho(r)}{\varepsilon_o} = -\frac{e^2 n(r)}{\varepsilon_o k_B T}\phi_s(r)$$

$$\phi(r) = \frac{q}{4\pi\varepsilon_o r}\exp\left(-\frac{r}{\lambda_D}\right)$$

Debye Length

$$\boxed{\lambda_D = \sqrt{\frac{\varepsilon_o k_B T}{e^2 n}}}$$

How Do We Model 10^9 particles?

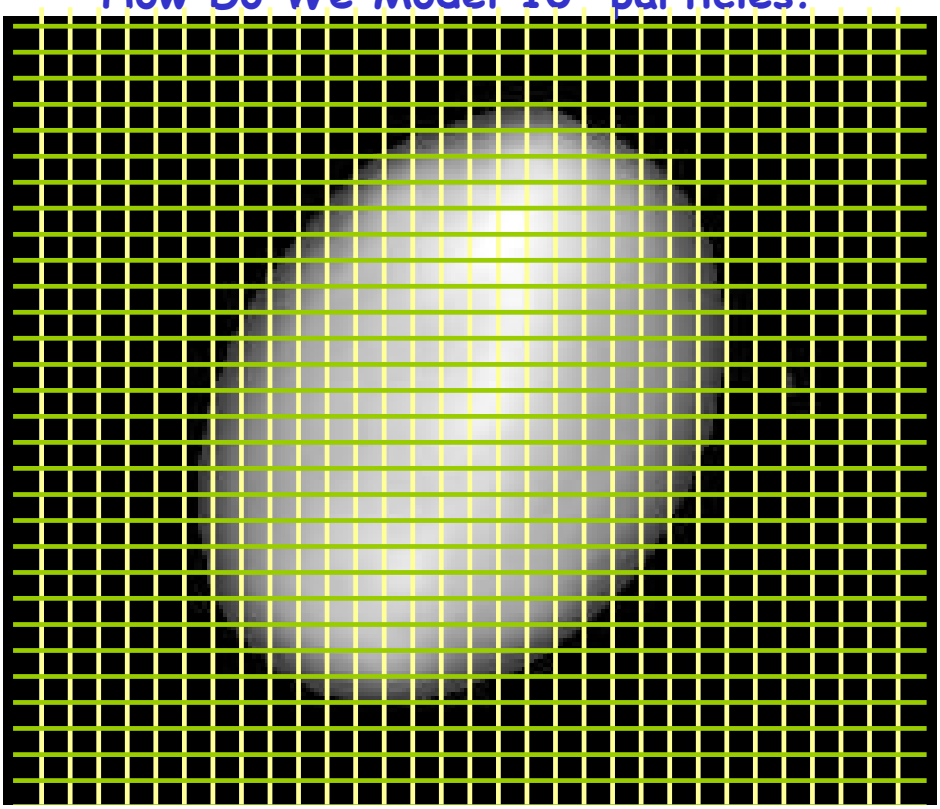

Galaxies Can Be Similarly Treated

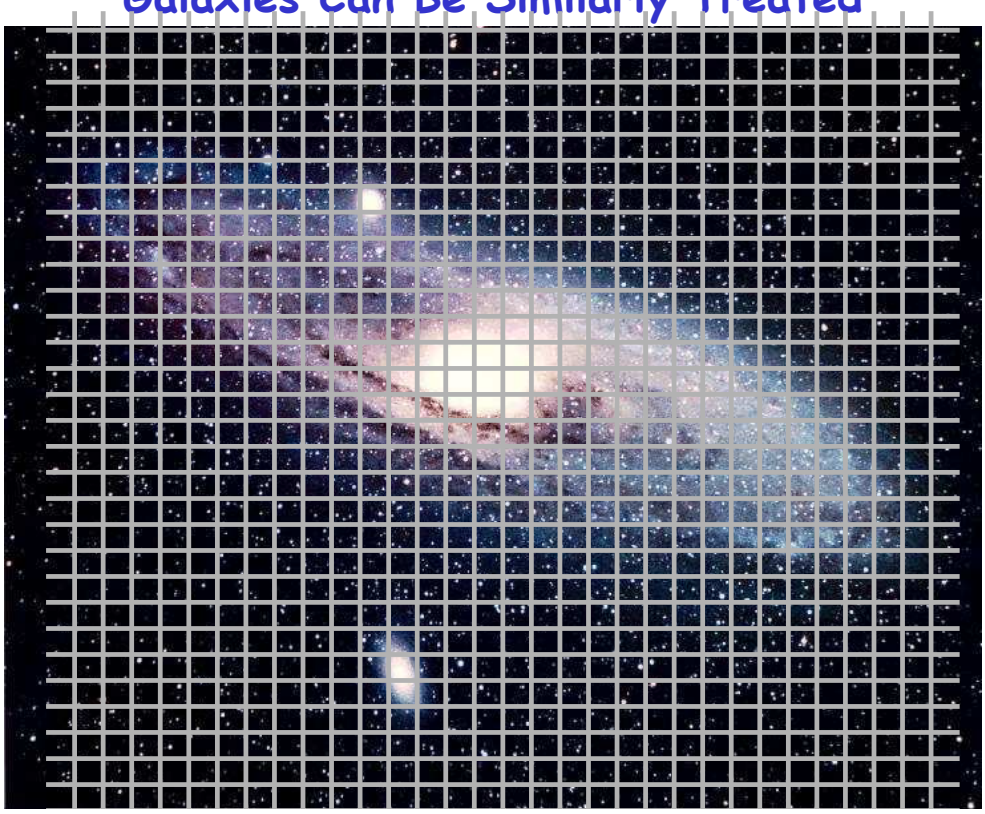

Debye Shielding

If:

Large number of particles (# particles in Debye sphere = $n\lambda_D^3 >> 1$)

$\lambda_D < R$ (Space-Charge-Dominated)

Force from "collective" potential >> force from nearest neighbors

Probability of individual particle-particle interaction (Coulomb collisions) << collective interaction

Can use grid to model space-charge-force

Grid needs to be small enough enough to resolve potential variations (Rule of thumb $\Delta x \sim \lambda_D/3$)

Otherwise, individual "collisions" important and need be modeled

Particle Tracking and Numerical Methods

Rami Kishek

Particle Trajectories: x-x' Phase Space

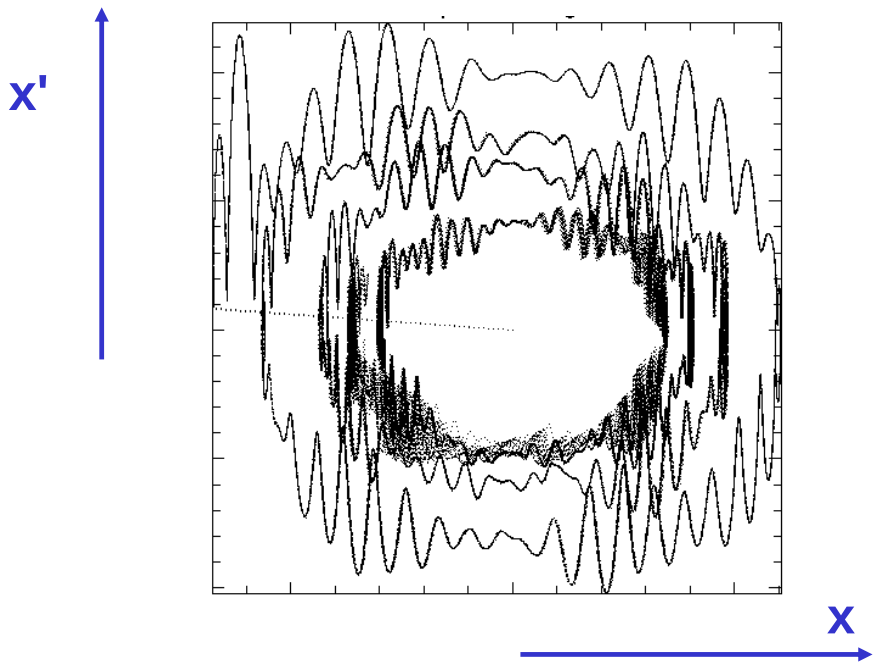

Pushing Particles (Tracking)

Maxwell's Equations:

$$\vec{\nabla} \times \vec{E} = -\frac{\partial \vec{B}}{\partial t} \qquad \vec{\nabla} \bullet \vec{E} = \frac{\rho}{\varepsilon_o}$$

$$\vec{\nabla} \times \vec{B} = \frac{1}{c^2}\frac{\partial \vec{E}}{\partial t} + \mu_o \vec{J} \qquad \vec{\nabla} \bullet \vec{B} = 0$$

Lorentz Force Law:

$$\vec{F} = \frac{d}{dt}\left(\gamma m \vec{v}\right) = q\left(\vec{E} + \vec{v} \times \vec{B}\right)$$

Computer Limitations

- Computers can only handle numbers (binary, no less).
- Computers can only perform simple arithmetic (no differentiation).
- Furthermore, computers can only handle a finite number of data. Continuous functions (made of infinite number of "points") must be discretized.
- Can only deal with bounded problems.

Particle Pushing

$$\vec{v} = \frac{d\vec{x}}{dt}$$

$$\vec{F} = \frac{d}{dt}\left(\gamma m \vec{v}\right)$$

Equations of Motion (Newton)

Know derivatives of function – want to predict function's future values

To determine position of a particle as a function of time in response to a given force, need to integrate equations of motion.

Note: Forces can be time-dependent.

Time Discretization

- Particle positions and velocities change continuously with respect to time, but computer can hold only finite number of quantities.
- Hence treat time (or s) as a discrete quantity: care about particle positions and velocities only at discrete instances of time.

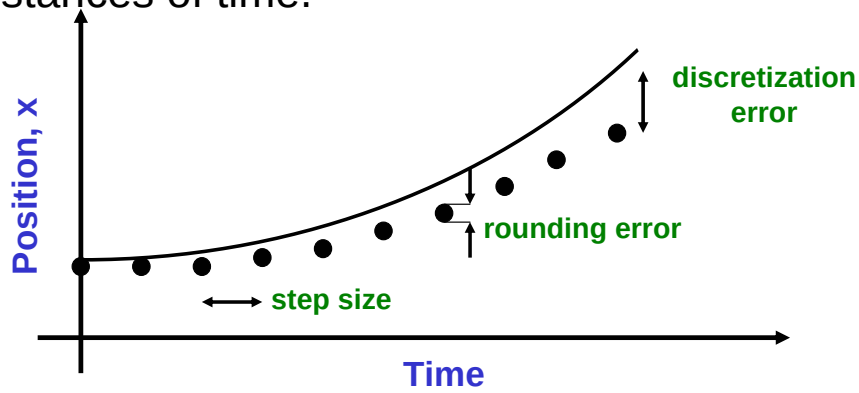

Euler Method

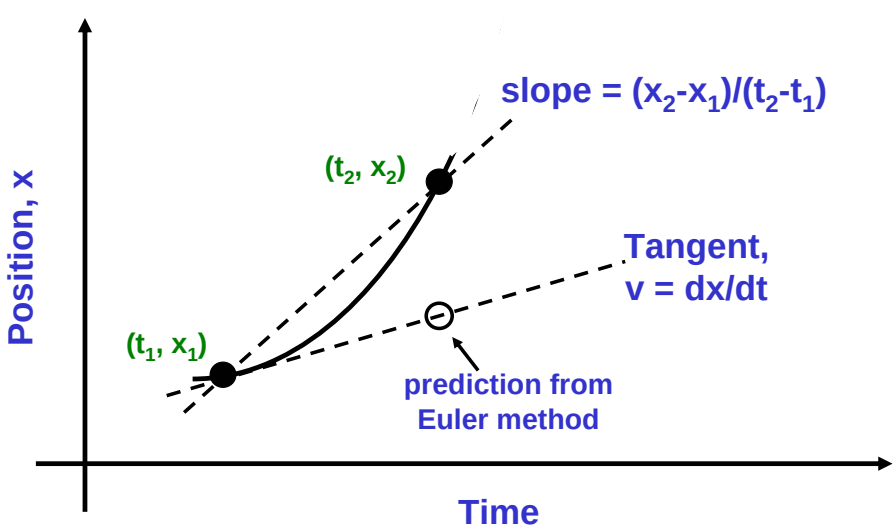

As $\Delta t = (t_2-t_1) \rightarrow 0$, then slope $\rightarrow$ dx/dt

Forward-, Backward-, & Central-Differences

$$f'(s) \approx \frac{f(s+\Delta s)-f(s)}{\Delta s}$$ Forward-Difference

$$f'(s) \approx \frac{f(s)-f(s-\Delta s)}{\Delta s}$$ Backward-Difference

$$f'(s) \approx \frac{f(s+\frac{\Delta s}{2})-f(s-\frac{\Delta s}{2})}{\Delta s}$$ Central-Difference

Forward- and Backward- Differences Converge as Δs

Central-Difference Converges as $(\Delta s)^2$

Accuracy of Difference Method

Taylor Expand arbitrary function:

$$f(s+\Delta s) = \cancel{f(s)} + \cancel{\Delta s f'(s)} + \cancel{\tfrac{\Delta s^2}{2!} f''(s)} + \cancel{\tfrac{\Delta s^3}{3!} f'''(s)} + \tfrac{\Delta s^4}{4!} f^{iv}(s) + O\left(\Delta s^5\right)$$

$$f(s-\Delta s) = \cancel{f(s)} - \cancel{\Delta s f'(s)} + \cancel{\tfrac{\Delta s^2}{2!} f''(s)} - \cancel{\tfrac{\Delta s^3}{3!} f'''(s)} + \tfrac{\Delta s^4}{4!} f^{iv}(s) + O\left(\Delta s^5\right)$$

Subtract 2 Equations:

$$f'(s) = \frac{f(s+\Delta s)-f(s-\Delta s)}{2\Delta s} - \frac{\Delta s^2}{6} f'''(s) + \ldots$$

Add 2 Equations:

$$f''(s) = \frac{f(s+\Delta s)+f(s-\Delta s)-2f(s)}{\Delta s^2} - \frac{\Delta s^2}{12} f^{iv}(s) + \ldots$$

Discretization Errors

Can reduce errors in 2 ways:

- Use smaller time steps
- Use higher-order integration technique which converges faster as a function of time step.

Examples,

Euler method converges as Δt or Δs

4th-order Runge-Kutta converges as $(\Delta t)^4$.

Center-Difference Methods converge as $(\Delta t)^2$.

LeapFrog Methods

Eqns of Motion: 2 first-order differential equation
center-difference expansion of each

$$x(t+\Delta t) \cong x(t) + (\Delta t)\, v\left(t + \Delta t/2\right)$$

$$\gamma m v\left(t + \Delta t/2\right) \cong \gamma m v\left(t - \Delta t/2\right) + (\Delta t)\, F(t)$$

Notes:

Positions and Velocities not known at same points.

Electric forces depend only on particle positions.

Get $(\Delta t)^2$ convergence for only one calculation per step per equation.

Pair not self-starting. Need to integrate backwards 1/2 step to start.

The Leap Frog

$$x(t+\Delta t) = x(t) + \Delta t \times v(t+\Delta t/2)$$

$$v(t+\Delta t/2) = v(t-\Delta t/2) + \Delta t \times F(t)/m$$

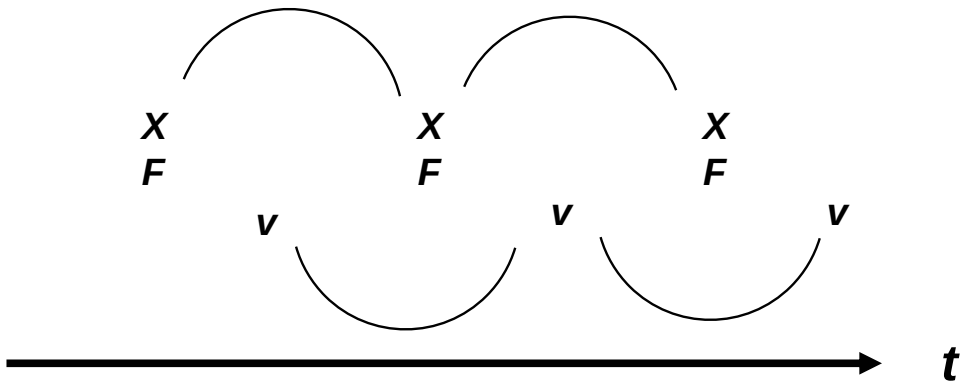

Note that the forces depend only on the particle positions.

Why use leapfrog ?

- Only second order but simple (and appropriate because of truncation errors in field solution).
- Solves an easy to visualize physical problem, i.e. gives the correct answer for a force which is constant over the integration interval
- Symplectic
- time-centered and reversible, I.e. simulation can be run backward
- Langdon called these characteristics “virtuous”.

Implications of Leapfrog

- To obtain useable output, velocity and position of particles must be measured at the same time.
- Therefore, at all instances of time in which diagnostic output is desired, the calculation must be advanced 1/2 step to synchronize position and velocity → semi-Leapfrog.
- This is expensive.

Integrating the envelope equation

- Can use same methods for general purpose integration

Computation in Beams: Field Solvers

Rami Kishek

Review:

How Do We Model 10^9 particles?

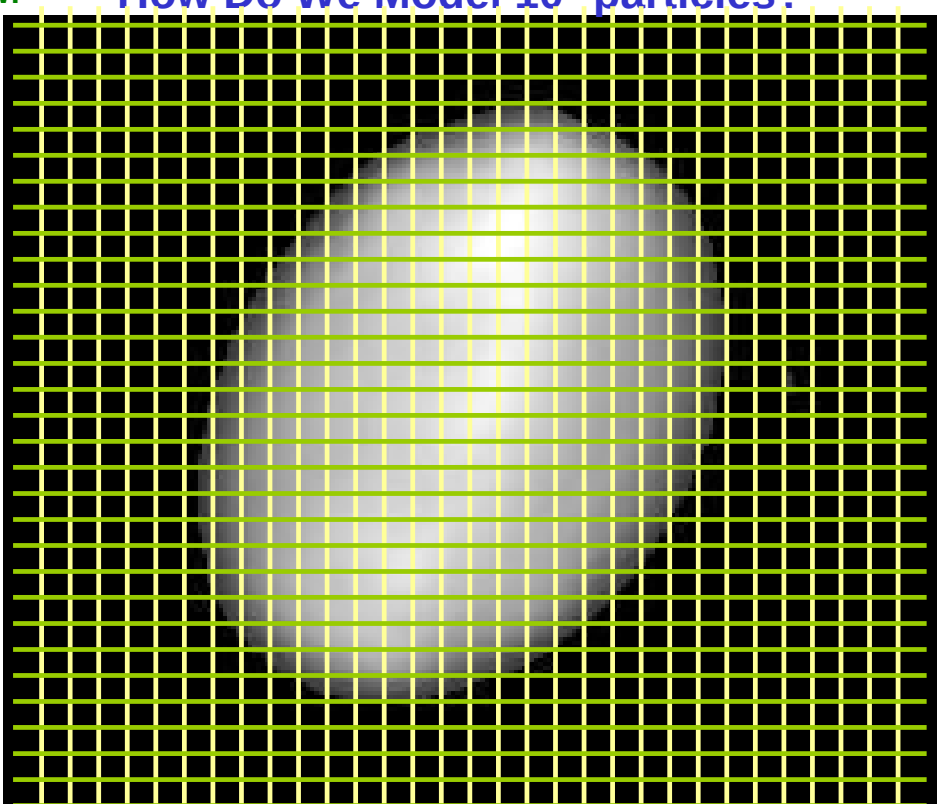

Solving for Fields

Humphries CPA 4.2, 4.5
Birdsall Chap 2

Maxwell's Equations:

$$\vec{\nabla} \times \vec{E} = -\frac{\partial \vec{B}}{\partial t} \qquad \vec{\nabla} \bullet \vec{E} = \frac{\rho}{\varepsilon_o}$$

$$\vec{\nabla} \times \vec{B} = \frac{1}{c^2}\frac{\partial \vec{E}}{\partial t} + \mu_o \vec{J} \qquad \vec{\nabla} \bullet \vec{B} = 0$$

Lorentz Force Law:

$$\vec{F} = \frac{d}{dt}\left(\gamma m \vec{v}\right) = q\left(\vec{E} + \vec{v} \times \vec{B}\right)$$

Static Approximation (steady state) $\frac{\partial}{\partial t} \to 0$:

$$\vec{\nabla} \times \vec{E} = 0 \frac{\partial \vec{B}}{\partial t} \qquad \vec{\nabla} \bullet \vec{E} = \frac{\rho}{\varepsilon_o}$$

Electrostatic

Source Terms

$$\vec{\nabla} \times \vec{B} = \mu_o \vec{J} + \mu_o \vec{J} \qquad \vec{\nabla} \bullet \vec{B} = 0$$

Magnetostatic

Electrostatic Case

First Equation, $\vec{\nabla} \times \vec{E} = 0$ allows us to define electrostatic potential, ϕ:

$$\vec{E} = -\vec{\nabla}\phi$$

$$\vec{\nabla} \bullet \vec{E} = -\vec{\nabla} \bullet \vec{\nabla}\phi$$

Poisson Eqn

$$\boxed{\nabla^2\phi = \frac{\partial^2\phi}{\partial x^2} + \frac{\partial^2\phi}{\partial y^2} + \frac{\partial^2\phi}{\partial z^2} = -\frac{\rho}{\varepsilon_o}}$$

If no space charge, $\rho = 0$,

$$\boxed{\nabla^2\phi = 0}$$

Laplace's Eqn

Solving for E-S Potential numerically

Divide space into grid.

Quantities (e.g., charge density, potential) defined on the grid.

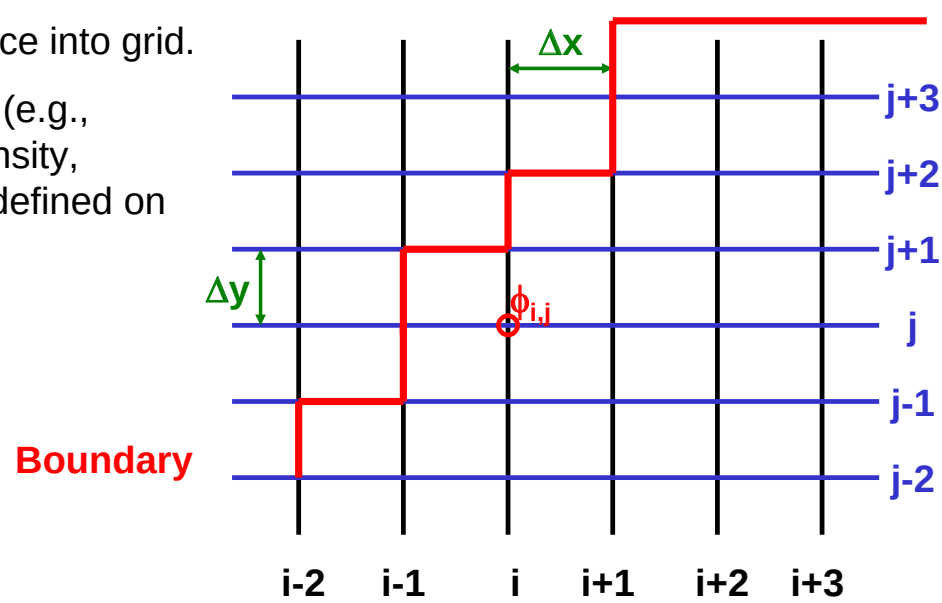

Boundary Conditions

Dirichlet B.C.: ϕ(border point) = constant

0 for conducting boundary

Neumann B.C.: $\frac{\partial \phi}{\partial x} = const$

Other Gridding Geometries Possible

HW Problem

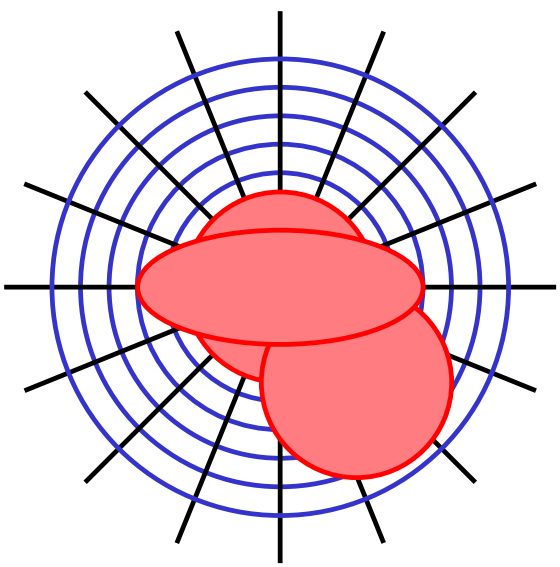

Alternative gridding may be more suitable

However, Pay a Price:

- **Difference equations more complex**
- **Resolution varies in different parts of beam**
- **Gridding may introduce unphysical behavior**

Adaptive Mesh (grid size changes with location to model details at higher resolution). Again more complex.

Forward-, Backward-, & Central-Differences

$$f'(x) \approx \frac{f(x+\Delta x)-f(x)}{\Delta x}$$ Forward-Difference

$$f'(x) \approx \frac{f(x)-f(x-\Delta x)}{\Delta x}$$ Backward-Difference

$$f'(x) \approx \frac{f(x+\frac{\Delta x}{2})-f(x-\frac{\Delta x}{2})}{\Delta x}$$ Central-Difference

Forward- and Backward- Differences Converge as Δx

Central-Difference Converges as $(\Delta x)^2$

Here $\quad ' \equiv \frac{\partial}{\partial x}$

Accuracy of Difference Method

Taylor Expand arbitrary function:

$$f(x+\Delta x) = \cancel{f(x)} + \cancel{\Delta x f'(x)} + \cancel{\frac{\Delta x^2}{2!} f''(x)} + \cancel{\frac{\Delta x^3}{3!} f'''(x)} + \frac{\Delta x^4}{4!} f^{iv}(x) + o\left(\Delta x^5\right)$$

$$f(x-\Delta x) = \cancel{f(x)} - \cancel{\Delta x f'(x)} + \cancel{\frac{\Delta x^2}{2!} f''(x)} - \cancel{\frac{\Delta x^3}{3!} f'''(x)} + \frac{\Delta x^4}{4!} f^{iv}(x) + o\left(\Delta x^5\right)$$

Subtract 2 Equations:

$$f'(x) = \frac{f(x+\Delta x)-f(x-\Delta x)}{2\Delta x} - \frac{\Delta x^2}{6} f'''(x) + \ldots$$

Add 2 Equations:

$$f''(x) = \frac{f(x+\Delta x)+f(x-\Delta x)-2f(x)}{\Delta x^2} - \frac{\Delta x^2}{12} f^{iv}(x) + \ldots$$

Transform Poisson's Equation

Derivative ⇒ Finite Difference

$$\phi(x,y) = \phi\left(i\Delta x, j\Delta y\right) = \phi\left(i,j\right) = \phi_{i,j}$$

$$\phi'_{i+\frac{1}{2},j} = \frac{\partial}{\partial x}\phi_{i+\frac{1}{2},j} \approx \frac{\phi_{i+1,j} - \phi_{i,j}}{\Delta x}$$

Central-Difference Estimate
Error ~ O(Δx^2)

$$\frac{\partial^2 \phi_{i,j}}{\partial x^2} \approx \frac{\phi'_{i+\frac{1}{2},j} - \phi'_{i-\frac{1}{2},j}}{\Delta x}$$

Error in 2nd derivative
~ O(Δx^2)

Finite-Difference Form of Laplacian Operator

$$\frac{\partial^2 \phi_{i,j}}{\partial x^2} \approx \frac{\left(\phi_{i+1,j} - \phi_{i,j}\right)/\Delta x - \left(\phi_{i,j} - \phi_{i-1,j}\right)/\Delta x}{\Delta x}$$

$$= \frac{\phi_{i+1,j} + \phi_{i-1,j} - 2\phi_{i,j}}{\left(\Delta x\right)^2}$$

2-D

$$\nabla^2 \phi_{i,j} \approx \frac{\phi_{i+1,j} + \phi_{i-1,j} - 2\phi_{i,j}}{\left(\Delta x\right)^2} + \frac{\phi_{i,j+1} + \phi_{i,j-1} - 2\phi_{i,j}}{\left(\Delta y\right)^2}$$

Typically, $\Delta x = \Delta y = \Delta$

$$\boxed{\phi_{i,j} \approx \frac{1}{4}\left(\phi_{i+1,j} + \phi_{i-1,j} + \phi_{i,j+1} + \phi_{i,j-1}\right)}$$

Potential at each point is average of that at neighboring points

$$\phi_{i,j} \approx \frac{1}{4}\left(\phi_{i+1,j} + \phi_{i-1,j} + \phi_{i,j+1} + \phi_{i,j-1}\right)$$

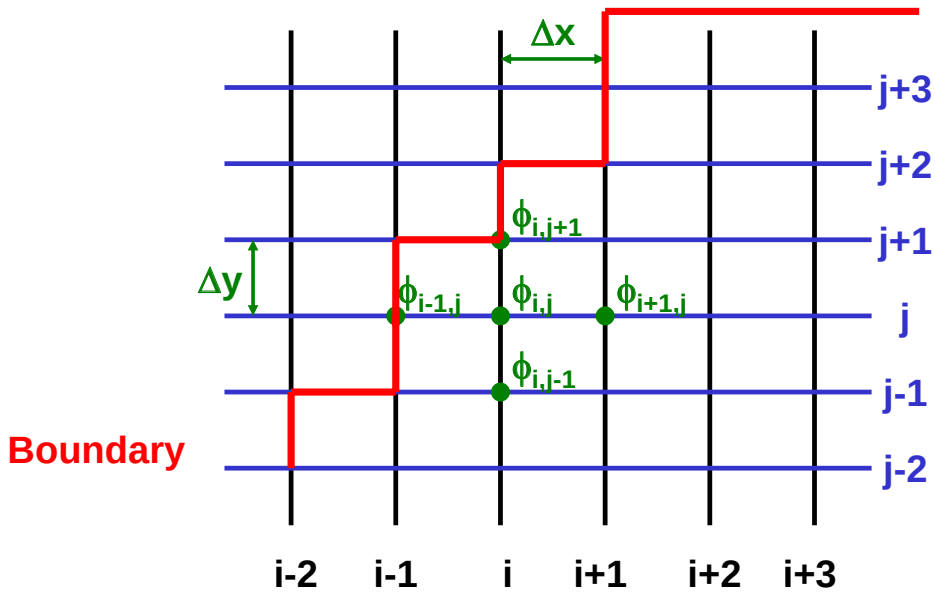

Poisson's Equation

Q_{ij} – charge in cell

$$\left(\phi_{i+1,j} + \phi_{i-1,j} + \phi_{i,j+1} + \phi_{i,j-1}\right) - 4\phi_{i,j} \approx -\frac{\rho_{i,j}\Delta^2}{\varepsilon_o}$$

$$\phi_{i,j} \approx \frac{1}{4}\left(\phi_{i+1,j} + \phi_{i-1,j} + \phi_{i,j+1} + \phi_{i,j-1}\right) + \frac{1}{4}\frac{Q_{i,j}}{\varepsilon_o}$$

Can generalize to 3-D …

Algorithms for Solving Coupled Difference Equations

A. Tridiagonal matrices: 1-D Problems

B. Finite-Difference Methods: (for higher-D)

- **Gauss-Seidel:** Iteration
- **Successive Over-Relaxation (SOR):** Enhanced Iteration
  Most general method.
- **Multi-grid** Methods: SOR with changing grid size each iteration.
- **Conjugate Gradient**: Sparse Matrices

C. Fourier Transforms.

A. Tridiagonal Matrices

1-D

$$\phi_{i-2} - 2\phi_{i-1} + \phi_i = -\frac{\Delta^2 \rho_{i-1}}{\varepsilon_o}$$

$$\phi_{i-1} - 2\phi_i + \phi_{i+1} = -\frac{\Delta^2 \rho_i}{\varepsilon_o}$$

$$\phi_i - 2\phi_{i+1} + \phi_{i+2} = -\frac{\Delta^2 \rho_{i+1}}{\varepsilon_o}$$

$$\begin{pmatrix} -2 & 1 & 0 & 0 & 0 & 0 \\ 1 & -2 & 1 & 0 & 0 & 0 \\ 0 & 1 & -2 & 1 & 0 & 0 \\ 0 & 0 & 1 & -2 & 1 & 0 \\ 0 & 0 & 0 & 1 & -2 & 1 \\ 0 & 0 & 0 & 0 & 1 & -2 \end{pmatrix} \begin{pmatrix} \phi_1 \\ \vdots \\ \phi_6 \end{pmatrix} = \boxed{\begin{pmatrix} -\phi_0 \\ 0 \\ 0 \\ 0 \\ 0 \\ -\phi_7 \end{pmatrix}} - \boxed{\frac{\Delta^2}{\varepsilon_o} \begin{pmatrix} \rho_1 \\ \vdots \\ \rho_6 \end{pmatrix}}$$

Source

Boundaries

B. Finite Difference Methods

1. Write Difference equations for each point on the grid.
2. Results in system of N coupled *algebraic* equations with N unknowns where N is the number of gridpoints.
3. Can solve, in principle at least.

In practice, for large N, or for complicated boundaries, system can be difficult to solve. For example, inversion of large matrix not computationally efficient.

Iterative Solution Procedure (Gauss-Seidel)

1. Initial guess of ϕ at all points.
2. Calculate charge density and load on grid.
3. Impose Boundary Conditions
4. Generate Next Guess by calculating potential at each point from existing data.
5. Iterate until solution converges (typically some 200 iterations).

Demonstration

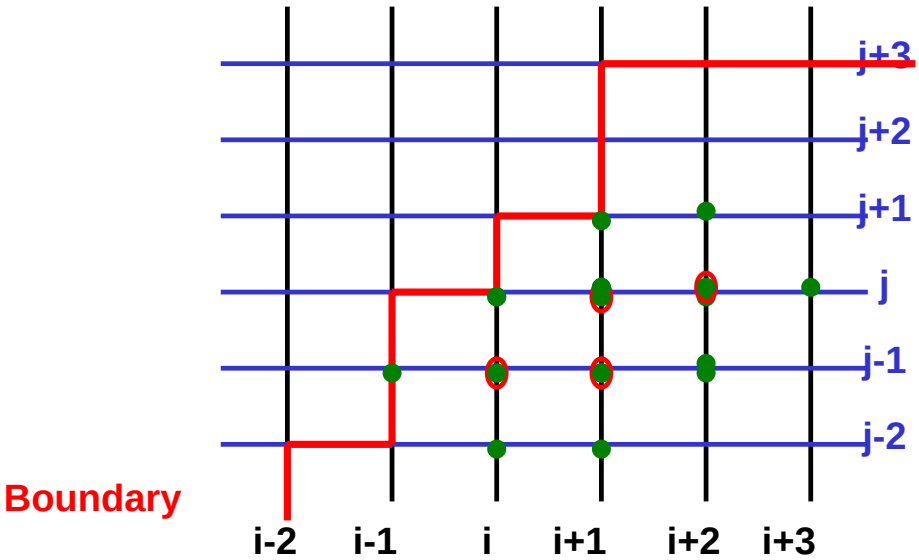

Successive Over-Relaxation (SOR) Method

Define Residual for each iteration, n:

$$
\begin{aligned}
{}^{n}R_{i,j} &= {}^{calc}\phi_{i,j} - {}^{n-1}\phi_{i,j} \\
&= \frac{1}{4}\left(\phi_{i+1,j} + \phi_{i-1,j} + \phi_{i,j+1} + \phi_{i,j-1}\right) - \phi_{i,j}
\end{aligned}
$$

$$
{}^{n}\phi = {}^{n-1}\phi + \omega\, {}^{n}R
$$

Over-relaxation coefficient, $1 \le \omega \le 2$

Obviously, solution converges when R = 0

Notes on SOR method

Check for yourselves:

$\omega = 1$ corresponds to simple averaging and iteration (Gauss-Seidl)

$\omega = 2$ corresponds to overshooting so as to achieve faster convergence. Gives more weight to new value of ϕ.

Convergence still SLOW!

E.g., for an $n \times n$ 2-D grid, calculation time ~ n^3, since need order n iterations to propagate errors out of mesh.

So Why use SOR?

Finite-Difference gives closed set of equations, so can solve in principle.

Solution can get messy for complicated geometries.

SOR does not care about complexity of boundaries!

Takes about as much time to solve a complicated problem as a simple one, for a given number of grid cells.

Multi-Grid Iteration

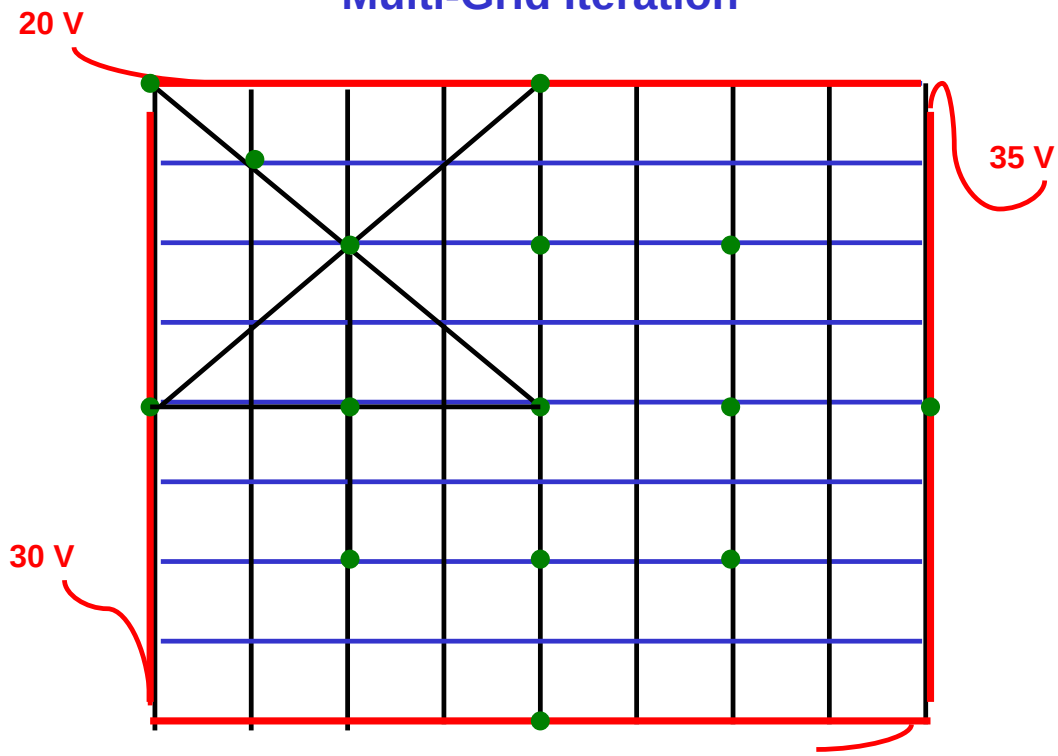

Faster than SOR for same resolution

C. FFT Methods

See Lund Notes

Much faster than SOR - no iterations are needed.

Basic idea:

Transform to Fourier Domain $\rho_{i,j} \rightarrow \rho\left(k_x, k_y\right)$

$$\phi_{i,j} \rightarrow \phi\left(k_x, k_y\right)$$

Differentiation becomes multiplication

$$\nabla^2 \phi_{i,j} \rightarrow -\left(k_x^2 + k_y^2\right)\phi\left(k_x, k_y\right)$$

$$\phi\left(k_x, k_y\right) = \frac{\rho\left(k_x, k_y\right)}{\varepsilon_o\left(k_x^2 + k_y^2\right)}$$

Transform Back to spatial domain

Why FFT?

Takes advantage of Fast Fourier Transform routines, hence converges much faster:

FFT of N points takes ~ N log N calculations

For n × n 2-D grid, total number of points $N = n^2$, so FFT converges as $n^2 \log n^2 = 2\, n^2 \log n$

Better than n^3

Limitation of FFT Method

Can only implement simple boundaries, e.g., round pipe.

To include conducting boundary, calculate equivalent image charge needed to produce zero-potential on it.

1. **Calculate a capacitance matrix relating potential on boundary points to image charges at the boundary.**
2. **Solve for the potential without any images.**
3. **Multiply the potential at the boundary points by the capacitance matrix to get the induced images.**
4. **Add the images to the total charge and recalculate the potential.**

Magnetostatic Calculations

Frequently desire to know magnetic field of a DC electromagnet. Know current configuration, want B-field.

Possible methods:

- Vector Potential
- Biot-Savart Law

$$\boxed{\vec{B} = \frac{\mu}{4\pi}\Sigma\left(\frac{Id\vec{s}\times\hat{r}}{r^2}\right)}$$

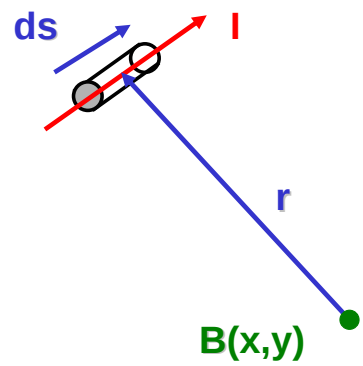

Electromagnetic

Use full set of equations.

$$\vec{\nabla}\times\vec{E} = -\frac{\partial\vec{B}}{\partial t} \qquad \vec{\nabla}\bullet\vec{E} = \frac{\rho}{\varepsilon_o} \rightarrow 0$$

$$\vec{\nabla}\times\vec{B} = \frac{1}{c^2}\frac{\partial\vec{E}}{\partial t} + \mu_o\vec{J} \rightarrow 0 \qquad \vec{\nabla}\bullet\vec{B} = 0$$

Absence of space charge leads to wave equation in free space

$$\frac{\partial^2\vec{E}}{\partial t^2} = -c^2\nabla\times\nabla\times\vec{E}$$

Wave Equation

$$\frac{\partial^2 \eta}{\partial t^2} = c^2 \frac{\partial^2 \eta}{\partial x^2}$$

Notes on Electromagnetic Calculations

- In general more difficult to solve.
- Time needs to be discretized as well.
- For leapfrog algorithms, x and v not known simultaneously. Hence, ρ, and **J**, and consequently **E** and **B** not known simultaneously either.
- Leads to instability if $c\,\Delta t > \Delta x$

Courant Condition: $$(c\Delta t)^2 \left(\frac{1}{\Delta x^2} + \frac{1}{\Delta y^2} \right) < 1$$

Particle-in-Cell Codes (PIC)

Rami Kishek

Particle-in-Cell (PIC)

Self-Consistent method for solving
Maxwell's Equations and **Lorentz Force Law**:

Uses **macroparticles** to sample actual particles

Represents **fields on a grid**.

Structure of a PIC Code

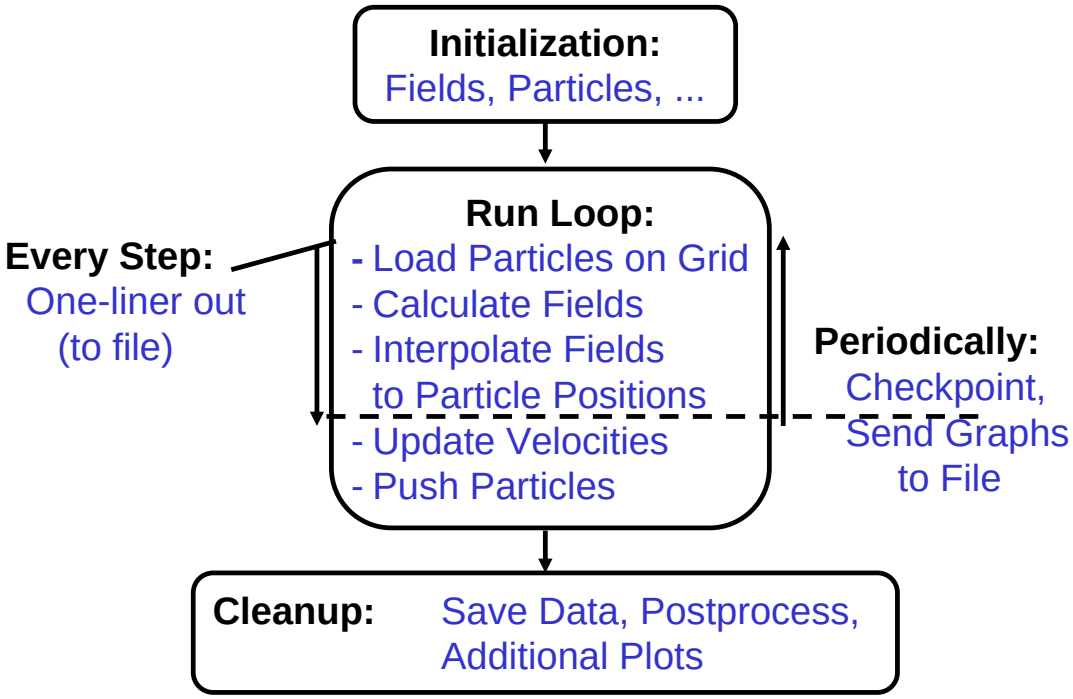

Components of a PIC code

- Field Calculation
- Particle Pushing
- Interpolation schemes
- Particle Loading
- Diagnostics and Output.

Interpolation Schemes

Nearest Gridpoint (NGP)

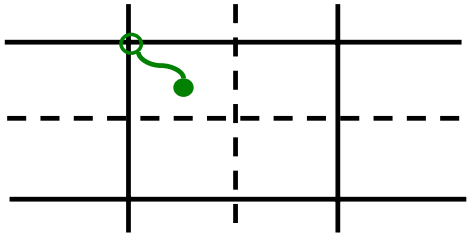

Cloud-in-cell

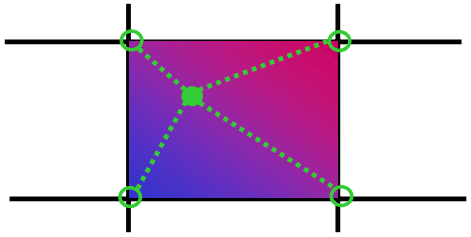

Higher-Order

Particle Loading

- Populating Phase Space
- Random number generation
- Initial distributions

Particle Simulation Caveat: Particle Loading

Populating Phase Space:

"Pseudo-Random" vs. "Quiet Start"

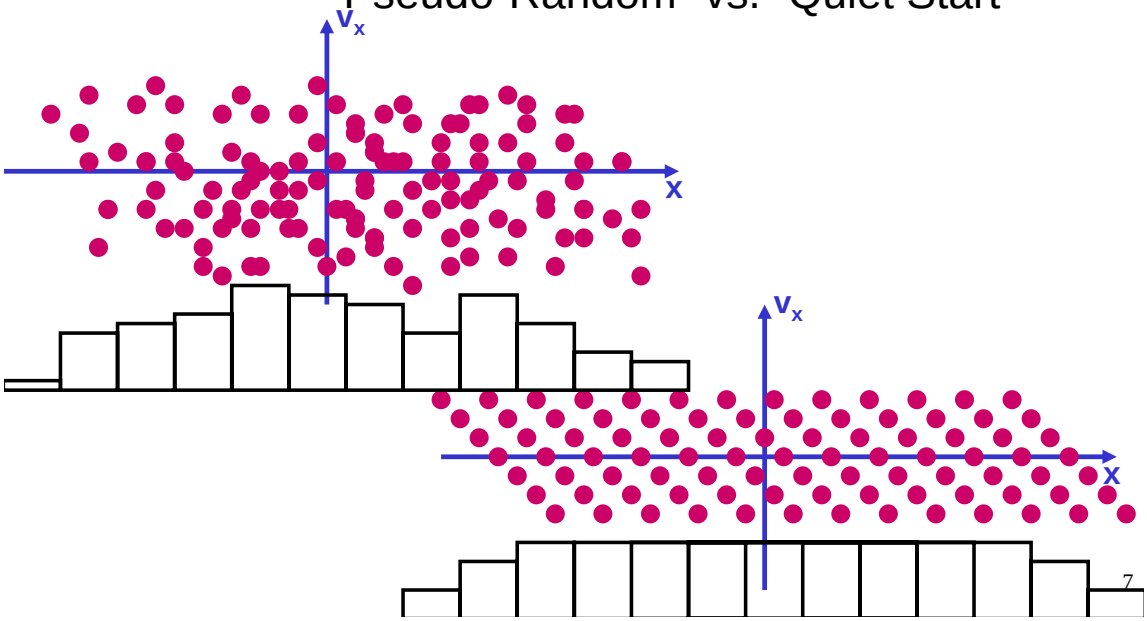

Particle Simulation Caveat: Particle Loading

Populating Phase Space:

"Pseudo-Random" vs. "Quiet Start"

The Dangers of "Quiet-Start"

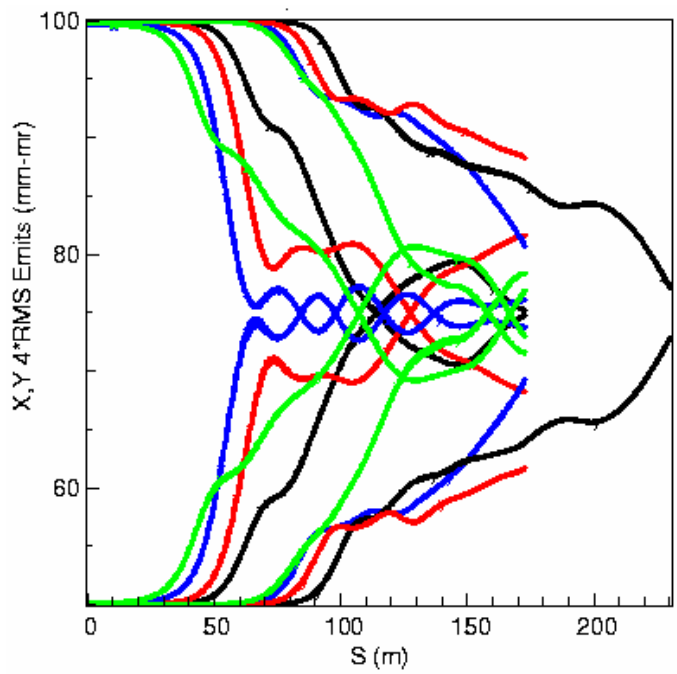

Enhancing Speed

- Symmetry
- Filtering

Self-Consistency

- With sufficient space charge, forces generated between particles need to be included in model.
- Motion of the particles will change these self-forces, hence the calculation needs to be updated as the particles move, e.g., every time step.
- Space charge forces can be represented in several different ways, e.g., as an averaged linear force, etc.
- We are primarily interested in a representation of space charge forces that is self-consistent with the particle model.

Output

- 1/2 Time step to synchronize position and velocity before recording output. Visualization is an important aspect.
- Real-time interactive graphics vs.. No Output!

One-liners: a Suitable Compromise

One line of text for each step listing values of selected variables. Useful for keeping an eye in case anything goes wrong, e.g.,

```
it =    30 zbeam =   0.4500 2*xrms =    9.52 emity =  58.55 nplive =     1000
it =    40 zbeam =   0.6000 2*xrms =    9.81 emity =  58.56 nplive =     1000
it =    50 zbeam =   0.7500 2*xrms =   10.11 emity =  58.56 nplive =     1000
```


Graphical Output

- Graphical output is for human consumption.
- Need graphics in order to condense the massive amounts of data generated by simulation.
- Need to display it in presentable form.
- Graphical output also useful for comparison of different simulations.

Sources of Error

- Macroparticle Statistics
- Discrete Time Step
- Discrete Potential (gridcells)
- Input and initialization errors; particle loading
- Modeling issues

Advanced Computing Topics

Rami Kishek

Parametric Resonance

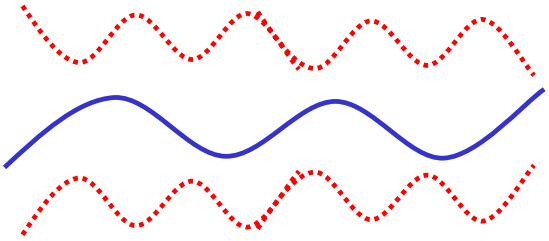

Envelope oscillations

Particle oscillations

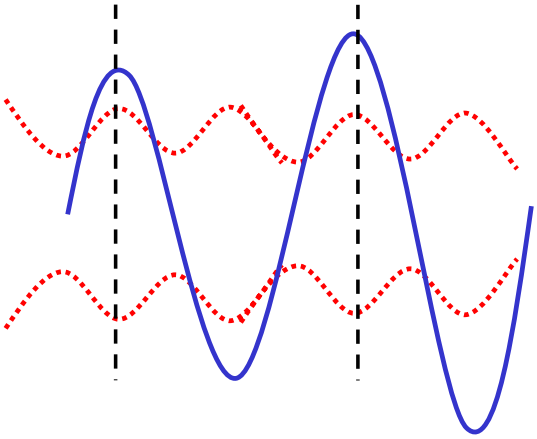

Envelope oscillations

Particle oscillations

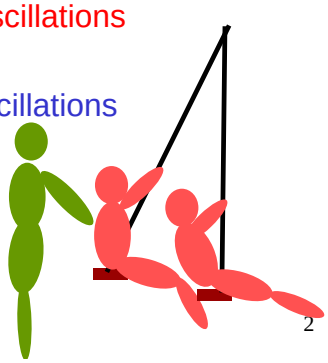

First UMER Experiments (during construction)

24 mA, 10 keV

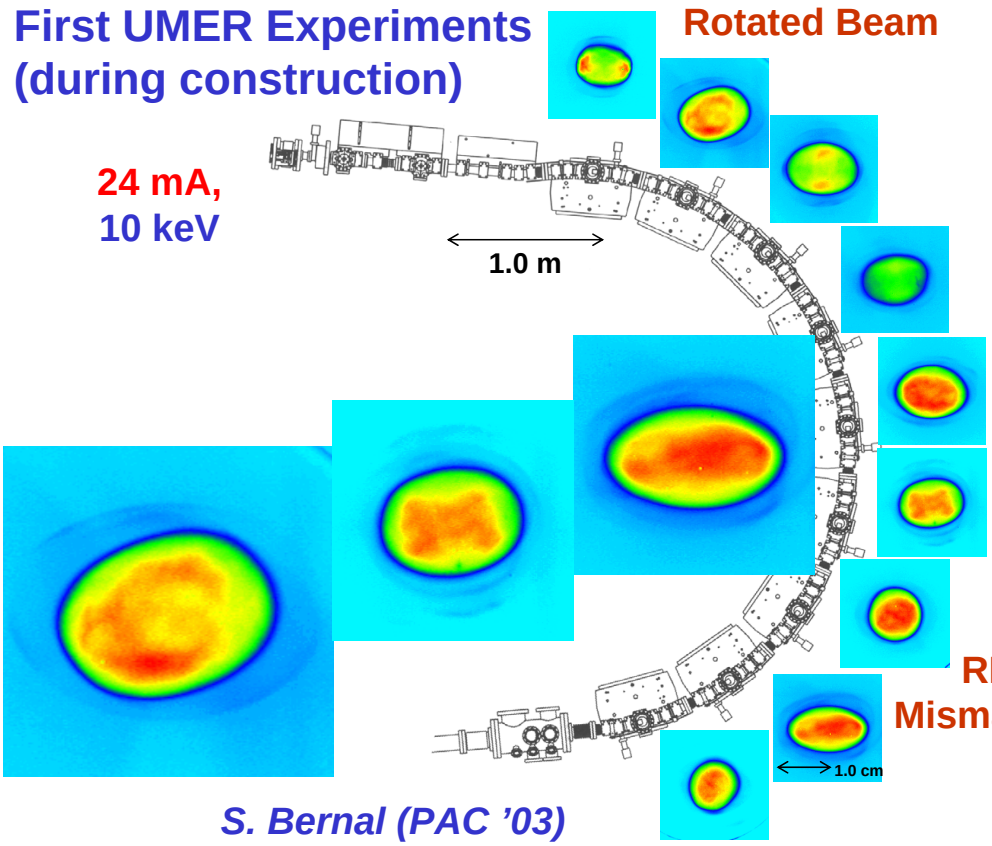

S. Bernal (PAC '03)

Dynamic Range Problem

- Interested in halos.
- Halos can contain as little as 10^{-5} particle density as in the main beam.
- Resolving that accurately requires very good particle statistics. For a PIC code, this means 10^9 particles, or more.

Possible Solutions

1. Enhance Speed of PIC codes:
   - Sub-Cycling: do not solve for fields at every step
   - Split-operator techniques (maps + PIC)
2. Particle-Core Models
3. Subtract out main beam particles, I.e., look only at halo or perturbation ➲ δf
4. Direct Solution in terms of particle "density" ➲ "Vlasov Solvers"
5. Hybrid Codes

2. Particle Core Model: Edge Lensing

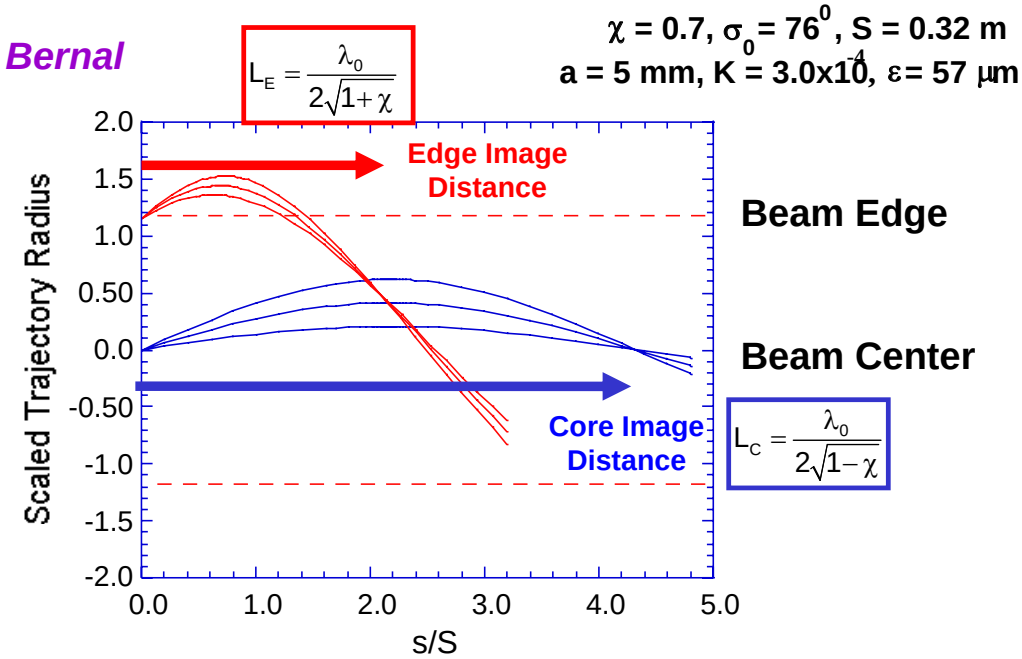

Theory / P-Core Model

Matrix Techniques and Maps

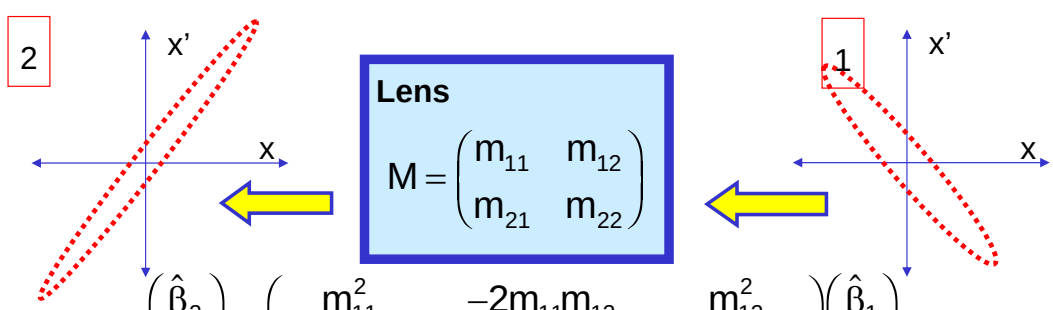

$$M = \begin{pmatrix} m_{11} & m_{12} \\ m_{21} & m_{22} \end{pmatrix}$$

$$\begin{pmatrix} \hat{\beta}_2 \\ \hat{\alpha}_2 \\ \hat{\gamma}_2 \end{pmatrix} = \begin{pmatrix} m_{11}^2 & -2m_{11}m_{12} & m_{12}^2 \\ -m_{11}m_{21} & 1+2m_{12}m_{21} & -m_{12}m_{22} \\ m_{21}^2 & -2m_{21}m_{22} & m_{22}^2 \end{pmatrix} \begin{pmatrix} \hat{\beta}_1 \\ \hat{\alpha}_1 \\ \hat{\gamma}_1 \end{pmatrix}$$

TRANSPORT: Library of lattice element matrices

TRACE: Advances beam ellipse using matrix models of lattice

MARYLIE: Lie mapping of lattice elements, can handle nonlinearity

Following slides courtesy of VNL …

Alex Friedman, Ron Davidson, Eric Sonnendrucker,
Wei W. Lee, Bill Sharp, & Dave Grote

3. Perturbative (δf) Method: PPPL code BEST

E.g., Electron-Proton 2-Stream Instability, growing from initial noise

Dipole "surface mode" can be destabilized by background electrons

For each particle,
$f_i = f_{i0} + \delta f_i$

Evolve δf_i step-by-step along orbit

In a nonlinear calculation, orbit is computed using full field $E_0 + \delta E$

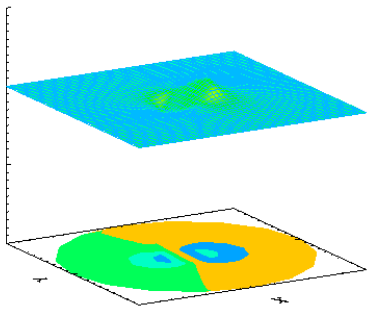

initial

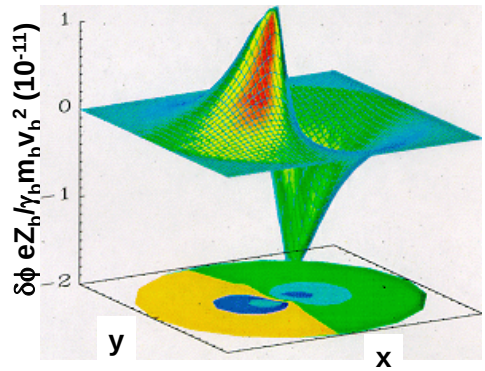

t= 200/ω_β

Offers reduced noise for detailed studies of instability, beam-plasma, and electron processes.

Review: Computation: Vlasov Solvers

No particles!

6-D (4-D) grid

- Define density in phase space, $f(x,y,z, v_x,v_y,v_z)$
- Evolve by numerically solving Vlasov Equation

Advantages:

- Get smooth distribution at all times, no numerical collisions.

Disadvantages:

- Grid very large compared to PIC code with same resolution (e.g. 128^2 = 16.3k; 128^4 = 268M).
- Advancing each cell requires interpolation every time step.

4. Semi-Lagrangian Vlasov Solver (SLV)

The distribution function $f(\underline{x},\underline{v})$ is retained at nodes of a 4-D mesh

The calculation reaches backward in time along a characteristic (orbit in phase space) to obtain the current value of f at each node

Thus, Low-density and high-density regions of phase space are tracked equally well; this is useful for halo studies

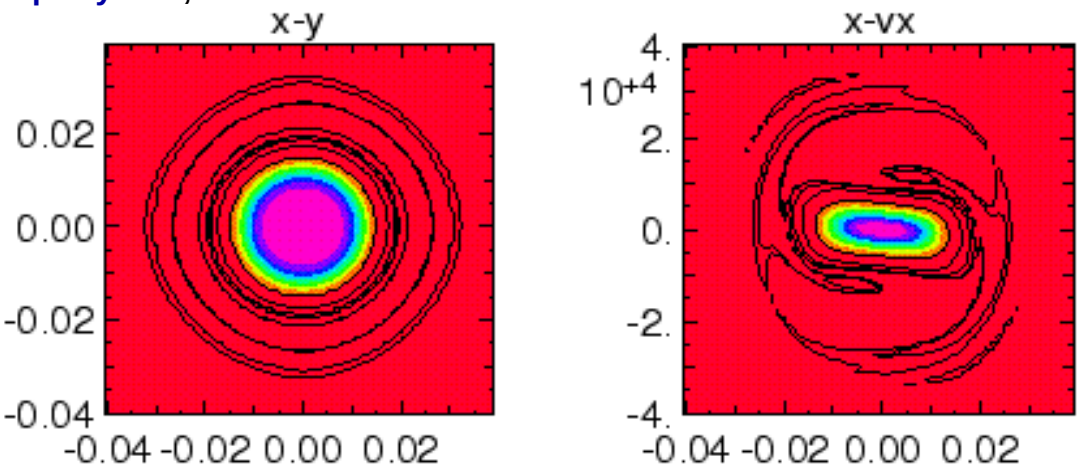

Black contour lines: 0.1, 0.01, 0.001, 0.0001, and 0.00001 of peak

5. Moment methods (e.g. CIRCE)

- Physics model:
  - longitudinal: hundreds of “slices” in a Lagrangian fluid model
  - transverse: each slice evolved using envelope and centroid equations
- Applications:
  - acceleration and compression schedules, “ears”
  - error tolerances
  - beam sensing and steering
- Limitations (perhaps not fundamental ...):
  - no model for emittance growth or phase-mixing of “mismatch”
  - no module impedance model
  - slow variation along beam assumed

The beam's current and velocity must be tailored to achieve compression and pulse shaping (CIRCE calculation)

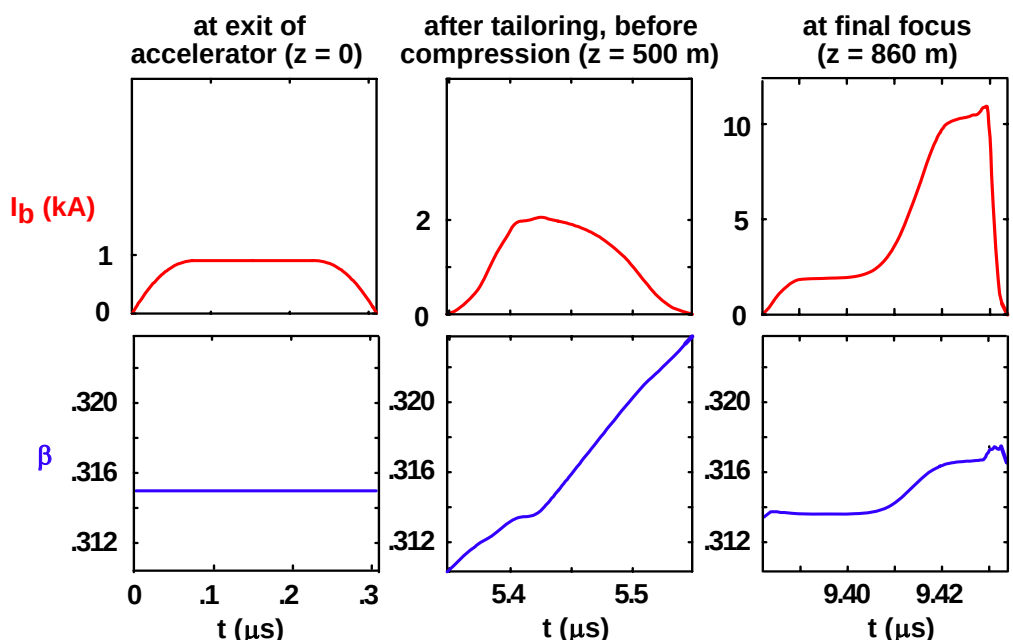

Testing: A Case Study on Validation

Rami Kishek

Quote of the Day

"After you break up with your girlfriend, it takes twice as much time to get over her as the time you actually spent together!"

- a friend of mine

"After you think you're done writing a program, it takes you twice as much time to debug it as the time you actually spent writing it."

- my rule of thumb

WARP Code

- Electrostatic Particle-in-Cell (PIC) Code.
- Flexible Geometries: 2-D (x-y, r-z) and 3-D.
- Contains various accelerator models for representing external lenses.
- Includes many different Poisson solvers (SOR, FFT, multi-grid, adaptive meshing). Subgrid interpolation allows for curved boundaries.
- Follows the beam around bends.

5-Beamlet Experiment

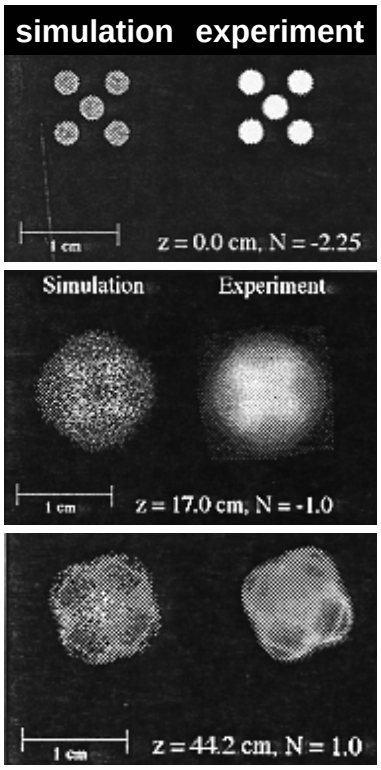

~ 1989

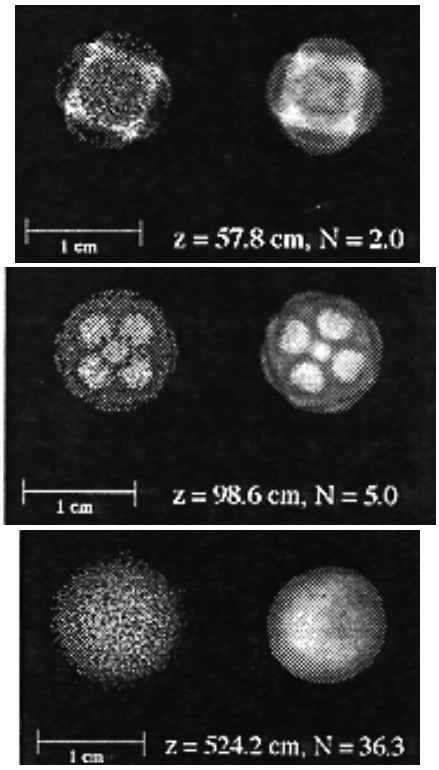

e-Beam Injector Experiment, 1998-1999

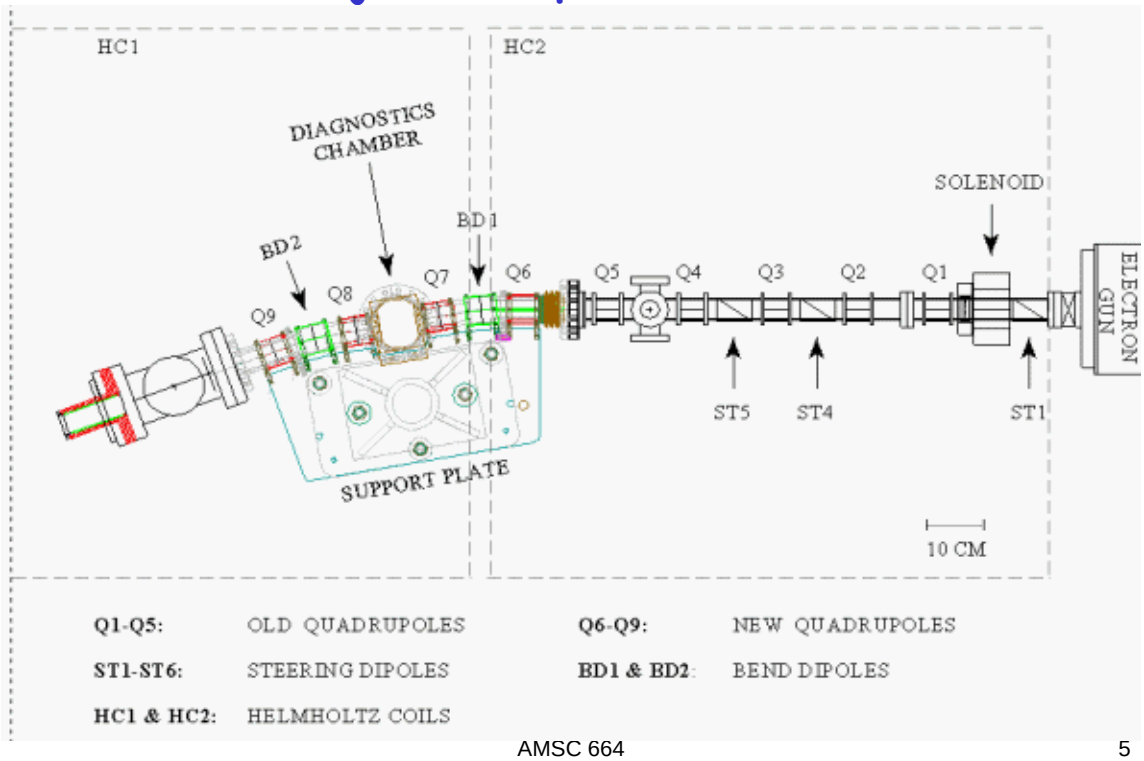

Experimental setup complicated

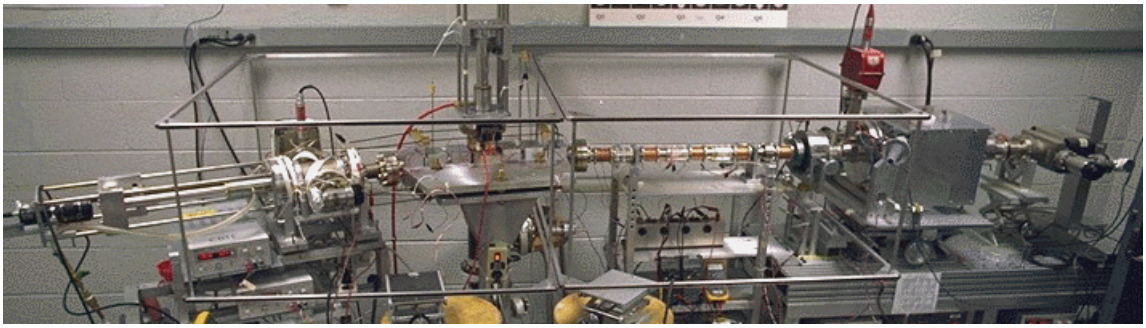

http://www.ireap.umd.edu/umer/ringdesign/protoinjexper.html

Phosphor screen photo used to determine size

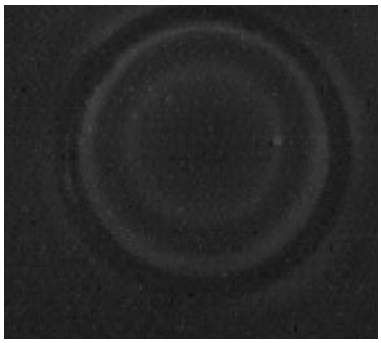

Profile across cross-section is hollowed:

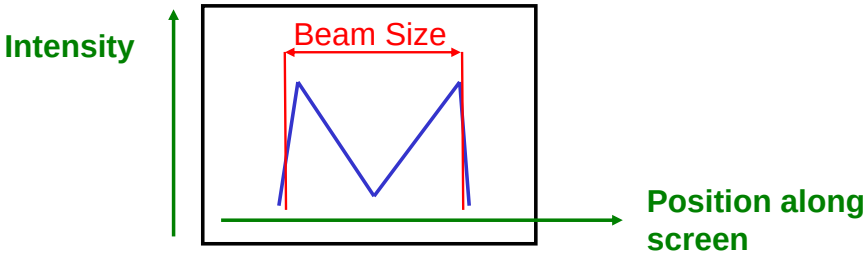

Initial Results Disagree

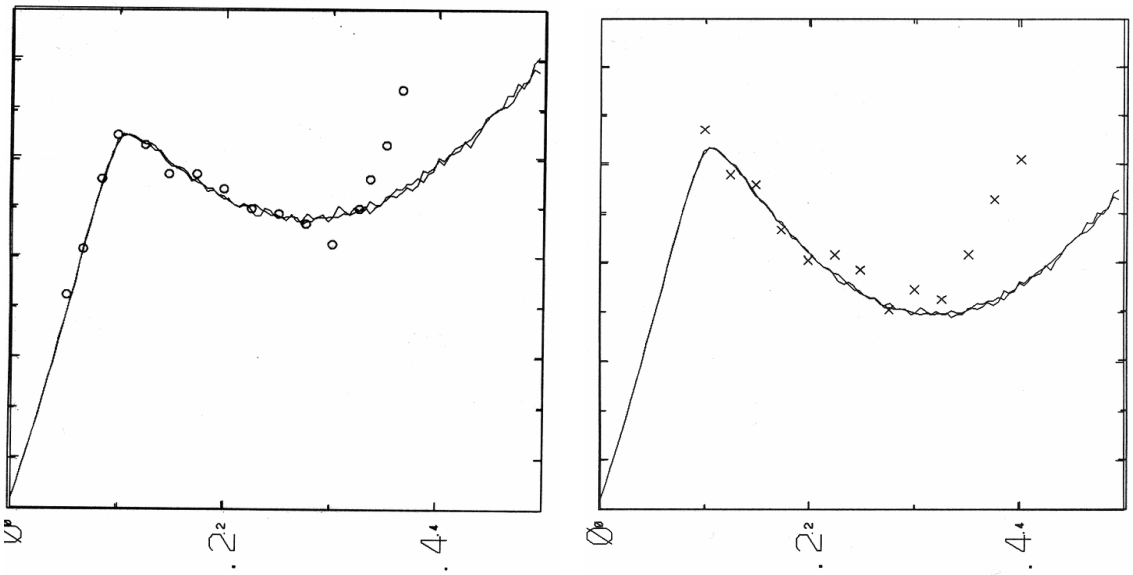

Simulation

Experiment

Attempted different models to reproduce data

1. Slightly varied initial conditions
2. Slightly varied magnet strength
3. Refined description of magnet fields
4. Added relativistic effects
5. Superimposed effect of beam ends

Beam Ends – a Clever Explanation

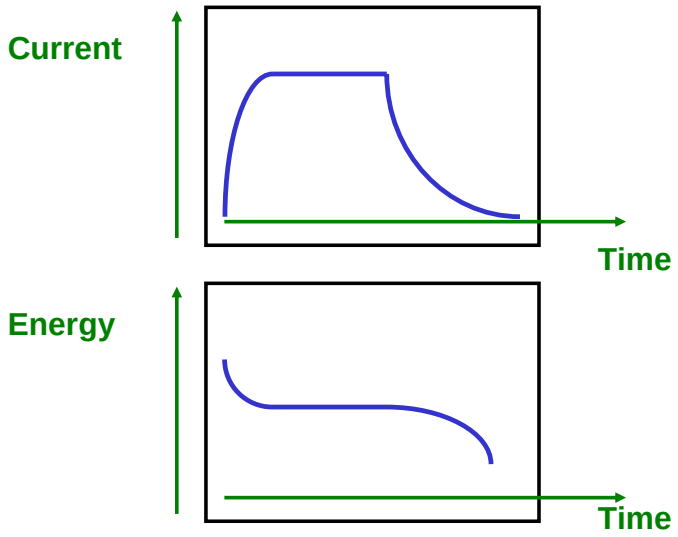

P-screen an Integrating Diagnostic

Near Perfect Fit

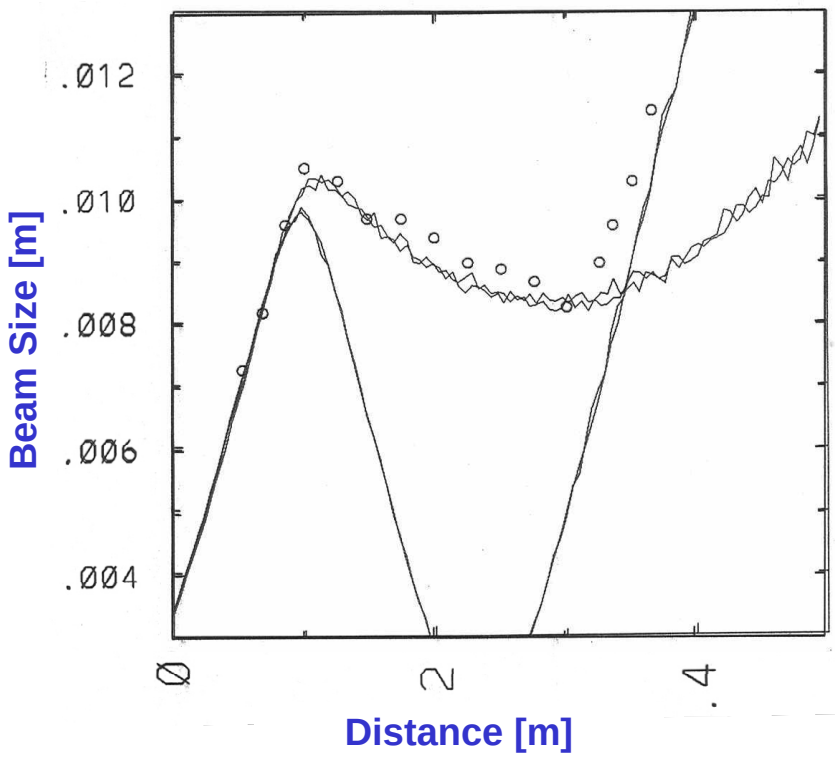

Beam Ends – an Explanation?

- Perfect agreement between simulation code and experiment …
- … without either of them agreeing with reality

- Testing the Hypothesis: Experiment with different pulse lengths

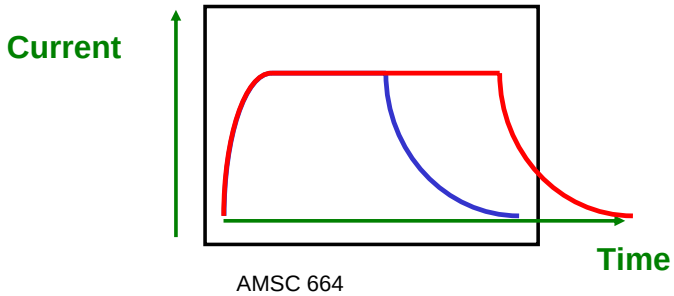

One day in the lab, however, caught a strong hint

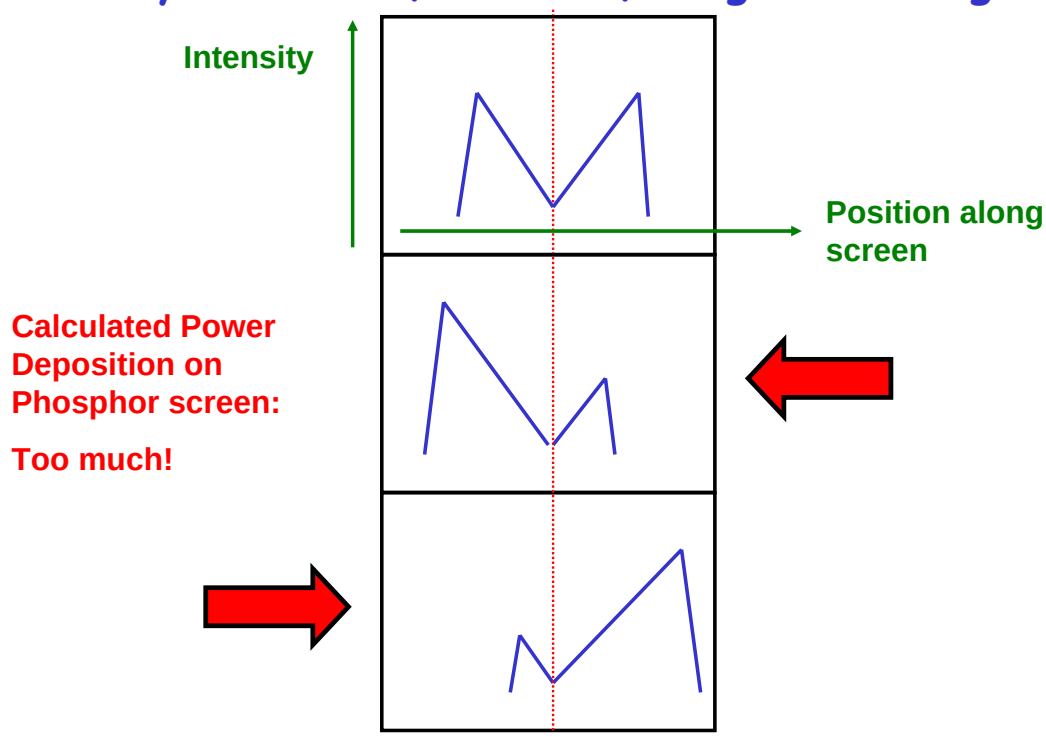

Attempted Explanations of Disagreement

- Wrong magnetic fields or initial conditions - Sensitivity Studies (Solenoid Strength, Initial Slope, Emittance)
- Possibility of head and tail particles smearing measurement - P-screen an Integrating Diagnostic
- Code problems? Benchmarked some other published experiment - OK.
- Experiment: P-screen damage? Power deposition

Opened Up Experiment: found many things wrong

1. Phosphor-screen was damaged
2. Initial conditions (measured using screen) were wrong (by factor of 2)!
3. Hence, magnets were also set for wrong values in experiment
4. Magnetic field used in simulation not exactly as experiment
5. Camera system dated to 1980s, needed replacement
6. Processing of experimental data slow – used image processing to automate and enhance

Another Problem: Solenoid Magnet Field Profile

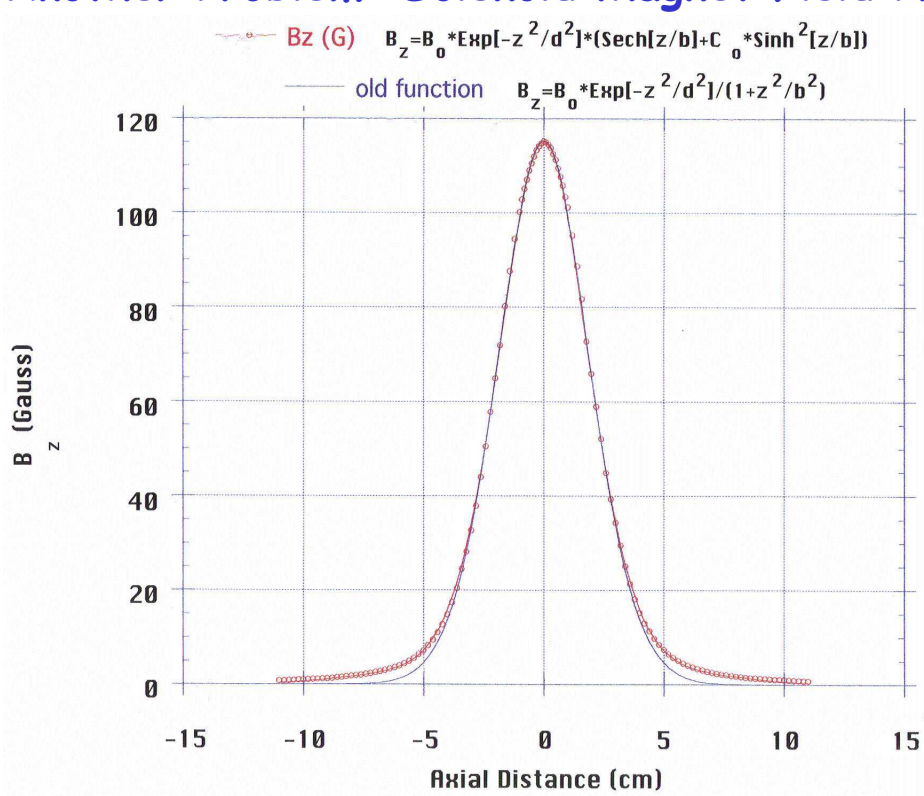

Revision of experiment and simulation resulted in much better agreement

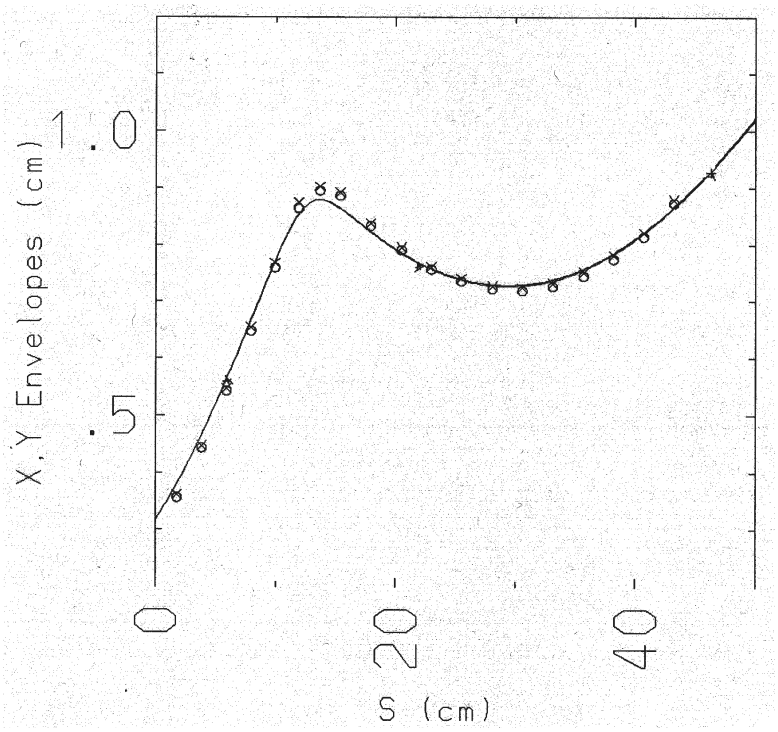

Agreement also in density profile

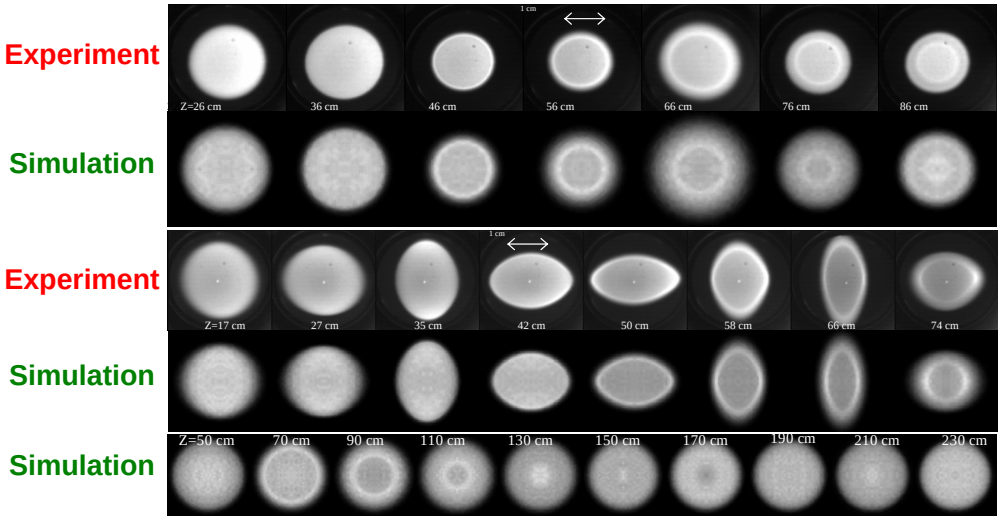

S. Bernal, et. al., PRL, **82**, 4002 (1999).

J.J. Barnard and S.M. Lund, USPAS, Jan. 2004

Simulation Techniques for Intense Beams

Outline

1. Why Numerical Simulation

2. Classes of Intense Beam Simulations
   - A. Particle Methods
   - B. Distribution Methods
   - C. Moment Methods.

3. Numerical Methods
   - A. Discritizations
     - Derivatives
     - Integrals
   - B. Application to Moment Methods
     - Euler and Runge-kutta advances
     - Example Application

4. Numerical Methods for Particle and Distribution Methods
   - A. Field discritizations
   - B. Particle Methods and "PIC" Codes for solving Vlasov's equation.
     - Leapfrog advance
     - Field solution
     - Particle weighting
     - Advance cycle
     - Initialization
     - Numerical convergance
     - Examples

C. Distribution Methods

- Similarities with particle methods

Will not cover in class - only mention qualitatively

- Distribution advance
- Examples

5. Overview of the WARP code

References.

Simulation Techniques for Intense Beams

§1 Overview: Why Numerical simulation?

- Builds intuition on intense beam dynamics.
  The primary purpose of simulation is to gain insight on trends, sensitivities, etc. – not specific numbers!
  In contrast to laboratory experiments:
  - Full nonintrusive beam diagnostics are possible
  - Effects can be turned on and off.

  This insight can also be applied to motivate approximations in analytical analysis.
- Allows analysis of more realistic situations that can be intractable in analytical analysis.
  - Realistic geometries
  - Non-ideal distributions
  - Combined effects
  - Large amplitude (nonlinear) effects.

- Expected performance of specific machines can be quantified.

- Computers and numerical methods / libraries are becoming more powerful enabling both analysis of more realistic problems and better numerical convergance.
  - Processor speed increasing
  - Parallel machine architectures
  - Memory larger

  } Hardware bigger and faster

  - Numerical methods improved
  - Libraries of debugged code modules

  } Software more developed

Although simulations are increasingly powerful and valuable in the analysis of intense beams, simulations should not be used to exclusion:

- Parametric scaling is <u>very</u> important in machine design. Often it is hardest to understand what specific choices should be made in physical aperture sizes, etc. Although scaling can be explored with simulation, Analytical analysis often best illustrates the tradeoffs, sensitivities, and relevant combinations of parameters.

- Concepts often fail due to limits of technology (fabrication tolerances, material failures, unanticipated properties, ...) and hence full laboratory testing is vital. Many understood classes of error can be probed with simulation though – unanticipated sources are most dangerous.

- Economic realities often severely limit what can be constructed and such limitations must be understood so you do not simulate something unobtainable.

The highest understanding and confidence is achived when results from analytic theory, numerical simulation, and experiment all converge.

These days numerical simulation skills also make you highly employable in many areas of accelerator and beam physics!

Numerous programing languages are employed in numerical simulations of intense beams. The most common today are:

Fortran, Fortran 90
C, C++
Java

Results are analyzed with a variety of graphics packages:

NCAR, gist, gnuplot, idl, narcisse, ...

Perhaps the most modern and flexible way simulation packages can be structured is to link routines programmed in fast, compiled code with an interactive interpreter such as:

python, basis, yorick

- Allows routines to be coded in mixed languages and (form python) in modern, object-oriented structure.
- Flexible reconfiguration of code modules possible to adapt for specific (unanticipated) needs
  - reduces need for recompilation and cumbersome structures for special uses.
  - aids cross-checking problems and debugging
- "Steering" of code during runs to address unanticipated effects.

Discussing particular programing languages and graphics packages is beyond the scope of this class. Here our goal is to survey numerical simulation methods employed without presenting details of specific implementations.

However,— We will show examples based on the "WARP" particle-in-cell code developed for intense beam simulation at LLNL and LBNL.

WARP - Named since it works on a "warped" Cartesian mesh with bends.

WARP is a family of particle-in-cell code tools built around a common python interpeter for flexable operation. It is optimized for the simulation of intense beams with self-consistent electrostatic space-charge forces

More on WARP later after discussion of methods etc.

J.J. Barnard and S. M. Lund
USPAS, Jan 2004

§2 Classes of Intense Beam Simulations

There are 3 distinct classes of modeling of intense ion beams applicable to numerical simulation

1/ Particle Methods
2/ Distribution Methods
3/ Moment Methods

All of these draw heavily on methods developed for the simulation of neutral plasmas.
The main differences:

- Lack of overall charge neutrality
  - Single species typical (though electron + ion simulations are common too.
- Directed motion of the beam.
- Applied field descriptions are setup for beam optical elements and accelerating structures.

Review/contrast these methods before discussing specific numerical implementations.

1/ Particle Methods

Classical point particles are advanced with self-consistent interactions given by the Maxwell Equations.

- Most general: If actual number of particles are used, this is approx. the physical beam.

Equations of motion (time domain, 3d, for generality)

i'th particle:

$$\boxed{\begin{aligned} \frac{d\vec{p}_i}{dt} &= \vec{F}_i = q\left(\vec{E} + \frac{d\vec{x}_i}{dt} \times \vec{B}\right) \\ m\gamma_i \frac{d\vec{x}_i}{dt} &= \vec{p}_i \,; \quad \gamma_i = \left[1 + \vec{p}_i^{\,2}/m^2c^2\right]^{1/2} \end{aligned}}$$

initial conditions:

$\{\vec{x}_i(t=0), \vec{p}_i(t=0)\}$

particle orbits

$\vec{x}_i(t), \vec{p}_i(t)$ solved as a function of time.

Fields (Electromagnetic in most general form)

$$\nabla \cdot \vec{E} = \frac{\rho}{\varepsilon_0}$$

charge density

$$\rho(\vec{x},t) = \rho_{ext}(\vec{x},t) + \sum_i q\,\delta[\vec{x} - \vec{x}_i(t)]$$

$$\nabla \times \vec{E} = -\frac{\partial \vec{B}}{\partial t}$$

external (applied)

particle beam

current density

$$\nabla \times \vec{B} = \mu_0 \vec{J} + \mu_0\varepsilon_0 \frac{\partial \vec{E}}{\partial t}$$

$$\vec{J}(\vec{x},t) = \vec{J}_{ext}(\vec{x},t) + \sum_i q \frac{d\vec{x}_i(t)}{dt}\,\delta[\vec{x} - \vec{x}_i(t)]$$

$$\nabla \cdot \vec{B} = 0$$

+ Boundary conditions on $\vec{E}, \vec{B}$.

2/ Distribution Methods:

- Based on reduced (statistical) continuum models of the beam.
- Two classes (microscopic) kinetic models and (macroscopic) fluid models.
- Here distribution means a function of cont. variables e.g. $f(\vec{x},\vec{p},t)$ in Vlasov model.

2a Kinetic Model (Vlasov, neglect collisions)

- Obtained from statistical averages of particle formulation

Equations of Motion

$$\boxed{\left\{\frac{\partial}{\partial t} + \vec{v}\cdot\frac{\partial}{\partial \vec{x}} + q\left(\vec{E} + \vec{v}\times\vec{B}\right)\right\} f(\vec{x},\vec{p},t) = 0}$$

$$\vec{v} = \frac{\vec{p}}{\gamma m} = \frac{\vec{p}/m}{\left(1+\vec{p}^2/m^2c^2\right)^{1/2}}$$

initial conditions:

$f(\vec{x},\vec{p},t=0)$

Distribution evolution

$f(\vec{x},\vec{p},t)$ evolved from $t=0$.

$\vec{x},\vec{p},t$ indep. variables.

Fields

Same as particle case with different expressions of ρ, $\vec{J}$:

$$\nabla\cdot\vec{E} = \frac{\rho}{\sqrt{\varepsilon_0}} \qquad \rho(\vec{x},t) = \rho_{ext}(\vec{x},t) + q\int d^3p\, f(\vec{x},\vec{p},t)$$

external (applied) — beam

$$\nabla\times\vec{E} = -\frac{\partial\vec{B}}{\partial t}$$

$$\nabla\times\vec{B} = \mu_0\vec{J} + \mu_0\varepsilon_0\frac{\partial\vec{E}}{\partial t} \qquad \vec{J}(\vec{x},t) = \vec{J}_{ext}(\vec{x},t) + q\int d^3p\, \vec{v}\, f(\vec{x},\vec{p},t)$$

$$\nabla\cdot\vec{B} = 0$$

+ Boundary conditions on $\vec{E}, \vec{B}$

The Vlasov equation is essentially a continuity equation for an incompressible "fluid" f in 6D phase-space. To see this, note that:

$$\frac{\partial}{\partial \vec{p}} \cdot \vec{v} \times \vec{B} = 0$$

so the Vlasov equation can be expressed as:

$$\boxed{\frac{\partial f}{\partial t} + \frac{\partial}{\partial \vec{x}} \cdot \underbrace{\left(\vec{v} f\right)}_{= d\vec{x}/dt|_{orbit}} + \frac{\partial}{\partial \vec{p}} \cdot \underbrace{\left(q\left[\vec{E} + \vec{v} \times \vec{B}\right] f\right)}_{= d\vec{p}/dt|_{orbit}} = 0}$$

Which is manifestly the form of a continuity equation in 6D phase-space. $\Rightarrow$ probability is not created or destroyed!

The effect of collisions can be added to this formulation by adding a collision operator:

$$\boxed{\frac{\partial f}{\partial t} + \vec{v} \cdot \frac{\partial}{\partial \vec{x}} f + q\left[\vec{E} + \vec{v} \times \vec{B}\right] \cdot \frac{\partial}{\partial \vec{p}} f = \left.\frac{\partial f}{\partial t}\right|_{coll}}$$

For most applications in beam physics

$$\left.\frac{\partial f}{\partial t}\right|_{coll}$$

can be neglected (see Intro. lectures). For exceptional cases specific forms of collision terms can be found in Nicholson, "Intro to Plasma Theory," Wiley 1983.

We will find later that the common Particle-in-Cell (PIC) is <u>not</u> really a particle method but rather a method that uses a collection of smoothed "macro" particles to simulate Vlasov's equation. This roughly can be 'understood' by noting that Vlasov's equation can be interpreted as

$$\frac{d}{dt} f(\vec{x}, \vec{p}, t) = 0$$

total derivative along a test particle.

$\Rightarrow$ Advance test particles in a continuous field "fluid" to erase collisions.

But Remember:

PIC is a method to solve Vlasov's equation <u>not</u> a discrete particle method.

This notion should become clear after these lectures.

2b Fluid Model

- Obtained from further averages of kinetic models.
- Described in terms of "macroscopic" variables (density, Flow velocity, Pressure, ...)
- Models must be closed (truncated) at some order via physically motivated assumptions (cold or negligible heat flow, ...)

Density n: $$n(\vec{x},t) = \int d^3p\, f(\vec{x},\vec{p},t)$$

Flow velocity $\vec{V}$: $$n\vec{V}(\vec{x},t) = \int d^3p\, \vec{v}\, f(\vec{x},\vec{p},t)$$

$\vec{P}$ $$n\vec{P}(\vec{x},t) = \int d^3p\, \vec{p}\, f(\vec{x},\vec{p},t)$$

Pressure Tensor $\mathcal{P}_{ij}$: $$n\mathcal{P}_{ij}(\vec{x},t) = \int d^3p\, [p_i - P_i(\vec{x},t)][v_j - V_j(\vec{x},t)] \cdot f(\vec{x},\vec{p},t)$$

Higher Rank Objects

Equations of Motion (Eulerian approach)

continuity: $$\frac{\partial}{\partial t} n + \frac{\partial}{\partial \vec{x}} \cdot [n\vec{V}] = 0$$

Force: ith comp. $$n\left(\frac{\partial}{\partial t} + \vec{V}\cdot\frac{\partial}{\partial \vec{x}}\right) P_i + \sum_j \frac{\partial}{\partial x_j} \mathcal{P}_{ij} = nq\left[\vec{E} + \vec{V}\times\vec{B}\right]_i$$

Higher order – Models must be truncated.
Simplist: cold fluid ($\mathcal{P}_{ij} \equiv 0$)

Field

Same as the kinetic and particle case with

$$\rho(\vec{x},t) = \rho_{ext}(\vec{x},t) + qn(\vec{x},t)$$

$$\vec{J}(\vec{x},t) = \vec{J}_{ext}(\vec{x},t) + qn(\vec{x},t)\,\vec{V}(\vec{x},t)$$

Aside: Lagrangian Formulations of Distribution Methods

In certain kinetic and especially fluid models it can be convenient to adopt so-called "Lagrangian" models.

Eulerian fluid model: flow quantities specified in terms of space ($\vec{x}$) and time (t). $\vec{V} = \vec{V}(\vec{x}, t)$.

Lagrangian fluid model: Identify parts of the flow with objects (material element) and follow the flow in time (t). (shape of elements must generally change in t)

In reality many particle methods are really hybrid Lagrangian too:

- Smoothing methods in the common PIC (Particle In Cell) method (to be covered) typically employ shaped particles that may be thought of as Lagrangian elements representing a Vlasov fluid.

<u>Example:</u> 1D Lagrangian model of the longitudinal evolution of a cold beam.

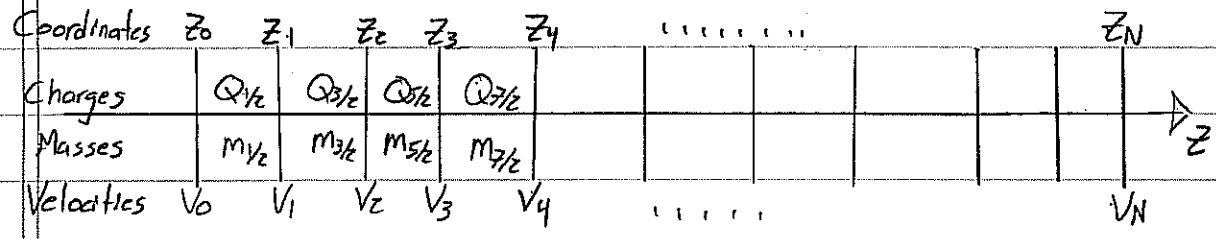

z_i	slice boundaries	$Q_{i+1/2}$	Fixed	$\frac{Q_{i+1/2}}{m_{i+1/2}} = \frac{q}{m}$	
V_i	velocities of slice boundaries.	$m_{i+1/2}$	Fixed		$= \text{const}$ for single species. (set initial cond.)

Solve the equations of motion:

$$\frac{dz_i(t)}{dt} = V_i(t)$$

$$\frac{dV_i(t)}{dt} = \left(\frac{q}{m}\right) E_z(z_i, t)$$

for all the slice boundaries. Several methods might be used to calculate E_z:

1) Take "slices" to have some radial extent modeled by a $\perp$ envelope etc. and deposit the $Q_{i+1/2}$ onto a grid and solve:

$$\nabla^2 \phi = -\frac{\rho}{\varepsilon_0} \qquad E_z = -\frac{\partial \phi}{\partial z}$$

subject to $E_z \to 0$ as $|z| \to \infty$

2) Employ a "g"-factor model

$$E_z = \frac{-g}{2\pi\varepsilon_0} \frac{\partial \lambda}{\partial z}$$

λ calculated from Q_i and radial extent of elements etc.

3) Pure-1d model and use Gauss' Law

//

3/ Moment Methods (with all phase space variations integrated over)

- Most reduced description of intense beam.
- Beam represented by a finite (closed and truncated) set of moments that are advanced from initial values.
  Here by moments, we mean functions of a single variable s or t.
- Such models usually are not fully self-consistent but are commonly used for lattice design.
  - Some special cases such as a stable $\perp$ KV equilibrium distribution are consistent with truncated moment description (rms envelope eqn.)
  - Typically derived from assumed distributions with self-similar evolution.

Many moment models exist. Illustrate with examples for $\perp$ beam evolution:

$$\langle \cdots \rangle_\perp = \frac{\int dx dy \int dx' dy' \cdots f}{\int dx dy \int dx' dy' f}$$

1st order moments

$\vec{x}_c = \langle \vec{x} \rangle_\perp$	centroid coordinate
$\vec{x}_c' = \langle \vec{x}' \rangle_\perp$	centroid angle
$\Delta = \langle \frac{\delta p}{p} \rangle_\perp \equiv \langle \delta \rangle_\perp$	off momentum
$\vdots$	$\vdots$

2nd order moments

x moments	y moments	x-y cross moments	dispersive moments
$\langle x^2 \rangle_\perp$	$\langle y^2 \rangle_\perp$	$\langle xy \rangle_\perp$	$\langle x\delta \rangle_\perp$, $\langle y\delta \rangle_\perp$
$\langle xx' \rangle_\perp$	$\langle yy' \rangle_\perp$	$\langle x'y \rangle_\perp$, $\langle xy' \rangle_\perp$	$\langle x'\delta \rangle_\perp$, $\langle y'\delta \rangle_\perp$
$\langle x'^2 \rangle_\perp$	$\langle y'^2 \rangle_\perp$	$\langle x'y' \rangle_\perp$	$\langle \delta^2 \rangle_\perp$
			....

Note:

Typically convenient to subtract centroid from higher order moments

$$\tilde{x} \equiv x - x_c \quad , \quad \tilde{x}' \equiv x' - x_c' \quad \ldots\ldots$$

$$\tilde{y} \equiv y - y_c \quad \quad \tilde{y}' \equiv y' - y_c'$$

$$\langle \tilde{x}^2 \rangle_\perp = \langle (x - x_c)^2 \rangle_\perp = \langle x^2 \rangle_\perp - x_c^2 \quad , \text{etc.}$$

3rd order moments

Analogous. $\langle x^3 \rangle_\perp$, $\langle x^2 y \rangle_\perp$, ...

Many quantities of physical interest are expressed in terms of moments:

Statistical Beam size:
$$\begin{cases} r_x = 2\langle \tilde{x}^2 \rangle_\perp^{1/2} \\ r_y = 2\langle \tilde{y}^2 \rangle_\perp^{1/2} \end{cases}$$

Statistical Emittances
$$\begin{cases} \varepsilon_x = 4\left[\langle \tilde{x}^2 \rangle_\perp \langle \tilde{x}'^2 \rangle_\perp - \langle \tilde{x}\tilde{x}' \rangle_\perp^2 \right]^{1/2} \\ \varepsilon_y = 4\left[\langle \tilde{y}^2 \rangle_\perp \langle \tilde{y}'^2 \rangle_\perp - \langle \tilde{y}\tilde{y}' \rangle_\perp^2 \right]^{1/2} \end{cases}$$

Equations of Motion

- Can be expressed in terms of moments or combinations of moments that are of physical interest.
- Moments are advanced from specified initial values.

Ex: $\delta = 0$, 2nd order truncation, zero x-y cross moments
linear focusing lattice, elliptical beam with uniform charge.

$$\frac{dx_c'}{ds} = -\kappa_x(s) x_c + \text{image terms} \quad ; \quad \frac{dx_c}{ds} = x_c'$$

$$\frac{dy_c'}{ds} = -\kappa_y(s) y_c + \text{image terms} \quad ; \quad \frac{dy_c}{ds} = y_c'$$

$$\frac{d}{ds}\begin{bmatrix} \langle \tilde{x}^2 \rangle_\perp \\ \langle \tilde{x}\tilde{x}' \rangle_\perp \\ \langle \tilde{x}'^2 \rangle_\perp \\ \langle \tilde{y}^2 \rangle_\perp \\ \langle \tilde{y}\tilde{y}' \rangle_\perp \\ \langle \tilde{y}'^2 \rangle_\perp \end{bmatrix} = \begin{bmatrix} 2\langle \tilde{x}\tilde{x}' \rangle_\perp \\ \langle \tilde{x}'^2 \rangle_\perp - \kappa_x(s)\langle \tilde{x}^2 \rangle_\perp + Q\langle \tilde{x}^2 \rangle^{1/2} / \left[4\langle \tilde{x}^2 \rangle_\perp^{1/2}\left(\langle \tilde{x}^2 \rangle_\perp^{1/2} + \langle \tilde{y}^2 \rangle_\perp^{1/2}\right)\right] \\ -2\kappa_x(s)\langle \tilde{x}\tilde{x}' \rangle_\perp + 2Q\langle \tilde{x}\tilde{x}' \rangle_\perp / \left[4\langle \tilde{x}^2 \rangle_\perp^{1/2}\left(\langle \tilde{x}^2 \rangle_\perp^{1/2} + \langle \tilde{y}^2 \rangle_\perp^{1/2}\right)\right] \\ 2\langle \tilde{y}\tilde{y}' \rangle_\perp \\ \langle \tilde{y}'^2 \rangle_\perp - \kappa_y(s)\langle \tilde{y}^2 \rangle_\perp + Q\langle \tilde{y}^2 \rangle^{1/2} / \left[4\langle \tilde{y}^2 \rangle_\perp^{1/2}\left(\langle \tilde{x}^2 \rangle_\perp^{1/2} + \langle \tilde{y}^2 \rangle_\perp^{1/2}\right)\right] \\ -2\kappa_y(s)\langle \tilde{y}\tilde{y}' \rangle_\perp + 2Q\langle \tilde{y}\tilde{y}' \rangle_\perp / \left[4\langle \tilde{y}^2 \rangle_\perp^{1/2}\left(\langle \tilde{x}^2 \rangle_\perp^{1/2} + \langle \tilde{y}^2 \rangle_\perp^{1/2}\right)\right] \end{bmatrix}$$

or using $\frac{d}{ds}\varepsilon_x^2 = 0 = \frac{d}{ds}\varepsilon_y^2$, the 2nd order moment equations can be equivalently expressed as:

$$\frac{d}{ds} r_x' + \kappa_x r_x - \frac{Q}{r_x + r_y} - \frac{\varepsilon_x^2}{r_x^3} = 0 \quad ; \quad \frac{d r_x}{ds} = r_x'$$

$$\frac{d}{ds} r_y' + \kappa_y r_y - \frac{Q}{r_x + r_y} - \frac{\varepsilon_y^2}{r_y^3} = 0 \quad ; \quad \frac{d r_y}{ds} = r_y'$$

Field

- In moment methods fields are typically calculated using averages over assumed distribution forms.
  - often analytic solutions employed.

Example

Envelope model employed above assumes an elliptical cross-section beam with uniform charge in free space.

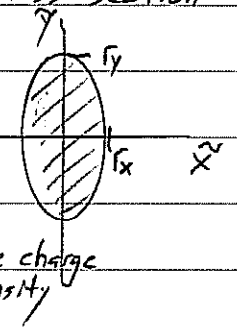

For: $\tilde{x}^2/r_x^2 + \tilde{y}^2/r_y^2 < 1$

λ = line charge density

$$E_{\tilde{x}} = \frac{\lambda \tilde{x}}{\pi\varepsilon_0 r_x (r_x + r_y)}, \quad E_{\tilde{y}} = \frac{\lambda \tilde{y}}{\pi\varepsilon_0 r_y (r_x + r_y)}$$

these forms are employed in the derivation of the moment equations of motion presented (KV Envelope Equation).

Moment models generally form an infinite chain of equations that do <u>not</u> truncate. To be useful the moments must be truncated. Truncations are usually carried out via field model assumptions. For example, the KV model field assumption above leads to a truncation of moments at 2nd order with

$$\varepsilon_x^2 = 16\left[\langle x^2\rangle_\perp \langle x'^2\rangle_\perp - \langle xx'\rangle_\perp^2\right] = \text{const.}$$

$$\varepsilon_y^2 = 16\left[\langle y^2\rangle_\perp \langle y'^2\rangle_\perp - \langle yy'\rangle_\perp^2\right] = \text{const.}$$

Beyond the 3 levels of modeling outlined above:

1/ Particle Methods

2/ Distribution Methods

3/ Moment Methods

There exist numerous "hybrid" models that combine features of several methods. Also, moments are typically calculated in particle and distribution methods as diagnostics.

- Hybrids: δf, gyro-kinetic, ... PIC with shaped particles; etc.

In general:

- Particle and Distribution methods are appropriate for higher levels of detail
- Moment methods are used for rapid iteration of machine design.
- Even within a single method (particle say) there exist many levels of description.
  - Electromagnetic, electrostatic + many field sol. numerical methods
  - 1d, 2d, 3d, ...

    ⋮
- Employing a hierarchy of models with full diagnostics allows cross-checking (both in numerics and physics) and aids understanding.
  - No single method is best in all cases.

J.J. Barnard and S. M. Lund
USPAS, Jan 2004

§3 Numerical Methods:

General approach is to discretize independent variables in each of the methods and solve for dependant variables which may in cases also be discretized.

time (or s)

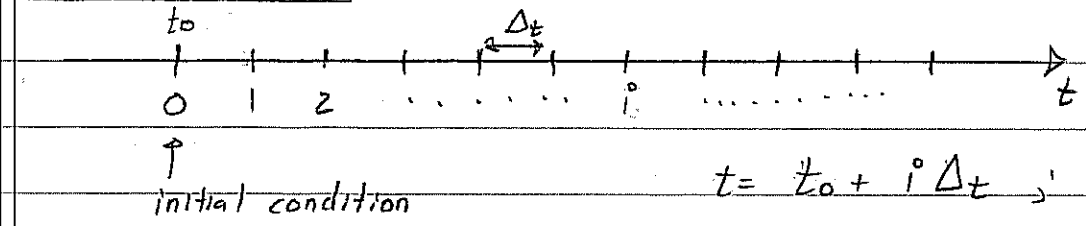

$$t = t_0 + i\,\Delta t \;;\quad i = 0, 1, 2, 3, \ldots$$

spatial coordinates (transverse)

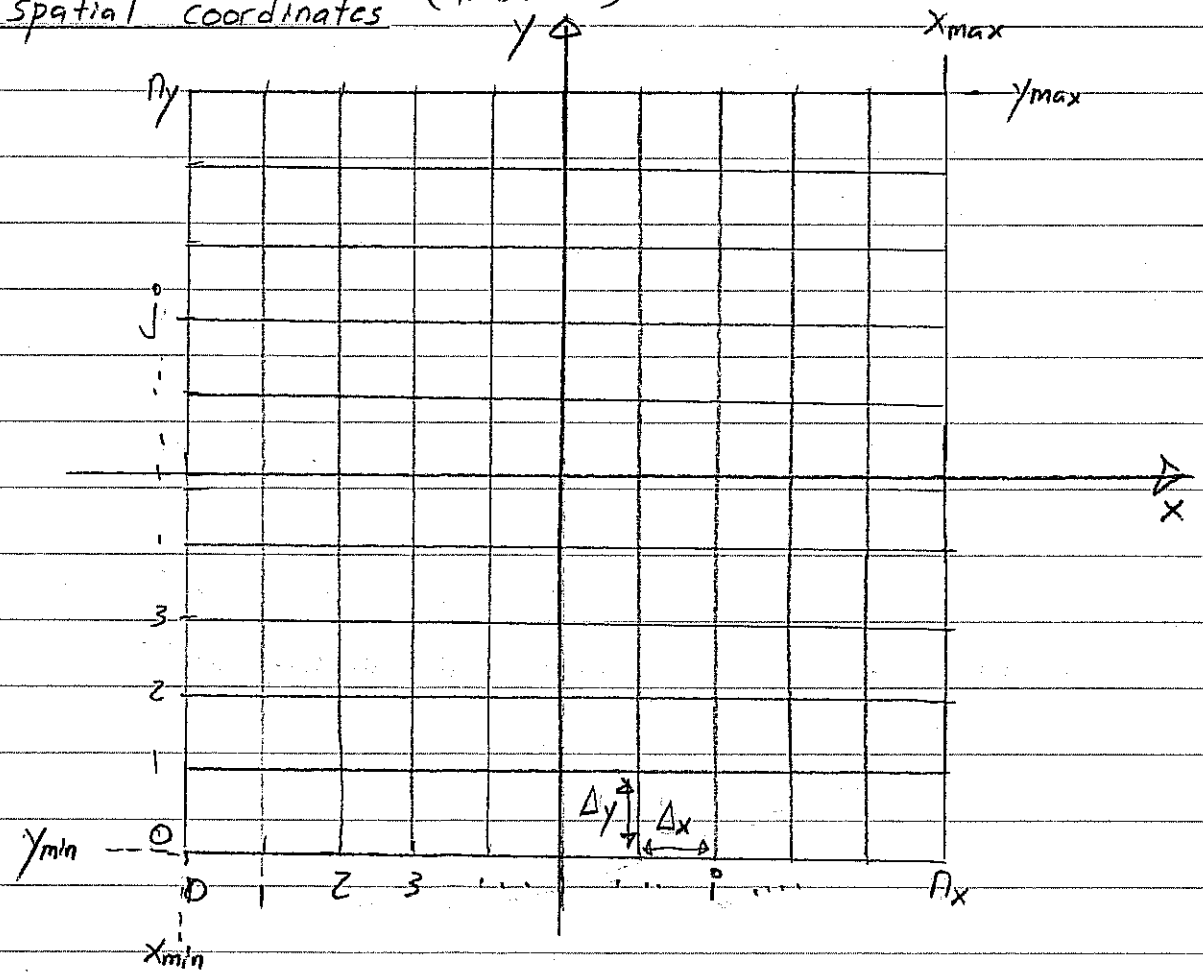

$$x_i = x_{min} + \Delta x \cdot i \;;\quad \Delta x = (x_{max} - x_{min})/n_x \;;\quad i = 0, 1, 2, \ldots n_x$$

$$y_j = y_{min} + \Delta y \cdot j \;;\quad \Delta y = (y_{min} - y_{max})/n_y \;;\quad j = 0, 1, 2, \ldots n_y$$

analogous for 3d, momentum coordinates, etc...

Spatial coordinates (longitudinal)

In typical applications may:

- Move a ⊥ thin "slice" of beam along the axial coordinate s of a reference particle.

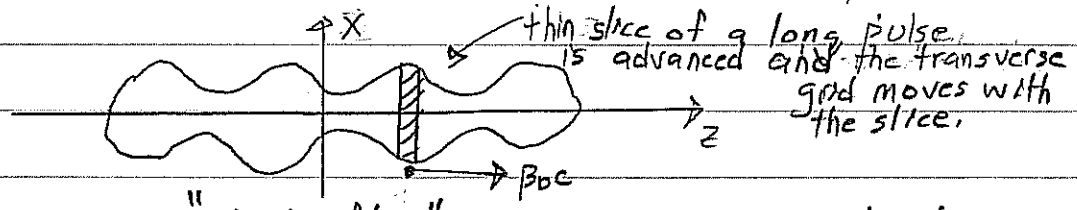

– This "steady flow" approximation is not always possible – some problems are intrinsic 3D.

- Simulate a steady state situation like in a mid-pulse diode where the beam fills the grid.

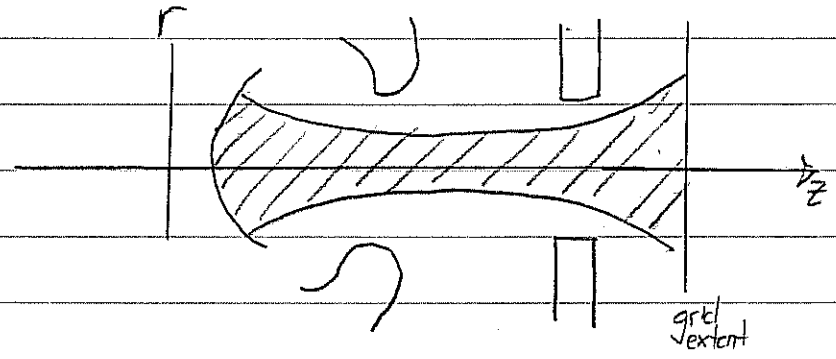

In these situations the mesh is stationary.

- Simulate a 3D beam with a moving mesh that follows a reference particle (possibly beam centroid).

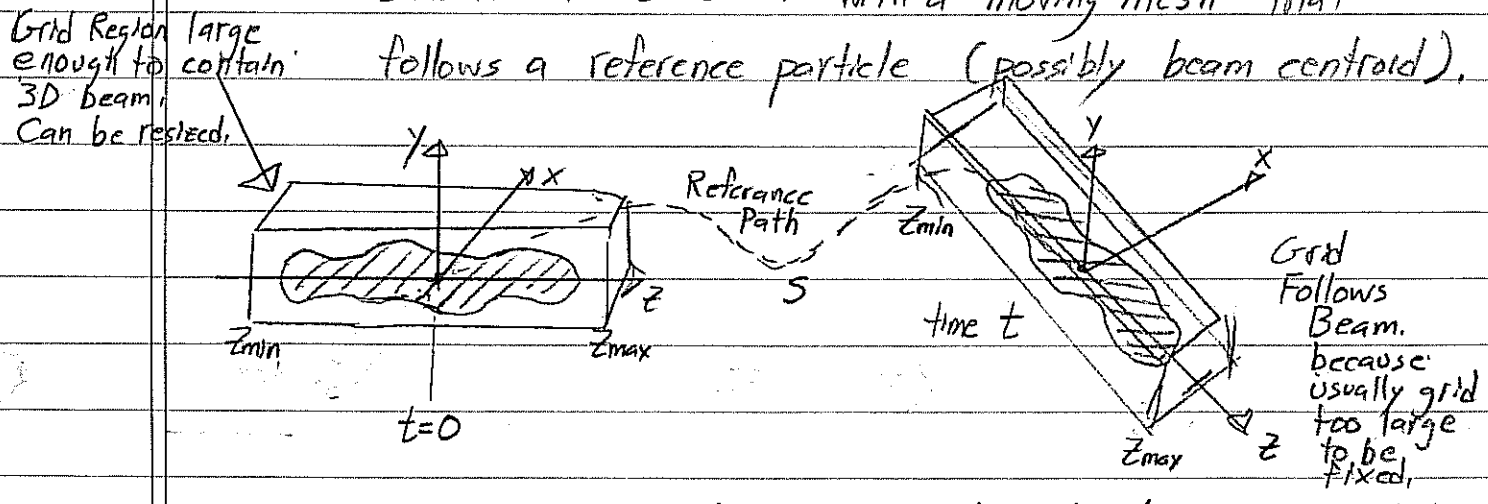

– Grid may be moved in discretized jumps so that applied fields maintain alignment with the grid.

Particle and distribution methods require further levels of discritization in field and other quantities to be rendered practical. Before discussing this we will first discuss basic discrete numerical operations employed. Then we will apply these operations to the simplist case, moment methods, before discussing the more complicated particle and distribution methods.

§3A: Discrete Numerical Operations

Let x represent a space or time coordinate and $f(x)$ some continuous function of x.

$$x_i = x_{min} + \Delta x \cdot i \quad ; \quad \Delta x = (x_{max} - x_{min})/n_x \; ; \quad i = 0, 1, 2, \ldots, n_x$$

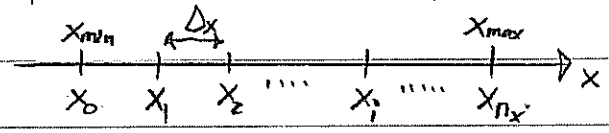

Denote

$$f_i \equiv f(x = x_i) \quad , \text{ etc.}$$

and taylor expand:

$$f_{i+1} = f_i + \left.\frac{\partial f}{\partial x}\right|_i \Delta x + \frac{1}{2!}\left.\frac{\partial^2 f}{\partial x^2}\right|_i \Delta x^2 + \frac{1}{3!}\left.\frac{\partial^3 f}{\partial x^3}\right|_i \Delta x^3 + \cdots$$

$$f_{i-1} = f_i - \left.\frac{\partial f}{\partial x}\right|_i \Delta x + \frac{1}{2!}\left.\frac{\partial^2 f}{\partial x^2}\right|_i \Delta x^2 - \frac{1}{3!}\left.\frac{\partial^3 f}{\partial x^3}\right|_i \Delta x^3 + \cdots$$

Derivatives

Low order derivatives follow immediately

$$\boxed{\begin{aligned} &\text{Foward:} \quad \left.\frac{\partial f}{\partial x}\right|_i = \frac{f_{i+1} - f_i}{\Delta_x} + \mathcal{O}(\Delta_x) \\ &\text{Backward:} \quad \left.\frac{\partial f}{\partial x}\right|_i = \frac{f_i - f_{i-1}}{\Delta_x} + \mathcal{O}(\Delta_x) \end{aligned}}$$

A more accurate, centered, schemes is obtained by subtracting the two expansions: But needs more grid points for accuracy.

$$\boxed{\begin{aligned} &\text{Centered:} \quad \left.\frac{\partial f}{\partial x}\right|_i = \frac{f_{i+1} - f_{i-1}}{2\Delta_x} + \mathcal{O}(\Delta_x^2) \\ &\text{(3 point)} \end{aligned}}$$

The expansions can be relabled ($i \to i+1$, etc) and the resulting equations analyzed to obtain 5-point and other higher-order forms such as:

$$\boxed{\text{5 Point:} \quad \left.\frac{\partial f}{\partial x}\right|_i = \frac{f_{i-2} - 8f_{i-1} + 8f_{i+1} - f_{i+2}}{12\Delta_x} + \mathcal{O}(\Delta_x^4)}$$

Still higher order forms are possible but rapidly become more combersome and require more points. Higher order derivatives can be similiarly obtained. For example, adding the two expansions shows:

$$\boxed{\left.\frac{\partial^2 f}{\partial x^2}\right|_i = \frac{f_{i+1} - 2f_i + f_{i-1}}{\Delta_x^2} + \mathcal{O}(\Delta_x^2)}$$

Integrals (Quadrature)

Take n_x even, then $\int_{x_{min}}^{x_{max}} dx\, f(\tilde{x})$ can be composed as sub-integrals of form:

$$\int_{x_{i-1}}^{x_{i+1}} d\tilde{x}\, f(\tilde{x})$$

Using a linear approximation: (Trapezoidal Rule)

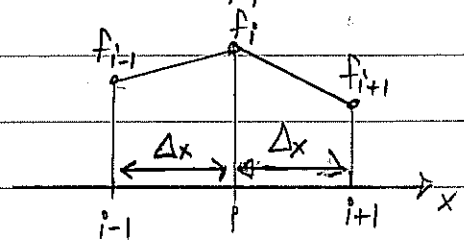

$$\boxed{\int_{x_{i-1}}^{x_{i+1}} d\tilde{x}\, f(\tilde{x}) = \frac{(f_{i-1} + 2f_i + f_{i+1})}{2}\Delta x + \mathcal{O}(\Delta x^3)}$$

Better approximations can be found (Simpsons' Rule) using Taylor series expansions and the previous discrete derivatives:

$$f(x) = f_i + \frac{f_{i+1} - f_{i-1}}{2\Delta x} x + \frac{f_{i+1} - 2f_i + f_{i-1}}{\Delta x^2} x^2 + \cdots$$

giving:

$$\boxed{\int_{x_{i-1}}^{x_{i+1}} dx\, f(x) = \frac{(f_{i+1} + 4f_i + f_{i-1})}{3}\Delta x + \mathcal{O}(\Delta x^5)}$$

Numerous other higher order formulas can be derived but are more complicated.

In the examples given, uniform meshes have been employed and formulas are readily generalized to multi-dimensions. In practice, nonuniform meshes are also often used since many applications need resolution concentrated in particular regions. Unfortunately, this makes the differencing formulas more complicated. Particularly with respect to ordering errors. An example of derivative calculations on a nonuniform 1d grid is included in the homework to illustrate methods.

§3B Numerical Solution of Moment Methods

We now have the tools to discuss the numerical solution of moment methods. The moment equations may always be written as an N-dimensional set of coupled 1st order ordinary differential equations:

$$\boxed{\begin{aligned} \vec{M} &= (x_c, \langle \tilde{x}^2 \rangle_\perp, \ldots\ldots) \\ \frac{d\vec{M}}{ds} &= \vec{F}(\vec{M}, s) \end{aligned}}$$

// Example:

Axisymmetric envelope equation for a continuously focused beam

$$\frac{d^2R}{ds^2} + k_{\beta 0}^2 R - \frac{Q}{R} - \frac{\varepsilon_x^2}{R^3} = 0 \quad , \quad k_{\beta 0}^2, Q, \varepsilon_x^2 \text{ constants.}$$

$$\frac{d}{ds}\begin{bmatrix} R' \\ R \end{bmatrix} = \begin{bmatrix} -k_{\beta 0}^2 R + \frac{Q}{R} + \frac{\varepsilon_x^2}{R^3} \\ R' \end{bmatrix}$$

///

Euler's Method:

Apply the forward diff. formula

$$\left.\frac{d\vec{M}}{ds}\right|_i = \frac{\vec{M}_{i+1} - \vec{M}_i}{\Delta_s} + \mathcal{O}(\Delta_s) = \vec{F}(\vec{M}_i, s_i)$$

1st order Euler Method:

$$\boxed{\vec{M}_{i+1} = \vec{M}_i + \Delta_s \vec{F}(\vec{M}_i, s_i) + \mathcal{O}(\Delta_s^2)}$$

The moments can then be advanced from their initial values.

Note that for N_s steps will lead to a total error $\sim N_s \cdot \mathcal{O}(\Delta_s^2) \sim \frac{(s_{max}-s_{min})}{\Delta_s} \cdot \mathcal{O}(\Delta_s^2) \sim \mathcal{O}(\Delta_s)$.

- Error decreases only linearly with step size.
- Numerical work for each step is only 1 evaluation of $\vec{F}$.

<u>Definition</u>

A discrete advance with error $\mathcal{O}(\Delta_s^n)$ is an $n-1$'th order method.

Thus Euler's method is a 1st order method.

Higher order methods are generally used for ODE's

$$\boxed{\frac{d\vec{M}}{ds} = \vec{F}(\vec{M}, s)}$$

<u>Runge-Kutta Method:</u>

Integrate:

$$\therefore \vec{M}_{i+1} = \vec{M}_i + \int_{s_i}^{s_{i+1}} ds\, \vec{F}(\vec{M}, s)$$

Approximate $\vec{F}$ by a taylor expansion through the midpoint of the interval. The linear term integrates to zero leaving: $\vec{F}(\vec{M}, s) = \vec{F}(\vec{M}_{i+1/2}, s_{i+1/2}) + \left.\frac{\partial \vec{F}}{\partial s}\right|_{i+1/2} \cdot s + \cdots$

$$\Rightarrow \vec{M}_{i+1} = \vec{M}_i + \vec{F}(\vec{M}_{i+1/2}, s_{i+1/2}) \cdot \Delta_s + \mathcal{O}(\Delta_s^3)$$

Note: only need $\vec{M}_{i+1/2}$ to $\mathcal{O}(\Delta_s^2)$ for $\mathcal{O}(\Delta_s^3)$ accuracy. Apply Euler's method for the 2-step procedure:

2nd Order Runge-Kutta Method:

$$\vec{k} \equiv \Delta_s \vec{F}(\vec{M}_i, s_i)$$

$$\vec{M}_{i+1} = \vec{M}_i + \Delta_s \cdot \vec{F}\left(\vec{M}_i + \frac{\vec{k}}{2}, s_i + \frac{\Delta_s}{2}\right) + \mathcal{O}(\Delta_s^3)$$

- Requires 2 evaluations of $\vec{F}$ per advance.
- 2nd order accurate in Δ_s.

Higher order Runge-Kutta Schemes are analogously derived from various quadrature formulas. Many such formulas are derived in standard numerical texts.

- Typically, methods with local error $\mathcal{O}(\Delta s^{N+1})$ will require N evaluations of $\vec{F}$.

For beam physics, many methods are employed to advance moments and particle orbits. A general survey of these methods is beyond the scope of this lecture. But some general comments can be made:

- Many high-order methods with adaptive stepsize exist that refine accuracy to specified tolerances and are optimized for specific classes of equations.
- Choice of methods often involves numerical work and stability considerations.
- Certain methods can be formulated to exactly preserve relevant single-particle invariants.
  - "Symplectic" methods preserve Hamiltonian structure of dynamics.
- Accelerator problems can be demanding due to multiple frequency scales and long tracking times/distances.

Numerical stability is key — but is difficult to analyze in general.

One simple test often used is a "Numerical Reversibility" check. In this method, the final value of an advance is used as an initial condition. Then the problem is run backwards to the original start point and deviations analyzed.

- Often a stringent test of accuracy.
- Will ultimately fail due to roundoff errors and cases where there is a sensitive dependance on initial conditions.
- Orbits can be wrong but qualitatively right ..... we will quantify this notion better later. So lack of full convergance does not necessarily mean that useless results will be obtained.

We now briefly overview an application of Moment equations, namely the KV envelope equations, to a practical high current transport lattice that was designed for heavy ion fusion applications at Lawrence Berkeley National Laboratory.

Moment Equation Application: Pep. RMS Envelope Equations

Neglect image charges and nonlinear self-fields (emittance constant) to obtain moment equations for the evolution of the beam envelope radii

$$\frac{d^2 r_x}{ds} + \kappa_q r_x - \frac{2Q}{r_x + r_y} - \frac{\varepsilon_x^2}{r_x^3} = 0$$

$$\frac{d^2 r_y}{ds} - \kappa_q r_y - \frac{2Q}{r_x + r_y} - \frac{\varepsilon_y^2}{r_y^3} = 0$$

statistical beam envelope radii

$$r_x = 2\sqrt{\langle x^2 \rangle}$$

$$r_y = 2\sqrt{\langle y^2 \rangle}$$

$$Q = \frac{qI}{2\pi\varepsilon_0 mc^3 \gamma_b^3 \beta_b^3}$$

... **Dimensionless Perveance**
measures space-charge strength

$$\varepsilon_x = 4[\langle x^2 \rangle \langle x'^2 \rangle - \langle xx' \rangle^2]^{1/2}$$

($\varepsilon_{xn} = \gamma_b \beta_b \varepsilon_x$ **normalized**)

... **RMS Edge Emittance**
measures x-x' phase-space area
~ (beam size)sqrt(thermal temperature)

The matched beam solution together with parametric constraints from engineering, higher-order theory, and simulations are used to design the lattice

S.M. Lund 11

Alternating Gradient Focusing Lattice with Syncopation

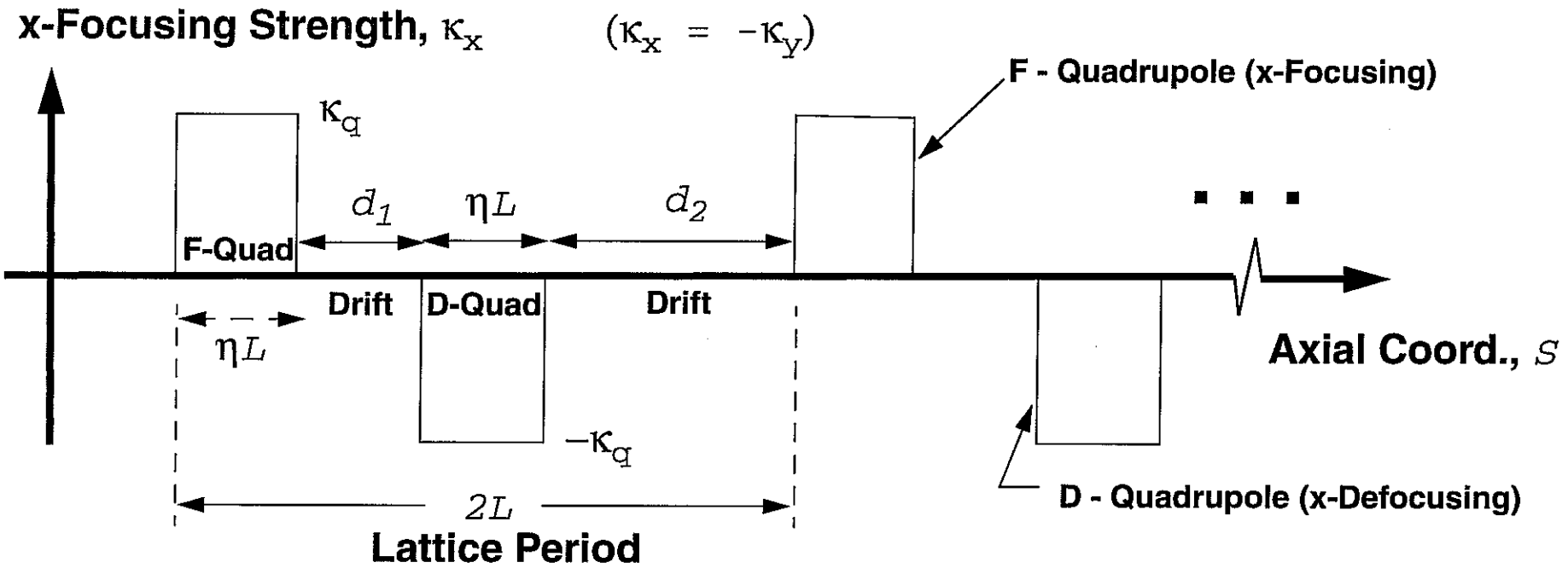

Drifts:

$$d_1 = \alpha(1-\eta)2L$$

$$d_2 = (1-\alpha)(1-\eta)2L$$

η = **Quadrupole Occupancy** $(0 < \eta < 1)$

α = **Syncopation Factor** $(0 < \alpha < 1)$

$\alpha = 1/2$ => **Symmetric FODO,** $d_1 = d_2$

$\alpha = 0,1$ => **F touches D**

Focusing Strength:

$$\kappa_q = \begin{cases} \dfrac{1}{[B\rho]}\left|\dfrac{dB_x}{dy}\right| & \text{, Magnetic Quadrupole} \\ \dfrac{1}{[B\rho]V_b}\left|\dfrac{dE_x}{dx}\right| & \text{, Electric Quadrupole} \end{cases}$$

Rigidity

$$[B\rho] = m\gamma_b V_b / q$$

S.M. Lund 12/

Matched Envelope Solution and Particle Phase Advances

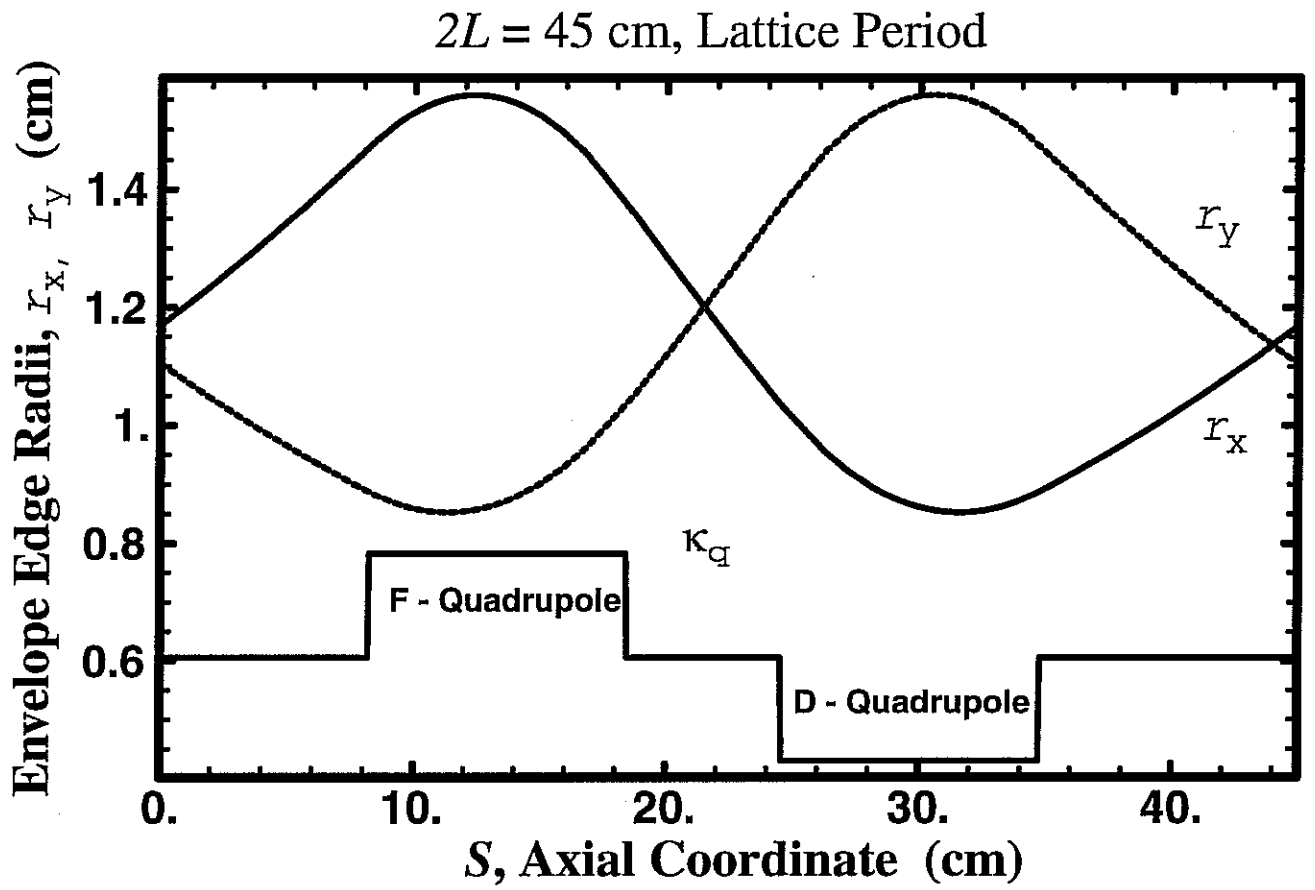

Ion

K^+, E = 2 meV

Current

I = 800 mA

Quadrupole:

occupancy
η = 0.453

syncopation factor
α = 0.248

Low Emittance Case: $\varepsilon_{x,rms}$ = 33.0 mm-mrad, rms edge

$\overline{r_x} = \overline{r_y}$ = 1.184 cm

Max[r_x] = **Max**[r_y] = 1.558 cm **Max**[r_x'] = -**Min**[r_y'] = 38.9 mrad $\sigma_{\beta 0}$ = 80°/Lattice-Period

Min[r_x] = **Min**[r_y] = 0.853 cm **Max**[r_y'] = -**Min**[r_x'] = 58.0 mrad σ_β = 6.88°/Lattice-Period

High Emittance Case: $\varepsilon_{x,rms}$ = 100.0 mm-mrad, rms edge

$\overline{r_x} = \overline{r_y}$ = 1.218 cm

Max[r_x] = **Max**[r_y] = 1.605 cm **Max**[r_x'] = -**Min**[r_y'] = 40.2 mrad $\sigma_{\beta 0}$ = 80°/Lattice-Period

Min[r_x] = **Min**[r_y] = 0.875 cm **Max**[r_y'] = -**Min**[r_x'] = 60.0 mrad σ_β = 19.8°/Lattice-Period

S.M. Lund 13/

J.J. Barnard and S.M. Lund
USPAS, Jan 04

§4 Numerical Solution of Particle and Distribution Methods

Particle methods – generally not used at high space-charge intensity

Distribution methods – pretered – mainly PIC – for high space-charge. We will motivate why now.

Particle Methods – Why they are not a good choice:

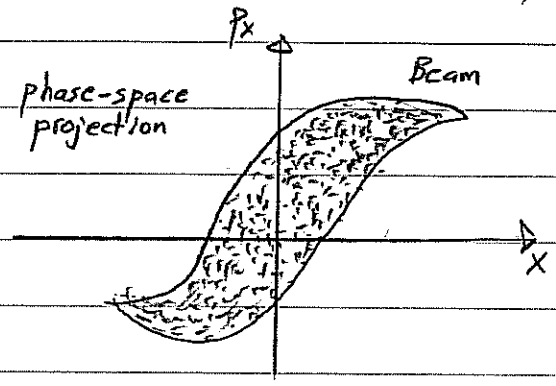

N particle coordinates $\{\vec{x}_i, \vec{p}_i\}$

Physical Beam: (typical)
$N \sim 10^{10} - 10^{14}$ particles

Although larger problems are possible every year with more powerful computers, processor speed and memory limitations presently limit us to

$$N \lesssim 10^8 \text{ particles.}$$

Represent the beam by "macroparticles" and advance macroparticles in time.

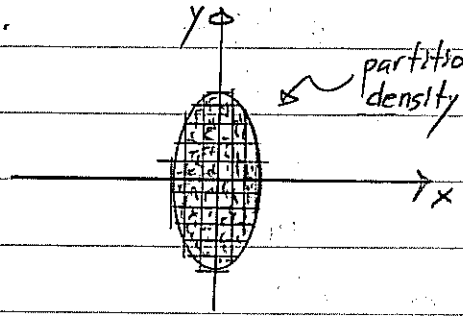

partition local density into macroparticles

- Same q/m ratio as real particle $\Rightarrow$ same single particle dynamics in applied field.
- Results in more collisions due to macroparticles having more close approaches.
  - Enhanced collisionality is unphysical
  - Controlled by smoothing the macroparticle interaction with the self-field. More on this later!

Distribution Methods

Vlasov as an example.

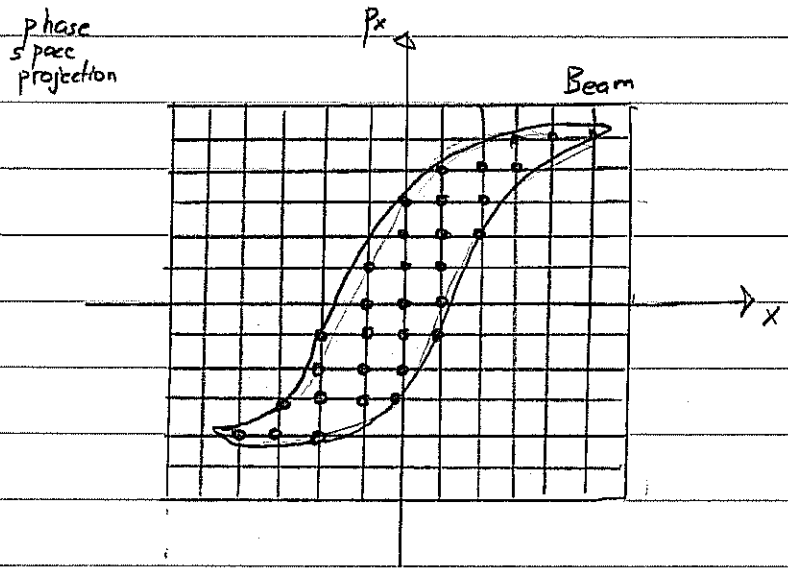

Discrete grid points $\{\vec{x}_i, \vec{p}_i\}$

Advance distribution $f(\vec{x}, \vec{p}, t)$ at discrete grid points in time.

- Continuum distribution advanced on a discrete phase-space mesh.
  - Extreme memory for high resolution. Ex. for 4d x-p_x, y-p_y with 100 mesh points on each axis $\Rightarrow 100^4 = 10^8$ values to store in fast memory.
- Discritization errors can lead to aliasing and unphysical behaviour (negative probability etc.).

Both particle and distribution methods can be broken up into 2 basic parts:

1) Moving particles or distribution evaluated at grid points through a finite time (or axial space) step.

2) Calculation of beam self-fields consistently with the distribution of particles.

In both methods, significant fractions of the run time may also be devoted to diagnostics:

- Moments – can be computationally intensive and may be accumulated frequently for evolution of evolution "histories."
- Phase space projections ("snapshot" in time)
- Fields (snapshot in time)

Diagnostics are also critical!

- Without appropriate diagnostics runs are useless even if correct.
- Must accumulate and present mass data in an understandable format.

Significant source code development may also be devoted to creating (loading) the initial distribution of particles to simulate.

- Such parts of the simulation will usually only take a small fraction of total run time.

Particle Methods – Integration of the Equations of Motion

Higher order methods require more storage and numerical work per time step

- Fieldsolves are expensive, especially in 3D, and several fieldsolves per step can be necessary for higher order accuracy.

$\therefore$

Typically, low-order methods are used for self-consistent space-charge. The "leapfrog" method is the most common.

- Only need to store prior position and velocity
- One field solve per timestep.

Illustrate for

Nonrelativistic equations of motion:

$$m\frac{d\vec{v}}{dt} = \vec{F} = q(\vec{E} + \vec{v}\times\vec{B})$$

$$\frac{d\vec{x}}{dt} = \vec{v}$$

Leapfrog advance (time centered)

1) $$m\frac{\vec{V}_{i+1/2} - \vec{V}_{i-1/2}}{\Delta t} = \vec{F}_i$$

2) $$\frac{\vec{X}_{i+1} - \vec{X}_i}{\Delta t} = \vec{V}_{i+1/2}$$

Note: $\vec{x}$ and $\vec{v}$ advanced out of phase.

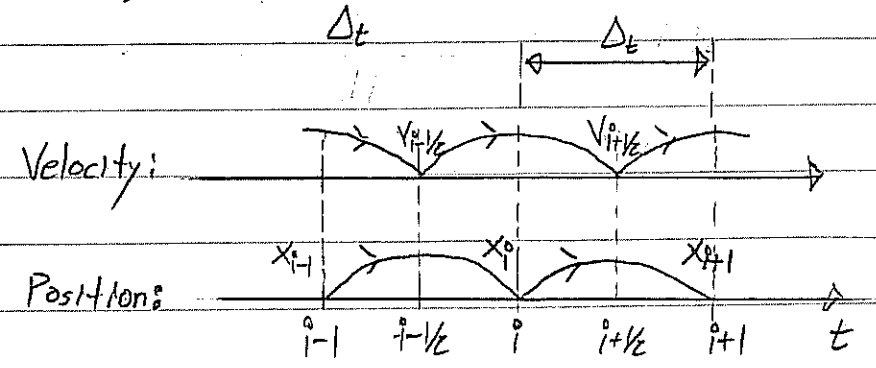

For purposes of analysis of the properties of the leapfrog method it is often convenient to write the map in an alternative form:

$$\begin{cases} \dfrac{\vec{x}_{i+1} - \vec{x}_i}{\Delta_t} = \vec{v}_{i+1/2} \\[2ex] i \to i-1 \quad \dfrac{\vec{x}_i - \vec{x}_{i-1}}{\Delta_t} = \vec{v}_{i-1/2} \end{cases}$$

Subtract the equations and apply the other formula:

$$\Rightarrow \quad m\,\frac{\vec{v}_{i+1/2} - \vec{v}_{i-1/2}}{\Delta_t} = \boxed{m\,\frac{\vec{x}_{i+1} - 2\vec{x}_i + \vec{x}_{i-1}}{\Delta_t^2} = \vec{F}_i}$$

Note:
$$\left.\frac{\partial^2 f}{\partial x^2}\right|_i = \frac{f_{i+1} - 2f_i + f_{i-1}}{\Delta_x^2} + \mathcal{O}(\Delta_x^2)$$
$\Rightarrow$ $\vec{x}_{i+1}$ fixed from $\vec{x}_i, \vec{x}_{i-1}, \vec{F}_i$ to $\mathcal{O}(\Delta_t^4)$

<u>Synchronization and desynchronization:</u>

Since $\vec{x}$ and $\vec{v}$ are not evaluated at the same time in the leapfrog method:

- Initial conditions <u>must be adjusted</u> to start the advance. Typically, $\vec{v}$ is pushed back a half cycle.

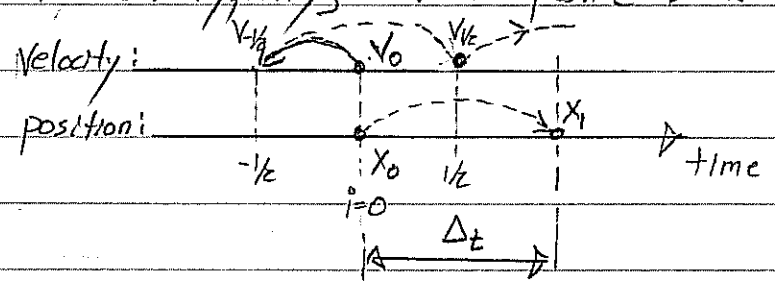

- When evaluating diagnostic quantities such as moments the particle coordinates and velocities should first be synchronized using a similar procedure.

Another complication is in evaluation of the force which has velocity dependence when magnetic fields are present since $\vec{x}$ and $\vec{v}$ are advanced out of phase in the leap-frog method.

$$\boxed{\vec{F} = q\vec{E} + q\underbrace{\vec{v}}_{\text{Velocity term}} \times \vec{B}}$$

Note:

- Electric field $\vec{E}$ accelerates.
- Magnetic field $\vec{B}$ bends particle trajectory without change in speed $\vec{v}$.

A commonly implemented time centered scheme for this is the following 3-step "Boris" method:

1) <u>Half-step acceleration</u> in electric field

$$\vec{V}^{(1)}_{i+1/2} = \vec{V}_{i-1/2} + \frac{q}{m}\vec{E}_i \cdot \frac{\Delta_t}{2}$$

2) <u>Rotation</u> in magnetic field. Here choose coordinates such that $\vec{B}_i = B_i\hat{z}$, $\omega_{ci} = qB_i/m$

$\parallel B_i$: $V^{(2)}_{z\,i+1/2} = V^{(1)}_{z\,i+1/2}$ [Parallel Magnetic Field to $\vec{v}$ does not bend trajectory]

$\perp B_i$: $$\begin{pmatrix} V^{(2)}_{x\,i+1/2} \\ V^{(2)}_{y\,i+1/2} \end{pmatrix} = \begin{bmatrix} \cos(\omega_{ci}\Delta_t) & \sin(\omega_{ci}\Delta_t) \\ -\sin(\omega_{ci}\Delta_t) & \cos(\omega_{ci}\Delta_t) \end{bmatrix} \begin{pmatrix} V^{(1)}_{x\,i+1/2} \\ V^{(1)}_{x\,i+1/2} \end{pmatrix}$$

3) <u>Half-step acceleration</u> in electric field

$$\vec{V}_{i+1/2} = \vec{V}^{(3)}_{i+1/2} = \vec{V}^{(2)}_{i+1/2} + \frac{q}{m}\vec{E}_i \cdot \frac{\Delta_t}{2}$$

Complication! On startup how does one generate the out of phase $\vec{x}, \vec{v}$ advance from initial conditions?

- Calculate $\vec{E}, \vec{B}$ with initial conditions.
- Move $\vec{v}$ backward a half-step $(-\Delta t/2)$
  - Rotate with $\vec{B}$ a half-step.
  - Deaccelerate a half-step in $\vec{E}$.

Similar comments hold for synchronization of $\vec{x}, \vec{v}$ for diagnostic accumulation.

Now we will look at the numerical properties of the leapfrog advance cycle.

- Only use a simple example to illustrate issues.

Leapfrog Advance Errors and Numerical Stability

To better understand the leapfrog method consider the simple harmonic oscillator:

$$\boxed{\frac{d^2x}{dt^2} = -\omega^2 x \qquad \omega = \text{const.}}$$

Exact Solution $\Rightarrow$ $x = C_0 \cos\omega t + C_1 \sin\omega t$ $\qquad$ C_0, C_1 constants

$= X_0 \cos(\omega t + \psi_0)$ $\qquad$ set from initial conds.

In the leapfrog method:

$$\boxed{\frac{x_{i+1} - 2x_i + x_{i-1}}{\Delta_t^2} = -\omega^2 x_i}$$

Try a solution of form

$$x_i = C_0 \cos\tilde{\omega} t_i + C_1 \sin\tilde{\omega} t_i$$

Substitute

$$x_i = C e^{j\tilde{\omega} i \Delta_t} \qquad j \equiv \sqrt{-1}$$

Use j to not confuse with other index choices.

$$\Rightarrow \quad e^{j\tilde{\omega}\Delta_t} - 2 + e^{-j\tilde{\omega}\Delta_t} = -\omega^2 \Delta_t^2$$

$$2 - 2\cos(\tilde{\omega}\Delta_t) = \omega^2 \Delta_t^2$$

$$\sin^2\left(\frac{\tilde{\omega}\Delta_t}{2}\right) = \frac{\omega^2 \Delta_t^2}{4} \qquad \text{take + root}$$

$$\Rightarrow \quad \boxed{\sin\left(\frac{\tilde{\omega}\Delta_t}{2}\right) = \frac{\omega\Delta_t}{2}}$$

This has solutions for $\omega\Delta_t < 2$ and it is straightforward to show (expansion) that for $\omega\Delta_t$ small:

$$\boxed{\tilde{\omega}\Delta_t = \omega\Delta_t + \frac{(\omega\Delta_t)^3}{24} + \mathcal{O}(\omega\Delta_t^5)}$$

It follows immediately for the leapfrog method:

- For $\omega \Delta_t < 2$ the method is <u>stable</u>
- There is <u>no</u> amplitude error in the integration
- For $\omega dt \ll 1$, the phase error is

Actual phase: $\psi \equiv \omega i \Delta_t$

Simulated phase: $\tilde{\psi} \equiv \tilde{\omega} i \Delta_t \simeq \omega i \Delta_t + \frac{(\omega \Delta_t)^3}{24} i$

Error phase: $\Delta\psi = \tilde{\psi} - \psi = \frac{(\omega \Delta_t)^3}{24} i$

Note: i to get to a fixed time $\sim 1/\Delta_t$ and therefore phase errors decrease as $\mathcal{O}(\Delta_t^2)$

// Example: $\omega = 2\pi/\tau$

$\Delta_t = 0.1\,\tau$: steps for a π phase error $\simeq 24\pi/(0.1 \cdot 2\pi)^3 \simeq 304 \Rightarrow \sim 30.4$ cycles

$\Delta_t = 0.01\,\tau$: steps for a π phase error $\simeq 24\pi/(0.01 \cdot 2\pi)^3 \simeq 3.04 \times 10^5 \Rightarrow \sim 3{,}040$ cycles

///

<u>Contrast: Numerical and Actual Orbit</u>

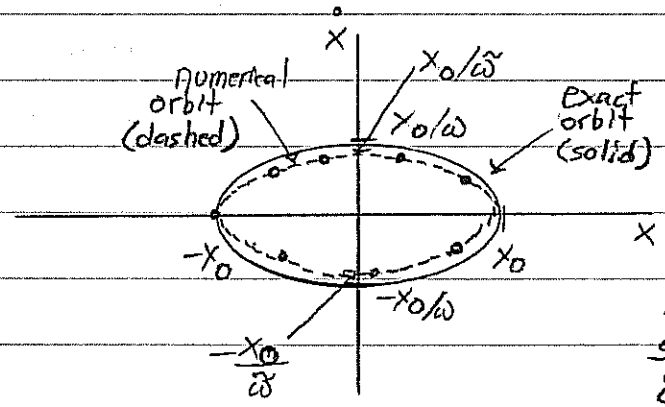

Emittances = (Phase space Areas)/π

exact: $\mathcal{E} = x_0^2/\omega$

Numerical $\tilde{\mathcal{E}} = x_0^2/\tilde{\omega}$

$$\frac{\tilde{\mathcal{E}}}{\mathcal{E}} \simeq 1 - \frac{(\omega \Delta_t)^2}{24}$$

The numerical orbit conserves phase space area regardless of the number of steps taken! <u>The slight differences between the numerical and actual orbit can be removed by rescaling ω to account for the discrete step.</u>

- More general analysis of the leapfrog map shows it has "symplectic" structure – meaning it preserves the Hamiltonian nature of the dynamics.
- Symplectic methods are important for long tracking problems (typical in accelerators) to obtain the right orbit structure – Runge-Kutta is not symplectic

Particle Methods – Field solution

The self-consistant calculation of self-fields is of primary importance to accurately simulate intense particle beams. Techniques outlined here are also applicable to distribution methods.

$$\vec{F} = q\vec{E} + q\vec{v} \times \vec{B}$$

Fields can be resolved into externally applied and self (i.e., beam generated) components:

$$\boxed{\begin{array}{ll} \vec{E} = \vec{E}_a + \vec{E}_s & \vec{E}_a, \vec{B}_a : \text{Applied} \\ \vec{B} = \vec{B}_a + \vec{B}_s & \vec{E}_s, \vec{B}_s : \text{Self} \end{array}}$$

- $\vec{E}_a, \vec{B}_a$ applied fields generated from magnets and electrodes
  - Sometimes calculated at high resolution in external codes and imported or specified via analytic formulae
  - Sometimes calculated from code fieldsolve via applied charges and currents and boundary conditions
- $\vec{E}_s, \vec{B}_s$ self fields generated from beam charges and currents.
  - At high beam intensities can be a large fraction (on average) of the applied fields
  - Important to calculate with realistic boundary conditions.

For simplicity, we restrict analysis to electrostatic problems to illustrate methods:

$$\vec{B} = \vec{B}_a \qquad \text{(specified via another code or theory)}$$
$$\vec{E} = \vec{E}_a + \vec{E}_s \qquad \left(\begin{array}{l}\vec{E}_a \text{ due to biased electrodes and} \\ \vec{E}_s \text{ due to beam space-charge}\end{array}\right)$$

The Maxwell equations to be solved for $\vec{E}$ are

$$\boxed{\begin{array}{ll} \nabla \cdot \vec{E} = \dfrac{\rho}{\varepsilon_0} & + \text{ Boundary conditions on } \vec{E}. \\ \nabla \times \vec{E} = 0 & \end{array}}$$

$\nabla \times \vec{E}$ implies that we can always take

$$\vec{E} = -\nabla \phi$$

and we have

$$\boxed{\begin{array}{ll} \nabla^2 \phi = -\dfrac{\rho}{\varepsilon_0} & + \text{ Boundary conditions on } \phi \\ \vec{E} = -\nabla \phi & \end{array}}$$

As an explicit example, it might be necessary to solve (2D) problems like:

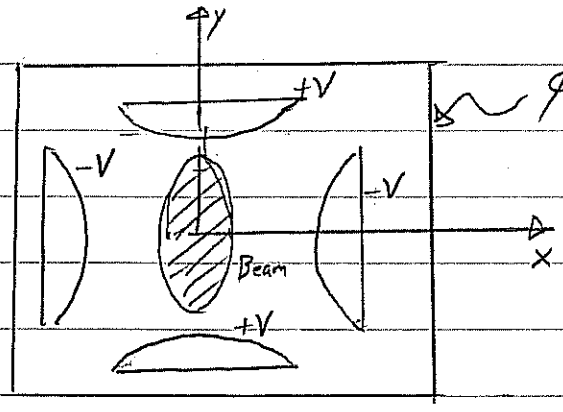

ϕ or $\frac{\partial \phi}{\partial n}$ specified on domain boundary or in infinite space.

Formally, the solution to ϕ can be constructed with a Green's Function: (Illustrated for Dirichlet Boundary Conditions)

$$\boxed{\begin{aligned} \nabla^2 G(\vec{x},\vec{x}') &= -4\pi\delta(\vec{x}-\vec{x}') \\ G(\vec{x},\vec{x}')\Big|_{\vec{x}' \text{ on boundaries}} &= 0 \end{aligned}}$$

which gives:

$$\boxed{\phi(\vec{x}) = \underbrace{\int_V d^3x' \frac{\rho(\vec{x}')}{4\pi\varepsilon_0} G(\vec{x},\vec{x}')}_{\substack{\text{Self-field component} \\ \equiv \phi_s \\ \vec{E}_s = -\frac{\partial\phi_s}{\partial\vec{x}}}} - \underbrace{\frac{1}{4\pi}\oint_S d^2x' \phi(\vec{x}')\frac{\partial G(\vec{x},\vec{x}')}{\partial n'}}_{\substack{\text{Applied Field from} \\ \text{electrode potentials} \\ \equiv \phi_a \\ \vec{E}_a = -\frac{\partial\phi_a}{\partial\vec{x}}}}}$$

$\hat{n}$ = normal to conductor surface

- ϕ_a can be calculated in advance and need not be recalculated.
  - may be analytical in simple situations.

Let: $q_M, \vec{x}_i$ = macro-particle charge and coordinate
N_p = Macro particle number.

$$\phi_s = \int d^3x' \frac{\rho(\vec{x}')}{4\pi\varepsilon_0} G(\vec{x},\vec{x}') = \sum_{i=1}^{N_p} \int d^3x' \frac{q_M \delta(\vec{x}'-\vec{x}_i)}{4\pi\varepsilon_0} G(\vec{x},\vec{x}')$$

$$\boxed{\phi_s = \sum_{i=1}^{N_p} \frac{q_M}{4\pi\varepsilon_0} G(\vec{x},\vec{x}_i)}$$

Then the field at the jth macro-particle is

$$\boxed{\vec{E}_{sj} = \left.\frac{\partial \phi_s}{\partial \vec{x}}\right|_{\vec{x}=\vec{x}_j} = \frac{q_M}{4\pi\varepsilon_0} \sum_{\substack{i=1 \\ i\neq j}}^{N_p} \left.\frac{\partial G(\vec{x}, \vec{x}_i)}{\partial \vec{x}}\right|_{\vec{x}=\vec{x}_j}}$$

This, in general, will be a numerically intensive expression to evaluate at <u>each</u> macroparticle.

- $N_p(N_p-1)$ terms to evaluate <u>and G itself will in general be complicated</u>, and may require many costly numerical operations for each term.

- Small number of macroparticles that this procedure may be carried out for will result in a noisy field
  - Enhanced, unphysically high, close approaches (collisions) can change the physics.

- Special "fast multipole" methods based on Greens' functions can reduce the scaling to $\sim N_p$ or $\sim N_p \ln N_p$. However the coefficient is large and smoothing is not easily implimented, usually rendering such methods inferior to gridded methods to be covered shortly.

// Example – Self Fields in free space:

$$G(\vec{x}, \vec{x}') = \frac{1}{|\vec{x}-\vec{x}'|} \quad ; \quad \vec{E}_{sj} = \frac{q_M}{4\pi\varepsilon_0} \sum_{i\neq j}^{N_p} \frac{(\vec{x}_j - \vec{x}_i)}{|\vec{x}_j - \vec{x}_i|^3}$$

//

An alternative Procedure is Needed to:

1) <u>Calculate fields efficiently</u>
2) <u>Smooth interactions</u> to compensate for limited particle numbers.

Approach:

Solve the Maxwell Equations on a discrete spatial grid and then smooth the interactions calculated from the gridded field. We will outline this method for 2D interactions, 3D is analogous.

$$x_i = x_{min} + \Delta x \cdot i \qquad \Delta x = (x_{max} - x_{min})/n_x \qquad i = 0, 1, 2, \ldots, n_x$$

$$y_i = y_{min} + \Delta y \cdot j \qquad \Delta y = (y_{max} - y_{min})/n_y \qquad j = 0, 1, 2, \ldots, n_y$$

$$\left.\begin{aligned} \vec{E}_{ij} &= \vec{E}(x_i, y_j) \\ \phi_{ij} &= \phi(x_i, y_j) \\ \rho_{ij} &= \rho(x_i, y_j) \end{aligned}\right\} \text{Field components, potential, and charge are gridded}$$

Ex

Beam in an electric quadrupole (2D)

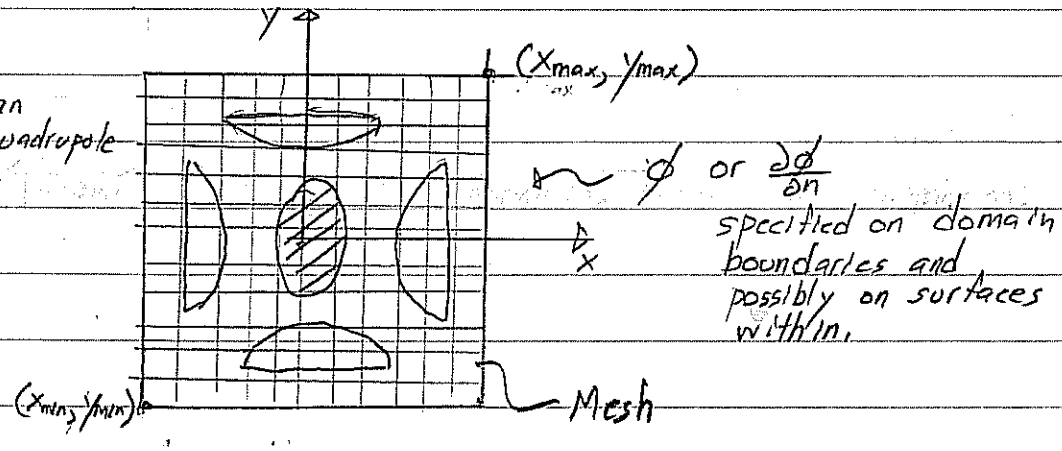

Note: ρ_{ij} must be calculated from macro-particle not necessarily on grid points. Also fields will ultimately be needed at macro-particle coordinates not on the grid. These issues will be covered later under "particle weighting"

For low order Differencing, the Poisson Equation becomes:

$$\boxed{\frac{\phi_{i+1,j} - 2\phi_{i,j} + \phi_{i-1,j}}{\Delta_x^2} + \frac{\phi_{i,j+1} - 2\phi_{i,j} + \phi_{i,j-1}}{\Delta_y^2} = -\frac{\rho_{i,j}}{\varepsilon_0}}$$

with the gridded field components calculated as:

$$\boxed{\begin{aligned} E_{x_{ij}} &= \frac{\phi_{i+1,j} - \phi_{i-1,j}}{2\Delta_x} \\ E_{y_{ij}} &= \frac{\phi_{i,j+1} - \phi_{i,j-1}}{2\Delta_y} \end{aligned}}$$

Boundary conditions must also be incorporated as equations of constraint.

1) <u>Dirichlet Conditions</u>: ϕ specified on surfaces.

Example: $\phi = V = \text{const}$ at right grid edge:

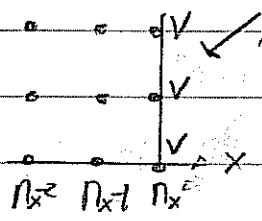

$\phi_{n_x,j} = V = \text{const}$

$i = n_x - 1$ cells:

$$\frac{V - 2\phi_{n_x-1,j} + \phi_{n_x-2,j}}{\Delta_x^2} + \frac{\phi_{n_x-1,j+1} - 2\phi_{n_x-1,j} + \phi_{n_x-1,j-1}}{\Delta_y^2} = \frac{-\rho_{n_x-1,j}}{\varepsilon_0} \quad ; \text{ etc.}$$

2) <u>Neumann Conditions</u>: $\partial\phi/\partial n$ specified on surfaces.

Example: $\partial\phi/\partial x = G = \text{const}$ at right grid edge:

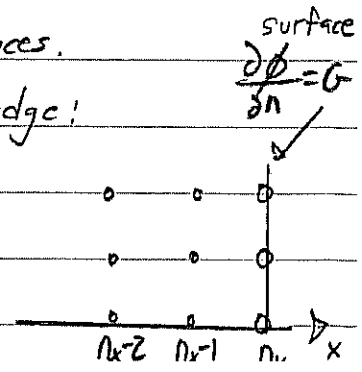

$$\boxed{\frac{\phi_{n_x-1,j} - \phi_{n_x,j}}{\Delta_x} = G}$$

The finite differenced Poisson equation and the boundary conditions can be expressed in Matrix Form:

$$\boxed{\bar{M} \cdot \vec{\phi} = \vec{S}}$$

$\bar{M}$ = coefficients matrix from <u>local</u> finite differences
This matrix will be sparse (i.e., most elements zero)

$\vec{\phi}$ = vector of potentials at grid points.

$\vec{S}$ = "source" terms resulting from 1) <u>beam charge deposited on the grid</u> (ρ_{ij}) and "known" potentials from 2) <u>boundary condition constraints</u>.

Formal solution found by Matrix inversion:

$$\boxed{\vec{\phi} = \bar{M}^{-1} \cdot \vec{S}}$$

Direct inversion of $\bar{M}^{-1}$ is not practical due to large dimension of problem. However:

- $\bar{M}$ will in general be very sparse due to the use of local, low-order finite differencing.
- Many fast, numerically efficient inversion methods exist for sparse matrices.
  - Specific method best used depends on type of differencing and boundary conditions.

To illustrate this procedure, consider a simple 1-d example with Dirichlet boundary conditions.

$$\frac{d^2\phi}{dx^2} = -\frac{\rho}{\varepsilon_0} \qquad \phi(x_\ell) = V_\ell \quad \text{left B.C.}$$
$$\phi(x_r) = V_r \quad \text{right B.C.}$$

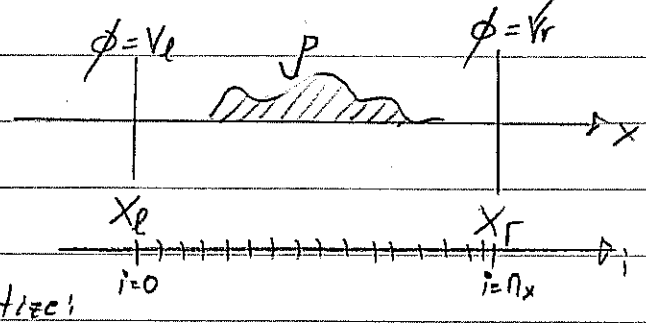

Discritize:

$$\frac{\phi_{i+1} - 2\phi_i + \phi_{i-1}}{\Delta_x^2} = -\frac{\rho_i}{\varepsilon_0}$$

$$x_i = x_\ell + \Delta_x \cdot i \,, \quad \Delta_x = (x_r - x_\ell)/n_x \,; \quad i = 0, 1, 2, \ldots, n_x$$

$$\phi_0 = V_\ell$$
$$\phi_{n_x} = V_r$$

note: ρ_0 is irrelevant – and will have a surface term to fix boundary cond.

$$\begin{bmatrix} -2 & 1 & & & & & \\ 1 & -2 & 1 & & & 0 & \\ & 1 & -2 & 1 & & & \\ & & & \ddots & & & \\ & & & 1 & -2 & 1 & \\ & 0 & & & 1 & -2 & 1 \\ & & & & & 1 & -2 \end{bmatrix} \begin{bmatrix} \phi_1 \\ \phi_2 \\ \phi_3 \\ \vdots \\ \phi_{n_x-3} \\ \phi_{n_x-2} \\ \phi_{n_x-1} \end{bmatrix} = -\frac{\Delta_x^2}{\varepsilon_0} \begin{bmatrix} \rho_1 + \frac{\varepsilon_0}{\Delta_x^2} V_\ell \\ \rho_2 \\ \rho_3 \\ \vdots \\ \rho_{n_x-3} \\ \rho_{n_x-2} \\ \rho_{n_x-1} + \frac{\varepsilon_0}{\Delta_x^2} V_r \end{bmatrix}$$

Matrix has tri-diagonal structure and may be rapidly inverted to find the ϕ_i.

- Sparse matrices need not be stored in full (waste of memory)

Many other methods exist to solve the discretized field equations. These methods fall into 3 broad classes:

1) Direct Matrix Methods
   - Fast Inversion of sparse matrices.

2) Spectral Methods
   - Fast Fourier Transform (FFT)
     - Periodic boundary conditions
     - sine transform [$\phi=0$ on grid boundary]
     - FFT + capacity matrix for arbitrary conductors
     - Free space boundary conditions

3) Relaxation Methods
   - Successive overrelaxation (SOR)
     - General boundary conditions and structures.
   - Multigrid (good, fast, accurate method for complicated boundaries)

Sometimes these methods may be combined. For example, one might employ spectral methods transversely and invert the tri-diagonal matrix longitudinally.

Other discretization procedures are also widely employed:
- Finite elements
- Variational
- Monte-Carlo ,,,,,,

The various methods of field solution are central to the efficient numerical solution of intense beams. It is not possible to review them all here. But before discussing particle weighting, we will first overview the important spectral methods and FFTs.

Spectral Methods and the FFT

The spectral approach combined with numerically efficient Fast Fourier Transforms (FFTs) is commonly used to solve the Maxwell Equations on a discrete spatial grid.

- Approach provides spectral information on fields that can smooth the interactions.

Illustrate in 1-d for simplicity (multidimensions analogous)

$$\boxed{\frac{d^2\phi}{dx^2} = \frac{-\rho}{\varepsilon_0}}$$

Continuous Fourier Transforms: (Reminder)

$$\boxed{\begin{aligned} \tilde{\phi}(k) &= \int_{-\infty}^{\infty} dx\, e^{ikx}\, \phi(x) & \tilde{\rho}(k) &= \int_{-\infty}^{\infty} dx\, e^{ikx}\, \rho(x) \\ \phi(x) &= \int_{-\infty}^{\infty} \frac{dk}{2\pi}\, e^{-ikx}\, \tilde{\phi}(k) & \rho(x) &= \int_{-\infty}^{\infty} \frac{dk}{2\pi}\, e^{-ikx}\, \tilde{\rho}(k) \end{aligned}}$$

Transform Poisson Eqn. $\Rightarrow$ $$k^2 \tilde{\phi}(k) = \frac{\tilde{\rho}(k)}{\varepsilon_0}$$

$$\boxed{\phi(x) = \int_{-\infty}^{\infty} \frac{dk}{2\pi}\, e^{-ikx}\, \frac{\tilde{\rho}(k)}{\varepsilon_0 k^2}}$$

Similar procedures work for the field on a discrete and <u>finite</u> spatial grid.

Discrete Fourier Transform:

$$x_j = x_{min} + \Delta_x \cdot j \quad , \quad dx = (x_{max} - x_{min})/n_x \; ; \; j = 0, 1, 2, \ldots n_x$$

$$\phi_j = \phi(x_j)$$

$n_x + 1$ grid points. (take even)

$$k_n \equiv \frac{2\pi n}{(n_x+1)\Delta_x} \qquad n = -\frac{(n_x+1)}{2}, \ldots\ldots, \frac{n_x+1}{2}$$

$$\tilde{\phi}(k_n) = \int_{-\infty}^{\infty} dx \, e^{ik_n x} \phi(x) \approx \Delta_x \sum_{j=0}^{n_x} e^{ik_n x_j} \phi_j$$

Discrete Transform:

$$\approx \Delta_x \sum_{j=0}^{n_x} e^{\frac{i 2\pi n j}{n_x+1}} \phi_j$$

$$\boxed{\begin{aligned} \tilde{\phi}_n &\equiv \tilde{\phi}(k_n) \\ &\equiv \Delta_x \sum_{j=0}^{n_x} e^{\frac{i 2\pi n j}{n_x+1}} \phi_j \end{aligned}}$$

Note that $\tilde{\phi}_n$ is periodic in n with period $n_x + 1$

$$\tilde{\phi}_{-n} = \tilde{\phi}_{n_x+1-n}$$

Let n vary from: $n = 0, 1, 2, \ldots, n_x$
so n and j have same ranges.

Then an inverse transform can be <u>exactly</u> constructed:

$$\boxed{\phi_j = \frac{1}{(n_x+1)\Delta_x} \sum_{n=0}^{n_x} e^{\frac{-i 2\pi n j}{n_x+1}} \tilde{\phi}_n}$$

The discrete transform constructed describes a periodic problem if indices are extended.

- Discretization errors (aliasing) can occur.

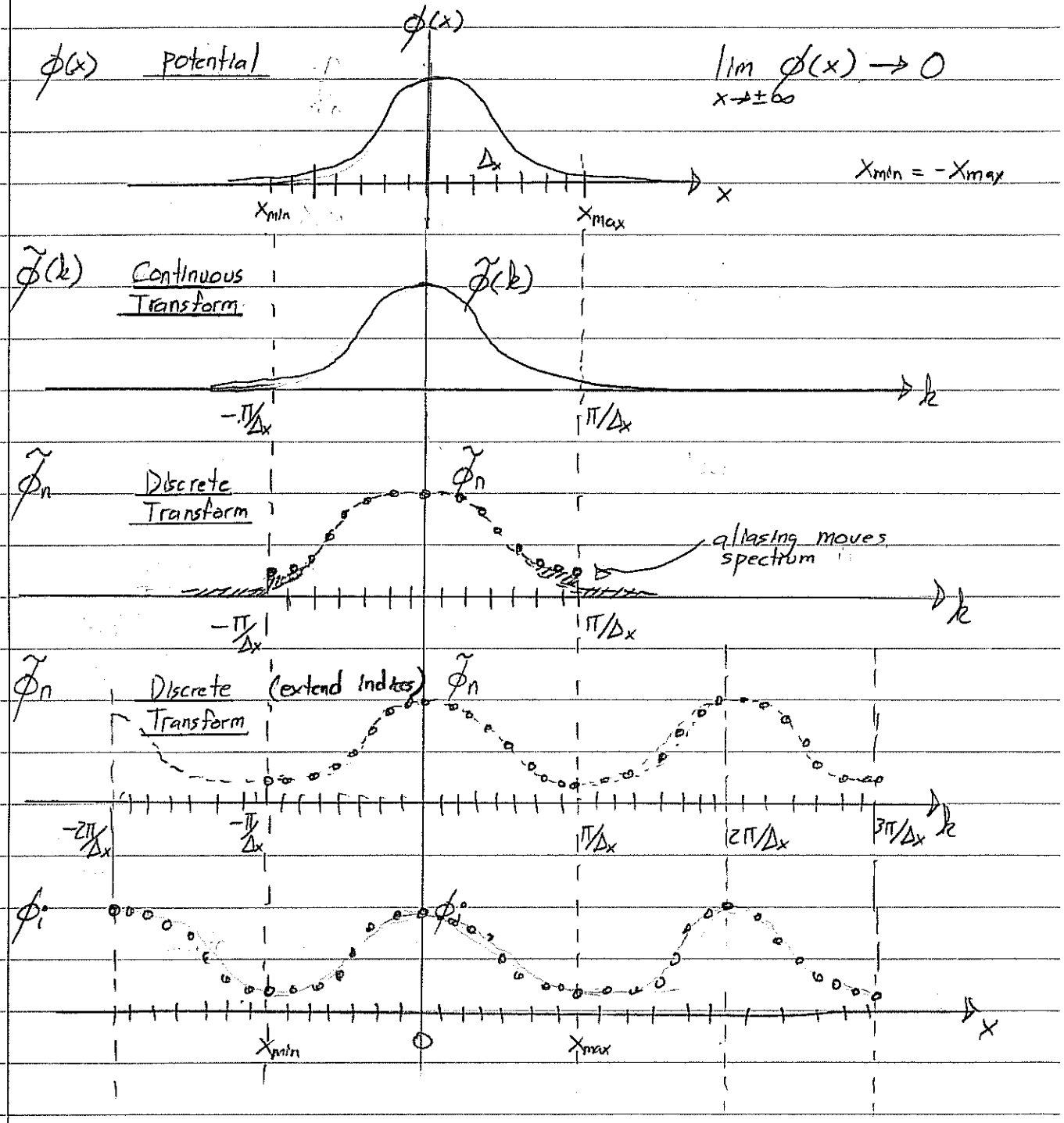

Application of Discrete Fourier transforms to solve Poisson's Equation:

$$E_x = -\frac{\partial \phi}{\partial x} \iff E_{x_j} = -\frac{\phi_{j+1} - \phi_{j-1}}{2\Delta x}$$

$$\frac{d^2\phi}{dx^2} = -\frac{\rho}{\varepsilon_0} \implies \frac{\phi_{j+1} - 2\phi_j + \phi_{j-1}}{\Delta x^2} = -\frac{\rho_j}{\varepsilon_0}$$

Applying the discrete transform one obtains:

$$\boxed{\begin{aligned} \tilde{E}_{x_n} &= -i K_n \tilde{\phi}_n \qquad K_n = k_n \left[\frac{\sin(k_n \Delta x)}{k_n \Delta x}\right] \\ &\qquad K_n = k_n \, \mathrm{dif}(k_n \Delta x) \\ &\qquad k_n \equiv \frac{2\pi n}{(n_x+1)\Delta x} \end{aligned}}$$

$$\mathrm{dif}(x) \equiv \frac{\sin x}{x} \quad \text{from diffraction theory}$$

and Poisson's eqn becomes

$$\boxed{\begin{aligned} \tilde{\phi}_n &= \frac{\tilde{\rho}_n}{\varepsilon_0 K_n^2} \qquad K_n^2 = k_n^2 \left[\frac{\sin\left(\frac{k_n \Delta x}{2}\right)}{\frac{k_n \Delta x}{2}}\right]^2 \\ &\qquad = k_n^2 \, \mathrm{dif}^2(k_n \Delta x/2) \end{aligned}}$$

Note:

- Factors of K_n^2 need only be calculated once per simulation (store values).

// Aside – Example Derivation of Discrete Transform Formula.

$$E_{x_j} = -\frac{\phi_{j+1} - \phi_{j-1}}{2\Delta_x}$$

$$\begin{cases} \phi_j = \dfrac{1}{(n_x+1)\Delta_x} \displaystyle\sum_{n=0}^{n_x} e^{\frac{-i2\pi n j}{n_x+1}} \tilde{\phi}_n \\ E_{x_j} = \dfrac{1}{(n_x+1)\Delta_x} \displaystyle\sum_{n=0}^{n_x} e^{\frac{-i2\pi n j}{n_x+1}} \tilde{E}_{x_n} \end{cases}$$

Substitute transforms in difference formula:

$$2\Delta_x \sum_{n=0}^{n_x} e^{\frac{-i2\pi n j}{n_x+1}} \tilde{E}_n =$$

$$= -\sum_{n=0}^{n_x} e^{\frac{-i2\pi n j}{n_x+1}} \tilde{\phi}_n \left\{ e^{\frac{-i2\pi n}{n_x+1}} - e^{\frac{i2\pi n}{n_x+1}} \right\}$$

$$\Delta_x \sum_{n=0}^{n_x} e^{\frac{-i2\pi n j}{n_x+1}} \tilde{E}_n = i \sum_{n=0}^{n_x} e^{\frac{-i2\pi n j}{n_x+1}} \sin\left(\frac{2\pi n}{n_x+1}\right) \tilde{\phi}_n$$

This equation must hold true for each complex term $\propto e^{\frac{-i2\pi n j}{n_x+1}}$ to be valid for general j.

$$\Rightarrow \quad \tilde{E}_n = \frac{i}{\Delta_x} \sin\left(\frac{2\pi n}{n_x+1}\right) \cdot \tilde{\phi}_n$$

$$k_n = \frac{2\pi n}{(n_x+1)\Delta_x}$$

$$\Rightarrow \quad \tilde{E}_n = i\, k_n \left[\frac{\sin(k_n \Delta_x)}{k_n \Delta_x}\right] \tilde{\phi}_n$$

//

Typical discrete Fourier Transform Field Solution (not optimized)

$$\rho_j \xrightarrow[\text{FT}]{\text{Foward Trans.}} \tilde{\rho}_n \xrightarrow[\cdot \frac{1}{k_n^2}]{\text{Multiply}} \tilde{\phi}_n \xrightarrow[\text{IFT}]{\text{Inverse Trans.}} \phi_j \xrightarrow{\text{Finite Diff.}} E_{xj}$$

The Fast Fourier Transform (FFT) makes this procedure numerically efficient.

- Discrete transform (no optimization) $\sim (n_x+1)^2$ complex operations.

- FFT exploits symmetries to reduce needed operations to $\sim (n_x+1)\ln(n_x+1)$.
  - Huge savings for large n_x.

- The needed symmetries exist only for certain numbers of grid points. In the simplest manifestations:

$$n_x + 1 = 2^p \qquad p = 1, 2, 3, \ldots$$

  - reduced gridding freedom.
  - other manifestations allow 2^p and products of prime numbers for more possibilities ..

The FFT can be combined with other procedures such as capacity matrices to implement boundary conditions for interior conductors, etc. This allows rapid field solutions in complicated geometries.

FFT is fastest method for simple geometry.

Particle Weighting

We have outlined methods to solve Electrostatic! Maxwell's equations on a discrete spatial grid. To complete the description we must:

- Specify how to deposit macro-particle charges and currents on the mesh.
- Specify how to interpolate fields on the spatial grid points to the macroparticle coordinates (not generally on the mesh) to apply in the particle advance.
- Smooth interactions resulting from the small number of macro-particles to reduce artifical collisions resulting from the use of an unphysically small number of macro-particles.

This is called the "particle weighting" problem.

Birdsall & Langdon pg 10

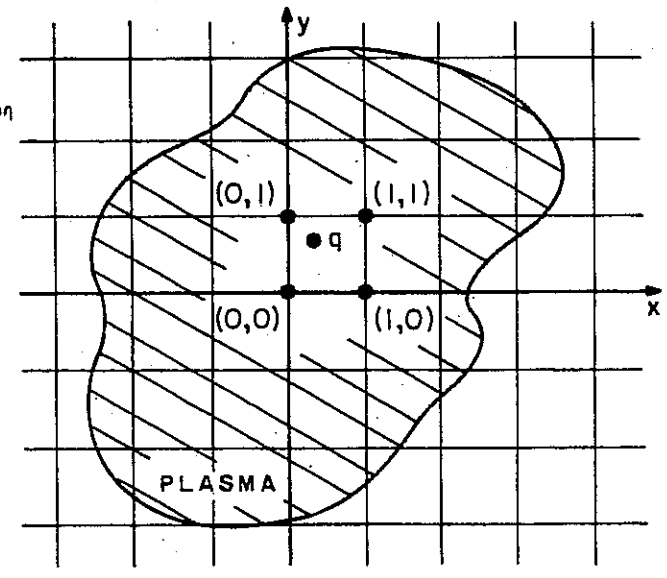

Figure 2-2b A mathematical grid is set into the plasma region in order to measure charge and current densities ρ, **J**; from these we will obtain the electric and magnetic fields **E**, **B** on the grid. A charged particle q at (x,y) will typically be counted in terms of ρ at the nearby grid points (0,0), (1,0); (1,1), (0,1) and in terms of **J** at the faces between these points. The force on q will also be obtained from the fields at these nearby points.

It is found that it is usually better to employ the same weighting schemes to both deposit the Macro-particles charges and currents on the mesh and to extrapolate the fields at gridded points to the Macro-particles.

- Avoids unphysical self-forces where the particle accelerates itself.

Many methods of particle weighting exist. Can be grouped into 4 catagories:

1) <u>Nearest Grid Point</u>
2) <u>Cloud in Cell</u> (CIC)
   - Shaped particles. Linear $\Rightarrow$ Particle-in-Cell PIC
3) <u>Multipole</u>
   - Dipole, subtracted dipole, etc.
4) <u>Higher order Methods</u>
   - Splines
   - $\vec{k}$ space cutoffs in discrete transforms

   ⋮

Possible hybrid methods also exist. We will illustrate methods 1) and 2) in 1D for electrostatic problems. Generalizations to higher dimensions are straightforward. Descriptions of methods can be found in the literature.

1) Nearest Grid Point:

Assign charges to the nearest grid cell.

- Fast and simple
- Noisy

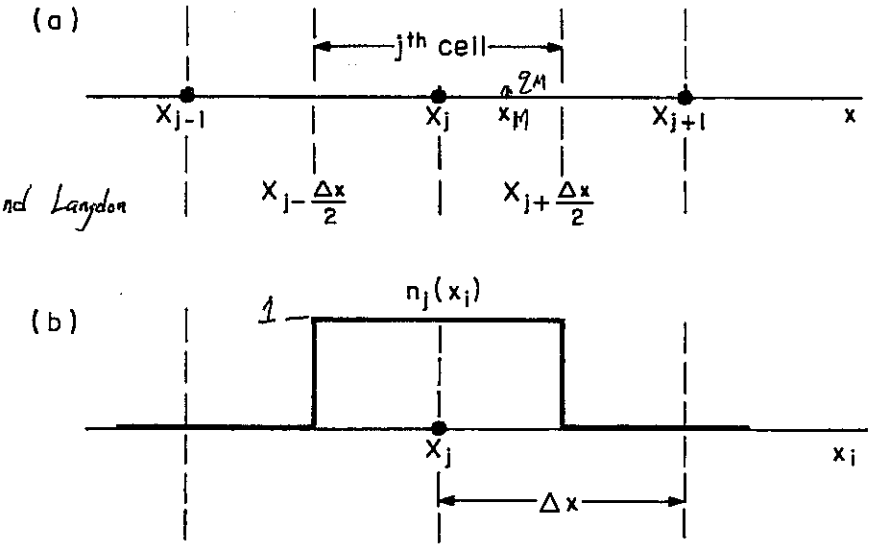

Birdsall and Langdon pg 20.

Figure 2-6a (a) Zero-order particle and field weighting, also called nearest-grid-point, or, NGP. Particles in the jth cell, that is, with positions $x_i \in X_j \pm \Delta x/2$, are assigned to X_j to obtain grid density $n(X_j)$. All of these particles are acted on by the field at X_j, $E(X_j)$. (b) The density $n_j(X_i)$ at point X_j due to a particle at x_M as the particle moves through the cell centered on X_j. This density may be interpreted as the effective particle shape.

q_M, x_M = charge and coordinate of Macro-particle

X_j = closest grid cell.

charge Deposition :	$q_j = q_M$
Field :	$E_x\big\|_{x=x_M} = E_{x_j}$

2) Cloud in Cell

Shaped macroparticles pass freely through each-other.

- Smoother than Nearest Grid Point.
- For linear interpolation results in simple, commonly used "Particle-in-Cell" (PIC) method.

Illustrate 1D PIC "Area" weighting:

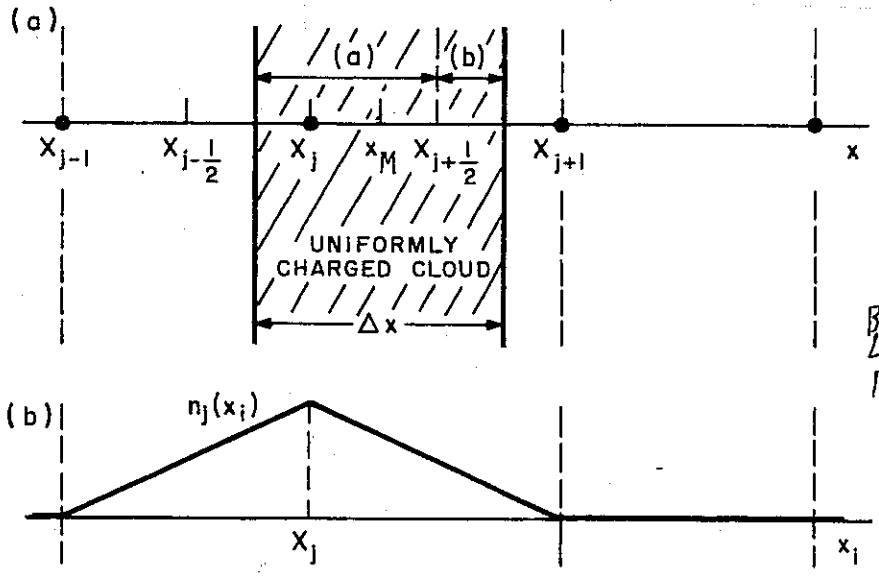

Birdsall & Langdon pg 21

Figure 2-6b (a) First-order particle weighting, or cloud-in-cell model CIC. The nominal finite-size charged particle, or cloud, is one cell wide, with center at x_i. This weighting puts that part of the cloud which is in the jth cell at X_j, fraction (a), and that part which is in the $(j+1)^{th}$ cell at X_{j+1}, fraction (b). This weighting is the same as applying NGP interpolation to each elemental part. (b) The grid density $n_j(x_i)$ at point x_i as the particle moves past X_j, again displaying the effective particle shape $S(x)$.

q_M, X_M = charge and coordinate of macro-particle

X_j = closest grid cell

Charge Deposition:

$$q_j = q_M \left[\frac{\Delta_x - (X_M - X_j)}{\Delta_x} \right] = \frac{X_{j+1} - X_M}{\Delta_x}$$

$$q_{j+1} = q_M \left[\frac{X_M - X_j}{\Delta_x} \right]$$

Field:

$$E_x \Big|_{x=x_M} = \left[\frac{X_{j+1} - X_M}{\Delta_x} \right] E_j + \left[\frac{X_M - X_j}{\Delta_x} \right] E_{j+1}$$

Computational Cycle for Particle Simulations

We now have (simplified) notions of the parts that make up a particle simulation.

1) Particle Moving
2) Field Solver on a discrete mesh
3) Weighting of particles and Fields to and from the mesh.

These are combined in a computational cycle:

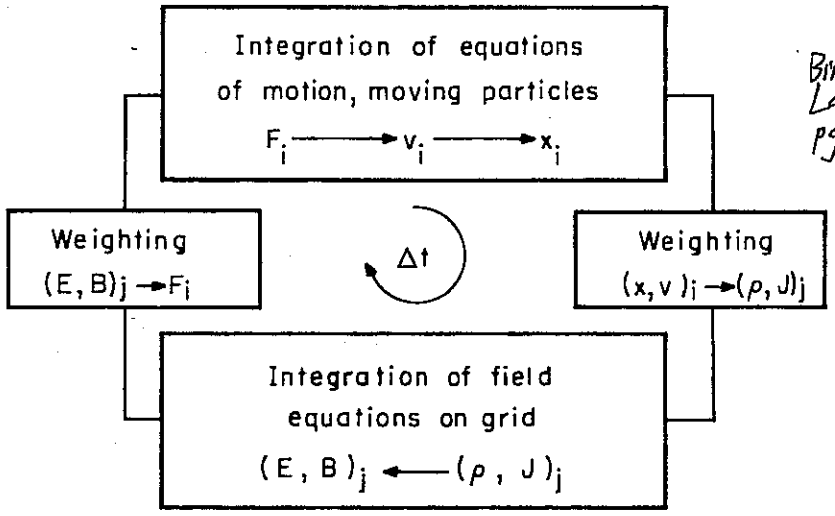

Birdsall & Langdon pg 11

Figure 2-3a A typical cycle, one time step, in a particle simulation program. The particles are numbered $i = 1, 2, \ldots, NP$; the grid indices are j, which become vectors in 2 and 3 dimensions.

At synchronization steps, particle coordinates, velocities, and fields will all be in-phase and diagnostics may be accumulated.

Diagnostics:

Depend on what is analyzed. Typical choices:

- Moments – statistical sums over the particle distribution (slices and full beam), often plotted as time histories as the beam evolves in the accelerator:

centroid: $x_c = \langle x \rangle_\perp$ .....

RMS Widths: Beam Size $r_x = 2\langle (x-x_c)^2 \rangle^{1/2}$, ... etc.

Emittance: $\varepsilon_x = 16\left[\langle (x-x_c)^2\rangle\langle (x'-x_c')^2\rangle - \langle (x-x_c)(x'-x_c')\rangle^2\right]^{1/2}$,

etc.

Here; $\langle \cdots \rangle_\perp = \frac{1}{N_s}\sum_i^{\text{slice}} \{\cdots\}_i$ ..... etc.

Slice emittance "history"

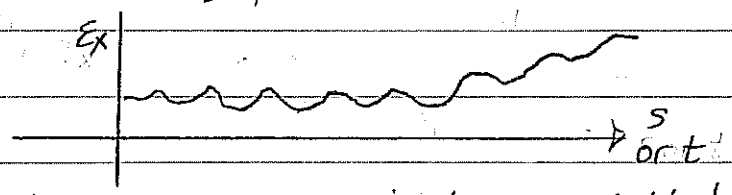

- Particle phase-space projections plotted as snapshots in time (x-x', y-y', x-y, x'-y', ...).

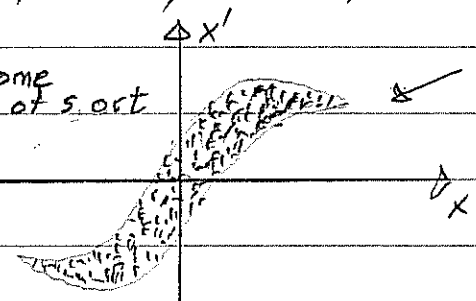

scatter plot of enough macro-particles to visualize the phase-volume and structure of the beam.

Plotting snapshots at periodic locations allows vizualization of the evolution of beam distortions:

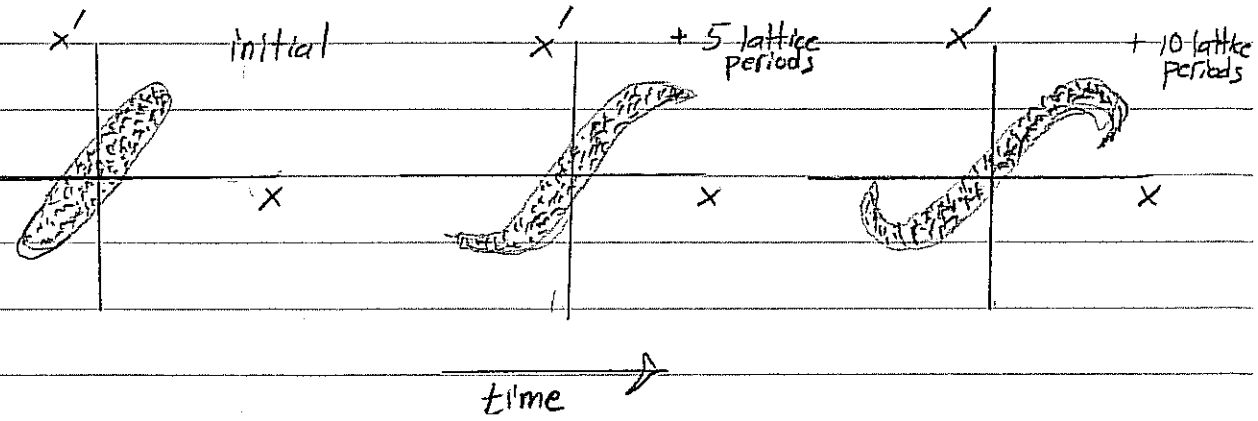

- <u>Field</u> Diagnostics:

Contours of self and applied fields illustrate field structure.

Examples:

1) Total potential contors of ϕ (self and applied) of an elliptical beam in an electric quadrupole formed by 4 biased rods.

same ϕ contours with beam particles plotted

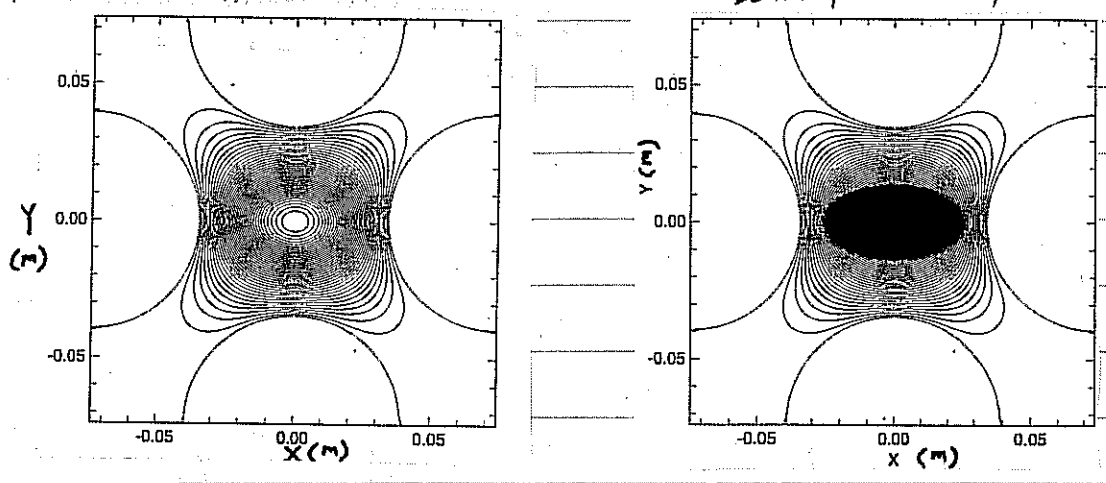

2) <u>Applied Field</u> Scalar magnetic potential contours of a permanant magnet lense illustrate the structure of applied field nonlinearities:

8 Block Permanent Magnet Quadrupole.

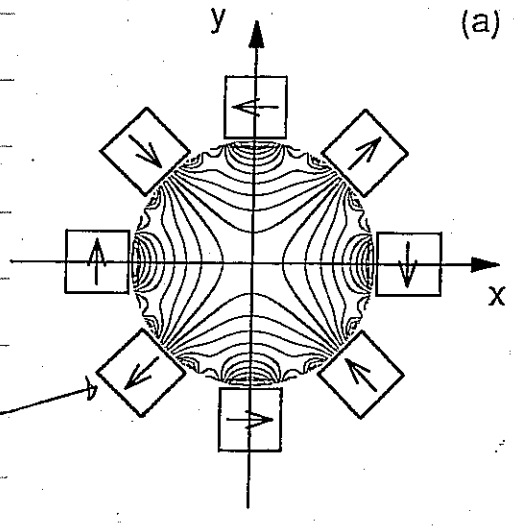

Note: contours deviate from hyperbolic near apeture edge.

Numerous other field diagnostics are possible:

- Field energy, multipole moments,

Particle Loads

To start the simulation, one must specify and "load" the initial distribution function.

In realistic accelerators, focusing elements are s-varying. In such situations there are in general no known equilibrium distribution functions. Moreover, it is unclear in most cases if the beam is even best thought of as an equilibrium + perturbations as is typical in plasma physics. Rather, in accelerators, the beam is injected from a source and may only reside in the machine (especially a linac) for a small number of characteristic oscillation periods and may not fully relax to an equilibrium-like state. In such situations, so-called "source-to-target" simulations where the particles are simulated off the source and tracked to the target can be most realistic if carried out with realistic focusing fields, accelerating waveforms, alignment errors, etc.

Unfortunately, such idealized source-to-target simulations can rarely be carried out due to computer limitations.

- Memory limits
- Numerical convergance and accuracy ....

Two ways around this limitation:

1) Load experimentally measured distribution at some point in the machine and advance as an initial condition.
2) Load an idealized initial distribution.

The 1st option can have practical difficulties:

- Diagnostics often are far from an ideal 6D "snapshot" of the beam phase-space.
  - Much information typically lost.
- Process of measuring the beam can itself change the beam.

Most commonly, some experimental measures such as:

- rms beam sizes r_x, r_y, r_x', r_y'
- rms emittances $\varepsilon_x, \varepsilon_y$

are loaded in the form of idealized distributions.

It can be insightful to initialize the beam in a simplified manner

- Fewer simultaneous processes can allow one to more clearly see how limits arise.
- Seed perturbations of relevance when analyzing resonance effects, instabilities, halo, etc.

In these situations it is often useful to load a round, continuously focused distribution such as:

- Thermal Equilibrium
- Waterbag
- KV

and then transform the particle coordinates to "match" the local focusing structure of the lattice using a local KV envelope solution:

$$\frac{d^2}{ds^2} r_x(s) + \kappa_x(s) r_x(s) - \frac{2Q(s)}{r_x(s)+r_y(s)} - \frac{\varepsilon_x^2(s)}{r_x^3(s)} = 0$$

$$\frac{d^2}{ds^2} r_y(s) + \kappa_y(s) r_y(s) - \frac{2Q(s)}{r_x(s)+r_y(s)} - \frac{\varepsilon_y^2(s)}{r_y^3(s)} = 0$$

$\kappa_x(s), \kappa_y(s)$ = lattice focusing constants
$Q(s)$ = local perveance (specified)
$\varepsilon_x(s), \varepsilon_y(s)$ = local emittances (specified)

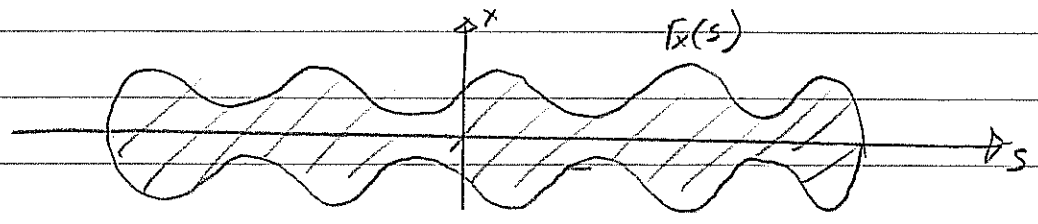

Procedure:

1st

Load in each $\perp$ slice round, continuous distribution:

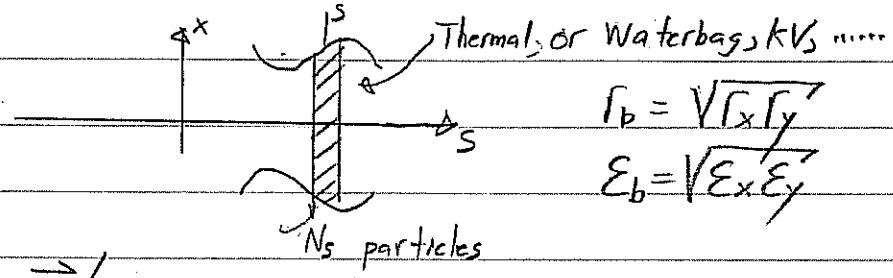

$$r_b = \sqrt{r_x r_y}$$

$$\varepsilon_b = \sqrt{\varepsilon_x \varepsilon_y}$$

$\Rightarrow$ $\vec{X}_i$, $\vec{X}_i'$ specified

2nd

Transform the spatial coordinates to match the elliptical envelope structure.

$$x_i \longrightarrow \frac{r_x}{r_b} x_i$$

$$y_i \longrightarrow \frac{r_y}{r_b} y_i$$

3rd

Transform the local thermal velocity spreads to obtain the right average thermal force.

$$x_i' \longrightarrow \frac{\varepsilon_x}{\varepsilon_b} \frac{r_b}{r_x} x_i'$$

$$y_i' \longrightarrow \frac{\varepsilon_y}{\varepsilon_b} \frac{r_b}{r_y} y_i'$$

4th

Add the correct coherent velocity to match the needed envelope angle.

$$x_i' \longrightarrow x_i' + r_x' \frac{x_i}{r_x}$$

$$y_i' \longrightarrow y_i' + r_y' \frac{y_i}{r_y}$$

// Aside – The semi-Gaussian Distribution

It is not necessary to always load something based on a transformation of an equilibrium distribution to get a good quiescent load. Note that for high space-charge intensities:

- Beam space charge will be more or less uniform out to the edge, where the density will rapidly fall to zero.

- If the beam is injected off a uniform tempeture source or has relaxed, one expects roughly uniform thermal velocity spread across the cross-section of the beam.

This suggests the so-called "semi-Gaussian" load specified as follows:

- Uniform density within an elliptical beam envelope.

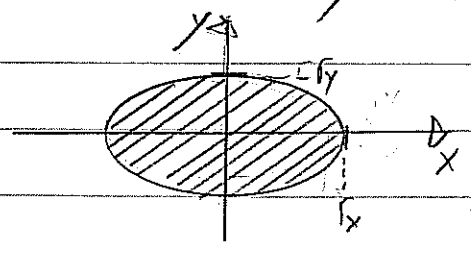

x_i, y_i uniformly distributed for $(x/r_x)^2 + (y/r_y)^2 \leq 1$.

- Gaussian distributed thermal velocity spread with the correct coherent velocity to match the needed envelope angles.

$$x_i' = r_x' \frac{x_i}{r_x} + \frac{\varepsilon_x}{2r_x} \tilde{r}_{x_i}$$

$$y_i' = r_y' \frac{y_i}{r_y} + \frac{\varepsilon_y}{2r_y} \tilde{r}_{y_i}$$

$\tilde{r}_{x,y_i}$ Gaussian distributed with unit variance $\left(\frac{1}{N_s}\sum_i^{slice} \tilde{r}_{x,y_i}^2 = 1\right)$

The semi-Gaussian load results in "squared" initial x-x' and y-y' phase space projections:

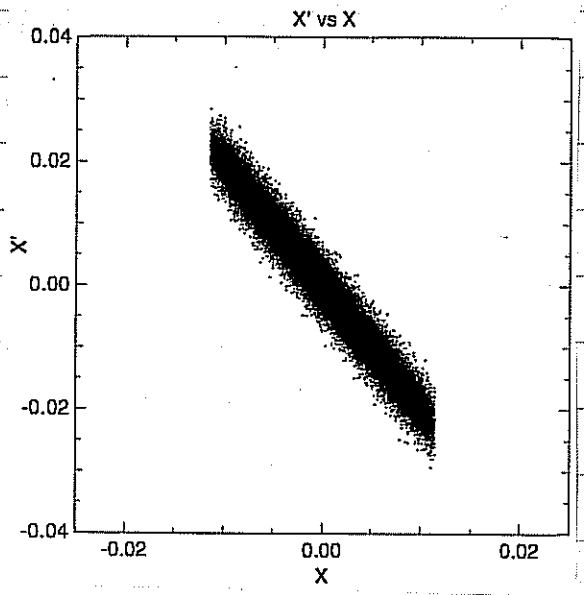

Initial load in a symmetric FODO AG Quadrupole transport lattice

The unphysical edges typically relax rapidly without perturbing the low order RMS structure of the beam (envelope match, emittance, etc.).

1 lattice period advance

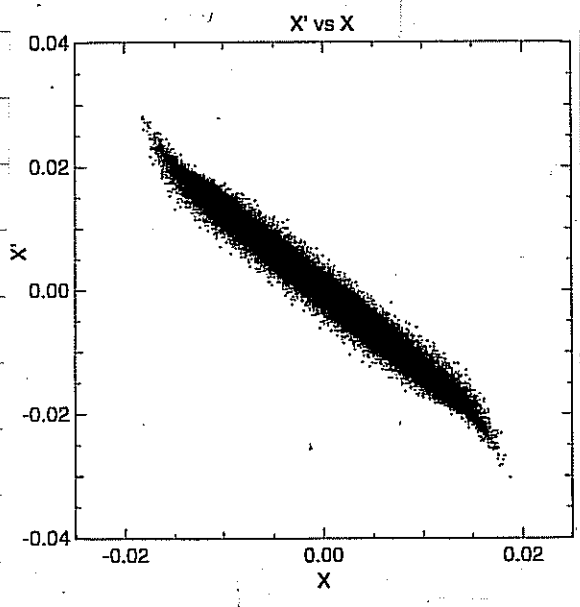

4 lattice period advance

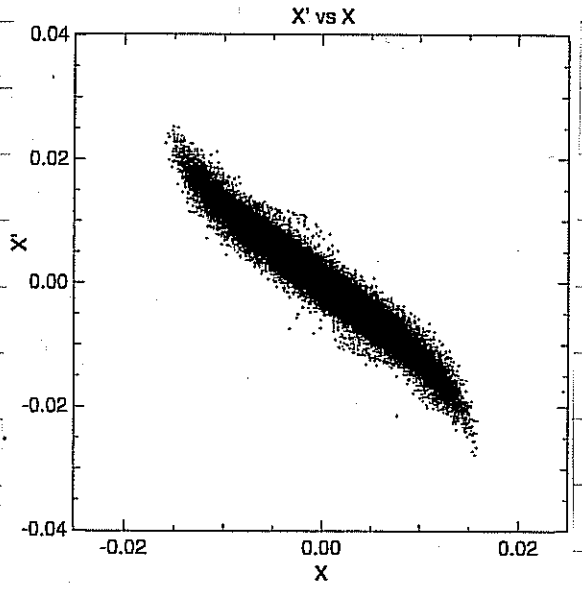

Numerous other loading techniques exist to address specific issues. //

Numerical Convergence

Numerical simulations must be checked for proper resolution and statistics to be confident that answers obtained are correct and physical.

Resolution on discritized quantities
- Time step in particle advance
- Spatial grid for fields

Statistics (number of macroparticles) to control noise.

More resolution and statistics require more computer time and memory. To be practical, one generally wishes to solve problems with the minimum resources required to achieve correct, converged answers. Unfortunately, there are no set rules on what resolution and statistics are required. This depends on what one is examining, how long the simulations are run, what numerical methods are employed, ...

Some general guidance:

- The statistical rms emittances:

$$\varepsilon_x = 4\left[\langle x^2\rangle_\perp \langle x'^2\rangle_\perp - \langle xx'\rangle_\perp^2\right]^{1/2}$$

$$\varepsilon_y = 4\left[\langle y^2\rangle_\perp \langle y'^2\rangle_\perp - \langle yy'\rangle_\perp\right]^{1/2}$$

often prove to be sensitive and easy to interpret measures of numerical differences when plotted as overlaid time histories.
  - picks up small phase space distortions induced by numerical errors.

general guidance continued ....

- To get started, find results from similar problems using similar methods.

- Benchmark code and methods against problems with known analytical solutions, established codes using both similar and different numerical methods, ...

- Recheck numerical convergence whenever runs differ significantly <u>or</u> when differing quantities are analyzed.

  - What is adequate for one measure of the beam (say image charge structure) may not be for another (say collective modes).

- Although it is common to increase resolution and statistics till relevant quantities do not vary, it is <u>also useful to purposefully analyze poor resolution and statistics regimes so the characteristics of unphysical numerical errors can be recognized.</u>

- Expect to make many setup, convergence, and debugging runs for each useful series of simulations carried out.

Specific Numerical Convergence Comments:

Time Resolution.

These comments are applicable to both spatial or time steps of the particle advance. We will frame estimates in terms of timesteps.

- Particle coordinates should not move through more than one cell in a single step. This is a standard "Courant" condition:

$$\boxed{\begin{aligned} v_x \Delta_t &< \Delta_x \\ v_y \Delta_t &< \Delta_y \\ v_z \Delta_t &< \Delta_z \end{aligned}}$$

for all particles.

- Enough steps should be taken to resolve variations in applied field structures.

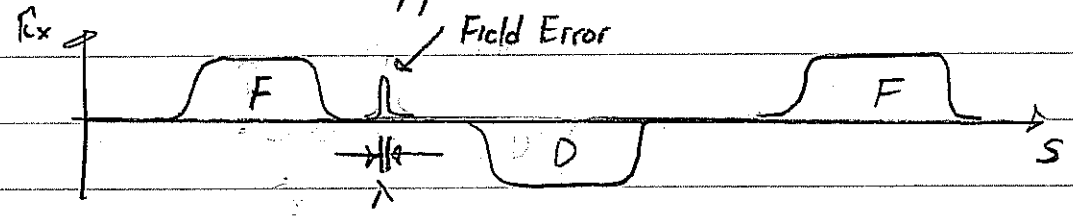

$$\boxed{v_s \Delta_t < \lambda \quad ; \quad \lambda = \text{shortest wavelength of field structures to be modeled}}$$

- Phase variations in collective waves (if of interest) should be resolved. For a leap-frog mover this requires:

$$\boxed{\begin{aligned} &\omega = \text{mode frequency component} \\ &\frac{\omega \Delta_t}{2\pi} < \frac{1}{2} \end{aligned}}$$

Spatial Resolution

For cold beams the beam edge can be sharp for most reasonable distribution functions:

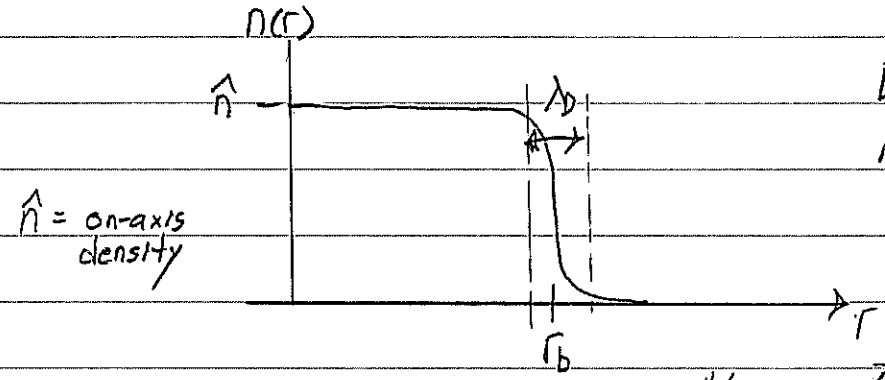

Density falls of in $\mathcal{O}(\lambda_D)$

Debye length: $\lambda_D = \dfrac{v_t}{\omega_p} = \left(\dfrac{\varepsilon_0 k_B T}{\hat{n} q^2}\right)^{1/2}$ $\qquad v_t = (k_B T/m)^{1/2}$, $\quad \omega_p = \left(\dfrac{q^2 \hat{n}}{\varepsilon_0 m}\right)^{1/2}$

$$r_b = \sim 5\lambda_D \rightarrow 30\lambda_D \quad \text{typical.}$$

To resolve edge physics, the mesh should have several cells across the rapid density variation near the edge of the beam.

$$\boxed{dx, dy < \frac{\lambda_{Dxy}}{2} \qquad \lambda_{Dxy} = \left(\frac{k_B T_{xy}}{m}\right)^{1/2} \qquad T_{xy} = \text{local kinetic temperature}}$$

The mesh should also resolve relevant spatial scales associated with processes of interest:

- If applied electrostatic fields are calculated from biased conductors, the mesh should resolve conductor structures or special corrections should be made.
- Self-field fluctuations induced by collective modes should be resolved.

Collective mode resolution: From Eigenfunctions to be presented later in the class:

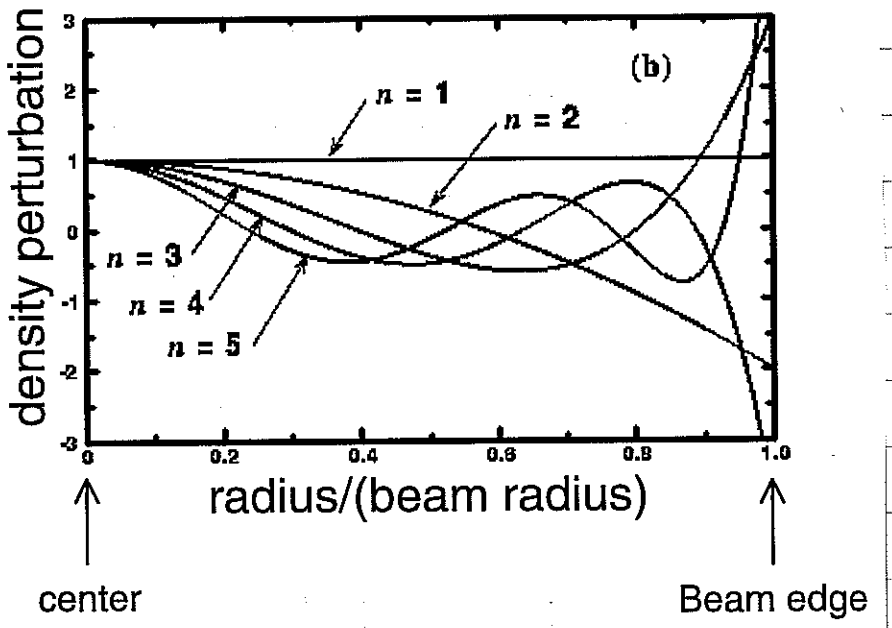

Collective mode density perturbations on a uniform density beam.

$\Rightarrow \quad dx, dy < \lambda \sim$ shortest characteristic wavelength of modes of interest.

Note that higher order modes (n larger) will become hard to resolve. Moreover, such perturbations also oscillate rapidly making time (s) stepsize resolution likewise difficult.

Statistics:

Collective effects typically require having a significant number of particles N_D within the characteristic screening radius characterized by the Debye length:

2D: $$N_D = \sum_i \int_{\substack{\text{circle} \\ |\vec{x}|<\lambda_D}} d^2x \, \delta^{(2)}(\vec{x}-\vec{x}_i) \gg 1$$

$\vec{x}_i$ = macro-particle coordinate.

3D: $$N_D = \sum_i \int_{\substack{\text{sphere} \\ |\vec{x}|<\lambda_D}} d^3x \, \delta^{(3)}(\vec{x}-\vec{x}_i) \gg 1$$

where:

$$\lambda_D = \frac{v_t}{\omega_p} = \left(\frac{\varepsilon_0 k_B T}{\hat{n} q^2}\right)^{1/2} \qquad v_t = (k_B T/m)^{1/2} \qquad \omega_p = \left(\frac{q^2 \hat{n}}{\varepsilon_0 m}\right)^{1/2}$$

$\sum_i \Rightarrow$ sum over all macro particles.

In simulations of higher order collective modes it may also be necessary to have a significant number of particles per cell on a mesh that resolves the relevant spatial variations of mode induced self-field fluctuations.

2D: $$N_{cell} = \sum_i \int_{cell} d^2x \, \delta^{(2)}(\vec{x}-\vec{x}_i) \gg 1$$

3D: $$N_{cell} = \sum_i \int_{cell} d^3x \, \delta^{(3)}(\vec{x}-\vec{x}_i) \gg 1$$

- Larger N_{cell} prevents local self-fields from being noise dominated.
- Larger N_{cell} leads to larger N_D, typically $N_D > N_{cell}$, since λ_D must be resolved on the grid.

Good statistics are <u>only</u> needed in the beam core with the possible exception of certain beam-halo problems and near the beam edge.

- Most beams will only occupy a fraction of the full grid.

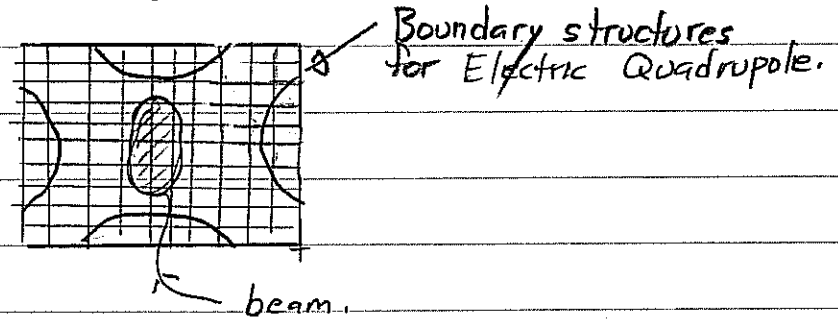

statistics should be evaluated in the cells that the beam occupies rather than average grid measures.

No comprehensive rules exist for how good the statistics must be. <u>Individual problems must be checked and verified.</u> Some general comments:

- What is adequate will typically depend on what is analyzed
  - Image fields may be resolved with few particles
  - Collective waves may take many particles if low noise (interpetable) diagnostic projections are needed.
- Longer runs generally require increased statistics
- Poor statistics result in unphysical collisionality that is often characterized by a linear rise in beam emittances with simulation time.

Classes of Particle Simulations.

How important is smoothing?

3D Beam: $N \sim 10^{10} - 10^{14}$ particles typical

Simulations: $N \lesssim 10^{8}$ practical (modern parallel computers), typical $10^{3} - 10^{6}$

Each simulation particle may represent: $10^{3} \rightarrow 10^{11}$ particles in the real beam for 3D simulations.

- Smoothing involved with particle weightings are key to obtaining physical answers and limiting collisionality.

Is the situation really this bad?

- Lower dimensonal models typically simulated.

3D Model

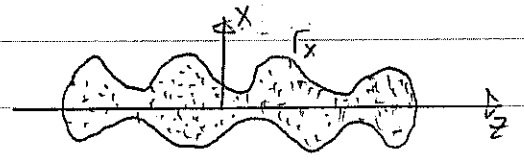

N point particles with smoothed interactions

Phase Space:

x, y, z
p_x, p_y, p_z } 6D

Physical charge – point charges

$$\rho = \sum_i q\, \delta(x-x_i)\,\delta(y-y_i)\,\delta(z-z_i)$$

Smoothed charge

$$\rho = \sum_i q_M\, f(x-x_i, y-y_i, z-z_i)$$

q_M: Macro particle charge

f: smoothed shape function

2D ⊥ Thin Slice Model

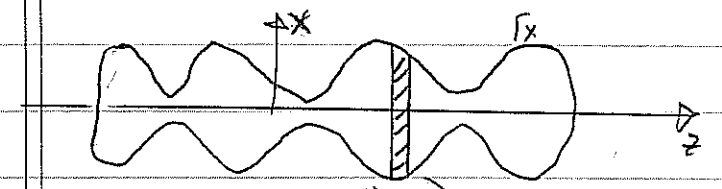

N line charges with smoothed interactions.

Thin slice

$\frac{\partial}{\partial z} \ll \nabla_\perp$

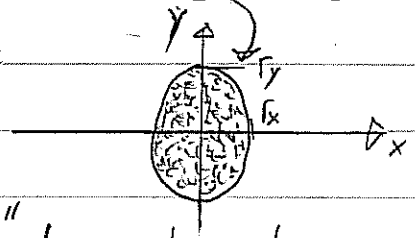

Phase Space:

$\left.\begin{matrix} x, y \\ p_x, p_y \end{matrix}\right\}$ 4D + possible 1D p_z

4D or 5D

"Physical" charge - line charges

$$\rho = \sum_i \lambda_p \delta(x-x_i)\delta(y-y_i)$$

Smoothed charge -

$$\rho = \sum_i \lambda_M f(x-x_i, y-y_i)$$

λ_M : Macro particle line charge

f : smoothing function

The slice must be tracked in s with each particle moving the same increment in s with each step so that a slice maps to a slice.

- If p_z is included the velocity distribution must be assumed "frozen in".

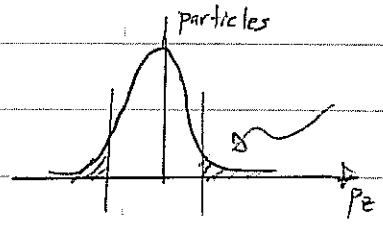

parts that would leave assumed replenished by particles from adjacent slices.

- Response to acceleration may be modeled with

- "Thick" slice models also possible with periodic boundary conditions on the "slice" to try to recover some 3D effects of a long pulse in a periodic lattice.

2D r-z Model

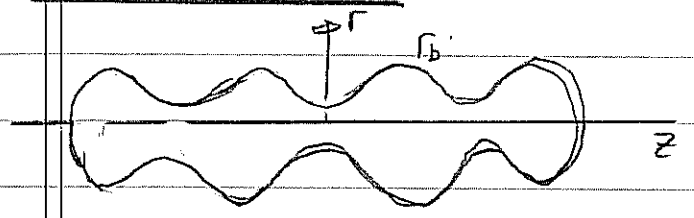

N charged Rings with smoothed interactions

$\partial/\partial\theta = 0$ Axisymmetric

Phase Space.

$\left.\begin{matrix} r, z \\ p_r, p_z \end{matrix}\right\}$ 4D + possible 1D p_θ (angular mom.)

4D or 5D.

physical charge – cylindrical rings

$$\rho = \sum_i \frac{Q_i}{2\pi} \frac{\delta(r-r_i)\,\delta(z-z_i)}{r_i}$$

Smoothed charge

$$\rho = \sum_i \frac{Q_M}{2\pi} \frac{f(r-r_i,\, z-z_i)}{r_i}$$

Q_M : Macro particle charge
f : Smoothing function.

- Used to model solinoidal transport of an initial axisymmetric beam.
- Sometimes used to model AG beams with an approximately equivalent, s-dependant focusing force. $\vec{x}_\perp'' = k_{\beta 0}^2(s)\,\vec{x}_\perp + \cdots\cdots$

1D Axisymmetric Model

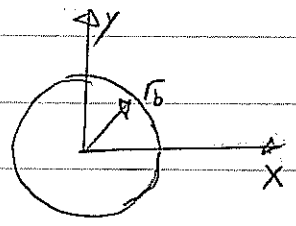

N charged cylinders with smoothed interactions

$\partial/\partial\theta = 0$

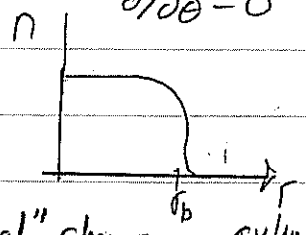

Phase – Space

$\left.\begin{matrix} r \\ p_r \end{matrix}\right\}$ 2D + possible p_θ, p_z

2D to 4D

"physical" charge – cylindrical sheets

$$\rho = \sum_i \frac{Q_i}{2\pi} \frac{\delta(r-r_i)}{r_i}$$

Smoothed charge

$$\rho = \sum_i \frac{Q_M}{2\pi} \frac{f(r-r_i)}{r_i}$$

Q_M : Macro charge
f : Smoothing function

- Simple model for continuously focused, axisymmetric beams

1D slab Model

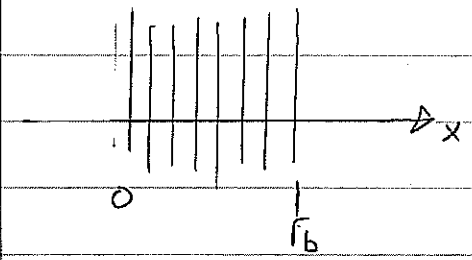

N charged slabs with smoothed interactions.

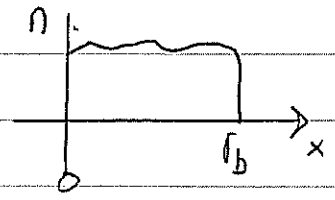

Phase-Space

$\left.\begin{matrix} x \\ p_x \end{matrix}\right\}$ 2D + possible p_y, p_z

2D to 4D

"physical" charge - sheets

$$\rho = \sum_i \sigma\, \delta(x - x_i)$$

smoothed charge

$$\rho = \sum_i \sigma_M\, f(x - x_i)$$

σ_M: macro particle charge
f: smoothing function

- Most simple model, but slab geometry is least physical.

It is not immediately clear how such different models can in many cases represent qualitatively similar collective interactions since force laws can change form with dimension. For example, in free space, we find that:

Model	Free space: Field due to ith "particle"
3D	$\vec{E} = \dfrac{q_i}{4\pi\varepsilon_0} \dfrac{(\vec{x} - \vec{x}_i)}{\lvert\vec{x} - \vec{x}_i\rvert^3}$
2D	$\vec{E} = \dfrac{\lambda_i}{2\pi\varepsilon_0} \dfrac{(\vec{x} - \vec{x}_i)}{\lvert\vec{x} - \vec{x}_i\rvert^2}$ $\quad \lambda_i$ = line-charge "particle"
1D	$E_x = \dfrac{\sigma_i}{2\varepsilon_0} \dfrac{(x - x_i)}{\lvert x - x_i\rvert}$ $\quad \sigma_i$ = sheet charge "particle"

The reason these radically different interactions can give similar physics is that the screening associated with collective interactions is found to be similiar:

- Debye screening has similiar characteristics in each dimension.

showed 2D form, in class. Will show in final that the 3D scaling obtains the same Debye length definition. $\Rightarrow$

$$\lambda_D = \frac{v_{thermal}}{\omega_p} = \left(\frac{\varepsilon_0 k_B T}{\hat{n} q^2}\right)^{1/2} \qquad v_t = (k_B T/m)^{1/2} \qquad \omega_p = \left(\frac{q^2 \hat{n}}{\varepsilon_0 m}\right)^{1/2}$$

- <u>It is much easier to have a significant number of particles within the characteristic screening distances for lower dimensional problems.</u>

  - Lower dimensional simulations can more easily resolve collective effects!
    (Sometimes people run 3D simulations for collective modes and present garbage answers due to resolution difficulties)

// Example

$q = Ze$ ions

$e = 1.6 \times 10^{-19}$ C

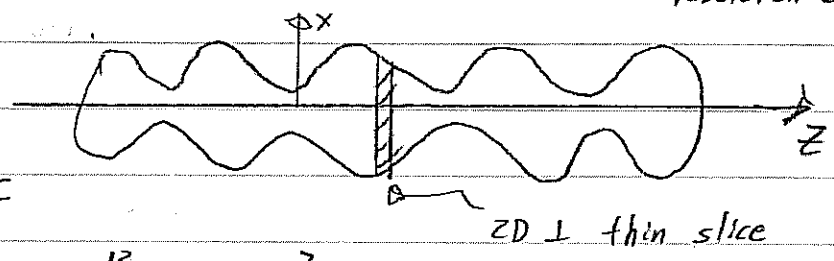

$\lambda \sim 10^{-13} \rightarrow 10^{-7}$ C/m typical for intense beams

$$\frac{\#\text{ particles}}{\text{cm}} = \frac{\lambda}{Ze \cdot 100} \sim \frac{10^4}{Z} \rightarrow \frac{10^{10}}{Z} \qquad q = Ze$$

charge state

- Smoothing still important in lower dimensions and real beam is 3D

Practical Considerations

Computer Memory

Computer memory dictates how large a problem can be run.

- If the problem will not fit into fast memory (RAM), computer performance will be severely compromised.
  - writes to hard disks are slow.

3 main contributions to memory:

1) Particle phase space coordinates
2) Gridded field.
3) General code overhead.

} Dominate for large problems

Generally, particle and field quantities are stored in double precision:

Representation	digits (Floating Point)	Bytes memory
Single Precision	8	4
Double Precision	16	8

Relevant case for most problems

1) Particle Phase Space Coordinates

N_p = # macro particles

D = Dimension of variables characterizing particles.

$$\boxed{\text{Memory} = 8 \times N_p \times D \quad \text{Bytes}}$$

The dimension D depends on the specific type of simulation!

Examples:

3D $D = 7$: x, y, z; $p_x, p_y, p_z, \gamma^{-1}$ (for opt.)

2D $D = 4$: $\perp$ slice in s: x, y; p_x, p_y

2) Gridded field

For electrostatic problems typically need only store ϕ and ρ on the mesh.

- Discrete Fourier Transform complex, but transform is of real functions. Proper optimization can be carried out using only ϕ and ρ arrays.
- Electric field is typically not stored and is calculated for each particle only where needed.
  - Some methods do store gridded $\vec{E}$ to optimize specific problems / computers.

$$N_m = \#\text{ mesh points.}$$
$$= (n_x+1)(n_y+1) \qquad \text{2D} \perp \text{Slice}$$
$$= (n_x+1)(n_y+1)(n_z+1) \qquad \text{3D}$$
$$\vdots$$

Bytes $8 \cdot 2$ ϕ, ρ

$$\boxed{\text{Memory} = 16 * N_m \text{ Bytes}}$$

Dimensonality is also critical in field solves. One typically finds:

1D Simulations:

Fieldsolve trivial - only a small fraction of the work involved in moving particles.

- Greens' functions can be used. (Gauss' Law)

2D Simulations

Fieldsolve is typically a small fraction of the work involved in moving particles if fast, gridded methods are used. (e.g. FFT). Special boundary conditions may increase this fraction.

Numerical Work	Method
Small fraction particle moving	FFT with periodic B.C.
	FFT with Capacity Matrix
	SOR
↓	⋮
Dominates particle moving	Green's Function

3D Simulations

Fieldsolve typically is comparable to or dominates the work involved in moving particles even if fast, gridded methods are employed.

- Fieldsolve efficiency of critical importance in 3D to optimize run time.
- You could teach whole classes just on 3D electrostatic field solve methods for Poisson's equation.

3) General Code Overhead

Some system memory is also used for:

- Scratch arrays for various numerical methods in fieldsolvers, movers, etc.
- Diagnostic routines, graphics packages, etc.

$$\boxed{\text{Memory} = M_{\text{overhead}} \sim \text{characteristic of given code} \quad \text{Typical } 1\text{MB} - \gtrsim 20\text{MB}}$$

Some modern graphics packages are large!

Total memory usuage (Electrostatic PIC)

$$\boxed{\text{Memory} = 8 \times N_p \times D + 16\, N_m + M_{overhead} \quad \text{Bytes}}$$

Machine RAM capacity should not be exceeded.

Speed of Computational Cycle:

The speed of the computational advance cycle is also extremely important and dictates the time that runs will take.

- Parts of the code that more time is spent in should be more carefully optimized to minimize operations
  - Particle mover
  - Field solver
  - Frequent diagnostics such as moments.

- Infrequent diagnostics, loaders, problem setup routines ect. often can be coded with less care since they are only executed infrequently. However, diagnostics often take much wall clock time to code!

It is often useful to benchmark the code in terms of

$$\boxed{t_{step} = \text{Time for a computational cycle in an "ordinary" run step.}}$$

Machine Architectures.

Problems may be simulated on:

1) Serial machines
   - sometimes small clusters of processors without specific need for parallel programing.

2) Parallel machines
   - multi-processors, possibly shared memory but more often linked memory via fast message processing.

Parallel machines have been recently improved with libraries that allow "natural" problem formulation with less effort and they promise to enable much larger simulations (resolution + statistics)
   - Several 100 Million particle simulations possible.

Beams problems may often be conveinently partitioned among processors using axial slices:

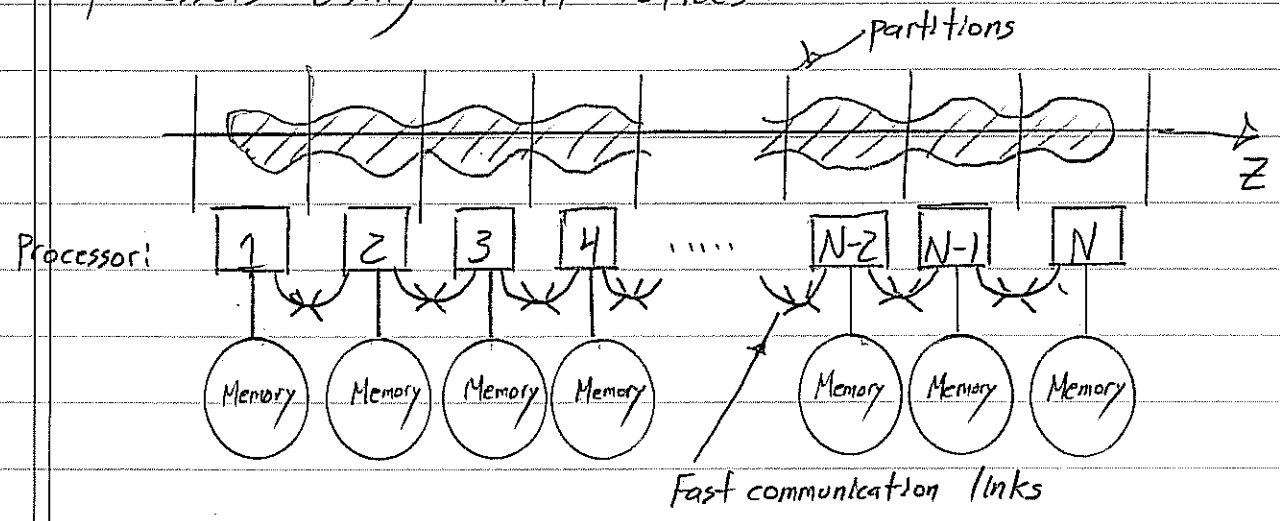

- Sharing of data at boundaries is needed for field solves
- Some problems will require the partitions to be adjusted (particle sorting) to maintain the load balance.
  - processors should ideally share load equally since the slowest will limit the advance.

Ideal parallelization will result in a linear speedup with processor number.

τ_{step} = time per "ordinary" step of computational cycle.

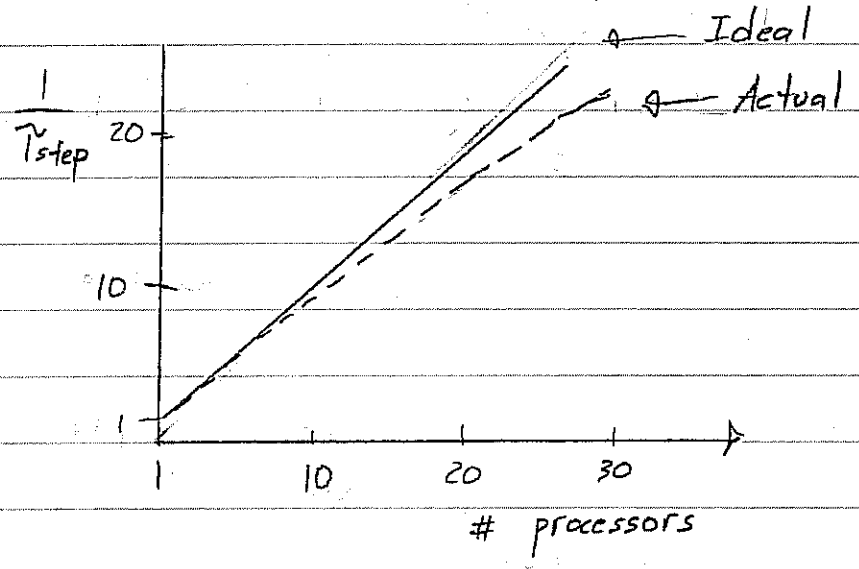

- Actual speedup will be less than ideal due to:
  - overhead in data transfers
  - less than ideal load balance among the processors, resorting of particles, etc.

Even with the significant advances in problem size and speed promised by parallel computers, the solution of realistic 3D beam problems with direct (not gridded) fields will remain far too large a problem to simulate in the forseeable future. Thus we will always try to exploit computer resources to the maximum extent possible

- Better numerical methods
- Parallelization

3D PIC simulations are being used to guide retrofits of an existing ESQ injector at LBL

1st principles, mid-pulse 3D simulations have been carried out to guide injector retrofits aimed at decreasing beam aberrations

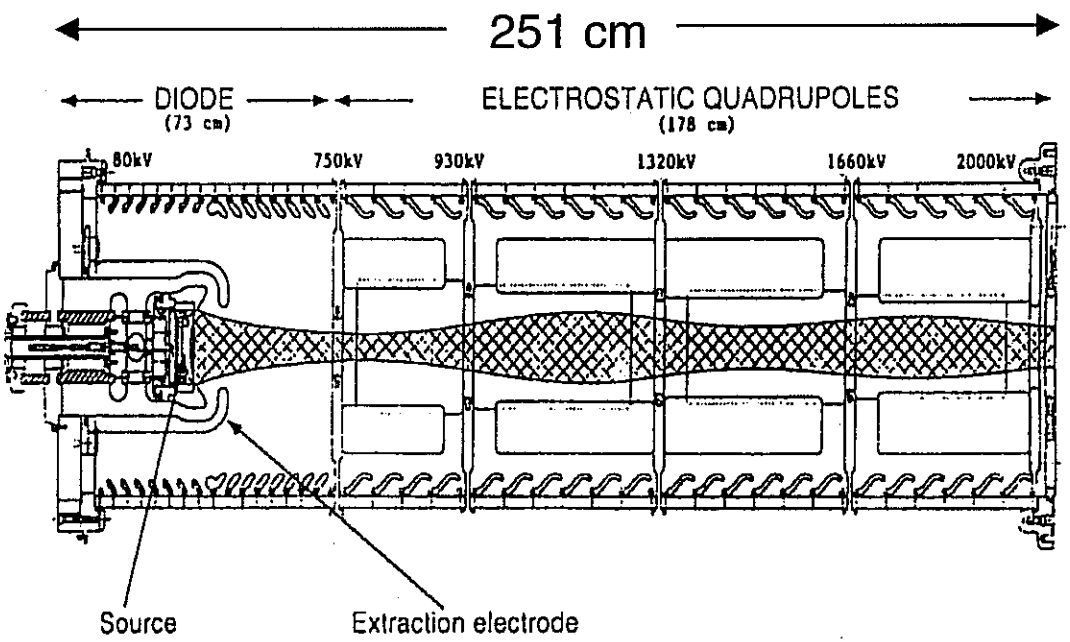

Multi-Shot Film Images of Beam at Injector Exit

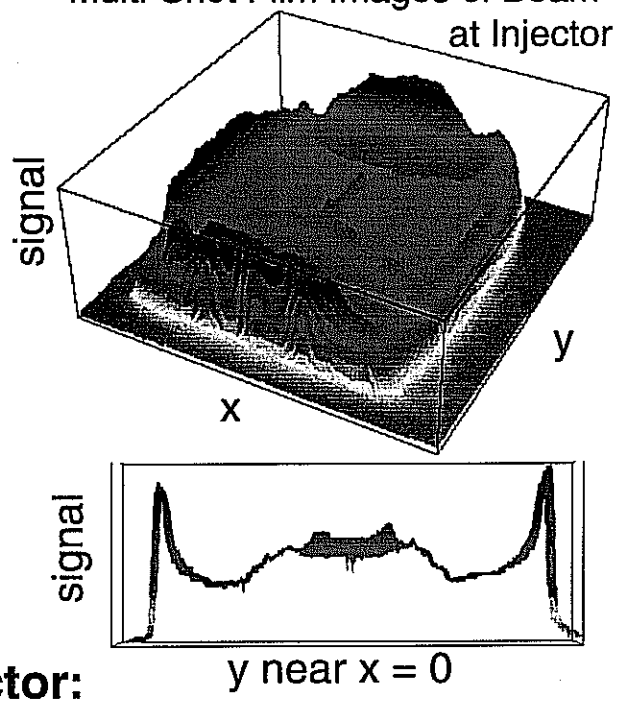

Parameters expected at exit of retrofitted injector:

Energy:	**E = 1.71 MeV**	
Current:	**I = 692 mA, K**	
Emittance:	**ε_n = 1.1 π mm-mrad**	**rms edge measure**
	~ 0.7 π mm-mrad	**measure eliminating empty entrained space**
Envelope:	**r_x = 56.3 mm**	**r_x' = 53.8 mrad**
	r_y = 55.7 mm	**r_y' = -44.8 mrad**

Example PIC Simulations

S.M. Lund 54

HCX Injector: Simulations show distribution distortions in the retrofitted injector should be more modest

Mid-pulse distribution projections at exit plane of injector

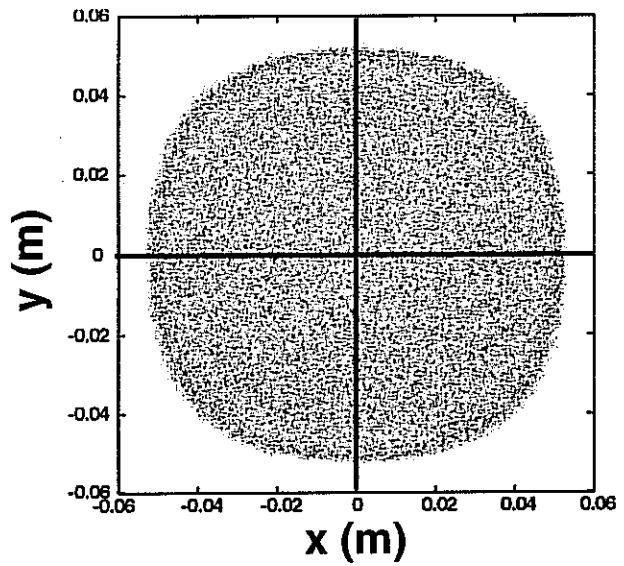

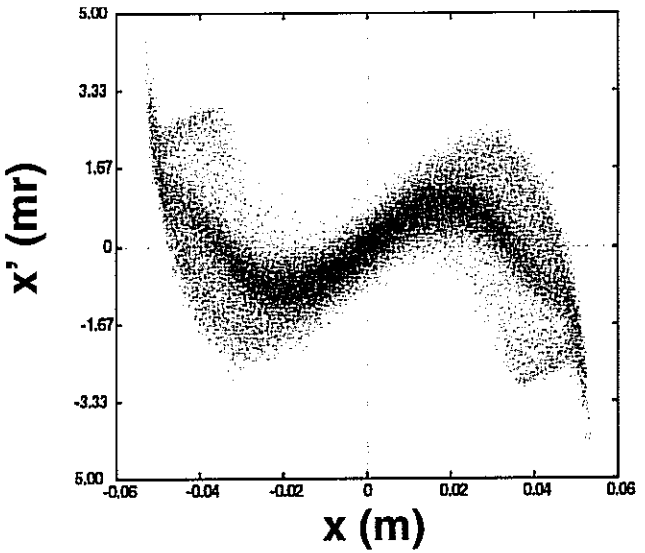

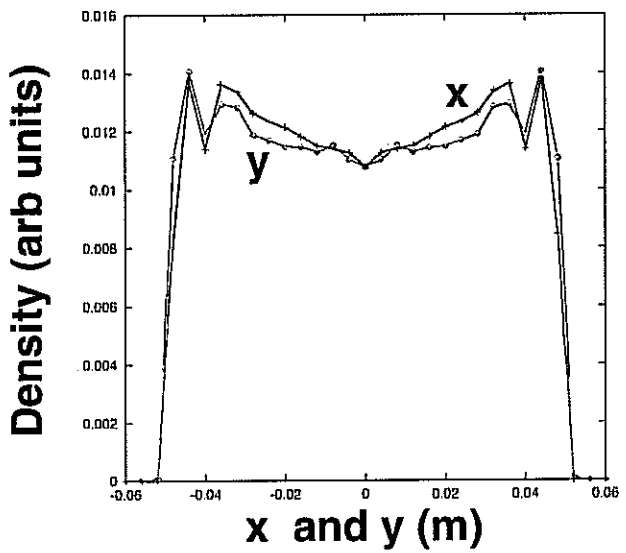

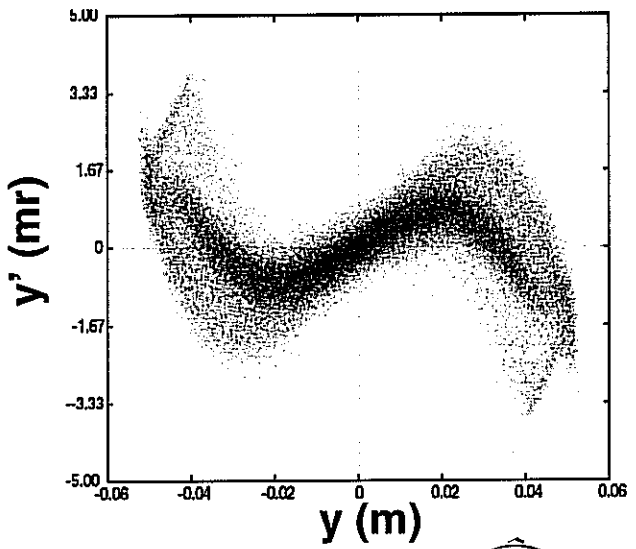

Overall convergence and divergence angles removed to illustrate distortions

SM Lund 55/

Simulations show how waveform rise-time determines beam head mismatch

Tuned 1d diode voltage waveform rise-time is 400 ns -- deviations from this lead to significant mismatch effects in the beam head and particle loss with resultant worries about breakdown, electron effects, etc.

Rise-time τ = 800 ns

beam head particle loss < 0.1%

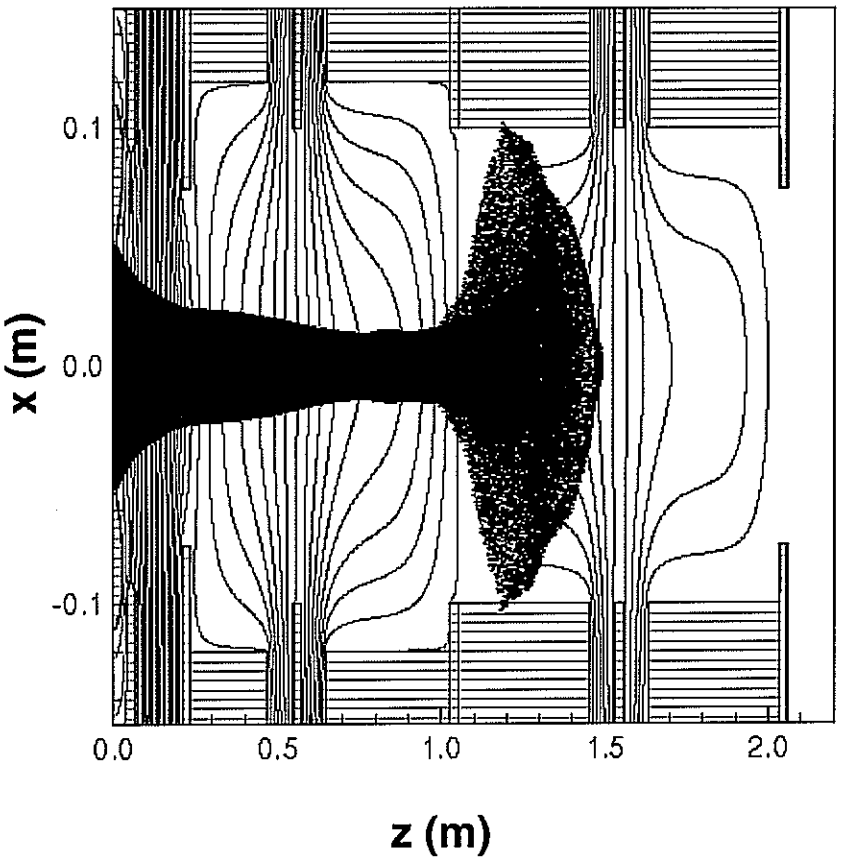

Rise-time τ = 400 ns

zero beam head particle loss

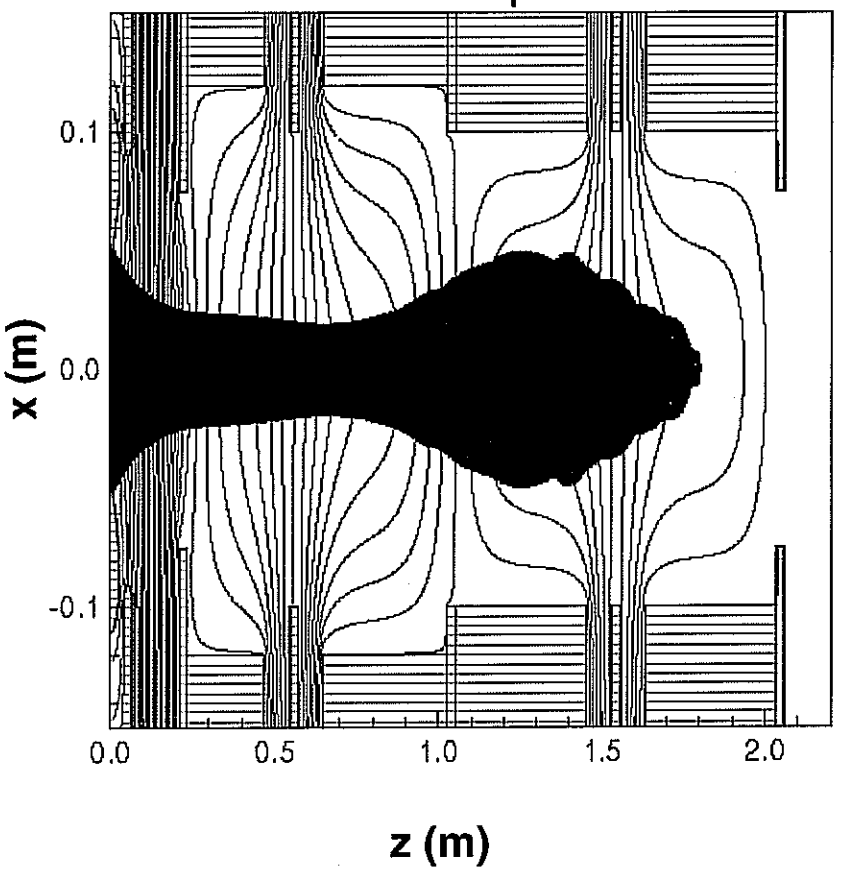

S.M. Lund 56

Initial distribution distortions will launch a spectrum of collective mode perturbations that evolve

Kinetic and fluid theories have been employed to analyze perturbations on a uniform density intense-beam equilibrium [Lund and Davidson, Phys. Plasmas, 5 3028 (1998)]

Small Amplitude Perturbations (arbitrary units, kinetic and fluid theory)

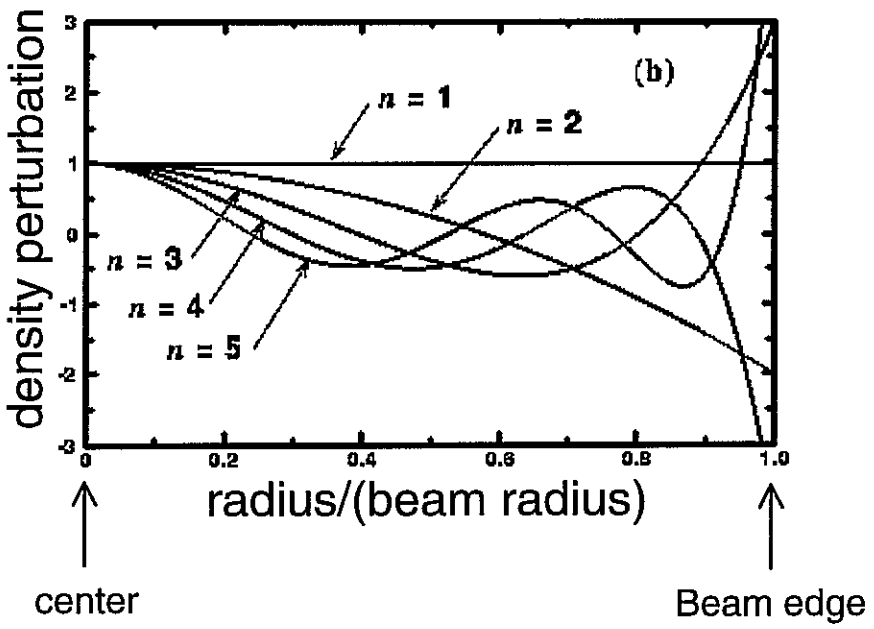

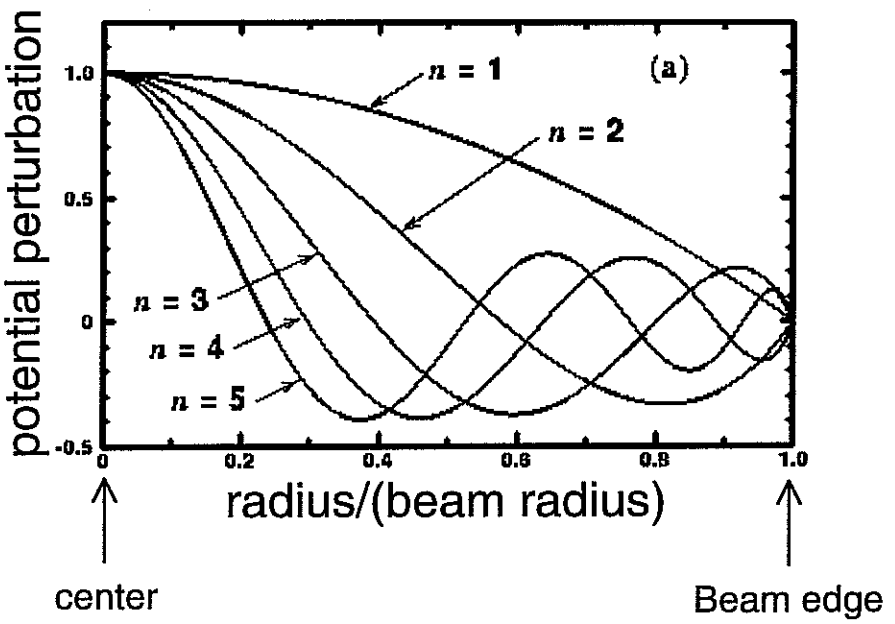

Mode Dispersion Relation (fast branch, from fluid theory)

$$\frac{\sigma_n}{\sigma_0} = \sqrt{2 + 2\left(\sigma/\sigma_0\right)^2 (2n^2 - 1)}$$

σ_n = mode phase advance

n = 1,2,3, ……

Example:

$\sigma_0 = 80^o$, $\sigma/\sigma_0 = 0.2$

$\sigma_1 = 115^o$, $\sigma_5 = 182^o$, ….

SM, Lund 57

Perturbations launched by initial distribution nonuniformities can phase-mix to a more uniform profile with increased emittance

Mode spectrum launched can undergo a rapid cascade, settling to a smaller amplitude and lower order distortion

- Approximate conservation constraints employed to bound emittance increases resulting from full relaxation to a uniform profile [Lund, Lee, and Barnard, Proc. Linac 2000, pg. 290]
- How will such evolutions influence the range and interpretation of measurements

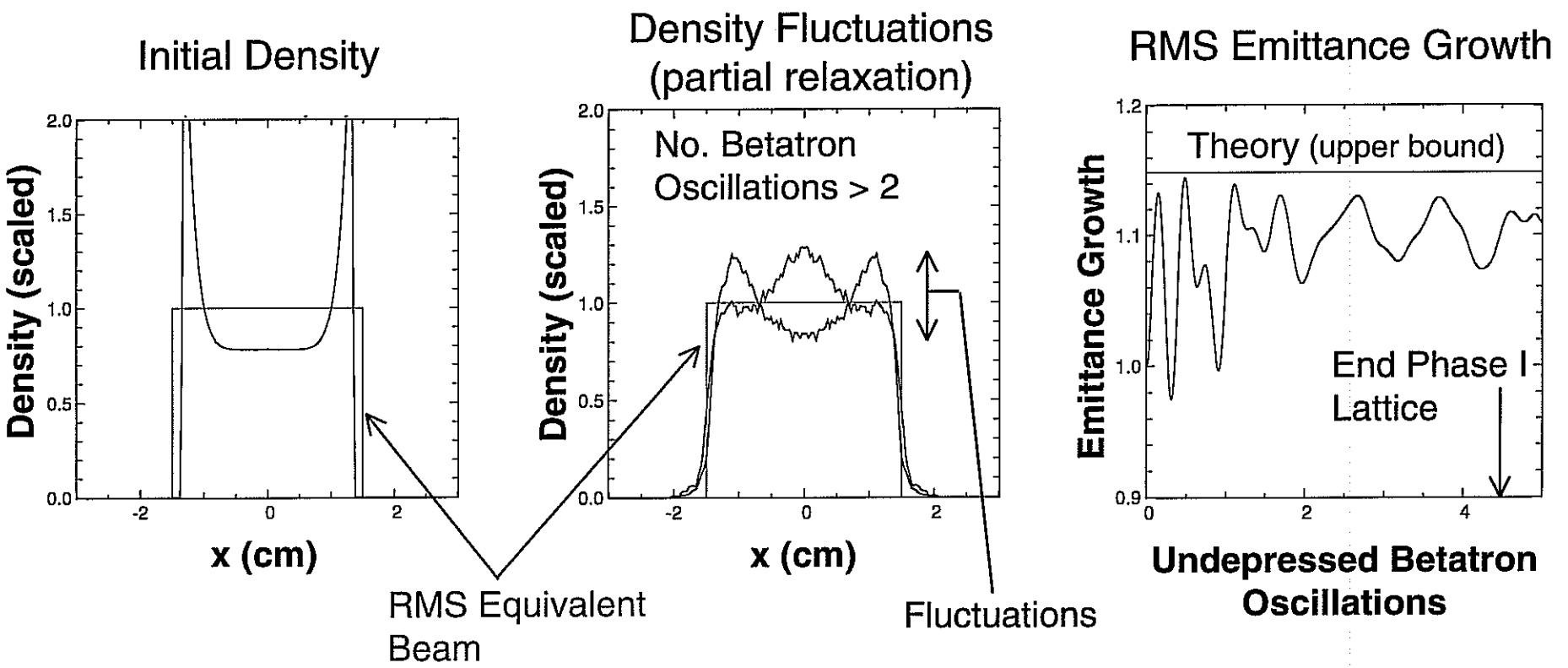

SM, Lund 58/

Analytic theory has been used to parametrically bound emittance growth due to the relaxation of space-charge nonunifomities

Approximate conservation constraints can be employed to estimate maximal emittance increases resulting from the relaxation of an initial nonuniform density profile to a final, uniform profile [Lund, Lee, and Barnard, Proceedings Linac 2000, Monterey, CA, pg. 290]

Initial Density

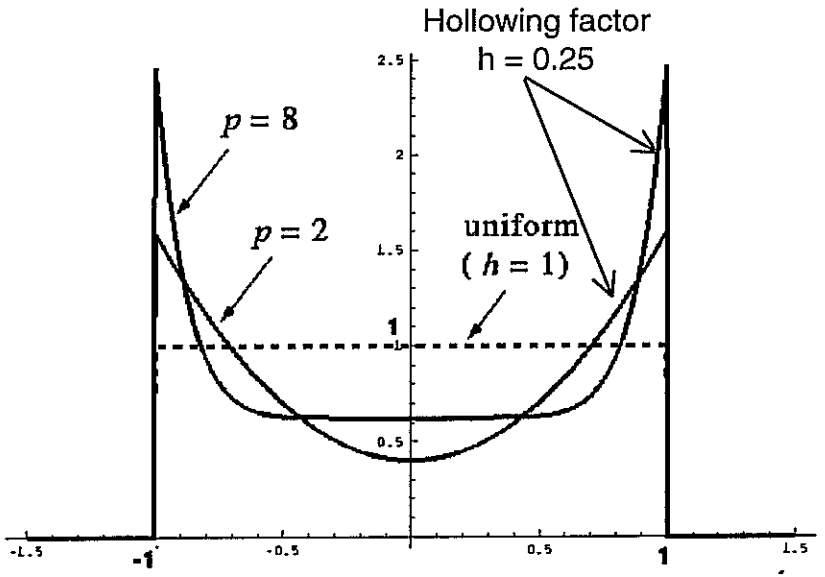

hollowing ~ r^p

h = ratio min to max density

Emittance Growth on Relaxation

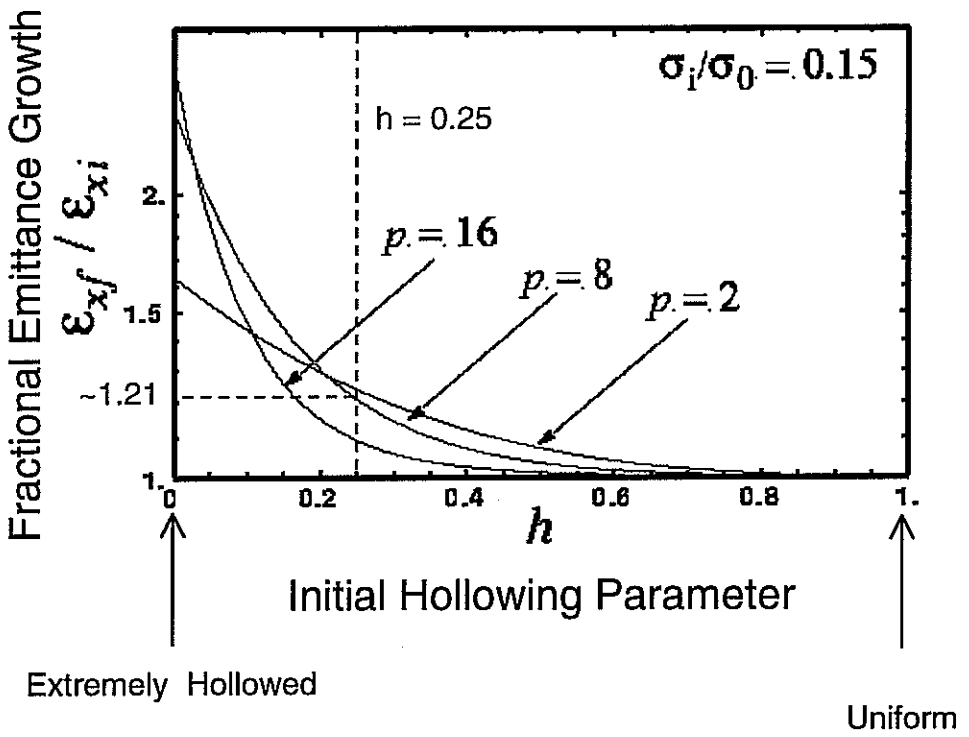

S.M. Lund 5/1

HCX Phase II: A wide range of parametric simulations have been carried out with realistic magnetic transport lattices

A syncopated magnetic transport lattice of ~ 50 lattice periods has been designed

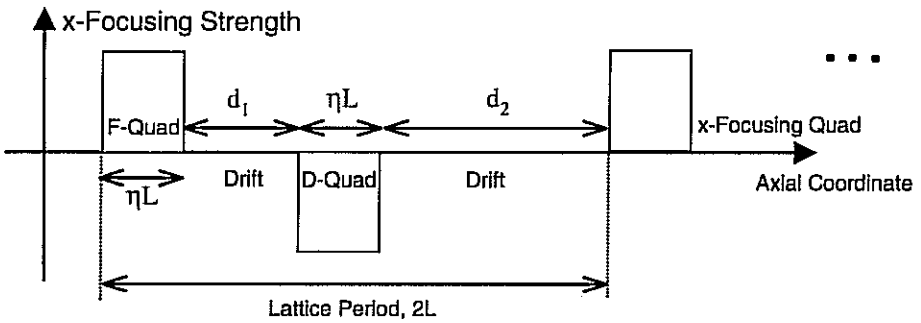

		HCX:
η = Quadrupole Occupancy	$(0 < \eta < 1)$	$\eta = 0.453$
α = Syncopation Factor	$(0 < \alpha < 1)$	$\alpha = 0.248$

Drifts:

$d_1 = \alpha(1-\eta)\eta L$

$d_2 = (1-\alpha)(1-\eta)\eta L$

Superconducting magnetic quadrupoles have been designed and prototyped

$r_p = 29.5$ mm $B_q' = 104$ T/m (max) $B_q \sim 6$ Tesla (wire)

$\ell = 136$ mm $\ell_{eff} = 101$ mm Integrated Field Error $< 15 \times 10^{-3}$

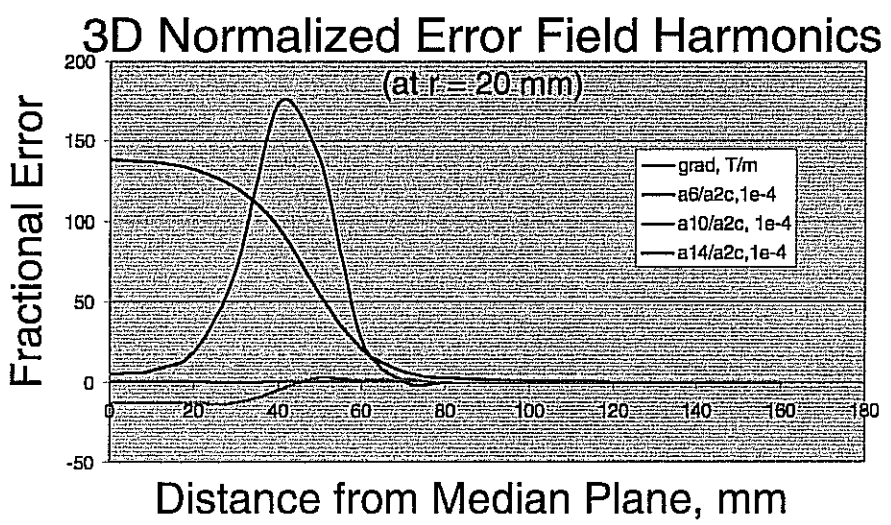

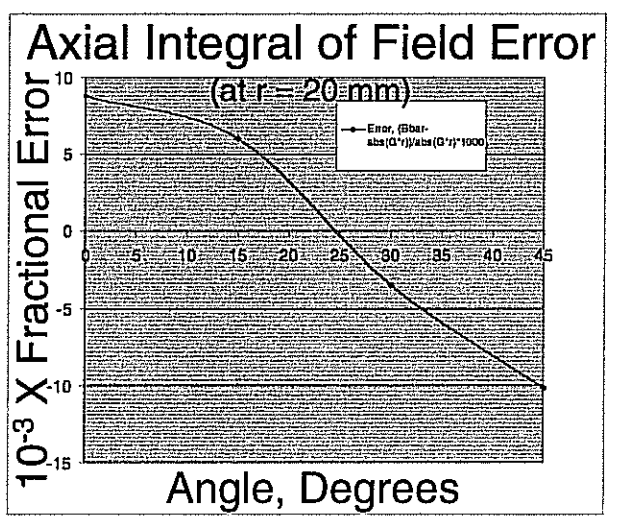

S.M. Lund 109

HCX Phase II: Processes influencing beam quality and control have been explored --- Example: Nonlinear applied fields and beam quality

Full 3D magnetic field is resolved as:

$$\vec{B} = \vec{B}_{quad} + \delta\vec{B} \qquad \delta\vec{B} \rightarrow s \cdot \delta\vec{B}$$

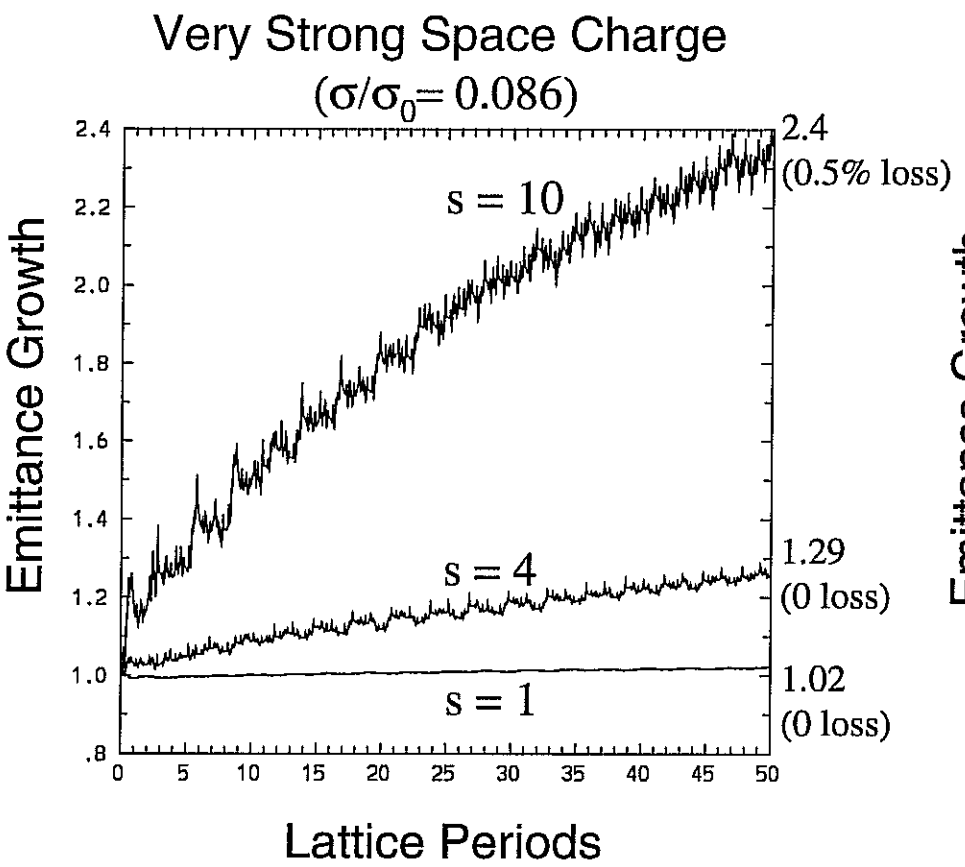

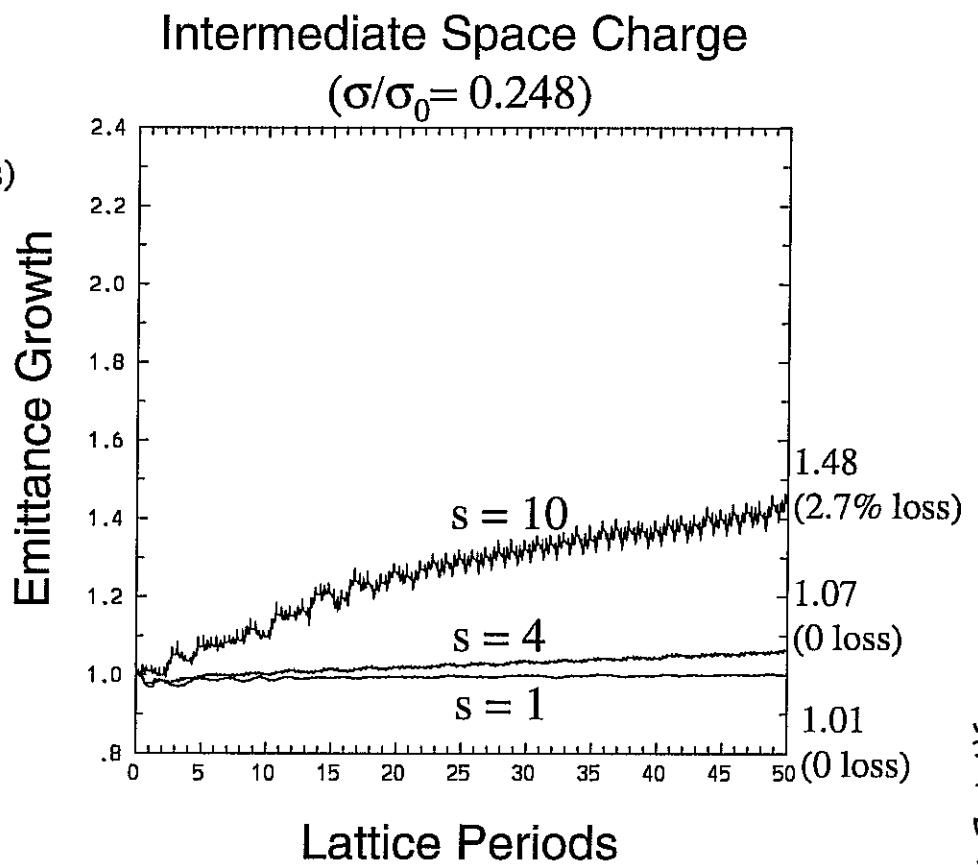

S.M. Lund 6/1

S.M. Lund 62

Initial KV Distribution

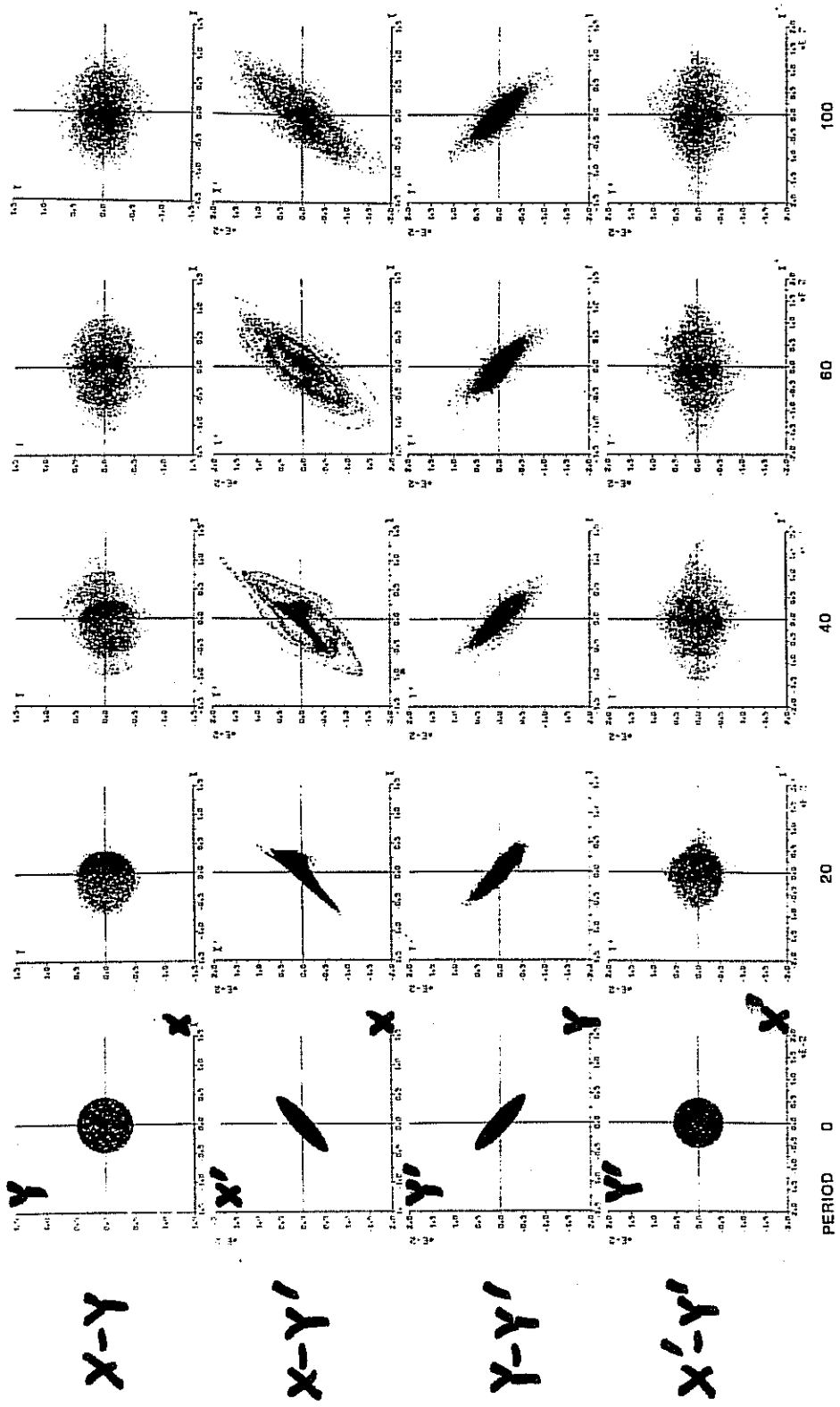

FIGURE 2 Transformation of an initial K-V distribution through the GSI FODO channel at $\sigma_0 = 90°$, $\sigma = 41°$.

J. Struckmeier, J. Klabunde, and M. Reiser, Part. Accel. 15, 47 (1984).

See also Reiser Text, pg 495.

Initial Gaussian Distribution

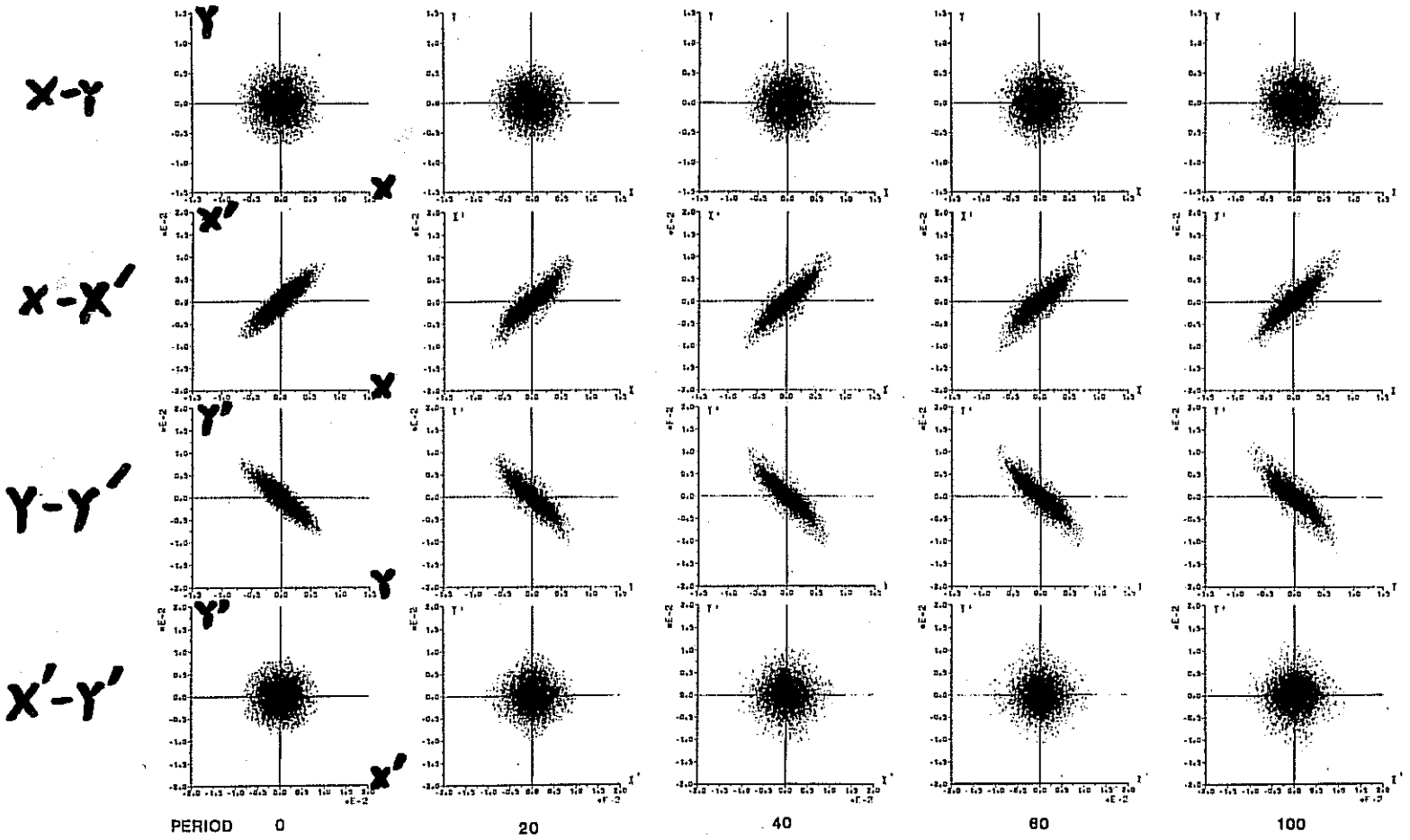

FIGURE 6 Transformation of an initial Gaussian distribution (rms-matched) through the GSI FODO channel at $\sigma_0 = 90°$, $\sigma = 41°$.

J. Struckmeier, J. Klabunde and M. Reiser, Part. Accel. 15, 47 (1984)

S.M. Lund 63/

S. M. Lund 64

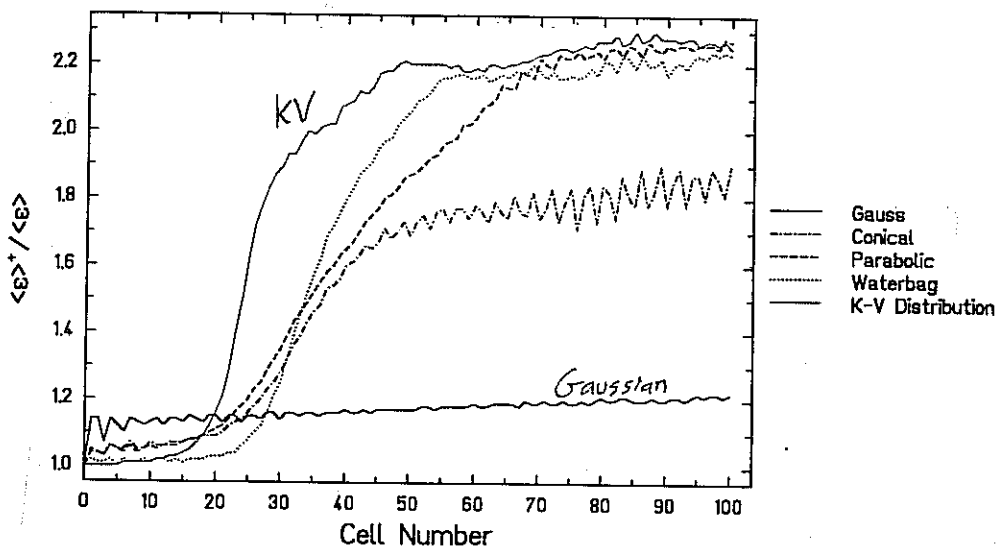

FIGURE 7 Emittance growth factors versus the number of cells obtained from particle simulations for initial K-V, waterbag, parabolic, conical and Gaussian distributions at $\sigma_0 = 90°$, $\sigma = 41°$.

From J. Struckmeier, J. Kabunde, and M. Reiser, Part. Accel. 15 47 (1984).

Distribution Methods — Direct Gridded Solution of Vlasov's Equation.

Consider the Vlasov equation as an example.

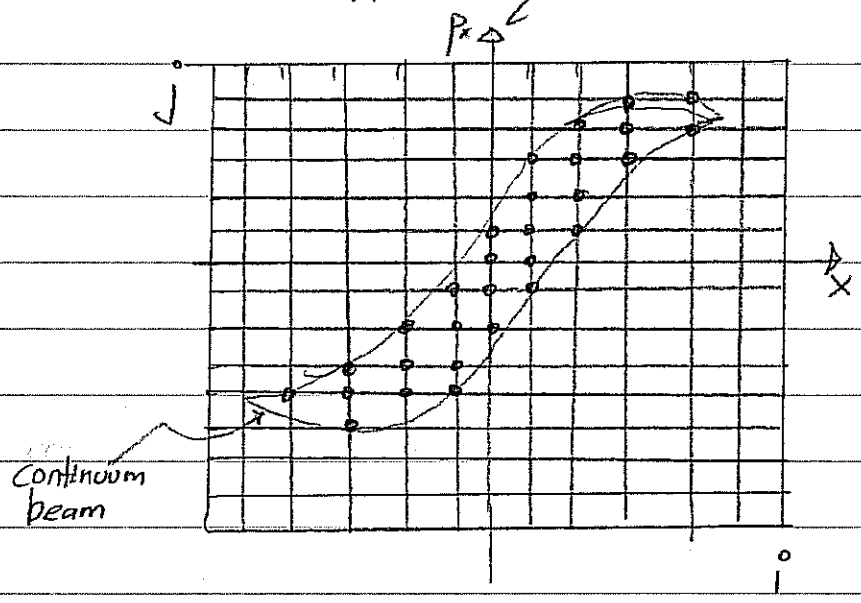

$$f(x_i, p_j, t) = f_{ij}(t)$$

The distribution is advanced at discrete grid points in time.

- Fields are typically solved using a discrete spatial mesh as for the particle methods described before.
  - Deposition on mesh is typically straightforward in Vlasov case (sum over momentum variables.

- The distribution advance cycle is different than for particle methods.
  - Numerical stability is key.
  - Characteristics and "semi-Lagrangian" methods can be employed.
  - Methods for solving for characteristics are familiar from dynamics/plasma physics.

Direct Vlasov Methods:

"Pros"

Reasons for Vlasov simulations:

- Low noise - only discretization effects without statistical effects
- Allows clear analysis of collective effects and tenuous distribution components.

"Cons"

Reasons why Vlasov simulations are presently employed less than PIC:

- Extreme memory requirements for needed grid resolution in multi-dimensional phase space.
  - Beams often have sharp edges in phase space that move in responce to varying applied focusing forces.
- Numerical stability tends to be more difficult than in particle methods.

No time to illustrate Vlasov and other distribution methods in this introductory course. We hope to cover these methods and other numerical fieldsolve techniques in a later expanded version of this class.

However ..... it is easy to generalize from what we have learned!

WARP Code Overview

Electrostatic Multi-dimensional PIC Code

WARP3d – x, y, z, p_x, p_y, p_z
Moves in t

Many Fieldsolvers!
SOR, Multigrid, FFT,
FFT + Tridiag, FFT + Cap Matrix, ..

WARPxy – x, y, p_x, p_y, p_z
Moves in s

WARPrz – r, z, p_r, p_z, p_θ
Moves in t

WARPenv – envelope solver
Used to seed / load PIC
r_x, r_y, r_x', r_y'
Advances in s

Hermes – Fluid II + Bridded
Space Charge Field

- Common diagnostic tools built around gist graphics
- Run with python interpreter

Example Script
"ag-slice.py"

Acknowledgements, References

Numerical Methods

1. Forman S. Acton, "Numerical Methods that Work," Harper and Row Publishers, New York, 1970.
2. Stephen Koonin, Computational Physics," Addison-Wesley Publishing Co., 1986.

Survey of Numerical Methods

3. W. Press, B. Flannery, S. Teukolsky, W. Vetterling, "Numerical Recipes, The Art of Scientific Computing," Cambridge University Press, 1986.

Particle Methods

4. C. K. Birdsall and A. B. Langdon, "Plasma Physics via Computer Simulation," McGraw-Hill Book Company, 1985.
5. R. W. Hockney and J. W. Eastwood, "Computer Simulation using Particles," Institute of Physic Publishing, 1988.

A special thanks to Alex Friedman, Dave Grote, Jean-Luc Vay, and Michiel de Hoon of the Lawrence Livermore and Lawrence Berkeley National Labs for help with these notes and general guidance. Also thanks are due for Irving Haber (NRL), Christine Celata (LBL), and Bill Fawley (LBL) for educating the authors on various simulation methods.

John Barnard
Steven Lund
USPAS
June 2006

Summary of JB lectures

START WITH MICROSCOPIC PHASE SPACE DENSITY

$$\boxed{N(\underline{x},\underline{v},t) = \sum_{i=1}^{N} \delta(\underline{x}-\underline{X}_i(t))\,\delta(\underline{v}-\underline{V}_i(t))}$$ Klimontovich Density

$\frac{\partial N}{\partial t}$ + LORENTZ EQUATIONS $\Rightarrow$ KLIMONTIVICH EQUATION:

$$\boxed{\frac{\partial N}{\partial t} + v\cdot\nabla_x N(\underline{x},\underline{v},t) - \frac{q}{m}(E^m + v\times B^m)\cdot\nabla_v N(\underline{x},\underline{v},t) = 0}$$

$$\boxed{\text{or } \frac{dN(\underline{x},\underline{v},t)}{dt} = 0}$$

Letting $N = f + \delta f$ $\quad f = \langle N\rangle$ $\quad f = \frac{\int N\, d^3x\, d^3v}{\Delta x^3\,\Delta v^3}$

$E^m = E + \delta E$ $\quad E = \langle E_m\rangle$

$B^m = B + \delta B$ $\quad B = \langle B_m\rangle$ $\quad n^{-1/3} \ll \Delta x \ll \lambda_D$

PERFORMING LOCAL AVERAGES TO OBTAIN SMOOTH & "SLIKEY" QUANTITIES:

$$\boxed{\frac{\partial f}{\partial t} + \underline{v}\cdot\frac{\partial f}{\partial \underline{x}} + \frac{d\underline{v}}{dt}\cdot\frac{\partial f}{\partial \underline{v}} = \frac{\partial f}{\partial t_c}} \sim \frac{f}{\tau_c}$$

We estimated $\frac{|\partial f/\partial t_c|}{\left|\frac{q\underline{E}}{m}\cdot\partial f/\partial \underline{v}\right|} \sim \frac{1}{16\,\lambda_D^3\, n_0} \ll 1$

$\lambda_D = v_{TH}/\omega_p \qquad v_{TH} \equiv \sqrt{\frac{kT}{m}} \qquad \omega_p \equiv \sqrt{\frac{q^2 n}{\varepsilon_0 m}}$

$$\frac{\partial f}{\partial t} + \underline{v}\cdot\frac{\partial f}{\partial \underline{x}} + \frac{d\underline{p}}{dt}\cdot\frac{\partial f}{\partial \underline{p}} = 0 \qquad \dot{p} = -\frac{\partial H}{\partial \underline{x}}\ ;\ \dot{x} = \frac{\partial H}{\partial \underline{p}}$$

$$\boxed{\frac{df}{dt} = 0}$$ LIOUVILLE'S EQUATION (INCOMPRESSIBILITY OF PHASE VOLUME)

DEFINE NORMALIZED EMITTANCES PROPORTIONAL TO $\Delta p_z \Delta z \propto \Delta E\,\Delta t$

$\Delta p_x \Delta x$

$\Delta p_y \Delta y$

SO THAT

$$\varepsilon_{Nx}^2 = \gamma^2\beta^2\left(\langle x^2\rangle\langle x'^2\rangle - \langle x x'\rangle^2\right)$$

$\Rightarrow$ CONSTANT IF FORCES ARE LINEAR IN X & FILAMENTATION IS ABSENT. (LINEAR WITHOUT COUPLING TO Z, OR Y).

WE DERIVED TWO SETS OF PARTICLE EQUATION OF MOTION:

PARAXIAL EQUATION (FOR AXISYMMETRIC SYSTEMS) $\left(\frac{\partial}{\partial\theta} = 0\right)$

STARTING WITH THE LORENTZ FORCE EQUATION $\frac{d\underline{p}}{dt} = q(\underline{E} + \underline{v} \times \underline{B})$ IN CYL. COORD.

$$\underbrace{\frac{d}{dt}(\gamma m \dot{r})}_{\text{INERTIAL}} - \underbrace{\gamma m r \dot{\theta}^2}_{\text{CENTRIFUGAL}} = q\left(\underbrace{\frac{V''}{2} r}_{E_r \text{ external (DIVERGENCE OF } E = 0)} + \underbrace{r\dot{\theta} B}_{v_\theta B_z}\right) + q\left(\underbrace{E_r^{self}}_{\text{SELF-FIELD}} + \underbrace{v_z B_\theta^{self}}_{\text{SELF-FIELD}}\right)$$

$$\boxed{\dot{r} \equiv \frac{dr}{dt}; \quad r' = \frac{dr}{ds} = \frac{\dot{r}}{\beta c}}$$

θ-component:

$$p_\theta = \gamma m r^2 \dot{\theta} + \frac{qB(z) r^2}{2} = \text{constant}$$

$$= \gamma m r^2 \beta c \theta' + \frac{qBr^2}{2} = \text{constant}$$

$$\underbrace{r''}_{\text{INERTIAL}} + \underbrace{\frac{\gamma'}{\beta^2\gamma} r'}_{\text{ACCELERATION (INERTIA)}} + \underbrace{\frac{\gamma''}{2\beta^2\gamma} r}_{E_r \text{ (CONVERGENCE OF FIELD LINES)}} + \underbrace{\left(\frac{\omega_c}{2\gamma\beta c}\right)^2 r}_{v_\theta B_z \text{ CENTRIFUGAL}} - \underbrace{\left(\frac{p_\theta}{\gamma\beta m c}\right)^2 \frac{1}{r}}_{\text{CENTRIFUGAL}} - \underbrace{\frac{q}{\gamma^3 m v_z^2} \frac{\lambda(r)}{2\pi\epsilon_0 r}}_{\text{SELF FIELD}} = 0$$

STATISTICAL AVERAGE OF THIS EQUATION

$$r_b'' + \frac{\gamma'}{\beta^2\gamma} r_b' + \frac{\gamma''}{2\beta^2\gamma} r_b + \left(\frac{\omega_c}{2\gamma\beta c}\right)^2 r_b - \frac{4\langle p_\theta\rangle^2}{(\gamma m\beta c)^2 r_b^3} - \frac{\varepsilon_r^2}{r_b^3} - \frac{Q}{r_b} = 0$$

$$\varepsilon_r^2 \equiv 4\left(\langle r^2\rangle\langle r'^2\rangle - \langle r r'\rangle^2 + \langle r^2\rangle\langle r^2\theta'^2\rangle - \langle r^2\theta'\rangle^2\right); \quad Q = \frac{q\lambda}{2\pi\epsilon_0 \gamma^3 \beta^2 m c^2}$$

$$= \varepsilon_x^2 - 4\langle r^2\theta'\rangle^2 \quad (\text{if } \rho = \rho(r) \text{ only})$$

EQUATION OF MOTION

AGAIN STARTING WITH $\frac{d\underline{p}}{dt} = q(\underline{E} + \underline{v} \times \underline{B})$

RETURN TO X, Y COORDINATES

$$x'' + \frac{1}{\gamma v_z}\frac{d}{ds}(\gamma v_z)x' = \frac{-q}{\gamma^3 m v_z^2}\frac{\partial \varphi}{\partial x} \pm \begin{cases} \frac{qB'}{\gamma m v_z} x & \text{for magnetic quads} \\ \frac{qE'}{\gamma m v_z^2} x & \text{for electric quads} \end{cases}$$

Let $\frac{\gamma m v_z}{q} = \frac{p}{q} \equiv [B\rho] \equiv$ RIGIDITY

$$y'' + \frac{1}{\gamma v_z}\frac{d}{ds}(\gamma v_z)y' = \frac{-q}{\gamma^3 m v_z^2}\frac{\partial \varphi}{\partial y} \mp \begin{cases} \frac{B'}{[B\rho]} y & \text{magnetic} \\ \frac{qE'}{\gamma m v_z^2} y & \text{electric} \end{cases}$$

ENVELOPE EQUATION

$$r_x^2 = 4\langle x^2\rangle; \quad r_y^2 = 4\langle y^2\rangle$$

$$r_x' = \frac{4\langle x x'\rangle}{r_x}$$

$$r_x'' = \frac{4\langle x x''\rangle}{r_x} + \frac{\varepsilon_x^2}{r_x^3}; \qquad \varepsilon_x^2 = 16(\langle x^2\rangle\langle x'^2\rangle - \langle x x'\rangle^2)$$

$$r_y'' = \frac{4\langle y y''\rangle}{r_y} + \frac{\varepsilon_y^2}{r_y^3} \qquad \varepsilon_y^2 = 16(\langle y^2\rangle\langle y'^2\rangle - \langle y y'\rangle^2)$$

for magnetic focusing:

$$r_x'' + \frac{1}{\gamma v_z}\frac{d}{ds}(\gamma v_z) r_x' + \frac{4q}{\gamma^3 m v_z^2}\frac{\langle x \frac{\partial \varphi}{\partial x}\rangle}{r_x} \pm \frac{B'}{[B\rho]} r_x - \frac{\varepsilon_x^2}{r_x^3} = 0$$

$$r_y'' + \frac{1}{\gamma v_z}\frac{d}{ds}(\gamma v_z) r_y' + \frac{4q}{\gamma^3 m v_z^2}\frac{\langle y \frac{\partial \varphi}{\partial y}\rangle}{r_y} \pm \frac{B'}{[B\rho]} r_x - \frac{\varepsilon_y^2}{r_y^3} = 0$$

(for electric focusing $\frac{B'}{[B\rho]} \to \frac{qE'}{\gamma m v_z^2}$)

National® Brand 42-182 100 SHEETS Made in U.S.A.

SPACE CHARGE TERM WITH ELLIPTICAL SYMMETRY

NOW DEFOCUSING IN ONE DIRECTION AND FOCUSING IN THE OTHER $\Rightarrow$ RADIAL SYMMETRY SHOULD BE REPLACED BY ELLIPTICAL SYMMETRY: $\rho = \rho\left(\frac{x^2}{r_x^2} + \frac{y^2}{r_y^2}\right)$

CAN BE SHOWN THAT $\left\langle x \frac{\partial \phi}{\partial x} \right\rangle = \frac{-\lambda}{4\pi\epsilon_0} \frac{r_x}{r_x + r_y}$

$$\left\langle y \frac{\partial \phi}{\partial y} \right\rangle = \frac{-\lambda}{4\pi\epsilon_0} \frac{r_y}{r_x + r_y}$$

USE $\phi(x,y) = \frac{-r_x r_y}{4\epsilon_0} \int_0^\infty \frac{\hat{\rho}(\chi)\, ds}{\sqrt{r_x^2+s}\sqrt{r_y^2+s}}$ to prove, where $\hat{\rho}(\chi) = \frac{d\rho}{d\chi}$

$\rho(x,y) = \hat{\rho}(\chi)\big|_{s=0}$

$\chi = \frac{x^2}{r_x^2+s} + \frac{y^2}{r_y^2+s}$

DEFINING $Q = \frac{2\lambda q}{4\pi\epsilon_0 \gamma^3 m v_z^2}$

$$\Rightarrow \boxed{\begin{aligned} & r_x'' + \frac{1}{\gamma v_z}\frac{d}{ds}(\gamma v_z) r_x' - \frac{2Q}{r_x + r_y} \mp \frac{B'}{[B\rho]} r_x - \frac{\varepsilon_x^2}{r_x^3} = 0 \\ & r_y'' + \frac{1}{\gamma v_z}\frac{d}{ds}(\gamma v_z) r_y' - \frac{2Q}{r_x + r_y} \pm \frac{B'}{[B\rho]} r_y - \frac{\varepsilon_y^2}{r_y^3} \end{aligned}}$$

(for Electric Focusing $\frac{B'}{[B\rho]} \to \frac{qE'}{\gamma m v_z^2}$)

(ANALOGUE TO CIRCULAR BEAM:

$\left\langle r \frac{\partial \phi}{\partial r} \right\rangle = \frac{-\lambda}{4\pi\epsilon_0}$ PROVED IN HOMOWORK)

ENVELOPE EQUATIONS DERIVED

RMS (ENVELOPES DEFINED IN TERMS OF RMS QUANTITIES; EMITTANCE NOT GUARANTEED TO BE CONSERVED).

1. PARAXIAL r_b ; $\rho(r)$
2. ELLIPTICAL r_x, r_y ; $\rho\left(\frac{x^2}{r_x^2}+\frac{y^2}{r_y^2}\right)$
3. LONGITUDINAL r_z FOR $E_z = \frac{-q}{4\pi\varepsilon_0}\frac{\partial\lambda}{\partial z} \propto z$; $[\lambda \propto (1-4z^2/r_z^2)]$
   $V \propto (z/r_z)$
4. ELLIPSOIDAL of BUNCHES $r_\perp, r_z$ (ALSO r_x, r_y, r_z c.f. Wangler, section 9.9).
   (ρ CONSTANT)
5. ELLIPTICAL WITH IMAGES r_x, r_y $\rho\left(\frac{x^2}{r_x^2}+\frac{y^2}{r_y^2}\right)$
6. BARRIER FRAME (PERIODIC SOLENOIDS OR CONTINUOUS FOCUSING) $\tilde{r}_x, \tilde{r}_y$ $\rho(r)$

KINETIC ENVELOPE EQUATIONS (CONSTRAINT EQUATION OF A PARTICULAR DISTRIBUTION FUNCTION; EMITTANCE CONSERVED)

1. KV FOR ELLIPTICAL UNIFORM BEAMS $f(x,x',y,y')$
   [IDENTICAL TO #2 ABOVE]
2. NEUFFER DISTRIBUTION FOR 1D $f(z,z')$
   [IDENTICAL TO #3 ABOVE]

MOMENT EQUATIONS

1. TRANSVERSE WITH CHROMATIC EFFECTS
   $\langle x^2\rangle, \langle x'^2\rangle, \langle xx'\rangle, \langle x^2\delta\rangle, \langle x'^2\delta\rangle, \langle xx'\delta\rangle, \ldots$

Summary of Current Limits From Different Focusing Methods

Einzel Lens

$$Q_{max} \cong \frac{3\pi^2}{8}\left(\frac{q\phi_0}{m v_0^2}\right)^2\left(\frac{r_b}{L}\right)^2$$

Solenoids

$$Q_{max} = \left(\frac{\omega_c r_b}{2\gamma\beta c}\right)^2$$

Quadrupole Focusing

$$Q_{max} \cong \frac{\eta\phi_0}{2\pi}\left(\frac{\sin\frac{\eta\pi}{2}}{\frac{\eta\pi}{2}}\right)\left[\frac{B r_b}{[B\rho]}\left[\frac{r_b}{r_p}\right] \quad \frac{2qV_q}{\gamma m v_z^2}\left[\frac{r_b^2}{r_p^2}\right]\right]$$

MAGNETIC

Electric

For Non-Relativistic Beams

$$\lambda_{max} \propto \frac{\phi_0^2}{V} \qquad \lambda_{max} \propto \frac{q}{m} B^2 r_p^2 \qquad \lambda_{max} \propto \begin{cases} B_1 V^{1/2} r_p \\ V_q \end{cases}$$

Note
ϕ_0 = Voltage between Einzel lenses
V_q = Voltage on a quad relative to ground
V = particle energy / q

Solenoids: $\log\{\lambda[Cm^{-1}]\} = -7.0$
Electrostatic quads: $\log\{\lambda[Cm^{-1}]\} = -5.8$
Magnetic quads: $\log\{\lambda[Cm^{-1}]\} = -8.9 + \frac{1}{2}\log\{E_{kin}[eV]\}$
Einzel lenses: $\log\{\lambda[Cm^{-1}]\} = 0.01 - \log\{E_{kin}[eV]\}$

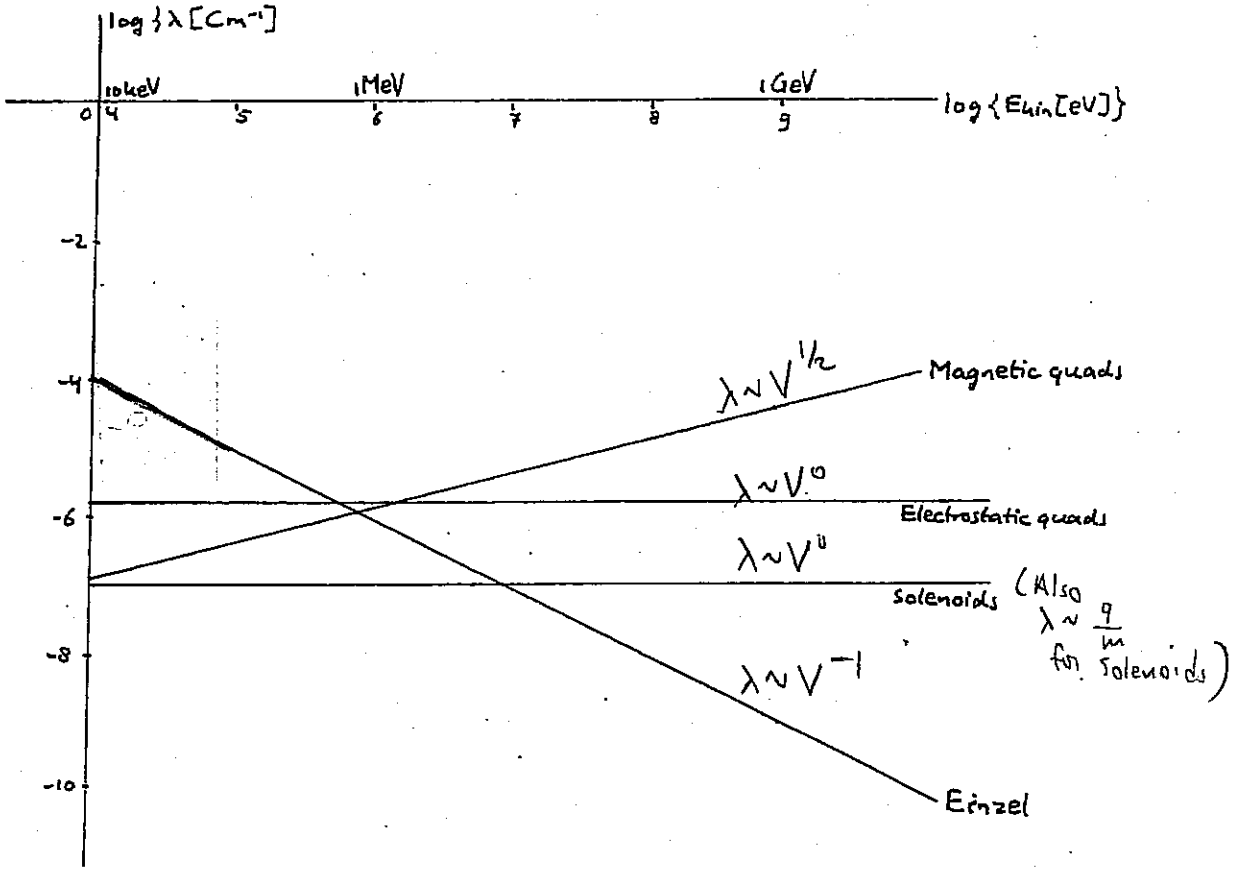

ESTIMATING SPOT SIZE

$$r_x'' + \frac{(\gamma_b \beta_b)'}{\gamma_b \beta_b} r_x + K_x r_x - \frac{2Q}{r_x + r_y} - \frac{\epsilon_x^2}{r_x^3} = 0$$

$$r_y'' + \frac{(\gamma_b \beta_b)'}{\gamma_b \beta_b} r_y + K_y r_y - \frac{2Q}{r_x + r_y} - \frac{\epsilon_y^2}{r_y^3} = 0$$

<u>IN CHAMBER</u>: NO EXTERNAL FOCUSING, NO ACCELERATION AND BEAM IS OFTEN CIRCULAR (BY DESIGN)

$$\Rightarrow \quad K_x = K_y = (\gamma_b \beta_b)' = 0 \qquad \& \quad r_x = r_y = r_b$$

$\Rightarrow$ ENVELOPE EQUATION IS:

$$r_b'' = \frac{Q}{r_b} + \frac{\epsilon^2}{r_b^3}$$

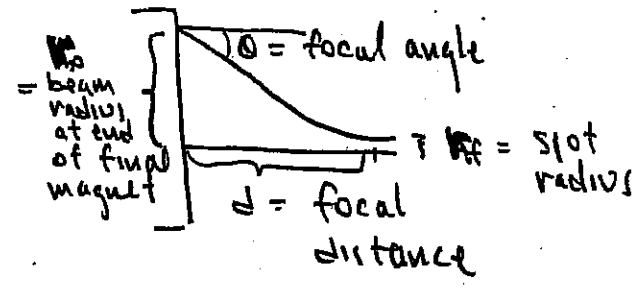

MULTIPLYING BY r_b' & INTEGRATING $\Rightarrow$

$$\frac{r_{bf}'^2}{2} - \frac{r_{bo}'^2}{2} = Q \ln \frac{r_{bf}}{r_{bo}} + \frac{\epsilon^2}{2 r_{bo}^2} - \frac{\epsilon^2}{2 r_{bf}^2}$$

<u>NOW</u> $r_{bo}' \cong \theta$ $\qquad r_{bf}$ = spot radius $\qquad r_{bf} << r_{bo}$

$r_{bf}' = 0 \qquad r_{bo} \cong d\theta$

$$\Rightarrow \boxed{\theta^2 \cong 2Q \ln\left(\frac{\theta d}{r_{bf}}\right) + \frac{\epsilon^2}{r_{bf}^2}}$$

WHEN $Q = 0$

$$r_{spot}^2 = \frac{\epsilon^2}{\theta^2} + r^2_{\text{CHROMATIC ABERRATION}} + \ldots$$

$$r^2_{\text{CHROMATIC}} = \alpha^2 d^2 \left(\frac{\delta p}{p}\right)^2 \theta^2$$

$\alpha \cong 6$ (system dependent)

LONGITUDINAL DYNAMICS SUMMARY

1 D VLASOV EQUATION

$$\frac{\partial \tilde{f}}{\partial s} + z' \frac{\partial f}{\partial z} + z'' \frac{\partial \tilde{f}}{\partial z'} = 0$$

$$E_z = \frac{-g}{4\pi\epsilon_0} \frac{\partial \lambda}{\partial z}$$ "g-factor" model

$$z'' = \frac{q E_z}{m v_0^2} \; ; \qquad \frac{\partial^2 \phi}{\partial z^2} + \frac{1}{r} \frac{\partial}{\partial r}\left(r \frac{\partial \phi}{\partial r}\right) = -\frac{\rho}{\epsilon_0}$$

CHILD-LANGMUIR IN 1-D DIODE

LEADS TO FLUID EQUATIONS

$\int$(Vlasov Equation) dz'

$$\frac{\partial \lambda}{\partial s} + \frac{\partial}{\partial z}(\lambda \bar{z}') = 0$$

$$\frac{\partial \bar{z}'}{\partial s} + \bar{z}' \frac{\partial \bar{z}'}{\partial z} + \frac{1}{\lambda} \frac{\partial}{\partial z}(\lambda \Delta z'^2) = \frac{q E_z}{m v_0^2}$$

1D E_z: $\Rightarrow$ CHILD LANGMUIR SOLUTION $\leftarrow$ NON-LINEAR SOLUTION TO FLUID EQUATIONS

g-factor: $\Rightarrow$ SPACE-CHARGE WAVES

$\hookrightarrow$ LONGITUDINAL OR REFLECTIVE WALL INSTABILITY (IF $E_1 = z^{\nu} I_1$)

$\Rightarrow$ SPACE-CHARGE RAREFACTION WAVES $\leftarrow$ NON-LINEAR SOLUTION TO FLUID EQNS.

$\Rightarrow$ PARABOLIC BUNCH COMPRESSION $\leftarrow$ NON-LINEAR SOLUTION TO FLUID EQUATIONS

$\Rightarrow$ "EAL" FIELDS

2D PIERCE ELECTRODE

TIME DEPENDENT LAMPEL TEFENBACC SOLUTION

VLASOV EQUATION ALSO $\Rightarrow$ ENVELOPE EQUATION $\iint$ Vlasov Equation $dz\, dz'$

$$\frac{d^2 r_z}{ds^2} = \frac{\epsilon_z^2}{r_z^3} + \frac{3}{2} \frac{g q Q_c}{4\pi\epsilon_0 m v^2} \frac{1}{r_z^2} - K(r) r_z$$

KINETIC SOLUTION TO VLASOV EQUATION & SATISFYING KMI ENVELOPE EQUATION

$\hookrightarrow$ NEWBER DISTRIBUTION

$$f(z,z') = \frac{3N}{2\pi\epsilon_z} \sqrt{1 - \frac{z^2}{r_z^2} - \frac{r_z^2 (z' - r_z' z / r_z)^2}{\epsilon_z}}$$

NORMAL MODES

LONGITUDINAL

SPACE-CHARGE WAVES (FLUID)

$\omega = \pm c_s k$ [IN COMOVING BEAM FRAME]

$$c_s = \sqrt{\frac{q g \lambda_0}{4\pi\epsilon_0 m}}$$ = SPACE CHARGE WAVE SPEED

TRANSVERSE

ENVELOPE MODES

CONTINUOUS FOCUSING (LONG BUNCHES)

BREATHING: $k_B^2 = 2k_{p0}^2 + 2k_p^2$

QUADRUPOLE $k_Q^2 = k_{p0}^2 + 3k_p^2$

(HERE $k_p^2 \equiv k_{p0}^2 - \frac{Q}{r_b^2}$)

(ANALOGOUS MODES IN BUNCHED BEAMS)

STEVE LOOKED AT MODES IN PERIODIC SYSTEMS (& CONTINUOUS FOCUSING

+ KINETIC MODES (GLUCKSTERN MODES)
+ FLUID MODES

INSTABILITIES

1. LONGITUDINAL (RESISTIVE WALL) INSTABILITY
   (FLUID INSTABILITY)

2. ELECTRON – ION INSTABILITY
   (CENTROID INSTABILITY)

STEVE TALKED ABOUT:

3. ENVELOPE INSTABILITIES

STEVE TALKED ABOUT:

4. KINETIC INSTABILITIES
   (DISTRIBUTION FUNCTION DEPENDENT)

5. SINGLE PARTICLE RESONANT INSTABILITIES
   - HALO
   - RING RESONANCES

HALO:

CORE TEST PARTICLE MODEL:

$$x'' = \begin{cases} -\left[k_{\beta 0}^2 - \frac{Q}{r_b^2}\right]x & \text{for } r < r_b \\ -\left[k_{\beta 0}^2 - \frac{Q}{r^2}\right]x & \text{for } r > r_b \end{cases}$$

$$r_b = r_{b0} + \delta r_b \cos(k_\beta s + \phi)$$

Gluckstern's phase-amplitude analysis:

$$x'' + \overbrace{\left[k_{\beta 0}^2 - \frac{Q}{r_{b0}^2}\right]}^{k_\beta^2} x = f(x)$$

Non linear + forcing part

$x = A\sin\psi \quad x' = k_\beta A\cos\psi$ ← PHASE/AMPLITUDE

$\psi = k_\beta s + \alpha$ If $f = 0$ A & ϕ would be constant

$\Rightarrow A' = \frac{1}{k_\beta r_{b0}} f\cos\psi \quad \alpha' = \frac{-1}{k_\beta r_{b0} A} f\sin\psi$

DEFINE RESONANT PHASE $\Psi_r = 2\psi - k_\beta s$

AVERAGE OVER ALL NON-RESONANT FREQUENCIES

$$A_r' = \frac{1}{k_\beta r_{b0}} \int_{-\pi}^{\pi} f\cos\psi \frac{d\psi}{2\pi}; \quad \alpha_r' = \frac{-1}{k_\beta A_r} \int_{-\pi}^{\pi} \frac{d\psi}{2\pi} f\sin\psi$$

$\rightarrow A_r', \Psi_r' \xrightarrow[(\omega = A_r^2)]{} \omega', \Psi_r' \rightarrow H(\omega, \Psi_r) \rightarrow$ CORE RESONANT PARTICLE TRAJECTORY & SEPARATRIX

Numerically determined frequency and amplitude of particle oscillations: linear rf focusing

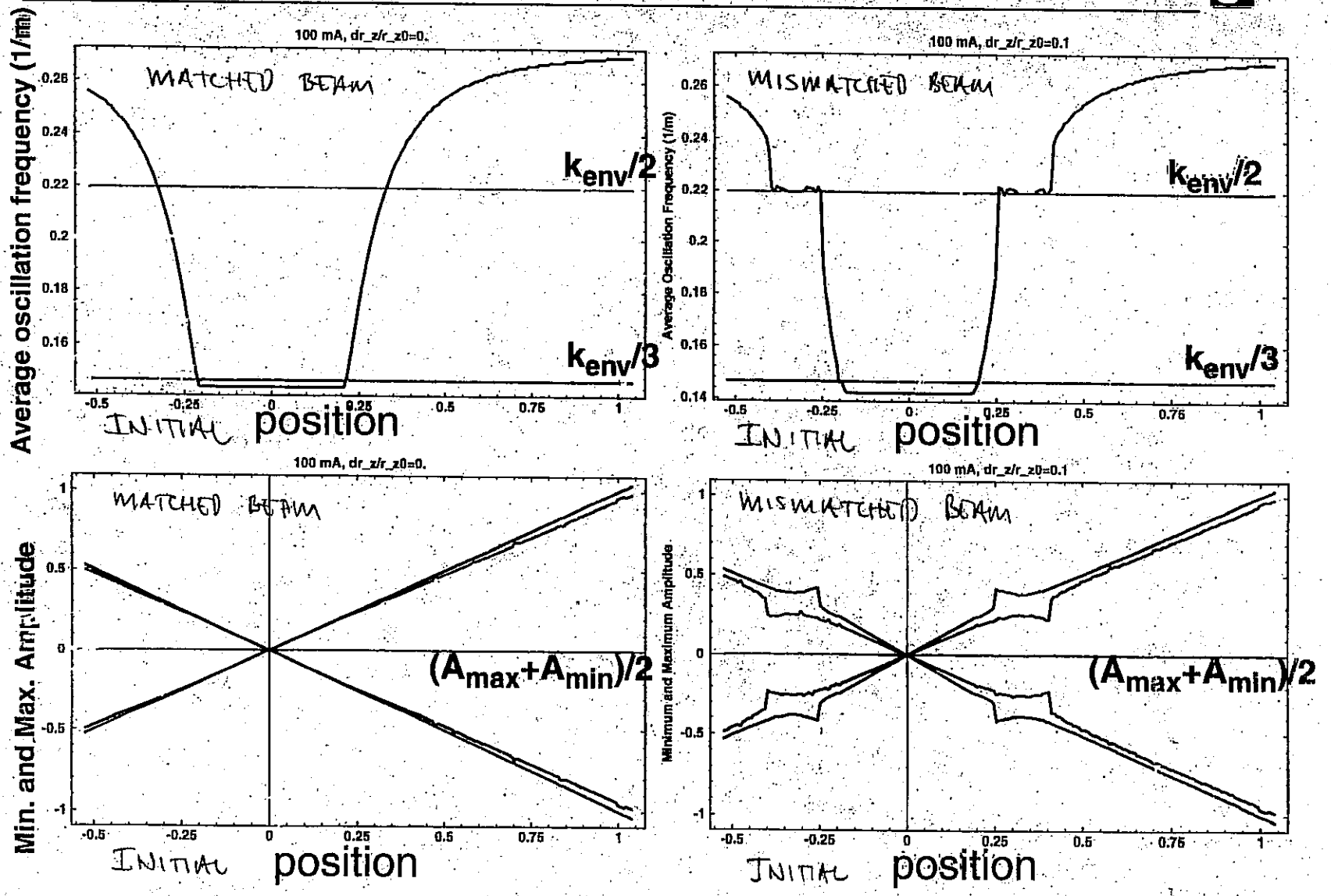

HI+ Heavy ion	Residual gas molecule	e- electron

Processes:

1. Coulomb collisons (intra-beam)

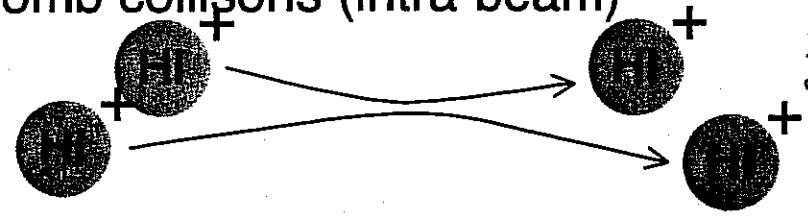

$$\frac{dT_\perp}{dt} = -\frac{1}{2}\frac{dT_\parallel}{dt} = -\frac{(T_\perp - T_\parallel)}{\tau}$$

$$\tau \sim \nu_c^{-1}$$

2. Coulomb collisions with residual gas

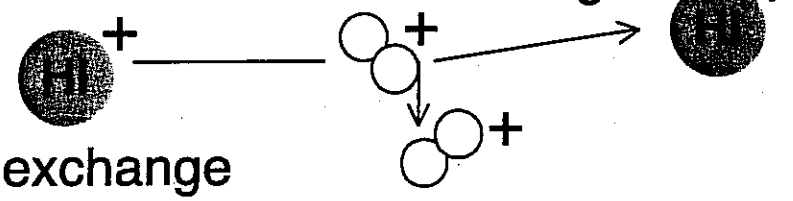

$$\frac{d\sigma_N}{ds} \sim n_g(\quad)$$

3. Charge exchange

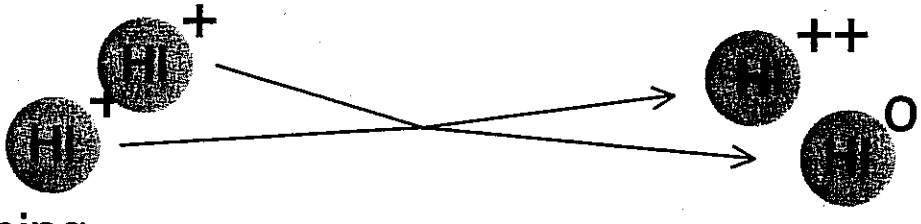

4. Stripping

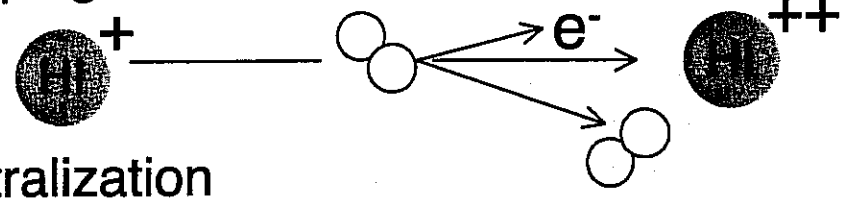

5. Neutralization

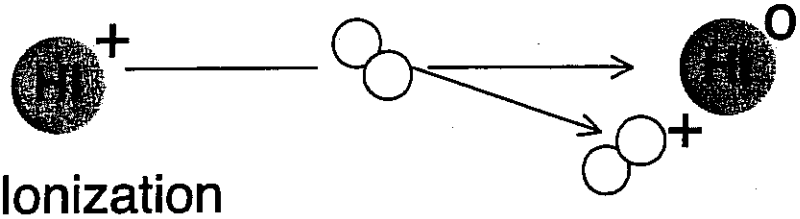

CHARGE CHANGING COLLISIONS

Beam loss

+

n_{HI} molecules

6. Gas Ionization

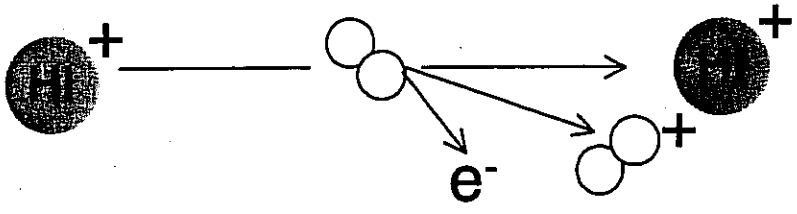

n_g molecules

SUMMARY OF ELECTRON, GAS, PRESSURE, & SCATTERING EFFECTS

1. COULOMB COLLISIONS WITHIN BEAM CAN TRANSFER ENERGY FROM ⊥ TO ∥ AND PROVIDE LOWER LIMIT ON $T_{\parallel}$, HIGHER THAN FROM ACCELERATIVE COOLING.

2. COULOMB INTERACTIONS WITH RESIDUAL GAS NUCLEI PROVIDE A SOURCE OF EMITTANCE GROWTH (BUT NOT IMPORTANT FOR HIGHER MASS AND LONGER RESIDENCE TIMES).

3. PRESSURE INSTABILITY FROM DESORPTION OF RESIDUAL GAS BY STRAYED BEAM IONS HITTING WALL OR BEAM-IONIZED RESIDUAL GAS ATOMS, FORCED TO WALL BY E-field of BEAM. LIMITS CURRENT IN RINGS OR HIGH REP RATE LINAC.

4. ELECTRONS CAN CASCADE AND REACH A "QUASI" EQUILIBRIUM POPULATION OF SIMILAR LINE CHARGE TO THE ION BEAM. ELECTRON-ION TWO STREAM INSTABILITY IS UNSTABLE, AND CAN LEAD TO TRANSVERSE INSTABILITY, SIMILAR TO WHAT IS OBSERVED IN SOME PROTON RINGS.

Inertial Fusion Energy (IFE) power plants of the future will consist of four parts

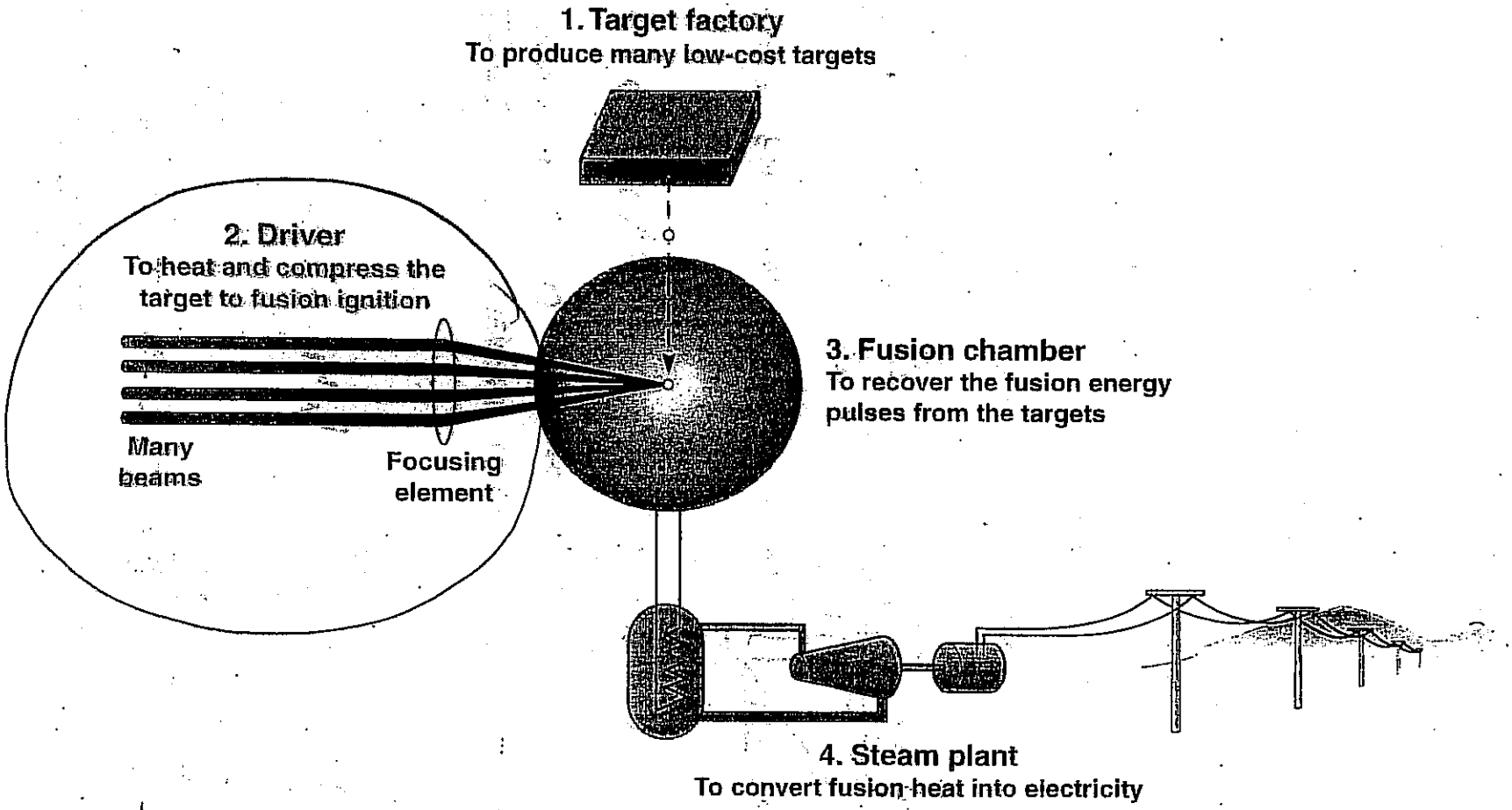

A power-plant driver would fire about five targets per second to produce as much electricity as today's 1000-megawatt power plant